FROM OXIDATIVE STRESS TO COGNITIVE DECLINE - TOWARDS NOVEL THERAPEUTIC APPROACHES, 2nd Edition

EDITED BY: Touqeer Ahmed and Nady Braidy

PUBLISHED IN: Frontiers in Molecular Neuroscience, Frontiers in Pharmacology, Frontiers in Neuroscience, Frontiers in Aging Neuroscience and Frontiers in Behavioural Neuroscience

frontiers Research Topics

ISSN 1664-8714
ISBN 978-2-8325-3410-6
DOI 10.3389/978-2-8325-3410-6

About Frontiers

Frontiers is more than just an open-access publisher of scholarly articles: it is a pioneering approach to the world of academia, radically improving the way scholarly research is managed. The grand vision of Frontiers is a world where all people have an equal opportunity to seek, share and generate knowledge. Frontiers provides immediate and permanent online open access to all its publications, but this alone is not enough to realize our grand goals.

Frontiers Journal Series

The Frontiers Journal Series is a multi-tier and interdisciplinary set of open-access, online journals, promising a paradigm shift from the current review, selection and dissemination processes in academic publishing. All Frontiers journals are driven by researchers for researchers; therefore, they constitute a service to the scholarly community. At the same time, the Frontiers Journal Series operates on a revolutionary invention, the tiered publishing system, initially addressing specific communities of scholars, and gradually climbing up to broader public understanding, thus serving the interests of the lay society, too.

Dedication to Quality

Each Frontiers article is a landmark of the highest quality, thanks to genuinely collaborative interactions between authors and review editors, who include some of the world's best academicians. Research must be certified by peers before entering a stream of knowledge that may eventually reach the public - and shape society; therefore, Frontiers only applies the most rigorous and unbiased reviews.
Frontiers revolutionizes research publishing by freely delivering the most outstanding research, evaluated with no bias from both the academic and social point of view. By applying the most advanced information technologies, Frontiers is catapulting scholarly publishing into a new generation.

What are Frontiers Research Topics?

Frontiers Research Topics are very popular trademarks of the Frontiers Journals Series: they are collections of at least ten articles, all centered on a particular subject. With their unique mix of varied contributions from Original Research to Review Articles, Frontiers Research Topics unify the most influential researchers, the latest key findings and historical advances in a hot research area! Find out more on how to host your own Frontiers Research Topic or contribute to one as an author by contacting the Frontiers Editorial Office: frontiersin.org/about/contact

FROM OXIDATIVE STRESS TO COGNITIVE DECLINE - TOWARDS NOVEL THERAPEUTIC APPROACHES, 2nd Edition

Topic Editors:
Touqeer Ahmed, National University of Sciences & Technology, Pakistan
Nady Braidy, University of New South Wales, Australia

Publisher's note: This is a 2nd edition due to an article retraction.

Citation: Ahmed, T., Braidy, N., eds. (2023). From Oxidative Stress to Cognitive Decline - Towards Novel Therapeutic Approaches, 2nd Edition. Lausanne: Frontiers Media SA. doi: 10.3389/978-2-8325-3410-6

Table of Contents

frontiers in Molecular Neuroscience

EDITORIAL
published: 12 April 2021
doi: 10.3389/fnmol.2021.650498

Editorial: From Oxidative Stress to Cognitive Decline - Towards Novel Therapeutic Approaches

Touqeer Ahmed[1]* *and Nady Braidy*[2]*

[1] Neurobiology Laboratory, Department of Healthcare Biotechnology, Atta-ur-Rahman School of Applied Biosciences, National University of Sciences and Technology, Islamabad, Pakistan, [2] Faculty of Medicine, Centre for Healthy Ageing, School of Psychiatry, University of New South Wales, Sydney, NSW, Australia

Keywords: oxidative stress, cognition, Alzheimer's disease, neurodegeneration, natural products

Editorial on the Research Topic

From Oxidative Stress to Cognitive Decline - Towards Novel Therapeutic Approaches

Oxidative stress is likely to play a major contributing role, or at least a causal role, in the etiology and pathogenesis of neurological disorders. So far, limited therapeutic options are available for people with these debilitating disorders. Oxidative stress is caused by multiple factors, including aging, greater vulnerability of easily oxidizable unsaturated fatty acids in the brain, higher metabolic activity by the brain, increased production of mitochondrial-derived free radicals, calcium dyshomeostasis, and glutamate-induced excitotoxicity. Moreover, environmental chemicals/toxins, heavy metals, and an imbalanced diet can contribute significantly to the accumulation of oxidative stress, potentially leading to reduced cellular viability, cognitive decline, and eventually death. In this special topic, a series of articles review recent trends in the molecular mechanisms of oxidative stress in the development and progression of neurodegenerative disorders, and highlight previously undescribed potential therapeutic options.

Oxidative stress represents a major factor which promotes neuronal degeneration, resulting in a wide variety of disorders, including mild cognitive impairment (MCI), which usually progresses to dementia. Arslan et al. systematically reviewed studies conducted on humans where several oxidative stress markers have been used as biomarkers in Alzheimer's disease (AD) at an early stage. The study found that non-invasive oxidative stress markers may be useful for the detection of MCI and AD, but are limited due to poor specificity and sensitivity. However, many of these markers may be used in combination with family history and other biochemical tests to detect the disease at an early stage. The study further showed that long-term use of selected vitamins and polyphenol-rich foods may be useful for managing AD pathology, although further work is needed to justify the use of natural antioxidants in clinic. Kandlur et al. reviewed the implications of age-associated oxidative damage on learning and memory and the molecular events, with special emphasis on associated epigenetic machinery. Increased understanding of these mechanisms may provide renewed insight in to the development of potential therapeutic targets within the oxidative system.

The cross-sectional study by Iqbal et al. further showed that, with increasing age, accumulation of metals was significantly associated with the tau and amyloid pathology. In addition, serum levels of various lipoproteins were associated with severity of MCI in a well-sized Pakistani population. Findings from this study can help in the translation of some commonly measured substances in serum levels to help in predicting the MCI. Hongo et al. explored carotenoid astaxanthin,

Edited by:
Eric J. Kremer,
Université de Montpellier, France

Reviewed by:
Melissa R. Andrews,
University of Southampton,
United Kingdom

***Correspondence:**
Touqeer Ahmed
touqeer.aahmed@gmail.com;
touqeer.ahmed@asab.nust.edu.pk
Nady Braidy
n.braidy@unsw.edu.au

Received: *07 January 2021*
Accepted: *05 March 2021*
Published: *12 April 2021*

Citation:
Ahmed T and Braidy N (2021) Editorial: From Oxidative Stress to Cognitive Decline - Towards Novel Therapeutic Approaches. Front. Mol. Neurosci. 14:650498. doi: 10.3389/fnmol.2021.650498

mitigated memory deficits, and significantly reversed pathological hallmarks of AD, including Aβ42 deposition, pTau formation, GSH decline, and PV-positive neuronal deficits. In line with the clinical findings by Iqbal et al. elevated GSH levels may ameliorate pathological processes in the AD.

AD is characterized by progressive loss of basal forebrain cholinergic neurons and reduced cortical choline acetyltransferase activity is associated with cognitive decline. Most of the drugs available for the management of symptoms for AD are cholinergic modulators, and targeting the cholinergic system may be beneficial in neurocognitive disorders. The original research article by Kowalczyk et al., showed that Bergapten (furanocoumarin), a naturally occurring compound found in the Apiaceae family, could enhance memory performance against scopolamine-induced memory impairment. More specifically, the study demonstrated that Bergapten (both the single and repeated doses) increased memory acquisition and consolidation, suggesting its beneficial effects on multiple cognitive domains. Clinical translation of Bergapten is a promising approach to attenuate oxidative damage due to aging and age-related disorders.

Stroke is the leading cause of morbidity and mortality worldwide and represents a major risk factor for dementia. More than 85% of the stroke cases are ischemic, which result in major loss in physiological activity of the brain, leading to complex pathophysiological events culminating in cognitive decline and death. Ali et al. explored the neuroprotective effects of atorvastatin, cephalexin, and mycophenolate against NF-κB in ischemic stroke, as compared to the standard NF-κB inhibitor caffeic acid phenethyl ester (CAPE). The study demonstrated that these novels NF-κB inhibitors could attenuate ischemic stroke-induced neuronal toxicity by targeting NF-κB, a potential therapeutic approach in ischemic stroke, suggesting a frontier for emerging research. Furthermore, Ling et al. used a mouse model of middle cerebral artery occlusion to show that treatment with melatonin prior to ischemic injury could protect against neuroinflammation and oxidative stress and modulate the endogenously produced antioxidant enzyme, thioredoxin (Trx) pathway. These findings suggest that melatonin can represent a pharmacophore for the development of therapeutic strategies for enhancing recovery, prevention, and progression of ischemic injury.

Subarachnoid hemorrhage (SAH) represents another cerebrovascular disease with significant detrimental effects on the brain and cognitive performance. SAH can lead to endothelial cell injury and blood-brain barrier (BBB) disruption. The original research article by Zhuang et al. demonstrated that hydrogen inhalation could protect against SAH-induced endothelial cell injury, BBB disruption, microthrombosis, and vasospasm in rats, and neurobehavioral effects at least in part by inhibition of activation of the ROS/NLRP3 axis. Liu H. et al. demonstrated that Bakuchiol, an analog of resveratrol, could protect against early brain injury following SAH by ameliorating BBB disruption, oxidative stress, and apoptosis via modulation of Trx1/TXNIP expression and the phosphorylation of AMPK. Taken together, hydrogen inhalation and naturally occurring compounds such as Bakuchiol represent promising therapeutic strategies for protection against brain injury after SAH.

In recent years, there has been a concerted effort to identify and develop potential drugs with multi-target and multi-pathway neuroprotective effects in the treatment of neurocognitive disorders. Abdul Hannan et al. reviewed recent literature on the neuroprotective effects of phytochemicals that can co-activate cellular antioxidant defense and TrkB signaling-mediated cell survival systems. Yang et al. demonstrated that Catalpol (CAT), an iridoid glycoside compound, showed neuroprotective effects by attenuating microglial-mediated neuroinflammatory response through the inhibition of the p53-mediated Bcl-2/Bax/caspase-3 apoptosis pathway and regulating Keap1/Nrf2 pathway. These results collectively indicate the potential of CAT as a highly effective therapeutic agent for neuroinflammatory and neuro-oxidative disorders. In the original research article by Zhang et al., the authors used a cell culture system to demonstrate that the polyphenol Fisetin can protect against hyperglycemia-induced neurotoxicity through the PI3K/Akt/CREB pathway. Fisetin, which is abundant in fruits such as strawberries, grape seed, apple, and onion, can cross the BBB and demonstrated limited adverse effects. Liu P. et al. demonstrated that harmine, an analogous β-carboline alkaloid compound, ameliorated cognitive impairment by inhibiting NLRP3 inflammasome activation and enhancing the BDNF/TrkB signaling pathway in diabetic rats, and represents a potential therapeutic drug for diabetes-induced cognitive dysfunction. Dong et al. demonstrated that nicotine could protect against exposure hydrogen peroxide toxicity *in vitro* through the activation of the α7-nAChR/Erk1/2 signaling pathway, which suggests that nicotine usage may be a novel strategy for the treatment of neurodegenerative disorders associated with increased oxidative stress.

Apart from pharmacological therapeutic strategies for the treatment of neurocognitive disorders, non-pharmacological strategies have been developed to improve brain plasticity and minimize the neurotoxicity effects of amyloid-beta (Aβ) peptide. The original research article by Dare et al. used a neurotoxicity model induced by Aβ in rats to demonstrate that physical and cognitive exercise could reverse recognition memory deficits, lower hippocampal lipid peroxidation, and maintain optimal acetylcholinesterase activity following exposure to pathophysiological concentrations of Aβ. This suggests that physical and cognitive exercises may partially reverse hippocampal tissue disorganization.

Taken together, the articles add to our recent work in the area of oxidative stress and neurodegenerative diseases. Collectively, they demonstrate that oxidative stress plays a central role in the pathobiology of neurodegenerative diseases and AD in particular. The articles are suggestive of the potential beneficial effects of antioxidant therapy for the prevention and treatment of neurodegenerative diseases. These findings are mostly from preclinical studies; further support from clinical data can authenticate the use of these agents.

AUTHOR CONTRIBUTIONS

TA and NB wrote the manuscript and approved it. All authors contributed to the article and approved the submitted version.

Conflict of Interest: The authors declare that the research was conducted in the absence of any commercial or financial relationships that could be construed as a potential conflict of interest.

frontiers in Neuroscience

ORIGINAL RESEARCH
published: 21 January 2020
doi: 10.3389/fnins.2019.01441

Hydrogen Inhalation Attenuates Oxidative Stress Related Endothelial Cells Injury After Subarachnoid Hemorrhage in Rats

*Kai Zhuang[1], Yu-Chun Zuo[2], Prativa Sherchan[3], Ji-Kai Wang[1], Xiao-Xin Yan[4] and Fei Liu[1]**

[1] Department of Neurosurgery, The Third Xiangya Hospital, Central South University, Changsha, China, [2] Department of Neurosurgery, Xiangya Hospital, Central South University, Changsha, China, [3] Department of Physiology and Pharmacology, School of Medicine, Loma Linda University, Loma Linda, CA, United States, [4] Department of Anatomy and Neurobiology, Xiangya School of Medicine, Central South University, Changsha, China

Background: Subarachnoid hemorrhage (SAH) is a devastating cerebrovascular disease with poor clinical outcome. Nucleotide binding and oligomerization domain-like receptor family pyrin domain-containing 3 (NLRP3) inflammasome serves a key role in inflammatory response, which may lead to endothelial cell injury and blood-brain barrier (BBB) disruption. Hydrogen (H_2) is considered a neuroprotective antioxidant. This study was set out to explore whether hydrogen inhalation protects against SAH induced endothelial cell injury, BBB disruption, microthrombosis and vasospasm in rats.

Methods: One hundred eighty-two male SD rats were used for the study. SAH was induced by endovascular perforation. H2 at a concentration of 3.3% was inhaled beginning at 0.5 h after SAH for duration of 30, 60 or 120 min, followed by single administration or once daily administration for 3 days. The temporal expression of NLRP3 and ASC in the brain was determined, with the effect of hydrogen inhalation evaluated. In addition, brain water content, oxidative stress markers, inflammasome, apoptotic markers, microthrombosis, and vasospasm were evaluated at 24 or 72 h after SAH.

Results: The expression of NLRP3 and ASC were upregulated after SAH associated with elevated expression of MDA, 8-OHdG, 4-HNE, HO-1, TLR4/NF-κB, inflammatory and apoptotic makers. Hydrogen inhalation reduced the expression of these inflammatory and apoptotic makers in the vessels, brain edema, microthrombi formation, and vasospasm in rats with SAH relative to control. Hydrogen inhalation also improved short-term and long-term neurological recovery after SAH.

Conclusion: Hydrogen inhalation can ameliorate oxidative stress related endothelial cells injury in the brain and improve neurobehavioral outcomes in rats following SAH. Mechanistically, the above beneficial effects might be related to, at least in part, the inhibition of activation of ROS/NLRP3 axis.

Keywords: subarachnoid hemorrhage, hydrogen, BBB, NLRP3 inflammasome, microthrombosis, vasospasm

OPEN ACCESS

Edited by:
Nady Braidy,
University of New South Wales, Australia

Reviewed by:
Ravinder Kaundal,
Icahn School of Medicine at Mount Sinai, United States
Mengliang Zhou,
Jinling Hospital, China

***Correspondence:**
Fei Liu
doctorlf@126.com

Specialty section:
This article was submitted to Neuropharmacology, a section of the journal Frontiers in Neuroscience

Received: *29 October 2019*
Accepted: *23 December 2019*
Published: *21 January 2020*

Citation:
Zhuang K, Zuo Y-C, Sherchan P, Wang J-K, Yan X-X and Liu F (2020) Hydrogen Inhalation Attenuates Oxidative Stress Related Endothelial Cells Injury After Subarachnoid Hemorrhage in Rats. Front. Neurosci. 13:1441. doi: 10.3389/fnins.2019.01441

INTRODUCTION

Subarachnoid hemorrhage (SAH) is a life threatening cerebrovascular disease with high morbidity and mortality. SAH mainly affects middle-aged patients and accounts for the highest fatality among all stroke subtypes, which places a huge burden on the economy and society (Suarez et al., 2006; Etminan, 2015). Early brain injury (EBI), a series of pathophysiological changes occurring within the first 72 h after SAH, has been considered a major cause of death and poor outcomes following SAH (Cahill et al., 2006; Caner et al., 2012; Sehba et al., 2012). Additionally, delayed cerebral ischemia (DCI) that occurs 4–14 days after SAH may progress to cerebral infarction and exacerbate brain injury, also causing mortality or severe disability. Recently, microthrombosis due to endothelial cell injury has been implicated as one of the mechanisms that contribute to DCI.

Oxidative stress resulted from oxy-hemoglobin stimulation post SAH is one of the factors involved in EBI (Ayer and Zhang, 2008; Crowley et al., 2008). The imbalance in free radical generation and clearance can lead to oxidative stress, which aggravates inflammatory response and cell death after SAH (Ayer and Zhang, 2008; Ducruet et al., 2010). Thus, anti-oxidative agents are expected to be protective against SAH, and may be a potential promising therapeutic strategy for SAH patients (Wang et al., 2012; Kuo et al., 2013; Zhang et al., 2014).

Inflammation mediated by produced chemokines and cytokines is another major factor responsible for EBI in SAH, (Caner et al., 2012; Chen et al., 2013; Sun et al., 2013). Mounting evidence indicates that NLRP3 inflammasome is a key component of the inflammatory response in various neurological diseases including SAH (Chen et al., 2013; Ma et al., 2014), ischemic stroke (Yang et al., 2014), traumatic brain injury (Liu et al., 2013), and Alzheimer's disease (Tan et al., 2013). Reactive oxygen species (ROS) generation, K^+ efflux, Cl^- efflux appear to be the three common upstream mediators of NLRP3, while activation of the adapter protein apoptosis-associated speck-like protein containing a CARD (ASC) is also involved (Tang et al., 2017). However, the role and mechanism of NLRP3 inflammasome in the pathogenesis of microthrombosis and vasospasm after SAH remain poorly understood.

Hydrogen (H_2) is an antioxidant gas that appears to be neuroprotective (Zhan et al., 2012; Zhuang et al., 2012; Zhuang et al., 2013). Recent studies show that hydrogen exerts anti-oxidant, anti-inflammatory, and anti-apoptotic properties. For instance, hydrogen can mitigate ischemia/reperfusion injury of kidney (Cardinal et al., 2010) and intestine (Wu et al., 2017). Hydrogen enriched saline can attenuate neuronal apoptosis and oxidative stress post SAH (Hong et al., 2014). A recent study showed beneficial effects of intraperitoneal injection of hydrogen-rich saline in an experimental SAH model, and hypothesized that the protective effect might involve NLRP3 inflammasome (Shao et al., 2016). Thus, it is necessary to explore whether hydrogen gas inhalation can reduce NLRP3 inflammasome and mitigate this downstream effects after SAH. Given the importance of vascular endothelial injury in the pathophysiology of SAH, the study was aimed to investigate whether hydrogen inhalation can reduce SAH induced microthrombosis and vasospasm via ameliorating endothelial cell inflammation and damage.

MATERIALS AND METHODS

Animals and Surgical Induction of SAH

Adult male Sprague–Dawley rats (250 g–280 g) were purchased from the SLAC Company (Changsha, China). Rats were housed in a room with constant temperature (25°C), humidity control and with a 12/12 h light/dark cycle, with standard animal chow and water provided freely. All the experimental procedures were approved by the Institutional Animal Care and Use Committee of Central South University and performed according to the Guide for the Care and Use of Laboratory Animals of the National Institutes of Health (eighth edition) and the ARRIVE guidelines.

Surgery was performed to induce SAH using a modified endovascular perforation method as previously described (Sugawara et al., 2008). Briefly, rats were anesthetized with pentobarbital (40 mg/kg, i.p.). The left common-, external-, and internal- carotid arteries were exposed, and a 3-centimeter-long sharpened 4–0 monofilament nylon suture was inserted into the left internal carotid artery through the external carotid artery stump until a resistance was felt, and the suture was advanced 3 mm further to perforate the bifurcation of anterior and middle cerebral artery (MCA). Sham-operated rats underwent above identical procedures except for the artery perforation.

Hydrogen Administration

Hydrogen (H_2) was administered to experimental rats by inhalation, which was started 0.5 h after the induction of SAH. Hydrogen administration was performed following procedures described in a previous study (Xin et al., 2017). Thus, rats were placed in a transparent chamber that had an inlet connected with 3.3% hydrogen gas inhaler (MIZ, MHG-2000, Japan). The concentration of oxygen in the chamber was maintained at 21% using supplemental oxygen which was monitored continuously with a gas analyzer. Hydrogen concentration in the chamber was maintained at 3.3% with continuous monitoring throughout the duration of inhalation. The animals without hydrogen treatment were placed in a chamber with room air only.

Animal Grouping and Treatments

The overall experimental design is shown schematically in **Figure 1**. The study was divided into four parts. The first part consisted of time course study; the second part was outcome study to evaluate effects of three different durations of H2 inhalation; the third part was outcome study to evaluate the effects of a single or once daily administration of H2 inhalation for 3 days; and the fourth part was to evaluate the long-term outcome after H2 inhalation.

Experiment 1

This experiment was designated to determine the temporal expression of NLRP3 and ASC in the ipsilateral left hemisphere at different time-points after SAH. Twenty-four rats were randomly divided into four groups: Sham group surviving 24 h (h) and

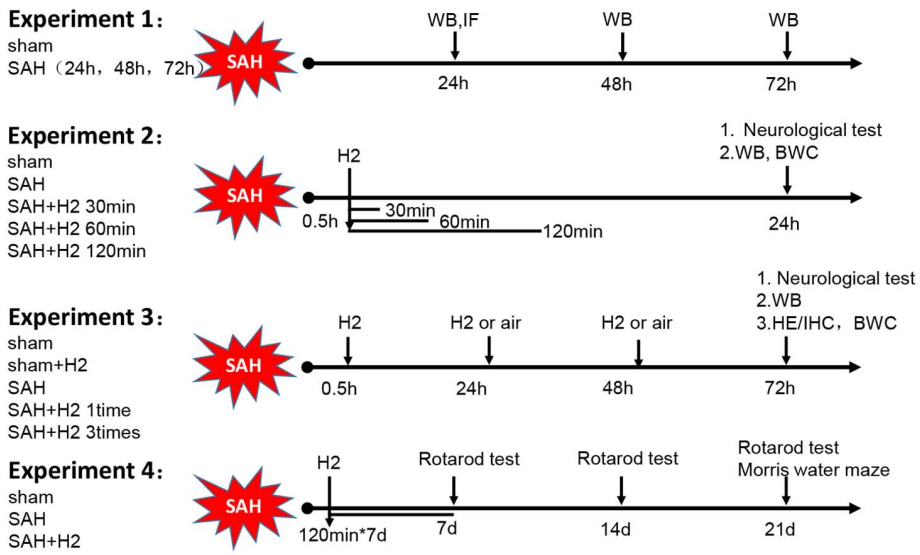

FIGURE 1 | Schematic illustration of experimental design. H2, hydrogen gas; WB, western blot; IF, immunofluorescence; IHC, immunohistochemistry; HE, Hematoxylin Eosin; BWC, Brain water content.

SAH groups surviving 24, 48, and 72 h post-surgery, respectively ($n = 6$/group). The animals were euthanized at the indicated time-points after SAH, with brain samples analyzed biochemically and histologically.

Experiment 2

This experiment was set to evaluate the effect of hydrogen inhalation for 30, 60, and 120 min on the expression of NLRP3 and ASC at 24 h after SAH. Thirty rats were randomly assigned into five groups ($n = 6$/group): Sham, SAH, SAH + H2 (30 min), SAH + H2 (60 min), and SAH + H2 (120 min). Hydrogen gas inhalation was started 0.5 h after SAH, and continued for 30, 60, and 120 min, respectively. Rats in Sham and SAH groups that were supplied with normal room air only. Neurobehavior was evaluated 24 h after surgery. Animals were allowed to survive 24 h, and then the brain samples were collected and subjected to immunoblotting study. Additionally, brain water content was measured in control and H2 treatment groups surviving 120 min, including 18 rats in the Sham, SAH and SAH + H2 groups, respectively ($n = 6$/group). Water contents in neuroanatomical structures were calculated using the formula: Water content (%) = (wet weight – dry weight)/wet weigh × 100%, wherein wet weigh was measured immediately following brain dissection, while dry weight was obtained following 24 h drying of the samples in the oven at 100°C.

Experiment 3

This experiment was to determine the effect of one time or three times administration of hydrogen gas inhalation on the expression of NLRP3 and ASC at 72 h after SAH. Thirty rats were randomly assigned to four groups ($n = 6$/group): Sham, Sham + H2, SAH, SAH + H2 (one time) and SAH + H2 (three times). Hydrogen gas inhalation was administered either one time (0.5 h after SAH) or three times (0.5, 24, and 48 h after SAH). Hydrogen gas concentration was maintained at 3.3% and was administered for duration of 120 min each time. Rats in Sham and SAH group were put in the same chamber with normal room air only. Neurobehavior was evaluated 72 h after surgery, followed by brain collection for western blot analysis. Additionally, 24 rats were divided into four groups ($n = 6$/group): Sham, Sham + H2, SAH, SAH + H2 (three times), the brains from these groups of animals were collected for immunohistochemistry. Besides, 18 rats were divided into three groups ($n = 6$/group): Sham, SAH, SAH + H2 (three times), brain water content was measured at 72 h.

Experiment 4

This experiment was set to explore the long-term beneficial effect of hydrogen inhalation after SAH. Eighteen rats were randomly assigned to three groups ($n = 6$/group): Sham, SAH and SAH + H2. Hydrogen inhalation was administered for 120 min once daily for 7 days. Rats in Sham and SAH groups served as surgical and vehicle controls, respectively. Neurological scores were evaluated using Rotarod test at 7, 14, and 21 days after SAH and water maze test was performed at 21–25 days after operation.

Measurement of SAH Grade

Subarachnoid hemorrhage grade was evaluated using a previously established scoring method, with 0–18 points scaling the degree of bleeding (Sugawara et al., 2008), which was carried out by two investigators who were blinded to the experiments. In sham-operated rats, the score was consistently 0. Only the operated animals with SAH grade greater than eight were included in the current study.

Neurobehavioral Evaluation

Neurobehavioral assessments were performed by an investigator who was blinded to the experiments and animal groups. Modified

Garcia test and beam balance test were performed at 24 and 72 h after SAH using as previously described (Sugawara et al., 2008). Rotarod test was performed at days 7, 14, and 21 after SAH to assess sensorimotor coordination and balance. Water maze test was performed at days 21–25 after SAH to evaluate spatial learning and memory as previously described (Lekic et al., 2010; Sherchan et al., 2011).

Measurement of Lipid Peroxidation

The left hemisphere from freshly removed brain was used for assessment of lipid peroxidation by measurement of malondialdehyde (MDA) using a commercial MDA kits (Cat#S0131, Beyotime, China), following the manufacturer's instruction. The absorbance of the supernatant was measured by spectrophotometry at 532 nm and quantified using a standard curve. All tests were conducted in triplicate. The MDA concentrations were expressed as fold increase relative to sham group.

Western Blot Analysis

Western blot was performed as previously described (Xiao et al., 2018). Briefly, proteins were extracted in lysates of the ipsilateral cortex or hippocampus (doublecortin levels) via homogenization using radioimmunoprecipitation (RIPA) buffer (Cat#P0013B, Beyotime, China). The primary antibodies were used with the following dilutions: NLRP3 (1:500, Cat#ab210491, Abcam, United States), ASC (1:500, Cat#sc-51414, Santa Cruz Biotechnology, United States), caspase-1 (1:500, Cat#22915-1-AP, Proteintech, United States), cleaved caspase-1 (1:1000, Cat#ab179515, Abcam, United States), IL-1β (1:500, Cat#16806-1-AP, Proteintech, China), DCX (1:1000, Cat#ab18723, Abcam, United States) TLR4 (1:1000, Cat#ab217274, Abcam, United States), NF-κB(p65) (1:1000, Cat#ab16502, Abcam, United States), phosph-(NF-κB)(p65) (1:1000, Cat#ab106129, Abcam, United States), SOD2 (1:1000, Cat#ab68155, Abcam, United States), 4-HNE (1:1000, Cat#ab46545, Abcam, United States), HO-1 (1:1000, Cat#ab13243, Abcam, United States), Bcl-2 (1:1000, Cat#ab59348, Abcam, United States), Bax (1:1000, Cat#ab32503, Abcam, United States), cleaved caspase-3 (1:500, Cat#9661, Cell Signaling Technology, United States), and GAPDH (1:1000, Cat#10494-1-AP, Proteintech, China).

Histological, Immunohistochemical and Immunofluorescent Stains

Brain samples were cut into 30 μm thick coronal sections and collected in serial sets as previously described using a cryostat (Leica CM3050S, Buffalo Grove, IL, United States). Consecutive sections from each animal were stained with cresyl violet (Nissl stain), hematoxylin/eosin (HE) and primary antibodies with the avidin-biotin complex (ABC) method or fluorescent-tagged secondary antibodies as previously described (Hu et al., 2017). The primary antibodies used including the following: NLRP3 (1:200, Cat#ab4207, Abcam, United States), ASC (1:200, Cat#sc-51414, Abcam, United States), 8-OHdG (1:200, Cat#ab48508, Abcam, United States), DCX (1:200, Cat#ab18723, Abcam, United States), and fibrinogen (1:500, Cat# LS-B11024, Lifespan, United States). The Nissl stain of the hippocampus was analyzed to assess the neurological damage, the molecular layer and hilus of CA1 were photographed for statistical analysis.

Co-labeling of Lectin and TUNEL Staining

Lectin and TUNEL co-labeling was performed using a double immunofluorescent method. Briefly, brain sections were incubated with biotinylated lectin (1:500, Cat#B-1175, Vector, United States) followed by AMCA Streptavidin (1:200, Vector, United States) to label vascular endothelium. TUNEL staining was performed using an *in situ* Cell Death Detection Kit (Cat#11684817910, Roche Inc., United States), which was performed following the manufacturer instructions to detect apoptosis as previously described (Xiao et al., 2018). Sections were dehydrated in increasing concentrations of ethanol and cleared in xylenes and then coverslippered. Fluorescently labeled sections were coverslippered with a commercial antifading mounting medium. All sections were examined on a light microscope, with images captured using a built-in imaging system (BX53, Olympus, Japan).

Statistical Analysis

Sample size was calculated by Sigma Plot, which indicated that the animal numbers $n = 6$/group was deemed sufficient for the experiments with no outliers identified. All measurement data were expressed as mean ± standard derivation (SD). Normal distribution of data was verified with Shapiro–Wilk normality test. One-way analysis of variance (ANOVA) was used in this study to compare differences among groups followed by Tukey's multiple-comparisons test using the SPSS 18.0 software (SPSS Inc., Chicago, IL, United States). The level of statistically significance difference was set with $p < 0.05$.

RESULTS

Animal Number and Mortality Rate

A total of 182 rats were used for the study which comprised of 48 rats in the Sham group and 134 rats in the SAH groups. None of the animals died in the sham group (0 of 48 rats). The overall mortality rate after SAH induction was 17.9% (24 of 134 rats) (**Supplementary Figure S1A**). There was no significant difference in mortality rates between SAH groups. At 24 h after SAH induction, blood clots were mainly observed around the Circle of Willis and ventral brainstem (**Supplementary Figure S1B**). There was no significant difference in the average SAH grades among SAH groups with or without hydrogen inhalation (**Supplementary Figure S1C**).

SAH Induced Upregulation of NLRP3 and ASC Expression in Ipsilateral Cerebrum

Modified Garcia score and beam balance test were performed to evaluate the neurological deficit (**Supplementary Figures S2A,B**). While western blot was performed to determine

the protein expression of NLRP3 and ASC in the left basal cortex, hippocampus and convex cortex (**Figure 2A**) at 24, 48, and 72 h after SAH. Levels of NLRP3 and ASC were peaked at 24 h after SAH and gradually decreased thereafter, although remained significantly elevated up to 72 h after SAH compared to sham group ($p < 0.05$; **Figures 2B,C**, respectively). Consistent with immunoblotting, double immunofluorescence showed that NLRP3 co-localized ASC in the brain at micro-vessels 24 h after SAH (**Figure 2D**).

H2 Inhalation Attenuated NLRP3 and ASC Overexpression, Improved Neurobehavior and Reduced Brain Water Content at 24 h After SAH

The modified Garcia score and beam balance score evaluated 24 h after SAH was significantly lower in the SAH groups than sham group, and H2 inhalation for 120 min significantly improved the Garcia score and beam balance neurological score compared with SAH group ($p < 0.05$; **Figure 3A**). At 24 h after SAH, the expression of NLRP3 and ASC was significantly increased in the left basal cortex, hippocampus and convex cortex ($p < 0.05$; **Figures 3B,C**). H2 inhalation for 120 min reduced the expression of NLRP3 and ASC in SAH + H2 group when compared with SAH group in the above cerebral subregions ($p < 0.05$; **Figures 3B,C**). Since H2 inhalation for 120 min was observed to be most effective, we chose 120 min time point inhalation for the next studies. The brain water content in the left hemisphere and right hemisphere were significantly increased in SAH group compared with sham group, while H2 inhalation for 120 min significantly reversed this change in SAH + H2 group compared with SAH group ($p < 0.05$; **Figure 3D**). However, the brain water content in cerebellum and brain stem show no significantly difference between sham, SAH and SAH + H2 groups ($p > 0.05$; **Figure 3D**).

H2 Inhalation Attenuated NLRP3 and ASC Overexpression, Improved Neurobehavior and Reduced Brain Water Content at 72 h After SAH

The modified Garcia and beam balance scores 72 h after SAH were significantly improved with one time administration and three times administration of hydrogen inhalation for 120 min duration each ($p < 0.05$; **Figure 4A**). H2 inhalation for three times significantly improved neurological scores 72 h after SAH compared with single administration ($p < 0.05$; **Figure 4B**). At 72 h after SAH, the expression of NLRP3 and ASC was significantly increased, and H2 inhalation for three times reduced the expression of NLRP3 and ASC as compared with SAH and SAH + H2 (one time) groups ($p < 0.05$; **Figure 4B**). The brain water content in the left hemisphere and right hemisphere were significantly reduced in SAH+H2 group compared with SAH group (**Supplementary Figure S2C**). Since H2 inhalation for three times each for 120 min was more effective, we chose hydrogen inhalation three times for the remaining studies.

H2 Inhalation Ameliorated Microthrombosis and Vasospasm 72 h After SAH

Immunohistochemistry staining for fibrinogen showed significantly increased microthrombi counts in both cortex and hippocampus after SAH which was reduced with H2 inhalation three times for 120 min each in the SAH + H2 group compared to SAH group ($p < 0.05$; **Figures 5A,B**). Hematoxylin and eosin staining showed significant vasoconstriction of the anterior cerebral artery (ACA), MCA, and basilar artery (BA) at 72 h after SAH. These changes were reversed in the group with H2 inhalation three times relative to the SAH + H2 group compared to SAH group ($p < 0.05$; **Figures 5C,D**).

H2 Inhalation Attenuated TUNEL Positivity and TLR4/NF-κB Activation at 72 h After SAH

Double staining of lectin and TUNEL staining showed increased TUNEL positive cells in the micro-vessels 72 h after SAH, which was reduced in the SAH + H2 group compared to SAH group (**Figures 6A,B**). Similarly, TUNEL positive cells in the macro-vessels was reduced in the SAH + H2 group compared to SAH group (**Figures 6C,D**). Given that oxidative stress may mediate DNA damage via TLR4/NF-κB pathway, we tested if H2 inhalation could affect TLR4 pathway. Immunoblotting data indicated that levels of TLR4 and phospho-NF-κB (p65), Bax and cleaved caspase-3 were significantly increased in SAH group compared with sham group, whereas the Bcl-2 was significantly reduced. After H2 inhalation, there was a trend of reversal of above changes ($p < 0.05$; **Figure 6E**).

H2 Inhalation Improved Long-Term Neurological Outcome After SAH

Memory and cognitive function deficit was related to the hippocampal injury after SAH. Nissl staining showed that H2 inhalation ameliorated neuronal injury in the hippocampus after SAH (**Figure 7A**). Specifically, the expression of doublecortin (DCX), a marker for immature neurons, was reduced after SAH and H2 inhalation reversed this change (**Figures 7B,C**, respectively). In Rotarod test, SAH group had a significantly shorter latency to fall compared with the sham group at 1, 2, and 3 weeks after SAH. H2 inhalation daily 120 min for 7 days improved the latency to fall in the SAH + H2 group compared to SAH group ($p < 0.05$; **Figure 7D**). In the Water Maze test, the escape latency and swim distance traveled to find the platform was longer in the SAH group compared to sham group. However, H2 inhalation significantly reduced escape latency on days 3 and 4 of testing and decreased swim distance during block three of testing in the SAH + H2 group compared to SAH group ($p < 0.05$; **Figures 7E–G**). In the probe trial, SAH group spent less time in the target quadrant when the platform was removed compared with sham group ($p < 0.05$; **Figure 7H**). Again, H2 inhalation improved the duration spent in probe quadrant in SAH + H2 group compared to SAH group.

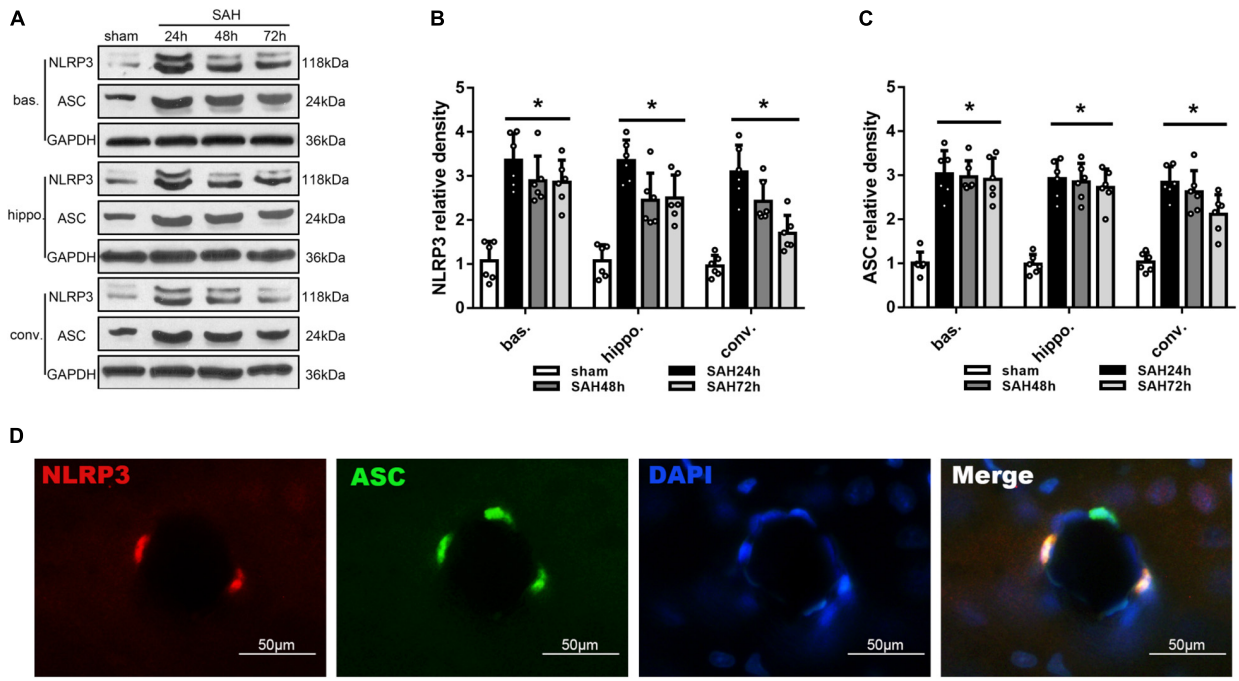

FIGURE 2 | Temporal expression of NLRP3 and ASC in different areas of the ipsilateral hemisphere after unilateral induction of SAH. **(A)** Representative western blots and Quantitative analysis of **(B)** NLRP3 and **(C)** ASC protein expression in the basal cortex (bas.), hippocampus (hippo.), and convex cortex (conv.) at 24, 48, and 72 h after SAH. Data are represented as mean ± SD of relative density. $n = 6$ per group.*$p < 0.05$ vs. sham. **(D)** Double immunofluorescence staining of NLRP3 and ASC. Scale bar = 50 μm.

H2 Inhalation Attenuated Oxidative Stress 72 h After SAH

Oxidative stress induced by SAH was considered as one of main cause of EBI, and may affect multiple cellular elements including endothelial cells. Lipid peroxidation reflected by the concentration of MDA and 8-OHdG may relate to oxidative stress induced DNA damage. We detected changes in the concentration of MDA (**Figure 8A**), 8-OHdG staining (**Figure 8B**) as well as the levels of SOD2, 4-HNE and HO-1 (**Figure 8C**) in the brain at 72 h after SAH. Thus, MDA concentration, 8-OHdG positive cells and the expression of 4-HNE and HO-1 were increased, while the expression of anti-oxidant protein SOD2 was decreased. Notably, these changes were reversed by hydrogen inhalation compared to SAH group.

H2 Inhalation Ameliorated NLRP3 Inflammasome Activation 72 h After SAH

The NLRP3 inflammasome is assembled when the cell is under oxidative stress, and the ROS directly can induce this assembly. Therefore, we speculated that H2 inhalation could reduce endothelial cells injury through inhibit NLRP3 inflammasome. As expected, levels of NLRP3, ASC, cleaved caspase-1, and IL-1β were increased in SAH group compared with the sham group ($p < 0.05$; **Figure 8D**). H2 inhalation reduced the expression of NLRP3, ASC, cleaved caspase-1, and IL-1β in SAH + H2 group compared with SAH group ($p < 0.05$; **Figure 8D**).

DISCUSSION

The present study extended evidence in support of a neuroprotective effect of hydrogen therapy for hemorrhagic cerebral stroke. Major findings of this study include (1) NLRP3 and ASC was upregulated after SAH with highest level noted at 24 h after SAH in the basal cortex, hippocampus and convex cortex; (2) H2 inhalation downregulated the expression of NLRP3 inflammasome proteins and improved neurobehavioral function after SAH. (3) H2 inhalation attenuated microthrombosis and vasospasm after SAH. (4) H2 inhalation improved long-term neurological function after SAH. (5) H2 inhalation reduced oxidative stress partially related to ROS/NLRP3 inflammasome axis.

Reactive oxygen species generated by mitochondrial dysfunction play a significant role in oxidative stress to various types of cells in the brain including microglia, astrocytes, neurons, and endothelial cells, which has been related to inflammation, apoptosis and neurological deficits after SAH (Ayer and Zhang, 2008; Sorce and Krause, 2009; Skowronska and Albrecht, 2013; Sahebkar et al., 2018; Su et al., 2018). The NLRP3 inflammasome composed of NLRP3, ASC and caspase-1, is responsible for the maturation and secretion of proinflammatory cytokines IL-1β and IL-18. A recent study showed that mitochondrial ROS, K^+ efflux, Cl^- efflux are essential and proximal upstream factors for NLRP3 inflammasome assembly (Tang et al., 2017). Inhibition of NLRP3 inflammasome formation has protective effect after SAH

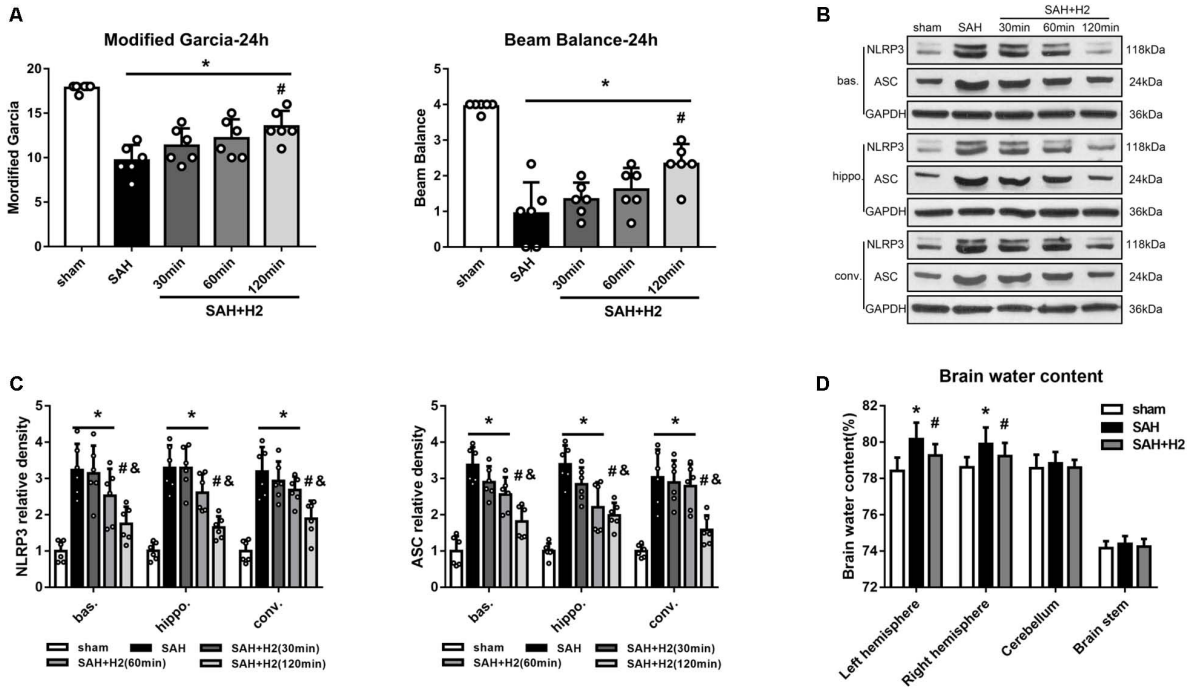

FIGURE 3 | Effect of hydrogen inhalation on neurological scores, NLRP3 and ASC expression and brain edema at 24 h after SAH. **(A)** Modified Garcia score and beam balance test score after hydrogen inhalation treatment for 30, 60, and 120 min duration after SAH. **(B)** Representative western blots and **(C)** quantitative analysis of NLRP3 and ASC protein expression in left basal cortex (bas.), hippocampus (hippo.), and convex cortex (conv.), respectively. **(D)** Brain water content in left hemisphere, right hemisphere, cerebellum and brain stem in sham, SAH and SAH + H2 group. Data represented as mean ± SD. $n = 6$ per group, $^*p < 0.05$ vs. sham; $\#p < 0.05$ vs. SAH; $\&p < 0.05$ vs. SAH + H2 (30 min).

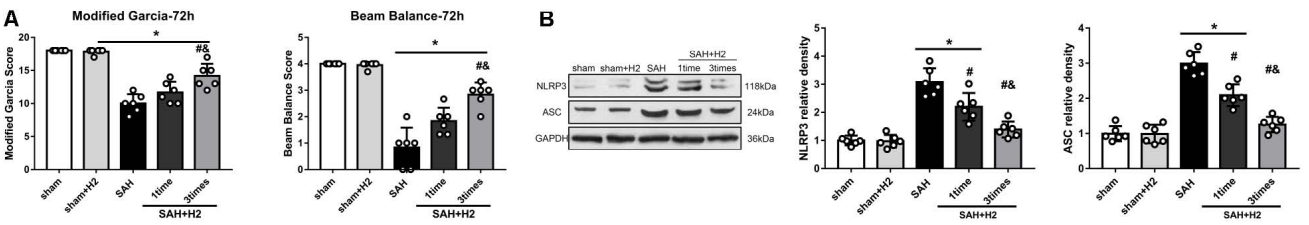

FIGURE 4 | Effect of hydrogen inhalation on neurological scores, NLRP3 and ASC expression and brain edema at 72 h after SAH. **(A)** Modified Garcia score and beam balance test score at 72 h after SAH with hydrogen inhalation single administration (one time) or once daily administration for 3 days (three times). **(B)** Representative western blots and quantitative analysis of NLRP3 and ASC expression in the left hemisphere at 72 h after surgery. Data represented as mean ± SD. $n = 6$ per group, $^*p < 0.05$ vs. sham; $\#p < 0.05$ vs. SAH. $\&p < 0.05$ vs. SAH + H2 (one time).

(Chen et al., 2013; Zhou et al., 2018). In this study, we measured NLRP3 and ASC expression in different brain regions after SAH including the left hippocampus, convex cortex and basal cortex samples. We observed NLRP3 upregulation in all these regions, indicating that SAH could induce mitochondrial ROS affected broad brain regions.

Hydrogen has been considered a therapeutic anti-oxidative agent for decades as it can easily penetrate the blood brain barrier via gaseous diffusion. Considering its explosive potential (safe concentration between 2 and 5%) (Zhan et al., 2012), we used 3.3% as the dosage in the current study. Previous study reported that hydrogen applied at 1 h after injury ameliorated oxidative stress and showed neuroprotective effect at 24 h, but failed to show beneficial effect at 72 h after SAH (Zhan et al., 2012). This suggests that the therapeutic window and treatment duration are important when designing hydrogen therapy. Hydrogen inhalation was started 30 min after SAH in our study, with different duration of hydrogen inhalation, single vs. multiple times inhalation also tested to determine the optimal regime for hydrogen inhalation. Our results suggest that hydrogen inhalation for 120 min once daily for 3 and 7 days can improve short-term and long-term neurobehavior outcomes after SAH.

Vasospasm has been considered as the main pathophysiological cause of delayed brain injury. Recently, microthrombosis has been shown to play a major role in DCI (Vergouwen et al., 2008). Indeed, autopsy studies observed

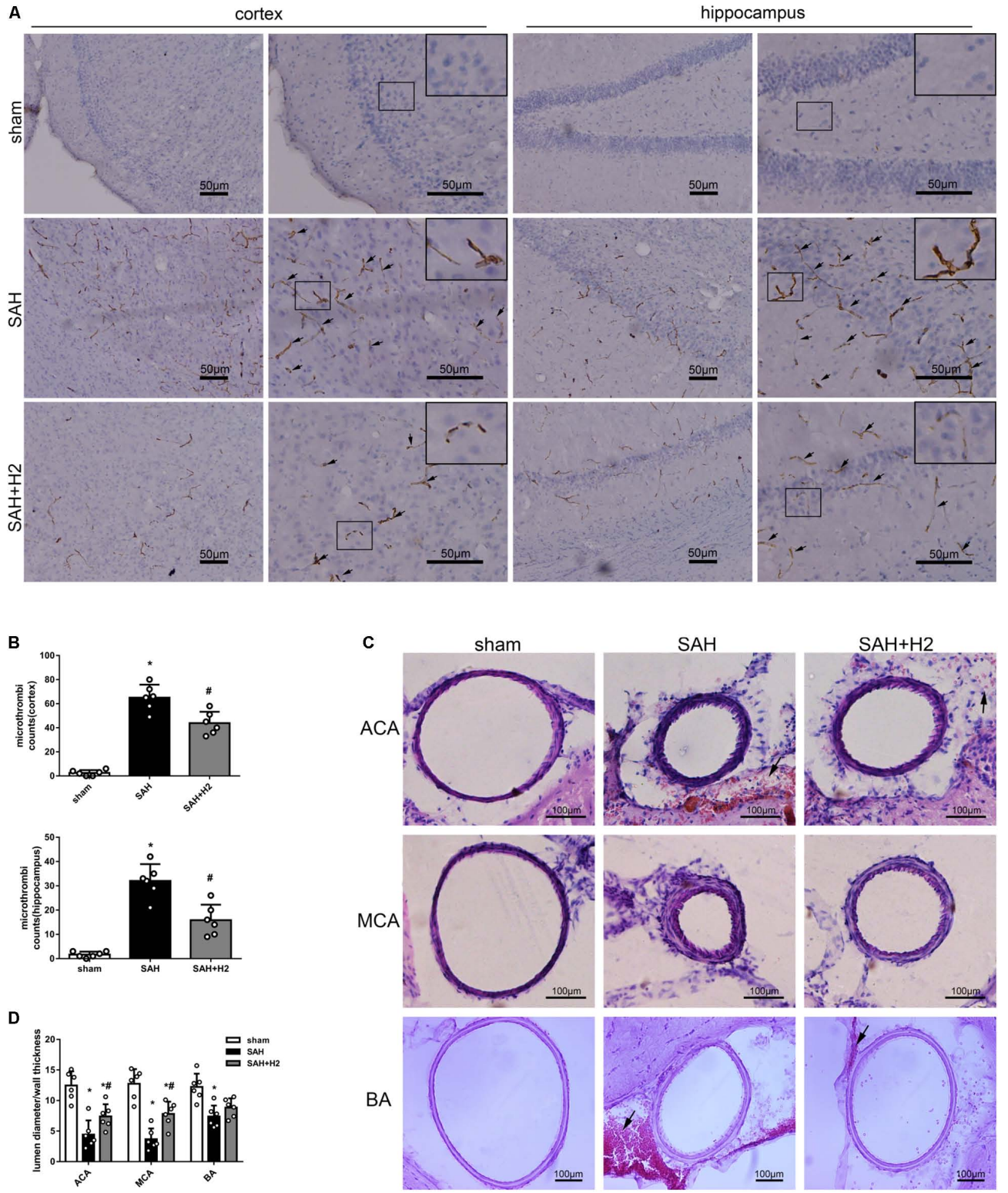

FIGURE 5 | Effect of hydrogen inhalation on microthrombosis and vasospasm at 72 h after SAH. **(A)** Representative images and **(B)** quantitative analysis of microthrombosis in the cortex and hippocampus at 72 h after SAH. Scale bar = 50 μm. **(C)** Representative images and **(D)** quantitative analysis of vasospasm of the anterior cerebral artery (ACA), middle cerebral artery (MCA), and basilar artery (BA) at 72 h after SAH. Scale bar = 100 μm. Data represented as mean ± SD. $n = 6$ per group, $^{*}p < 0.05$ vs. sham; $\#p < 0.05$ vs. SAH.

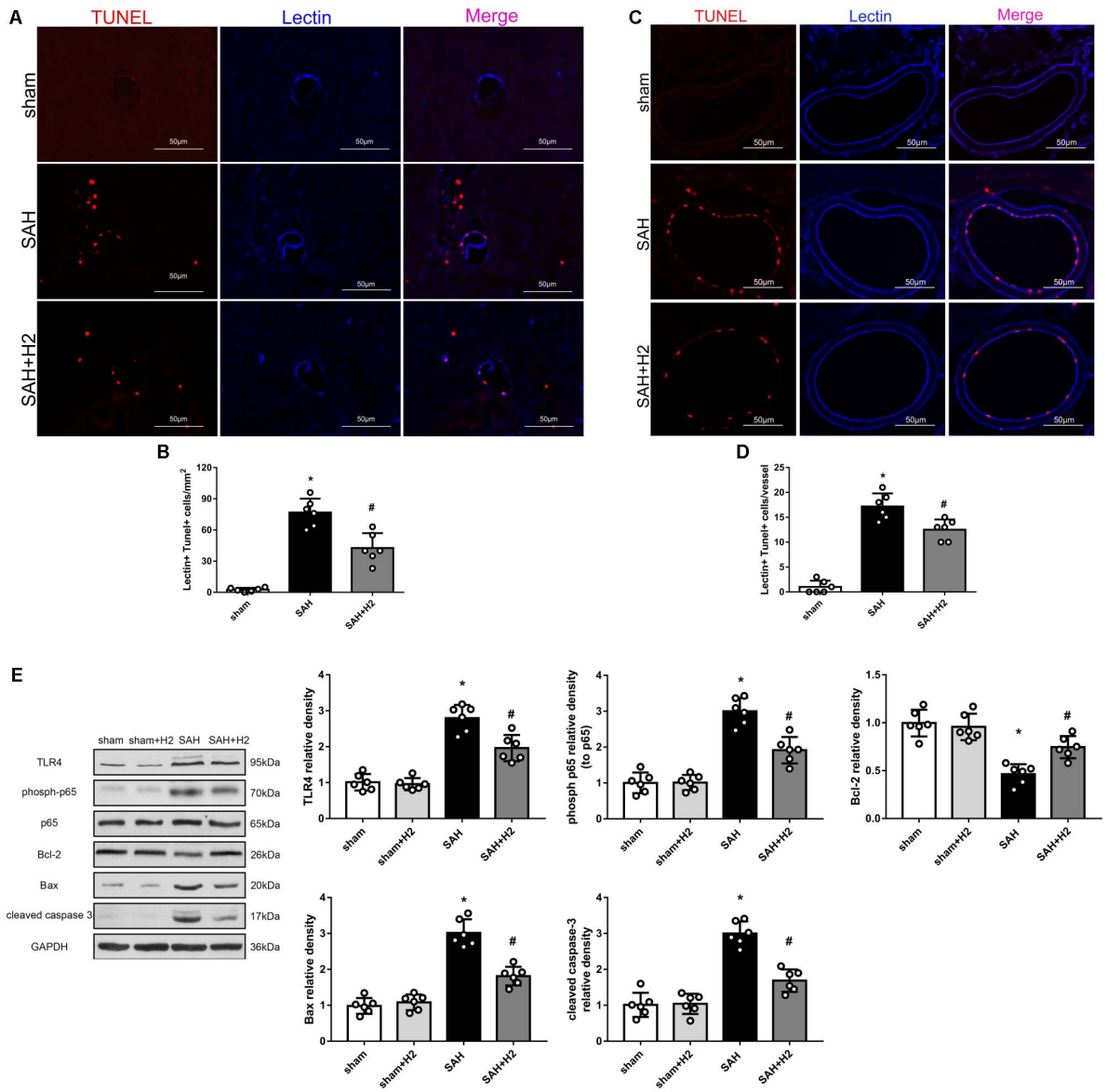

FIGURE 6 | Effect of hydrogen inhalation on endothelium injury in the micro- and macro-vessels at 72 h after SAH. **(A)** Representative immunofluorescence images and **(B)** quantitative analysis of lectin and TUNEL staining in brain micro-vessels. **(C)** Representative images and **(D)** quantitative analysis of lectin and TUNEL staining in brain macro-vessels. **(E)** Representative western blots and quantitative analysis of TLR4, phosoh-p65, Bcl-2, Bax and cleaved caspase-3 in left hemisphere at 72 h. Data represented as mean ± SD. $n = 6$ per group, $^*p < 0.05$ vs. sham; $\#p < 0.05$ vs. SAH.

ischemic regions rich of microthrombi, while vasospasm was neither necessary nor sufficient to induce delayed ischemic deficits (Suzuki et al., 1990; Vergouwen et al., 2008). Endothelial cell death and coagulation induced by inflammation have been well established (Muroi et al., 2014; Frontera et al., 2017), and considered the main cause of microthrombosis (Sabri et al., 2012). We found co-labeling of the endothelial marker lectin and TUNEL, indicating DNA damage in endothelial cells after SAH. We also observed NLRP3 expression in the endothelial cells after SAH suggestive of endothelial inflammation. Interestingly, we found that both microvessels and macrovessels were affected after SAH, and hydrogen inhalation could ameliorate these changes in the vascular profiles.

Oxidative stress to lipids and proteins are a part of the pathophysiology of SAH and can result in cellular damage and dysfunction (Facchinetti et al., 1998; Zhan et al., 2012). Elevation of MDA and 8-OHdG are reported after SAH (Mo et al., 2018). In this study we also observed increased levels of MDA and 8-OHdG in the brain after SAH, and hydrogen inhalation significantly reversed these changes. Therefore, hydrogen inhalation can provide antioxidative protective effect on lipids and proteins after SAH.

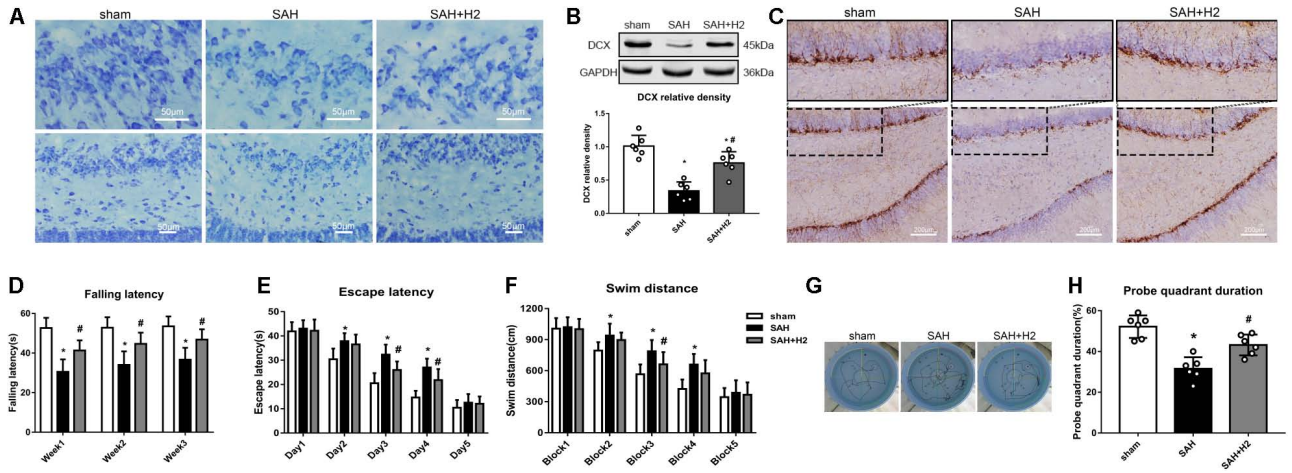

FIGURE 7 | Effect of hydrogen inhalation on long term neurobehavior after SAH. **(A)** Representative images of Nissl staining in the hippocampus. **(B)** Representative western blot images and quantitative analysis of doublecortin (DCX) expression. **(C)** Immunohistochemistry images of DCX in the hippocampus. **(D)** Rotarod test performed at weeks 1, 2, and 3 after SAH. **(E)** Escape latency and **(F)** Swim distance and **(G)** Representative trace images of water maze test performed at 3 weeks after SAH. **(H)** Probe quadrant duration in the probe trial test. Data represented as mean ± SD. $n = 6$ per group. $^*p < 0.05$ vs. sham group; $\#p < 0.05$ vs. SAH group.

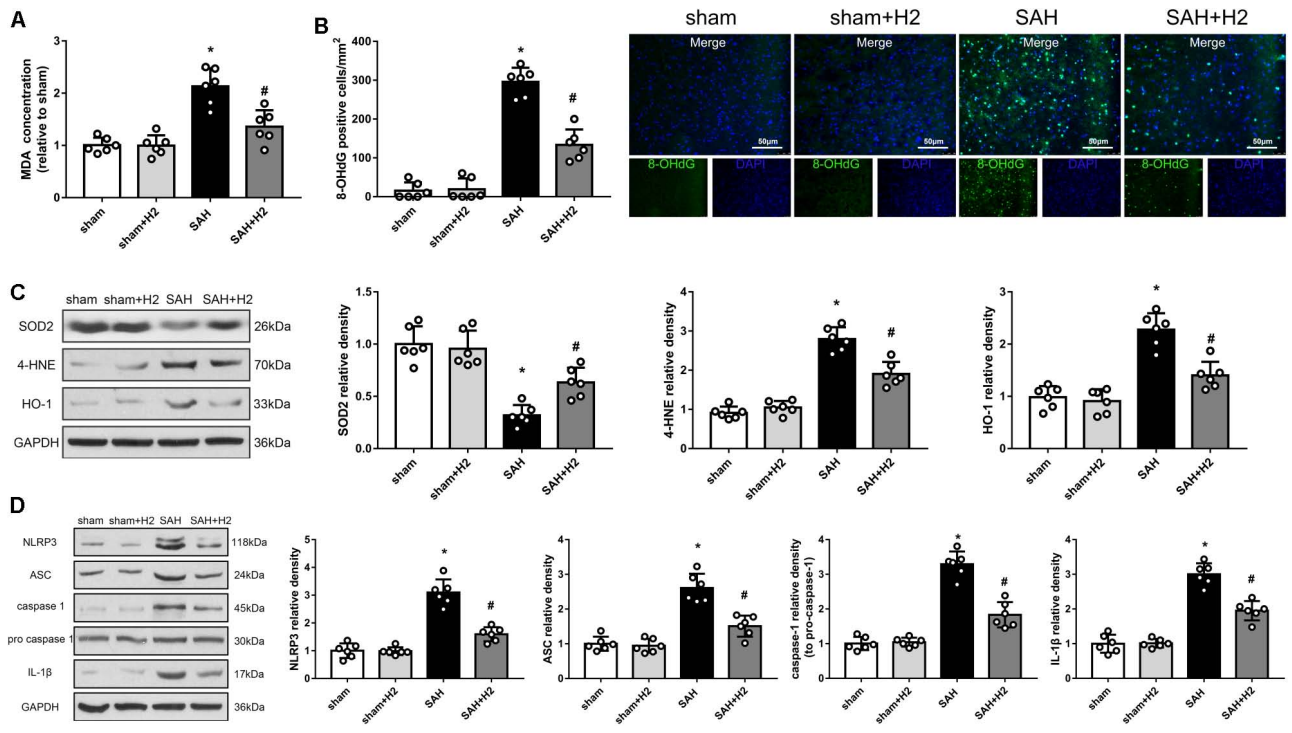

FIGURE 8 | Modulation of hydrogen inhalation on ROS/NLRP3 axis. **(A)** The concentration of MDA in different groups. **(B)** Quantitative analysis and representative images of 8-OHdG staining at 72 h after SAH. **(C)** Representative western blots and quantitative analysis of SOD2, 4-HNE, HO-1 in the left hemisphere 72 h after surgery. **(D)** Representative western blots and quantitative analysis of NLRP3, ASC, cleaved caspase-1, caspase-1, and IL-1β in the left hemisphere. Data represented as mean ± SD. $n = 6$ per group, $^*p < 0.05$ vs. sham; $\#p < 0.05$ vs. SAH.

Inflammation is a significant causal factor in EBI after SAH, as suggested by evidence of the involvement of NLRP3 inflammasome and TLR4/NF-κB in SAH (Kawakita et al., 2017; Zhou et al., 2018), which may related to the early as well as late neuronal injuries (Zhou et al., 2007; You et al., 2013; Kawakita et al., 2017; Okada and Suzuki, 2017). Other study showed that the regulation of TLR4/NF-κB pathway by melatonin alleviated secondary brain damage and neurobehavioral dysfunction in

SAH model (Wang et al., 2013). Recently, hydrogen rich saline was reported to attenuate EBI by repressing NLRP3 and NF-κB related inflammation (Shao et al., 2016). Consistently, in this study we observed that hydrogen inhalation decreased levels of NLRP3 inflammasome and the TLR4/NF-κB pathway proteins after SAH.

Cellular damage including apoptosis is associated with EBI in cerebral stroke (Hasegawa et al., 2011). Specifically, endothelial cells play an essential role in maintaining the blood brain barrier, while endothelial dysfunction contributes to vascular disease and stroke (Roquer et al., 2009). Inflammation and apoptosis can induce endothelial damage after stroke (Suzuki and Urano, 2011; Xu et al., 2017). Our results showed that NLRP3 in the endothelial cells after SAH could be mitigated by hydrogen inhalation. We also showed a beneficial effect of hydrogen inhalation in antagonizing DNA fragmentation as indicated by TUNEL positivity in vascular cells induced by experimental SAH. Moreover, we also observed that immature neurons in the hippocampal dentate gyrus were reduced after SAH, and hydrogen inhalation attenuated damage to immature neurons.

Previous studies have shown that hydrogen therapy could improve neurological outcome in animal models of ischemic and hemorrhagic cerebral stroke (Zhan et al., 2012; Zhuang et al., 2012; Shao et al., 2016; Wang et al., 2016; Ono et al., 2017). Hydrogen inhalation can attenuate postoperative cognitive impairment by regulating inflammation and apoptosis in a rat model (Xin et al., 2017). However, long-term outcomes following hydrogen inhalation after SAH has not been previously studied. In this study, we observed that hydrogen inhalation daily for 7 days after SAH improved long-term neurological function evaluated by Rotarod test and water maze test in SAH rats. Consistently, we observed that hydrogen inhalation decreased inflammation and apoptosis markers after SAH which was associated with reduced vasospasm, microthrombosis, cellular injury and improved neurological function after SAH in rats.

Hydrogen products including hydrogen gas and hydrogen saline have broad applications for brain injuries derived from ischemia/reperfusion (Cui et al., 2016; Wang et al., 2016; Yu et al., 2017) and hemorrhage (Hong et al., 2014) in both animal models (Li et al., 2015) and clinical patients (Ono et al., 2017). There are several advantages of hydrogen gas application for clinical use. First, inhalation is a convenient method for hydrogen administration in the clinical setting. Moreover, hydrogen gas is stable without restraints by temperature and humidity. However, there are some limitations in the present study. For example, *in vitro* experiments would be useful to verify inhibition of NLRP3 inflammasome in endothelial cells by hydrogen is relevant to its overall neuroprotective effects after SAH. Further studies are also needed to elucidate the mechanisms by which hydrogen inhalation ameliorates microthrombosis and vasospasm. Moreover, while our findings support an involvement of TLR4/NF-κB pathway in the brain injury after SAH (Wang et al., 2013; Shao et al., 2016), the link of this signaling to hydrogen remains to be explore in detail. Nonetheless, the data presented in the current study support that hydrogen is a promising therapy in clinical management of cerebral strokes.

CONCLUSION

Based on the findings in the current study, we conclude that hydrogen inhalation can improve neurobehavioral outcomes after SAH, which may be related to, at least in part, the effect of this gas in ameliorating microthrombosis and vasospasm, NLRP3 inflammasome formation, activation of the TLR4/NF-κB pathway, and DNA damage in endothelial cells.

DATA AVAILABILITY STATEMENT

All datasets generated for this study are included in the article/**Supplementary Material**.

ETHICS STATEMENT

The animal study was reviewed and approved by the Institutional Animal Care and Use Committee of Central South University.

AUTHOR CONTRIBUTIONS

KZ, Y-CZ, FL, and X-XY participated in the experimental design and manuscript preparation. KZ, Y-CZ, and J-KW performed the experiments. KZ and J-KW collected and analyzed the data. Y-CZ, X-XY, and FL interpreted the data. KZ and Y-CZ drafted the manuscript. PS revised the manuscript and proofread the language. All authors read and approved the final manuscript.

FUNDING

This project was funded by the National Natural Science Foundation of China (Grants 81571150 and 81870944).

SUPPLEMENTARY MATERIAL

The Supplementary Material for this article can be found online at: https://www.frontiersin.org/articles/10.3389/fnins.2019.01441/full#supplementary-material

FIGURE S1 | (A) The number of rats used in each group and mortality. WB, western blot; IF, immunofluorescence; IHC, immunohistochemistry; BWC, Brain water content. **(B)** Representative images of the brain samples from each group at 24 h after surgery. Subarachnoid blood clots were observed mainly around the Circle of Willis and ventral brainstem. No blood was present in the sham group. **(C)** The SAH grade in sham, SAH, and SAH + H2 group.

FIGURE S2 | (A) Modified Garcia score and **(B)** beam balance test score at 24, 48, and 72 h after SAH. **(C)** Brain water content in left hemisphere, right hemisphere, cerebellum and brain stem in sham, SAH and SAH + H2 group at 72 h. Data represented as mean ± SD. $n = 6$ per group, $^{*}p < 0.05$ vs. sham; $\#p < 0.05$ vs. SAH.

REFERENCES

Ayer, R. E., and Zhang, J. H. (2008). Oxidative stress in subarachnoid haemorrhage: significance in acute brain injury and vasospasm. *Acta Neurochir. Suppl.* 104, 33–41. doi: 10.1007/978-3-211-75718-5_7

Cahill, J., Calvert, J. W., and Zhang, J. H. (2006). Mechanisms of early brain injury after subarachnoid hemorrhage. *J. Cereb. Blood Flow Metab.* 26, 1341–1353.

Caner, B., Hou, J., Altay, O., Fujii, M., and Zhang, J. H. (2012). Transition of research focus from vasospasm to early brain injury after subarachnoid hemorrhage. *J. Neurochem.* 123(Suppl. 2), 12–21. doi: 10.1111/j.1471-4159.2012.07939.x

Cardinal, J. S., Zhan, J., Wang, Y., Sugimoto, R., Tsung, A., Mccurry, K. R., et al. (2010). Oral hydrogen water prevents chronic allograft nephropathy in rats. *Kidney Int.* 77, 101–109. doi: 10.1038/ki.2009.421

Chen, S., Ma, Q., Krafft, P. R., Hu, Q., Rolland, W. II, Sherchan, P., et al. (2013). P2X7R/cryopyrin inflammasome axis inhibition reduces neuroinflammation after SAH. *Neurobiol. Dis.* 58, 296–307. doi: 10.1016/j.nbd.2013.06.011

Crowley, R. W., Medel, R., Kassell, N. F., and Dumont, A. S. (2008). New insights into the causes and therapy of cerebral vasospasm following subarachnoid hemorrhage. *Drug Discov. Today* 13, 254–260. doi: 10.1016/j.drudis.2007.11.010

Cui, J., Chen, X., Zhai, X., Shi, D., Zhang, R., Zhi, X., et al. (2016). Inhalation of water electrolysis-derived hydrogen ameliorates cerebral ischemia-reperfusion injury in rats - A possible new hydrogen resource for clinical use. *Neuroscience* 335, 232–241. doi: 10.1016/j.neuroscience.2016.08.021

Ducruet, A. F., Gigante, P. R., Hickman, Z. L., Zacharia, B. E., Arias, E. J., Grobelny, B. T., et al. (2010). Genetic determinants of cerebral vasospasm, delayed cerebral ischemia, and outcome after aneurysmal subarachnoid hemorrhage. *J. Cereb. Blood Flow Metab.* 30, 676–688. doi: 10.1038/jcbfm.2009.278

Etminan, N. (2015). Aneurysmal subarachnoid hemorrhage–status quo and perspective. *Transl. Stroke Res.* 6, 167–170. doi: 10.1007/s12975-015-0398-6

Facchinetti, F., Dawson, V. L., and Dawson, T. M. (1998). Free radicals as mediators of neuronal injury. *Cell Mol. Neurobiol.* 18, 667–682.

Frontera, J. A., Provencio, J. J., Sehba, F. A., Mcintyre, T. M., Nowacki, A. S., Gordon, E., et al. (2017). The role of platelet activation and inflammation in early brain injury following subarachnoid hemorrhage. *Neurocrit. Care* 26, 48–57. doi: 10.1007/s12028-016-0292-4

Hasegawa, Y., Suzuki, H., Sozen, T., Altay, O., and Zhang, J. H. (2011). Apoptotic mechanisms for neuronal cells in early brain injury after subarachnoid hemorrhage. *Acta Neurochir. Suppl.* 110, 43–48. doi: 10.1007/978-3-7091-0353-1_8

Hong, Y., Shao, A., Wang, J., Chen, S., Wu, H., Mcbride, D. W., et al. (2014). Neuroprotective effect of hydrogen-rich saline against neurologic damage and apoptosis in early brain injury following subarachnoid hemorrhage: possible role of the Akt/GSK3beta signaling pathway. *PLoS One* 9:e96212. doi: 10.1371/journal.pone.0096212

Hu, X., Hu, Z. L., Li, Z., Ruan, C. S., Qiu, W. Y., Pan, A., et al. (2017). Sortilin fragments deposit at senile plaques in human cerebrum. *Front. Neuroanat.* 11:45. doi: 10.3389/fnana.2017.00045

Kawakita, F., Fujimoto, M., Liu, L., Nakano, F., Nakatsuka, Y., and Suzuki, H. (2017). Effects of toll-like receptor 4 antagonists against cerebral vasospasm after experimental subarachnoid hemorrhage in mice. *Mol. Neurobiol.* 54, 6624–6633. doi: 10.1007/s12035-016-0178-7

Kuo, C. P., Wen, L. L., Chen, C. M., Huh, B., Cherng, C. H., Wong, C. S., et al. (2013). Attenuation of neurological injury with early baicalein treatment following subarachnoid hemorrhage in rats. *J. Neurosurg.* 119, 1028–1037. doi: 10.3171/2013.4.JNS121919

Lekic, T., Hartman, R., Rojas, H., Manaenko, A., Chen, W., Ayer, R., et al. (2010). Protective effect of melatonin upon neuropathology, striatal function, and memory ability after intracerebral hemorrhage in rats. *J. Neurotrauma* 27, 627–637. doi: 10.1089/neu.2009.1163

Li, X. J., Li, C. K., Wei, L. Y., Lu, N., Wang, G. H., Zhao, H. G., et al. (2015). Hydrogen sulfide intervention in focal cerebral ischemia/reperfusion injury in rats. *Neural Regen. Res.* 10, 932–937. doi: 10.4103/1673-5374.158353

Liu, H. D., Li, W., Chen, Z. R., Hu, Y. C., Zhang, D. D., Shen, W., et al. (2013). Expression of the NLRP3 inflammasome in cerebral cortex after traumatic brain injury in a rat model. *Neurochem. Res.* 38, 2072–2083. doi: 10.1007/s11064-013-1115-z

Ma, Q., Chen, S., Hu, Q., Feng, H., Zhang, J. H., and Tang, J. (2014). NLRP3 inflammasome contributes to inflammation after intracerebral hemorrhage. *Ann. Neurol.* 75, 209–219. doi: 10.1002/ana.24070

Mo, J., Enkhjargal, B., Travis, Z. D., Zhou, K., Wu, P., Zhang, G., et al. (2018). AVE 0991 attenuates oxidative stress and neuronal apoptosis via Mas/PKA/CREB/UCP-2 pathway after subarachnoid hemorrhage in rats. *Redox Biol.* 20, 75–86. doi: 10.1016/j.redox.2018.09.022

Muroi, C., Fujioka, M., Mishima, K., Irie, K., Fujimura, Y., Nakano, T., et al. (2014). Effect of ADAMTS-13 on cerebrovascular microthrombosis and neuronal injury after experimental subarachnoid hemorrhage. *J. Thromb. Haemost.* 12, 505–514. doi: 10.1111/jth.12511

Okada, T., and Suzuki, H. (2017). Toll-like receptor 4 as a possible therapeutic target for delayed brain injuries after aneurysmal subarachnoid hemorrhage. *Neural Regen Res.* 12, 193–196. doi: 10.4103/1673-5374.200795

Ono, H., Nishijima, Y., Ohta, S., Sakamoto, M., Kinone, K., Horikosi, T., et al. (2017). Hydrogen gas inhalation treatment in acute cerebral infarction: a randomized controlled clinical study on safety and neuroprotection. *J. Stroke Cerebrovasc. Dis.* 26, 2587–2594. doi: 10.1016/j.jstrokecerebrovasdis.2017.06.012

Roquer, J., Segura, T., Serena, J., and Castillo, J. (2009). Endothelial dysfunction, vascular disease and stroke: the ARTICO study. *Cerebrovasc Dis.* 27(Suppl. 1), 25–37. doi: 10.1159/000200439

Sabri, M., Ai, J., Lakovic, K., D'abbondanza, J., Ilodigwe, D., and Macdonald, R. L. (2012). Mechanisms of microthrombi formation after experimental subarachnoid hemorrhage. *Neuroscience* 224, 26–37. doi: 10.1016/j.neuroscience.2012.08.002

Sahebkar, A., Panahi, Y., Yaribeygi, H., and Javadi, B. (2018). Oxidative stress in neurodegenerative diseases: a review. *CNS Neurol Disord. Drug Targets* 7, 207–215.

Sehba, F. A., Hou, J., Pluta, R. M., and Zhang, J. H. (2012). The importance of early brain injury after subarachnoid hemorrhage. *Prog. Neurobiol.* 97, 14–37. doi: 10.1016/j.pneurobio.2012.02.003

Shao, A., Wu, H., Hong, Y., Tu, S., Sun, X., Wu, Q., et al. (2016). Hydrogen-rich saline attenuated subarachnoid hemorrhage-induced early brain injury in rats by suppressing inflammatory response: possible involvement of NF-kappaB pathway and NLRP3 inflammasome. *Mol. Neurobiol.* 53, 3462–3476. doi: 10.1007/s12035-015-9242-y

Sherchan, P., Lekic, T., Suzuki, H., Hasegawa, Y., Rolland, W., Duris, K., et al. (2011). Minocycline improves functional outcomes, memory deficits, and histopathology after endovascular perforation-induced subarachnoid hemorrhage in rats. *J. Neurotrauma* 28, 2503–2512. doi: 10.1089/neu.2011.1864

Skowronska, M., and Albrecht, J. (2013). Oxidative and nitrosative stress in ammonia neurotoxicity. *Neurochem. Int.* 62, 731–737. doi: 10.1016/j.neuint.2012.10.013

Sorce, S., and Krause, K. H. (2009). NOX enzymes in the central nervous system: from signaling to disease. *Antioxid Redox Signal.* 11, 2481–2504. doi: 10.1089/ARS.2009.2578

Su, Q., Zheng, B., Wang, C. Y., Yang, Y. Z., Luo, W. W., Ma, S. M., et al. (2018). Oxidative stress induces neuronal apoptosis through suppressing transcription factor EB phosphorylation at Ser467. *Cell Physiol. Biochem.* 46, 1536–1554. doi: 10.1159/000489198

Suarez, J. I., Tarr, R. W., and Selman, W. R. (2006). Aneurysmal subarachnoid hemorrhage. *N. Engl. J. Med.* 354, 387–396.

Sugawara, T., Ayer, R., Jadhav, V., and Zhang, J. H. (2008). A new grading system evaluating bleeding scale in filament perforation subarachnoid hemorrhage rat model. *J. Neurosci. Methods* 167, 327–334. doi: 10.1016/j.jneumeth.2007.08.004

Sun, X., Ji, C., Hu, T., Wang, Z., and Chen, G. (2013). Tamoxifen as an effective neuroprotectant against early brain injury and learning deficits induced by subarachnoid hemorrhage: possible involvement of inflammatory signaling. *J. Neuroinflam.* 10:157. doi: 10.1186/1742-2094-10-157

Suzuki, S., Kimura, M., Souma, M., Ohkima, H., Shimizu, T., and Iwabuchi, T. (1990). Cerebral microthrombosis in symptomatic cerebral vasospasm–a quantitative histological study in autopsy cases. *Neurol Med. Chir.* 30, 309–316. doi: 10.2176/nmc.30.309

Suzuki, Y., and Urano, T. (2011). Novel situations of endothelial injury in stroke–mechanisms of stroke and strategy of drug development: novel mechanism of the expression and amplification of cell surface-associated fibrinolytic activity

demonstrated by real-time imaging analysis. *J. Pharmacol. Sci.* 116, 19–24. doi: 10.1254/jphs.10r23fm

Tan, M. S., Yu, J. T., Jiang, T., Zhu, X. C., and Tan, L. (2013). The NLRP3 inflammasome in Alzheimer's disease. *Mol. Neurobiol.* 48, 875–882. doi: 10.1007/s12035-013-8475-x

Tang, T., Lang, X., Xu, C., Wang, X., Gong, T., Yang, Y., et al. (2017). CLICs-dependent chloride efflux is an essential and proximal upstream event for NLRP3 inflammasome activation. *Nat. Commun.* 8:202. doi: 10.1038/s41467-017-00227-x

Vergouwen, M. D., Vermeulen, M., Coert, B. A., Stroes, E. S., and Roos, Y. B. (2008). Microthrombosis after aneurysmal subarachnoid hemorrhage: an additional explanation for delayed cerebral ischemia. *J. Cereb. Blood Flow Metab.* 28, 1761–1770. doi: 10.1038/jcbfm.2008.74

Wang, X., Zhang, L., Zhao, W., and Liu, T. (2016). The protective effects of hydrogen on HO-1 expression in the brainafter focal cerebral ischemia reperfusion in rats. *Turk J. Med. Sci.* 46, 1534–1539. doi: 10.3906/sag-1502-3

Wang, Z., Ma, C., Meng, C. J., Zhu, G. Q., Sun, X. B., Huo, L., et al. (2012). Melatonin activates the Nrf2-ARE pathway when it protects against early brain injury in a subarachnoid hemorrhage model. *J. Pineal. Res.* 53, 129–137. doi: 10.1111/j.1600-079X.2012.00978.x

Wang, Z., Wu, L., You, W., Ji, C., and Chen, G. (2013). Melatonin alleviates secondary brain damage and neurobehavioral dysfunction after experimental subarachnoid hemorrhage: possible involvement of TLR4-mediated inflammatory pathway. *J. Pineal. Res.* 55, 399–408. doi: 10.1111/jpi.12087

Wu, M. J., Chen, M., Sang, S., Hou, L. L., Tian, M. L., Li, K., et al. (2017). Protective effects of hydrogen rich water on the intestinal ischemia/reperfusion injury due to intestinal intussusception in a rat model. *Med. Gas Res.* 7, 101–106. doi: 10.4103/2045-9912.208515

Xiao, Y., Li, G., Chen, Y., Zuo, Y., Rashid, K., He, T., et al. (2018). Milk fat globule-epidermal growth factor-8 pretreatment attenuates apoptosis and inflammation via the integrin-beta3 pathway after surgical brain injury in rats. *Front. Neurol.* 9:96. doi: 10.3389/fneur.2018.00096

Xin, Y., Liu, H., Zhang, P., Chang, L., and Xie, K. (2017). Molecular hydrogen inhalation attenuates postoperative cognitive impairment in rats. *Neuroreport* 28, 694–700. doi: 10.1097/WNR.0000000000000824

Xu, Y., Wang, Y., Yan, S., Yang, Q., Zhou, Y., Zeng, X., et al. (2017). Regulation of endothelial intracellular adenosine via adenosine kinase epigenetically modulates vascular inflammation. *Nat. Commun.* 8:943. doi: 10.1038/s41467-017-00986-7

Yang, F., Wang, Z., Wei, X., Han, H., Meng, X., Zhang, Y., et al. (2014). NLRP3 deficiency ameliorates neurovascular damage in experimental ischemic stroke. *J. Cereb. Blood Flow Metab.* 34, 660–667. doi: 10.1038/jcbfm.2013.242

You, W. C., Wang, C. X., Pan, Y. X., Zhang, X., Zhou, X. M., Zhang, X. S., et al. (2013). Activation of nuclear factor-kappaB in the brain after experimental subarachnoid hemorrhage and its potential role in delayed brain injury. *PLoS One* 8:e60290. doi: 10.1371/journal.pone.0060290

Yu, Q., Wang, B., Zhao, T., Zhang, X., Tao, L., Shi, J., et al. (2017). NaHS protects against the impairments induced by oxygen-glucose deprivation in different ages of primary hippocampal neurons. *Front. Cell Neurosci.* 11:67. doi: 10.3389/fncel.2017.00067

Zhan, Y., Chen, C., Suzuki, H., Hu, Q., Zhi, X., and Zhang, J. H. (2012). Hydrogen gas ameliorates oxidative stress in early brain injury after subarachnoid hemorrhage in rats. *Crit. Care Med.* 40, 1291–1296. doi: 10.1097/CCM.0b013e31823da96d

Zhang, X. S., Zhang, X., Zhou, M. L., Zhou, X. M., Li, N., Li, W., et al. (2014). Amelioration of oxidative stress and protection against early brain injury by astaxanthin after experimental subarachnoid hemorrhage. *J. Neurosurg.* 121, 42–54. doi: 10.3171/2014.2.JNS13730

Zhou, K., Enkhjargal, B., Xie, Z., Sun, C., Wu, L., Malaguit, J., et al. (2018). Dihydrolipoic acid inhibits lysosomal rupture and NLRP3 through lysosome-associated membrane Protein-1/Calcium/Calmodulin-Dependent protein kinase II/TAK1 pathways after subarachnoid hemorrhage in rat. *Stroke* 49, 175–183. doi: 10.1161/STROKEAHA.117.018593

Zhou, M. L., Shi, J. X., Hang, C. H., Cheng, H. L., Qi, X. P., Mao, L., et al. (2007). Potential contribution of nuclear factor-kappaB to cerebral vasospasm after experimental subarachnoid hemorrhage in rabbits. *J. Cereb. Blood Flow Metab.* 27, 1583–1592. doi: 10.1038/sj.jcbfm.9600456

Zhuang, Z., Sun, X. J., Zhang, X., Liu, H. D., You, W. C., Ma, C. Y., et al. (2013). Nuclear factor-kappaB/Bcl-XL pathway is involved in the protective effect of hydrogen-rich saline on the brain following experimental subarachnoid hemorrhage in rabbits. *J. Neurosci. Res.* 91, 1599–1608. doi: 10.1002/jnr.23281

Zhuang, Z., Zhou, M. L., You, W. C., Zhu, L., Ma, C. Y., Sun, X. J., et al. (2012). Hydrogen-rich saline alleviates early brain injury via reducing oxidative stress and brain edema following experimental subarachnoid hemorrhage in rabbits. *BMC Neurosci.* 13:47. doi: 10.1186/1471-2202-13-47

Conflict of Interest: The authors declare that the research was conducted in the absence of any commercial or financial relationships that could be construed as a potential conflict of interest.

frontiers in Pharmacology

ORIGINAL RESEARCH
published: 11 March 2020
doi: 10.3389/fphar.2020.00307

Astaxanthin Ameliorated Parvalbumin-Positive Neuron Deficits and Alzheimer's Disease-Related Pathological Progression in the Hippocampus of *App*$^{NL-G-F/NL-G-F}$ Mice

Nobuko Hongo[1], *Yusaku Takamura*[1], *Hiroshi Nishimaru*[1], *Jumpei Matsumoto*[1], *Kazuyuki Tobe*[2], *Takashi Saito*[3,4], *Takaomi C. Saido*[3] *and Hisao Nishijo*[1]*

[1] System Emotional Science, Faculty of Medicine, University of Toyama, Toyama, Japan, [2] First Department of Internal Medicine, Faculty of Medicine, University of Toyama, Toyama, Japan, [3] Laboratory for Proteolytic Neuroscience, RIKEN Center for Brain Science, Wako-shi, Japan, [4] Department of Neurocognitive Science, Institute of Brain Science, Nagoya City University Graduate School of Medical Science, Nagoya, Japan

OPEN ACCESS

Edited by:
Nady Braidy, University of New South Wales, Australia

Reviewed by:
Vikas Mishra, Babasaheb Bhimrao Ambedkar University, India
Boyer D. Winters, University of Guelph, Canada

***Correspondence:**
Hisao Nishijo
nishijo@med.u-toyama.ac.jp

Specialty section:
This article was submitted to Neuropharmacology, a section of the journal Frontiers in Pharmacology

Received: *25 December 2019*
Accepted: *02 March 2020*
Published: *11 March 2020*

Citation:
Hongo N, Takamura Y, Nishimaru H, Matsumoto J, Tobe K, Saito T, Saido TC and Nishijo H (2020) Astaxanthin Ameliorated Parvalbumin-Positive Neuron Deficits and Alzheimer's Disease-Related Pathological Progression in the Hippocampus of App$^{NL-G-F/NL-G-F}$ *Mice. Front. Pharmacol. 11:307. doi: 10.3389/fphar.2020.00307*

Growing evidence suggests that oxidative stress due to amyloid β (Aβ) accumulation is involved in Alzheimer's disease (AD) through the formation of amyloid plaque, which leads to hyperphosphorylation of tau, microglial activation, and cognitive deficits. The dysfunction or phenotypic loss of parvalbumin (PV)-positive neurons has been implicated in cognitive deficits. Astaxanthin is one of carotenoids and known as a highly potent antioxidant. We hypothesized that astaxanthin's antioxidant effects may prevent the onset of cognitive deficits in AD by preventing AD pathological processes associated with oxidative stress. In the present study, we investigated the effects of astaxanthin intake on the cognitive and pathological progression of AD in a mouse model of AD. The *App*$^{NL-G-F/NL-G-F}$ mice were fed with or without astaxanthin from 5-to-6 weeks old, and cognitive functions were evaluated using a Barnes maze test at 6 months old. PV-positive neurons were investigated in the hippocampus. Aβ42 deposits, accumulation of microglia, and phosphorylated tau (pTau) were immunohistochemically analyzed in the hippocampus. The hippocampal anti-oxidant status was also investigated. The Barnes maze test indicated that astaxanthin significantly ameliorated memory deficits. Astaxanthin reduced Aβ42 deposition and pTau-positive areal fraction, while it increased PV-positive neuron density and microglial accumulation per unit fraction of Aβ42 deposition in the hippocampus. Furthermore, astaxanthin increased total glutathione (GSH) levels, although 4-hydroxy-2,3-trans-nonenal (4-HNE) protein adduct levels (oxidative stress marker) remained high in the astaxanthin supplemented mice. The results indicated that astaxanthin ameliorated memory deficits and significantly reversed AD pathological processes (Aβ42 deposition, pTau formation, GSH decrease, and PV-positive neuronal

deficits). The elevated GSH levels and resultant recovery of PV-positive neuron density, as well as microglial activation, may prevent these pathological processes.

Keywords: astaxanthin, Alzheimer's disease, amyloid β, parvalbumin-positive neuron, hippocampus, hyperphosphorylated tau, glutathione, 4-HNE protein

INTRODUCTION

Alzheimer's disease (AD) is the prevailing form of dementia, in which memory loss is the first symptom reported by patients (Jahn, 2013). The histopathologic features of the brain with AD are senile plaques that are composed of aggregated β-amyloid peptides (Aβ) and associated proteins and neurofibrillary tangles that are composed of phosphorylated tau (pTau) (Selkoe and Hardy, 2016). There are two major forms of Aβ: Aβ40 and Aβ42. Aβ42 is more neurotoxic due to its higher hydrophobicity, which promotes oligomerization and aggregation (Blennow and Zetterberg, 2018). Aβ deposition also induces microglial activation, which may ameliorate neurodegeneration due to Aβ accumulation (Deczkowska et al., 2018; Edwards, 2019). Accumulating evidence suggests that oxidative stress is implicated in AD; Aβ generates reactive oxygen species leading to mitochondrial dysfunctions *in vitro* (Lustbader et al., 2004; Manczak et al., 2010). A human study on mild cognitive impairment and AD reported that reduction of glutathione (GSH) with anti-oxidative action was observed in the hippocampus and frontal cortex, which was correlated with cognitive deficits (Mandal et al., 2015), while 4-hydroxy-2,3-trans-nonenal (4-HNE) protein adduct levels (a marker of lipid peroxidation) were elevated in AD patients (Markesbery and Lovell, 1998; Zarkovic, 2003).

A subclass of GABAergic interneurons co-expresses the calcium-binding protein parvalbumin (PV). Fast-spiking PV-positive neurons facilitate sensory and cognitive information processing by controlling pyramidal neuron activity and generating gamma oscillation (Bartos et al., 2007; Sohal et al., 2009; Nguyen et al., 2011; Nakamura et al., 2015). PV-positive neurons are sensitive to oxidative stress (Jiang et al., 2013; Kann et al., 2014; Steullet et al., 2017), and number of PV-positive neurons was reduced in the hippocampus of AD mouse models as well as AD patients (Takahashi et al., 2010). Furthermore, reduction of gamma oscillation associated with its dysfunction or phenotype loss was reported in human AD patients (Stam et al., 2002) and human amyloid precursor protein (hAPP) transgenic mice (Verret et al., 2012), which may be implicated in cognitive deficits in the hAPP mice and possibly in AD patients (Verret et al., 2012).

Astaxanthin is one of the carotenoids, naturally distributed in crustanceans, such as shrimps and crabs, and fish such as salmons and sea bream (Miki et al., 1982; Matsuno, 2001), and known as a highly potent antioxidant (Miki, 1991; Rodrigues et al., 2012). Recent clinical studies reported that astaxanthin may improve cognitive functions in aged individuals (Katagiri et al., 2012) and that astaxanthin supplementation decreased Aβ and phospholipid peroxides in red blood cells in healthy senior subjects (Nakagawa et al., 2011; Kiko et al., 2012). The previous available data suggest that astaxanthin may have a therapeutic or preventive effect on the progression of AD. Therefore, we hypothesized that astaxanthin's anti-oxidant effects may contribute to the prevention of the onset of cognitive deficits in AD through its effects on Aβ accumulation, pTau, microglia, and PV-positive neurons. In the present study, the effects of astaxanthin intake on cognitive functions, histopathological progression of AD, and PV-positive neurons were investigated in a mouse model of AD with single App knock-in, which is free from side effects due to overexpression of amyloid precursor protein (APP) (Saito et al., 2014; Sasaguri et al., 2017; Hashimoto et al., 2019)

MATERIALS AND METHODS

Experimental Schedule

Our previous study reported that cortical Aβ deposition in $App^{NL\text{-}G\text{-}F/NL\text{-}G\text{-}F}$ mice ($App^{NL\text{-}G\text{-}F}$ mice) used in this study began by 2 months old and the $App^{NL\text{-}G\text{-}F}$ mice developed cognitive impairment at 6 months old, while microgliosis was observed at 9 months old (Saito et al., 2014). In order to evaluate preventive effects of astaxanthin on AD-related pathological progression, administration of astaxanthin to $App^{NL\text{-}G\text{-}F}$ mice started before formation of Aβ deposition, and the mice were tested with a behavioral test for spatial memory (Barnes maze test) at 6 months old (see below for the details). To analyze effects of astaxanthin on histochemical and biochemical findings in the brain including microgliosis, the mice were sacrificed at 9 months old (see below for the details). Thus, feeding of astaxanthin-containing diet started after weaning at 5-to-6 weeks, and continued until sacrifice at 9 months old (see below for the details), while the mice were subjected to the Barnes maze test at 6 months old.

Animals and Diets

The original lines of $App^{NL\text{-}G\text{-}F}$ mice were obtained from the RIKEN Center for Brain Science (Wako, Japan) and back-crossed onto a C57BL/6J background. After weaning at 5-to-6 weeks, male $App^{NL\text{-}G\text{-}F}$ mice were divided into two diet groups and fed normal chow (MF, Oriental Yeast Co. Ltd., Tokyo, Japan) with or without 0.02% astaxanthin as free form (w/w), which was derived from *Haematococcus pluvialis* (Fuji chemical industries Co., Ltd, Toyama, Japan). Age-matched male wild type (WT) C57BL/6J mice (Japan SCL Inc., Hamamatsu, Japan) were fed normal chow without astaxanthin. Thus, three groups of the mice were used in this study: (1) WT mice fed with normal chow without astaxanthin (control-fed WT mice, n = 25), (2) $App^{NL\text{-}G\text{-}F}$ mice fed with normal chow without astaxanthin

(control-fed App^{NL-G-F} mice, n = 23), and (3) App^{NL-G-F} mice fed with normal chow with astaxanthin (astaxanthin-fed App^{NL-G-F} mice, n = 24).

The App^{NL-G-F} and WT mice were socially housed with mice on the same diet and the same genotype group in a constant temperature environment (22 ± 1°C) with a 12/12-h light/dark cycle (lights were turned on from 07:00 to 19:00). Food and water were available *ad libitum*. All mice were tested with a Barnes maze test at 6 months old and the same mice were sacrificed for immunohistochemical analyses and biochemical assays at 9 months old (see below) (**Figure 1A**). All experimental procedures were conducted according to the guidelines for care and use of laboratory animals approved by the University of Toyama and the National Institutes of Health's Guide for the Care and Use of Laboratory Animals. This study was approved by the Ethics Committee for Animal Experiments at the University of Toyama (Permit No. A2013MED-53).

Barnes Maze Test

A total of 72 mice were tested with the Barnes maze test (control-fed WT mice, n = 25; control-fed App^{NL-G-F} mice, n = 23; astaxanthin-fed App^{NL-G-F} mice, n = 24). In an initial training session, two trials per day were performed continuously for 9 days (**Figure 1B**). In the training session, each mouse was placed in the center of a grey circular table (diam. = 1.0 m), which had 12 holes around the perimeter (**Figure 1C**). The circular open table was 75 cm above the floor and illuminated with 1,080 W lights. The mouse could escape into a black escape box (17 × 13 ×

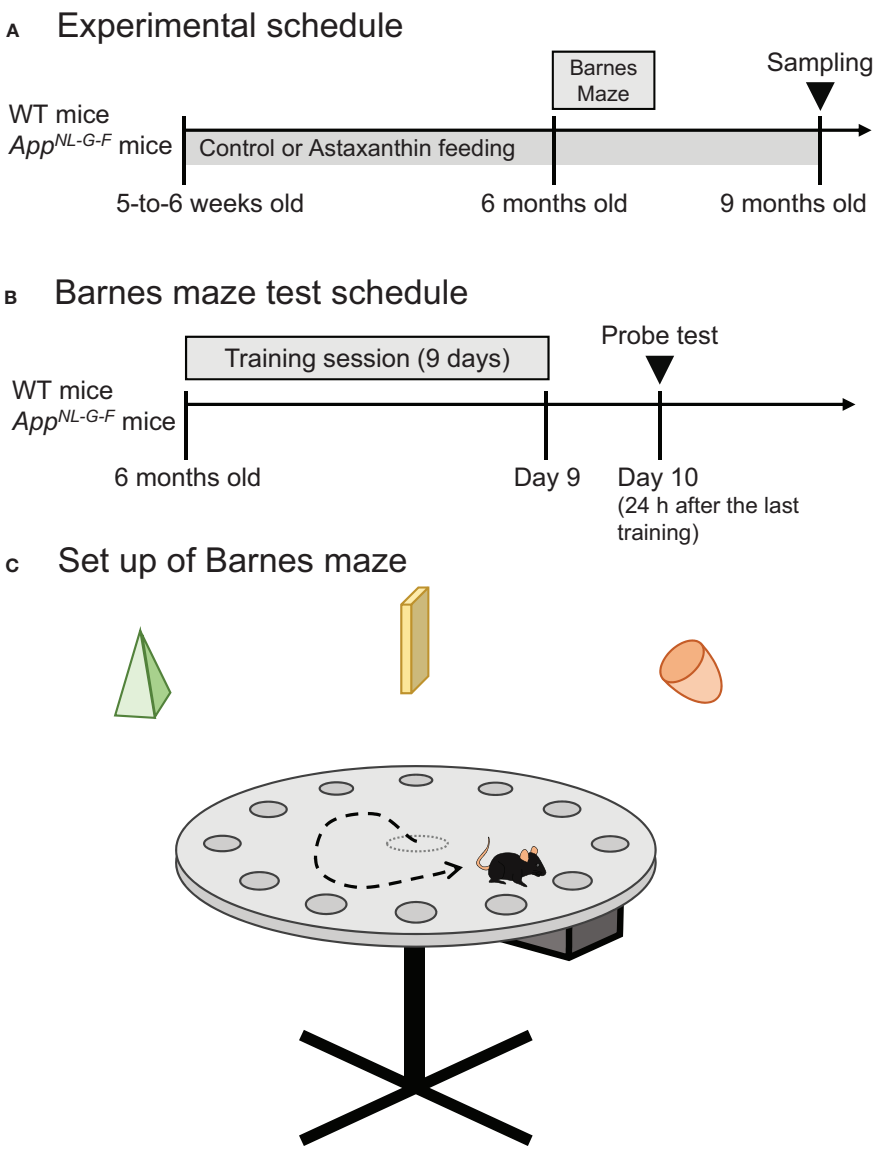

FIGURE 1 | Experimental schedule and Barnes maze test. **(A)** Experimental schedule. **(B)** Barnes maze test schedule. **(C)** Set up of the Barnes maze test. Three extramaze (distant) cues were placed over the maze.

7 cm) with paper bedding, which was located under one of the holes. The location of the hole with the escape box (goal) was the same in a given mouse but randomly different across individual mice. After each trial, the maze surface and escape box were cleaned with 70% ethanol. The maze was rotated daily, with the spatial location of the goal hole consistent in reference to the extra-maze room cues to prevent a bias according to intra-maze local cues. Escape latencies to the goal hole in the training session were measured by Time BCM (O'hara & Co., Tokyo, Japan).

One day after the last training day, each mouse was tested with a probe test (PT) (**Figure 1B**). Each mouse was placed on the table without the escape box for 3 min. In the PT, two parameters were evaluated. The goal hole region was defined as a belt-shaped area with a width of 4.7 cm around the goal hole (diam. = 5.0 cm). The number of visits to the goal hole region was defined as the number of times the center of gravity of a given mouse image crossed the goal hole region during 3 min of the PT. The goal hole time (sec) was defined as the time during which the center of gravity of a given mouse image stayed in the goal hole region. Data of the mice that fell off the table were excluded from the analysis.

Sampling and Preparation of Brain Specimens

Brain specimens were prepared from the mice used for the Barnes maze test. Under deep anesthesia with a mixture of three different anesthetics (medetomidine, midazolam, and butorphanol; 0.75, 4.0, and 5.0 mg/kg body weight, respectively; i.p.), the mice were transcardially perfused with heparinized saline (0.9% NaCl). After perfusion, the brain was removed from the skull. The 47 right hemispheres were used for the measurements of biochemical markers (4-HNE, GSH, and Aβ42). The hippocampus and prefrontal cortex (PFC) corresponding to the prelimbic and infralimbic areas were dissected from the right hemisphere and stored −80°C. The hippocampus and PFC were sonicated in 50 mM Tris-HCl buffer, pH 7.6, 150 mM NaCl, and the protease inhibitor cocktail (complete protease cocktail, Merck KGaA, Darmstadt, Germany) and centrifuged at 200,000 × g for 20 min at 4°C. The supernatant was collected as soluble fraction. The remaining pellet was sonicated in 50 mM Tris-HCl buffer, pH 7.6, containing 6 M guanidine–HCl and 150 mM NaCl, and centrifuged at 200,000 × g for 20 min at 4°C. The supernatant was collected as insoluble fraction. The protein content of each fraction was determined by BCA assay kit (Thermo Fisher Scientific Inc., MA, USA). Soluble and/or insoluble fractions were used for measurements of Aβ42, 4-HNE protein adduct, and total GSH (see below).

The 42 left hemispheres were used for PV immunohistochemistry, while 15 right and left hemispheres were used for immunohistochemistry of Aβ42, pTau, and Iba1 in the brain sections. These hemispheres were fixed in 4% paraformaldehyde dissolved in 0.1 M phosphate buffer (PB; pH 7.4) overnight, and used for immunohistochemistry (see below).

Quantitative Measurement of Aβ Deposition (ELISA)

A total of 36 mice were used (control-fed WT mice, n = 14; control-fed $App^{NL\text{-}G\text{-}F}$ mice, n = 9; astaxanthin-fed $App^{NL\text{-}G\text{-}F}$ mice, n = 13). The insoluble fraction samples were used to measure the amounts of Aβ42 by sandwich ELISA (Human β Amyloid (1–42) ELISA Kit Wako, FUJIFILM Wako Pure Chemical Corporation, Osaka, Japan).

Quantification of 4-HNE Protein Adduct (Slot Blot)

A total of 32 mice were used (control-fed WT mice, n = 12; control-fed $App^{NL\text{-}G\text{-}F}$ mice, n = 10; astaxanthin-fed $App^{NL\text{-}G\text{-}F}$ mice, n = 10). The soluble and insoluble fraction samples were loaded on the PVDF membrane (Immobilon P, Merck KGaA, Darmstadt, Germany) using the slot blot manifold. For standard 4-HNE protein adduct, BSA at the concentration of 1 mg/ml was treated with 100 μmol/L 4-HNE at 37°C for 4 h. Four-HNE monoclonal antibody (clone HNEJ-2, JaICA, Shizuoka, Japan) was used as the first antibody. Peroxide labeled-anti mouse IgG antibody (SeraCare Life Sciences Inc., MA, USA) was used as the secondary antibody. The amount of 4-HNE protein adduct was quantified by a luminol reagent kit (ECL, GE Healthcare, Ill, USA). The luminescence was detected by cooled CCD imager (LAS400, GE Healthcare) and analyzed using ImageJ ver.1.8.0 (Rasband, W.S., ImageJ, NIH, Bethesda, USA, https://imagej.nih.gov/ij/, 1997–2018.).

Quantitative Measurement of Total GSH

A total of 29 mice were used (control-fed WT mice, n = 10; control-fed $App^{NL\text{-}G\text{-}F}$ mice, n = 9; astaxanthin-fed $App^{NL\text{-}G\text{-}F}$ mice, n = 10). Sulfosalicylic acid (1% of final concentration) was added to the soluble fraction. The mixture was centrifuged at 8000 × g for 10 min at 4°C. The 1 N NaOH was added to the supernatant to 9% volume for deacidification. The sample was reacted with 25 μg/ml DTNB (5-5'-dithiobis[2-nitrobenzoic acid], Dojindo Laboratories, Kumamoto, Japan), 40 μg/ml NADPH, and 1 U/ml GSH reductase (Oriental Yeast Co. Ltd., Tokyo, Japan) for 10 min at 37°C. Then, total GSH was measured by colorimetric absorbance at 405 nm.

Immunohistochemistry and Analysis of PV-Positive Neurons

A total of 42 mice were used (control-fed WT mice, n = 13; control-fed $App^{NL\text{-}G\text{-}F}$ mice, n = 14; astaxanthin-fed $App^{NL\text{-}G\text{-}F}$ mice, n = 15). PV-positive neurons were stained following the same protocol described in our previous studies (Nguyen et al., 2011; Urakawa et al., 2013; Nakamura et al., 2015; Jargalsaikhan et al., 2017). Briefly, the fixed blocks of the left hemispheres were cut into 40-μm-thick sections. Five serial sections were collected for every 200 μm; one was used for PV staining, and one was used for cresyl-violet staining. The sections were stained with mouse monoclonal anti-PV antibodies (1:10,000 dilution in 1% horse serum PBS, Sigma, St. Louis, MO, USA).

PV-positive neurons were analyzed according to our previous studies (Nakamura et al., 2015; Jargalsaikhan et al., 2017). Briefly, the brain sections were observed using an all-in-one fluorescence microscope system (BZ-9000, Keyence Corporation, Osaka, Japan). PV-positive neurons were counted in the five sections in the hippocampus at −1.60, −1.76, −1.92, −2.08, and −2.24 mm posteriorly from the bregma based on the mouse brain atlas

(Hof et al., 2000). The PV-positive neurons were counted using a stereological technique with systematic random sampling (StereoInvestigator v.7.53.1, MicroBrightField, Williston, VT, USA) (Sterio, 1984; Nakamura et al., 2015; Jargalsaikhan et al., 2017). The grid size for the analysis was set at 1741.60 × 719.55-μm, while the size for the counting frames with inclusion and exclusion lines was set at 200 × 200-μm. The software highlighted only PV-positive cell bodies within the counting frame without contact with the exclusion lines. We counted PV-positive objects in the counting frame only if they came into focus within a predetermined 5-μm thick optical dissector that was positioned 2 μm below the surface of the mounted section using the Z-axis microcator. The PV-positive neuron density was computed in each mouse.

Immunofluorescent Staining and Analysis of Aβ42 and Iba1

A total of 15 mice were used (control-fed WT mice, n = 5; control-fed $App^{NL\text{-}G\text{-}F}$ mice, n = 5; astaxanthin-fed $App^{NL\text{-}G\text{-}F}$ mice, n = 5). Fixed right hemispheres were embedded in paraffin. Immunofluorescent staining was performed by Biopathology Institute Co., Ltd. (Oita, Japan). Anti-β-amyloid (1–42) antibody (rabbit IgG, AB5078P, MILLIPORE) and anti-Iba1 antibody (Goat IgG, ab5076, Abcam) were used as the primary antibodies. Anti-rabbit Alexa-594 and anti-goat Alexa 488 were used as the secondary antibodies. Finally, the brain sections were mounted on glass slides using mount media with DAPI (SlowFade Gold Antifade Reagent With DAPI, Thermo Fisher Scientific Inc., MA, USA).

Microscopic images of Aβ42 and Iba1 in the hippocampal sections at −1.80, −2.12, and −2.44 mm posteriorly from the bregma were captured under an identical, experimenter-blinded condition, using a fluorescent microscope (BX52, Olympus Corporation, Tokyo, Japan). The images were analyzed using ImageJ. Area fractions of Aβ42 of all images were estimated with binary data with the same threshold level (17,926/65,536). Area fractions of all Iba1 images were estimated with binary data with the same threshold level (17,408/65,536), excluding fractions below 19.6 μm^2 particles.

Immunohistochemistry and Analysis of Phosphorylated Tau (pTau)

A total of 15 mice were used (control-fed WT mice, n = 5; control-fed $App^{NL\text{-}G\text{-}F}$ mice, n = 5; astaxanthin-fed $App^{NL\text{-}G\text{-}F}$ mice, n = 5). Fixed hemispheres were embedded in paraffin. Immunohistochemical staining was performed by Biopathology Institute Co., Ltd. (Oita, Japan). MAPT/Tau (Ser198/Ser199/Ser202/Thr205) antibody (LS-C48043-50, Life Span Bioscience, Inc.) was used as the primary antibody. Then, the sections were treated with a polymer constituted with Fab' fragment of anti-rabbit IgG antibody and peroxidase (Nichirei-histfine simple stain Max PO, Nichirei bioscience Inc., Tokyo, Japan). pTau was visualized with 3, 3'-diaminobenzidine and hydrogen peroxide. Finally, the sections were stained with hematoxylin-eosin.

Microscopic images of pTau in the hippocampal sections at −1.84, −2.16, and −2.48 mm posteriorly from the bregma were analyzed using ImageJ to estimate the fraction of pTau-positive areas. Stained regions of pTau were isolated by colorimetric intensity adjustment and then binarized with the threshold level (37,266/65,536), excluding fractions below 19.6 μm^2 particles. Image processing and analyzing parameters were identical across the sections.

Statistical Data Analysis

Data in the training session of the Barns maze test were compared among the three groups using repeated measures two-way ANOVA, followed by the Tukey *post hoc* test. The other data were compared among the three groups using one-way ANOVA, followed by the Tukey *post hoc* test. Additionally, pTau data were compared using pairwise t-test with Bonferroni adjustment (**Figure 8D**). The relationships between the two parameters were analyzed using simple regression analysis (**Figures 9A–C**, correlations between histological parameters for Iba1, pTau, and Aβ42; **Figures 9D–F**, correlations between the behavioral parameter in the PT of the Barnes maze test and histological parameters). $P < 0.05$ was considered statistically significant. The statistical analyses were performed using R ver.3.4.3 (R Core Team, 2017).

RESULTS

Barnes Maze Test

The Barnes maze test was used to assess the memory functions of the three groups of mice at 6 months old (**Figure 2**). In the initial training session, the average latency to escape to the goal hole gradually decreased across the 9 days in the three groups of the mice (**Figure 2A**). The statistical analysis by repeated measures two-way ANOVA (group × day) indicated that there was no significant main effect of group [$F(2, 69) = 2.231$, $P = 0.115$], nor interaction between group and day [$F(16, 552) = 1.175$, $P = 0.284$].

To assess spatial reference memory after the training, the escape box was removed in the PT 24 h after the last training day (**Figure 2B**). A comparison of the number of visits to the goal region by one-way ANOVA indicated that there was a significant difference in the number of visits to the goal region among the three groups [$F(2, 67) = 3.912$, $P = 0.0247$]. Post hoc multiple comparisons indicated that the number of visits to the goal region was significantly smaller in the control-fed $App^{NL\text{-}G\text{-}F}$ mice than the astaxanthin-fed $App^{NL\text{-}G\text{-}F}$ mice (Tukey test, $P = 0.03603$) and tended to be smaller than the control-fed WT mice (Tukey test, $P = 0.05397$). On the other hand, average goal hole time in the PT of the control-fed WT, control-fed $App^{NL\text{-}G\text{-}F}$, and astaxanthin-fed $App^{NL\text{-}G\text{-}F}$ mice were 32.96 ± 2.35 (mean ± SEM), 26.05 ± 2.50, and 27.44 ± 2.28 sec, respectively. There was no significant difference among the three groups [$F(2, 67) = 2.4152$, $P = 0.09709$].

PV-Positive Neuron Density

Figure 3A shows examples of PV-stained hippocampal sections in the three groups of mice at 9 months old. The mean densities of PV-positive neurons in the three groups are shown in **Figure 3B**. The mean density of PV-positive neurons in the control-fed $App^{NL\text{-}G\text{-}F}$ mice was decreased to about 75% of those in the control-fed WT mice and 70% of those in the astaxanthin-fed $App^{NL\text{-}G\text{-}F}$ mice. A statistical analysis using one-way ANOVA indicated that there was a significant main effect of group [F(2,

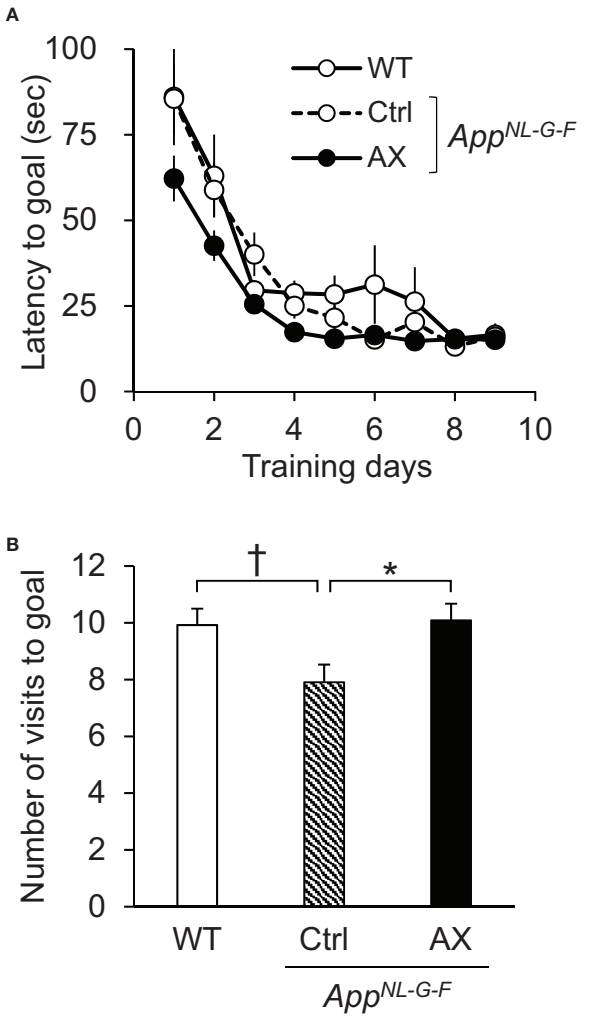

FIGURE 2 | Performance in the Barnes maze test. **(A)** Average latency to escape to the goal hole in the training session. **(B)** Comparison of the number of visits to the goal region in the probe test (PT). WT, wild type C57BL/6J mice; App^{NL-G-F}, $App^{NL-G-F/NL-G-F}$ mice; Ctrl, control-fed group; AX, astaxanthin-fed group. $^{*}P < 0.05$; $^{\dagger}P < 0.1$.

39) = 4.1877, $P = 0.0225$]. Post hoc tests indicated that the mean cell density was significantly higher in the astaxanthin-fed App^{NL-G-F} mice than in the control-fed App^{NL-G-F} mice (Tukey test, $P = 0.01922$).

Quantification of Aβ42 Levels by ELISA

The Aβ42 levels in the hippocampus and PFC were quantified in the App^{NL-G-F} and WT mice at 9 months old by ELISA (**Figure 4**). In the hippocampus (**Figure 4A**), there was a significant difference in Aβ42 levels among the three groups [F(2.0, 12.8) = 36.811, $P < 0.0001$]. Post hoc multiple comparisons indicated that Aβ42 levels were significantly higher in the control-fed App^{NL-G-F} mice (Tukey test, $P < 0.0001$) and astaxanthin-fed App^{NL-G-F} mice (Tukey test, $P < 0.0001$) than in the control-fed WT mice. Furthermore, Aβ42 levels were significantly higher in the control-fed App^{NL-G-F} mice than in the astaxanthin-fed App^{NL-G-F} mice (Tukey test, $P = 0.02925$). In the PFC (**Figure 4B**), Aβ42 levels were also increased in the App^{NL-G-F} mice. There was a significant difference in Aβ42 levels among the three groups [F(2.0, 12.8) = 17.298, $P = 0.0002$]. Post hoc multiple comparisons indicated that Aβ42 levels were significantly higher in the control-fed App^{NL-G-F} mice (Tukey test, $P = 0.00069$) and astaxanthin-fed App^{NL-G-F} mice (Tukey test, $P = 0.00089$) than in the control-fed WT mice.

Oxidative and Anti-Oxidant Status in the Hippocampus

Oxidative stress due to Aβ42 accumulation was assessed by quantifying 4-HNE bound to proteins (**Figures 5A, B**). Examples of slot blot analyses of 4-HNE protein adduct in three mice from each group are shown in **Figure 5A**. A statistical analysis (one-way ANOVA) indicated a significant difference among the three groups [F(2.0, 15.1)=11.722, $P = 0.00084$] (**Figure 5B**). Post hoc multiple comparisons indicated that 4-HNE protein adduct levels were significantly higher in the control-fed App^{NL-G-F} mice (Tukey test, $P = 0.00350$) and astaxanthin-fed App^{NL-G-F} mice (Tukey test, $P = 0.00960$) than in the control-fed WT mice.

To assess anti-oxidant status in the hippocampus, we compared total GSH levels in the hippocampus among the three groups of the mice (**Figure 5C**). A statistical analysis (one-way ANOVA) indicated a significant difference among the three groups [F(2, 26)=11.61, $P = 0.00025$]. Post hoc multiple comparisons indicated that the total GSH levels in the hippocampus were significantly lower in the control-fed App^{NL-G-F} mice than that in the control-fed WT mice (Tukey test, $P = 0.00020$) and astaxanthin-fed App^{NL-G-F} (Tukey test, $P = 0.00767$), and there was no significant difference in the total GSH levels between the control-fed WT and the astaxanthin-fed App^{NL-G-F} mice (Tukey test, $P = 0.32454$).

Aβ42 Deposition and Microglial Accumulation

We analyzed the relationships between Aβ42 deposition and microglial accumulation (**Figures 6** and **7**). Triple staining was performed using DAPI, antibody to Aβ42, and antibody to Iba1 (a marker of microgliosis) in the control-fed WT (**Figure 6A**), control-fed App^{NL-G-F} (**Figure 6B**), and astaxanthin-fed App^{NL-G-F} mice (**Figure 6C**). Aβ42 deposition (red) in the hippocampus colocalized with microglia (green) in the control-fed App^{NL-G-F} mice. A statistical analysis of Aβ42 deposition by one-way ANOVA indicated a significant difference among the three groups [F(2, 12)=88.226, $P < 0.0001$] (**Figure 7A**). Post hoc multiple comparisons indicated that β42 deposition increased more in the control-fed App^{NL-G-F} mice than in the control-fed WT mice (Tukey test, $P < 0.0001$) and astaxanthin-fed App^{NL-G-F} mice (Tukey test, $P < 0.0001$). A statistical analysis of the microglial accumulation (Iba1 staining) by one-way ANOVA also indicated a significant difference among the three groups [F(2, 5.55)=52.963, $P = 0.00024$] (**Figure 7B**). Post hoc multiple comparisons indicated that Iba1 fraction was greater in the control-fed App^{NL-G-F} mice (Tukey test, $P < 0.0001$) and astaxanthin-fed App^{NL-G-F} mice (Tukey test, $P = 0.00566$) than in the control-fed WT mice. Furthermore,

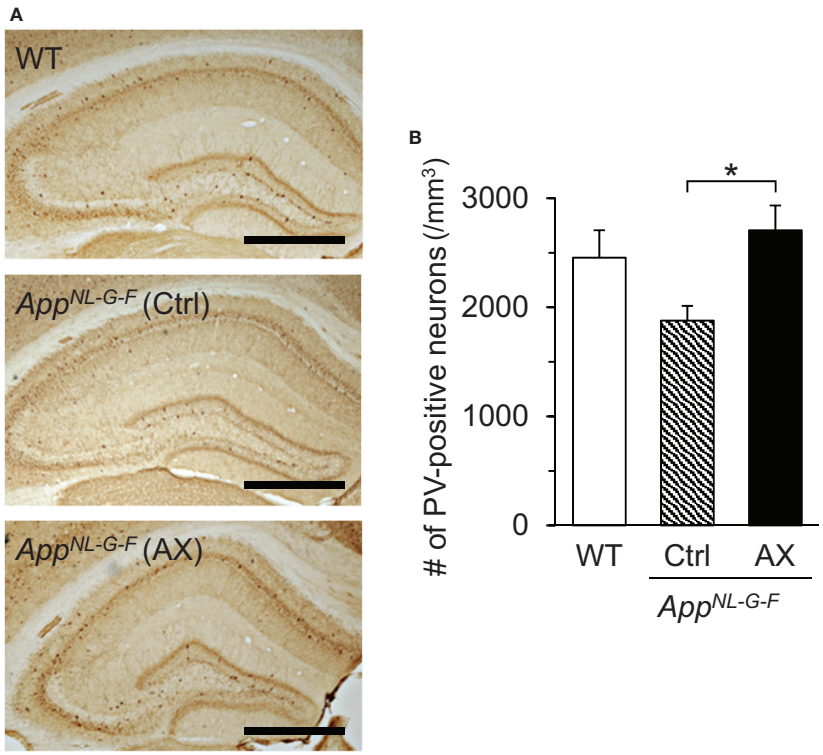

FIGURE 3 | Comparison of the parvalbumin (PV)-positive neuron density in the hippocampus among the three groups of the mice. **(A)** Microscopic images of the hippocampus. The typical PV-immunohistochemical sections of the hippocampus in the control-fed WT, control-fed App^{NL-G-F} (Ctrl), and astaxanthin-fed App^{NL-G-F} (AX) mice are shown. The bar indicates 1,000 μm. **(B)** Comparison of PV-positive neuron density in the hippocampus. WT, wild type C57BL/6J mice; App^{NL-G-F}, $App^{NL-G-F/NL-G-F}$ mice; Ctrl, control-fed group; AX, astaxanthin-fed group. *$P < 0.05$.

Iba1-fraction was smaller in the astaxanthin-fed App^{NL-G-F} mice than in the control-fed App^{NL-G-F} mice (Tukey test, $P = 0.00033$). Finally, we analyzed the colocalization of Aβ42 deposition and microglia. A statistical analysis of area fraction ratio of Iba1 against Aβ42 by one-way ANOVA also indicated a significant difference among the three groups [$F(2, 12)=44.812$, $P < 0.0001$] (**Figure 7C**). Post hoc multiple comparisons indicated that fraction ratios of Iba1 were greater in the control-fed App^{NL-G-F} mice (Tukey test, $P = 0.04796$) and astaxanthin-fed App^{NL-G-F} mice (Tukey test, $P < 0.0001$) than in the control-fed WT mice. Furthermore, fraction ratios of Iba1 were greater in the astaxanthin-fed App^{NL-G-F} mice than in the control-fed App^{NL-G-F} mice (Tukey test, $P = 0.00008$). These results indicated that microglia were more strongly accumulated in the astaxanthin-fed App^{NL-G-F} mice than the control-fed App^{NL-G-F} mice.

Phosphorylated Tau Accumulation

The deposits of Aβ and the neurofibrillary tangles composed of hyperphosphorylated tau protein (pTau) are the neuropathological hallmarks of AD, and tauopathy is enhanced following Aβ amyloidosis (Hardy and Selkoe, 2002; Perrin et al., 2009; Hashimoto et al., 2019). Therefore, we immunohistochemically investigated the effects of astaxanthin on the tauopathy in the control-fed WT (**Figure 8A**), control-fed App^{NL-G-F} (**Figure 8B**), and astaxanthin-fed App^{NL-G-F} mice (**Figure 8C**). A statistical analysis of the pTau fraction using one-way ANOVA indicated that the difference among the three groups tended to be significant [$F(2, 7.10)=3.6094$, $P = 0.08285$]. Multiple comparisons by pairwise t-tests with Bonferroni correction indicated that pTau fraction tended to be higher in the control-fed App^{NL-G-F} mice than the control-fed WT mice ($P = 0.062$) and that pTau fraction was significantly smaller in the astaxanthin-fed App^{NL-G-F} mice than the control-fed App^{NL-G-F} mice ($P = 0.038$) (**Figure 8D**).

Correlation Analyses

The above parameters in the AD pathology could be correlated each other according to the amyloid cascade theory. The area fraction of Aβ42 was significantly and positively correlated with Iba1 fraction [$F(1, 13) = 30.0$, $P = 0.00011$] (**Figure 9A**) and pTau fraction [$F(1, 13) = 12.9$, $P = 0.00333$] (**Figure 9B**). Iba1 fraction was significantly and positively correlated with pTau fraction [$F(1, 13) = 10.2$, $P = 0.00696$] (**Figure 9C**). Furthermore, the relationships between spatial reference memory in the PT in the Barnes maze test (number of visits to the goal region) and the above parameters were analyzed. The number of visits to the goal region was significantly and negatively correlated with Aβ42 fraction [$F(1, 13) = 10.7$, $P = 0.00607$] (**Figure 9D**), Iba1 fraction [$F(1, 13) = 7.7$, $P = 0.01563$] (**Figure 9E**), and pTau fraction [$F(1, 13) = 11.9$, $P = 0.00431$] (**Figure 9F**).

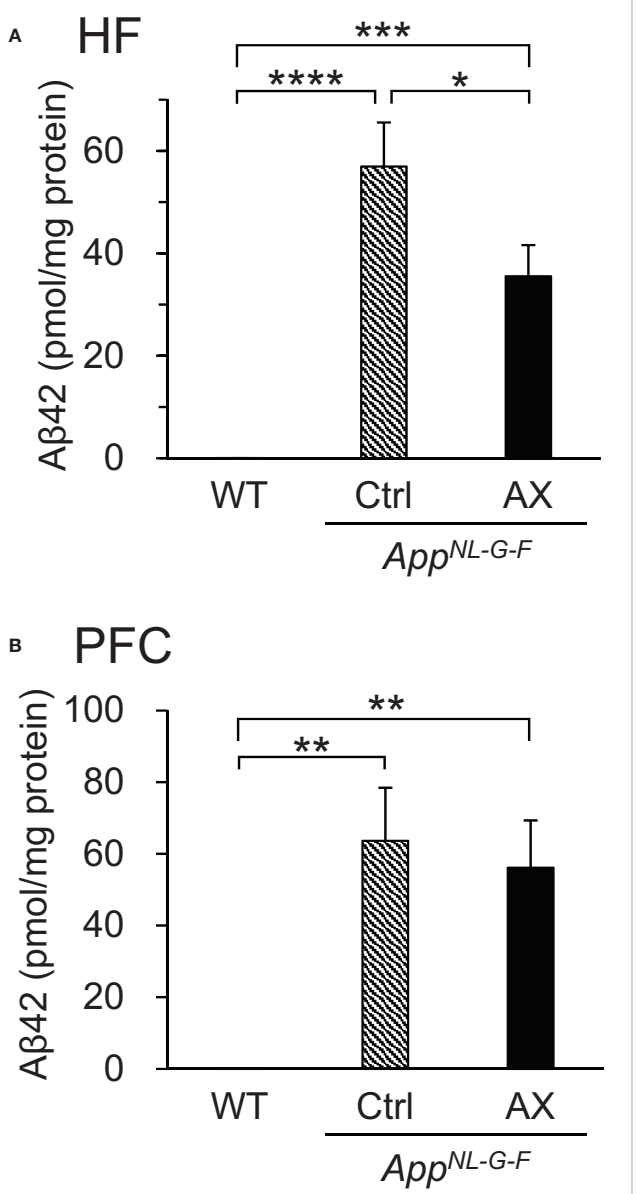

FIGURE 4 | Comparison of Aβ42 levels quantified by ELISA among the three groups of mice. **(A)** Comparison of Aβ42 levels in the hippocampus (HF). **(B)** Comparison of Aβ42 levels in the prefrontal cortex (PFC). WT, wild type C57BL/6J mice; $App^{NL\text{-}G\text{-}F}$, $App^{NL\text{-}G\text{-}F/NL\text{-}G\text{-}F}$ mice; Ctrl, control-fed group; AX, astaxanthin-fed group. $^{*}P < 0.05$; $^{**}P < 0.01$; $^{***}P < 0.001$; $^{****}P < 0.0001$.

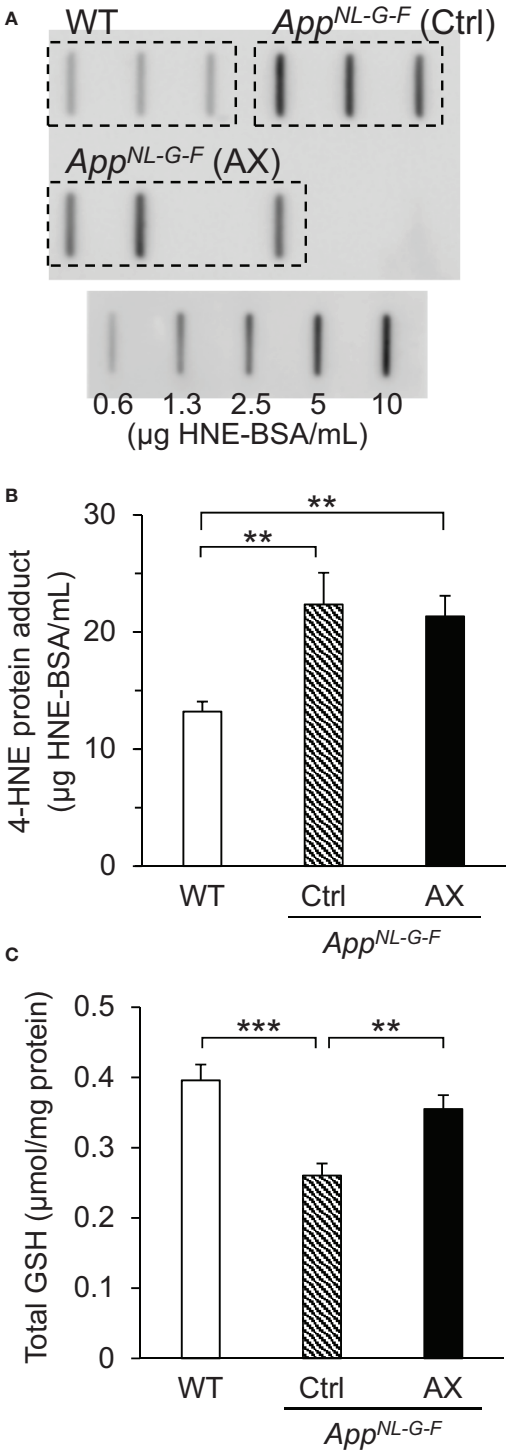

FIGURE 5 | Comparison of oxidative and anti-oxidant status in the hippocampus among the three groups of mice. **(A)** Examples of slot bot images. **(B)** Comparison of 4-hydroxy-2,3-trans-nonenal (4-HNE) protein adduct levels (oxidative stress marker) quantified by slot blot analysis. **(C)** Comparison of total glutathione (GSH) levels measured by GSH reductase recycling and Ellman's reagent. WT, wild type C57BL/6J mice; $App^{NL\text{-}G\text{-}F}$, $App^{NL\text{-}G\text{-}F/NL\text{-}G\text{-}F}$ mice; Ctrl, control-fed group; AX, astaxanthin-fed group. $^{**}P < 0.01$; $^{***}P < 0.001$.

DISCUSSION

Pathology in the Mouse AD Model

In the current study, we used a new mouse model of AD, the $App^{NL\text{-}G\text{-}F}$ mice that carries three *App* knock-in mutations associated with familial AD. This knock-in approach allows to express APP at a similar level to WT mice, and to generate elevated levels of pathogenic Aβ (Aβ42). Thus, it is unlikely that the potential artifacts due to APP overexpression occur in this mouse model (Saito et al., 2014). In this mouse model, (1)

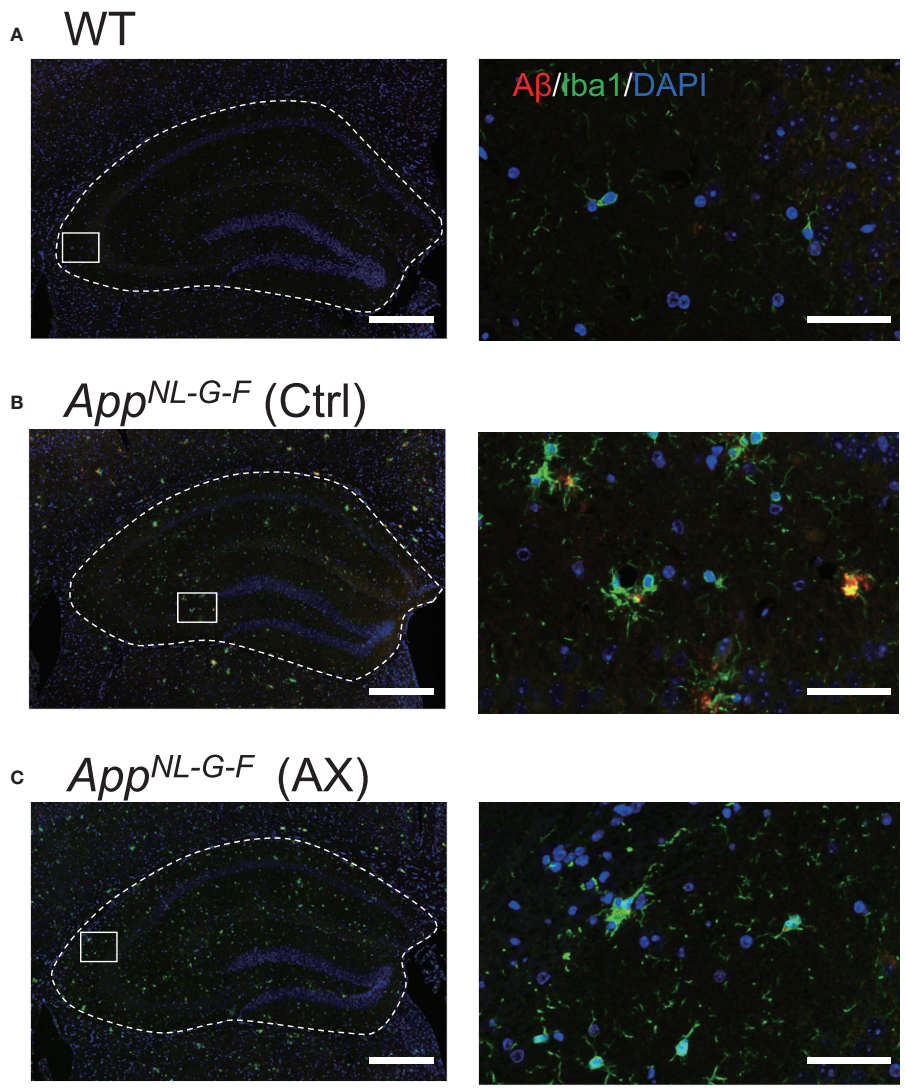

FIGURE 6 | Co-localization of Aβ42 and Iba1 in *App*$^{NL-G-F}$ mice. Typical immunohistofluorescence images of Aβ42 and Iba1 in the hippocampus of the control-fed WT **(A)**, control-fed *App*$^{NL-G-F}$ (Ctrl) **(B)** and astaxanthin-fed *App*$^{NL-G-F}$ (AX) **(C)** mice are shown. Red, green, and blue colors in each image indicate Aβ42, Iba1, and DAPI, respectively. The images on the right indicate enlarged images of the inset in the left images. Bars in the left and right panels represent 1,000 and 50 μm, respectively.

cortical Aβ deposition in the mice began by 2 months and was almost saturated by 7 months old, (2) the microgliosis and astrocytosis were observed at 9 months old, and (3) the memory impairment occurred by 6 months old (Saito et al., 2014). In the present study, astaxanthin supplementation to the experimental mice started from 5-to-6 weeks old before Aβ deposition started, and the mice were sacrificed at 9 months old so that the protective effects of astaxanthin on the onset and progression of AD could be analyzed.

In this model, we observed mild memory decline, accumulation of Aβ42 in the hippocampus and PFC, a mild increase in pTau fraction, and microglial accumulation (an increase in Iba1 fraction) in the *App*$^{NL-G-F}$ mice, which is consistent with the previous studies (Saito et al., 2014; Masuda et al., 2016; Hashimoto et al., 2019). These deficits in memory functions may not be ascribed to confounding effects outside the brain such as deficits in visual acuity and locomotor activity in the *App*$^{NL-G-F}$ mice since a previous study reported that motor and visual capabilities of *App*$^{NL-G-F}$ and WT mice were comparable at 24 months old (Sakakibara et al., 2019). We further indicated that 4-HNE protein adduct levels (a marker of lipid peroxidation), which were elevated in AD patients (Markesbery and Lovell, 1998; Zarkovic, 2003) and are toxic to normal cellular functions (Csala et al., 2015), were increased in the *App*$^{NL-G-F}$ mice. In addition, total GSH levels were decreased in the *App*$^{NL-G-F}$ mice, consistent with human AD patients (Mandal et al., 2015). A decrease in the PV-positive neuron density in the control-fed *App*$^{NL-G-F}$ mice may be ascribed to these changes in oxidative and anti-oxidant status due to Aβ42 accumulation in the control-fed *App*$^{NL-G-F}$ mice. Consistently, oligomers of Aβ42 have been

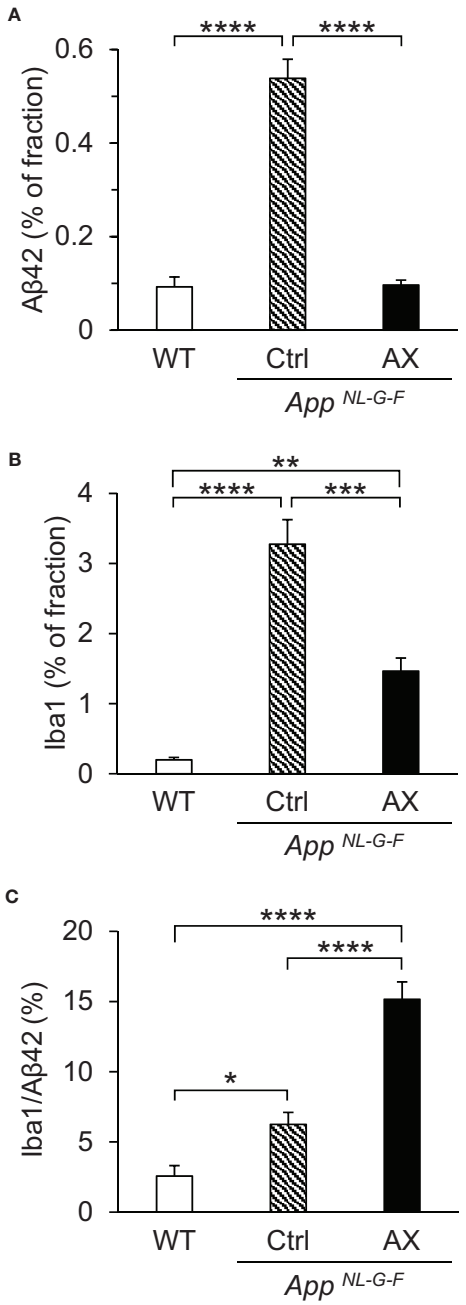

FIGURE 7 | Comparison of the area fraction of Aβ42 **(A)**, area fraction of Iba1 **(B)**, and area fraction ratio of Iba1 against Aβ42 **(C)** in the hippocampus among the three groups of the mice. The hippocampal sections with immunohistochemical staining were analyzed by ImageJ. WT, wild type C57BL/6J mice; $App^{NL\text{-}G\text{-}F}$, $App^{NL\text{-}G\text{-}F/NL\text{-}G\text{-}F}$ mice; Ctrl, control-fed group; AX, astaxanthin-fed group. $^{*}P < 0.05$; $^{**}P < 0.01$; $^{***}P < 0.001$; $^{****}P < 0.0001$.

reported to generate reactive oxygen species, which further induced membrane lipid peroxidation, intracellular Ca^{2+} entry associated with pore formation in the membrane, a decrease in membrane fluidity, and deficits in long-term potentiation (Yasumoto et al., 2019). The correlational analyses indicated that Aβ42 fraction was positively correlated with pTau and Iba1 fraction, while memory functions (number of visits to the goal region) were negatively correlated with Aβ and pTau fractions. These findings in this mouse AD model represent characteristics of human AD pathological findings and support the amyloid cascade theory of AD, in which accumulation of pathogenic Aβ induces amyloid plaques, hyperphosphorylation of tau (tauopathy), and microglial activation (Hardy and Selkoe, 2002; Selkoe and Hardy, 2016; Sasaguri et al., 2017; Edwards, 2019; Hashimoto et al., 2019).

Protective Mechanisms of Astaxanthin

The present results indicated that astaxanthin decreased Aβ42 deposition and prevented memory decline in the $App^{NL\text{-}G\text{-}F}$ mice. Consistently, two recent studies reported that astaxanthin reduced Aβ40 levels in a 3xTg AD mouse model (Fanaee-Danesh et al., 2019) and reduced Aβ42 levels in rats with intracerebroventricular injections of Aβ42 (Rahman et al., 2019). The present study further indicated that astaxanthin decreased pTau and the Iba1 fraction, while it increased hippocampal PV-positive neuron density and total GSH levels. Furthermore, the correlation analyses showed that Aβ42 and pTau fractions were significantly negatively correlated with hippocampus-dependent cognitive functions. On the other hand, it is reported that astaxanthin crosses the blood-brain barrier (Grimmig et al., 2017) and is detectable in brain tissues after oral administration (Choi et al., 2011). These results provide clues to discuss several mechanisms in which astaxanthin suppressed the progression of AD in the $App^{NL\text{-}G\text{-}F}$ mice.

First, astaxanthin increased the hippocampal PV-positive neuron density in the astaxanthin-fed $App^{NL\text{-}G\text{-}F}$ mice, which may be attributed to an increase in total GSH in the astaxanthin-fed $App^{NL\text{-}G\text{-}F}$ mice. Previous studies reported that astaxanthin increased GSH biosynthesis through the nuclear factor erythroid-related factor 2 and the antioxidant responsive element (Nrf2-ARE) pathway in the rat brain with subarachnoid hemorrhage (Wu Q. et al., 2014), and also increased brain GSH levels in other brain disorders due to chemical oxidative stress and amygdalar kindling in rozdents (Wu W. et al., 2014; Lu et al., 2015). GSH is an endogenous antioxidant that protects body tissues from oxidative damages, while PV-positive neurons were sensitive to oxidative stress (see Introduction). Therefore, elevated levels of GSH may increase the PV-positive neuron density in the astaxanthin-fed $App^{NL\text{-}G\text{-}F}$ mice. Second, PV-positive neurons play a critical role in the generation of gamma oscillations (Bartos et al., 2007; Sohal et al., 2009; Nguyen et al., 2011; Nakamura et al., 2015). In the AD mouse model, as well as AD patients, reduction of gamma oscillations and dysfunctions of PV-positive neurons were reported (Stam et al., 2002; Verret et al., 2012). A recent study reported that optogenetic or sensory induction of gamma oscillations resulted in reduction of Aβ peptides in the hippocampus of a mouse model of AD (5XFAD mice), which was attributed to microglial activation and resultant increase in microglial uptake of Aβ (Iaccarino et al., 2016). Thus, PV-positive neurons may reduce Aβ levels through its effect on microglia. In the present study, astaxanthin decreased Iba1 fraction in the $App^{NL\text{-}G\text{-}F}$ mice. Since microglia accumulate around Aβ

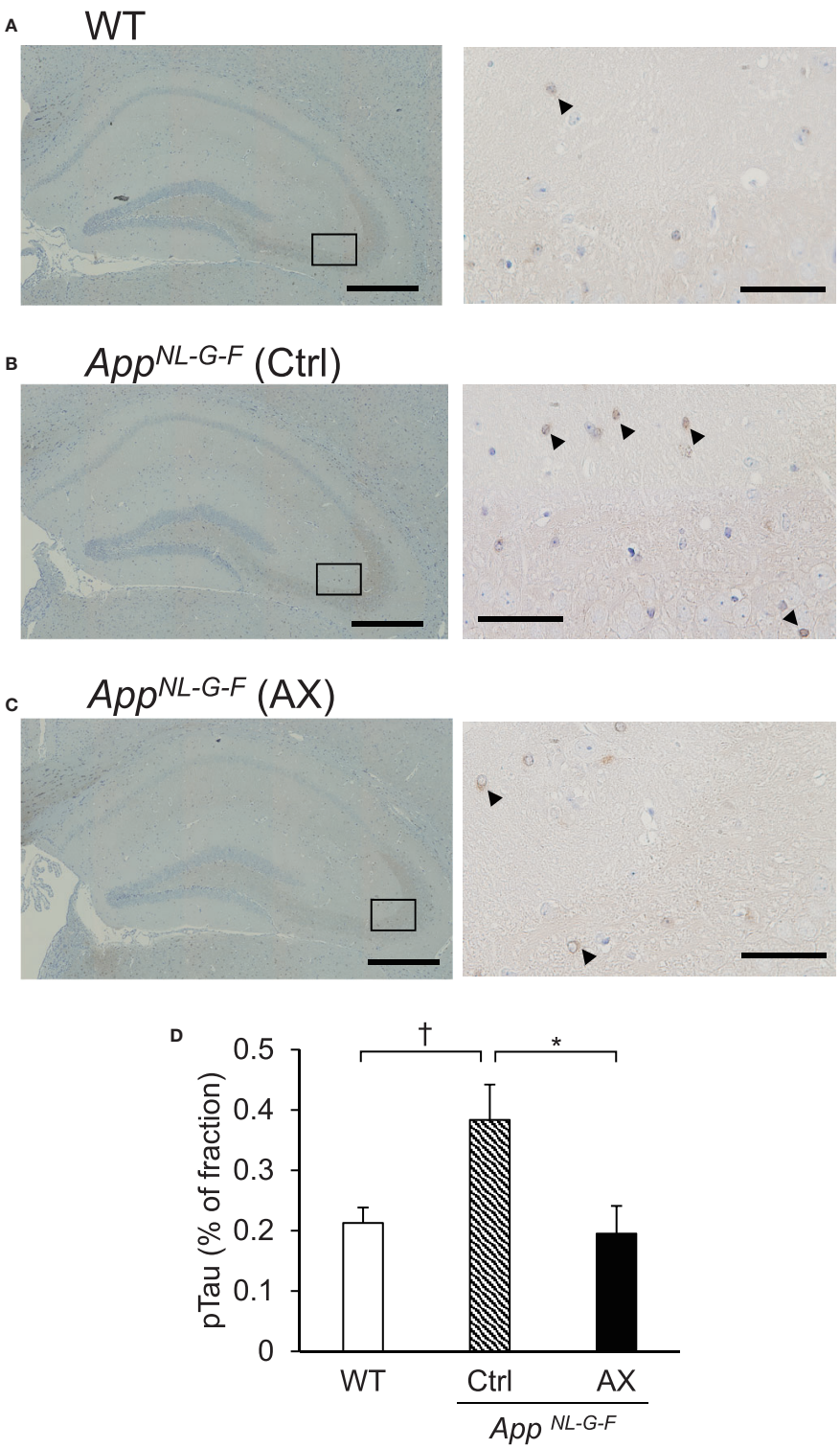

FIGURE 8 | Comparison of area fraction of phosphorylated tau (pTau) in the hippocampus among the three groups of the mice. Typical images of pTau-positive cells in the hippocampus of the control-fed WT **(A)**, control-fed $App^{NL\text{-}G\text{-}F}$ (Ctrl) **(B)**, and astaxanthin-fed $App^{NL\text{-}G\text{-}F}$ (AX) **(C)** mice are shown. The images on the right indicate enlarged images of the inset in the left images. Bars in the left and right panels represent 1,000 and 50 μm, respectively. Arrowheads indicate pTau-positive cells. **(D)** Comparison of pTau fraction in the hippocampus among the three groups of the mice. The area fraction of pTau was analyzed using ImageJ. WT, wild type C57BL/6J mice; $App^{NL\text{-}G\text{-}F}$, $App^{NL\text{-}G\text{-}F/NL\text{-}G\text{-}F}$ mice; Ctrl, control-fed group; AX, astaxanthin-fed group. $^{\dagger}P < 0.1$; $^{*}P < 0.05$.

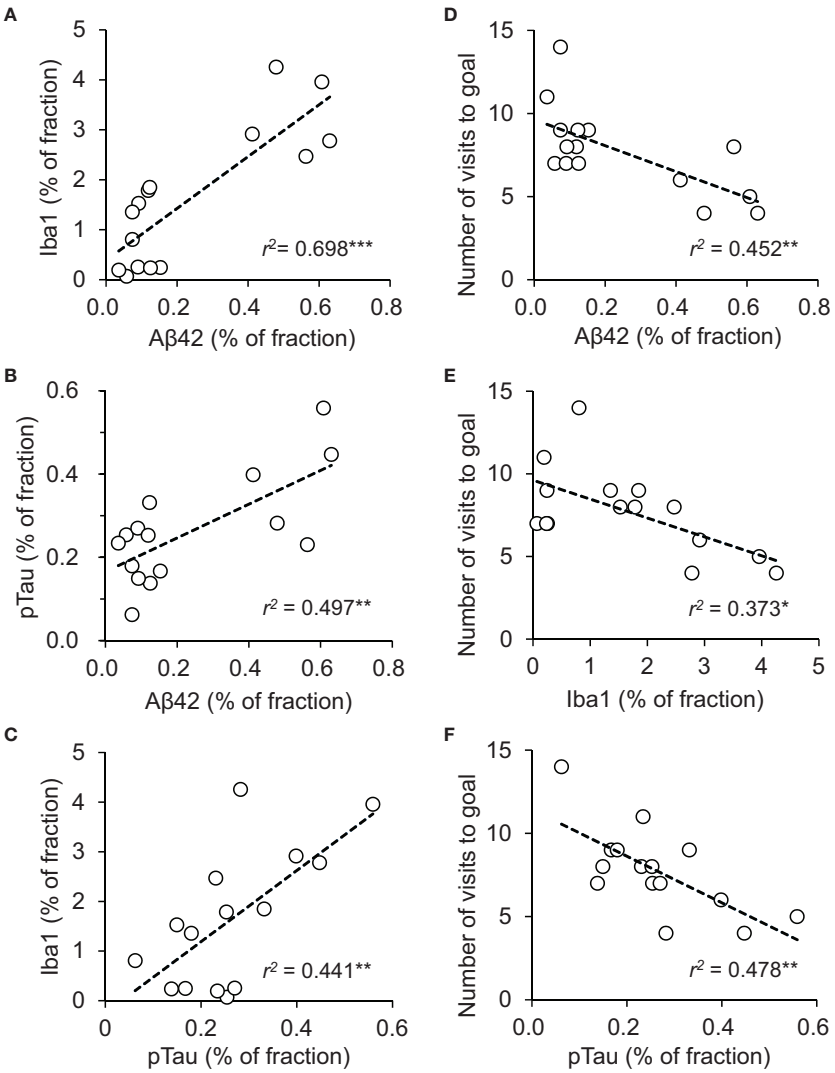

FIGURE 9 | Relationships among Aβ42 fractions, Iba1 fractions, and phosphorylated tau (pTau) fractions in the hippocampus and performance in the probe test (PT) in the Barnes maze test across the three groups of the mice. **(A)** Significant positive correlation between Aβ42 and Iba1 fractions. **(B)** Significant positive correlation between Aβ42 and pTau fractions. **(C)** Significant positive correlation between pTau and Iba1 fractions. **(D)** Significant negative correlation between Aβ42 fraction in the hippocampus and number of visits to the goal region in the Barnes maze PT. **(E)** Significant negative correlation between Iba1 fraction in the hippocampus and number of visits to the goal region in the Barnes maze PT. **(F)** Significant negative correlation between pTau fraction in the hippocampus and number of visits to the goal region in the Barnes maze PT. "r" indicates Pearson's product-moment correlation coefficient in the simple linear regression analysis. $^{*}P < 0.05$; $^{**}P < 0.01$; $^{***}P = 0.001$.

deposition (Hellwig et al., 2015), a decrease in Iba1 fraction may be attributed to a decrease in Aβ42 deposition in the astaxanthin-fed $App^{NL\text{-}G\text{-}F}$ mice. On the other hand, the fraction ratios of Iba1 against Aβ42 were greater in the astaxanthin-fed $App^{NL\text{-}G\text{-}F}$ mice than the control-fed $App^{NL\text{-}G\text{-}F}$ mice. This suggests that microglia were more strongly activated and sensitive to Aβ deposition in the astaxanthin-fed $App^{NL\text{-}G\text{-}F}$ mice. This activation of microglia, which may be attributed to gamma oscillation by PV-positive neurons (see above), may decrease Aβ deposition in the astaxanthin-fed $App^{NL\text{-}G\text{-}F}$ mice. Third, astaxanthin decreased pTau fraction in the astaxanthin-fed $App^{NL\text{-}G\text{-}F}$ mice compared with the control-fed $App^{NL\text{-}G\text{-}F}$ mice. In the present study, the pTau fraction was positively correlated with Aβ42 fraction, which is consistent with the amyloid cascade theory. These findings suggest that astaxanthin decreased pTau levels through its effects on Aβ42. Furthermore, recent studies reported that astaxanthin promoted Nrf2/ARE signaling in various experimental models (Li et al., 2013; Wu Q. et al., 2014; Zhu et al., 2018), while Nrf2 signaling reduces pTau by

activating autophagy-mediated degradation of pTau in the mouse brain (Jo et al., 2014). These findings suggest that astaxanthin may also reduce pTau through its effects on autophagy.

It has been recommended that anti-Aβ treatments should be tested in and applied to patients in an early phase of AD, before the formation of Aβ plaque (i.e., patients without brain damage) (Perrin et al., 2009; Sperling et al., 2011; McDade and Bateman, 2017). Since astaxanthin extracted from *Haematococcus pluvialis* was widely supplied for human consumption as a safe natural compound (Ambati et al., 2014), the present findings suggest that astaxanthin could be applied to such aged people without dementia or those with family risks of AD prior to the onset of AD symptoms. Further studies are required to elucidate mechanisms of astaxanthin effects on Aβ pathology, and translational research studies using human subjects are also required to test the usefulness of astaxanthin in the prevention of AD.

In the present study, the WT mice were fed only normal chow without 0.02% astaxanthin, but not normal chow with 0.02% astaxanthin. A previous study reported that feeding of 0.02% astaxanthin-containing diet for 8 weeks did not affect adult hippocampal neurogenesis in male WT C57BL/6J mice (Yook et al., 2016). Other studies also reported that administration of astaxanthin [80 mg/kg/day, oral gavage for 10 weeks (Yang et al., 2019); 25 mg/kg/day, oral gavage for 10 weeks (4 day/week) (Zhou et al., 2015)] did not affect spatial learning and memory in a Morris water maze test in WT mice. However, a higher dose of astaxanthin (0.5% astaxanthin-containing diet) for 8 weeks enhanced neurogenesis and improved special memory in male WT C57BL/6J mice (Yook et al., 2016). These findings suggest that feeding of normal chow with 0.02% astaxanthin might not affect spatial learning and memory in a Barnes maze test in WT mice although normal chow with astaxanthin in doses higher than 0.02% might enhance learning and memory even in WT mice. Further studies are required to investigate effects of astaxanthin on learning and memory functions in WT mice.

DATA AVAILABILITY STATEMENT

The datasets generated for this study are available on request to the corresponding author.

ETHICS STATEMENT

The animal study was reviewed and approved by the Ethics Committee for Animal Experiments at the University of Toyama.

AUTHOR CONTRIBUTIONS

HisN and KT designed the experiment. NH and YT performed the experiment. NH, YT, and HisN analyzed the data and wrote the manuscript. NH, YT, HisN, HirN, JM, KT, TS, and TCS revised the manuscript. All authors discussed the results, and approved the final manuscript.

FUNDING

This study was supported partly by research funds from Fuji chemical industries Co., Ltd., and University of Toyama. The funder had no role in study design, data collection and analysis, decision to submit the paper, or preparation of the manuscript.

REFERENCES

Ambati, R. R., Phang, S. M., Ravi, S., and Aswathanarayana, R. G. (2014). Astaxanthin: sources, extraction, stability, biological activities and its commercial applications–a review. *Mar Drugs* 12, 128–152. doi: 10.3390/md12010128

Bartos, M., Vida, I., and Jonas, P. (2007). Synaptic mechanisms of synchronized gamma oscillations in inhibitory interneuron networks. *Nat. Rev. Neurosci.* 8, 45–56. doi: 10.1038/nrn2044

Blennow, K. , and Zetterberg, H. (2018). The Past and the Future of Alzheimer's Disease Fluid Biomarkers. *J. Alzheimers Dis.* 62, 1125–1140. doi: 10.3233/JAD-170773

Choi, H. D., Kang, H. E., Yang, S. H., Lee, M. G., and Shin, W. G. (2011). Pharmacokinetics and first-pass metabolism of astaxanthin in rats. *Br. J. Nutr.* 105, 220–227. doi: 10.1017/S0007114510003454

Csala, M., Kardon, T., Legeza, B., Lizák, B., Mandl, J., Margittai, É., et al. (2015). On the role of 4-hydroxynonenal in health and disease. *Biochim. Biophys. Acta* 1852, 826–838. doi: 10.1016/j.bbadis.2015.01.015

Deczkowska, A., Keren-Shaul, H., Weiner, A., Colonna, M., Schwartz, M., and Amit, I. (2018). Disease-Associated Microglia: A Universal Immune Sensor of Neurodegeneration. *Cell* 173, 1073–1081. doi: 10.1016/j.cell.2018.05.003

Edwards, F. A. (2019). A Unifying Hypothesis for Alzheimer's Disease: From Plaques to Neurodegeneration. *Trends Neurosci.* 42, 310–322. doi: 10.1016/j.tins.2019.03.003

Fanaee-Danesh, E., Gali, C. C., Tadic, J., Zandl-Lang, M., Carmen Kober, A., Agujetas, V. R., et al. (2019). Astaxanthin exerts protective effects similar to bexarotene in Alzheimer's disease by modulating amyloid-beta and cholesterol homeostasis in blood-brain barrier endothelial cells. *Biochim. Biophys. Acta Mol. Basis Dis.* 1865, 2224–2245. doi: 10.1016/j.bbadis.2019.04.019

Grimmig, B., Kim, S. H., Nash, K., Bickford, P. C., and Douglas Shytle, R. (2017). Neuroprotective mechanisms of astaxanthin: a potential therapeutic role in preserving cognitive function in age and neurodegeneration. *Geroscience* 39, 19–32. doi: 10.1007/s11357-017-9958-x

Hardy, J., and Selkoe, D. J. (2002). The amyloid hypothesis of Alzheimer's disease progress and problems on the road to therapeutics. *Science* 297, 353–356. doi: 10.1126/science.1072994

Hashimoto, S., Matsuba, Y., Kamano, N., Mihira, N., Sahara, N., Takano, J., et al. (2019). Tau binding protein CAPON induces tau aggregation and neurodegeneration. *Nat. Commun.* 10, 2394. doi: 10.1038/s41467-019-10278-x

Hellwig, S., Masuch, A., Nestel, S., Katzmarski, N., Meyer-Luehmann, M., and Biber, K. (2015). Forebrain microglia from wild-type but not adult 5xFAD mice prevent amyloid-beta plaque formation in organotypic hippocampal slice cultures. *Sci. Rep.* 5, 14624. doi: 10.1038/srep14624

Hof, P. R., Young, W. G., Bloom, F. E., Belichenko, P. V., and Celio, M. R. (2000). *Comparative cytoarchitectonic atlas of the C57BL/6 and 129/ Sv mouse brains* (New York, Elsevier: Amsterdam).

Iaccarino, H. F., Singer, A. C., Martorell, A. J., Rudenko, A., Gao, F., Gillingham, T. Z., et al. (2016). Gamma frequency entrainment attenuates amyloid load and modifies microglia. *Nature* 540, 230–235. doi: 10.1038/nature20587

Jahn, H. (2013). Memory loss in Alzheimer's disease. *Dialogues Clin. Neurosci.* 15, 445–454.

Jargalsaikhan, U., Nishimaru, H., Matsumoto, J., Takamura, Y., Nakamura, T., Hori, E., et al. (2017). Ingestion of dried-bonito broth (dashi) facilitates PV-parvalbumin-immunoreactive neurons in the brain, and affects emotional behaviors in mice. *Nutr. Neurosci.* 20, 571–586. doi: 10.1080/1028415X.2016.1208429

Jiang, Z., Rompala, G. R., Zhang, S., Cowell, R. M., and Nakazawa, K. (2013). Social isolation exacerbates schizophrenia-like phenotypes via oxidative stress in cortical interneurons. *Biol. Psychiatry* 73, 1024–1034. doi: 10.1016/j.biopsych.2012.12.004

Jo, C., Gundemir, S., Pritchard, S., Jin, Y. N., Rahman, I., and Johnson, G. V. (2014). Nrf2 reduces levels of phosphorylated tau protein by inducing autophagy adaptor protein NDP52. *Nat. Commun.* 5, 3496. doi: 10.1038/ncomms4496

Kann, O., Papageorgiou, I. E., and Draguhn, A. (2014). Highly energized inhibitory interneurons are a central element for information processing in cortical networks. *J. Cereb Blood Flow Metab.* 34, 1270–1282. doi: 10.1038/jcbfm.2014.104

Katagiri, M., Satoh, A., Tsuji, S., and Shirasawa, T. (2012). Effects of astaxanthin-rich Haematococcus pluvialis extract on cognitive function: a randomised, double-blind, placebo-controlled study. *J. Clin. Biochem. Nutr.* 51, 102–107. doi: 10.3164/jcbn.D-11-00017

Kiko, T., Nakagawa, K., Satoh, A., Tsuduki, T., Furukawa, K., Arai, H., et al. (2012). Amyloid β levels in human red blood cells. *PloS One* 7, e49620. doi: 10.1371/journal.pone.0049620

Li, Z., Dong, X., Liu, H., Chen, X., Shi, H., Fan, Y., et al. (2013). Astaxanthin protects ARPE-19 cells from oxidative stress via upregulation of Nrf2-regulated phase II enzymes through activation of PI3K/Akt. *Mol. Vis.* 19, 1656–1666.

Lu, Y., Xie, T., He, X. X., Mao, Z. F., Jia, L. J., Wang, W. P., et al. (2015). Astaxanthin rescues neuron loss and attenuates oxidative stress induced by amygdala kindling in adult rat hippocampus. *Neurosci. Lett.* 597, 49–53. doi: 10.1016/j.neulet.2015.04.018

Lustbader, J. W., Cirilli, M., Lin, C., Xu, H. W., Takuma, K., Wang, N., et al. (2004). ABAD directly links Abeta to mitochondrial toxicity in Alzheimer's disease. *Science* 304, 448–452. doi: 10.1126/science.1091230

Manczak, M., Mao, P., Calkins, M. J., Cornea, A., Reddy, A. P., Murphy, M. P., et al. (2010). Mitochondria-targeted antioxidants protect against amyloid-beta toxicity in Alzheimer's disease neurons. *J. Alzheimers Dis.* 20, Suppl 2, S609–S631. doi: 10.3233/JAD-2010-100564

Mandal, P. K., Saharan, S., Tripathi, M., and Murari, G. (2015). Brain glutathione levels–a novel biomarker for mild cognitive impairment and Alzheimer's disease. *Biol. Psychiatry* 78, 702–710. doi: 10.1016/j.biopsych.2015.04.005

Markesbery, W. R., and Lovell, M. A. (1998). Four-hydroxynonenal, a product of lipid peroxidation, is increased in the brain in Alzheimer's disease. *Neurobiol. Aging* 19, 33–36. doi: 10.1016/S0197-4580(98)00009-8

Masuda, A., Kobayashi, Y., Kogo, N., Saito, T., Saido, T. C., and Itohara, S. (2016). Cognitive deficits in single App knock-in mouse models. *Neurobiol. Learn Mem.* 135, 73–82. doi: 10.1016/j.nlm.2016.07.001

Matsuno, T. (2001). Aquatic animal carotenoids. *Fish Sci.* 67, 771–783. doi: 10.1046/j.1444-2906.2001.00323.x

McDade, E., and Bateman, R. J. (2017). Stop Alzheimer's before it starts. *Nature* 547, 153–155. doi: 10.1038/547153a

Miki, W., Yamaguchi, K., and Konosu, S. (1982). Comparison of carotenoids in the ovaries of marine fish and shellfish. *Comp. Biochem. Physiol. B.* 71, 7–11. doi: 10.1016/0305-0491(82)90167-5

Miki, W. (1991). Biological functions and activities of animal carotenoids. *Pure Appl. Chem.* 63, 141–146. doi: 10.1351/pac199163010141

Nakagawa, K., Kiko, T., Miyazawa, T., Carpentero Burdeos, G., Kimura, F., Satoh, A., et al. (2011). Antioxidant effect of astaxanthin on phospholipid peroxidation in human erythrocytes. *Br. J. Nutr.* 105, 1563–1571. doi: 10.1017/S0007114510005398

Nakamura, T., Matsumoto, J., Takamura, Y., Ishii, Y., Sasahara, M., Ono, T., et al. (2015). Relationships among parvalbumin-immunoreactive neuron density, phase-locked gamma oscillations, and autistic/schizophrenic symptoms in PDGFR-β knock-out and control mice. *PloS One* 10, e0119258. doi: 10.1371/journal.pone.0119258

Nguyen, P. T., Nakamura, T., Hori, E., Urakawa, S., Uwano, T., Zhao, J., et al. (2011). Cognitive and socio-emotional deficits in platelet-derived growth factor receptor-β gene knockout mice. *PloS One* 6, e18004. doi: 10.1371/journal.pone.0018004

Perrin, R. J., Fagan, A. M., and Holtzman, D. M. (2009). Multimodal techniques for diagnosis and prognosis of Alzheimer's disease. *Nature* 461, 916–922. doi: 10.1038/nature08538

R Core Team. (2017). R: A Language and Environment for Statistical Computing. https://www.R-project.org/.

Rahman, S. O., Panda, B. P., Parvez, S., Kaundal, M., Hussain, S., Akhtar, M., et al. (2019). Neuroprotective role of astaxanthin in hippocampal insulin resistance induced by Aβ peptides in animal model of Alzheimer's disease. *BioMed. Pharmacother.* 110, 47–58. doi: 10.1016/j.biopha.2018.11.043

Rodrigues, E., Mariutti, L. R., and Mercadante, A. Z. (2012). Scavenging capacity of marine carotenoids against reactive oxygen and nitrogen species in a membrane-mimicking system. *Mar Drugs* 10, 1784–1798. doi: 10.3390/md10081784

Saito, T., Matsuba, Y., Mihira, N., Takano, J., Nilsson, P., Itohara, S., et al. (2014). Single App knock-in mouse models of Alzheimer's disease. *Nat. Neurosci.* 17, 661–663. doi: 10.1038/nn.3697

Sakakibara, Y., Sekiya, M., Saito, T., Saido, T. C., and Iijima, K. M. (2019). Amyloid-β plaque formation and reactive gliosis are required for induction of cognitive deficits in App knock-in mouse models of Alzheimer's disease. *BMC Neurosci.* 20, 13. doi: 10.1186/s12868-019-0496-6

Sasaguri, H., Nilsson, P., Hashimoto, S., Nagata, K., Saito, T., De Strooper, B., et al. (2017). APP mouse models for Alzheimer's disease preclinical studies. *EMBO J.* 36, 2473–2487. doi: 10.15252/embj.201797397

Selkoe, D. J., and Hardy, J. (2016). The amyloid hypothesis of Alzheimer's disease at 25 years. *EMBO Mol. Med.* 8, 595–608. doi: 10.15252/emmm.201606210

Sohal, V. S., Zhang, F., Yizhar, O., and Deisseroth, K. (2009). Parvalbumin neurons and gamma rhythms enhance cortical circuit performance. *Nature* 459, 698–702. doi: 10.1038/nature07991

Sperling, R. A., Jack, C. R., and Aisen, P. S. (2011). Testing the right target and right drug at the right stage. *Sci. Transl. Med.* 3, 111cm33. doi: 10.1126/scitranslmed.3002609

Stam, C. J., van Cappellen van Walsum, A. M., Pijnenburg, Y. A., Berendse, H. W., de Munck, J. C., Scheltens, P., et al. (2002). Generalized synchronization of MEG recordings in Alzheimer's Disease: evidence for involvement of the gamma band. *J. Clin. Neurophysiol.* 19, 562–574. doi: 10.1097/00004691-200212000-00010

Sterio, D. C. (1984). The unbiased estimation of number and sizes of arbitrary particles using the disector. *J. Microsc.* 134, 127–136. doi: 10.1111/j.1365-2818.1984.tb02501.x

Steullet, P., Cabungcal, J. H., Coyle, J., Didriksen, M., Gill, K., Grace, A. A., et al. (2017). Oxidative stress-driven parvalbumin interneuron impairment as a common mechanism in models of schizophrenia. *Mol. Psychiatry* 22, 936–943. doi: 10.1038/mp.2017.47

Takahashi, H., Brasnjevic, I., Rutten, B. P., Van Der Kolk, N., Perl, D. P., Bouras, C., et al. (2010). Hippocampal interneuron loss in an APP/PS1 double mutant mouse and in Alzheimer's disease. *Brain Struct. Funct.* 214, 145–160. doi: 10.1007/s00429-010-0242-4

Urakawa, S., Takamoto, K., Hori, E., Sakai, N., Ono, T., and Nishijo, H. (2013). Rearing in enriched environment increases parvalbumin-positive small neurons in the amygdala and decreases anxiety-like behavior of male rats. *BMC Neurosci.* 14, 13. doi: 10.1186/1471-2202-14-13

Verret, L., Mann, E. O., Hang, G. B., Barth, A. M., Cobos, I., Ho, K., et al. (2012). Inhibitory interneuron deficit links altered network activity and cognitive dysfunction in Alzheimer model. *Cell* 149, 708–721. doi: 10.1016/j.cell.2012.02.046

Wu, Q., Zhang, X. S., Wang, H. D., Zhang, X., Yu, Q., Li, W., et al. (2014). Astaxanthin activates nuclear factor erythroid-related factor 2 and the antioxidant responsive element (Nrf2-ARE) pathway in the brain after subarachnoid hemorrhage in rats and attenuates early brain injury. *Marine Drugs* 12, 6125–6141. doi: 10.3390/md12126125

Wu, W., Wang, X., Xiang, Q., Meng, X., Peng, Y., Du, N., et al. (2014). Astaxanthin alleviates brain aging in rats by attenuating oxidative stress and increasing BDNF levels. *Food Funct.* 5, 158–166. doi: 10.1039/c3fo60400d

Yang, X., Guo, A. L., Pang, Y. P., Cheng, X. J., Xu, T., Li, X. R., et al. (2019). Astaxanthin Attenuates Environmental Tobacco Smoke-Induced Cognitive Deficits: A Critical Role of p38 MAPK. *Mar Drugs* 17, 24. doi: 10.3390/md17010024

Yasumoto, T., Takamura, Y., Tsuji, M., Nakayama-Watanabe, T., Imamura, K., Inoue, H., et al. (2019). High molecular weight amyloid β1-42 oligomers induce

neurotoxicity via plasma membrane damage. *FASEB J.* 33, 9220–9234. doi: 10.1096/fj.201900604R

Yook, J. S., Okamoto, M., Rakwal, R., Shibato, J., Lee, M. C., Matsui, T., et al. (2016). Astaxanthin supplementation enhances adult hippocampal neurogenesis and spatial memory in mice. *Mol. Nutr. Food Res.* 60, 589–599. doi: 10.1002/mnfr.201500634

Zarkovic, K. (2003). 4-hydroxynonenal and neurodegenerative diseases. *Mol. Asppects Med.* 24, 293–303. doi: 10.1016/S0098-2997(03)00024-4

Zhou, X., Zhang, F., Hu, X., Chen, J., Wen, X., Sun, Y., et al. (2015). Inhibition of inflammation by astaxanthin alleviates cognition deficits in diabetic mice. *Physiol. Behav.* 151, 412–420. doi: 10.1016/j.physbeh.2015.08.015

Zhu, X., Chen, Y., Chen, Q., Yang, H., and Xie, X. (2018). Astaxanthin Promotes Nrf2/ARE Signaling to Alleviate Renal Fibronectin and Collagen IV Accumulation in Diabetic Rats. *J. Diabetes Res.* 2018, 6730315. doi: 10.1155/2018/6730315

Conflict of Interest: This study was supported partly by research funds from Fuji chemical industries Co., Ltd. Astaxanthin was provided from Fuji chemical industries Co., Ltd. NH is an employee of Fuji chemical industries Co., Ltd.

The remaining authors declare that the research was conducted in the absence of any commercial or financial relationships that could be construed as a potential conflict of interest.

frontiers in Molecular Neuroscience

REVIEW
published: 18 March 2020
doi: 10.3389/fnmol.2020.00041

Oxidative Stress in Cognitive and Epigenetic Aging: A Retrospective Glance

*Aditi Kandlur, Kapaettu Satyamoorthy and Gireesh Gangadharan**

Department of Cell and Molecular Biology, Manipal School of Life Sciences, Manipal Academy of Higher Education, Manipal, India

Brain aging is the critical and common factor among several neurodegenerative disorders and dementia. Cellular, biochemical and molecular studies have shown intimate links between oxidative stress and cognitive dysfunction during aging and age-associated neuronal diseases. Brain aging is accompanied by oxidative damage of nuclear as well as mitochondrial DNA, and diminished repair. Recent studies have reported epigenetic alterations during aging of the brain which involves reactive oxygen species (ROS) that regulates various systems through distinct mechanisms. However, there are studies which depict differing roles of reactive oxidant species as a major factor during aging. In this review, we describe the evidence to show how oxidative stress is intricately linked to age-associated cognitive decline. The review will primarily focus on implications of age-associated oxidative damage on learning and memory, and the cellular events, with special emphasis on associated epigenetic machinery. A comprehensive understanding of these mechanisms may provide a perspective on the development of potential therapeutic targets within the oxidative system.

Keywords: oxidative stress, brain aging, learning and memory, cognitive decline, epigenetic aging, molecular mechanisms

OPEN ACCESS

Edited by:
Touqeer Ahmed, National University of Sciences & Technology, Pakistan

Reviewed by:
Selva Rivas - Arancibia, National Autonomous University of Mexico, Mexico
Ian James Martins, Edith Cowan University, Australia

***Correspondence:**
Gireesh Gangadharan
gireesh.g@manipal.edu

Received: *16 January 2020*
Accepted: *02 March 2020*
Published: *18 March 2020*

Citation:
Kandlur A, Satyamoorthy K and Gangadharan G (2020) Oxidative Stress in Cognitive and Epigenetic Aging: A Retrospective Glance. Front. Mol. Neurosci. 13:41. doi: 10.3389/fnmol.2020.00041

INTRODUCTION

Aging involves the systemic loss of functioning in a time-dependent manner (Childs et al., 2015). There is increased focus on deciphering the mechanisms that prevail during aging. This is due to the increase in the life expectancy of individuals over these past few decades. The World Population Prospects 2019 report states an increase in the average life expectancy at birth to 72.6 years in 2019. The same report indicates that by 2050, the global number of individuals aged 65 years and more, will surpass the number of youths aged 15 to 24 years. The number of older individuals is projected to grow more than double the number of children below 5 years of age, by 2050 (United Nations, 2019). Aging is a key factor in several neurodegenerative disorders such as Alzheimer's and Parkinson's diseases (Hindle, 2010; Uddin et al., 2018). An aging brain is reported to show more cases of amyloid plaques, α-synuclein accumulation, loss of brain volume, loss of neurons, and neurofibrillary tangles (Elobeid et al., 2016). The hippocampus and the frontal lobes are the most commonly affected brain regions, therefore bringing about observable phenotypes pertaining to cognition, learning, memory, and attention (Peters, 2006). Brain being a metabolically robust active organ, is a large consumer of oxygen as well as producer of reactive oxygen species (ROS) (Halliwell, 1992). Although there are many theories to explain the mechanism of aging, the

free radical theory forms a basis to explain a great deal about how the reactive oxidants interact with the components of the cells to bring about a long-lasting accumulated damage and result in aging (Harman, 1968; Sohal and Brunk, 1992; Cutler and Mattson, 2006; Oswald et al., 2018). There seems to be a converging viewpoint regarding the epigenetic machinery that would be influenced by the changes in the oxidative microenvironment of cells. However, with the role of a double-edged sword, reactive oxidant species proves to be a necessary evil which also has been shown to be involved in various essential functions of the neuronal cells such as polarization of neurons, neurite outgrowth and axon specification, activity-induced synaptic growth and plasticity (Oswald et al., 2018). This review will highlight the roles played by the oxidative environment in the cells as aging proceeds and how it affects learning and memory as well as its significance in neurodegenerative diseases. The review will also include the underlying cellular events with an emphasis on the associated epigenetic machinery.

OXIDATIVE STRESS AND COGNITIVE AGING

Cognition is the collective set of abilities that involves various information processing, storage, and retrieval. This envelopes the concept of intelligence or metacognition, which involves the capacity to learn from experience and the ability to adapt to the surrounding environment or situations (Sternberg and Sternberg, 2011). There is a visible deterioration in cognition in aged individuals, in terms of fluid abilities or intelligence. This involves the application of crystallized abilities (skills and memories that are acquired) based on context/situation. These cognitive abilities that decline with age include attention, language skills, executive cognitive function, visuospatial abilities (perceiving spatial orientation of objects and visuoperceptual judgment), and certain types of memory such as working memory, prospective memory (to remember to perform a task in future) among others. There is also a well-defined and gradual decline in learning capacities (Critchley, 1984; Lezak et al., 2012; Murman, 2015). There are variations in the course of cognitive aging due to genetic as well as environmental factors. Such factors affect the cell's characteristic resilience to accumulation of damage that are brought about by stressors of aging (Barter and Foster, 2018). In terms of memory, episodic memory is the most effected with aging. This type of memory would include the memories of events in a spatio-temporal context (where and when it occurred) and with aging, retrieval becomes more difficult. On the other hand, semantic memory that covers memory of general knowledge of vocabulary, facts, etc. which does not require quick retrieval actions are retained quite well (Levine et al., 2002; Kinugawa et al., 2013). The hippocampus of the limbic system is the critical focal point or structure for the cognitive aspects such as acquiring information (learning), consolidation and recall of declarative (episodic and semantic) memories (Eichenbaum, 2001). It is an important region concerned in the spatial memory maps formation (Papp et al., 2007). The loss of memory retention and recall may be due to age dependent loss of hippocampal functioning. The memory in the hippocampus is presumed to be time-limited, in the manner that it stores memories fast and also undergoes faster overwriting, this in turn might represent a higher decay rate of such aspects of memory. However, the remote memory remains to be integrated into the neocortical regions, with the ventromedial prefrontal cortex becoming a major sector for memory consolidation in the limbic system-cortex axis (Nieuwenhuis and Takashima, 2011; Talamini and Gorree, 2012). This decline in cognitive abilities that accompanies aging may be partly due to brain atrophy that occurs in the temporal and frontal regions (Peters, 2006; Castelli et al., 2019).

Oxidative stress and its associated damage being involved in the age-dependent cognitive loss have been highlighted through numerous investigations to be the basis of pathogenesis. Comparison between young and aged animal brains showed higher levels of ROS and oxidative stress markers (Sohal et al., 1994; Liu et al., 2003; Serrano and Klann, 2004). The appearance of behavioral deficits or cognitive impairments in temporal and spatial memory, learning and retention of memory displayed strong associations with increasing oxidative species and stress in aged animal models (Carney et al., 1991; Fukui et al., 2001).

The conditions that prevail during aging are higher levels of oxidant species, oxidative stress and a shortfall in the antioxidant levels. To counter the effects of drop in antioxidant levels, the aged mice models that overexpress extracellular superoxide dismutase (EC-SOD) showed alleviation in spatial learning and memory related hippocampal long-term potentiation (LTP) that declines with age (Hu et al., 2006). They also showed better working memory as well as retention capacities when compared to the aged wild-type mice (Kamsler et al., 2007). On the other hand, to counter the effects of ROS, an antioxidant rich diet was able to reverse metabolic deficiencies of ascorbic acid, arachidonic acid, α-tocopherol. It even decreased the age-associated increase in the SOD activity, lipid peroxidation as well as inflammatory cytokine IL-1β. This might suggest the oxidative stress due to changes in the cellular environment might have an impact on the LTP (O'Donnell and Lynch, 1998). Age-associated cognitive impairment in terms of object recognition and associative fear memory has been observed in the *klotho* mouse model of aging. These mice showed higher levels of oxidative damage in lipid and DNA in the hippocampus and cerebral cortex. They also showed increased activity of antioxidants Cu/Zn-SOD and glutathione peroxidase (GPx) to compensate the increased ROS levels, the hippocampus also showed higher apoptotic gene expression. These mice when treated with α-tocopherol showed recovery of memory and reduced lipid peroxidation as well as cell death in the hippocampus, indicating oxidative stress caused apoptosis which later progressed into memory impairment (Nagai et al., 2002). A similar study with aging rats and vitamin E deficient rats showed decreased learning as well as memory retention ability whereas younger rats supplemented with vitamin E displayed accelerated learning and capabilities. This could be that the learning ability declined gradually during aging due to chronic exposure to oxidative stress.

The decrease in the memory retention capacity was due to oxidative stress induced delayed type of apoptosis that was observed in the CA1 hippocampal region. Vitamin E administration ameliorated the memory deficit. The vitamin E deficient rats showed higher levels of thiobarbituric acid reactive substances (TBARS), lipid hydroperoxides and protein carbonyls in the synaptic membranes. Synaptic membranes showed decreased ζ-potential causing a deficit in depolarization of the membrane and causing faulty neurotransmission (Fukui et al., 2001). Another study highlighted increased oxidative stress with aging in terms of increased TBARS with corresponding increase in Cu/Zn-SOD and mitochondrial Mn-SOD activity. The aged mice also displayed impaired mitochondrial electron transfer in certain complexes- complex I and III (brain NADH-cytochrome c reductase), complex IV (brain cytochrome oxidase) and brain citrate synthase. The study describes that neurodegeneration and longevity can be predicted through the neuromuscular functioning and the oxidative stress markers. It highlights the existence of a relationship between the oxidative stress and the behavioral performance in terms of exploration (Navarro et al., 2002). In the case of apoE knockout studies, it has been observed that there is a combined influence on cognitive aging through systemic oxidative stress and inflammatory vascular dysfunction (Evola et al., 2010). The age-related impairment of cognition involved oxidative molecular damages in the brain being one of the factors implicating cortical involvement. The same study established that the functional associations fall short to establish causal links that oxidative damage alone is able to cause age associated cognitive decline (Forster et al., 1996). Oxidative stress causing damage to mitochondria has been recently been implicated in neuronal degeneration as well as decline in cognition in Alzheimer's subjects (Reddy, 2006). In case of implicated neurons in Alzheimer's, oxidative damage is brought about by the free radicals generated by the entry of mutant APP and soluble Aβ into mitochondria and cause further impair mitochondrial metabolism (Manczak et al., 2006). Mild cognitive impairment (MCI) patient samples that precedes Alzheimer's shows a vast amount of oxidative damage in the brain in terms of lipid peroxidation, protein carbonyls, and malondialdehyde (Keller et al., 2005). Another study showed a strong correlation between decreased antioxidant levels and increased lipid peroxidation, also stating that the depleted antioxidant systems may be the end result of the increased oxidant species levels (Padurariu et al., 2010). Large scale cohort studies in humans such as EVA revealed a strong link as to oxidative stress being involved in cognitive decline with aging (Berr et al., 2000).

CELLULAR AND MOLECULAR IMPLICATIONS OF OXIDATIVE AGING

A prominent sign of an aging cell is the imbalance between the constantly produced reactive oxidant species and the diminishing antioxidant capacity (Halliwell, 1992). To have a better outlook on the role of oxidative stress during normal aging as well as disease conditions such as neurodegenerative disorders that accompany aging, we here discuss various levels of implications imposed by aging in the oxidative microenvironment- cellular, organellar, genetic as well as epigenetic.

Oxidative Damage Sources and Their Implications

DNA is an important carrier of heritable genetic information that faces the limitation of chemical stability that is constantly prone to changes (Lindahl, 1993). Considering the large genome size and the slower rate of replication when compared to the prokaryotes, it can be estimated that human cells have a turnover rate of 2,000–10,000 DNA purine bases on a daily basis due to hydrolytic depurination followed by excision repair. In this context, it has been hypothesized that long-lived, non-dividing human nerve cells would lose $\sim 10^8$ purines or ∼3% of its total purine residues from its DNA in an individual's lifetime (Lindahl and Nyberg, 1972).

DNA undergoes oxidative damage due to a series of sources reactive oxygen and nitrogen species (RONS), reactive carbonyl species, products of lipid peroxidation (De Bont and van Larebeke, 2004). The ROS are superoxide ($O_2^{-\cdot}$), singlet oxygen ($^1O_2$), hydrogen peroxide (H_2O_2), and hydroxyl radicals ($OH^{\cdot}$). Reactive nitrogen species include nitrous anhydride (N_2O_3) and peroxynitrite ($ONOO^-$). They bring about deaminating reactions on guanosine and adenosine (Burcham, 1999) (see **Table 1**).

Level of DNA Breaks With Oxygen Tension

Oxidative damage causes profound effects on the genetic composition by affecting the nuclear and mitochondrial DNA. The relative amounts of such damages if quantified can give an idea regarding the levels of oxidative stress faced by the cell, especially during aging. This has been done previously by various groups using different techniques such as HPLC-EC or GC/MS (see **Table 2**).

Cellular and Organellar Changes

The aging cell displays certain nucleocytoplasmic features which describe the events that precede and that follow the oxidative damage in various organelles as well as other subcellular compartments. As a part of the normal respiration, ROS such as superoxide is produced from the oxygen consumed, these reactive species interact with iron–sulfur clusters and release free iron, which triggers the downstream release of more reactive oxidant species (Boveris, 1984). Hydrogen peroxide from superoxide produce highly reactive hydroxyl radical that drive the oxidative damage toward the DNA, lipids, and proteins (Halliwell and Gutteridge, 1985). Mitochondria is a major internal source for ROS and hence is also a major target of oxidative damage (Chance et al., 1979); progressive impairment of mitochondria has been implicated in aging and neurodegenerative disorders such as Alzheimer's (Swerdlow and Khan, 2004; Mecocci et al., 2018). The mitochondrial DNA (mtDNA) is vulnerable to the insults of ROS as they lack histones. The mtDNA has been reported to show increasing levels of oxidized nucleoside 8-hydroxy-2′-deoxyguanosine (OH8dG)

TABLE 1 | Oxidizing species – their targets and products.

Oxidizing species (source)	Target	Oxidative damage product	References
Superoxide anions	Guanine	5-Diamino-4*H*-imidazolone (Iz) and 8-oxo-7,8-dihydroguanine (8-oxoG)	Misiaszek et al. (2004)
Singlet oxygen	Guanine	8-Oxo-7,8-dihydroguanine and spiroiminodihydantoin	DeFedericis et al. (2006)
Hydroxyl radicals	Adenine/adenosine	5-Formamido-6-aminopyrimidine type product (FAPy) adenine and adenosine; 8-hydroxyadenine or -adenosine	Steenken (1989)
	Cytosine	5-Hydroxy-5,6-dihydrocytos-6-yl and 6-hydroxy-5,6-dihydrocytos-5-yl	Chabita et al. (1996)
	5-Methylcytosine	5,6-Dihydroxy-5,6-dihydro-5-methylcytosine; 1-carbamoyl-4,5-dihydroxy-5-methyl-2-oxo-imidazolidine; aminocarbonyl[2-amino]-carbamic acid and *N*-formamide and 4-amino-1-5-dihydro-5-methyl-2-*H*-imidazol-2-one	Bienvenu and Cadet (1996), Bienvenu et al. (1996)
Nitrous anhydride	Adenine	Hypoxanthine	Burney et al. (1999)
	Cytosine	Uracil	
	5-Methylcytosine	Thymine	
	Guanine	Xanthine	
Peroxynitrite	Deoxyguanosine	8-Nitro-deoxyguanosine	Douki and Cadet (1996), Burcham (1999)
	Deoxyadenosine	8-Oxo-7,8-dihydro-2′-deoxyadenosine	Douki and Cadet (1996)
	Guanine	8-Nitroguanine	Love (2006)

with oxidative damage that gradually increases with aging and has been observed in Alzheimer's as well (Mecocci et al., 1993, 1994). Apart from mitochondrial DNA damage, models of premature aging also shows a disruption in DNA repair through defective repair proteins such as Ku86 as well as impairment of transcription-coupled repair of RNA polymerase II stalling lesions (Vogel et al., 1999; De Boer et al., 2002). The age-associated oxidative stress may be a common pathogenetic factor in the neurodegenerative disorders that show occurrence of cytoplasmic aggregates, which may be due to p62 and cytokeratins accumulation and aggregation with misfolded proteins (Zatloukal et al., 2002). In case of comorbidities of Alzheimer's such as Idiopathic normal pressure hydrocephalus, there have been reported mitochondria-endoplasmic reticulum contact (MERC) sites. These sites are said to be in a feedback-loop type regulation, wherein these sites can regulate the amyloid β-peptide (Aβ peptide) and the peptide can regulate these sites. These MERC sites were reported to increase in patients with dementia (Leal et al., 2018). Lysosomes exhibit increased accumulation of partially digested or damaged matter carried from the inhibited proteasomal activity. Proteasome inhibition also brought about an increase in the levels of mitochondrial ROS, loss of mitochondrial homeostasis and led to increased autophagy that might lead to brain aging (Sullivan et al., 2004). This has been observed in pathological conditions of Alzheimer's, where there is accumulation of soluble Aβ peptide in the lysosomes (Ditaranto et al., 2001). The damage by oxidative stress is seen to build up on nuclear pores. It alters nucleocytoplasmic transport as it affects nuclear lamina components. Aging also caused loss of nuclear pore protein such as Nup93. Aged neurons of rats possessed leaky nuclei and also accumulation of intranuclear tubulin bIII which caused severe chromatin aberrations (D'Angelo et al., 2009). Phosphorylated tau which is characteristic of Alzheimer's alters the transport across the nucleocytoplasmic axis. This was shown to occur by direct interactions with a nuclear pore protein Nup98 in the pore complex and alter nucleocytoplasmic transport in the hippocampal neurons (Eftekharzadeh et al., 2018).

In terms of energy metabolism, the metabolite NAD^+ and its associated histone deacetylase (HDAC) enzymes- sirtuins show significant decrease in aging and associated increased oxidative stress, causing catabolic breakdown of NAD^+ (Braidy et al., 2011). Neuronal and axonal protection was achieved through increased NAD^+ generation as well as downstream activation of the sirtuins, SIRT1 (Bedalov and Simon, 2004). These characteristics are affected in neurodegenerative diseases such as Alzheimer's and Parkinson's (Raff et al., 2002). NAD^+ depletion in aging could be due to PARP [poly (ADP-ribose) polymerase], which has been reported to show increased expression in cells from Alzheimer's and Parkinson's patients (Cosi et al., 1996; Love et al., 1999; Bürkle et al., 2004). On the genetic level, brain aging attributes certain cognition specific changes. Cognition in terms of synaptic plasticity and memory are regulated by the expression of certain immediate-early genes such as *arc*, *bdnf*, *zif268*, *c-fos*, and *Egr1* (Penner et al., 2010; Gallo et al., 2018). Most of the immediate early genes are involved to be regulating functions of Ca^{2+} regulation, myelin turnover, vesicular transport, synaptic plasticity as well as energy metabolism and they are known to decrease in transcription with aging (Blalock et al., 2003). Reduced expression of these genes in adult brain hampers memory consolidation and occurs in normal aging as well as memory disorders (Linnarsson et al., 1997; Rosi et al., 2005; Rowe et al., 2007).

Changes at the Epigenetic Level

A longitudinal study on a sample size of 104, performed with data on episodic memory as a parameter for tests, showed

TABLE 2 | Relative amounts of oxidative damages on nucleic acids in aging.

Type of oxidative damage	Rate of production	Sample studied	Rate of repair required/hits on DNA	Technique used to measure oxidative damage	Species	Age groups	Source of oxidative stress	References
8-Hydroxydeoxyguanosine (8OHdG)	236 fmol/μg of DNA	Liver	165 ± 66 pmol kg^{-1} day^{-1}	HPLC- electrochemical detection	Rat	24 months	Naturally occurring	Fraga et al. (1990)
	37.5 ± 3.2 fmol/μg of DNA	Kidney						
	16.7 ± 1.1 fmol/μg of DNA	Intestine						
	13.1 ± 2.5 fmol/μg of DNA	Brain						
	13.2 ± 0.9 fmol/μg of DNA	Testes						
	3.2 residues/10^6 bp	Liver	20% cleavage per μg DNA	HPLC- electrochemical detection	Mouse	4 months	Naturally occurring	Klungland et al. (1999)
	8–73 per 10^6 dG residues	Liver	Not mentioned	HPLC- electrochemical detection	Rat	6 months	Naturally occurring	Richter et al. (1988)
8-Hydroxyguanosine (8OHG)	3645 ± 1166 pmol kg^{-1} day^{-1}	Urine	Not mentioned	HPLC- electrochemical detection	Rat	24 months	Naturally occurring	Fraga et al. (1990)
8-Oxoguanine (8-oxoG)	76.2 ± 6.15 nmol/mmol creatinine	Urine	Not mentioned	HPLC and GC/MS	Rat	14 months	Naturally occurring	Foksinski et al. (2004)
	84.99 ± 5.91 nmol/mmol creatinine		34,000 repair events/cell/day		Mouse	12 months		
	8.4 ± 1.21 nmol/mmol creatinine		2,800 repair events/cell/day		Human	40 years		
8-Oxo-deoxyguanosine(8-oxodG)	0.037 ± 0.004 per 10^5dG residues	Liver	47,000 lesions/cell/day	HPLC- electrochemical detection	Mouse	4–8 months	γ-Irradiation (0.5–50 Gy	Hamilton et al. (2001)
	0.012 ± 0.003 per 10^5dG residues	Brain	Not mentioned					
	0.012 ± 0.004 per 10^5dG residues	Heart	Not mentioned					
	0.033 ± 0.005 per 10^5dG residues	Liver	Not mentioned		Rat	4–6 months	Naturally occurring	
	0.012 ± 0.003 per 10^5dG residues	Brain	Not mentioned					
	0.010 ± 0.002 per 10^5dG residues	Heart	Not mentioned					
	0.064 ± 0.004 per 10^5dG residues	Prostate	Not mentioned		Human	60–78 years	Naturally occurring	
8-Oxo-deoxyguanosine(8-oxodG)	7.22 ± 1.05 nmol/mmol creatinine	Urine	Not mentioned	HPLC and GC/MS	Rat	14 months	Naturally occurring	Foksinski et al. (2004)
	13.2 ± 1.23 nmol/mmol creatinine		34000 repair events/cell/day		Mouse	12 months		
	2.1 ± 0.44 nmol/mmol creatinine		2800 repair events/cell/day		Human	40 years		
8-Oxo-deoxyadenosine(8-oxodA)	59 per 10^5 nucleosides	Aqueous solution of DNA	Not mentioned	HPLC- electrochemical detection	–	–	Peroxynitrite solution	Douki and Cadet (1996)

that the epigenetic DNA-methylation age predicted dementia significantly when compared to the chronological age (Degerman et al., 2017). The same study has also shown associations with the epigenetic age with cognitive impairment, deteriorating working memory. The group that displayed maintained cognition at an older age of 70–80 had a younger epigenetic age when compared to the baseline levels of those at the age of 55–65. Apart from modifications that happens during gene expression, learning and memory are said to be driven by an "epigenetic code." Changes in this could lead to cognitive impairment particularly in learning and memory. Various signature patterns have been observed to be involved in the behavior patterns and these are the behavioral changes that are seen to be prominent in the process of aging (see **Table 3**). It is highly likely that the epigenetic landscape involved in such behavioral aspects of learning and memory is affected with aging.

DNA methylation is one among the epigenetic regulators of gene expression and is controlled through family of enzymes, DNMTs (DNA methyl transferases). They take part in establishing spatial memory and also in fear conditioning (Miller and Sweatt, 2007; Feng et al., 2010). DNMTs catalyze the methylation of the nucleotide cytosine at its 5th carbon to form 5-methyl cytosine (5mC). These 5mC are usually found in CpG dinucleotides in stretches of DNA termed "CpG islands." The mammalian brain shows approximately 62% methylated CpGs (Fasolino and Zhou, 2017). These islands have been studied to regulate gene expression through mechanisms such as CpG methylation (Kotambail et al., 2017). DNMTs rely on methyl group donors such as L-methylfolate via SAM (Stahl, 2010), however, there is deficiency of folate observed in aging as well as cases of dementia (Robins Wahlin et al., 2001; Reynolds, 2002), parallel to the decrease in global methylation with aging. Increased methylation at the *PP1* gene and decreased methylation at the *reelin* gene underlie conditioned fear memory (Miller and Sweatt, 2007). Similarly, *BDNF* has been studied to be strongly linked to enduring fear memories through the suppression of its fourth exon by promoter methylation (Alonso et al., 2005; Bekinschtein et al., 2008). While methylation at promoters of first and sixth exons led to increased transcription of the gene (Lubin et al., 2008). These changes are reversed within 24 h and occur in the hippocampus where memory formation occurs. However, memory storage in the prefrontal cortex was coinciding with persistent methylation at the CpG rich promoter of *calcineurin* (Miller et al., 2010). These studies showed that treatment with DNMT inhibitors at the hippocampus gave mixed results due to the dual role of methyl adding and removing activities whereas treatment at the prefrontal cortex prevented retrieval of the fear memory. These modifications also interact and lead to other epigenetic regulators such as HDACs to bring about suppression of the genes. Apart from methylation, hydroxymethyl cytosine formed by the oxidative environment as well as through the catalytic activity of methylcytosine dioxygenase TET1 (Jessop and Toledo-Rodriguez, 2018), is known to bring about changes in the expression of certain genes such as *Tdg, Apobec1, Smug,* and *Mbd4*. This has been studied to affect long-term associative memory, its formation as well as consolidation (Kaas et al., 2013). Chromatin remodeling occurs through covalent modifications to the histone core proteins- acetylation, phosphorylation in establishing long-term memory. Mitogen- and stress-activated protein kinase-1 (MSK1) is a major phosphorylating kinase that target H3 histones and other signaling molecules such as cAMP response element-binding protein (CREB) and other transcription factors involved in synaptic plasticity and memory (Deak et al., 1998; Soloaga et al., 2003). MSK1 shows high expression in the hippocampus and the double knockout models lack in long-term contextual fear memory but are not affected in terms of short-term associative memory of fear. These models also show a deficit in spatial learning and display an impairment in passive avoidance learning. The kinase acts on ERK to regulate histone modifications post fear training- H3 phosphorylation at Ser 10 and acetylation at Lys 14, which indicate transcriptional activation (Chwang et al., 2007).

Upregulated histone acetylation post-treatment with HDAC inhibitors has been shown to enhance memory formation and LTP (Levenson et al., 2004). Other similar studies pertaining to histone acetylation have been shown to be linked to activated gene expression of those that regulate cognition

TABLE 3 | Prominent behavior changes in aging and underlying epigenetic code.

Epigenetic code/modification	Genes affected	Behavior changes/cognitive parameter affected	References
DNA cytosine methylation (MeC)	*PP1; reelin; BDNF; calcineurin; Arc; Egr1; Fos; Homer1; Nr4a2*	Conditioned fear memory; long-term associative memory formation and consolidation	Miller and Sweatt (2007), Bekinschtein et al. (2008), Lubin et al. (2008), Miller et al. (2010), Kaas et al. (2013)
Cytosine hydroxymethylation (OHMeC)	*Tdg; Apobec1; Smug; Mbd4*	Long-term associative memory formation and consolidation	Kaas et al. (2013)
H3 phosphorylation at Ser 10 and acetylation at K14	Not mentioned	Conditioned fear memory- long-term memory consolidation	Chwang et al. (2007)
H4 acetylation at K12	*Fmn2*	Associative learning, conditioned fear memory	Peleg et al. (2010)
H3 and H4 acetylation	*Nr4a1; Nr4a2; NGFI-B*	Contextual fear conditioned memory	Vecsey et al. (2007)
H3 acetylation at K9 and H4 acetylation	Not mentioned	Spatial learning and memory	Castellano et al. (2012)
H2B acetylation at Lys 5, 12, 15, 20 and H4 acetylation at Lys 12	*bdnf, cFos, FosB* and *zif268*	Spatial memory and consolidation	Bousiges et al. (2010)

pertaining functions such as increased hippocampal synaptic connectivity/plasticity, LTP (Levenson et al., 2004; Vecsey et al., 2007; Peleg et al., 2010). Acetylation at H3 and H4 are generally linked with associative learning, conditioned fear memory-long-term storage and consolidation which have been studied to decrease with aging (Chwang et al., 2007; Vecsey et al., 2007; Peleg et al., 2010). These modifications usually occur at promoter regions of genes such as *Fmn2* (formin 2), *Nr4a1*, *Nr4a2* (nuclear receptor subfamily 4 group A member 1 and 2), *NGFI-B* (nerve growth factor I-B) which are known to take part in regulation of cytoskeletal structures, LTP, hippocampal dependent memory storage. Similar study revealed a multiple background changes in the epigenome with aging and highlighted that with aging there is also a region-wise change. It showed H3 acetylation at Lys 9 to be decreased in hippocampal CA1 region, no changes in DG (dentate gyrus) or CA3, whereas, H4 acetylation showed an opposite regulation with aging, increased in CA1 and reduced in DG. These changes were noted as with normal aging accompanied cognitive impairment in terms of spatial learning and memory (Castellano et al., 2012). H2B acetylation at Lys 5, 12, 15, 20, and H4 acetylation at Lys 12 affect spatial memory and its consolidation. These changes affect genes such as *bdnf, cFos, FosB,* and *zif268* (Bousiges et al., 2010).

Oxidative stress in form of ROS induced DNA lesions can influence and alter the methylome landscape in a cell, by means of DNA oxidation and TET-mediated hydroxymethylation (Kriaucionis and Heintz, 2009; Tahiliani et al., 2009). These lesions are pyrimidine hydroxylation products and 5-methylcytosine (5mC). They could interfere with the actual 5-hmC signals by their structural similarities (Lewandowska and Bartoszek, 2011). DNA lesions such as 8-oxoguanine could be repaired through mechanisms of base excision repair (BER) through enzyme 8-oxoG glycosylase (OGG1), however, it has also been shown to be involved in demethylation of methyl-CpGs from 5mC to cytosine, this could lead to changes in the epigenetic signatures of the genes and hence their expression (Zhou et al., 2016). CpG sites demethylation plays roles in memory formation as well as consolidation in hippocampus and the cingulate cortex (Duke et al., 2017). Oxidative stress could also lead to oxidation followed by deamination of the oxidized 5mC (Zuo et al., 1995). Cytosine and 5-methylcytosine give rise to varied products under the stress of ROS such as hydroxyl anions (see **Table 1**). Oxidation of cytosine would be a major factor as it enables its deamination to bring about GC → AT transitions.

Studies showed that hippocampal cells from Alzheimer's patients had decreased global methylation as well as hydroxymethylation (Chouliaras et al., 2013). Oxidative stress has the ability to alter methylation and histone acetylation, and hence may be a determinant regulatory factor that affects the epigenetics of cells (Gu et al., 2013). Another example of a reactive oxidant species regulating epigenetics of the aging brain is nitric oxide (NO). NO at appropriate concentrations reported to be neuroprotective; however, at excess concentrations, it has been shown to react with superoxide to form the highly reactive peroxynitrite contributing to the oxidative stress (Radi, 2013; Dubey et al., 2017). Sirt1 is known to regulate the production of NO *via* the acetylation of endothelial nitric oxide synthase (eNOS) (Donato et al., 2011; Martins, 2017b). The age associated decrease in Sirt1 seems to bring about deregulation of NO synthesis which in turn has a profound impact on various downstream targets of NO including DNA methylation, histone acetylases as well as histone methyltransferases (Socco et al., 2017). NO has been shown to have intricate connections with *BDNF*, which is involved in cognition (learning, memory, and its consolidation), synaptic plasticity, and LTP (Paul and Ekambaram, 2011; Kolarow et al., 2014; Dubey et al., 2017). *BDNF* regulates post-synaptically the production of NO in the hippocampal neurons at the dendrites and the soma through TrkB and TrkC based signaling (Kolarow et al., 2014). Reduced *BDNF* levels in the brain has been studied in the context of downstream result of deregulated NO synthesis, and also resulting cognitive impairment (Canossa et al., 2002; Banoujaafar et al., 2016). In the cortex and the hippocampus, NO shows gradual decline with aging (Reckelhoff et al., 1994; Lima-Cabello et al., 2016). Clinical samples of blood plasma in aged individuals have been studied to show higher levels of NO and has been implicated to loss of auditory-verbal as well as visual-spatial based working memory along with impairment of short term declarative memory (Talarowska et al., 2012). Aβ protein disrupts NO activity while impairing the synapses and LTP in Alzheimer's disease (Paul and Ekambaram, 2011).

The oxidative environment does seem to play an influence in regulating epigenetic machinery and the resulting epigenome of the aging cell. This affects certain characteristics of the cellular system in terms of plasticity and transmission efficacy that ultimately alter cognition to become prone to a gradual decline (**Figure 1**).

EVOLVING THEORIES OF AGING

The long-established theory that was made to attempt explaining the mechanism underlying aging explains it as the accumulating cellular and molecular damage through reactive oxidant species, is well known as the Free radical theory (Harman, 1956). There are now several theories as well as updated versions to this theory with better explanations to the demerits. One among them which is finding favors among many in the field of aging research is the damage theory. A strong argument that the damage theory poses is that the although antioxidants such as mitochondrial SOD seem to ameliorate conditions that prevail in oxidative stress situations, they don't seem to extend the life span through overexpression (Mockett et al., 2010). A recent theory that explains the mechanisms that prevail during aging is the epigenetic oxidative redox shift (EORS) theory. It attempts to explain the shift in metabolism with aging. It states the probable increased glycolysis that is brought about through the impaired mitochondrial system, which would ultimately result in increased ROS production. This is carried out by the upregulation of the redox-sensitive transcription factors. The upstream shift is said to be toward oxidized

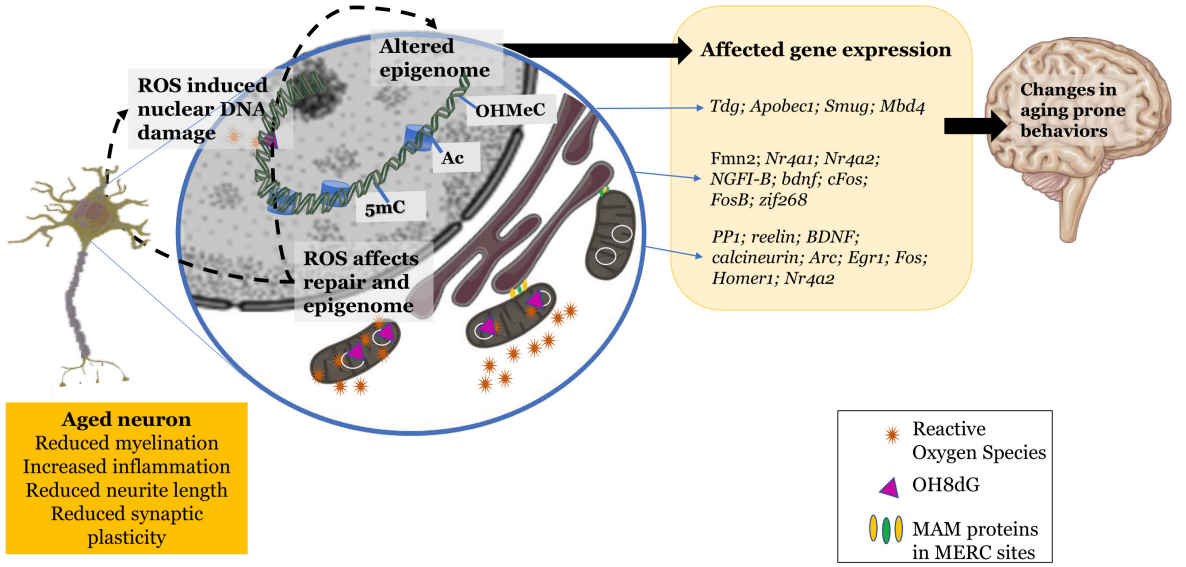

FIGURE 1 | Changes exhibited by the aging neuron: increased reactive oxidant species production, mitochondrial and nuclear DNA damage, dysfunctional mitochondrial-endoplasmic reticular sites. These changes in the redox environment in the cytosol as well as nucleus trigger epigenetic changes leading to altered gene expression and further leading to changes in aging prone behaviors. Schematic parts of the figure were taken from Servier Medical art (https://smart.servier.com/) licensed under an Unported license of Creative Commons Attribution 3.0.

metabolic shift (Jones, 2006) which is due to reduced bursts of energy requirement that is resultant of sedentary lifestyle or lower physical activity. The shift is epigenetically regulated through chromatin modulators - HDACs such as sirtuins, histone acetylases as well as DNMTs. This is accompanied by insulin resistance (Brewer, 2010).

MOLECULAR TARGETS - A STRATEGY AIMING FOR THERAPY

The process of oxidative damage has opened avenues for probable targets that either aid in apoptotic inhibition, reducing ROS, modulate chromatin architecture to keep learning and memory associated genes active in transcription. Some of them have been listed below. Quinone reductase 2 is one among the many genes that undergo changes in their hippocampal expression pattern with aging. Its overexpression is reported to be involved in learning deficits that occur in the case of age-related memory impairment. Its selective inhibitors, S26695 and S29434, were able to protect against the toxin menadione-induced apoptosis, preserving and enhancing learning abilities. Similarly, knockout models showed improved motor learning skills (Benoit et al., 2010).

Human TFAM protein was overexpressed in transgenic mice which suppressed ROS sourced from the mitochondria as well as the inflammatory IL-1β response. It increased the mean EPSP (excitatory postsynaptic potential) when compared to the wild-type aged mice, it ameliorated the working memory as well the hippocampal LTP (Hayashi et al., 2008). Treatment with spin-trapping compound N-*tert*-butyl-α-phenylnitrone (PBN) helped to cut down the increasing reserves of ROS and prevented early loss of glutamine synthetase activity. The treatment also reduced error rate in radial arm tests indicating that cognitive dysfunction does result from the accumulation of oxidant species, oxidized proteins and products; this impairment in cognition induced through oxidative stress is rescued through the treatment with spin trap moieties, however, this was later observed to be species specific (Carney et al., 1991). Epigenetic mechanisms such as histone deacetylation could be inhibited *via* HDAC inhibitors such as suberoylanilide hydroxamic acid (SAHA). This inhibits class I HDACs and has been observed to induce expression of learning and memory genes in aged mice (Peleg et al., 2010). The same compound along with other HDAC inhibitors such as sodium valproate and sodium butyrate have been studied to rescue the long-term memory deficits in case of contextual memory in Alzheimer's disease mice models (Kilgore et al., 2010). HDACI I2 and W2 brought about increased mRNA levels of Aβ degradation enzymes as well as decreased Aβ levels and rescued learning and memory deficits in aged mice Alzheimer's model- hAPP 3x Tg AD. The HDACI W2 also decreased tau phosphorylation at amino acid position threonine-181 (Sung et al., 2013).

Another possible target which could also bring about epigenetic regulation through HDAC sirtuins is NAD^+. NAD^+ is essential as a cofactor, a hydride donor in several metabolic functions necessary for cell's survival, a key player in energy metabolism- glycolysis, tricarboxylic acid cycle, mitochondrial oxidative phosphorylation (OXPHOS) as well as fatty acid β-oxidation (Wallace, 2012; Fang et al., 2017). NAD^+ serves as a substrate for SIRT1, to perform its gene regulatory function. Increased levels of NAD^+ has been shown to promote more

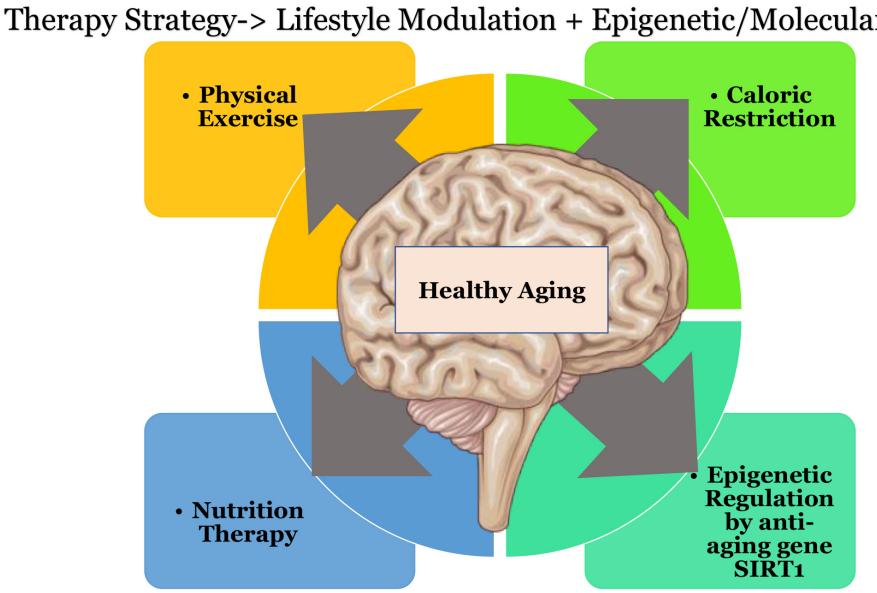

FIGURE 2 | Possible therapeutic directions that could result in healthier aging of the brain. Schematic parts of the figure were taken from Servier Medical art (https://smart.servier.com/) licensed under an Unported license of Creative Commons Attribution 3.0.

effective SIRT1 activity (Araki et al., 2004; Milne and Denu, 2008; Massudi et al., 2012b). NAD^+ is seen to be affected with chronic exposure to oxidative stress, which leads to its catabolism (Furukawa et al., 2007; Massudi et al., 2012a). SIRT1 correspondingly showed decreased activity with progressing age (Braidy et al., 2011).

On the other hand, Sirt1 levels could be regulated by means of certain activators and inhibitors (such as bacterial lipopolysaccharides-LPS). Its activators such as resveratrol have applications in stabilizing cases of epilepsy as well as epilepticus (Martins, 2017a). This could be potential alternative in molecular therapeutic strategies.

L-Arginine as a donor of NO is considered for potential therapeutic application. It showed neuroprotective roles along with NO to bring about amelioration of age induced memory impairment (Paul et al., 2005; Paul and Ekambaram, 2011; Hosseini et al., 2012). It also attenuated oxidative stress as well as DNA damage in models of sporadic Alzheimer's disease (Dubey et al., 2017).

Future Direction: Toward Healthier Aging

Therapeutic strategies may be devised using multiple approaches to curb the effects of oxidative stress, this could be in the form of caloric restriction (Martins, 2017c) coupled with exercise. Physical exercise has been shown to increase the levels of blood flow in the brain vasculature and also to influence *BDNF* based neuroplasticity (Banoujaafar et al., 2016). Other approaches could involve nutrition therapy to supplement key players that help in epigenetic regulation with amino acids such as L-arginine, diet with Sirt1 activators, or downstream metabolites such as NAD^+, or through quinone reductase inhibitors. Individual therapeutic strategies do not seem to show promising or effective results as there seems to exist a background interconnectivity in the treatment modules toward healthy aging of the brain, that would affect multiple pathways downstream (as shown in **Figure 2**). Keeping in mind that "we are what we eat" (Twiss, 2007) and that there is "no clear-cut definition of normal aging" (Vauzour et al., 2017) due to individual based differences. There could be substantial opportunities toward discovering pathways to healthy aging.

CONCLUSION

When observing the cellular background of cognitive decline, various aspects come into the picture that seem to be the basis of pathogenesis- oxidative stress and its associated damage, vast changes in the metabolic landscape, epigenetic variations, all of which accompany organellar dysfunction and the shortfall in repair and recovery mechanisms. Most of the studies highlight the significant association between aging and oxidative stress; however, still more studies have to be conducted that can show a direct causal link between the two. There is an increasing number of studies that point toward the epigenetic regulation of cognition through several mechanisms that affect the genes involved in learning and memory. Such that there might be a histone code that is involved in the regulation of cognition that may be impacted during aging. All the studies converge to a point that highlight the presence of oxidative stress in the aging cells, cognition in particular is affected via various mechanisms at the gene, nucleocytoplasmic and mostly the epigenetic level. Each component could pose as targets for therapy for symptomatic therapy but for a holistic approach several strategies that also involve epigenetic machinery would prove to be ideal. There is a

need for longitudinal studies *in vivo* and in humans to understand an overall perspective to understanding the placement of aging and its associated diseases. Longitudinal studies in aging animal models (natural and/or induced) and further into humans involving a combined therapeutic strategy of regulated lifestyle modules that incorporate the above-mentioned therapeutic concepts could help understand the fundamental pathology of aging and hence determine effective regulation of healthy aging. There also seems to be several lacunae in understanding the models (D-galactose induced, accelerated senescence, delayed aging, transgenic) to understand aging does not account for the complete pathology of aging (Mitchell et al., 2015). As aging has multiple confounding factors that play a role in determining the level of damage (multiple morbidities) (Santulli et al., 2015), it would be necessary to understand the combined effects of multiple factors to establish causal links between aging and oxidative stress and also the associated cognitive impairment.

AUTHOR CONTRIBUTIONS

AK synthesized and generally organized the manuscript, **Figures 1**, **2**, and **Tables 1–3**. GG and KS supervised and edited the manuscript. AK declared that substantially contributed to the review article in object.

FUNDING

This work was supported by Ramalingaswami Re-entry Fellowship, Department of Biotechnology, Government of India (No. BT/RLF/Re-entry/49/2018), Vision Group on Science and Technology, Government of Karnataka (GRD No. 818), and the Manipal Academy of Higher Education Institutional Intramural funding (MAHE/DREG/PHD/IMF/2019) to GG and DST-UKIERI fund to KS. AK thanks Manipal Academy of Higher Education for the Dr. TMA Pai Ph.D. scholarship and the Indian Council of Medical Research for the Junior Research Fellowship (ICMR-JRF).

ACKNOWLEDGMENTS

We would like to thank Manipal School of Life Sciences, Manipal Academy of Higher Education (MAHE), Manipal for the infrastructure and support.

REFERENCES

Alonso, M., Bekinschtein, P., Cammarota, M., Vianna, M. R. M., Izquierdo, I., and Medina, J. H. (2005). Endogenous BDNF is required for long-term memory formation in the rat parietal cortex. *Learn. Mem.* 12, 504–510. doi: 10.1101/lm.27305

Araki, T., Sasaki, Y., and Milbrandt, J. (2004). Increased nuclear NAD biosynthesis and SIRT1 activation prevent axonal degeneration. *Science* 305, 1010–1013. doi: 10.1126/science.1098014

Banoujaafar, H., Monnier, A., Pernet, N., Quirié, A., Garnier, P., Prigent-Tessier, A., et al. (2016). Brain BDNF levels are dependent on cerebrovascular endothelium-derived nitric oxide. *Eur. J. Neurosci.* 44, 2226–2235. doi: 10.1111/ejn.13301

Barter, J. D., and Foster, T. C. (2018). Aging in the brain: new roles of epigenetics in cognitive decline. *Neuroscientist* 24, 516–525. doi: 10.1177/1073858418780971

Bedalov, A., and Simon, J. A. (2004). NAD to the rescue. *Science* 305, 954–955. doi: 10.1126/science.1102497

Bekinschtein, P., Cammarota, M., Katche, C., Slipczuk, L., Rossato, J. I., Goldin, A., et al. (2008). BDNF is essential to promote persistence of long-term memory storage. *Proc. Natl. Acad. Sci. U.S.A.* 105, 2711–2716. doi: 10.1073/pnas.0711863105

Benoit, C.-E., Bastianetto, S., Brouillette, J., Tse, Y., Boutin, J. A., Delagrange, P., et al. (2010). Loss of quinone reductase 2 function selectively facilitates learning behaviors. *J. Neurosci.* 30, 12690–12700. doi: 10.1523/JNEUROSCI.2808-10.2010

Berr, C., Balansard, B., Arnaud, J., Roussel, A.-M., Alpérovitch, A., and Group, E. V. A. S. (2000). Cognitive decline is associated with systemic oxidative stress: the EVA study. *J. Am. Geriatr. Soc.* 48, 1285–1291. doi: 10.1111/j.1532-5415.2000.tb02603.x

Bienvenu, C., and Cadet, J. (1996). Synthesis and kinetic study of the deamination of the cis diastereomers of 5,6-dihydroxy-5,6-dihydro-5-methyl-2'-deoxycytidine. *J. Org. Chem.* 61, 2632–2637. doi: 10.1021/jo951900e

Bienvenu, C., Wagner, J. R., and Cadet, J. (1996). Photosensitized oxidation of 5-Methyl-2'-deoxycytidine by 2-Methyl-1,4-naphthoquinone: characterization of 5-(Hydroperoxymethyl)-2'-deoxycytidine and stable methyl group oxidation products. *J. Am. Chem. Soc.* 118, 11406–11411. doi: 10.1021/ja962073h

Blalock, E. M., Chen, K.-C., Sharrow, K., Herman, J. P., Porter, N. M., Foster, T. C., et al. (2003). Gene microarrays in hippocampal aging: statistical profiling identifies novel processes correlated with cognitive impairment. *J. Neurosci.* 23, 3807–3819. doi: 10.1523/jneurosci.23-09-03807.2003

Bousiges, O., Vasconcelos, A. P., de Neidl, R., Cosquer, B., Herbeaux, K., Panteleeva, I., et al. (2010). Spatial memory consolidation is associated with induction of several lysine-acetyltransferase (histone acetyltransferase) expression levels and H2B/H4 acetylation-dependent transcriptional events in the rat hippocampus. *Neuropsychopharmacology* 35, 2521–2537. doi: 10.1038/npp.2010.117

Boveris, A. (1984). Determination of the production of superoxide radicals and hydrogen peroxide in mitochondria. *Oxygen Radic. Biol. Syst.* 105, 429–435. doi: 10.1016/s0076-6879(84)05060-6

Braidy, N., Guillemin, G. J., Mansour, H., Chan-Ling, T., Poljak, A., and Grant, R. (2011). Age related changes in NAD+ metabolism oxidative stress and Sirt1 activity in wistar rats. *PLoS One* 6:e19194. doi: 10.1371/journal.pone.0019194

Brewer, G. J. (2010). Epigenetic oxidative redox shift (EORS) theory of aging unifies the free radical and insulin signaling theories. *Exp. Gerontol.* 45, 173–179. doi: 10.1016/j.exger.2009.11.007

Burcham, P. C. (1999). Internal hazards: baseline DNA damage by endogenous products of normal metabolism. *Mutat. Res. Toxicol. Environ. Mutagen.* 443, 11–36. doi: 10.1016/s1383-5742(99)00008-3

Bürkle, A., Beneke, S., and Muiras, M.-L. (2004). Poly (ADP-ribosyl) ation and aging. *Exp. Gerontol.* 39, 1599–1601.

Burney, S., Caulfield, J. L., Niles, J. C., Wishnok, J. S., and Tannenbaum, S. R. (1999). The chemistry of DNA damage from nitric oxide and peroxynitrite. *Mutat. Res. Mol. Mech. Mutagen.* 424, 37–49.

Canossa, M., Giordano, E., Cappello, S., Guarnieri, C., and Ferri, S. (2002). Nitric oxide down-regulates brain-derived neurotrophic factor secretion in cultured hippocampal neurons. *Proc. Natl. Acad. Sci. U.S.A.* 99, 3282–3287. doi: 10.1073/pnas.042504299

Carney, J. M., Starke-Reed, P. E., Oliver, C. N., Landum, R. W., Cheng, M. S., Wu, J. F., et al. (1991). Reversal of age-related increase in brain protein oxidation, decrease in enzyme activity, and loss in temporal and spatial memory by chronic administration of the spin-trapping compound N-tert-butyl-alpha-phenylnitrone. *Proc. Natl. Acad. Sci. U.S.A.* 88, 3633–3636. doi: 10.1073/pnas.88.9.3633

Castellano, J. F., Fletcher, B. R., Kelley-Bell, B., Kim, D. H., Gallagher, M., and Rapp, P. R. (2012). Age-related memory impairment is associated with disrupted multivariate epigenetic coordination in the hippocampus. *PLoS One* 7:e33249. doi: 10.1371/journal.pone.0033249

Castelli, V., Benedetti, E., Antonosante, A., Catanesi, M., Pitari, G., Ippoliti, R., et al. (2019). Neuronal cells rearrangement during aging and neurodegenerative disease: metabolism, oxidative stress and organelles dynamic. *Front. Mol. Neurosci.* 12:132. doi: 10.3389/fnmol.2019.00132

Chabita, K., Saha, A., Mandal, P. C., Bhattacharyya, S. N., Rath, M. C., and Mukherjee, T. (1996). Reactions of OH and eaq- adducts of cytosine and its nucleosides or nucleotides with Cu (II) ions in dilute aqueous solutions: a steady-state and pulse radiolysis study. *Radiat. Res.* 146, 514–524.

Chance, B., Sies, H., and Boveris, A. (1979). Hydroperoxide metabolism in mammalian organs. *Physiol. Rev.* 59, 527–605. doi: 10.1152/physrev.1979.59.3.527

Childs, B. G., Durik, M., Baker, D. J., and Van Deursen, J. M. (2015). Cellular senescence in aging and age-related disease: from mechanisms to therapy. *Nat. Med.* 21, 1424–1435. doi: 10.1038/nm.4000.Cellular

Chouliaras, L., Mastroeni, D., Delvaux, E., Grover, A., Kenis, G., Hof, P. R., et al. (2013). Consistent decrease in global DNA methylation and hydroxymethylation in the hippocampus of Alzheimer's disease patients. *Neurobiol. Aging* 34, 2091–2099. doi: 10.1016/j.neurobiolaging.2013.02.021

Chwang, W. B., Arthur, J. S., Schumacher, A., and Sweatt, J. D. (2007). The nuclear kinase mitogen-and stress-activated protein kinase 1 regulates hippocampal chromatin remodeling in memory formation. *J. Neurosci.* 27, 12732–12742. doi: 10.1523/jneurosci.2522-07.2007

Cosi, C., Colpaert, F., Koek, W., Degryse, A., and Marien, M. (1996). Poly(ADP-ribose) polymerase inhibitors protect against MPTP-induced depletions of striatal dopamine and cortical noradrenaline in C57B1/6 mice. *Brain Res.* 729, 264–269. doi: 10.1016/s0006-8993(96)00571-9

Critchley, M. (1984). And all the daughters of musick shall be brought low: language function in the elderly. *Arch. Neurol.* 41, 1135–1139. doi: 10.1001/archneur.1984.04050220029009

Cutler, R. G., and Mattson, M. P. (2006). Introduction: the adversities of aging. *Ageing Res. Rev.* 5, 221–238. doi: 10.1016/j.arr.2006.05.002

D'Angelo, M. A., Raices, M., Panowski, S. H., and Hetzer, M. W. (2009). Age-dependent deterioration of nuclear pore complexes causes a loss of nuclear integrity in postmitotic cells. *Cell* 136, 284–295. doi: 10.1016/j.cell.2008.11.037

De Boer, J., Andressoo, J. O., de Wit, J., Huijmans, J., Beems, R. B., van Steeg, H., et al. (2002). Premature aging in mice deficient in DNA repair and transcription. *Science* 296, 1276–1279. doi: 10.1126/science.1070174

De Bont, R., and van Larebeke, N. (2004). Endogenous DNA damage in humans: a review of quantitative data. *Mutagenesis* 19, 169–185. doi: 10.1093/mutage/geh025

Deak, M., Clifton, A. D., Lucocq, J. M., and Alessi, D. R. (1998). Mitogen-and stress-activated protein kinase-1 (MSK1) is directly activated by MAPK and SAPK2/p38, and may mediate activation of CREB. *EMBO J.* 17, 4426–4441. doi: 10.1093/emboj/17.15.4426

DeFedericis, H.-C., Patrzyc, H. B., Rajecki, M. J., Budzinski, E. E., Iijima, H., Dawidzik, J. B., et al. (2006). Singlet oxygen-induced DNA damage. *Radiat. Res.* 165, 445–451.

Degerman, S., Josefsson, M., Adolfsson, A. N., Wennstedt, S., Landfors, M., Haider, Z., et al. (2017). Maintained memory in aging is associated with young epigenetic age. *Neurobiol. Aging* 55, 167–171. doi: 10.1016/j.neurobiolaging.2017.02.009

Ditaranto, K., Tekirian, T. L., and Yang, A. J. (2001). Lysosomal membrane damage in soluble Aβ-mediated cell death in Alzheimer's disease. *Neurobiol. Dis.* 8, 19–31. doi: 10.1006/nbdi.2000.0364

Donato, A. J., Magerko, K. A., Lawson, B. R., Durrant, J. R., Lesniewski, L. A., and Seals, D. R. (2011). SIRT-1 and vascular endothelial dysfunction with ageing in mice and humans. *J. Physiol.* 589, 4545–4554. doi: 10.1113/jphysiol.2011.211219

Douki, T., and Cadet, J. (1996). Peroxynitrite mediated oxidation of purine bases of nucleosides and isolated DNA. *Free Radic. Res.* 24, 369–380. doi: 10.3109/10715769609088035

Dubey, H., Gulati, K., and Ray, A. (2017). Effects of Nitric Oxide (NO) modulators on cognitive function and brain oxidative stress in experimental model of Alzheimer's Disease in rats. *J. Pharmacol. Rep.* 2:126.

Duke, C. G., Kennedy, A. J., Gavin, C. F., Day, J. J., and Sweatt, J. D. (2017). Experience-dependent epigenomic reorganization in the hippocampus. *Learn. Mem.* 24, 278–288. doi: 10.1101/lm.045112.117

Eftekharzadeh, B., Daigle, J. G., Kapinos, L. E., Coyne, A., Schiantarelli, J., Carlomagno, Y., et al. (2018). Tau protein disrupts nucleocytoplasmic transport in Alzheimer's disease. *Neuron* 99, 925.e–940.e. doi: 10.1016/j.neuron.2018.07.039

Eichenbaum, H. (2001). The hippocampus and declarative memory: cognitive mechanisms and neural codes. *Behav. Brain Res.* 127, 199–207. doi: 10.1016/s0166-4328(01)00365-5

Elobeid, A., Libard, S., Leino, M., Popova, S. N., and Alafuzoff, I. (2016). Altered proteins in the aging brain. *J. Neuropathol. Exp. Neurol.* 75, 316–325. doi: 10.1093/jnen/nlw002

Evola, M., Hall, A., Wall, T., Young, A., and Grammas, P. (2010). Oxidative stress impairs learning and memory in apoE knockout mice. *Pharmacol. Biochem. Behav.* 96, 181–186. doi: 10.1016/j.pbb.2010.05.003

Fang, E. F., Lautrup, S., Hou, Y., Demarest, T. G., Croteau, D. L., Mattson, M. P., et al. (2017). NAD+ in aging: molecular mechanisms and translational implications. *Trends Mol. Med.* 23, 899–916. doi: 10.1016/j.molmed.2017.08.001

Fasolino, M., and Zhou, Z. (2017). The crucial role of DNA Methylation and MeCP2 in neuronal function. *Genes* 8:141. doi: 10.3390/genes8050141

Feng, J., Zhou, Y., Campbell, S. L., Le, T., Li, E., Sweatt, J. D., et al. (2010). Dnmt1 and Dnmt3a maintain DNA methylation and regulate synaptic function in adult forebrain neurons. *Nat. Neurosci.* 13, 423–430. doi: 10.1038/nn.2514

Foksinski, M., Rozalski, R., Guz, J., Ruszkowska, B., Sztukowska, P., Piwowarski, M., et al. (2004). Urinary excretion of DNA repair products correlates with metabolic rates as well as with maximum life spans of different mammalian species. *Free Radic. Biol. Med.* 37, 1449–1454. doi: 10.1016/j.freeradbiomed.2004.07.014

Forster, M. J., Dubey, A., Dawson, K. M., Stutts, W. A., Lal, H., and Sohal, R. S. (1996). Age-related losses of cognitive function and motor skills in mice are associated with oxidative protein damage in the brain. *Proc. Natl. Acad. Sci. U.S.A.* 93, 4765–4769. doi: 10.1073/pnas.93.10.4765

Fraga, C. G., Shigenaga, M. K., Park, J. W., Degan, P., and Ames, B. N. (1990). Oxidative damage to DNA during aging: 8-hydroxy-2'-deoxyguanosine in rat organ DNA and urine. *Proc. Natl. Acad. Sci. U.S.A.* 87, 4533–4537. doi: 10.1073/pnas.87.12.4533

Fukui, K., Onodera, K., Shinkai, T., Suzuki, S., and Urano, S. (2001). Impairment of learning and memory in rats caused by oxidative stress and aging, and changes in antioxidative defense systems. *Ann. N. Y. Acad. Sci.* 928, 168–175. doi: 10.1111/j.1749-6632.2001.tb05646.x

Furukawa, A., Tada-Oikawa, S., Kawanishi, S., and Oikawa, S. (2007). H2O2 accelerates cellular senescence by accumulation of acetylated p53 via decrease in the function of SIRT1 by NAD+ depletion. *Cell. Physiol. Biochem.* 20, 45–54.

Gallo, F. T., Katche, C., Morici, J. F., Medina, J. H., and Weisstaub, N. V. (2018). Immediate early genes, memory and psychiatric disorders: focus on c-Fos, Egr1 and Arc. *Front. Behav. Neurosci.* 12:79. doi: 10.3389/fnbeh.2018.00079

Gu, X., Sun, J., Li, S., Wu, X., and Li, L. (2013). Oxidative stress induces DNA demethylation and histone acetylation in SH-SY5Y cells: potential epigenetic mechanisms in gene transcription in Aβ production. *Neurobiol. Aging* 34, 1069–1079. doi: 10.1016/j.neurobiolaging.2012.10.013

Halliwell, B. (1992). Reactive oxygen species and the central nervous system. *J. Neurochem.* 59, 1609–1623. doi: 10.1111/j.1471-4159.1992.tb10990.x

Halliwell, B., and Gutteridge, J. M. C. (1985). *Free Radicals in Biology and Medicine*. Oxford: Clarendon Press.

Hamilton, M. L., Guo, Z., Fuller, C. D., Van Remmen, H., Ward, W. F., Austad, S. N., et al. (2001). A reliable assessment of 8-oxo-2-deoxyguanosine levels in nuclear and mitochondrial DNA using the sodium iodide method to isolate DNA. *Nucleic Acids Res.* 29, 2117–2126. doi: 10.1093/nar/29.10.2117

Harman, D. (1956). Aging: a theory based on free radical and radiation chemistry. *J. Gerontol.* 11, 298–300. doi: 10.1093/geronj/11.3.298

Harman, D. (1968). Free radical theory of aging: effect of free radical reaction inhibitors on the mortality rate of male LAF1 mice. *J. Gerontol.* 23, 476–482. doi: 10.1093/geronj/23.4.476

Hayashi, Y., Yoshida, M., Yamato, M., Ide, T., Wu, Z., Ochi-Shindou, M., et al. (2008). Reverse of age-dependent memory impairment and mitochondrial DNA damage in microglia by an overexpression of human mitochondrial

transcription factor a in mice. *J. Neurosci.* 28, 8624–8634. doi: 10.1523/JNEUROSCI.1957-08.2008

Hindle, J. V. (2010). Ageing, neurodegeneration and Parkinson's disease. *Age Ageing* 39, 156–161. doi: 10.1093/ageing/afp223

Hosseini, M., Pourganji, M., Khodabandehloo, F., Soukhtanloo, M., and Zabihi, H. (2012). Protective effect of l-arginine against oxidative damage as a possible mechanism of its Bene. cial properties on spatial learning in ovariectomized rats. *Basic Clin. Neurosci.* 3, 36–44.

Hu, D., Serrano, F., Oury, T. D., and Klann, E. (2006). Aging-dependent alterations in synaptic plasticity and memory in mice that overexpress extracellular superoxide dismutase. *J. Neurosci.* 26, 3933–3941. doi: 10.1523/JNEUROSCI.5566-05.2006

Jessop, P., and Toledo-Rodriguez, M. (2018). Hippocampal TET1 and TET2 expression and DNA hydroxymethylation are affected by physical exercise in aged mice. *Front. Cell Dev. Biol.* 6:45. doi: 10.3389/fcell.2018.00045

Jones, D. P. (2006). Redefining oxidative stress. *Antioxid. Redox Signal.* 8, 1865–1879. doi: 10.1089/ars.2006.8.1865

Kaas, G. A., Zhong, C., Eason, D. E., Ross, D. L., Vachhani, R. V., Ming, G., et al. (2013). TET1 Controls CNS 5-methylcytosine hydroxylation, Active DNA Demethylation, gene transcription, and memory formation. *Neuron* 79, 1086–1093. doi: 10.1016/j.neuron.2013.08.032

Kamsler, A., Avital, A., Greenberger, V., and Segal, M. (2007). Aged SOD overexpressing mice exhibit enhanced spatial memory while lacking *Hippocampal neurogenesis*. *Antioxid. Redox Signal.* 9, 181–189. doi: 10.1089/ars.2007.9.181

Keller, J. N., Schmitt, F. A., Scheff, S. W., Ding, Q., Chen, Q., Butterfield, D. A., et al. (2005). Evidence of increased oxidative damage in subjects with mild cognitive impairment. *Neurology* 64, 1152–1156. doi: 10.1212/01.WNL.0000156156.13641.BA

Kilgore, M., Miller, C. A., Fass, D. M., Hennig, K. M., Haggarty, S. J., Sweatt, J. D., et al. (2010). Inhibitors of class 1 histone deacetylases reverse contextual memory deficits in a mouse model of Alzheimer's disease. *Neuropsychopharmacology* 35, 870–880. doi: 10.1038/npp.2009.197

Kinugawa, K., Schumm, S., Pollina, M., Depre, M., Jungbluth, C., Doulazmi, M., et al. (2013). Aging-related episodic memory decline: are emotions the key? *Front. Behav. Neurosci.* 7:2. doi: 10.3389/fnbeh.2013.00002

Klungland, A., Rosewell, I., Hollenbach, S., Larsen, E., Daly, G., Epe, B., et al. (1999). Accumulation of premutagenic DNA lesions in mice defective in removal of oxidative base damage. *Proc. Natl. Acad. Sci. U.S.A.* 96, 13300–13305. doi: 10.1073/pnas.96.23.13300

Kolarow, R., Kuhlmann, C. R. W., Munsch, T., Zehendner, C., Brigadski, T., Luhmann, H. J., et al. (2014). BDNF-induced nitric oxide signals in cultured rat hippocampal neurons: time course, mechanism of generation, and effect on neurotrophin secretion. *Front. Cell. Neurosci.* 8:323. doi: 10.3389/fncel.2014.00323

Kotambail, A., Bhat, S., Jayaprakash, C., Fernandes, R., Varghese, V., and Satyamoorthy, K. (2017). Epigenetics and human diseases. *Hum. Genom. Appl.* 20, 73–100.

Kriaucionis, S., and Heintz, N. (2009). The nuclear DNA base 5-hydroxymethylcytosine is present in Purkinje neurons and the brain. *Science* 324, 929–930. doi: 10.1126/science.1169786

Leal, N. S., Dentoni, G., Schreiner, B., Kämäräinen, O.-P., Partanen, N., Herukka, S.-K., et al. (2018). Alterations in mitochondria-endoplasmic reticulum connectivity in human brain biopsies from idiopathic normal pressure hydrocephalus patients. *Acta Neuropathol. Commun.* 6:102. doi: 10.1186/s40478-018-0605-602

Levenson, J. M., O'Riordan, K. J., Brown, K. D., Trinh, M. A., Molfese, D. L., and Sweatt, J. D. (2004). Regulation of histone acetylation during memory formation in the hippocampus. *J. Biol. Chem.* 279, 40545–40559. doi: 10.1074/jbc.m402229200

Levine, B., Svoboda, E., Hay, J. F., Winocur, G., and Moscovitch, M. (2002). Aging and autobiographical memory: dissociating episodic from semantic retrieval. *Psychol. Aging* 17, 677–689. doi: 10.1037/0882-7974.17.4.677

Lewandowska, J., and Bartoszek, A. (2011). DNA methylation in cancer development, diagnosis and therapy—multiple opportunities for genotoxic agents to act as methylome disruptors or remediators. *Mutagenesis* 26, 475–487. doi: 10.1093/mutage/ger019

Lezak, M., Howieson, D., and Loring, D. (2012). *Neuropsychological Assessment*, 5th Edn, Oxford: Oxford University Press.

Lima-Cabello, E., Garcia-Guirado, F., Calvo-Medina, R., El Bekay, R., Perez-Costillas, L., Quintero-Navarro, C., et al. (2016). An abnormal nitric oxide metabolism contributes to brain oxidative stress in the mouse model for the fragile X syndrome, a possible role in intellectual disability. *Oxid. Med. Cell. Longev.* 2016:8548910. doi: 10.1155/2016/8548910

Lindahl, T. (1993). Instability and decay of the primary structure of DNA. *Nature* 362, 709–715. doi: 10.1038/362709a0

Lindahl, T., and Nyberg, B. (1972). Rate of depurination of native deoxyribonucleic acid. *Biochemistry* 11, 3610–3618. doi: 10.1021/bi00769a018

Linnarsson, S., Björklund, A., and Ernfors, P. (1997). Learning Deficit in BDNF Mutant Mice. *Eur. J. Neurosci.* 9, 2581–2587. doi: 10.1111/j.1460-9568.1997.tb01687.x

Liu, R., Liu, I. Y., Bi, X., Thompson, R. F., Doctrow, S. R., Malfroy, B., et al. (2003). Reversal of age-related learning deficits and brain oxidative stress in mice with superoxide dismutase/catalase mimetics. *Proc. Natl. Acad. Sci. U.S.A.* 100, 8526–8531. doi: 10.1073/pnas.1332809100

Love, S. (2006). Oxidative stress in brain ischemia. *Brain Pathol.* 9, 119–131. doi: 10.1111/j.1750-3639.1999.tb00214.x

Love, S., Barber, R., and Wilcock, G. K. (1999). Increased poly (ADP-ribosyl) ation of nuclear proteins in Alzheimer's disease. *Brain* 122, 247–253. doi: 10.1093/brain/122.2.247

Lubin, F. D., Roth, T. L., and Sweatt, J. D. (2008). Epigenetic regulation of BDNF gene transcription in the consolidation of fear memory. *J. Neurosci.* 28, 10576–10586. doi: 10.1523/JNEUROSCI.1786-08.2008

Manczak, M., Anekonda, T. S., Henson, E., Park, B. S., Quinn, J., and Reddy, P. H. (2006). Mitochondria are a direct site of Aβ accumulation in Alzheimer's disease neurons: implications for free radical generation and oxidative damage in disease progression. *Hum. Mol. Genet.* 15, 1437–1449. doi: 10.1093/hmg/ddl066

Martins, I. (2017a). Antimicrobial activity inactivation and toxic immune reactions induce Epilepsy in humans. *J. Med. Discov.* 2:jmd17040. doi: 10.24262/jmd.2.4.17040

Martins, I. (2017b). Single gene inactivation with implications to diabetes and multiple organ dysfunction syndrome. *J. Clin. Epigenetics* 03, 1–8. doi: 10.21767/2472-1158.100058

Martins, I. J. (2017c). Nutrition therapy regulates caffeine metabolism with relevance to NAFLD and induction of type 3 diabetes. *J. Diabetes Metab. Disord.* 4, 1–9. doi: 10.24966/dmd-201x/100019

Massudi, H., Grant, R., Braidy, N., Guest, J., Farnsworth, B., and Guillemin, G. J. (2012a). Age-associated changes in oxidative stress and NAD+ metabolism in human tissue. *PLoS One* 7:e42357. doi: 10.1371/journal.pone.0042357

Massudi, H., Grant, R., Guillemin, G. J., and Braidy, N. (2012b). NAD+ metabolism and oxidative stress: the golden nucleotide on a crown of thorns. *Redox Rep.* 17, 28–46. doi: 10.1179/1351000212Y.0000000001

Mecocci, P., Boccardi, V., Cecchetti, R., Bastiani, P., Scamosci, M., Ruggiero, C., et al. (2018). A long journey into aging, brain aging, and Alzheimer's Disease following the oxidative stress tracks. *J. Alzheimer Dis.* 62, 1319–1335. doi: 10.3233/JAD-170732

Mecocci, P., MacGarvey, U., and Beal, M. F. (1994). Oxidative damage to mitochondrial DNA is increased in Alzheimer's disease. *Ann. Neurol. Off. J. Am. Neurol. Assoc. Child Neurol. Soc.* 36, 747–751. doi: 10.1152/ajpendo.00387.2010

Mecocci, P., MacGarvey, U., Kaufman, A. E., Koontz, D., Shoffner, J. M., Wallace, D. C., et al. (1993). Oxidative damage to mitochondrial DNA shows marked age-dependent increases in human brain. *Ann. Neurol. Off. J. Am. Neurol. Assoc. Child Neurol. Soc.* 34, 609–616. doi: 10.1002/ana.410340416

Miller, C. A., Gavin, C. F., White, J. A., Parrish, R. R., Honasoge, A., Yancey, C. R., et al. (2010). Cortical DNA methylation maintains remote memory. *Nat. Neurosci.* 13, 664–666. doi: 10.1038/nn.2560

Miller, C. A., and Sweatt, J. D. (2007). Covalent modification of DNA regulates memory formation. *Neuron* 53, 857–869. doi: 10.1016/j.neuron.2007.02.022

Milne, J. C., and Denu, J. M. (2008). The Sirtuin family: therapeutic targets to treat diseases of aging. *Curr. Opin. Chem. Biol.* 12, 11–17. doi: 10.1016/j.cbpa.2008.01.019

Misiaszek, R., Crean, C., Joffe, A., Geacintov, N. E., and Shafirovich, V. (2004). Oxidative DNA damage associated with combination of guanine and

superoxide radicals and repair mechanisms via radical trapping. *J. Biol. Chem.* 279, 32106–32115. doi: 10.1074/jbc.m313904200

Mitchell, S. J., Scheibye-Knudsen, M., Longo, D. L., and de Cabo, R. (2015). Animal models of aging research: implications for human aging and age-related diseases. *Annu. Rev. Anim. Biosci.* 3, 283–303. doi: 10.1146/annurev-animal-022114-110829

Mockett, R. J., Sohal, B. H., and Sohal, R. S. (2010). Expression of multiple copies of mitochondrially targeted catalase or genomic Mn superoxide dismutase transgenes does not extend the life span of Drosophila melanogaster. *Free Radic. Biol. Med.* 49, 2028–2031. doi: 10.1016/j.freeradbiomed.2010.09.029

Murman, D. L. (2015). The impact of age on cognition. *Semin. Hear.* 36, 111–121. doi: 10.1055/s-0035-1555115

Nagai, T., Yamada, K., Kim, H.-C., Kim, Y.-S., Noda, Y., Imura, A., et al. (2002). Cognition impairment in the genetic model of aging klotho gene mutant mice: a role of oxidative stress. *FASEB J.* 17, 50–52. doi: 10.1096/fj.02-0448fje

Navarro, A., Sánchez Del Pino, M. J., Gómez, C., Peralta, J. L., and Boveris, A. (2002). Behavioral dysfunction, brain oxidative stress, and impaired mitochondrial electron transfer in aging mice. *Am. J. Physiol. Integr. Comp. Physiol.* 282, R985–R992. doi: 10.1152/ajpregu.00537.2001

Nieuwenhuis, I. L. C., and Takashima, A. (2011). The role of the ventromedial prefrontal cortex in memory consolidation. *Behav. Brain Res.* 218, 325–334. doi: 10.1016/j.bbr.2010.12.009

O'Donnell, E., and Lynch, M. A. (1998). Dietary antioxidant supplementation reverses age-related neuronal changes. *Neurobiol. Aging* 19, 461–467. doi: 10.1016/s0197-4580(98)00082-7

Oswald, M. C. W., Garnham, N., Sweeney, S. T., and Landgraf, M. (2018). Regulation of neuronal development and function by ROS. *FEBS Lett.* 592, 679–691. doi: 10.1002/1873-3468.12972

Padurariu, M., Ciobica, A., Hritcu, L., Stoica, B., Bild, W., and Stefanescu, C. (2010). Changes of some oxidative stress markers in the serum of patients with mild cognitive impairment and Alzheimer's disease. *Neurosci. Lett.* 469, 6–10. doi: 10.1016/j.neulet.2009.11.033

Papp, G., Witter, M. P., and Treves, A. (2007). The CA3 network as a memory store for spatial representations. *Learn. Mem.* 14, 732–744. doi: 10.1101/lm.687407

Paul, V., and Ekambaram, P. (2011). Involvement of nitric oxide in learning & memory processes. *Indian J. Med. Res.* 133, 471–478.

Paul, V., Reddy, L., and Ekambaram, P. (2005). A reversal by L-arginine and sodium nitroprusside of ageing-induced memory impairment in rats by increasing nitric oxide concentration in the hippocampus. *Indian J. Physiol. Pharmacol.* 49:179.

Peleg, S., Sananbenesi, F., Zovoilis, A., Burkhardt, S., Bahari-Javan, S., Agis-Balboa, R. C., et al. (2010). Altered histone acetylation is associated with age-dependent memory impairment in mice. *Science* 328, 753–756. doi: 10.1126/science.1186088

Penner, M. R., Roth, T. L., Barnes, C. A., and Sweatt, J. D. (2010). An epigenetic hypothesis of aging-related cognitive dysfunction. *Front. Aging Neurosci.* 2:9. doi: 10.3389/fnagi.2010.00009

Peters, R. (2006). Ageing and the brain. *Postgrad. Med. J.* 82, 84–88.

Radi, R. (2013). Peroxynitrite, a stealthy biological oxidant. *J. Biol. Chem.* 288, 26464–26472. doi: 10.1074/jbc.R113.472936

Raff, M. C., Whitmore, A. V., and Finn, J. T. (2002). Axonal self-destruction and neurodegeneration. *Science* 296, 868–871. doi: 10.1126/science.1068613

Reckelhoff, J. F., Kellum, J. A., Blanchard, E. J., Bacon, E. E., Wesley, A. J., and Kruckeberg, W. C. (1994). Changes in nitric oxide precursor, L-arginine, and metabolites, nitrate and nitrite, with aging. *Life Sci.* 55, 1895–1902. doi: 10.1016/0024-3205(94)00521-4

Reddy, P. (2006). Mitochondrial oxidative damage in aging and Alzheimer's disease: implications for mitochondrially targeted antioxidant therapeutics. *J. Biomed. Biotechnol.* 2006:31372. doi: 10.1155/JBB/2006/31372

Reynolds, E. H. (2002). Folic acid, ageing, depression, and dementia. *BMJ* 324, 1512–1515. doi: 10.1136/bmj.324.7352.1512

Richter, C., Park, J. W., and Ames, B. N. (1988). Normal oxidative damage to mitochondrial and nuclear DNA is extensive. *Proc. Natl. Acad. Sci. U.S.A.* 85, 6465–6467. doi: 10.1073/pnas.85.17.6465

Robins Wahlin, T.-B., Wahlin, A., Winblad, B., and Bäckman, L. (2001). The influence of serum vitamin B12 and folate status on cognitive functioning in very old age. *Biol. Psychol.* 56, 247–265. doi: 10.1016/s0301-0511(01)00079-5

Rosi, S., Ramirez-Amaya, V., Vazdarjanova, A., Worley, P. F., Barnes, C. A., and Wenk, G. L. (2005). Neuroinflammation alters the hippocampal pattern of behaviorally induced Arc expression. *J. Neurosci.* 25, 723–731. doi: 10.1523/JNEUROSCI.4469-04.2005

Rowe, W. B., Blalock, E. M., Chen, K.-C., Kadish, I., Wang, D., Barrett, J. E., et al. (2007). Hippocampal expression analyses reveal selective association of immediate-early, neuroenergetic, and myelinogenic pathways with cognitive impairment in aged rats. *J. Neurosci.* 27, 3098–3110. doi: 10.1523/JNEUROSCI.4163-06.2007

Santulli, G., Borras, C., Bousquet, J., Calzà, L., Cano, A., Illario, M., et al. (2015). Models for preclinical studies in aging-related disorders: one is not for all. *Transl. Med.* 13, 4–12.

Serrano, F., and Klann, E. (2004). Reactive oxygen species and synaptic plasticity in the aging hippocampus. *Ageing Res. Rev.* 3, 431–443. doi: 10.1016/j.arr.2004.05.002

Socco, S., Bovee, R. C., Palczewski, M. B., Hickok, J. R., and Thomas, D. D. (2017). Epigenetics: The third pillar of nitric oxide signaling. *Pharmacol. Res.* 121, 52–58. doi: 10.1016/j.phrs.2017.04.011

Sohal, R. S., and Brunk, U. T. (1992). Mitochondrial production of pro-oxidants and cellular senescence. *Mutat. Res.* 275, 295–304. doi: 10.1016/0921-8734(92)90033-l

Sohal, R. S., Ku, H.-H., Agarwal, S., Forster, M. J., and Lal, H. (1994). Oxidative damage, mitochondrial oxidant generation and antioxidant defenses during aging and in response to food restriction in the mouse. *Mech. Ageing Dev.* 74, 121–133. doi: 10.1016/0047-6374(94)90104-x

Soloaga, A., Thomson, S., Wiggin, G. R., Rampersaud, N., Dyson, M. H., Hazzalin, C. A., et al. (2003). MSK2 and MSK1 mediate the mitogen-and stress-induced phosphorylation of histone H3 and HMG-14. *EMBO J.* 22, 2788–2797. doi: 10.1093/emboj/cdg273

Stahl, S. M. (2010). Methylated spirits: epigenetic hypotheses of psychiatric disorders. *CNS Spectr.* 15, 220–230. doi: 10.1017/S1092852900000055

Steenken, S. (1989). Purine bases, nucleosides, and nucleotides: aqueous solution redox chemistry and transformation reactions of their radical cations and e-and OH adducts. *Chem. Rev.* 89, 503–520. doi: 10.1021/cr00093a003

Sternberg, R. J., and Sternberg, K. (2011). *Cognitive Psychology*, 6th Edn, California: California State University.

Sullivan, P. G., Dragicevic, N. B., Deng, J.-H., Bai, Y., Dimayuga, E., Ding, Q., et al. (2004). Proteasome inhibition alters neural mitochondrial homeostasis and mitochondria turnover. *J. Biol. Chem.* 279, 20699–20707. doi: 10.1074/jbc.m313579200

Sung, Y. M., Lee, T., Yoon, H., DiBattista, A. M., Song, J. M., Sohn, Y., et al. (2013). Mercaptoacetamide-based class II HDAC inhibitor lowers Aβ levels and improves learning and memory in a mouse model of Alzheimer's disease. *Exp. Neurol.* 239, 192–201. doi: 10.1016/j.expneurol.2012.10.005

Swerdlow, R. H., and Khan, S. M. (2004). A "mitochondrial cascade hypothesis" for sporadic Alzheimer's disease. *Med. Hypotheses* 63, 8–20. doi: 10.1016/j.mehy.2003.12.045

Tahiliani, M., Koh, K. P., Shen, Y., Pastor, W. A., Bandukwala, H., Brudno, Y., et al. (2009). Conversion of 5-methylcytosine to 5-hydroxymethylcytosine in mammalian DNA by MLL partner TET1. *Science* 324, 930–935. doi: 10.1126/science.1170116

Talamini, L. M., and Gorree, E. (2012). Aging memories: differential decay of episodic memory components. *Learn. Mem.* 19, 239–246. doi: 10.1101/lm.024281.111

Talarowska, M., Gałecki, P., Maes, M., Orzechowska, A., Chamielec, M., Bartosz, G., et al. (2012). Nitric oxide plasma concentration associated with cognitive impairment in patients with recurrent depressive disorder. *Neurosci. Lett.* 510, 127–131. doi: 10.1016/j.neulet.2012.01.018

Twiss, K. C. (2007). *We Are What We Eat. The Archaeology of Food and Identity*. Illinois: Southern Illinois University.

Uddin, M. S., Stachowiak, A., Mamun, A., Al Tzvetkov, N. T., Takeda, S., Atanasov, A. G., et al. (2018). Autophagy and Alzheimer's Disease: from molecular mechanisms to therapeutic implications. *Front. Aging Neurosci.* 10:4. doi: 10.3389/fnagi.2018.00004

United Nations (2019). *World Population Prospects 2019: Highlights (ST/ESA/SER.A/423)*. New York, NY: United Nations.

Vauzour, D., Camprubi-Robles, M., Miquel-Kergoat, S., Andres-Lacueva, C., Bánáti, D., Barberger-Gateau, P., et al. (2017). Nutrition for the ageing brain: towards evidence for an optimal diet. *Ageing Res. Rev.* 35, 222–240. doi: 10.1016/j.arr.2016.09.010

Vecsey, C. G., Hawk, J. D., Lattal, K. M., Stein, J. M., Fabian, S. A., Attner, M. A., et al. (2007). Histone deacetylase inhibitors enhance memory and synaptic plasticity via CREB:CBP-dependent transcriptional activation. *J. Neurosci.* 27, 6128–6140. doi: 10.1523/JNEUROSCI.0296-07.2007

Vogel, H., Lim, D.-S., Karsenty, G., Finegold, M., and Hasty, P. (1999). Deletion of Ku86 causes early onset of senescence in mice. *Proc. Natl. Acad. Sci. U.S.A.* 96, 10770–10775. doi: 10.1073/pnas.96.19.10770

Wallace, D. C. (2012). Mitochondria and cancer. *Nat. Rev. Cancer* 12, 685–698. doi: 10.1038/nrc3365

Zatloukal, K., Stumptner, C., Fuchsbichler, A., Heid, H., Schnoelzer, M., Kenner, L., et al. (2002). p62 Is a common component of cytoplasmic inclusions in protein aggregation diseases. *Am. J. Pathol.* 160, 255–263. doi: 10.1016/s0002-9440(10)64369-6

Zhou, X., Zhuang, Z., Wang, W., He, L., Wu, H., Cao, Y., et al. (2016). OGG1 is essential in oxidative stress induced DNA demethylation. *Cell. Signal.* 28, 1163–1171. doi: 10.1016/j.cellsig.2016.05.021

Zuo, S., Boorstein, R. J., and Teebor, G. W. (1995). Oxidative damage to 5-methylcytosine in DNA. *Nucleic Acids Res.* 23, 3239–3243. doi: 10.1093/nar/23.16.3239

Conflict of Interest: The authors declare that the research was conducted in the absence of any commercial or financial relationships that could be construed as a potential conflict of interest.

frontiers in Neuroscience

ORIGINAL RESEARCH
published: 19 March 2020
doi: 10.3389/fnins.2020.00241

Fisetin Prevents HT22 Cells From High Glucose-Induced Neurotoxicity *via* PI3K/Akt/CREB Signaling Pathway

Shenshen Zhang[1,2], Ran Xue[1,2], Yaping Geng[1,2], Hao Wang[1,2] and Wenjie Li[2]*

[1] Precision Nutrition Innovation Center, College of Public Health, Zhengzhou University, Zhengzhou, China, [2] Department of Nutrition and Food Hygiene, College of Public Health, Zhengzhou University, Zhengzhou, China

Hyperglycemia has been widely considered as a key risk factor for diabetic encephalopathy which can cause neuronal apoptosis and cognitive deficits. The flavonoid compound, fisetin, possesses potential neuroprotective effects and also enhances learning and memory. However, the role of fisetin in hyperglycemia-induced neuronal cytotoxicity has not been fully elucidated. In the present study, HT22 murine hippocampal neuronal cell line was used to establish the injured cell model. Cell proliferation and cytotoxicity assay, Hoechst 33258 staining, qRT-PCR, western blot analysis, and specific inhibitor were used to investigate the effect and molecular mechanisms of fisetin on high glucose (HG)-induced neurotoxicity in HT22 cells. Our results showed that 125 μM and 48 h of treatment was identified as optimal damage parameter of HG. Fisetin significantly improved HG-inhibited cell viability. The levels of LDH, malondialdehyde (MDA), and superoxide dismutase (SOD) were noticeably modulated by fisetin, which alleviated HG-induced HT22 cell oxidative damage. Besides, the apoptosis of HT22 cells was rescued by fisetin pretreatment. In addition, fisetin also prevented HG-induced downregulation of the mRNA expression of *Bdnf*, *Gdnf*, synaptophysin (*Syp*), and glutamate ionotropic receptor AMPA type subunit 1 (*Gria1*) in cells. More importantly, the decreased phosphorylation of phosphoinositide 3 kinase (PI3K), Akt, and cAMP-response element binding protein (CREB) was rescued by fisetin treatment and that neuroprotective effect of fisetin was partially blocked by PI3K inhibitor, LY294002. These findings indicate that fisetin has potent neuroprotective effect and prevents HG-induced neurotoxicity by activation of PI3K/Akt/CREB pathway.

Keywords: fisetin, HT22 cell, high glucose, neurotoxicity, neuroprotection

OPEN ACCESS

Edited by:
Touqeer Ahmed, National University of Sciences and Technology, Pakistan

Reviewed by:
Sun Young Park, Pusan National University, South Korea
Dong-Sung Lee, Chosun University, South Korea

****Correspondence:***
Shenshen Zhang
zsslb2005@163.com

Specialty section:
This article was submitted to Neuropharmacology, a section of the journal Frontiers in Neuroscience

Received: *30 October 2019*
Accepted: *03 March 2020*
Published: *19 March 2020*

Citation:
Zhang S, Xue R, Geng Y, Wang H and Li W (2020) Fisetin Prevents HT22 Cells From High Glucose-Induced Neurotoxicity via PI3K/Akt/CREB Signaling Pathway. Front. Neurosci. 14:241. doi: 10.3389/fnins.2020.00241

INTRODUCTION

Diabetic encephalopathy is one of the most common crippling complications resulting from diabetes mellitus (DM) affecting central nervous system (Zenker et al., 2013; Simo et al., 2017). Accumulated evidences have demonstrated that DM patients have a significantly higher risk of suffering from cognitive dysfunction (Biessels et al., 2006; Biessels and Despa, 2018).

Abbreviations: Akt, protein kinase B; BBB, blood–brain barrier; BDNF, brain derived neurotrophic factor; CREB, cAMP-response element binding protein; GDNF, glial cell line-derived neurotrophic factor; GluR1, glutamate receptor 1; Gria1, glutamate ionotropic receptor AMPA type subunit 1; HG, high glucose; PI3K, phosphoinositide 3 kinase; SYP, synaptophysin.

Thus, the importance of diabetic encephalopathy is increasingly being recognized. Currently, loads of researches focus on searching for safe and effective agents to prevent the loss of cognitive function for DM patients.

Several prospective studies have shown that high blood glucose level is a key risk factor in DM-induced cognitive dysfunction and dementia (Kaeidi et al., 2019; Zhang et al., 2019; Sharma et al., 2020). The neuronal glucose level in the central nervous system can be induced up to four-fold increase by hyperglycemia in diabetes (Zhu et al., 2018). The abnormal intracellular glucose metabolism possesses multiple toxic effects on brain, such as formation of advanced glycated end products (AGEs), generation of ROS, and activation of polyol, diacylglycerol, and hexosamine pathways, leading to cognitive dysfunction (Seto et al., 2015). Nonetheless, no specific means is able to protect against the neurotoxicity of hyperglycemia. It is noteworthy that the cellular senescence and apoptosis is a crucial neurotoxicity induced by hyperglycemia (Arunachalam et al., 2014). Thus, therapeutically targeting hyperglycemia-induced damage of nerve cells and explicit the molecular mechanism would be a novel strategy for treating diabetic neuropathy.

The CREB is a transcription regulatory and abundant in brain, particular in neurons. The activation of CREB pathway is closely correlated with the number of surviving neurons, which play important roles in learning and memory in brain (Caracciolo et al., 2018). CREB can also regulate various targeting molecular, including the BDNF, which is essential for neuronal development and survival, synaptic plasticity, and cognitive function (Feng et al., 2019). In neuronal cells, the activation of CREB can be stimulated by the phosphorylation of the upstream PI3K and its effector Akt. Zhang W. et al. (2018) addressed that administration of diterpene ginkgolides could protect against cerebral ischemia/reperfusion damage in rats by upregulating the activation of CREB and Nrf2 through PI3K/Akt signaling pathway. Pretreatment of SH-SY5Y cells with rifampicin remarkably enhanced the phosphorylation of PI3K, Akt, and CREB, exhibiting neuroprotective effects against rotenone-induced apoptosis (Wu et al., 2018). Insulin resistance-induced hyperglycemia downregulated the Akt/CREB signaling pathway caused the obstacle of neuronal pathology in hippocampus neurons and cognitive deficits (Xiang et al., 2015). It should be noted that PI3K/Akt/CREB signaling would be a promising target pathway for treatment of diabetic neuropathies in brain.

Diabetes mellitus-induced cognitive dysfunction is a great problem for public health. Despite the therapeutic benefits of antidiabetic agents for the treatment of DM-induced cognitive dysfunction, most of these pharmaceutical agents are associated with various undesirable side-effects (Meneses et al., 2015). Recently, medicinal natural extracts appear to offer effective effects in improving DM-related complications with minimal toxicity and side-effects. Fisetin (3,3′,4′,7-tetrahydroxy flavone), a ubiquitous flavonoid, widely exists in strawberries, grape seed, apple, onion, and persimmon (Ma et al., 2018). The chemical structural formula is shown in **Figure 1**. It has been reported that fisetin possesses neuroprotection potentials, antioxidant, antitumor, anti-inflammation by affecting multiple molecular and signaling pathways (Nabavi et al., 2016; Zhang et al., 2016). Furthermore, fisetin exhibits high brain uptake potential. Krasieva et al. (2015) observed that fisetin can be rapidly detected in the nucleoli of HT22 cells during incubation and in the brain of mice after oral and ip administration. Maher (2009) also found that fisetin exhibits high brain uptake potential. Fisetin can reduce cognitive deficits in old SAMP8 mice while improving impaired synaptic function, age-associated stress, and inflammation (Currais et al., 2018). However, the effect of fisetin on hyperglycemia-induced neurotoxicity has not been fully addressed. In the present study, we investigated the neuroprotective effect of fisetin on HG-induced cell apoptosis in HT22 cells, and whether fisetin protected HT22 cells against HG-induced neurotoxicity *via* PI3K/Akt/CREB signaling pathway would be studied.

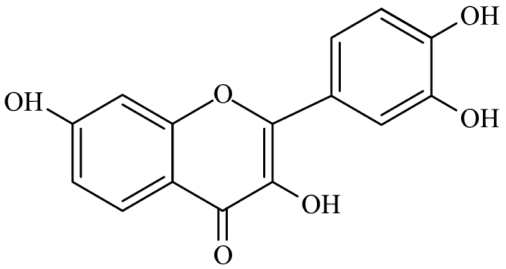

FIGURE 1 | The chemical structural formula of fisetin.

MATERIALS AND METHODS

Reagents

Fisetin, glucose and dimethyl sulfoxide (DMSO) were obtained from Sigma–Aldrich (St. Louis, MO, United States). Fisetin (the purity is > 98%) was dissolved in < 0.1% of DMSO solution. LY294002 (the specific inhibitor of PI3K) was bought from MedChemExpress (Shanghai, China). Cell counting kit-8 (CCK-8) was purchased from Dojindo China Co., Ltd. (Shanghai, China). LDH cytotoxicity assay kit, lipid peroxidation [malondialdehyde (MDA)] assay kit, superoxide dismutase (SOD) assay kit, and Hoechst 33258 were obtained from Beyotime (Shanghai, China). Dulbecco's modified eagle's medium (DMEM) and phosphate-buffered saline (PBS) were purchased from Biological Industries (Shanghai, China). Fetal bovine serum (FBS) was purchased from Gibco (Grand Island, NY, United States). Antibody against PI3K (#4257), Phospho-PI3Kp85/p55 (#4228), Akt (#4691), Phospho-Akt (#4060), CREB (#4820), and p-CREB (#9198) were obtained from Cell Signaling Technology (Beverly, MA, United States). Antibody against β-actin was purchase from Absin (Shanghai, China).

Cell Culture

HT22 cells, a mouse hippocampal neuronal cell line, were a gift offered by prof. Deng (Medical School, Hunan University of Chinese Medicine). Optimal growth and survival rate of HT22 cells require 25 mM basal glucose (Fan et al., 2016). Hence, cells were cultivated in HG DMEM medium supplemented with

10% FBS, 100 U/mL penicillin, and 100 mg/mL streptomycin (Solarbio, Beijing, China) in a humidified incubator (5% CO_2, 37°C).

Cell Viability Assay

The cell viability of HT22 cells was determined using the CCK-8 assay. Briefly, cells were seeded into 96-well plates at a density of 1×10^4/well for 12 h. After treatment with HG (25–175 mM) or fisetin (0–20 μM) for indicated time, CCK-8 solution was added to each well and incubated for another 2 h in the incubator. Mannitol was osmotic pressure control group. Then, absorbance was measured using a microplate reader (Molecular Devices, San Jose, CA, United States). Cell viability was expressed as the percentage of Abs 570 nm of vehicle control.

Detection of Superoxide Dismutase (SOD) Activity, Malondialdehyde (MDA) Content, and LDH Leakage Rate

After treatment, HT22 cells were lyzed with lysis buffer (Beyotime Biotechnology, Jiangsu, China) after which SOD activity, MDA content, and LDH leakage rate were detected according to the manufacturer's instruction and normalized to the total protein content, respectively.

Hoechst 33258 Staining Assay

To observe the morphological changes in the nuclear chromatin of HT22 cells, the chromatin-specific dye Hoechst 33258 staining was used to stain the nuclei. Cells were seeded in six-well plates at a density of 1×10^5 cells/well and then treated with HG in the presence or absence of fisetin for 48 h. Subsequently, the culture medium was removed, washed thrice with PBS, and then fixed with 4% paraformaldehyde for 20 min. After washed three times with PBS, cells were stained with 50 μg/mL Hoechst 33258 solution for 15 min in the dark. Finally, HT22 cells were observed and photographed using the fluorescence microscope (Nikon, Tokyo, Japan). The apoptosis rate of HT22 cells was quantified by the ratio of cells with fragmented and densely stained nuclei to all cells.

Quantitative Real-Time PCR (qPCR)

HT22 cells treated with HG in the presence or absence of fisetin were harvested for qPCR. Total RNA was purified from HT22 cells using Trizol reagent (Pufei Biotechnology, Shanghai, China). Total cDNA synthesis was performed using PrimeScript™ RT Master Mix (Takara, Dalian, China) according to the manufacturer's instructions. QPCR was performed to detect transcript levels of *Bdnf*, *Gdnf*, *Syp*, and *Gria1* using the One Step TB Green™ PrimeScript™ RT-PCR Kit (Takara, Dalian, China). Primer sequences are as follows (**Table 1**).

TABLE 1 | Primers sequences used for quantitative PCR.

Gene	Primers
Bdnf	Forward-5′ CGGCCCAACGAAGAAAACCATAA3′, Reverse-5′ GGCGCCGAACCCTCATAGACAT3′
Gdnf	Forward-5′ GATATTGCAGCGGTTCCTG3′, Reverse-5′ CCTGGCCTACTTTGTCACTTG3′
Gria1	Forward-5′ATGTGGAAGCAAGGACTCCG3′, Reverse-5′ CCACATTGCTCAGGCTCAGA3′
Syp	Forward-5′TGTGCCAACAAGACGGAGAG3′, Reverse-5′TTTAACGCAGGAGGGTGCAT3′

Western Blotting

HT22 cells were collected and total cell lysates were prepared using Phosphorylated Protein Extraction Kit (KeyGen Biotech, Nanjing, China). Equal amounts of protein extracts were mixed (5:1) with loading buffer for electrophoresis in acylamide SDS gels. After electrophoresis, samples were transferred onto polyvinylidene fluoride membrane (Millipore, MA, United States). The proteins were exposed to the specific primary antibodies against the target protein. Cross-reactivity was observed using species-specific secondary antibodies labeled with horseradish peroxidase (HRP) and ECL Plus kit in gel imaging analysis system (Biorad, CA, United States). The quantitative analysis of each bolt was carried out by Quantity One 1-D analysis software (Biorad, CA, United States).

Statistical Analysis

Statistical analyses were carried out with GraphPad Prism software, version 6.0. All data were presented as the means ± SEM. Differences between the groups were tested by one-way analysis of variance (ANOVA) followed by Student's test. $P < 0.05$ was considered statistically significant.

RESULTS

Effect of Fisetin or HG on HT22 Cells Viability

HT22 cells were treated with a serial concentrations of fisetin (0–25 μM) for 48 h; 25 μM of fisetin reduced cell viability to 78.64 ± 0.48% of that in the control group. At the concentration of below 20 μM (cell viability ≥ 90.05 ± 5.89%), there was no significant difference between fisetin treatment group and control ($P > 0.05$) (**Figure 2A**). Therefore, lower concentration (0–20 μM) of fisetin was used which was safe and had no influence on the survival of HT22 cells; 25–175 mM of HG (DMEM with HG containing 25 mM glucose) treated HT22 cell for 24 or 48 h, respectively. Mannitol (150 mM) was osmotic pressure control group. The results showed that cell viability was remarkably decreased with the increasing concentration of fisetin at 48 h. Glucose at 125 and 150 mM decreased cell viability to 51.33 ± 2.73 and 49.07 ± 3.41% ($P < 0.001$), respectively (**Figure 2B**). Thus, 125 mM of HG was a sub-toxic concentration to construct HT22 cell damage model in the subsequent experiments.

Effects of Fisetin on HG-Induced Cytotoxicity in HT22 Cells

To determine whether fisetin could protect neurons from HG injury, HT22 cells were pretreated with fisetin (0–25 μM) for 1 h followed by indicated concentration of HG (125 mM) for 48 h. As shown in **Figure 3A**, treatment with HG significant inhibited HT22 cells proliferation (51.08 ± 3.74%), while treatment with

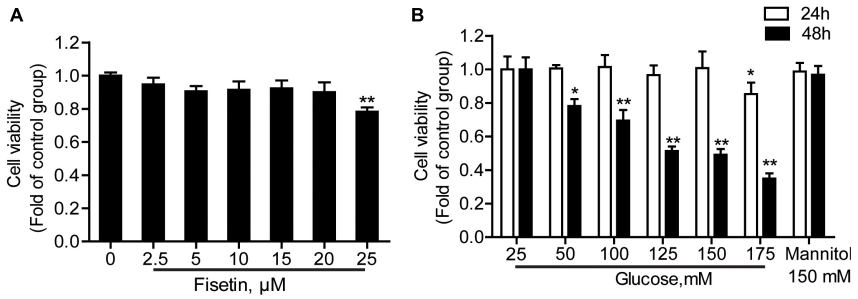

FIGURE 2 | Effect of different concentrations of fisetin or glucoseon HT22 cell viability. **(A)** HT22 cells were incubated with fisetin at different concentrations (2.5, 5, 10,15, 20, 25 μM) for 48 h. **(B)** CCK-8 assay for cell viability in HT22 cells treated with different concentrations of glucose (25, 50, 100, 125, 150, 175 mM). The data are presented as the mean ± SEM, $n = 4$; *$P < 0.05$, **$P < 0.01$ *vs.* the 25 mM glucose (control) group.

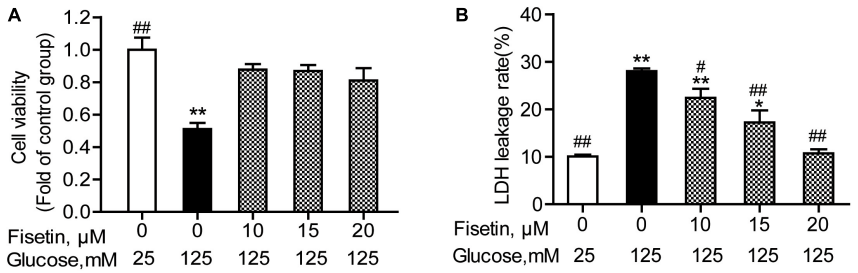

FIGURE 3 | Effect of fisetin on high glucose (HG)-induced neurotoxicity in HT22 cells. HT22 cells were pretreated with fisetin (10, 15, 20 μM) or vehicle control for 1 h followed by high glucose (125 mM) for 48 h **(A)** cell viability is shown in OD value. **(B)** The LDH leakage rate of HT22 cells after treatment with indicated concentration of fisetin and HG. Data were expressed as mean ± SEM of four independent experiments. *$P < 0.05$, **$P < 0.01$ *vs.* the 25 mM glucose (control) group; #$P < 0.05$, ##$P < 0.01$ *vs.* 125 mM glucose (HG) group.

fisetin strikingly increased cell viability and almost make it recover to the normal level.

The LDH leakage rate was elevated after HG stimulation, and treatment with 125 mM of HG alone increased the LDH leakage rate to 28.04 ± 1.03% ($P < 0.001$), compared to control group. Pretreatment with fisetin, the LDH leakage rate was rescued to base line at 20 μM fisetin (10.7 ± 1.02%, $P < 0.001$) compared to the HG-treated group (**Figure 3B**). All these results strongly suggested that fisetin could protect HT22 cells from HG-induced cytotoxicity.

Effect of Fisetin on HG-Induced Oxidative State in HT22 Cells

The antioxidant activity of fisetin was evaluated, including SOD activity and MDA content. As expected, the results showed that compared with the vehicle control, HG treatment alone significantly inhibited SOD activity to 9.43 ± 0.25 U/mg prot ($P < 0.001$), but increased MDA content to 8.28 ± 0.96 mmol/mg prot ($P = 0.005$) (**Figure 4**). Whereas fisetin pretreatment dramatically reversed this trend, the SOD activity of 20 μM fisetin was 14.65 ± 0.30 U/mg prot, obviously higher than HG-alone treated group ($P < 0.001$). The MDA contents of fisetin (10, 15, 20 μM) pretreated groups were dramatically suppressed compared with HG group ($P = 0.016$, 0.003, 0.005, respectively). These results showed that pretreatment with fisetin protected HT22 cells against HG-induced cell oxidative damage.

Fisetin Protects Against HG-Induced HT22 Cells Apoptosis

Hoechst 33258 staining was used to quantify the levels of apoptosis in each group. As shown in **Figure 5**, the control group cell apoptosis rate is 2.55 ± 0.45%. HG treatment alone significantly promoted HT22 cells apoptosis (18.28 ± 0.34%) compared to the control group ($P < 0.001$). As expected, pretreatment with fisetin effectively attenuated the apoptosis induced by HG in HT22 cells. Compared with HG group, the cell apoptotic rate was significantly decreased to 2.92 ± 0.49% at 20 μM of fisetin ($P < 0.001$).

Changes in HG-Induced Gene Expression by Fisetin Treatment

To elucidate the neuroprotective effect of fisetin against HG, we explored the expressions of several neurotrophic factors. As shown in **Figure 6**, the qRT-PCR results revealed that there was significant decrease in the mRNA expression of *Bdnf*, *Gdnf*, and *Gria1* in HG treated group (0.36 ± 0.01, 0.49 ± 0.028, 0.34 ± 0.06, respectively), compared with control group ($P < 0.05$); *Syp* was also decreased to 0.48 ± 0.08, but not significant ($P = 0.12$). However, when HT22 cells were pretreated with fisetin for 1 h before incubation with HG, the mRNA expression of *Bdnf*, *Gdnf*, *Syp*, and *Gria1* was markedly upregulated in a dose-dependent manner compared with HG group ($P < 0.05$). Fisetin could dramatically neutralize the damage effect of HG on HT22 cells.

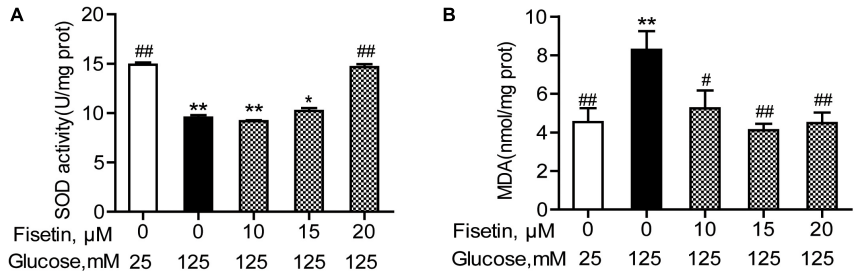

FIGURE 4 | Fisetin alleviates high glucose (HG)-induced oxidative damage in HT22 cells. Cells were pretreated with 10–20 μM of fisetin or vehicle control for 1 h and then exposed to 125 mM of high glucose for 48 h. **(A)** SOD activity and **(B)** MDA content were determined using the test kits. Data were expressed as mean ± SEM, $n = 4$. $^{*}P < 0.05$, $^{**}P < 0.01$ *vs.* the 25 mM glucose (control) group; $\#P < 0.05$, $\#\#P < 0.01$ *vs.* 125 mM glucose (HG) group.

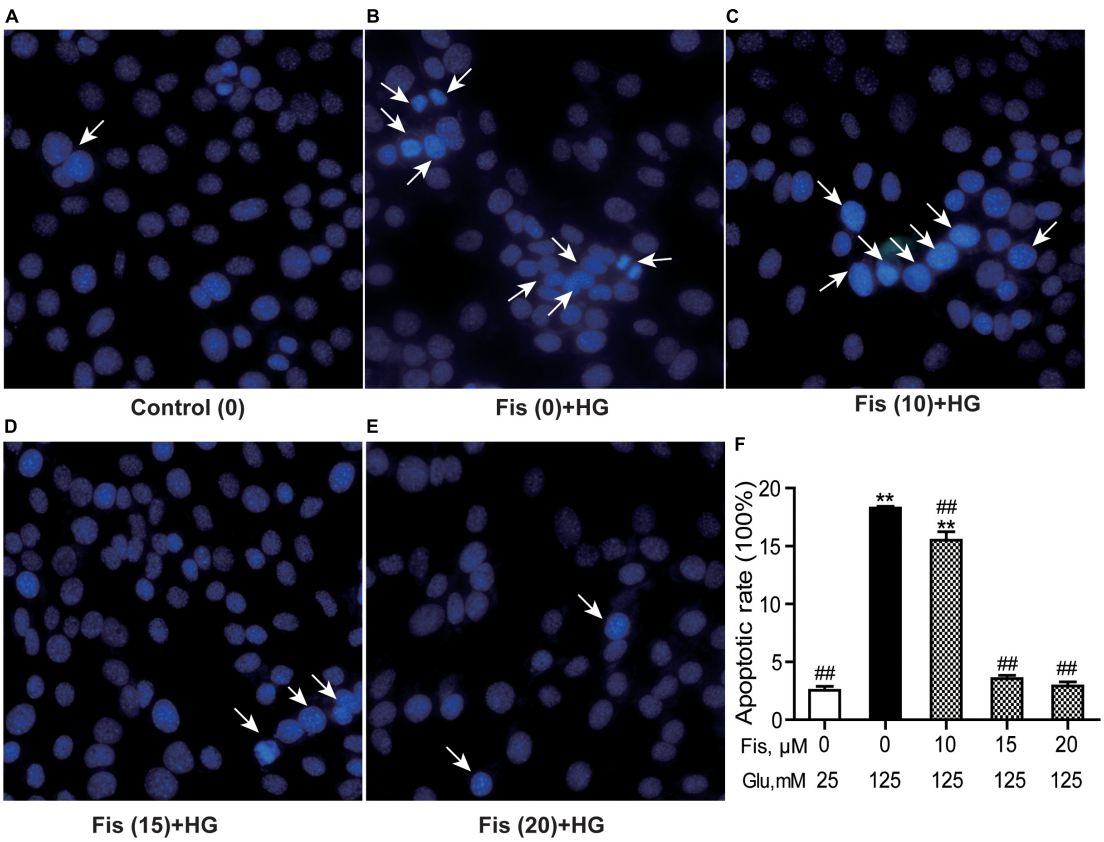

FIGURE 5 | Protective effects of fisetin against high glucose (HG)-induced apoptosis in HT22 cells. HT22 cells were stimulated with high glucose (125 mM) for 48 h in the presence or absence of fisetin. The nuclear structure of each group was stained with Hoechst 33258. **(A)** Control, **(B)** HG, **(C)** Fisetin (10 μM) + HG, **(D)** Fisetin (15 μM) + HG, **(E)** Fisetin (20 μM) + HG. **(F)** Quantitative analysis of high glucose induced apoptosis in each group. Fis: fisetin, Glu: glucose. $^{**}P < 0.01$ *vs.* the 25 mM glucose (control) group; $\#\#P < 0.01$ *vs.* 125 mM glucose (HG) group.

Fisetin Enhances Phosphorylation of CREB, Akt, and PI3K in HG-Induced HT22 Cells

To illustrate the molecular mechanisms responsible for the improvement of HG-induced cytotoxicity by fisetin, the activation of PI3K/Akt/CREB pathway was assessed *via* Western blotting assay. As shown in **Figure 7**, the p-PI3K/PI3K ratio, p-Akt/Akt ratio, and p-CREB/CREB ratio of the control group were set as 1. The relative level of p-PI3K/PI3K, p-Akt/Akt, and p-CREB/CREB inhibited after exposure to HG compared to the control group ($P < 0.05$). However, pretreatment with fisetin obviously rescued the HG-inhibited expressions of p-CREB and p-Akt ($P < 0.05$ and $P < 0.01$). In addition, the expression of p-PI3K exhibited an upward tendency compared with the HG group, but not significant (**Figure 7**).

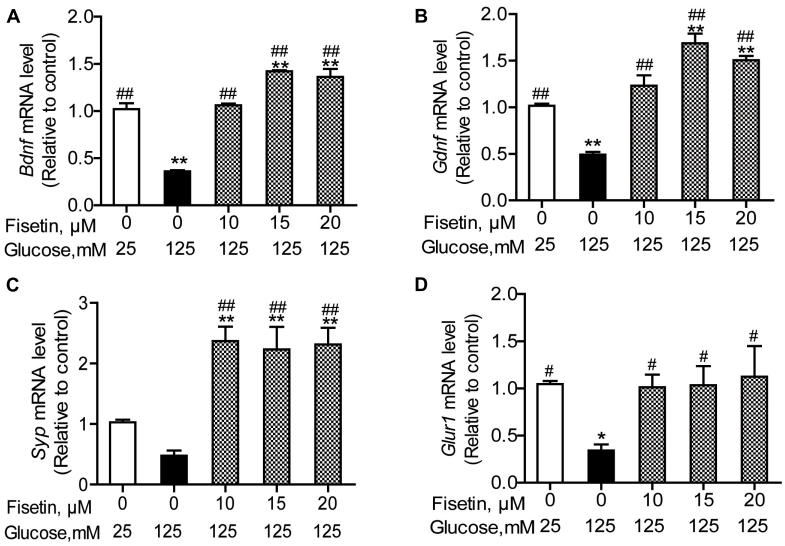

FIGURE 6 | Effect of fisetin on relative mRNA expression levels of Bdnf **(A)**, Gdnf **(B)**, Syp **(C)**, and Gria1 **(D)** in HT22 cells. Cells were preincubated with or without fisetin for 1 h, and then incubated with high glucose (125 mM) for 48 h. *Bdnf*, *Gdnf*, *Syp*, and *Gria1* mRNA levels were examined by quantitative PCR. Data were expressed as mean ± SEM, $n = 4$. *$P < 0.05$, **$P < 0.01$ *vs.* the 25 mM glucose (control) group; #$P < 0.05$, ##$P < 0.01$ *vs.* 125 mM glucose (HG) group.

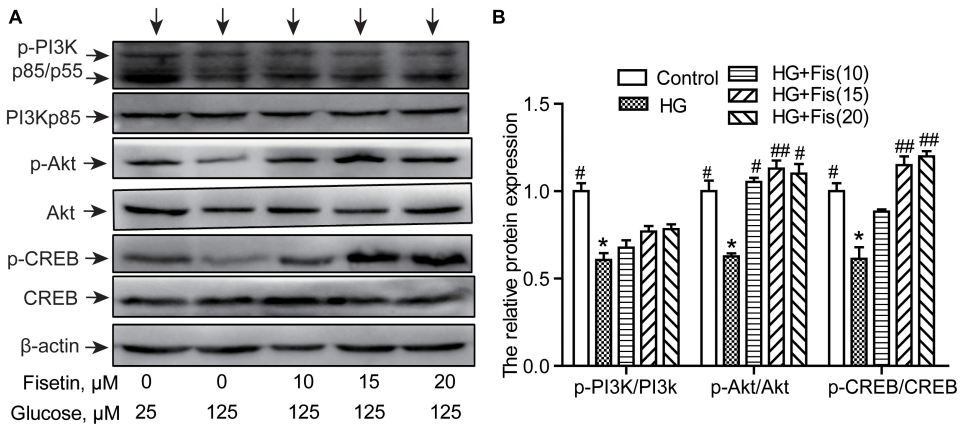

FIGURE 7 | Effect of fisetin on the PI3K/Akt/CREB signaling pathway. **(A)** Western blot analysis of the expression of phosphorylated PI3K, Akt, CREB, and total PI3K, Akt, CREB in HT22 cells. **(B)** The histograms showing their relative expression (phosphorylation was expressed as ratio with respect to their total form). The results were expressed as mean ± SEM ($n = 3$). *$P < 0.05$, **$P < 0.01$ *vs.* the 25 mM glucose (control) group; #$P < 0.05$, ##$P < 0.01$ *vs.* 125 mM glucose (HG) group.

Suppression of the PI3K/Akt/CREB Signaling Pathway Reverses Fisetin's Neuroprotection in HG-Induced HT22 Cells

It is well known that CREB can regulate memory, learning, and synaptic transmission as well as neuron survival, differentiation, and axon growth in brain (Sun et al., 2017). To further determine whether the protection of fisetin against HG-induced neurotoxicity was through the activation of PI3K/Akt/CREB signaling pathway, we pretreated HT22 cells with LY294002 (10 μM), a specific PI3K/Akt pathway inhibitor, for 30 min before addition of fisetin. As shown in **Figures 8A,B**, the control group was set as 1, the ratio of p-PI3K/PI3K, p-Akt/Akt, and p-CREB/CREB of HG group was 0.70 ± 0.01, 0.63 ± 0.03, 0.58 ± 0.04, respectively. Pretreatment with fisetin for 1 h followed by HG could markedly improve protein levels of phosphorylated PI3K, Akt, CREB, and cell viability compared to HG-treated HT22 cells ($P < 0.05$). Unfortunately, this improvement effect of fisetin on p-Akt was almost eliminated by the pre-incubated with inhibitor LY294002 (the ratio is 0.46 ± 0.03). Compared to HG + Fis group, the enhancement of p-CREB and cell viability by fisetin was partially suppressed by LY294002 preincubation in HG + Fis + LY ($P < 0.05$). These results indicated that fisetin protects against HG-induced HT22 cell damage partially through PI3K/Akt/CREB signaling pathway.

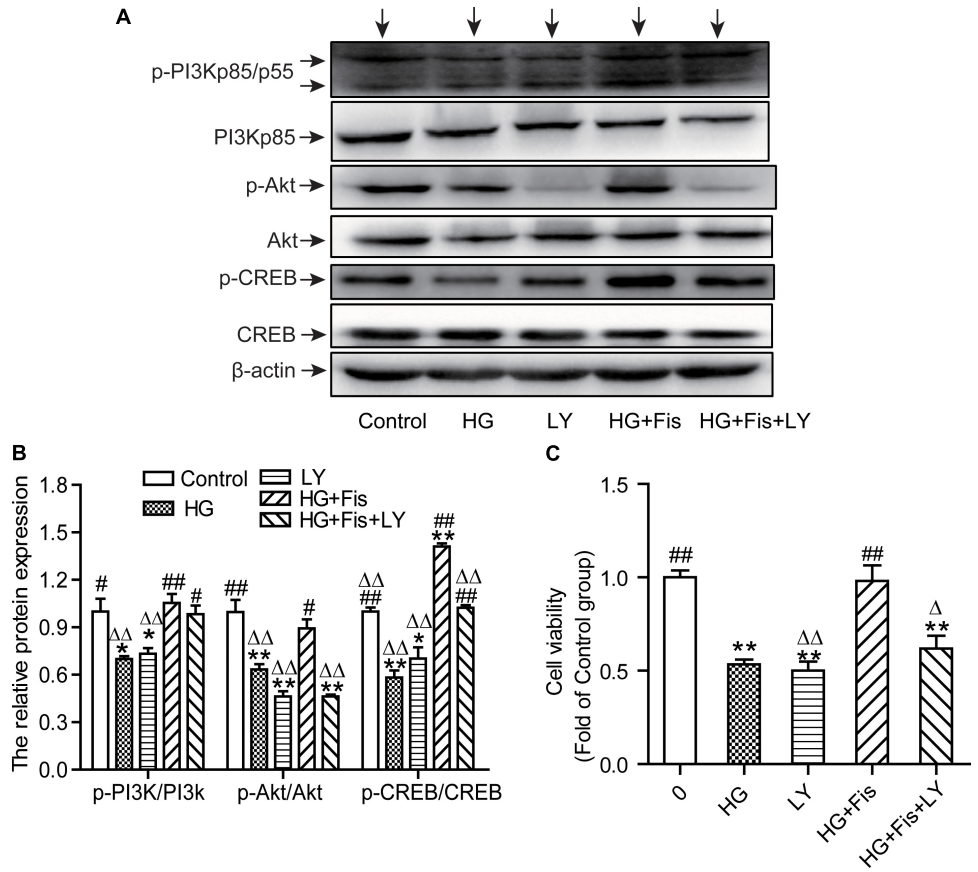

FIGURE 8 | LY294002 blocked the protection of fisetin against high glucose (HG)-induced cytotoxicity. **(A)** Protein expressions were tested. **(B)** Quantitative analysis of the blots was shown in panel after normalized by Quantity One Software. **(C)** Cell viability was determined by CCK-8 assay. Data were expressed as mean ± SEM (n = 3). Ctr: normal HT22 cells, HG: HT22 cells exposed to high glucose (125 mM) for 48 h, LY: HT22 cells incubated with LY294002 at 10 μM, HG + Fis: high glucose (125 mM) incubated cells pre-incubated with fisetin (20 μM) for 1 h. HG + Fis + LY: HT22 cells preincubated with LY294002 (10 μM) for 30 min followed by fisetin (20 μM) and high glucose (125 mM). $^{*}P < 0.05$, $^{**}P < 0.01$ *vs.* the 25 mM glucose (control) group; $\#P < 0.05$, $\#\#P < 0.01$ *vs.* 125 mM glucose (HG) group; $\Delta P < 0.05$, $\Delta\Delta P < 0.01$ *vs.* HG + Fis group.

DISCUSSION

Diabetes mellitus-associated neuronal dysfunction is one of the most common crippling complications affecting peripheral nerves of diabetic patients. High blood glucose, the characteristics of DM, has been demonstrated to possess negative effects on cognitive function and brain structure. Chronic high blood glucose could alter the substrate transport, lactate homeostasis, and glutamate/glutamine cycling in hippocampus, leading to cognitive deficits (Zhang et al., 2019). Fisetin, a natural flavonoid, is an orally active, novel neuroprotective and cognition-enhancing molecular, possessing high BBB penetration potential. Flavonoid fisetin was screened out from *Rhus verniciflua*, which could protect HT22 cells against glutamate-induced neurotoxicity through attenuating oxidative stress (Cho et al., 2012). Similarly, another study found fisetin prevented fluoride and dexamethasone co-induced oxidative damage in HT-22 cells (Inkielewicz-Stepniak et al., 2012). However, its role in DM-induced cognitive dysfunction has not been explained. The present study was attempted to understand the molecular mechanisms underlying neuroprotective effect of fisetin on HG-treated HT22 cells.

In the present study, we demonstrated that fisetin pretreatment protected against HG-induced neurotoxicity in HT22 cells *via* the activation of PI3K/Akt/CREB signaling pathway. Fisetin dramatically attenuated HG-induced LDH release, MDA overproduction, decreased SOD activity, and cell apoptosis. Inhibition of PI3K/Akt/CREB signaling pathway by PI3K inhibitor LY294002 partially abolished fisetin-provided protection effects on HG-induced cell apoptosis. In general, the present results indicated that fisetin may possess the ability to protect against hyperglycemia-induced neurotoxicity.

In our study, we used HG-exposed HT22 cells as hyperglycemia-induced neurotoxicity model *in vitro*. First, the concentration of HG and fisetin for *in vitro* studies was detected on the basis of cytotoxicity studies. It was found that 125 mM of HG treated HT22 cells for 48 h could decrease cell viability by about 50%. Moreover, the concentration for fisetin was studied on the basis of CCK-8 assay wherein exposure to 20 μM of fisetin for 48 h did not cause any significant

change in cell viability of HT22 cells. Therefore, 125 mM of HG was employed as the sub-toxic dose for HT22 cells in the present study. In addition, 20 μM of fisetin would be selected to investigate the neuroprotective effect in the following study. These results confirmed that the HG-induced neurotoxicity model was established successfully.

Tremendous studies have found that fisetin is effective in treatment of diabetic neuropathy, age-related neurodegenerative diseases and brain injury (Sandireddy et al., 2016; Chen et al., 2018; Currais et al., 2018). One important reason may be that fisetin has high brain uptake potential and BBB penetration (Maher, 2009). There is an ongoing debate about whether fisetin can reach the central nervous system that is sufficient to affect brain function. An *in vivo* study using two-photon exited fluorescence imaging indicated that intraperitoneal injection or oral administration of fisetin is rapidly distributed to brain parenchyma (Krasieva et al., 2015). He et al. (2018) demonstrated that oral fisetin exhibits better bioavailability and BBB permeability than structurally related flavonoids, quecetin, luteolin, and myricetin. The unpublished results from Maher's laboratory indicated that sulfated and/or glucuronidated forms of fisetin reach concentrations of 30 μM in the cerebrospinal fluid with a plasma half life of 8 h in macaques fed a single oral dose of 25 mg/kg·bw (Maher, 2017). Hence, fisetin is likely to exhibit excellent BBB penetration and neuroprotection property. We explored the effect of fisetin on neurons in detail. In this study, fisetin played a protective role in HT22 cells against HG-induced neural damages. When HT22 cells were pretreated with fisetin for 1 h, the notable reduced cell viability induced by HG was restored to the basal level and the LDH release was also attenuated. Oxidative stress has been widely considered as a crucial element in the adverse effects of hyperglycemia to various tissues, including neuronal cells. Zhang L. et al. (2018) discovered that fisetin alleviated oxidative stress and BBB distortion after traumatic brain injury through the activation of the Nrf2/ARE pathway. Our study showed that HG increased the oxidative stress through suppressing SOD activity and elevating MDA production. However, fisetin pretreatment dramatically improved SOD activity while alleviating MDA over-production, playing a significant protective role in HT22 cells. This finding indicated that fisetin alleviated oxidant stress in HG-induced cell damage. Additionally, one of the potential mechanisms for hyperglycemia-induced neural cell death is connected with apoptosis that was assessed by many investigations (Namazi Sarvestani et al., 2018; Kaeidi et al., 2019). Taurine reduced HG-induced the number of apoptotic cell *via* Akt/Bad pathway in HT22 cells which further balanced the levels of Bcl-2 and Bax (Wu et al., 2019). Namazi Sarvestani et al. (2018) found that HG induced neurotoxicity and apoptosis in PC12 cells by increasing the protein expression of pro-apoptotic Bax and caspase 3 and decreasing Bcl-2 protein expression. In our experiment, we obtained the consistent results that stimulation of HT22 cells by HG enhanced cell apoptotic rates compared to control group, while fisetin could significantly attenuated HG-induced apoptosis in HT22 cells. It is suggested that anti-apoptosis participates in the protective effects of fisetin against HG-induced neuronal injury.

To confirm the neuroprotective effect of fisetin, the mRNA expression of *Bdnf*, *Gdnf*, *Syp*, and *Gria1* was tested. BDNF is a highly conserved neurotrophin with pivotal role in neuronal survival, neurogenesis, synaptogenesis, and neuroplasticity (Mizui et al., 2016; De Assis et al., 2018). The expression of BDNF gene (*Bdnf*) is closely linked to all aspects of neuronal functioning, including complex processes of cognition (Morgan et al., 2015). The elevation of BDNF is beneficial for improvements in neuroplasticity and lower ratios of cognitive deficits (Phillips et al., 2014). GDNF is associated with the modulation of synaptic plasticity and the formation of neural circuits (Airaksinen and Saarma, 2002). In ischemia/reperfusion rats, Wharton's jelly-derived mesenchymal stem cells obviously increased gene expression of GDNF and BDNF and improved the functional learning and memory (Abd El Motteleb et al., 2018). In the present study, it was found that *Bdnf* and *Gdnf* gene expression was notably inhibited in HT22 cells cultured with HG, while fisetin pretreatment dramatically upregulated *Bdnf* and *Gdnf* expression, even higher than control group. Besides, it is widely believed that SYP can mediate synaptic structure and play a part in synaptic plasticity through phosphorylation and release of neurotransmitters (Liu et al., 2016). Chronic fluoride exposures reduced SYP expression and induced aberrant changes of GSK-3β/β-catenin signaling, leading to neuronal apoptosis and impaired synaptic plasticity (Jiang et al., 2019). In addition, it is well known that the *Gria1* gene, ionotropic receptor AMPA type subunit 1, is closely associated with depression and status epilepticus. *Gria1* knockout mice exhibit a phenotype relevant for neuropsychiatric disorders, including reduced synaptic plasticity and attentional deficits (Ang et al., 2018). In our research, we found that *Syp* and *Gria1* gene expression was suppressed by HG, but significantly rescued by fisetin pretreatment. It is suggested that the neuroprotective effect of fisetin should be associated with the improvement of neuronal function-related genes expression.

Diabetes mellitus-related cognitive deficits are one of the typical central nervous system complications, while the underlying molecular mechanisms by which hyperglycemia damage cognitive ability are still uncertain. Research has showed that PI3K/Akt signaling pathway acts as a key regulator in neuronal cell death and survival *via* stimulating multiple downstream targets (Zhang W. et al., 2018). 6-Hydroxydopamine (6-OHDA) and rotenone are both commonly used as neurotoxin in the study of PD. Fisetin could alleviate 6-OHDA- or rotenone-induced cytoxicity and oxidative stress in SH-SY5Y cells by activating PI3K/Akt signaling (Watanabe et al., 2018; Rajendran and Ramachandran, 2019). Whether this signaling pathway has any effect in the protection effect of fisetin on hyperglycemia-induced neurotoxicity is not clear. Akt can phosphorylate a number of downstream molecules related to cell survival and proliferation like CREB (Hu et al., 2017). CREB, a transcriptional activator after being phosphorylated, is essential for memory formation, neuronal plasticity, and apoptosis in hippocampal neurons (Kim et al., 2013). Ahmad et al. (2017) discovered

that the suppressed p-PI3K, p-Akt, and p-GSK3β expression in $A\beta_{1-42}$-treated mice was reversed by fisetin. In the present study, we found the involvement of the PI3K/Akt/CREB signaling in the protection effect of fisetin on HG-induced HT22 cell injury. Exposure to HG alone in HT22 cells was found to significantly decrease the ratio of p-PI3K/PI3K, p-Akt/Akt, and p-CREB/CREB. Fisetin noticeably ameliorated HG-induced deactivation of Akt and CREB, whereas this action was almost blocked by LY294002, the specific inhibitor of PI3K, especially on the activation of Akt. The phosphorylation of CREB and cell viability was partially eliminated. Thus, we speculated that Akt and CREB is the downstream of PI3K and there may be other pathways activating CREB. Taken together, these findings indicated that the neuroprotection of fisetin against HG may partly lie in the reactivation of the PI3K/Akt/CREB signaling.

Fisetin is present in human diet and has benefit to nervous system. In recent years, human clinical trial with fisetin has been performed for brain ischemic stroke with encouraging outcomes (Feng et al., 2019). There is no evidence for either short- or long-term toxicity of fisetin (Currais et al., 2014). These positive outcomes provide foundation for the development of fisetin as new drug and conduct further clinical studies. Although fisetin exhibits rapid absorption and wide distribution into tissues (kidneys, intestines, liver, and brain) and efficiently cross the BBB, its clinical application is mainly limited because of poor water solubility and high lipophilicity (Krasieva et al., 2015; Mehta et al., 2018). Luckily, novel drug delivery systems can improve the activity and overcoming problems associated with fisetin. The fisetin nanoemulsion intraperitoneally injection has a 24-fold increase in fisetin relative bioavailability, without any difference in systemic exposure compared to free fisetin (Ragelle et al., 2012). This technique will definitely help fisetin develop into a new approach for pharmacological treatment for intractable diabetic neuropathy. However, to translate the neuroprotection potential of fisetin to clinical use, well-designed clinical trials along with the reliable analytical markers are required. More detailed and deeper investigation focused toward human trials, optimization of desired physiological responses in targeted patients and molecular targets of fisetin are required. These studies will contribute to the development of fisetin as therapeutics for diabetic encephalopathy in the future.

CONCLUSION

In summary, the current study demonstrates that fisetin is able to elevate cell viability, alleviate oxidative damage, inhibit neuron apoptosis, and improve nerve functional parameters in HT22 cells under HG-induced neurotoxicity. The activation of PI3K/Akt/CREB pathway is involved in neuroprotection of fisetin. The present study provides further support that eating more foods rich in fisetin may be beneficial for nervous system. Based on the neuroprotective activity and high BBB permeability, fisetin might be developed into a new approach for pharmacological treatment of intractable diabetic neuropathy. In future research, we plan to develop further *in vivo* studies and clinical trials to reveal the neuroprotection effects and underlying mechanisms of fisetin against HG-induced cognitive dysfunction.

DATA AVAILABILITY STATEMENT

All datasets generated for this study are included in the article/supplementary material.

AUTHOR CONTRIBUTIONS

SZ and RX designed the experiments. HW and WL contributed to the conception of the work, contributed to the figure preparation, and modified the grammar mistakes. SZ, RX, and YG acquired data for cell experiments and analyzed the final results. SZ wrote the first draft of the manuscript. RX and YG wrote sections of the manuscript. All authors contributed to the manuscript revision and approved the submitted version.

FUNDING

This work was supported by the National Natural Science Foundation of China (NSFC, No. 81903314), Key Scientific Research Project of Colleges and Universities in Henan Province (Grant No. 17A330006), and China Postdoctoral Science Foundation (Grant No. 2017M622379).

ACKNOWLEDGMENTS

We gratefully acknowledge Prof. Wang for his support on the experimental platform and equipment in Precision Nutrition Innovation Center.

REFERENCES

Abd El Motteleb, D. M., Hussein, S., Hasan, M. M., and Mosaad, H. (2018). Comparison between the effect of human Wharton's jelly-derived mesenchymal stem cells and levetiracetam on brain infarcts in rats. *J. Cell. Biochem.* 119, 9790–9800. doi: 10.1002/jcb.27297

Ahmad, A., Ali, T., Park, H. Y., Badshah, H., Rehman, S. U., and Kim, M. O. (2017). Neuroprotective effect of fisetin against amyloid-beta-induced cognitive/synaptic dysfunction, neuroinflammation, and neurodegeneration in adult mice. *Mol. Neurobiol.* 54, 2269–2285. doi: 10.1007/s12035-016-9795-4

Airaksinen, M. S., and Saarma, M. (2002). The GDNF family: signalling, biological functions and therapeutic value. *Nat. Rev. Neurosci.* 3, 383–394. doi: 10.1038/nrn812

Ang, G., McKillop, L. E., Purple, R., Blanco-Duque, C., Peirson, S. N., Foster, R. G., et al. (2018). Absent sleep EEG spindle activity in GluA1 (Gria1) knockout mice: relevance to neuropsychiatric disorders. *Transl. Psychiatry* 8:154. doi: 10.1038/s41398-018-0199-2

Arunachalam, G., Samuel, S. M., Marei, I., Ding, H., and Triggle, C. R. (2014). Metformin modulates hyperglycaemia-induced endothelial senescence and apoptosis through SIRT1. *Br. J. Pharmacol.* 171, 523–535. doi: 10.1111/bph.12496

Biessels, G. J., and Despa, F. (2018). Cognitive decline and dementia in diabetes mellitus: mechanisms and clinical implications. *Nat. Rev. Endocrinol.* 14, 591–604. doi: 10.1038/s41574-018-0048-7

Biessels, G. J., Staekenborg, S., Brunner, E., Brayne, C., and Scheltens, P. (2006). Risk of dementia in diabetes mellitus: a systematic review. *Lancet Neurol.* 5, 64–74. doi: 10.1016/s1474-4422(05)70284-2

Caracciolo, L., Marosi, M., Mazzitelli, J., Latifi, S., Sano, Y., Galvan, L., et al. (2018). CREB controls cortical circuit plasticity and functional recovery after stroke. *Nat. Commun.* 9:2250. doi: 10.1038/s41467-018-04445-9

Chen, Y. P., Sivalingam, K., Shibu, M. A., Peramaiyan, R., Day, C. H., Shen, C. Y., et al. (2018). Protective effect of fisetin against angiotensin II-induced apoptosis by activation of IGF-IR-PI3K-Akt signaling in H9c2 cells and spontaneous hypertension rats. *Phytomedicine* 57, 1–8. doi: 10.1016/j.phymed.2018.09.179

Cho, N., Choi, J. H., Yang, H., Jeong, E. J., Lee, K. Y., Kim, Y. C., et al. (2012). Neuroprotective and anti-inflammatory effects of flavonoids isolated from Rhus verniciflua in neuronal HT22 and microglial BV2 cell lines. *Food Chem. Toxicol.* 50, 1940–1945. doi: 10.1016/j.fct.2012.03.052

Currais, A., Farrokhi, C., Dargusch, R., Armando, A., Quehenberger, O., Schubert, D., et al. (2018). Fisetin reduces the impact of aging on behavior and physiology in the rapidly aging SAMP8 mouse. *J. Gerontol. A Biol. Sci. Med. Sci.* 73, 299–307. doi: 10.1093/gerona/glx104

Currais, A., Prior, M., Dargusch, R., Armando, A., Ehren, J., Schubert, D., et al. (2014). Modulation of p25 and inflammatory pathways by fisetin maintains cognitive function in Alzheimer's disease transgenic mice. *Aging Cell* 13, 379–390. doi: 10.1111/acel.12185

De Assis, G. G., Gasanov, E. V., de Sousa, M. B. C., Kozacz, A., and Murawska-Cialowicz, E. (2018). Brain derived neutrophic factor, a link of aerobic metabolism to neuroplasticity. *J. Physiol. Pharmacol.* 69, 351–358. doi: 10.26402/jpp.2018.3.12

Fan, F., Liu, T., Wang, X., Ren, D., Liu, H., Zhang, P., et al. (2016). ClC-3 expression and its association with hyperglycemia induced HT22 hippocampal neuronal cell apoptosis. *J. Diabetes Res.* 2016:2984380. doi: 10.1155/2016/2984380

Feng, H., Wang, C., He, W., Wu, X., Li, S., Zeng, Z., et al. (2019). Roflumilast ameliorates cognitive impairment in APP/PS1 mice via cAMP/CREB/BDNF signaling and anti-neuroinflammatory effects. *Metab. Brain Dis.* 34, 583–591. doi: 10.1007/s11011-018-0374-4

He, W. B., Abe, K., and Akaishi, T. (2018). Oral administration of fisetin promotes the induction of hippocampal long-term potentiation in vivo. *J. Pharmacol. Sci.* 136, 42–45. doi: 10.1016/j.jphs.2017.12.008

Hu, M., Liu, Z., Lv, P., Wang, H., Zhu, Y., Qi, Q., et al. (2017). Autophagy and Akt/CREB signalling play an important role in the neuroprotective effect of nimodipine in a rat model of vascular dementia. Behav. Brain Res. 325(Pt A), 79–86. doi: 10.1016/j.bbr.2016.11.053

Inkielewicz-Stepniak, I., Radomski, M. W., and Wozniak, M. (2012). Fisetin prevents fluoride- and dexamethasone-induced oxidative damage in osteoblast and hippocampal cells. *Food Chem. Toxicol.* 50, 583–589. doi: 10.1016/j.fct.2011.12.015

Jiang, P., Li, G., Zhou, X., Wang, C., Qiao, Y., Liao, D., et al. (2019). Chronic fluoride exposure induces neuronal apoptosis and impairs neurogenesis and synaptic plasticity: role of GSK-3beta/beta-catenin pathway. *Chemosphere* 214, 430–435. doi: 10.1016/j.chemosphere.2018.09.095

Kaeidi, A., Hajializadeh, Z., Jahandari, F., and Fatemi, I. (2019). Leptin attenuates oxidative stress and neuronal apoptosis in hyperglycemic condition. *Fundam. Clin. Pharmacol.* 33, 75–83. doi: 10.1111/fcp.12411

Kim, J., Kwon, J. T., Kim, H. S., and Han, J. H. (2013). CREB and neuronal selection for memory trace. *Front. Neural Circuits* 7:44. doi: 10.3389/fncir.2013.00044

Krasieva, T. B., Ehren, J., O'Sullivan, T., Tromberg, B. J., and Maher, P. (2015). Cell and brain tissue imaging of the flavonoid fisetin using label-free two-photon microscopy. *Neurochem. Int.* 89, 243–248. doi: 10.1016/j.neuint.2015.08.003

Liu, S. J., Yang, C., Zhang, Y., Su, R. Y., Chen, J. L., Jiao, M. M., et al. (2016). Neuroprotective effect of beta-asarone against Alzheimer's disease: regulation of synaptic plasticity by increased expression of SYP and GluR1. *Drug Des. Devel. Ther.* 10, 1461–1469.

Ma, T., Kandhare, A. D., Mukherjee-Kandhare, A. A., and Bodhankar, S. L. (2018). Fisetin, a plant flavonoid ameliorates doxorubicin-induced cardiotoxicity in experimental rats: the decisive role of caspase-3, COX-II, cTn-I, iNOs and TNF-alpha. *Mol. Biol. Rep.* 46, 105–118. doi: 10.1007/s11033-018-4450-y

Maher, P. (2009). Modulation of multiple pathways involved in the maintenance of neuronal function during aging by fisetin. *Genes Nutr.* 4, 297–307. doi: 10.1007/s12263-009-0142-5

Maher, P. (2017). Protective effects of fisetin and other berry flavonoids in Parkinson's disease. *Food Funct.* 8, 3033–3042. doi: 10.1039/c7fo00809k

Mehta, P., Pawar, A., Mahadik, K., and Bothiraja, C. (2018). Emerging novel drug delivery strategies for bioactive flavonol fisetin in biomedicine. *Biomed. Pharmacother.* 106, 1282–1291. doi: 10.1016/j.biopha.2018.07.079

Meneses, M. J., Silva, B. M., Sousa, M., Sa, R., Oliveira, P. F., and Alves, M. G. (2015). Antidiabetic drugs: mechanisms of action and potential outcomes on cellular metabolism. *Curr. Pharm. Des.* 21, 3606–3620. doi: 10.2174/1381612821666150710145753

Mizui, T., Ishikawa, Y., Kumanogoh, H., and Kojima, M. (2016). Neurobiological actions by three distinct subtypes of brain-derived neurotrophic factor: multi-ligand model of growth factor signaling. *Pharmacol. Res.* 105, 93–98. doi: 10.1016/j.phrs.2015.12.019

Morgan, J. A., Corrigan, F., and Baune, B. T. (2015). Effects of physical exercise on central nervous system functions: a review of brain region specific adaptations. *J. Mol. Psychiatry* 3:3. doi: 10.1186/s40303-015-0010-8

Nabavi, S. F., Braidy, N., Habtemariam, S., Sureda, A., Manayi, A., and Nabavi, S. M. (2016). Neuroprotective effects of fisetin in Alzheimer's and Parkinson's diseases: from chemistry to medicine. *Curr. Top. Med. Chem.* 16, 1910–1915. doi: 10.2174/1568026616666160204121725

Namazi Sarvestani, N., Saberi Firouzi, S., Falak, R., Karimi, M. Y., Davoodzadeh Gholami, M., Rangbar, A., et al. (2018). Phosphodiesterase 4 and 7 inhibitors produce protective effects against high glucose-induced neurotoxicity in PC12 cells via modulation of the oxidative stress, apoptosis and inflammation pathways. *Metab. Brain Dis.* 33, 1293–1306. doi: 10.1007/s11011-018-0241-3

Phillips, C., Baktir, M. A., Srivatsan, M., and Salehi, A. (2014). Neuroprotective effects of physical activity on the brain: a closer look at trophic factor signaling. *Front. Cell. Neurosci.* 8:170. doi: 10.3389/fncel.2014.00170

Ragelle, H., Crauste-Manciet, S., Seguin, J., Brossard, D., Scherman, D., Arnaud, P., et al. (2012). Nanoemulsion formulation of fisetin improves bioavailability and antitumour activity in mice. *Int. J. Pharm.* 427, 452–459. doi: 10.1016/j.ijpharm.2012.02.025

Rajendran, M., and Ramachandran, R. (2019). Fisetin protects against rotenone-induced neurotoxicity through signaling pathway. *Front. Biosci. (Elite Ed.)* 11, 20–28. doi: 10.2741/e843

Sandireddy, R., Yerra, V. G., Komirishetti, P., Areti, A., and Kumar, A. (2016). Fisetin imparts neuroprotection in experimental diabetic neuropathy by modulating Nrf2 and NF-kappaB pathways. *Cell. Mol. Neurobiol.* 36, 883–892. doi: 10.1007/s10571-015-0272-9

Seto, S. W., Yang, G. Y., Kiat, H., Bensoussan, A., Kwan, Y. W., and Chang, D. (2015). Diabetes mellitus, cognitive impairment, and traditional Chinese medicine. *Int. J. Endocrinol.* 2015:810439.

Sharma, G., Parihar, A., Talaiya, T., Dubey, K., Porwal, B., and Parihar, M. S. (2020). Cognitive impairments in type 2 diabetes, risk factors and preventive strategies. *J. Basic Clin. Physiol. Pharmacol.* doi: 10.1515/jbcpp-2019-0105 [Epub ahead of print].

Simo, R., Ciudin, A., Simo-Servat, O., and Hernandez, C. (2017). Cognitive impairment and dementia: a new emerging complication of type 2 diabetes-the diabetologist's perspective. *Acta Diabetol.* 54, 417–424. doi: 10.1007/s00592-017-0970-5

Sun, H., Wu, H., Liu, J., Wen, J., Zhu, Z., and Li, H. (2017). Prenatal stress impairs spatial learning and memory associated with lower mRNA level of the CAMKII and CREB in the adult female rat hippocampus. *Neurochem. Res.* 42, 1496–1503. doi: 10.1007/s11064-017-2206-z

Watanabe, R., Kurose, T., Morishige, Y., and Fujimori, K. (2018). Protective effects of fisetin against 6-OHDA-induced apoptosis by activation of PI3K-Akt signaling in human neuroblastoma SH-SY5Y Cells. *Neurochem. Res.* 43, 488–499. doi: 10.1007/s11064-017-2445-z

Wu, P., Chen, X., Inam, U. L., Shi, X., Zhang, M., Li, K., et al. (2019). Taurine ameliorates high glucose induced apoptosis in HT-22 cells.

Adv. Exp. Med. Biol. 1155, 889–903. doi: 10.1007/978-981-13-8023-5_75

Wu, X., Liang, Y., Jing, X., Lin, D., Chen, Y., Zhou, T., et al. (2018). Rifampicin prevents SH-SY5Y cells from rotenone-induced apoptosis via the PI3K/Akt/GSK-3beta/CREB signaling pathway. *Neurochem. Res.* 43, 886–893. doi: 10.1007/s11064-018-2494-y

Xiang, Q., Zhang, J., Li, C. Y., Wang, Y., Zeng, M. J., Cai, Z. X., et al. (2015). Insulin resistance-induced hyperglycemia decreased the activation of Akt/CREB in hippocampus neurons: molecular evidence for mechanism of diabetes-induced cognitive dysfunction. *Neuropeptides* 54, 9–15. doi: 10.1016/j.npep.2015.08.009

Zenker, J., Ziegler, D., and Chrast, R. (2013). Novel pathogenic pathways in diabetic neuropathy. *Trends Neurosci.* 36, 439–449. doi: 10.1016/j.tins.2013.04.008

Zhang, L., Huang, Y., Zhuo, W., Zhu, Y., Zhu, B., and Chen, Z. (2016). Fisetin, a dietary phytochemical, overcomes Erlotinib-resistance of lung adenocarcinoma cells through inhibition of MAPK and AKT pathways. *Am. J. Transl. Res.* 8, 4857–4868.

Zhang, L., Wang, H., Zhou, Y., Zhu, Y., and Fei, M. (2018). Fisetin alleviates oxidative stress after traumatic brain injury via the Nrf2-ARE pathway. *Neurochem. Int.* 118, 304–313. doi: 10.1016/j.neuint.2018.05.011

Zhang, S., Xue, R., and Hu, R. (2019). The neuroprotective effect and action mechanism of polyphenols in diabetes mellitus-related cognitive dysfunction. *Eur. J. Nutr.* doi: 10.1007/s00394-019-02078-2 [Epub ahead of print].

Zhang, W., Song, J. K., Yan, R., Li, L., Xiao, Z. Y., Zhou, W. X., et al. (2018). Diterpene ginkgolides protect against cerebral ischemia/reperfusion damage in rats by activating Nrf2 and CREB through PI3K/Akt signaling. *Acta Pharmacol. Sin.* 39, 1259–1272. doi: 10.1038/aps.2017.149

Zhu, W. W., Xiao, F., Tang, Y. Y., Zou, W., Li, X., Zhang, P., et al. (2018). Spermidine prevents high glucose-induced senescence in HT-22 cells by upregulation of CB1 receptor. *Clin. Exp. Pharmacol. Physiol.* 45, 832–840. doi: 10.1111/1440-1681.12955

Conflict of Interest: The authors declare that the research was conducted in the absence of any commercial or financial relationships that could be construed as a potential conflict of interest.

frontiers in Pharmacology

ORIGINAL RESEARCH
published: 01 May 2020
doi: 10.3389/fphar.2020.00535

Harmine Ameliorates Cognitive Impairment by Inhibiting NLRP3 Inflammasome Activation and Enhancing the BDNF/TrkB Signaling Pathway in STZ-Induced Diabetic Rats

Peifang Liu[1†], Hui Li[2†], Yueqiu Wang[2†], Xiaolin Su[3], Yang Li[2], Meiling Yan[4], Lan Ma[5] and Hui Che[2*]*

[1] Department of Neurology, The Second Affiliated Hospital of Harbin Medical University, Harbin, China, [2] Department of Endocrinology, The Second Affiliated Hospital of Harbin Medical University, Harbin, China, [3] Department of Biochemistry and Molecular Biology, Indiana University School of Medicine, Indianapolis, IN, United States, [4] The Center for Drug Research and Development, Guangdong Pharmaceutical University, Guangzhou, China, [5] Department of Geriatrics, The Second Affiliated Hospital of Harbin Medical University, Harbin, China

OPEN ACCESS

Edited by:
Touqeer Ahmed,
National University of Sciences & Technology, Pakistan

Reviewed by:
Mohammad Shamsul Ola,
King Saud University, Saudi Arabia
Tahir Ali,
University of Calgary, Canada

***Correspondence:**
Hui Che
chehui1203@163.com
Lan Ma
Lilyma70@163.com

[†]These authors have contributed equally to this work

Specialty section:
This article was submitted to Neuropharmacology, a section of the journal Frontiers in Pharmacology

Received: 23 December 2019
Accepted: 06 April 2020
Published: 01 May 2020

Citation:
Liu P, Li H, Wang Y, Su X, Li Y, Yan M, Ma L and Che H (2020) Harmine Ameliorates Cognitive Impairment by Inhibiting NLRP3 Inflammasome Activation and Enhancing the BDNF/TrkB Signaling Pathway in STZ-Induced Diabetic Rats. Front. Pharmacol. 11:535. doi: 10.3389/fphar.2020.00535

Diabetes mellitus (DM) is considered a risk factor for cognitive dysfunction. Harmine not only effectively improves the symptoms of DM but also provides neuroprotective effects in central nervous system diseases. However, whether harmine has an effect on diabetes-induced cognitive dysfunction and the underlying mechanisms remain unknown. In this study, the learning and memory abilities of rats were evaluated by the Morris water maze test. Changes in the nucleotide-binding oligomerization domain-containing protein (NOD)-like receptor family, pyrin domain containing 3 (NLRP3) inflammasome and brain-derived neurotrophic factor (BDNF)/TrkB signaling pathway were determined in both streptozotocin (STZ)-induced diabetic rats and high glucose (HG)-treated SH-SY5Y cells by western blotting and histochemistry. Herein, we found that harmine administration significantly ameliorated learning and memory impairment in diabetic rats. Further study showed that harmine inhibited NLRP3 inflammasome activation, as demonstrated by reduced NLRP3, ASC, cleaved caspase-1, IL-1β, and IL-18 levels, in the cortex of harmine-treated rats with DM. Harmine was observed to have similar beneficial effects in HG-treated neuronal cells. Moreover, we found that harmine treatment enhanced BDNF and phosphorylated TrkB levels in both the cortex of STZ-induced diabetic rats and HG-treated cells. These data indicate that harmine mitigates cognitive impairment by inhibiting NLRP3 inflammasome activation and enhancing the BDNF/TrkB signaling pathway. Thus, our findings suggest that harmine is a potential therapeutic drug for diabetes-induced cognitive dysfunction.

Keywords: harmine, diabetes mellitus, cognitive dysfunction, NLRP3 inflammasome, BDNF

INTRODUCTION

Diabetes mellitus (DM) is a chronic metabolic disease and a global epidemic (Sun et al., 2020). In 2019, the number of people suffering from DM worldwide was estimated to be 463 million, and this number is predicted to rise to 700 million in 2045 (International Diabetes Federation, https://www.diabetesatlas.org/). Epidemiological surveys have revealed that DM patients are at a higher risk to develop dementia (Morris et al., 2014; Zhang et al., 2018; Chornenkyy et al., 2019). Clinical studies have also shown that dementia and DM share many pathological features, such as cerebral atrophy and neurodegeneration (Korf et al., 2007; Kumar et al., 2008). Hyperglycemia, impaired insulin signaling, vascular dysfunction, and inflammation are considered to be contributors to diabetic-induced neurodegeneration and cognitive dysfunction (Sonnen et al., 2009; Kimura, 2016; Duarte et al., 2020).

Recent studies have clearly shown that the inflammasome is involved in the pathogenesis of central nervous system diseases by triggering interleukin (IL)-1β and IL-18 maturation (Ahmed et al., 2017; White et al., 2017; Du et al., 2018). The nucleotide-binding oligomerization domain-containing protein (NOD)-like receptor family, pyrin domain containing 3 (NLRP3) inflammasome is a well-known inflammasome that is associated with multiple neurodegenerative diseases. However, inactivation of the NLRP3 inflammasome can ameliorate these diseases (Lu et al., 2016; Sarkar et al., 2017; La Rosa et al., 2019; Swanson et al., 2019; Fox et al., 2020). DM-related studies have also revealed that NLRP3 inflammasome activation is involved in several diabetic complications, such as diabetic cardiomyopathy, diabetic nephropathy, and diabetic retinopathy (Yu et al., 2020). NLRP3 inflammasome activation is observed in the brains of db/db mice, a diabetic model that exhibits cognitive dysfunction (Zhai et al., 2018). Moreover, high glucose (HG) has been found to induce NLRP3 inflammasome activation in neurons (Ward and Ergul, 2016). These findings suggest that the NLRP3 inflammasome might be associated with the progression of diabetes-induced cognitive dysfunction.

Harmine is an analogous β-carboline alkaloid compound and possesses various biological functions. For example, harmine has been found to influence β-cell proliferation and induce adipocyte thermogenesis in the progression of DM (Dirice et al., 2016; Nie et al., 2016). Harmine can treat multiple cancers by increasing cell apoptosis, inhibiting CDKs and suppressing the AKT/mTOR signaling pathway (Song et al., 2004; Ding et al., 2019; Wu et al., 2019). Moreover, harmine also has a variety of effects, including antioxidative, anti-inflammatory, anti-hypertensive, and antidepressant effects, in the central nervous system (Li et al., 2018). Previous studies have revealed that harmine can ameliorate learning and memory impairment in scopolamine-induced animals (He et al., 2015; Li et al., 2018). However, whether harmine can improve cognitive dysfunction in diabetic rats is still unclear.

Abbreviations: ASC, adaptor protein apoptosis-associated speck-like protein; BDNF, brain-derived neurotrophic factor; DM, diabetes mellitus; FBG, fasting blood glucose; Har, harmine; HG, high glucose; IL-1β, Interleukin-1β; IL-18, Interleukin-18; ND, non-diabetes; NLRP3, nucleotide-binding oligomerization domain-containing protein (NOD)-like receptor family, pyrin domain containing 3; p-TrkB, phosphorylated TrkB; STZ, Streptozotin.

The aim of the present study was to evaluate the possible effect of harmine on the cognitive dysfunction induced by DM and to explore the underlying molecular mechanisms. Our *in vivo* and *in vitro* experiments provided strong evidence that harmine is a neuroprotective agent that acts by inhibiting NLRP3 inflammasome activation and enhancing BDNF/TrkB signaling pathway.

MATERIALS AND METHODS

Model of Diabetes Mellitus and Pharmacotherapy

Male Sprague-Dawley rats (weight, 180–220 g) were obtained from the Animal Center of the Second Affiliated Hospital of Harbin Medical University (China). The rats were housed in a temperature (23 ± 1°C)- and humidity (55 ± 5%)-controlled environment with free access to food and water. A model of diabetes mellitus (DM) was established as described in our previous studies (Meng et al., 2019; Che et al., 2020). Briefly, the rats received a single intraperitoneal injection of 60 mg/kg streptozotocin (STZ) dissolved in citrate buffer (pH = 4.5). Fasting blood glucose (FBG) levels were detected 3 days after STZ injection. Rats with FBG levels >16.7 mmol/L were considered diabetic. Diabetic model rats were randomly divided into the DM group and the DM plus harmine treatment (DM + har) group. Beginning on day 4 after STZ injection, the rats in the DM + har group (n = 8) were given harmine (20 mg/kg) by oral gavage for 12 weeks. The rats in the DM group (n = 8) and nondiabetic (ND) group (n = 8) were orally administered an equal volume of 0.9% saline solution daily.

Morris Water Maze

To determine the effect of harmine on cognitive function in diabetic rats, we subjected the rats to the Morris water maze test after 12 weeks of intervention. Briefly, the escape platform was placed in the first quadrant (2 cm under the surface of the water). On the first day, each rat was placed into the water facing the pool wall and then allowed to find the escape platform within 120 s by itself. If the rat failed to find the target within a specified time, one of the experimenters guided it to the platform and allowed it to rest for at least 20 s. Training was performed for 5 days. The probe trial, in which the escape platform was removed from the first quadrant, and each rat underwent a 120 s swim trial, was performed on the sixth day. The swim distance, escape latency, number of platform crossings in the target quadrant, and time spent in the target quadrant were recorded by the DigBehav-Morris Water Maze Video Analysis System.

Cell Culture and Treatment

Human SH-SY5Y neuroblastoma cells were cultured at a density of 1×10^6 cells/well in 6-well plates with Dulbecco's modified Eagle's medium containing 10% fetal bovine serum (FBS), 100 units/ml penicillin, and 100 μg/ml streptomycin. The cells were incubated in a common incubator with 5% CO_2 and 95% O_2 at 37°C. The medium was replaced every two days. When the

SH-SY5Y cells were approximately 70%–80% confluent, they were exposed to HG (33 mM) conditions and treated with or without harmine (1 μM) for 48 h.

Western Blot Analysis

Protein samples were extracted from rats from the different groups and SH-SY5Y cells for immunoblotting analysis. Briefly, the rats were anesthetized with 10% chloral hydrate (500 mg/kg, intraperitoneal) and then killed by cervical dislocation. The brain tissues were removed and homogenized in 1,000 μl RIPA buffer containing 10 μl protease inhibitor cocktail per 100 mg brain tissue. The homogenates were placed on ice for 30 min. After centrifugation at 13,500 rpm at 4°C for 30 min, the supernatants were collected. The cells were seeded in 6-well plates and treated with or without harmine. After being washed three times with PBS, the cells were lysed with RIPA buffer containing 1% protease inhibitor cocktail. The concentrations of the protein samples were assessed with the BCA kit according to the manufacturer's instructions. The proteins were separated on 10% SDS gels, transferred onto NC membranes, and incubated in 5% bovine serum albumin for 2 h. The membranes were incubated with primary antibodies against nucleotide-binding oligomerization domain-containing protein (NOD)-like receptor family, pyrin domain containing 3 (NLRP3) (1:500, Bioss, China), adaptor protein apoptosis-associated speck-like protein (ASC) (1:200, Abcam, USA), caspase-1 (1:200, Abcam, USA), interleukin-18 (IL-18) (1:200, Abcam, USA), IL-1β (1:200, Abcam, USA), brain-derived neurotrophic factor (BDNF) (1:500, Bioss, China), TrkB (1:500, Bioss, China), phosphorylated TrkB (p-TrkB) (1:200, Bioss, China), and GAPDH (1:1000) 4°C overnight. On the next day, the membranes were incubated with secondary antibodies at room temperature for 1 h. The bands were captured on the Odyssey Infrared Imaging System (LI-COR) and quantified with Odyssey software by measuring the band intensity (area × OD) and normalizing it to that of GAPDH.

Immunofluorescence Analysis

The cells were fixed in 4% paraformaldehyde, permeabilized, and blocked in 10% serum with 0.01% triton for 1 h at room temperature. The samples were then incubated with primary antibodies against NLRP3 (1:200, Bioss, China) and BDNF (1:200, Bioss, China) overnight at 4°C. An undiluted Alexa Fluor® 568 (red)-conjugated goat anti-rabbit IgG or Alexa Fluor® 488 (green)-conjugated anti-rabbit IgG secondary antibody was used. Images were captured with a Zeiss microscope and quantified with Image Pro Plus 6 software.

Immunohistochemical Staining

Rats from the different groups (n = 3 in each group) were anesthetized with 10% chloral hydrate (500 mg/kg, intraperitoneal), and the whole body of each rat was perfused through the left ventricle with 4% paraformaldehyde (pH 7.4). The cortex and hippocampi were removed from the brain of each rat and fixed in 4% paraformaldehyde overnight at 4°C. After dehydration in a concentration gradient of ethanol solutions and dimethylbenzene, the brain tissue samples were embedded in paraffin and cut into 5-μm-thick cross sections. The specimens were then deparaffinized and blocked with bovine serum albumin. The following primary antibodies were used in this study: NLRP3 (1:200, Bioss, China), caspase-1 (1:200, Abcam, USA), IL-18 (1:200, Abcam, USA), and IL-1β (1:200, Abcam, USA). Incubation was performed overnight at 4°C. After incubation with secondary antibodies at 37°C for 30 min, the sections were stained with diaminobenzidine and hematoxylin. Images were captured by microscopy (Zeiss, Germany). Ten images per rat were randomly selected, and at least thirty images per group were analyzed to determine the ratio of positive signal/image by using Image Pro Plus 6 software.

Statistical Analysis

The data are expressed as the mean ± SEM. One-way repeated measure analysis of variance (ANOVA) was used to analyze differences in day-to-day performance in the MWM test. Student's t-test was used to analyze the differences between two groups. All statistical analyses were performed with SPSS 22.0 software. $P < 0.05$ was considered statistically significant.

RESULTS

Harmine Ameliorates Learning and Memory Impairment in STZ-Induced Diabetic Rats

To examine the effect of harmine on the learning and memory abilities of streptozocin (STZ)-induced diabetic rats, we subjected different groups of rats to the Morris water maze test. As illustrated in **Figure 1A**, in the training session, the diabetic rats swam a longer distance to reach the hidden platform than the non-diabetes (ND) rats. However, harmine administration significantly shortened the swimming distance of the diabetic rats. Moreover, the diabetic rats exhibited a longer escape latency than the ND rats, and this increase in escape latency was reversed by harmine administration (**Figure 1B**). In the probe trial, the number of platform crossings in the target quadrant exhibited by the diabetic rats was decreased compared with that exhibited by the ND rats. In addition, the diabetic rats spent less time in the target quadrant than the ND rats. Importantly, harmine administration increased both the number of platform crossings and the time spent in the target quadrant compared with those exhibited by the diabetic rats (**Figures 1C, D**). These data indicated that harmine can ameliorate learning and memory impairments induced by diabetes.

Harmine Reduces NLRP3 Inflammasome Activation in STZ-Induced Diabetic Rats

Next, we aimed to evaluate the effect of harmine on the nucleotide-binding oligomerization domain-containing protein (NOD)-like receptor family, pyrin domain containing 3 (NLRP3) inflammasome activation in STZ-induced diabetic rats. As shown in **Figures 2A, C**, the levels of major NLRP3 inflammasome components and effectors, including the NLRP3 receptor and the adaptor protein apoptosis-associated speck-like

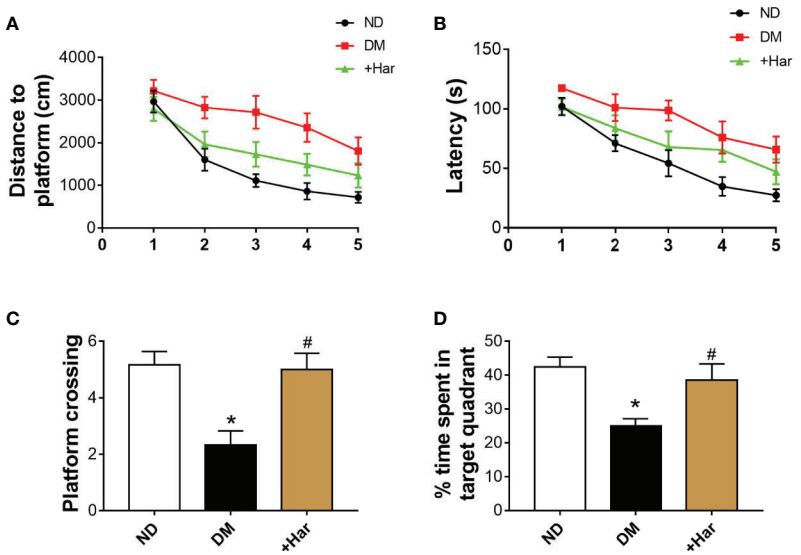

FIGURE 1 | Harmine ameliorates learning and memory impairments in streptozotocin (STZ)–induced diabetic rats. **(A)** Distances to platform in the different groups on day 1 to day 5 were compared (ANOVA: Day 1: $P = 0.535$; Day 2: $P = 0.18$; Day 3: $P = 0.005$; Day 4: $P = 0.005$; Day 5: $P = 0.031$). **(B)** Latencies for the rats in the different groups to reach the platform on day 1 to day 5 were compared (ANOVA: Day 1: $P = 0.127$; Day 2: $P = 0.133$; Day 3: $P = 0.034$; Day 4: $P = 0.041$; Day 5: $P = 0.034$). **(C)** The number of platform crossings in target quadrant in the probe trial. n = 6 in each group. $^{*}P < 0.05$ vs sham, $^{\#}P < 0.05$ vs DM. **(D)** The percentage of time spent in target quadrant in the probe trial. n = 6 rats in each group. $^{*}P < 0.05$ vs sham, $^{\#}P < 0.05$ vs DM. DM, diabetes mellitus; Har, harmine; ND, non-diabetes.

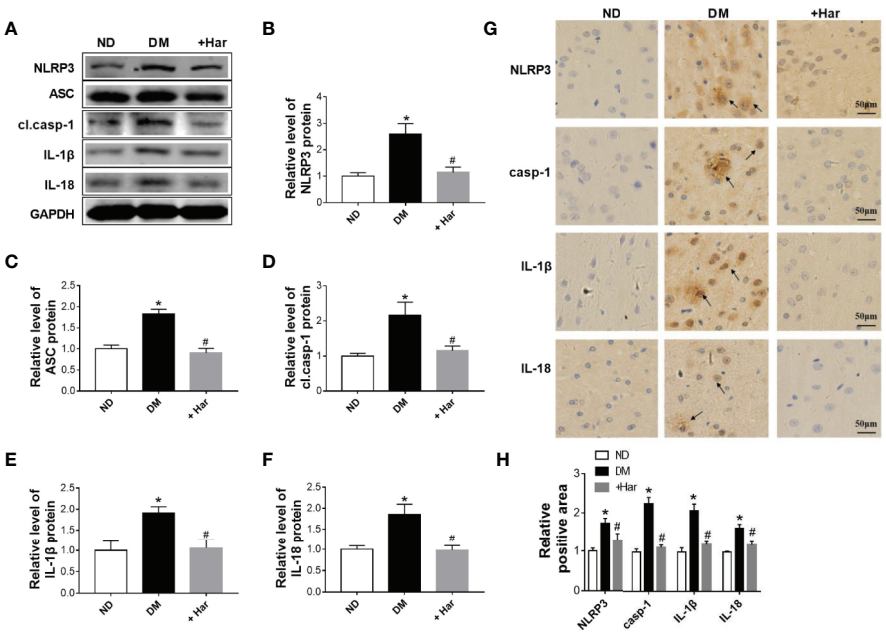

FIGURE 2 | The effect of harmine on the NLRP3 inflammasome in streptozotocin (STZ)–induced diabetic rats. **(A–F)** Western blot analysis of NLRP3, ASC, cl.casp-1, IL-1β, and IL-18 levels in the cortex of STZ-induced diabetic rats after harmine administration. Western blot images **(A)** and related histograms **(B–F)**. n =3 in each group. $^{*}P < 0.05$ vs sham, $^{\#}P < 0.05$ vs DM. **(G)** Immunohistochemical staining analysis showed that harmine reduced the expression of NLRP3, casp-1, IL-1β, and IL-18 in the cortex of diabetic rats. **(H)** Histogram of the data in G. DM, diabetes mellitus; casp-1, caspase-1; cl. casp-1, cleaved caspase-1; Har, harmine; ND, non-diabetes.

protein (ASC), were significantly increased in the brains of the diabetic rats compared with the ND rats. Moreover, NLRP3 inflammasome activation was observed in the diabetic rats, as demonstrated by higher levels of cleaved caspase-1, interleukin (IL)-1β, and IL-18. Importantly, we found that these changes were markedly reversed by harmine administration (**Figures 2A, D–F**). Moreover, immunohistochemical analysis further confirmed that the levels of the NLRP3 receptor, caspase-1, IL-1β, and IL-18 were significantly decreased by harmine treatment (**Figures 2G, H**). These results suggested that harmine can inhibit NLRP3 inflammasome activation in STZ-induced diabetic rats.

Effect of Harmine on NLRP3 Inflammasome Activation in HG-Treated SH-SY5Y Cells

To further observe the function of harmine on NLRP3 inflammasome activation, western blotting and immunofluorescence were used to assess changes in the NLRP3 inflammasome in high glucose (HG)-treated neuronal cells treated with or without harmine. As shown in **Figures 3A–C**, the expression of NLRP3 and ASC was found to be markedly higher in the HG-treated cells than in the control cells, and this increase in expression was reversed by harmine treatment. Moreover, HG conditions significantly upregulated cleaved caspase-1, IL-1β, and IL-18 levels. However, this effect was blocked by harmine treatment (**Figures 3A, D–F**). A similar change in NLRP3 was also observed by immunofluorescence (**Figures 3G, H**). These results suggested that harmine can inhibit NLRP3 inflammasome activation in HG-treated neuronal cells.

Harmine Significantly Enhances BDNF/TrkB Signaling Both *In Vivo* and *In Vitro*

Previous studies have shown that BDNF/TrkB signaling is involved in the progression of diabetes-induced cognitive dysfunction. To determine the effect of harmine on BDNF/TrkB signaling, we measured the changes in BDNF and TrkB in the different groups. The results showed that STZ injection significantly reduced the level of BDNF in the brains of rats, and that this effect was reversed by harmine treatment (**Figures 4A, B**). As shown in **Figure 4C**, the level of phosphorylated TrkB (p-TrkB) was also lower in the DM group than in the ND group. However, the harmine-treated rats exhibited a higher level of p-TrkB than the DM rats.

In addition, we detected the effect of harmine on BDNF/TrkB signaling *in vitro*. Using western blotting, we found that the level of BDNF was much lower in the HG-treated cells than in the control cells, and was upregulated by harmine treatment (**Figure 5A**). Similar changes in BDNF were also observed by immunofluorescence (**Figures 5B, C**). Furthermore, we observed that the harmine-treated cells exhibited a higher level of p-TrkB than the HG-treated cells (**Figure 5D**). These data demonstrated that harmine can enhance the BDNF/TrkB signaling pathway both *in vivo* and *in vitro*.

DISCUSSION

The present study is the first to demonstrate that harmine can attenuate cognitive dysfunction in STZ-induced diabetic rats. Moreover, harmine was found to inhibit NLRP3 inflammasome

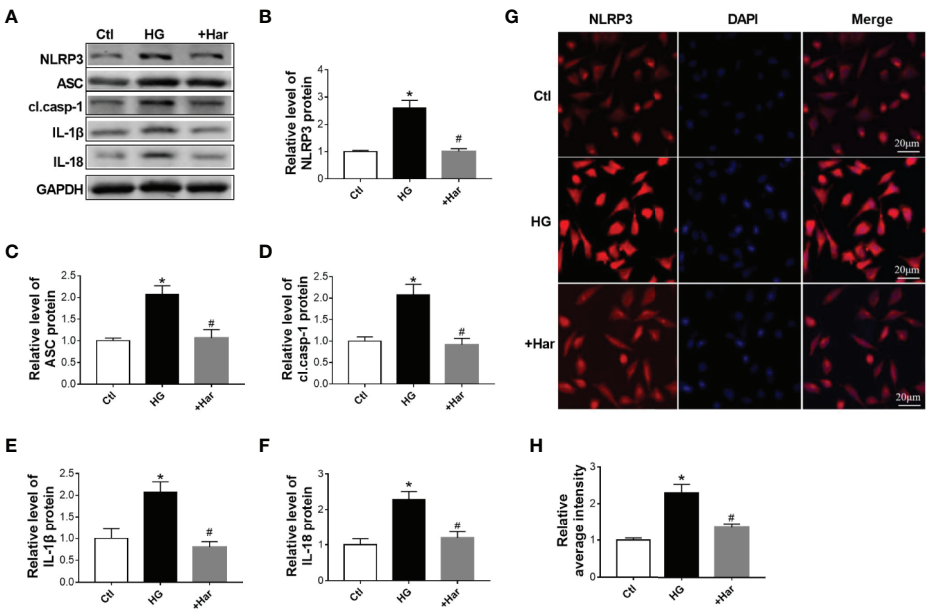

FIGURE 3 | The effect of harmine on the NLRP3 inflammasome in high glucose (HG)–treated cells. **(A–F)** Western blot analysis of NLRP3, ASC, cl. casp-1, IL-1β, and IL-18 levels in HG-treated SH-SY5Y cells after harmine administration. Western blot images **(A)** and related histograms **(B–F)**. $^{*}P < 0.05$ vs sham, $^{\#}P < 0.05$ vs HG. The data are presented as the mean ± SEM of 4 batches of cells per group. **(G)** Representative images showing staining for NLRP3 (red) and DAPI (blue) after exposure to harmine. **(H)** Histogram of the data in G. HG, high glucose; casp-1, caspase-1; cl. casp-1, cleaved caspase-1; Har, harmine.

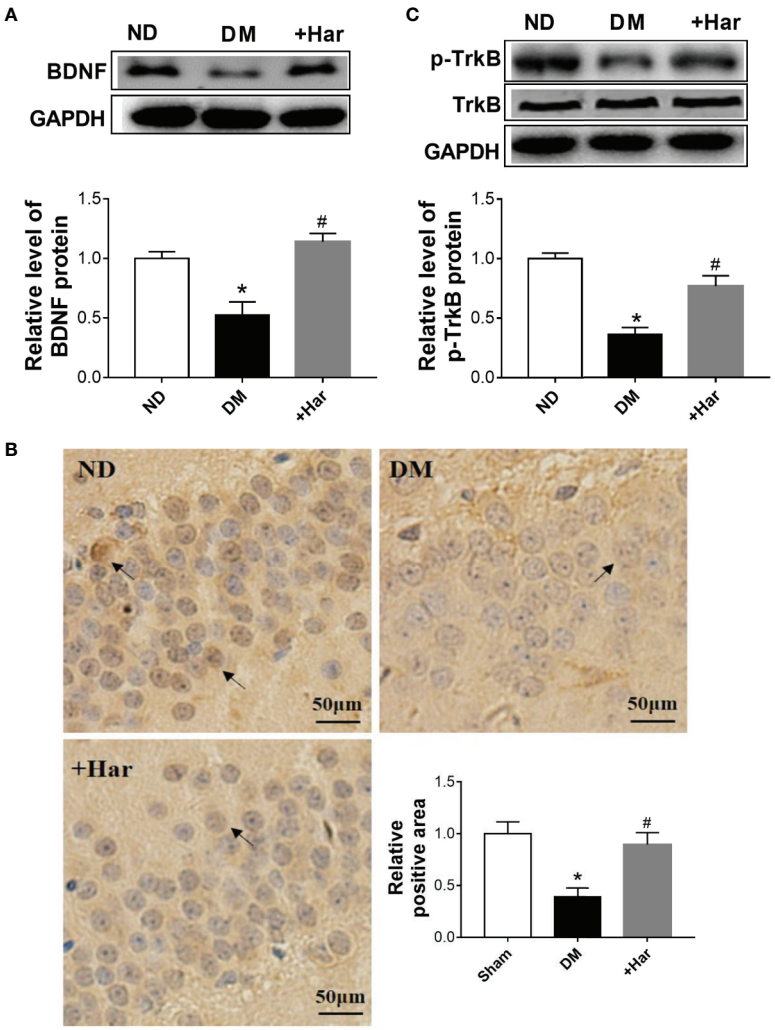

FIGURE 4 | The effect of harmine on brain-derived neurotrophic factor (BDNF)/TrkB in vivo. **(A)** Harmine increased the level of BDNF in the cortex of streptozotocin (STZ)–induced diabetic rats, as detected by western blotting. Top, western blot images of BDNF. Bottom, related histogram. n = 3 in each group. $^{*}P < 0.05$ vs sham, $^{\#}P < 0.05$ vs DM. **(B)** Immunohistochemical analysis of BDNF in the hippocampi of diabetic rats after harmine treatment. Lower right panel, quantification of the BDNF-positive area in the brain. **(C)** Western blot analysis of p-TrkB in the cortex of STZ-induced diabetic rats after harmine treatment. Top, western blot images. Bottom, related histogram. n = 3 in each group. $^{*}P < 0.05$ vs sham, $^{\#}P < 0.05$ vs DM. DM, diabetes mellitus; Har, harmine; p-TrkB, phosphorylated TrkBl; ND, non-diabetes.

activation and enhance the BDNF/TrkB signaling pathway in both STZ-induced diabetic rats and HG-treated neuronal cells.

Recently, studies have demonstrated a strong relationship between DM and dementia. Aging, hyperglycemia, insulin resistance, and inflammation are considered common pathogenic factors for DM and dementia. For example, hyperglycemia has been implicated as an important factor in neuronal cell death, synaptic plasticity dysfunction, and learning and memory impairment (Chen et al., 2019). Insulin resistance is involved in the progression of cognitive dysfunction through promoting Aβ accumulation and tau aggregation. Moreover, growing evidence suggests that inflammation plays a vital role in the relationship between DM and dementia. It has been found that the levels of inflammation-related markers, such as IL-1β, IL-18, and IL-6, are increased in both DM and dementia patients. Notably, IL-1β has been found to be associated with Aβ accumulation, tau hyperphosphorylation, β cell proliferation, and insulin secretion (Boni-Schnetzler et al., 2018; Li et al., 2020). It is widely acknowledged that NLRP3 inflammasome activation contributes to DM and dementia by triggering IL-1β maturation. NLRP3 inflammasome activation along with cognitive dysfunction has been observed in diabetic mice (Zhai et al., 2018). NLRP3 inflammasome inhibition improves cognitive dysfunction in diabetic rats following stroke (Ward et al., 2019). HG conditions can induce NLRP3 inflammasome activation in HT22 cells (Ward and Ergul, 2016). Concordant with previous findings, we found that the NLRP3 inflammasome was more strongly activated in the brains of the diabetic rats than the ND rats, as evidenced by the increased concentrations of NLRP3, ASC, caspase-1, IL-1β, and IL-18. Importantly, harmine

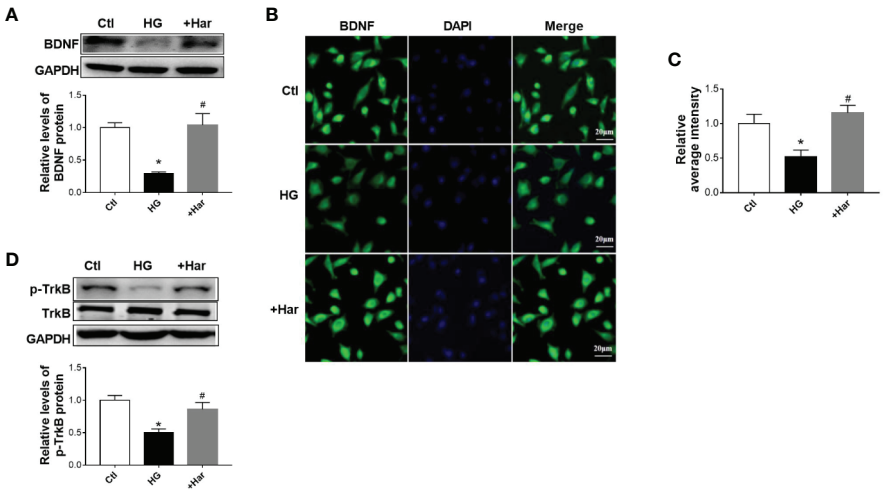

FIGURE 5 | The effect of harmine on brain-derived neurotrophic factor (BDNF)/TrkB in vitro. **(A)** Harmine increased the level of BDNF in HG-treated cells, as detected by western blotting. Top, western blot images. Bottom, related histogram. n =3 in each group. $^{*}P < 0.05$ vs control, $^{\#}P < 0.05$ vs HG. **(B)** Immunohistochemical staining analysis showing the expression of BDNF. **(C)** Histogram of the data in B. **(D)** Western blot analysis of p-TrkB in SH-SY5Y cells exposed to HG conditions. Top, western blot images. Bottom, related histogram. n =3 in each group. $^{*}P < 0.05$ vs control, $^{\#}P < 0.05$ vs HG. HG, high glucose; Har, harmine; p-TrkB, phosphorylated TrkB.

administration significantly inhibited NLRP3 inflammasome activation and improved cognitive dysfunction in the diabetic rats. We also observed that HG conditions induced NLRP3 inflammasome activation and IL-1β and IL-18 maturation in SH-SY5Y neuronal cells, and that this effect was also blocked by harmine treatment. These results thus demonstrate that harmine exerts a neuroprotective effect by influencing the NLRP3 inflammasome both *in vivo* and *in vitro*.

The neurotrophic factor brain-derived neurotrophic factor (BDNF)/TrkB signaling pathway contributes to neuronal migration, neuronal survival, synaptic plasticity, and memory (Carabalona et al., 2016; Tomassoni-Ardori et al., 2019). Decreased levels of BDNF and TrkB are observed in rats with diabetes-induced cognitive dysfunction. However, enhancement of the BDNF/TrkB pathway alleviates cognitive impairment in diabetic rats (Yang and Gao, 2017) and protects against neuronal apoptosis and synaptic plasticity dysfunction under HG conditions (Zhong et al., 2019). Recent studies have established a link between the NLRP3 inflammasome and BDNF. IL-1β can suppress BDNF-dependent synaptic plasticity and cognitive decline through disturbing the BDNF signaling pathway (Tapia-Arancibia et al., 2008; Tong et al., 2012). Notably, NLRP3 inflammasome inhibition can upregulate BDNF expression by suppressing IL-1β (Fu et al., 2020). Consistent with previous studies, our data showed that BDNF levels were downregulated by DM, and upregulated by harmine administration. In addition, TrkB (BDNF receptor) levels were reduced in the diabetic group than in the control group. Importantly, harmine administration inhibited the NLRP3 inflammasome, significantly enhanced the BDNF/TrkB signaling pathway and ameliorated cognitive dysfunction in diabetic rats.

Our study provides evidence to show that harmine can mitigate cognitive impairment in STZ-induced diabetic rats and exert neuroprotective effects through inhibiting NLRP3 inflammasome activation and enhancing the BDNF/TrkB signaling pathway. We thus provide novel insight and potential targets for diabetes-induced cognitive dysfunction.

DATA AVAILABILITY STATEMENT

All datasets generated for this study are included in the article/supplementary material.

ETHICS STATEMENT

All animal procedures in the current study were performed in accordance with the guidelines of the Institutional Animal Care and Use Committee of Harbin Medical University (No. SYDW 2019-123).

AUTHOR CONTRIBUTIONS

LM and HC were responsible for study design, analysis, and article writing. PL and MY performed the animal experiments. PL, YW, YL, and HL performed the experiments *in vitro*. LM, HC, and XS revised the manuscript.

FUNDING

This work was supported by the National Natural Science Foundation of China (81600935), the China Postdoctoral Science Foundation (2017M621308), and the Natural Science Foundation of Heilongjiang Province (QC2017108), and the Major Program of Natural Science Foundation of Heilongjiang Province (ZD2018017).

REFERENCES

Ahmed, M. E., Iyer, S., Thangavel, R., Kempuraj, D., Selvakumar, G. P., Raikwar, S. P., et al. (2017). Co-Localization of Glia Maturation Factor with NLRP3 Inflammasome and Autophagosome Markers in Human Alzheimer's Disease Brain. *J. Alzheimers Dis.* 60, 1143–1160. doi: 10.3233/JAD-170634

Boni-Schnetzler, M., Hauselmann, S. P., Dalmas, E., Meier, D. T., Thienel, C., Traub, S., et al. (2018). β Cell-Specific Deletion of the IL-1 Receptor Antagonist Impairs β Cell Proliferation and Insulin Secretion. *Cell Rep.* 22, 1774–1786. doi: 10.1016/j.celrep.2018.01.063

Carabalona, A., Hu, D. J., and Vallee, R. B. (2016). KIF1A inhibition immortalizes brain stem cells but blocks BDNF-mediated neuronal migration. *Nat. Neurosci.* 19, 253–262. doi: 10.1038/nn.4213

Che, H., Wang, Y., Li, H., Li, Y., Sahil, A., Lv, J., et al. (2020). Melatonin alleviates cardiac fibrosis via inhibiting lncRNA MALAT1/miR-141-mediated NLRP3 inflammasome and TGF-beta1/Smads signaling in diabetic cardiomyopathy. *FASEB J.* 34, 5282–5298. doi: 10.1096/fj.201902692R

Chen, Z., Guo, H., Lu, Z., Sun, K., and Jin, Q. (2019). Hyperglycemia aggravates spinal cord injury through endoplasmic reticulum stress mediated neuronal apoptosis, gliosis and activation. *BioMed. Pharmacother.* 112, 108672. doi: 10.1016/j.biopha.2019.108672

Chornenkyy, Y., Wang, W. X., Wei, A., and Nelson, P. T. (2019). Alzheimer's disease and type 2 diabetes mellitus are distinct diseases with potential overlapping metabolic dysfunction upstream of observed cognitive decline. *Brain Pathol.* 29, 3–17. doi: 10.1111/bpa.12655

Ding, Y., He, J., Huang, J., Yu, T., Shi, X., Zhang, T., et al. (2019). Harmine induces anticancer activity in breast cancer cells via targeting TAZ. *Int. J. Oncol.* 54, 1995–2004. doi: 10.3892/ijo.2019.4777

Dirice, E., Walpita, D., Vetere, A., Meier, B. C., Kahraman, S., Hu, J., et al. (2016). Inhibition of DYRK1A Stimulates Human beta-Cell Proliferation. *Diabetes* 65, 1660–1671. doi: 10.2337/db15-1127

Du, S. Q., Wang, X. R., Zhu, W., Ye, Y., Yang, J. W., Ma, S. M., et al. (2018). Acupuncture inhibits TXNIP-associated oxidative stress and inflammation to attenuate cognitive impairment in vascular dementia rats. *CNS Neurosci. Ther.* 24, 39–46. doi: 10.1111/cns.12773

Duarte, A. I., Candeias, E., Alves, I. N., Mena, D., Silva, D. F., Machado, N. J., et al. (2020). Liraglutide Protects Against Brain Amyloid-beta1-42 Accumulation in Female Mice with Early Alzheimer's Disease-Like Pathology by Partially Rescuing Oxidative/Nitrosative Stress and Inflammation. *Int. J. Mol. Sci.* 21, E1746. doi: 10.3390/ijms21051746

Fox, D., Mathur, A., Xue, Y., Liu, Y., Tan, W. H., Feng, S., et al. (2020). Bacillus cereus non-haemolytic enterotoxin activates the NLRP3 inflammasome. *Nat. Commun.* 11, 760. doi: 10.1038/s41467-020-14534-3

Fu, Q., Li, J., Qiu, L., Ruan, J., Mao, M., Li, S., et al. (2020). Inhibiting NLRP3 inflammasome with MCC950 ameliorates perioperative neurocognitive disorders, suppressing neuroinflammation in the hippocampus in aged mice. *Int. Immunopharmacol.* 82, 106317. doi: 10.1016/j.intimp.2020.106317

He, D., Wu, H., Wei, Y., Liu, W., Huang, F., Shi, H., et al. (2015). Effects of harmine, an acetylcholinesterase inhibitor, on spatial learning and memory of APP/PS1 transgenic mice and scopolamine-induced memory impairment mice. *Eur. J. Pharmacol.* 768, 96–107. doi: 10.1016/j.ejphar.2015.10.037.

Kimura, N. (2016). Diabetes Mellitus Induces Alzheimer's Disease Pathology: Histopathological Evidence from Animal Models. *Int. J. Mol. Sci.* 17, 503. doi: 10.3390/ijms17040503

Korf, E. S., van Straaten, E. C., de Leeuw, F. E., van der Flier, W. M., Barkhof, F., Pantoni, L., et al. (2007). Diabetes mellitus, hypertension and medial temporal lobe atrophy: the LADIS study. *Diabetes Med.* 24, 166–171. doi: 10.1111/j.1464-5491.2007.02049.x

Kumar, A., Haroon, E., Darwin, C., Pham, D., Ajilore, O., Rodriguez, G., et al. (2008). Gray matter prefrontal changes in type 2 diabetes detected using MRI. *J. Magn Reson Imaging.* 27, 14–19. doi: 10.1002/jmri.21224

La Rosa, F., Saresella, M., Marventano, I., Piancone, F., Ripamonti, E., Al-Daghri, N., et al. (2019). Stavudine Reduces NLRP3 Inflammasome Activation and Modulates Amyloid-beta Autophagy. *J. Alzheimers Dis.* 72, 401–412. doi: 10.3233/JAD-181259

Li, S. P., Wang, Y. W., Qi, S. L., Zhang, Y. P., Deng, G., Ding, W. Z., et al. (2018). Analogous beta-Carboline Alkaloids Harmaline and Harmine Ameliorate Scopolamine-Induced Cognition Dysfunction by Attenuating Acetylcholinesterase Activity, Oxidative Stress, and Inflammation in Mice. *Front. Pharmacol.* 9, 346. doi: 10.3389/fphar.2018.00346

Li, Y., Xu, P., Shan, J., Sun, W., Ji, X., Chi, T., et al. (2020). Interaction between hyperphosphorylated tau and pyroptosis in forskolin and streptozotocin induced AD models. *BioMed. Pharmacother.* 121, 109618. doi: 10.1016/j.biopha.2019.109618

Lu, Y., Xiao, G., and Luo, W. (2016). Minocycline Suppresses NLRP3 Inflammasome Activation in Experimental Ischemic Stroke. *Neuroimmunomodulation* 23, 230–238. doi: 10.1159/000452172.

Meng, S., Yang, F., Wang, Y., Qin, Y., Xian, H., Che, H., et al. (2019). Silymarin ameliorates diabetic cardiomyopathy via inhibiting TGF-beta1/Smad signaling. *Cell Biol. Int.* 43, 65–72. doi: 10.1002/cbin.11079

Morris, J. K., Vidoni, E. D., Honea, R. A., and Burns, J. M. (2014). Impaired glycemia increases disease progression in mild cognitive impairment. *Neurobiol. Aging.* 35, 585–589. doi: 10.1016/j.neurobiolaging.2013.09.033

Nie, T., Hui, X., Mao, L., Nie, B., Li, K., Sun, W., et al. (2016). Harmine Induces Adipocyte Thermogenesis through RAC1-MEK-ERK-CHD4 Axis. *Sci. Rep.* 6, 36382. doi: 10.1038/srep36382

Sarkar, S., Malovic, E., Harishchandra, D. S., Ghaisas, S., Panicker, N., Charli, A., et al. (2017). Mitochondrial impairment in microglia amplifies NLRP3 inflammasome proinflammatory signaling in cell culture and animal models of Parkinson's disease. *NPJ Parkinsons Dis.* 3, 30. doi: 10.1038/s41531-017-0032-2.

Song, Y., Kesuma, D., Wang, J., Deng, Y., Duan, J., Wang, J. H., et al. (2004). Specific inhibition of cyclin-dependent kinases and cell proliferation by harmine. *Biochem. Biophys. Res. Commun.* 317, 128–132. doi: 10.1016/j.bbrc.2004.03.019

Sonnen, J. A., Larson, E. B., Brickell, K., Crane, P. K., Woltjer, R., Montine, T. J., et al. (2009). Different patterns of cerebral injury in dementia with or without diabetes. *Arch. Neurol.* 66, 315–322. doi: 10.1001/archneurol.2008.579.

Sun, Y., Ma, C., Sun, H., Wang, H., Peng, W., Zhou, Z., et al. (2020). Metabolism: A Novel Shared Link between Diabetes Mellitus and Alzheimer's Disease. *J. Diabetes Res.* 2020, 4981814. doi: 10.1155/2020/4981814.

Swanson, K. V., Deng, M., and Ting, J. P. (2019). The NLRP3 inflammasome: molecular activation and regulation to therapeutics. *Nat. Rev. Immunol.* 19, 477–489. doi: 10.1038/s41577-019-0165-0.

Tapia-Arancibia, L., Aliaga, E., Silhol, M., and Arancibia, S. (2008). New insights into brain BDNF function in normal aging and Alzheimer disease. *Brain Res. Rev.* 59, 201–220. doi: 10.1016/j.brainresrev.2008.07.007

Tomassoni-Ardori, F., Fulgenzi, G., Becker, J., Barrick, C., Palko, M. E., Kuhn, S., et al. (2019). Rbfox1 up-regulation impairs BDNF-dependent hippocampal LTP by dysregulating TrkB isoform expression levels. *Elife* 8, e49673. doi: 10.7554/eLife.49673

Tong, L., Prieto, G. A., Kramar, E. A., Smith, E. D., Cribbs, D. H., Lynch, G., et al. (2012). Brain-derived neurotrophic factor-dependent synaptic plasticity is suppressed by interleukin-1beta via p38 mitogen-activated protein kinase. *J. Neurosci.* 32, 17714–17724. doi: 10.1523/JNEUROSCI.1253-12.2012

Ward, R., and Ergul, A. (2016). Relationship of endothelin-1 and NLRP3 inflammasome activation in HT22 hippocampal cells in diabetes. *Life Sci.* 159, 97–103. doi: 10.1016/j.lfs.2016.02.043

Ward, R., Li, W., Abdul, Y., Jackson, L., Dong, G., Jamil, S., et al. (2019). NLRP3 inflammasome inhibition with MCC950 improves diabetes-mediated cognitive impairment and vasoneuronal remodeling after ischemia. *Pharmacol. Res.* 142, 237–250. doi: 10.1016/j.phrs.2019.01.035.

White, C. S., Lawrence, C. B., Brough, D., and Rivers-Auty, J. (2017). Inflammasomes as therapeutic targets for Alzheimer's disease. *Brain Pathol.* 27, 223–234. doi: 10.1111/bpa.12478.

Wu, L. W., Zhang, J. K., Rao, M., Zhang, Z. Y., Zhu, H. J., and Zhang, C. (2019). Harmine suppresses the proliferation of pancreatic cancer cells and sensitizes pancreatic cancer to gemcitabine treatment. *Onco Targets Ther.* 12, 4585–4593. doi: 10.2147/OTT.S205097.

Yang, Y., and Gao, L. (2017). Celecoxib Alleviates Memory Deficits by Downregulation of COX-2 Expression and Upregulation of the BDNF-TrkB Signaling Pathway in a Diabetic Rat Model. *J. Mol. Neurosci.* 62, 188–198. doi: 10.1007/s12031-017-0922-0.

Yu, Z. W., Zhang, J., Li, X., Wang, Y., Fu, Y. H., and Gao, X. Y. (2020). A new research hot spot: The role of NLRP3 inflammasome activation, a key step in pyroptosis, in diabetes and diabetic complications. *Life Sci.* 240, 117138. doi: 10.1016/j.lfs.2019.117138.

Zhai, Y., Meng, X., Ye, T., Xie, W., Sun, G., and Sun, X. (2018). Inhibiting the NLRP3 Inflammasome Activation with MCC950 Ameliorates Diabetic Encephalopathy in db/db Mice. *Molecules* 23, E522. doi: 10.3390/molecules23030522.

Zhang, D. A., Lam, V., Chu, V., and Li, M. (2018). Type 2 Diabetes with Comorbid Depression in Relation to Cognitive Impairment: an Opportunity for Prevention? *Mol. Neurobiol.* 55, 85–89. doi: 10.1007/s12035-017-0719-8.

Zhong, Y., Zhu, Y., He, T., Li, W., Li, Q., and Miao, Y. (2019). Brain-derived neurotrophic factor inhibits hyperglycemia-induced apoptosis and downregulation of synaptic plasticity-related proteins in hippocampal neurons via the PI3K/Akt pathway. *Int. J. Mol. Med.* 43, 294–304. doi: 10.3892/ijmm.2018.3933

Conflict of Interest: The authors declare that the research was conducted in the absence of any commercial or financial relationships that could be construed as a potential conflict of interest.

frontiers in Pharmacology

ORIGINAL RESEARCH
published: 14 May 2020
doi: 10.3389/fphar.2020.00690

Neuroprotective Effect of Catalpol *via* Anti-Oxidative, Anti-Inflammatory, and Anti-Apoptotic Mechanisms

Chunjing Yang[1,2,3], *Zhengyuan Shi*[1,2,3], *Longtai You*[4], *Yuanyuan Du*[4], *Jian Ni*[5]* *and Dan Yan*[1,2,3]*

[1] Department of Pharmacy, Beijing Shijitan Hospital, Capital Medical University, Beijing, China, [2] Beijing Key Laboratory of Bio-characteristic Profiling for Evaluation of Rational Drug Use, Beijing, China, [3] International Cooperation & Joint Laboratory of Bio-characteristic Profiling for Evaluation of Rational Drug Use, Beijing, China, [4] School of Chinese Materia Medica, Beijing University of Chinese Medicine, Beijing, China, [5] Beijing Research Institute of Chinese Medicine, Beijing University of Chinese Medicine, Beijing, China

OPEN ACCESS

Edited by:
Touqeer Ahmed,
National University of Sciences & Technology, Pakistan

Reviewed by:
Ravinder Kaundal,
Icahn School of Medicine at Mount Sinai, United States
Rajesh Ramasamy,
Universiti Putra Malaysia, Malaysia

***Correspondence:**
Jian Ni
njtcm@263.net
Dan Yan
pharmsci@126.com

Specialty section:
This article was submitted to Neuropharmacology, a section of the journal Frontiers in Pharmacology

Received: 06 November 2019
Accepted: 27 April 2020
Published: 14 May 2020

Citation:
Yang C, Shi Z, You L, Du Y, Ni J and Yan D (2020) Neuroprotective Effect of Catalpol via Anti-Oxidative, Anti-Inflammatory, and Anti-Apoptotic Mechanisms. Front. Pharmacol. 11:690. doi: 10.3389/fphar.2020.00690

Neuroinflammation and neuro-oxidative damage are now considered to be key factors in the neurological diseases. Therefore, it is important to study anti-inflammatory and neuroprotective agents. The present study investigated the anti-inflammatory and neuroprotective effects of catalpol (CAT), and the potential molecular mechanisms involved. The findings revealed that CAT markedly downregulated pro-inflammatory mediator nitric oxide (NO) and cytokines, including interleukin (IL)-6 and tumor necrosis factor (TNF)-a in lipopolysaccharide (LPS)-treated BV2 microglial cells. Moreover, CAT significantly decreased the levels of intracellular reactive oxygen species (ROS) and malondialdehyde (MDA), increased superoxide dismutase (SOD) activity and glutathione (GSH) level, reversed apoptosis, and restored mitochondrial membrane potential (MMP) in primary cortical neurons stimulated with hydrogen peroxide (H_2O_2). Furthermore, mechanistic studies showed that CAT inhibited nuclear factor-κB (NF-κB) pathway and p53-mediated Bcl-2/Bax/casaspe-3 apoptotic pathway. Moreover, it targeted the Kelch-like ECH-associated protein 1(Keap1)/Nuclear factor E2-related factor 2 (Nrf2) pathway. In summary, CAT may exert neuroprotective potential by attenuating microglial-mediated neuroinflammatory response through inhibition of the NF-κB signaling pathway. It blocked cortical neuronal oxidative damage by inhibiting p53-mediated Bcl-2/Bax/casaspe-3 apoptosis pathway and regulating Keap1/Nrf2 pathway. These results collectively indicate the potential of CAT as a highly effective therapeutic agent for neuroinflammatory and neuro-oxidative disorders.

Keywords: anti-inflammation, anti-oxidative, catalpol, nuclear factor-κB, Kelch-like ECH-associated protein 1/ Nuclear factor E2-related factor 2

INTRODUCTION

Inhibition of neuroinflammation and neuro-oxidation is a critical action mode in the treatment of neurological diseases such as Alzheimer's disease, Parkinson's disease, and Huntington's disease (Kim et al., 2018; Mesika and Reichmann, 2019). Microglia act as important innate immune cells in the central nervous system (Kim et al., 2017). At rest, microglia are scavengers in the central nervous system to remove damaged neurons and pathogens. However, upon stress and injury, microglia produce neurotoxic molecules, which induce neuronal cell damage and the production of neurodegenerative diseases. Neuron cell membranes have high levels of unsaturated fatty acids, high oxygen consumption, and weak antioxidant defense capacity. Therefore, oxidative stress is extremely susceptible to damage to the nervous system, resulting in neurodegenerative diseases (Islam, 2017; Singh et al., 2019). The cerebral cortex is a superior center that regulates or controls body movement, and is involved in functional roles in cognition, learning, and memory (Frey et al., 1993). Primary cortical neurons are cells extracted from the cerebral cortex. They are one of the major cells in the cerebral cortex. In recent years, a growing number of studies have shown that damage to cortical neurons caused by oxidative stress is involved in the development of many neurological diseases, such as Alzheimer's disease and Parkinson's disease (Dinda et al., 2019; Hajizadeh Moghaddam et al., 2020). Therefore, it has become a novel strategy to find a potential drug with multi-target and multi-pathway neuroprotective effect in the treatment of neurological diseases.

Catalpol (CAT), an iridoid glycoside compound, is isolated from Radix *Rehmanniae*. Numerous studies have suggested that CAT exhibits anti-inflammatory and anti-oxidative effects. *In vitro,* it attenuates hydrogen peroxide (H_2O_2)-induced apoptosis of PC12 cells (Jiang et al., 2004). Moreover, the antioxidant property of CAT has been well studied in gerbils (Li et al., 2004). It has been reported that CAT inhibited the production of free radicals and promoted antioxidant capacity in human umbilical vein endothelial cells (Hu et al., 2010). Studies have also shown that CAT enhanced recovery of cerebral function after cerebral ischemia, through a mechanism involving anti-inflammation (Zhu et al., 2015). However, the anti-neuroinflammatory and anti-oxidative effects of CAT on BV2 microglia and primary cortical neuron cells remain unclear. Therefore, the aim of the present study was to investigate whether CAT could protect BV2 microglia from lipopolysaccharide (LPS)-induced inflammation, and whether it could protect primary cortical neuron cells from H_2O_2-mediated oxidative stress. The oxidative parameters determined in appropriate cell models were reactive oxygen species (ROS), mitochondrial membrane potential (MMP), glutathione (GSH), malondialdehyde (MDA), and superoxide dismutase (SOD), while the inflammatory indices were nitric oxide (NO), tumor necrosis factor (TNF)-α, and interleukin (IL)-6. The chemical structure of CAT is shown in **Figure 1**.

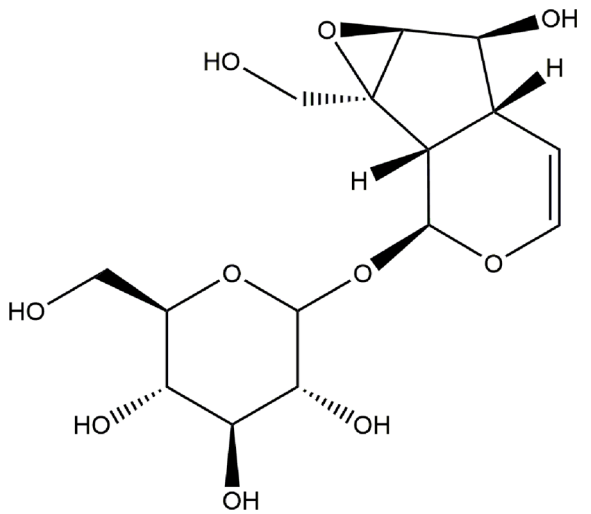

FIGURE 1 | Chemical structure of CAT.

MATERIALS AND METHODS

Drugs and Chemicals

Catalpol (CAT; ≧98% purity) was provided by Shanghai Yuanye Bio-Technology Co. Ltd. (Shanghai, China). Dulbecco's modified eagle's medium/F-12 (DMEM/F-12) and fetal bovine serum (FBS) were bought from Corning (NY, USA). Hanks' balanced salt solution (HBSS), minimum essential medium (MEM), glucose solution, neurobasal medium, B27, L-glutamine, and trypsin were purchased from Life Technologies (NY, USA). Horse serum was bought from Hyclone (Logan, Utah, USA). LPS (from *E. coli,* isotype 055:B5) was obtained from Sigma Chemical Co. (St. Louis, MO, USA), while H_2O_2 was provided by Beijing Chemical Works (Beijing, China). Phosphate buffered saline (PBS), dimethyl sulfoxide (DMSO), and 3-(4, 5 -dimethylthiazol-2-yl)-2, 5-dipheny-ltetrazolium bromide (MTT) were obtained from Solarbio (Beijing, China). NO assay kit was provided by Applygen Co. (Beijing, China). TNF-α and enzyme-linked immunosorbent assay (ELISA) kits for IL-6 were purchased from BOSTER (Wuhan, China). Annexin V-FITC apoptosis, DAPI, ROS, and MMP were supplied by Beyotime (Nanjing, China). MDA, SOD, and GSH were obtained from Jiancheng (Nanjing, China). The antibodies for Bax, Bcl-2, caspase 3, cleaved-caspase 3, p53, Kelch-like ECH-associated protein 1 (Keap1), Nuclear factor E2-related factor 2 (Nrf2), quinone oxidoreductase 1 (NQO1), heme oxygenase-1 (HO-1), and NF-κB p65 and IκB-α and the phosphorylated forms of nuclear factor-κB (NF-κB) p65, IκB-α were products of Cell Signaling Technology (Massachusetts, USA).

BV2 Microglia Cell Culture

The BV2 microglial cells (Chinese Academy of Sciences, Shanghai, China) were cultured in high glucose DMEM/F-12

medium containing 10% heat-inactivated FBS and 1% penicillin (10,000 U/ml) and streptomycin (10,000 μg/ml) in a humidified atmosphere with 5% CO_2 at 37°C

Isolation and Culture of Primary Cortical Neurons

All animal protocols used in this study were approved by the animal Care and Use Committee of the Beijing Shijitan Hospital. Primary cortical neuron cells were obtained from the brain of E14 C57BL/6 mouse embryos bought from SPF Biotechnology Co. Ltd., Beijing, China. Dissected cortical tissue from embryonic 14-day old mouse was minced and incubated with 0.125% trypsin in Ca^{2+}- and Mg^{2+}-free HBSS for about 20 min at 37°C. Then, the trypsin was carefully removed and the plating media (MEM media supplemented with 20% horse serum, 0.5 mM glutamine, 1.35 g glucose, 1% penicillin-streptomycin) was added to re-suspend the cells. Tissue chunks were removed using a 40 μM cell strainer. The single-cell suspension was cultured on poly-D-lysine-coated plates in the plating media. After 4–8 h, the plating media was replaced with the feeding medium i.e. neurobasal medium supplemented with 2% B27, 0.5 mM glutamine, 1% penicillin (10,000 U/ml), and streptomycin (10,000 μg/ml). Half of the medium was aspirated from each well and replaced with fresh feeding medium (warmed to 37°C) every 2 days until the neurons were mature (Beaudoin et al., 2012).

Cell Viability Assay

The effect of CAT on the viabilities of BV2 microglia and primary cortical neurons was determined using MTT assay. The BV2 microglial cells were plated into 96-well plates at a density of 2.0×10^5 cells/ml. After 24 h, the cells were pre-treated for 24 h with CAT at concentrations of 0, 1, 5, 25, 50, and 100 μM. The control was treated with DMSO (0.05%) in place of CAT. After 24 h, 100 μl of MTT working solution (0.5 mg/ml) was added to each well. After 2–4 h, the culture supernatant was replaced with 100 μl of DMSO to dissolve the purple formazan crystals formed. The optical density (OD) of each formazan solution was read at 570 nm in a microplate reader (Thermo, Multiskan GO, USA).

Primary cortical neurons were cultured in 96-well plates at a density of 1.0×10^4 cells/well. On the seventh day, the cells were treated with CAT at concentrations of 0, 12.5, 25, 50, and 100 μM, and also with different concentrations of H_2O_2 for 24 h. Cells in the untreated control received DMSO (0.1%). After 24 h, 100 μl of MTT working solution (0.5 mg/ml) was added to each well. Following incubation for 2–4 h, the culture supernatant was replaced with 100 μl of DMSO to dissolve the resultant purple formazan crystals. The OD of each formazan solution was read at 570 nm in a microplate reader (Thermo, Multiskan GO, USA).

Assay of NO Production

NO production was measured using NO assay kit based on the Griess reaction. The BV2 microglial cells (2.0×10^5 cells/ml) were cultured in 96-well plates and pretreated with CAT for 2 h before treatment with LPS (0.5 μg/ml). After 18 h, NO level was measured in the culture supernatant using the Griess reaction. The OD of the mixture was read at 540 nm in a microplate reader.

ELISA Assays

The effect of CAT on the expressions of TNF-α and IL-6 in the culture supernatant was determined with ELISA kits. In this assay, BV2 microglia were cultured in 96-well plates at a density of 1.0×10^5 cells/ml, and were pretreated with CAT for 2 h before treatment with LPS (0.5 μg/ml). After incubation for 18 h, the expression of TNF-α and IL-6 in the culture supernatant were determined using their corresponding ELISA kits in line with the manufacturers' instructions. The OD of the mixture was read at 450 nm in a microplate reader.

Measurement of Intracellular ROS

ROS are produced at the beginning of the inflammation phase. Therefore, the effect of CAT on intracellular ROS accumulation was measured. The generation of intracellular ROS was determined using DCFH-DA fluorescent dye (Wang and Joseph, 1999). The DCFH-DA probe is a non-polar compound which lightly diffuses into cells, where it is hydrolyzed by intracellular esterase to generate DCFH which is trapped within the cells and becomes intracellularly oxidized to form the highly fluorescent compound 2, 7-dichlorofluorescein (DCF) which is measured flow cytometrically. In this assay, primary cultured cortical neurons were seeded in six-well plates. Following various treatments, the cells were incubated with 10 μM DCFH-DA for 30 min at 37°C in the dark. Subsequently, the cells were harvested, washed twice with PBS, and re-suspended for fluorescence analysis using a flow cytometer.

DAPI Staining

Apoptosis was measured with DAPI staining (Lin et al., 2015). The primary cultured cortical neurons were fixed with 4% paraformaldehyde for 10 min after treatments. Then, the cells were washed with PBS and permeabilized using DAPI staining solution for 5 min. Thereafter, the cells were washed with PBS and examined under fluorescence microscope.

Annexin V-FITC and PI Double Staining

The apoptotic cells in each group were treated with CAT at doses of 12.5, 25, and 50 μM before stimulation with H_2O_2 (50 μM) for 2 h. Then, the apoptotic cells were determined using Annexin V-Alexa FITC detection kit, according to the manufacturer's protocol. Fluorescence was measured with flow cytometry (You et al., 2018).

Assay of MMP

Changes in MMP were determined with JC-1 by measuring red *vs.* green fluorescence (healthy cells with high MMP give out red fluorescence [JC-1-aggregate], while apoptotic/dead cells emit green fluorescence [JC-1-monomer] because of lack of MMP). Primary cultured cortical neurons were cultured in six-well plates and treated with different concentrations of CAT (50, 25, and 12.5 μM) before stimulation with H_2O_2 (50 μM) for 2 h.

The cells were then harvested *via* trypsinization, and washed with PBS. Thereafter, the cells were exposed to JC-1 staining solution, incubated for 20 min at 37°C in a CO_2 incubator, washed with PBS to remove unbound dye, and re-suspended in PBS. The fluorescence intensity was measured with flow cytometry.

Measurement of Levels of GSH, MDA, and SOD

The generation of GSH was determined with GSH assay kit (Jiancheng, Nanjing, China). Primary cultured cortical neurons were cultured in six-well plates and treated with different concentrations of CAT (50, 25, and 12.5 μM) before stimulation with H_2O_2 (50 μM) for 2 h. The cells were then harvested *via* trypsinization, washed with PBS, and broken up using ultrasound cell breaker. The resultant cell suspension was used for measurement of GSH, MDA, and SOD with assay kits, in accordance with the manufacturer's instruction.

Western-Blot

The cells were lysed using RIPA (Beijing Dingguo Changsheng Biotechnology Co. Ltd.). The concentration of total protein in the lysate was determined with bicinchoninic acid (BCA) assay. Protein samples were subjected to 10% SDS–polyacrylamide gel electrophoresis. The proteins were electro-transferred from the gels to PVDF membranes to form blots.

The membranes were blocked with 5% (v/v) dried milk and incubated at 4°C overnight with anti-Bax, anti-Bcl-2, anti-caspase 3, anti-cleaved caspase 3, anti-p53, anti-Keap1, anti-Nrf2, anti-NQO1, anti-HO-1 (Cell Signaling Technology, USA), anti-p-NF-κB p65, anti- NF-κB p65, anti-IκBα, and anti-p-IκBα (Cell Signaling Technology, USA). Thereafter, the membranes were incubated with HRP-conjugated goat anti-mouse IgG for 1 h at room temperature. β-Actin and GAPDH (Cell Signa ling Technology, Inc.) were used as the reference proteins.

Statistical Analysis

Each experiment was repeated at least in triplicate and data were shown as mean ± SD. The data obtained were subjected to statistical analyses using SPSS 17.0 software. Statistical differences were determined with one-way ANOVA and LSD test. Differences were considered significant at $^{*}p < 0.05$, $^{**}p < 0.01$ *vs.* H_2O_2; $^{\#}p < 0.05$, $^{\#\#}p < 0.01$ *vs.* control.

RESULTS

Effect of CAT and H_2O_2 on Cell Viability

Normal primary cortical neurons (**Figure 2**) were used for the next experiments. In order to eliminate experimental errors caused by non-specific cytotoxicity, cell viability testing was carried out. Compared with the control group, CAT at concentrations lower than, or equal to 25 μM had no effect on the viability of BV2 microglia. Thus, CAT was used in subsequent experiments at concentrations of 1, 5, and 25 μM (**Figure 3A**). Moreover, CAT at concentrations lower than, or equal to 50 μM had no effect on the viability of primary cortical neurons. Thus, CAT was used in subsequent studies at concentrations of 12.5, 25, and 50 μM (**Figure 3B**).

The neuronal viabilities were 62 and 27% at H_2O_2 concentrations of 50 and 100 μM, respectively. When the cells were stimulated with 50 μM H_2O_2 for 2 h, they became swollen and rounded, and there were many cell fragments. Moreover, the interwoven cellular network disappeared. The higher the concentrations of H_2O_2, the more the degree of cell death. Therefore, 2 h of stimulation with H_2O_2 (50 μM) was used in subsequent studies (**Figures 3C, D**).

CAT Inhibited LPS-Induced NO, TNFα, and IL-6 Production in BV2 Microglia

In order to study the effect of CAT on LPS-induced inflammatory responses, and the molecular mechanisms

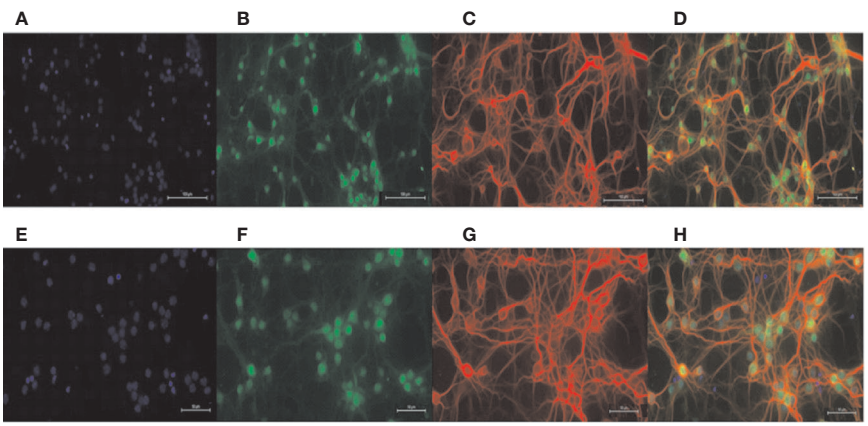

FIGURE 2 | Identification of primary neurons. DAPI staining labeled all nuclei **(A, E)**; NEUN staining labeled primary neuron nuclei **(B, F)**; MAP-2 staining labeled primary neuron dendrites **(C, G)**; merged Figure **(D, H)**. Scale = 100 μM **(A–D)**; scale = 50 μM **(E–H)**.

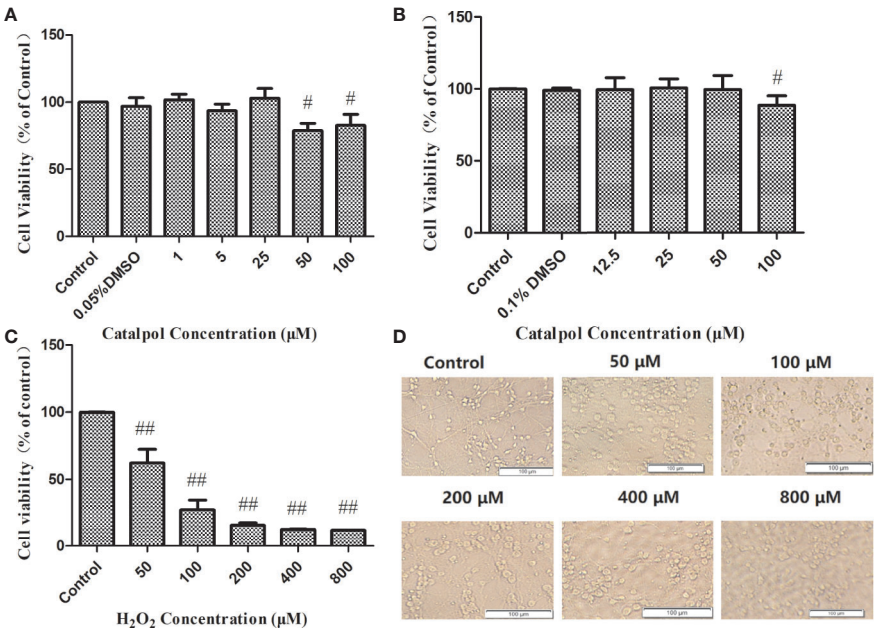

FIGURE 3 | Cell viability of BV2 **(A)** and primary neurons **(B)** treated with CAT in three independent experiments. Cell viability of primary cortical neurons treated with H_2O_2 and the corresponding morphology **(C, D)**. MTT assay data are presented as mean ± SD. ($^{\#}p < 0.05$, $^{\#\#}p < 0.01$ *vs.* Control).

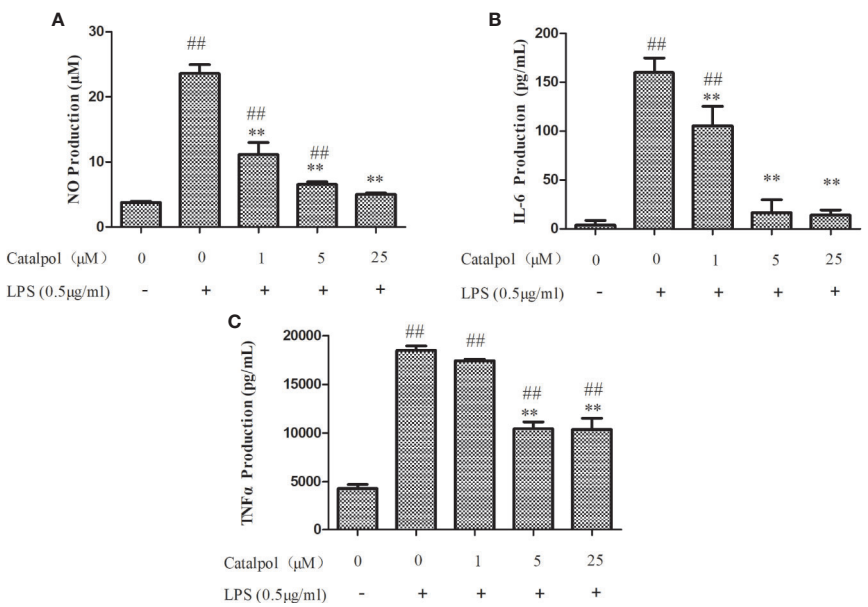

FIGURE 4 | Effect of CAT on levels of NO **(A)**, IL-6 **(B)**, and TNF-α **(C)** in LPS-stimulated BV2 microglial cells. BV2 microglia were pretreated with different concentrations of CAT (1, 5, and 25 μM) for 2 h before treatment with LPS (0.5 μg/ml) for 18 h. Data are presented as mean ± SD of three independent experiments ($^{**}p < 0.01$ *vs*. LPS; $^{\#\#}p < 0.01$ *vs*. control).

involved, the ability of CAT to regulate NO production in response to LPS stimulation was first investigated. The LPS-stimulated group exhibited significantly increased NO production, when compared with the control group. However, as shown in **Figure 4A**, CAT significantly suppressed NO production (11.13, 6.55, and 5.02 μM) at 1, 5, and 25 μM, respectively. Thus, CAT treatment inhibited LPS-induced NO production in a dose-dependent manner (1–25 μM).

Based on inhibitory effect of CAT on NO production, the regulatory effect of CAT on pro-inflammatory cytokines (TNF-α and IL-6) in BV2 microglia was determined. Stimulation with LPS markedly induced the expression of IL-6 in BV2 microglia. In contrast, CAT significantly downregulated IL-6 expression (105.44, 16.88, and 14.17 pg/ml at CAT doses of 1, 5, and 25 μM, respectively; **Figure 4B**). As shown in **Figure 4C**, LPS stimulation markedly increased the expression of TNF-α in BV2 microglia. However, CAT significantly inhibited TNF-α production (10441 and 10359 pg/ml at doses of 5 and 25 μM, respectively). Thus, CAT treatment markedly inhibited LPS-induced expressions of IL-6 and TNF-α, indicating its good ability of anti-inflammatory effect.

CAT Reversed H_2O_2-Induced ROS and MDA Production, and GSH and SOD Reduction

As shown in **Figure 5A**, H_2O_2 stimulation markedly increased the levels of ROS in primary cortical neurons. However, treatment with CAT at doses of 12.5–50 μM led to marked inhibition of H_2O_2-induced expression of ROS ($p < 0.01$), indicating that CAT exerted good anti-oxidative effect.

Figure 5B showed that H_2O_2 significantly increased the expression of MDA, when compared with control group. Treatment with CAT at doses of 25–50 μM CAT significantly decreased the production of MDA ($p < 0.05$, $p < 0.01$). Besides, the level of GSH and SOD activity were markedly lowered after H_2O_2 treatment. However, CAT (25–50 μM) significantly increased GSH level and SOD activity ($p < 0.01$, **Figures 5C, D**).

Effect of CAT on Apoptosis and MMP of Oxidative Stress-Injured Primary Cortical Neurons

As shown in **Figure 6A**, apoptotic cells with aggregation of chromatin and nuclei were observed under a fluorescence microscope following DAPI staining in the H_2O_2 stimulation group. However, after treatment with CAT, the number of apoptotic cells decreased in a dose-dependent manner. The apoptotic cells were quantified using flow cytometry assays. **Figures 6B, C** show that the percentage of apoptotic cells (early and late apoptotic cells) were significantly higher in cells stimulated with H_2O_2, relative to the control group. However, CAT at doses of 25–50 μM, significantly reversed H_2O_2-induced apoptosis in primary cortical neurons ($p < 0.05$).

Quantitative measurement of MMP was done to determine cell death in primary cortical neurons stimulated with H_2O_2. As shown in **Figure 6D**, H_2O_2 significantly induced loss of MMP. However, treatment with CAT (25–50 μM) led to significant reversal of the H_2O_2-induced MMP reduction in primary cortical neurons ($p < 0.05$). Thus, the apoptosis of primary cortical neurons might have been caused by the loss of MMP function.

Effect of CAT on Levels of Nrf2/HO-1 Pathway-Related Proteins in Primary Cortical Neurons

Figure 7 displayed that H_2O_2 markedly decreased the expressions of Nrf2, NQO1, and HO-1, but increased the expression of Keap1 ($p < 0.01$). However, treatment with CAT significantly enhanced

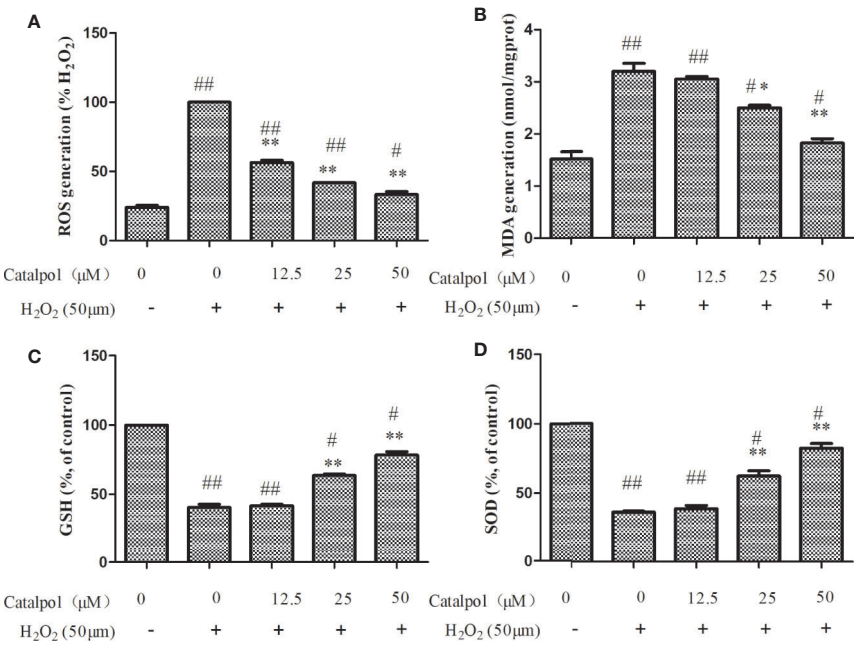

FIGURE 5 | Effect of CAT on levels of ROS **(A)**, MDA **(B)**, GSH **(C)**, and SOD **(D)** in H_2O_2-stimulated primary cortical neurons. Primary cortical neurons were pretreated with different concentrations of CAT (12.5, 25, and 50 μM) before stimulation with H_2O_2 (50 μM) for 2 h. Data are presented as mean ± SD of three independent experiments (*$p < 0.05$,**$p < 0.01$ *vs*. H_2O_2; #$p < 0.05$, ##$p < 0.01$ *vs*. Control).

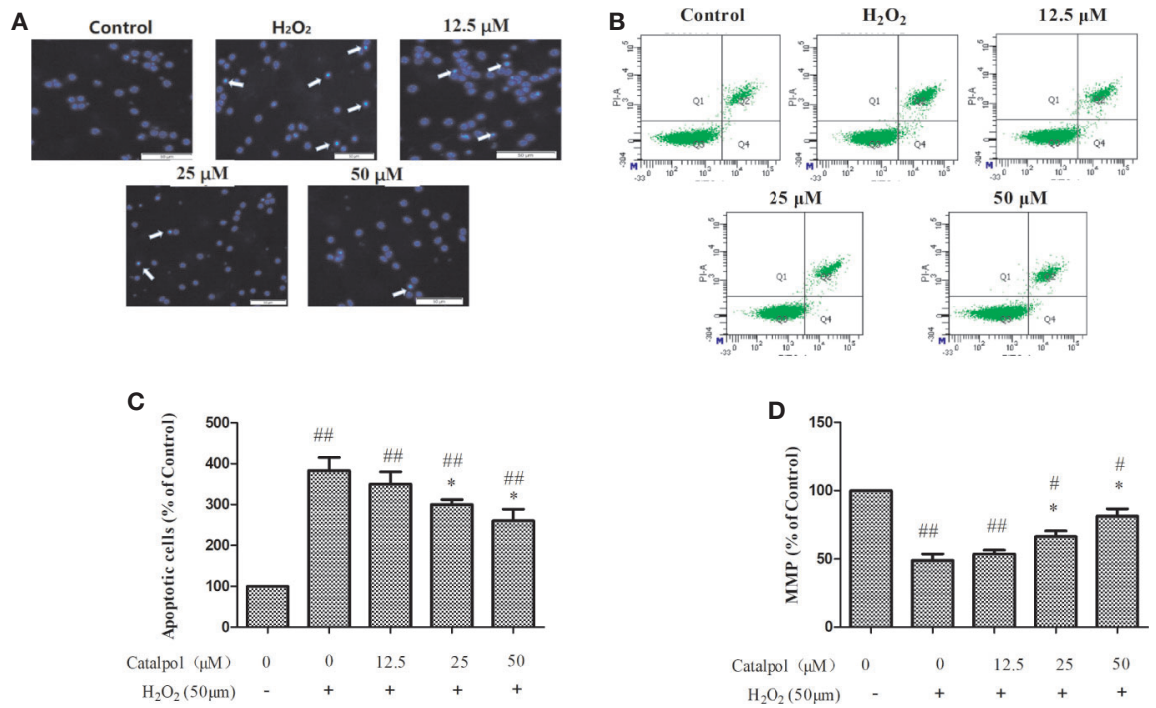

FIGURE 6 | Apoptosis **(A–C)** and MMP **(D)** of H_2O_2-stimulated primary cortical neurons after treatment with CAT (12.5, 25, and 50 μM). Apoptosis was determined using DAPI staining (×50, arrow markers represent the apoptotic cells) and flow cytometry assays. Data are expressed as mean ± SD of three independent experiments (*$p < 0.05$ *vs*. H_2O_2; $^{\#}p < 0.05$, $^{\#\#}p < 0.01$ *vs*. control).

the protein levels of Nrf2, NQO1, and HO-1 ($p < 0.05$, $p < 0.01$), and lowered the protein level of Keap1 ($p < 0.01$).

Effect of CAT on Levels of Apoptosis-Related Proteins in Primary Cortical Neurons

In order to further study the potential mechanism involved in the protection of the primary cortical neurons by CAT, the expressions of apoptosis-related proteins were measured with western blot. Results on **Figure 8** show that H_2O_2 markedly increased the expressions of p53, Bax, and caspase 3, but decreased the expression of Bcl-2 ($p < 0.01$). However, treatment with CAT significantly decreased the protein levels of p53, Bax, and caspase 3 ($p < 0.05$, $p < 0.01$), while the protein level of Bcl-2 was increased ($p < 0.01$). Since caspase 3 cleavage is a better indicator of apoptosis than an increase in total caspase 3, the expression of cleaved-caspase 3 was also assayed. Results showed that H_2O_2 significantly increased the expression of cleaved-caspase 3. However, CAT treatment (12.5, 25, and 50 μM) led to significant downregulations of the expression of cleaved caspase 3 ($p < 0.01$).

Effect of CAT on Levels of NF-κB-Related Proteins in BV2 Microglia

The potential mechanism involved in the protection BV2 microglia by CAT was investigated by assaying the expressions of *NF-κB*-related proteins using western blot. The results (**Figure 9**) showed that LPS markedly upregulated the value of p-IκBα/IκBα and p-p65/p65 ($p < 0.01$). However, treatment with CAT (5 and 25 μM) significantly downregulated the protein expressions of p-IκBα/IκBα and p-p65/p65 ($p < 0.01$).

DISCUSSION

Majority of nerve injuries are caused by complex of biochemical phenomena, such as protein aggregation, reactions of free radicals, glutamate excitotoxicity, inflammation, and oxidative stress. A damage such as nerve cell apoptosis or death is irreversible. It is thought that neuroprotective effects involve mechanisms such as inhibition of inflammation, excitotoxicity, oxidation, neuronal apoptosis, mitochondrial dysfunction, and calcium influx into cells (Tuttolomondo et al., 2015). In addition, neuro-inflammation and neuro-oxidation contribute to several neurodegenerative disorders, such as Parkinson's disease, Attention-deficit hyperactivity disorder, Huntington's disease, and Alzheimer's disease (McGeer and McGeer, 2004; Lopresti, 2015; Leffa et al., 2018; Li et al., 2020). Thus, it is necessary to study drugs that exert anti-oxidative and anti-inflammatory effects.

The complexity of structures in the brain make *in vivo* studies challenging. Cell lines derived from central nervous system

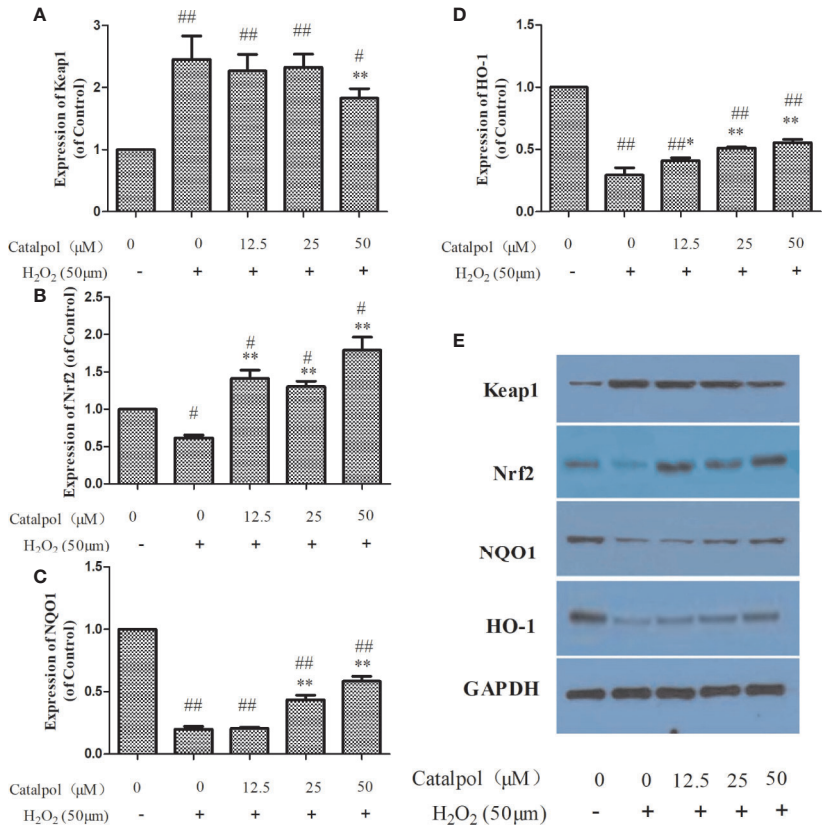

FIGURE 7 | Effect of CAT (12.5, 25, and 50 μM) on the expressions of Keap1, Nrf2, NQO1 and HO-1 in oxidative stress-injured primary cortical neurons. The columns show quantification of Keap1 **(A)**, Nrf2 **(B)**, NQO1 **(C)**, and HO-1 **(D)**. Representative western blot image **(E)** showing the relative expressions of Keap1, Nrf2, NQO1, and HO-1 in the groups. Data are expressed as mean ± SD of three independent experiments (*$p < 0.05$, **$p < 0.01$ *vs.* H_2O_2; #$p < 0.05$, ##$p < 0.01$ *vs.* Control).

precursors have limitations because the neurons derived from these lines fail to reflect the characteristics of central neurons, including the ability to form well-defined axons, dendrites, and synapses. In contrast, the primary cortical neurons reflect these characteristics. They have the advantages of single influencing factors, few interfering factors (such as blood circulation, body fluids, endocrine system, and blood-brain barrier), high repeatability, and ease of analysis of results. Therefore, primary cortical neurons were used as a model for *in vitro* studies (Reis, 2005). In this study, primary cortical neurons were stimulated with H2O2 to establish a cell model of oxidative stress damage. In the process of extracting primary cortical neurons, they become mixed up with many other cells such as astrocytes and vascular endothelial cells. Thus, differential adherence method and B27TM additive without OA were used to purify the cells (Xie et al., 2000). Neuronal cells were identified with double immunofluorescence staining. The results showed that the cell function was normal at the ninth day of culture and could be used for experiments.

SOD and GSH are predominant antioxidants involved in the neutralization of oxygen free radicals (Bose and Agrawal, 2006; Zhao et al., 2013). ROS are active oxygen radicals which directly reflect oxidative stress in cells. MDA reflects the severity of free radical attack, being the end product of lipid peroxidation in cell membranes. Thus, SOD, GSH, ROS, and MDA were used to assess the oxidative stress levels in primary cortical neurons. In this study, CAT increased the production of SOD and GSH, and decreased the production of MDA in H_2O_2-stimulated primary cortical neurons. Similar effects have been reported by other researches (Shu et al., 2016). For example, CAT increased the level of SOD and GSH, and decreased the level of MDA in the spleen and liver of aged mice (Zhang et al., 2008). In addition, results obtained in the present study showed that CAT at a concentration of 12.5 μM significantly reduced ROS levels but not MDA levels. There are two ways through which drugs exert antioxidant effects: direct clearance of free radicals, and production of antioxidant biomolecules, for example GSH and SOD (Paulina et al., 2013). Thus, it is likely that CAT at low concentration directly acted on ROS, but failed to recover the endogenous antioxidant defense system (GSH and SOD), resulting in its failure to significantly reduce the production of MDA. There is a dynamic balance between ROS production and antioxidant defense system in the body. When this balance is impaired, oxidative stress response results. When stimulated with H_2O_2, cells tend to produce excessive ROS, which then cause apoptosis. It is generally

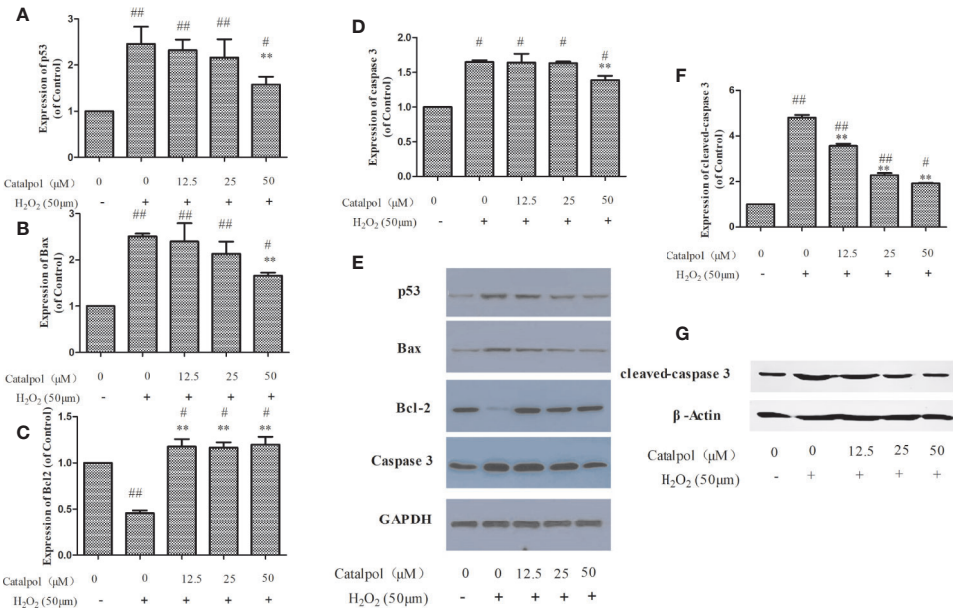

FIGURE 8 | Effect of CAT (12.5, 25, and 50 μM) on the expressions of p53, Bax, Bcl2, caspase 3, and cleaved-caspase 3 in oxidative stress-injured primary cortical neurons. The columns show quantifications of p53 **(A)**, Bax **(B)**, Bcl2 **(C)**, caspase 3 **(D)**, and cleaved-caspase 3 **(F)**. Representative western blot images **(E, G)** show the expressions of p53, Bax, Bcl2, caspase 3, and cleaved-caspase 3 in the groups. Data are expressed as mean ± SD of three independent experiments (**$p < 0.01$ *vs.* H_2O_2; #$p < 0.05$, ##$p < 0.01$ *vs.* control).

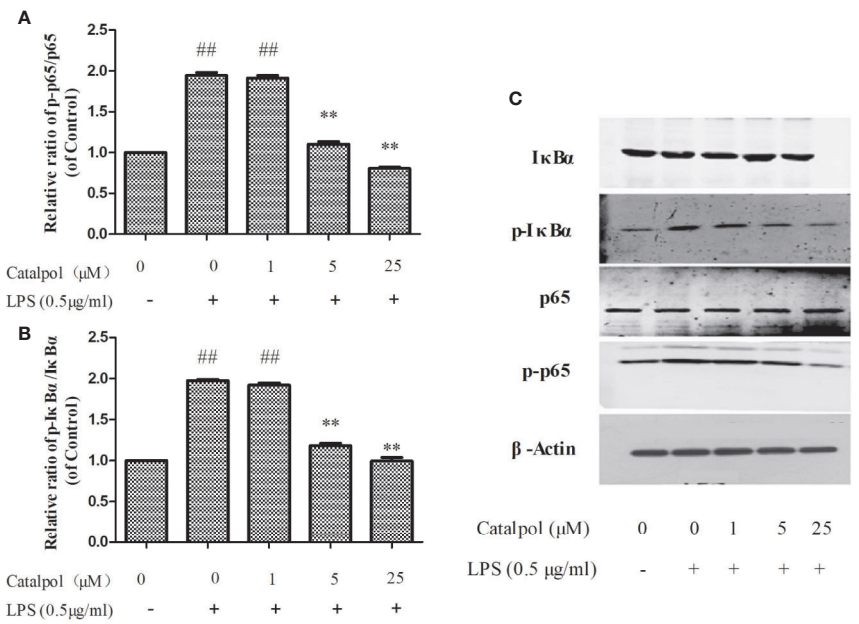

FIGURE 9 | Effect of CAT (1, 5, and 25 μM) on the protein expression of NF-κB in BV2 cells. The columns show levels of p-p65/p65 **(A)** and p-IκBα/IκBα **(B)**. Representative western blot image **(C)** showing the expressions of IκBα, p-IκBα, p65, and p-p65 in all groups. Data are expressed as mean ± SD of three independent experiments (**$p < 0.01$ vs. LPS; ##$p < 0.01$ *vs.* control).

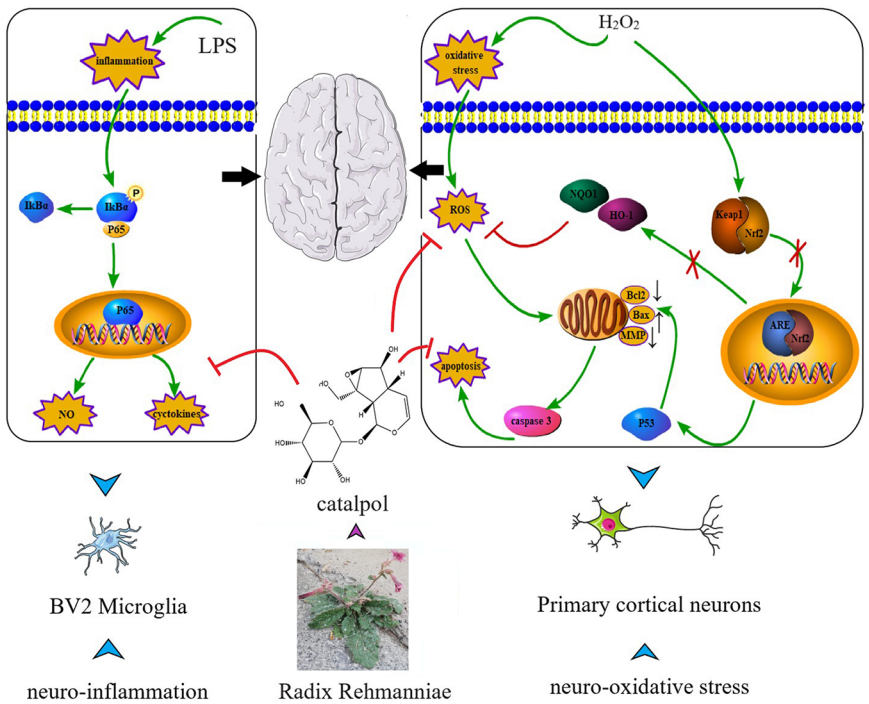

FIGURE 10 | Schematic diagram of the targets of CAT.

believed that there are two mechanisms through which apoptosis may be induced: receptor-mediated pathway (exogenous pathway) and mitochondrial-dependent pathway (endogenous pathway). Mitochondrial-dependent apoptosis begins in the mitochondria and is regulated by endogenous ROS. Excessive ROS may act on different targets in this pathway. For example, ROS damage biomacromolecules in the mitochondrial membrane, leading to decreased MMP and opening of permeability transition pore, thereby deforming the mitochondrion. These events lead to further generation of ROS (a vicious cycle), and ultimately lead to apoptosis (Hanikoglu et al., 2019). The high level of ROS production leads to serious oxidative damage to DNA, activation of p53 and accumulation p53 in the nucleus (Harris and Levine, 2005). It has been reported that P53 induces apoptosis by regulating the expressions of apoptosis-related proteins such as Bcl-2 and Bax (Nkpaa et al., 2019). In normal cells, caspase-3 exists in an inactive state. When the cell is stimulated, caspase-3 is activated by enzymatic cleavage during apoptosis. Cleaved-caspase 3 is a better indicator of apoptosis than an increase in total caspase 3. Thus, the expressions of cleaved-caspase 3 and caspase 3 were determined in this study. Caspase-3 protein is a key downstream enzyme of the apoptotic pathway. It is involved in apoptosis in a variety of pathways, and it is considered to be the core enzyme that induces apoptosis. It was found that CAT inhibited H_2O_2-induced apoptosis of primary cortical neurons by regulating apoptosis-related proteins such as Bcl-2 and Bax. With H_2O_2 stimulation, the protein expressions of p53, Bax, caspase-3, and cleaved-caspase 3 were increased, while the expression of anti-apoptotic protein Bcl-2 was decreased. However, these protein expression profiles were reversed with CAT treatment.

It is known that Nrf2 is a transcription factor which participates in redox homeostasis by regulating the expressions of regulating anti-oxidative genes. It is present in most cell types of the brain, including neuronal cells, and it is a key member of the Keap1/Nrf2 signaling pathway. Indeed, it is likely that Nrf2 signaling is involved in the protection of neurons (Cuadrado et al., 2019). Under resting conditions, Nrf2 binds to cytoplasmic protein Keap1. When oxidative stress occurs, Nrf2 is phosphorylated, separated from Keap1, and transferred from the cytoplasm to the nucleus. Then, Nrf2 binds to the antioxidant response element (ARE) and up-regulates the expressions of NQO1, HO-1 and other factors, thereby exerting its anti-oxidative effect (Jin et al., 2015). In this study, the expression of Keap1 protein in the model group was significantly increased, while the expression of Nrf2 protein was significantly decreased. However, CAT decreased the expression of Keap1 and increased the expression of Nrf2, indicating that regulated the activation of Nrf2. It is also known that activated Nrf2 dissociates from Keap1, and is transferred from the cytoplasm to the nucleus and combines with the ARE to further induce the expression of HO-1, NQO1, and other proteins, thereby exerting anti-oxidative stress effects. Therefore, the Keap1-Nrf2-ARE signaling pathway, or part thereof, is involved in the antioxidant mechanism of CAT.

Microglia have common features with macrophages, and they have been implicated as predominant cells involved in regulation of inflammation-mediated neuronal damage. LPS is

a thick layer of the outer membrane of gram-negative bacteria cell-wall. It plays an important role in chronic inflammation of the brain (Cuschieri and Maier, 2007). Microglia produces inflammatory mediators such as NO, as well as pro-inflammatory cytokines such as TNF-α and IL-6. These neurotoxic products induce neuronal cell damage and the production of nervous system disease (Bachiller et al., 2018; Hansen et al., 2018). In addition, pro-inflammatory cytokines trigger the production of ROS (Higashimoto et al., 2006). In the present study, pretreatment with CAT inhibited LPS-induced productions of NO, TNFα, and IL-6 in BV2 microglia through the NF-κB pathway. The NF-κBp65 is present in the cytoplasm of resting cells, and it combines with inhibitor IκBα. However, IκB protein regulated by IκB kinase complex in the cytoplasm is rapidly phosphorylated and degraded when NF-κB is activated by LPS, resulting in nuclear translocation of NF-κB dimers (Yun et al., 2008). The nuclear translocation of NF-κB dimers is involved in the expressions of genes linked to inflammation and apoptosis. The NF-κB is an important transcription factor which is expressed in brain cells, including neurons, microglia, and astrocytes, and it participates in several brain functions (Oneill and Kaltschmidt, 1997). It has been reported that NO regulates NF-κB transcription (Meffert and Baltimore, 2005). Moreover, it has been shown that CAT inhibited LPS and IFN-γ-induced inflammatory responses in astrocyte primary cultures (Bi et al., 2012). Thus, CAT exhibits neuroprotective effect by inhibiting neuro-inflammation.

Catalpol (CAT) has been studied extensively for its multiple pharmacological activities both *in vitro* and *in vivo*, including anti-diabetic, cardiovascular protective, neuroprotective, anticancer, hepatoprotective, anti-inflammatory, and anti-oxidant effects (Bai et al., 2019; Bhattamisra et al., 2019). Numerous studies have suggested the anti-inflammatory and anti-oxidative effects of CAT, such as in PC12 cells (Jiang et al., 2004), human umbilical vein endothelial cells (Hu et al., 2010), cardiac myocytes (Hu et al., 2016), and animal models of acute ischemic stroke (Zhu et al., 2015; Zheng et al., 2017). Although the pharmacological effects of CAT in the treatment of some diseases have been gradually discovered, its role and underlying mechanism in the treatment of neurological diseases are still unclear. Interestingly, in this study, we observed that CAT (particularly in higher dose) markedly downregulated the levels of NO, IL-6, and TNF-a in lipopolysaccharide (LPS)-treated BV2 microglial cells. Moreover, CAT significantly decreased the levels of ROS and MDA, increased SOD activity and GSH level, reversed apoptosis, and restored MMP in primary cortical neurons stimulated with H_2O_2. More importantly, NF-κB and p53-mediated Bcl-2/Bax/casaspe-3 apoptotic pathways were inhibited by CAT. Keap1/Nrf2 pathway was activated by CAT. These findings conclude that CAT has neuroprotective effect by attenuating microglial-mediated neuroinflammatory response and cortical neuronal oxidative damage (**Figure 10**). Therefore, CAT is a potential drug in the treatment of neurological diseases through activating the multi-signal pathways.

CONCLUSION

The present study has demonstrated the neuroprotective effects of CAT (particularly in higher dose) in attenuating LPS-induced neuroinflammation *via* inhibition of the NF-κB signaling pathway in BV2 microglia, and in H_2O_2-induced oxidative stress through activation of the Nrf2/HO-1 signaling pathway and inactivation p53-mediated Bcl-2/Bax/casaspe-3 apoptosis pathway in primary cortical neurons. Due to the anti –inflammatory, anti-oxidative, and anti-apoptotic effects of CAT in nerve cells, CAT may be a potential agent for the treatment of neurological disease.

DATA AVAILABILITY STATEMENT

All datasets generated for this study are included in the article/ supplementary material.

ETHICS STATEMENT

The Animal Care and Use Committee of the Beijing Shijitan Hospital approved all animal protocols.

AUTHOR CONTRIBUTIONS

JN, DY, and CY designed the research. ZS, LY, and YD performed the experiments. JN, DY, and CY conducted the data analysis. All authors have reviewed and approved the final version of the manuscript.

FUNDING

This work was supported by the Ministry of National Science and Technique (2014ZX09304306) and "Top youth team" of excellent talents in Beijing (2018000021223TD09).

REFERENCES

Bachiller, S., Jiménez-Ferrer, I., Paulus, A., Yang, Y., Swanberg, M., Deierborg, T., et al. (2018). Microglia in Neurological Diseases: A Road Map to Brain-Disease Dependent-Inflammatory Response. *Front. Cell Neurosci.* 12, 488. doi: 10.3389/fncel.2018.00488

Bai, Y., Zhu, R., Tian, Y., Li, R., Chen, B., Zhang, H., et al. (2019). Catalpol in diabetes and its complications: a review of pharmacology, pharmacokinetics, and safety. *Molecules* 24, 3302. doi: 10.3390/molecules24183302

Beaudoin, G. M., Lee, S. H., Singh, D., Yuan, Y., Ng, Y. G., Reichardt, L. F., et al. (2012). Culturing pyramidal neurons from the early postnatal mouse

hippocampus and cortex. *Nat. Protoc.* 7, 1741–1754. doi: 10.1038/nprot.2012.099

Bhattamisra, S. K., Yap, K. H., Rao, V., and Choudhury, H. (2019). Multiple biological effects of an iridoid glucoside, catalpol and its underlying molecular mechanisms. *Biomolecules* 10, 32. doi: 10.3390/biom10010032

Bi, J., Jiang, B., and Zorn, A. (2012). Catalpol inhibits LPS plus IFN-γ-induced inflammatory response in astrocytes primary cultures. *Toxicol. In Vitro.* 27, 543–550. doi: 10.1016/j.tiv.2012.09.023

Bose, K. S., and Agrawal, B. K. (2006). Effect of long term supplementation of tomatoes (cooked) on levels of antioxidant enzymes, lipid peroxidation rate, lipid profile and glycated haemoglobin in Type 2 diabetes mellitus. *West Indian Med. J.* 200655, 274–278. doi: 10.1590/S0043-31442006000400010

Cuadrado, A., Rojo, A. I., and Wells, G. (2019). Therapeutic targeting of the NRF2 and KEAP1 partnership in chronic diseases. *Nat. Rev. Drug discovery.* 18, 295–317. doi: 10.1038/s41573-018-0008-x

Cuschieri, J., and Maier, R. V. (2007). Oxidative stress, lipid rafts, and macrophage reprogramming. *Antioxid. Redox Signal.* 9, 1485–1498. doi: 10.1089/ars.2007.1670

Dinda, B., Dinda, M., Kulsi, G., Chakraborty, A., and Dinda, S. (2019). Therapeutic potentials of plant iridoids in Alzheimer's and Parkinson's diseases: A review. *Eur. J. Med. Chem.* 169, 185–199. doi: 10.1016/j.ejmech.2019.03.009

Frey, U., Huang, Y., and Kandel, E. (1993). Effects of cAMP simulate a late stage of LTP in hippocampal CA1 neurons. *Science.* 260, 1661–1664. doi: 10.1126/science.8389057

Hajizadeh Moghaddam, A., Ahmadnia, H., Jelodar, S. K., and Ranjbar, M. (2020). Hesperetin nanoparticles attenuate anxiogenic-like behavior and cerebral oxidative stress through the upregulation of antioxidant enzyme expression in experimental dementia of Alzheimer's type. *Neurol. Res.* 42, 477–486. doi: 10.1080/01616412.2020.1747716

Hanikoglu, A., Ozben, H., Hanikoglu, F., and Ozben, T. (2019). Hybrid compounds & oxidative stress induced apoptosis in cancer therapy. *Curr. Med. Chem.* 27, 2118–2132. doi: 10.2174/0929867325666180719145819

Hansen, D. V., Hanson, J. E., and Sheng, M. (2018). Microglia Alzheimer's disease. *J. Cell Biol.* 217, 459–472. doi: 10.1083/jcb.201709069

Harris, S. L., and Levine, A. J. (2005). The p53 pathway: positive and negative feedback loops. *Oncogene.* 24, 2899–2908. doi: 10.1038/sj.onc.1208615

Higashimoto, T., Panopoulos, A., Hsieh, C. L., and Zandi, E. (2006). TNFα induces chromosomal abnormalities independent of ROS through IKK, JNK, p38 and caspase pathways. *Cytokine.* 34, 0–50. doi: 10.1016/j.cyto.2006.03.015

Hu, L. A., Sun, Y. K., and Hu, J. (2010). Catalpol inhibits apoptosis in hydrogen peroxide-induced endothelium by activating the PI3K/Akt signaling pathway and modulating expression of Bcl-2 and Bax. *Eur. J. Pharmacol.* 628, 155–163. doi: 10.1016/j.ejphar.2009.11.046

Hu, L. A., Sun, Y. K., Zhang, H. S., Zhang, J. G., and Hu, J. (2016). Catalpol inhibits apoptosis in hydrogen peroxide-induced cardiac myocytes through a mitochondrial-dependent caspase pathway. *Biosci. Rep.* 36, e00348. doi: 10.1042/BSR20160132

Islam, M. T. (2017). Oxidative stress and mitochondrial dysfunction-linked neurodegenerative disorders. *Neurol. Res.* 39, 73–82. doi: 10.1080/01616412.2016.1251711

Jiang, B., Liu, J. H., Bao, Y. M., and An, L. J. (2004). Catalpol inhibits apoptosis in hydrogen peroxide-induced PC12 cells by preventing cytochrome c release and inactivating of caspase cascade. *Toxicon.* 43, 53–59. doi: 10.1016/j.toxicon.2003.10.017

Jin, X., Liu, Q., and Jia, L. (2015). Pinocembrin Attenuates 6-OHDA-induced Neuronal Cell Death Through Nrf2/ARE Pathway in SH-SY5Y Cells. *Cell. Mol. Neurobiol.* 35, 323–333. doi: 10.1007/s10571-014-0128-8

Kim, Y. S., Woo, J., and Lee, C. J. (2017). Decreased glial GABA and tonic inhibition in cerebellum of mouse model for attention-deficit/hyperactivity disorder (ADHD). *Exp. Neurobiol.* 26, 206. doi: 10.5607/en.2017.26.4.206

Kim, N., Do, J., Bae, J. S., Jin, H. K., Kim, J. H., Inn, K. S., et al. (2018). Piperlongumine inhibits neuroinflammation via regulating NF-κB signaling pathways in lipopolysaccharide-stimulated BV2 microglia cells. *J. Pharmacol. Sci.* 137, 195–201. doi: 10.1016/j.jphs.2018.06.004

Leffa, D. T., Torres, I., and Rohde, L. A. (2018). A review on the role of inflammation in attention-deficit/hyperactivity disorder. *Neuroimmunomodulati.* 25, 328–333. doi: 10.1159/000489635

Li, D. Q., Duan, Y. L., Bao, Y. M., Liu, C. P., Liu, Y., and An, L. J. (2004). Neuroprotection of catalpol in transient global ischemia in gerbils. *Neurosci. Res.* 50, 169–177. doi: 10.1016/j.neures.2004.06.009

Li, J. M., Zhao, Y., Sun, Y., and Kong, L. D. (2020). Potential effect of herbal antidepressants on cognitive deficit: pharmacological activity and possible molecular mechanism. *J. Ethnopharmacol.* 257, 112830. doi: 10.1016/j.jep.2020.112830. 112830.

Lin, R., Li, Z. F., Lin, J., Ye, J., Cai, Q., and Chen, L. (2015). Ethanolic extract of Tulipa edulis Bak induces apoptosis in SGC-7901 human gastric carcinoma cells via the mitochondrial signaling pathway. *Oncol. Lett.* 10, 2371. doi: 10.3892/ol.2015.3501

Lopresti, A. L. (2015). Oxidative and nitrosative stress in ADHD: possible causes and the potential of antioxidant-targeted therapies. *Atten. Defic. Hyperact. Disord.* 7, 237. doi: 10.1007/s12402-015-0170-5

McGeer, P. L., and McGeer, E. G. (2004). Inflammation and the degenerative diseases of aging. *Ann. N Y Acad. Sci.* 1035, 104–116. doi: 10.1196/annals.1332.007

Meffert, M. K., and Baltimore, D. (2005). Physiological functions for brain NF-kB. *Trends Neurosci.* 28, 37–43. doi: 10.1016/j.tins.2004.11.002

Mesika, R., and Reichmann, D. (2019). When safeguarding goes wrong: Impact of oxidative stress on protein homeostasis in health and neurodegenerative disorders. *Adv. Protein Chem. Struct. Biol.* 114, 221–264. doi: 10.1016/bs.apcsb.2018.11.001

Nkpaa, K. W., Awogbindin, I. O., and Amadi, B. A. (2019). Ethanol exacerbates manganese-induced neurobehavioral deficits, striatal oxidative stress, and apoptosis via regulation of p53, caspase-3, and bax/bcl-2 ratio-dependent pathway. *Biol. Trace Elem. Res.* 191, 135–148. doi: 10.1007/s12011-018-1587-4

Oneill, L. A. J., and Kaltschmidt, C. (1997). NF-kappa B: A crucial transcription factor for glial and neuronal cell function. *Trends Neurosci.* 20, 252–258. doi: 10.1016/S0166-2236(96)01035-1

Paulina, T., Kai, K., and Janusz, B. (2013). Role of antioxidant enzymes and small molecular weight antioxidants in the pathogenesis of age-related macular degeneration (AMD). *Biogerontology.* 14, 461–482. doi: 10.1007/s10522-013-9463-2

Reis, G. F. (2005). Adenylate cyclase-mediated forms of neuronal plasticity in hippocampal area CA1 are reduced with aging. *J. Neurophysiol.* 93, 3381–3389. doi: 10.1152/jn.00827.2003

Shu, M., Hu, X., and Hung, Z. (2016). Effects of tanshinone IIA on fibrosis in a rat model of cirrhosis through heme oxygenase-1, inflammation, oxidative stress and apoptosis. *Mol. Med. Rep.* 13, 3036–3042. doi: 10.3892/mmr.2016.4886

Singh, A., Kukreti, R., Saso, L., and Kukreti, S. (2019). Oxidative stress: a key modulator in neurodegenerative diseases. *Molecules* 24, 1583. doi: 10.3390/molecules24081583

Tuttolomondo, A., Pecoraro, R., Arnao, V., Maugeri, R., Iacopino, D. G., and Pinto, A. (2015). Developing drug strategies for the neuroprotective treatment of acute ischemic stroke. *Expert. Rev. Neurother.* 15, 1271–1284. doi: 10.1586/14737175.2015.1101345

Wang, H., and Joseph, J. A. (1999). Quantifying cellular oxidative stress by dichlorofluorescein assay using microplate reader. *Free Radic. Biol. Med.* 27, 612–616. doi: 10.1016/s0891-5849(99)00107-0

Xie, C., Markesbery, W. R., and Lovell, M. A. (2000). Survival of hippocampal and cortical neurons in a mixture of MEM+ and B27-supplemented neurobasal medium. *Free Radi. Bio. Med.* 28, 665–672. doi: 10.1016/S0891-5849(99)00268-3

You, L. T., Dong, X. X., Ni, B. R., Fu, J., Yang, C. J., Yin, X. B., et al. (2018). Triptolide Induces Apoptosis Through Fas Death and Mitochondrial Pathways in HepaRG Cell Line. *Front. Pharmacol.* 9, 813. doi: 10.3389/fphar.2018.00813

Yun, K. J., Kim, J. Y., Kim, J. B., Lee, K. W., Jeong, S. Y., Park, H. J., et al. (2008). Inhibition of LPS-induced NO and PGE2 production by asiatic acid via NF-κB inactivation in RAW 264.7 macrophages: possible involvement of the IKK and MAPK pathways. *Int. Immunopharmacol.* 8, 431–441. doi: 10.1016/j.intimp.2007.11.003

Zhang, X. L., Zhang, A. H., Jiang, B., Bao, Y. M., Wang, J. Y., and An, L. J. (2008). Further pharmacological evidence of the neuroprotective effect of catalpol from Rehmannia glutinosa. *Phytomedicine.* 15, 484–490. doi: 10.1016/j.phymed.2008.01.001

Zhao, F., Huang, W., Ousman, T., Zhang, B., Han, Y., Clotaire, D. Z., et al. (2013). Triptolide induces growth inhibition and apoptosis of human Laryngocarcinoma

cells by enhancing p53 activities and suppressing E6-mediated p53 degradation. *PloS One* 8, e80784. doi: 10.1371/journal.pone.0080784

Zheng, X. W., Yang, W. T., Chen, S., Xu, Q. Q., Shan, C. S., Zheng, G. Q., et al. (2017). Neuroprotection of catalpol for experimental acute focal ischemic stroke: preclinical evidence and possible mechanisms of antioxidation, anti-Inflammation, and antiapoptosis. *Oxid. Med. Cell Longev.* 2017, 5058609. doi: 10.1155/2017/5058609

Zhu, J., Chen, X., and Wang, H. (2015). Catalpol protects mice against renal ischemia/reperfusion injury via suppressing PI3K/Akt-eNOS signaling and inflammation. *Int. J. Clin. Exp. Med.* 8, 2038.

Conflict of Interest: The authors declare that the research was conducted in the absence of any commercial or financial relationships that could be construed as a potential conflict of interest.

frontiers in Pharmacology

ORIGINAL RESEARCH
published: 15 May 2020
doi: 10.3389/fphar.2020.00712

Bakuchiol Attenuates Oxidative Stress and Neuron Damage by Regulating Trx1/TXNIP and the Phosphorylation of AMPK After Subarachnoid Hemorrhage in Mice

Haixiao Liu[1,2†], Wei Guo[1†], Hao Guo[1†], Lei Zhao[1], Liang Yue[1], Xia Li[1], Dayun Feng[1], Jianing Luo[1], Xun Wu[1], Wenxing Cui[1] and Yan Qu[1]*

[1] Department of Neurosurgery, Tangdu Hospital, The Fourth Military Medical University, Xi'an, China, [2] Department of Pathology, University of Texas Southwestern Medical Center, Dallas, TX, United States

OPEN ACCESS

Edited by:
Touqeer Ahmed,
National University of Sciences & Technology, Pakistan

Reviewed by:
Budbazar Enkhjargal,
Boston University, United States
Baoliang Sun,
Shandong First Medical University, China

***Correspondence:**
Yan Qu
yanqu0123@fmmu.edu.cn

[†]These authors have contributed equally to this work

Specialty section:
This article was submitted to Neuropharmacology, a section of the journal Frontiers in Pharmacology

Received: 30 January 2020
Accepted: 30 April 2020
Published: 15 May 2020

Citation:
Liu H, Guo W, Guo H, Zhao L, Yue L, Li X, Feng D, Luo J, Wu X, Cui W and Qu Y (2020) Bakuchiol Attenuates Oxidative Stress and Neuron Damage by Regulating Trx1/TXNIP and the Phosphorylation of AMPK After Subarachnoid Hemorrhage in Mice. Front. Pharmacol. 11:712. doi: 10.3389/fphar.2020.00712

Subarachnoid hemorrhage (SAH) is a fatal cerebrovascular condition with complex pathophysiology that reduces brain perfusion and causes cerebral functional impairments. An increasing number of studies indicate that early brain injury (EBI), which occurs within the first 72 h of SAH, plays a crucial role in the poor prognosis of SAH. Bakuchiol (Bak) has been demonstrated to have multiorgan protective effects owing to its antioxidative and anti-inflammatory properties. The present study was designed to investigate the effects of Bak on EBI after SAH and its underlying mechanisms. In this study, 428 adult male C57BL/6J mice weighing 20 to 25 g were observed to investigate the effects of Bak administration in an SAH animal model. The neurological function and brain edema were assessed. Content of MDA/3-NT/8-OHdG/superoxide anion and the activity of SOD and GSH-Px were tested. The function of the blood-brain barrier (BBB) and the protein levels of claudin-5, occludin, zonula occludens-1, and matrix metalloproteinase-9 were observed. TUNEL staining and Fluoro-Jade C staining were conducted to evaluate the death of neurons. Ultrastructural changes of the neurons were observed under the transmission electron microscope. Finally, the roles of Trx, TXNIP, and AMPK in the protective effect of Bak were investigated. The data showed that Bak administration 1) increased the survival rate and alleviated neurological functional deficits; 2) alleviated BBB disruption and brain edema; 3) attenuated oxidative stress by reducing reactive oxygen species, MDA, 3-NT, 8-OHdG, gp91^{phox}, and 4-HNE; increased the activities of SOD and GSH-Px; and alleviated the damage to the ultrastructure of mitochondria; 4) inhibited cellular apoptosis by regulating the protein levels of Bcl-2, Bax, and cleaved caspase-3; and 5) upregulated the protein levels of Trx1 as well as the phosphorylation of AMPK and downregulated the protein levels of TXNIP. Moreover, the protective effects of Bak were partially reversed by PX-12 and compound C. To summarize, Bak attenuates EBI after SAH by alleviating BBB disruption, oxidative

stress, and apoptosis *via* regulating Trx1/TXNIP expression and the phosphorylation of AMPK. Its powerful protective effects might make Bak a promising novel drug for the treatment of EBI after SAH.

Keywords: bakuchiol, subarachnoid hemorrhage, early brain injury, oxidative stress, apoptosis, thioredoxin, AMP-activated protein kinase

INTRODUCTION

Although the treatment of subarachnoid hemorrhage (SAH), a severe subtype of stroke, has been discussed a lot in recent years, the mortality and morbidity of SAH remain high and it leads to the loss of many years of productive life (Macdonald and Schweizer, 2017). The loss of neurological function results from the primary injury directly caused by the hemorrhage and secondary injury following the primary injury (Macdonald, 2014).

Recently, an increasing number of studies have indicated that early brain injury (EBI), which occurs within the first 72 h of SAH, plays a crucial role in the poor prognosis of SAH (Liu L. et al., 2017; Macdonald and Schweizer, 2017). EBI is the primary cause of SAH-associated histological injuries, function deficits, and death (Sehba et al., 2012). Therefore, the targeting of EBI might be the most effective method for the treatment of SAH. During EBI, hemorrhage causes many pathophysiology problems, including the increase in intracranial pressure, the decrease in cerebral blood flow, and the global cerebral ischemia (Fujii et al., 2013). A complex mechanism, including blood-brain barrier (BBB) disruption, neuroinflammation, oxidative stress, and neuronal apoptosis is involved in the process of injury after SAH, which ultimately leads to cell death and severe damage to neurological functions (Lucke-Wold et al., 2016).

Bakuchiol (Bak), [(1E,3S)-3-ethenyl-3,7-dimethyl-1,6-oct adien-1-yl] phenol, an analog of resveratrol, is a prenylated phenolic monoterpene isolated from the seeds of *Psoralea corylifolia* L. (Leguminosae) (Feng et al., 2016; Xin et al., 2019) **Figure 1A**. It was initially identified in *Otholobium pubescens*, a kind of Peruvian medicinal plant used for the treatment of diabetes (Krenisky et al., 1999). Recently, Bak has been demonstrated to have numerous pharmacological properties, including the antioxidative and anti-inflammatory, antidiabetic, antiaging, and anticancer properties (Choi et al., 2010; Seo et al., 2013; Chaudhuri and Bojanowski, 2014; Li L. et al., 2017; Lim et al., 2019; Xin et al., 2019). For example, Bak maintains the activities of mitochondrial respiratory enzyme and protects the functions of mitochondrial against oxidative stress injury (Haraguchi et al., 2000). Bak treatment could also alleviate the edema, inflammation, and oxidative stress in the sepsis-induced acute lung injury (Zhang et al., 2017). Besides, Bak treatment could attenuate myocardial ischemia-reperfusion injury by attenuating mitochondrial oxidative damage and apoptosis *via* the activation of the SIRT1/PGC-1α signaling pathway (Feng et al., 2016). This strong antioxidative effect might be mediated by the terpenoid chain in its structure *via* a radical scavenging way (Adhikari et al., 2003). However, the effects of Bak on SAH remain unclear.

The present study aims to investigate the effects of Bak on EBI after SAH. The protective effects of Bak on BBB integrity, oxidative stress, cellular apoptosis, and neurological function during EBI were explored in an endovascular perforation SAH model in C57BL/6J mice. The roles of thioredoxin (Trx)/thioredoxin-interacting protein (TXNIP) and AMP-activated protein kinase (AMPK), which are crucial for the regulation of molecules in intracellular oxidative stress, were then studied by using their selective inhibitor, PX-12 and compound C (CC).

MATERIALS AND METHODS

Animals and Ethics

Healthy adult male C57BL/6J mice weighing 20–25 g were obtained from the Animal Center of the Fourth Military Medical University. The mice were maintained on a 12 h light/dark cycle at approximately 22°C under pathogen-free conditions with given free access to food and water. All experiments were performed according to *The Guide for the Care and Use of Laboratory Animals* published by the US National Institutes of Health (National Institutes of Health Publication, No. 85–23, revised 1996) and had been approved by the Ethics Committee of the Fourth Military Medical University (NO. TDLL2017-04-192).

Reagents

Bak, dihydroethidium (DHE), and 4′,6-diamino-2-phenylindole (DAPI) were purchased from Sigma-Aldrich (St. Louis, MO, USA). 1-Methylpropyl 2-imidazolyl disulfide (PX-12) was purchased from Selleck Chem (Houston, TX, USA). CC (ab146597) and rabbit polyclonal antibodies against $gp91^{phox}$ (ab80508), 4-hydroxynonenal (4-HNE) (ab46545), cleaved caspase-3 (ab2302), claudin-5 (ab15106), occludin (ab216327), and zonula occludens-1 (ZO-1) (ab96587) were purchased from Abcam (Cambridge, UK). Rabbit monoclonal antibodies against B-cell lymphoma-2 (Bcl-2) (2870), Bcl-2-associated X protein (Bax) (14796), matrix metalloproteinase-9 (MMP-9) (13667S), Trx-1 (2429S), TXNIP (14715S), AMPK (2532S), and phospho-AMPK (Thr172) (D4D6D) were purchased from Cell Signaling Technology (Beverly, MA, USA). Rabbit polyclonal antibody against β-actin (AC006) was purchased from ABclonal Biotech (College Park, Maryland, USA). A terminal deoxynucleotidyl transferase uridine triphosphate (UTP) nick-end labeling (TUNEL) kit was purchased from Roche (Mannheim,

Germany). Fluoro-Jade C (FJC) was purchased from Millipore (Temecula, USA). The enzyme-linked immune sorbent assay (ELISA) kits used to measure 8-hydroxy-2-deoxyguanosine (8-OHdG) and 3-nitrotyrosine (3-NT) levels were purchased from Cell Biolabs (San Diego, CA, USA). The kits used to measure glutathione peroxidase (GSH-Px), superoxide dismutase (SOD), and malondialdehyde (MDA) levels were purchased from the Institute of Jiancheng Bioengineering (Nanjing, Jiangsu, China). Human resource planning (HRP)-conjugated goat anti-rabbit secondary antibody was purchased from Bioworld Co. (Shanghai, China).

Experimental Designs

First, mice were randomly assigned to four groups: the sham, SAH, SAH + vehicle, and SAH + Bak groups (**Figure 1B**). Sham or SAH operation was conducted in the appropriate groups. Bak was diluted to a concentration of 10 mg/ml in normal saline with a 2% volume of ethanol. Drugs were administered orally by gavage at a dosage of 50 mg/kg/day for seven consecutive days before the injury. The mice in the vehicle group were given equal doses of 2% ethanol dissolved in normal saline. Second, PX-12 (25 mg/kg), a selective Trx inhibitor, and CC (2 mg/kg), a selective AMPK inhibitor, were administered to mice in the SAH + Bak + PX-12 and SAH + Bak + CC groups through tail vein injection immediately after SAH. The sham + Bak group was also introduced to observe the effects of Bak on normal animals. Tissues were collected 24 or 72 h after injury for the following experiments. All of the experiments and statistical analyses were conducted by researchers blinded to the grouping.

Subarachnoid Hemorrhage Animal Model

An endovascular perforation SAH model was developed by a method that has been described previously (Sozen et al., 2009; Kooijman et al., 2014). Briefly, animals were anesthetized with a mixture of isoflurane in 30% oxygen and 70% nitrous oxide (3% induction, 1.5% maintenance, v/v). Then, the left common carotid artery bifurcation was exposed, and the left external carotid artery was ligated and dissected. A nylon suture was inserted into the left internal carotid artery through the left external carotid artery stump and the left common carotid artery bifurcation. Resistance was encountered when the suture was located near the anterior communicating artery (ACA). The suture was then advanced approximately 3 more millimeters (total depth of 13–14 mm) to perforate the ACA. The suture was maintained in this position for 30 s before its withdrawal. A similar operation was performed on mice in the sham group, except that the suture was pierced less than 8 mm to avoid perforation of the ACA. The temperature was continuously monitored during the surgery. The animals were kept warm using a heating plate to maintain body temperature at 36.5–37.5°C during surgery and within 2 h after surgery. Meloxicam was given as analgesic after surgery, and 5% glucose dissolved in normal saline was given as nutritional support. To ensure the uniformity of damage, the mice with an SAH grading score ≤ 7 were excluded.

Survival Rate and Subarachnoid Hemorrhage Grade

Twenty mice in each group were used to evaluate the postinjury survival rate. These animals were observed for 7 days after sham or SAH operation under pathogen-free conditions with free access to food and water. They were then euthanized after 7 days.

SAH grading scores were evaluated when the animals were sacrificed using a previously reported method (Sugawara et al., 2008). Briefly, the basal cisterns of the animals were divided into six segments (**Figure 1C**) and the Willis circle and basilar arteries were observed. Subarachnoid blood clotting and the arteries on each segment were evaluated and scored from 0 to 3 score (grade 0: no subarachnoid blood; grade 1: minimal subarachnoid blood; grade 2: moderate blood clot with recognizable arteries; grade 3: blood clot obliterating all arteries within the segment). The SAH grading score was the sum of the scores of each segment.

Neurological Score

Neurological function was assessed using a modified Garcia's neurological scoring system (Garcia et al., 1995; Zhao et al., 2017) at 24 or 72 h after surgery. In brief, the evaluation consisted of six tests of the following: spontaneous activity (0–3), symmetry in the movement of all four limbs (0–3), symmetry in the movement of forelimbs (0–3), climbing (0–3), response to trunk stimulation (0–3), and response to whisker stimulation (0–3). The maximum score was 18; the minimum score was 0. Higher scores indicated better function.

Brain Water Content

The brain water content was tested by a previously described method (Xi et al., 2001; Jin et al., 2017) using the following formula: the brain water content (%) = [(wet weight − dry weight)/wet weight] ×100%. The mice were deeply anesthetized and sacrificed 24 or 72 h after surgery. Their brains were removed 24 or 72 h after injury and divided into four parts: the left hemisphere, the right hemisphere, the cerebellum, and the brain stem. Then, the water contents of each part were tested separately. Tissues were weighed immediately to obtain the wet weight, followed by drying at 95 to 100°C for 72 h and then weighing to obtain the dry weight.

Evans Blue Extravasation

Evans blue (EB) extravasations were tested 24 and 72 h after injury using a spectrophotometer (λ = 610 nm) to evaluate the permeability of the BBB. Briefly, 4 ml/kg of 2% (w/v) EB dye was injected into the right tail vein 3 h before the mice were sacrificed. Then, the animals were perfused transcardially with 50 ml of ice-cold 0.1 M phosphate-buffered saline (PBS, pH 7.4) under anesthesia to remove intravascular EB dye. The ipsilateral cortex was removed and homogenized in PBS and an equal volume of trichloroacetic acid to precipitate the protein. After 5 min, the samples were centrifuged, and the supernatants were extracted and used to measure the absorbance (Zhang et al., 2014; Zhang et al., 2015a).

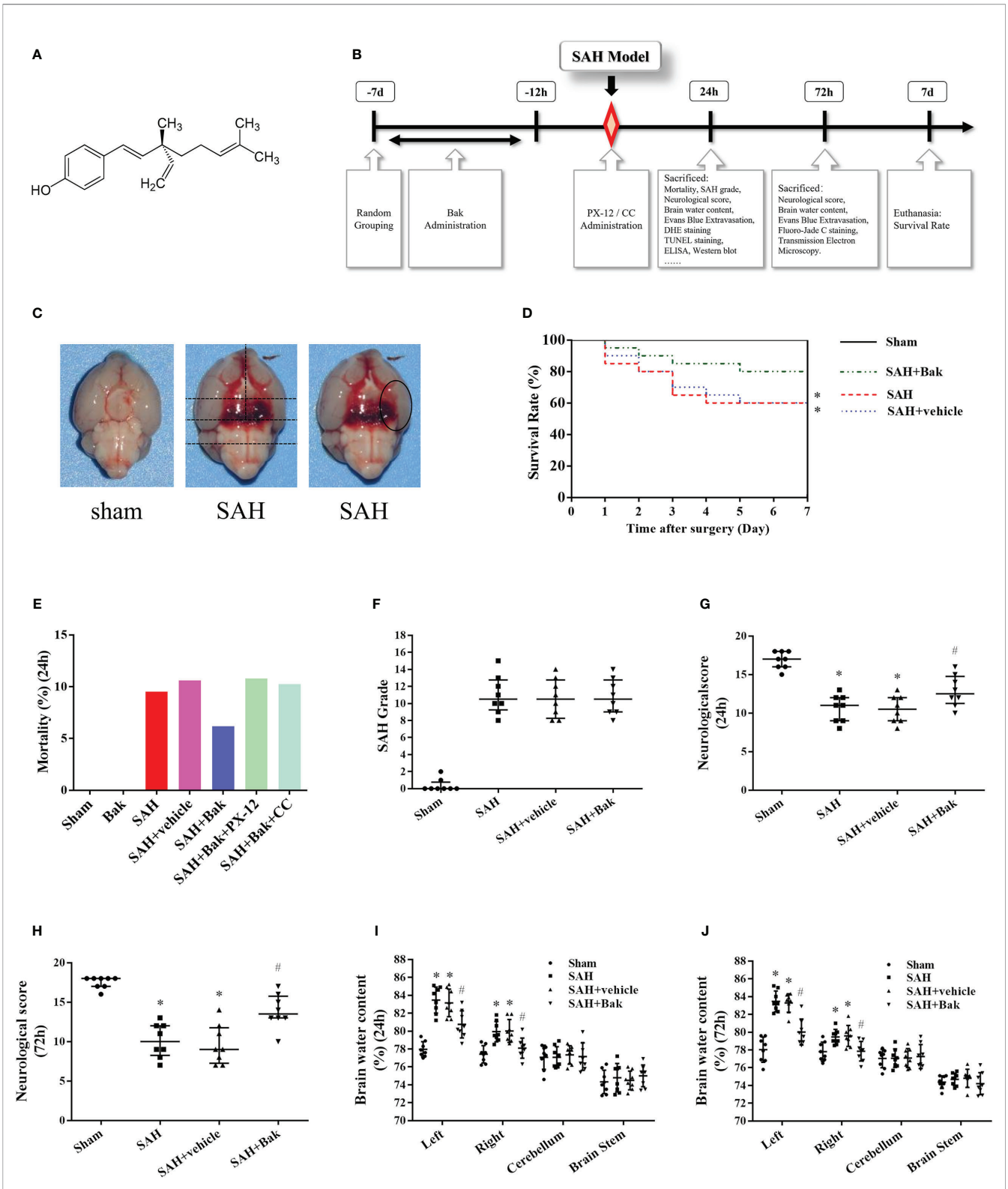

FIGURE 1 | Continued

FIGURE 1 | Experimental protocol and effect of Bak on mortality, neurological score, and brain water content in each group. **(A)** The chemical structure of Bak. **(B)** Experimental protocol. **(C)** The brain after SAH or sham. Blood clots can be seen in the ventral brain after SAH. The method to evaluate the SAH grading scores and the area observed after staining were showed. **(D)** Effect of Bak on the 7-day survival rate after SAH. Survival percentages in each day after injury are shown. Values are expressed as survival percentage. n = 20 for each group. **(E)** The mortality in each group. **(F)** SAH grading scores in each group. n = 8 for each group. **(G, H)** The neurological scores at 24 and 72 h after SAH. n=8 for each group. **(I, J)** Brain water content at 24 and 72 h after SAH. The brains are divided into four parts: the left hemisphere, the right hemisphere, the cerebellum, and the brain stem. The water content of each part is shown separately. n=8 for each group. Values of SAH grading score and neurological score are expressed as median and 25th–75th percentiles. Other values are expressed as mean ± SD. $^{*}P < 0.05$ *vs*. sham group, $^{\#}P < 0.05$ *vs*. SAH + vehicle group. Bak, bakuchiol; SAH, subarachnoid hemorrhage.

Dihydroethidium Staining

DHE staining was conducted to detect the superoxide anion, which reflected the oxidant stress levels in the tissue. Animals were perfused transcardially with PBS under anesthesia 24 h after SAH. Samples were immediately frozen at −80°C and sliced into 15 μm thick coronal brain slice with a freezing microtome (CM 1950, Leica, German). With reference to *The Mouse Brain in Stereotaxic Coordinates (Second Edition) (ACADEMIC PRESS)*, the slices at 0.58–2.5 mm posterior to bregma were selected. The slices were dyed with DHE for 30 min. Then, the ventral side of the left hemisphere was observed with a laser scanning confocal microscope (A1 Si, Nikon, Japan) (**Figure 1C**). The representative images were obtained from the slices located at about 2 mm posterior to bregma.

Assay of Malondialdehyde Content and the Superoxide Dismutase and Glutathione Peroxidase Activities

The brains were removed after their perfusion with PBS 24 h after SAH, and the ipsilateral cortex was homogenized to detect the levels of MDA and the activities of oxidative stress-related enzymes (SOD and GSH-Px). According to the instructions of commercial kits, the MDA levels were tested by the reaction of MDA with thiobarbituric acid under acidic conditions and a high temperature, following which the absorbance was detected. SOD activity was tested by WST-1 method following the instruction of commercial kits. The GSH-Px activity was tested by detecting the reduction of NADPH in the reaction system following the instructions of a commercial kit.

Concentrations of 3-Nitrotyrosine and 8-Hydroxy-2-Deoxyguanosine

ELISA kits were used to evaluate the levels of 3-NT and 8-OHdG in injured tissues at 24 h after SAH. Briefly, samples or standards were incubated with primary antibody at 4°C overnight, secondary antibody at room temperature for 1 h, and a substrate solution at the room temperature for 15 min in the dark. Finally, a solution to terminate the reaction was added to each sample. A SpectraMax M2 spectrometer (Molecular Devices, Sunnyvale, CA, USA) was used to measure the absorbance and calculate the protein level.

Transmission Electron Microscopic Observation

Samples were prepared following previously reported methods (Li X. et al., 2017). Briefly, 72 h after SAH induction, the mice were anesthetized and perfused with 50 ml of ice-cold PBS and 60 ml of ice-cold 4% paraformaldehyde (PFA). Then, the brains were removed. The injured cortical tissues were cut perpendicular to the long axis and trimmed into 1.5mm×1.5mm×3mm blocks. Then, the specimens were fixed for 12 h in 4% glutaraldehyde, postfixed for 1 h in 1% osmium tetroxide, dehydrated through graded ethanol, and embedded in resin. Specimens were cut into 80 nm sections by an ultramicrotome (Leica, Vienna, Austria). The ultrathin sections were fixed on 200 slot grids coated with Pioloform membranes and observed with a JEM-1400 electron microscope (JEOL, Tokyo, Japan). Micrographs were captured with a charge-coupled device camera (Olympus, Tokyo, Japan).

Terminal Deoxynucleotidyl Transferase Uridine Triphosphate Nick-End Labeling Assay

A TUNEL kit was used to detect cell apoptosis in the injured cortex. The animals were perfused with PBS and PFA 24 h after the injury as described above. Their brains were cautiously removed, fixed in 4% PFA for 12 h and dehydrated in sucrose solutions at different concentrations (10, 20, and 30%). The tissues were sliced into 25 μm thick slices with a freezing microtome. The slices were incubated with 0.3% hydrogen peroxide for 30 min at room temperature, 0.25% pancreatin for 45 min at 37°C, TUNEL reaction solution for 60 min at 37°C and DAPI (5 μg/ml) staining solution for 10 min at 37°C in a humidified box in the dark. With reference to *The Mouse Brain in Stereotaxic Coordinates (Second Edition) (ACADEMIC PRESS)*, the slices at 0.58–2.5 mm posterior to bregma were selected. The ventral side of the left hemisphere was observed with a confocal microscope (**Figure 1C**). The representative images were obtained from the slices located at about 2 mm posterior to bregma. The apoptotic index was reflected by the ratio of TUNEL-positive cells to DAPI-positive cells.

Fluoro-Jade C Staining

FJC staining was performed to detect neuronal degeneration in the tissues 72 h after injury (Bai et al., 2018). Briefly, the tissues were perfused, collected, fixed, dehydrated, and sliced as described above. The observed slices and areas were selected according to the method described above. Selected sections were incubated with 1% NaOH in 80% ethanol for 5 min and then rehydrated with 70% ethanol for 2 min and distilled water for 2 min. The slices were then incubated with 0.06% $KMnO_4$ for 10 min, rinsed with distilled water for 3 min, and incubated with a 0.0001% FJC solution for 15 min. Finally, the slices were washed three times with distilled water for 1 min each. The ventral side of the left hemisphere was observed and images were obtained

using a confocal microscope (**Figure 1C**). FJC-positive neurons were counted and calculated.

Western Blot Analysis

The ipsilateral cortical samples collected 24 h after injury were sonicated and homogenized in a mixture of lysis buffer and 1% protease inhibitor for 30 min and then centrifuged for 15 min at 12,000 rpm. Equal amounts of protein (25 μg) were separated on 8–15% sodium dodecyl sulfate (SDS)-polyacrylamide gels and transferred onto polyvinylidene difluoride (PVDF) membranes (Millipore Corporation, USA). The PVDF membranes were blocked in 5% nonfat dry milk/TBST (Tris-buffered saline, 0.1% Tween 20) for 90 min at room temperature and then incubated with rabbit anti-claudin-5 (1:1,000), anti-occludin (1:1,000), anti-ZO-1 (1:1,000), anti-MMP-9 (1:1,000), anti-gp91phox (1:500), anti-4-HNE (1:500), anti-Bcl-2 (1:1,000), anti-Bax (1:1,000), anti-cleaved caspase-3 (1:1,000), anti-Trx 1 (1:1,000), anti-TXNIP (1:1,000), anti-AMPK (1:1,000), anti-phospho-AMPK (1:1,000), and anti-β-actin (1:1,000) primary antibodies overnight at 4℃, followed by HRP-conjugated goat anti-rabbit (1:5,000) secondary antibody for 90 min at room temperature. Finally, the membranes were detected with the Bio-Rad imaging system (Bio-Rad, Hercules, CA, USA).

Statistical Analysis

GraphPad Prism 6 (GraphPad Software, San Diego, CA, USA) and SPSS 18.0 (SPSS, Chicago, IL, USA) was used for analysis. The survival rate was analyzed with the log-rank (Mantel-Cox) test. SAH grading scores and neurological scores are expressed as medians and 25th–75th percentiles and were analyzed by the Kruskal–Wallis one-way analysis of variance (ANOVA) on ranks, followed by Tukey's *post hoc* analysis. Means ± SDs are provided to describe other data. One-way ANOVA, followed by Tukey's *post hoc* analysis, and Bonferroni multiple comparison tests were used for intergroup comparisons. Multiple group comparisons were tested by one-way ANOVA followed by Tukey's honest significant difference (HSD) *post hoc* test. Differences for which $P < 0.05$ were considered statistically significant.

RESULTS

Bak Increases the Survival Rate and Alleviates Neurological Functional Deficits and Brain Edema After Subarachnoid Hemorrhage

The numbers of animals in each group used in the present study were described in **Table 1**. The overall mortality rate within 24 h after surgery in the sham, Bak, SAH, SAH + vehicle, SAH + Bak, SAH + Bak + PX-12, and SAH + Bak + CC groups were 0% (0/92), 0% (0/6), 9.5% (10/105), 10.6% (12/113), 6.2% (7/113), 10.8% (4/37), and 10.3% (4/39), respectively (**Figure 1E**). No animal was excluded from the experiment to observe the 7-day survival rate. The survived animals with insufficient brain injury were excluded from other experiments. Finally, 10, 9, 14, 3, and 4 animals were excluded in the SAH, SAH + vehicle, SAH + Bak, SAH + Bak + PX-12, and SAH + Bak + CC groups, respectively; 9, 12, 7, 4, 5 animals died before being sacrificed in the SAH, SAH + vehicle, SAH + Bak, SAH + Bak + PX-12, and SAH + Bak + CC groups, respectively (**Table 1**).

The 7-day survival rates in the sham, SAH, SAH + vehicle, and SAH + Bak groups were 100, 60, 60, and 80%, respectively (**Figure 1D**). Blood clots were clearly visible around the Willis circle and ventral brainstem of animals in the SAH, SAH + vehicle, and SAH + Bak groups. There was no significant difference in SAH grading scores between the SAH, SAH + vehicle, and SAH + Bak groups (**Figure 1F**).

Functional deficits, which were evaluated by neurological scores, and the degree of brain edema, which was evaluated by determining the brain water content, were measured 24 and 72 h after injury. SAH caused apparent neurological deficits and brain

TABLE 1 | The numbers of animals in each group.

	sham	sham+Bak	SAH	SAH			
				Vehicle	Bak	Bak+PX-12	Bak+CC
Included							
Survival rate	20	0	20	20	20	0	0
Brain water content	16	0	16	16	16	8	8
Evans blue extravasation	14	0	14	14	14	7	7
DHE staining	6	0	6	6	6	0	0
Oxidative stress marker detection	6	0	6	6	6	6	6
Western Blot	12	6	6	12	12	6	6
TUNEL	6	0	6	6	6	0	0
FJC staining	6	0	6	6	6	0	0
Transmission electron microscopy	6	0	6	6	6	3	3
In total	92	6	86	92	92	30	30
Died before being sacrificed	0	0	9	12	7	4	5
Excluded*	0	0	10	9	14	3	4

**No animal was excluded from the experiment to observe the survival rate. The animal with a SAH grading score ≤ 7 were excluded in other experiments. Bak, bakuchiol; SAH, subarachnoid hemorrhage; PX-12, 1-methylpropyl 2-imidazolyl disulfide; CC, compound C; DHE, dihydroethidium; TUNEL, terminal deoxynucleotidyl transferase UTP nick-end labeling; FJC, Fluoro-Jade C.*

edema. There were no significant differences in neurological scores or brain water content between the SAH and SAH + vehicle groups. Bak significantly improved neurological deficits and decreased the brain water content at 24 and 72 h after SAH (**Figures 1G–J**). The data of 24 h—brain water content/neurological scores and 72 h—brain water content/neurological scores were collected from different batches of animals. Thus, the difference between the injuries at 24 and 72 h was not compared.

Bak Protects Blood-Brain Barrier Integrity After Subarachnoid Hemorrhage

EB extravasation was tested 24 and 72 h after injury to evaluate the permeability of BBB. A sharp increase in EB extravasation was observed in the SAH and SAH + vehicle groups (*vs.* the sham group, $P < 0.05$), which was alleviated by Bak (**Figure 2B**). In addition, decreases in levels of the tight junction proteins claudin-5, occludin, and ZO-1 were observed in the SAH and SAH + vehicle groups (*vs.* the sham group, $P < 0.05$) 24 h after injury, which were offset by Bak. The MMP-9 level was increased in the SAH group (*vs.* the sham group, $P < 0.05$), but significantly reduced by Bak (**Figures 2A, C–F**).

Bak Ameliorates Oxidative Stress After Subarachnoid Hemorrhage

The proportion of DHE-positive cells was dramatically increased after SAH and significantly decreased by Bak (**Figures 3A, C**). The levels of MDA were significantly increased after SAH but significantly decreased following Bak administration (**Figure 3D**). In addition, the SOD and GSH-Px activities were impaired by SAH and remarkably enhanced by Bak administration (**Figures 3E, F**). Moreover, the levels of 3-NT and 8-OHdG were also increased after SAH and decreased significantly by Bak administration (**Figures 3G, H**). The protein levels of $gp91^{phox}$ and 4-HNE in the injured cortices were also increased 24 h after SAH and reduced by Bak treatment (**Figures 3B, I, J**).

Bak Attenuates Neuronal Damage After Subarachnoid Hemorrhage

TUNEL staining was performed to observe cellular apoptosis. The proportion of apoptotic cells was significantly increased after SAH. Bak significantly decreased the apoptotic index (**Figures 4A, B**). Previously, it was believed that the apoptosis mainly occurred on neurons after stroke. However, the latest research showed that the apoptosis and cell loss also occurred on glial cells (Chen et al., 2017; Ma et al., 2017; Sekerdag et al., 2018). Thus the FJC staining was further performed to quantify the degenerated neurons. The number of FJC-positive degenerated cells was significantly increased after SAH. This degeneration was alleviated by Bak administration (**Figures 4C, D**).

The protein levels of Bax, Bcl-2, and cleaved caspase-3 in injured tissues were tested by western blotting. The protein levels

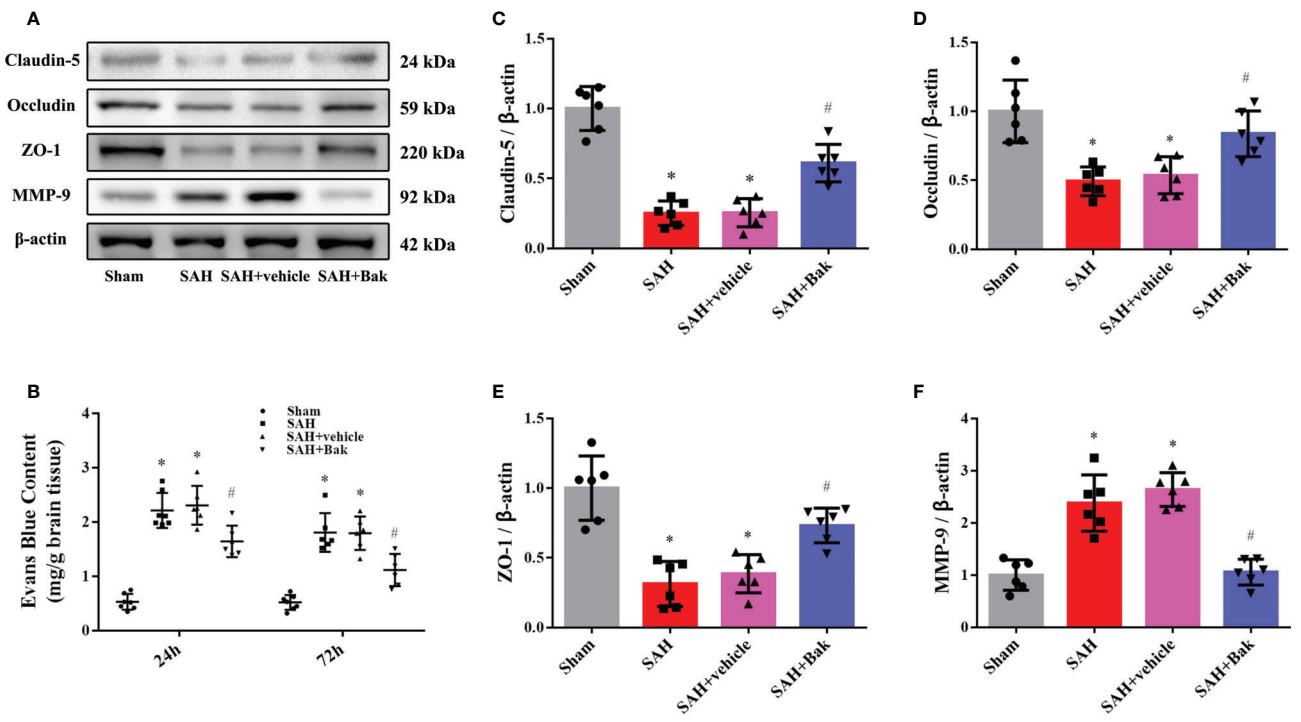

FIGURE 2 | The effect of Bak on BBB integrity after SAH. **(A)** Representative western blot images of the level of claudin-5, occludin, ZO-1, and MMP-9 at 24 h after SAH. n=6 for each group. **(B)** The EB extravasations at 24 and 72 h after injury. n=7 for each group. **(C–F)** Statistical analysis of the protein level of claudin-5, occludin, ZO-1, and MMP-9. Values are expressed as mean ± SD. *$P < 0.05$ *vs*. sham group, #$P < 0.05$ *vs*. SAH + vehicle group. Bak, bakuchiol; SAH, subarachnoid hemorrhage; BBB, blood-brain barrier; ZO-1, zonula occludens-1; MMP-9, matrix metalloproteinase-9; EB, Evans blue.

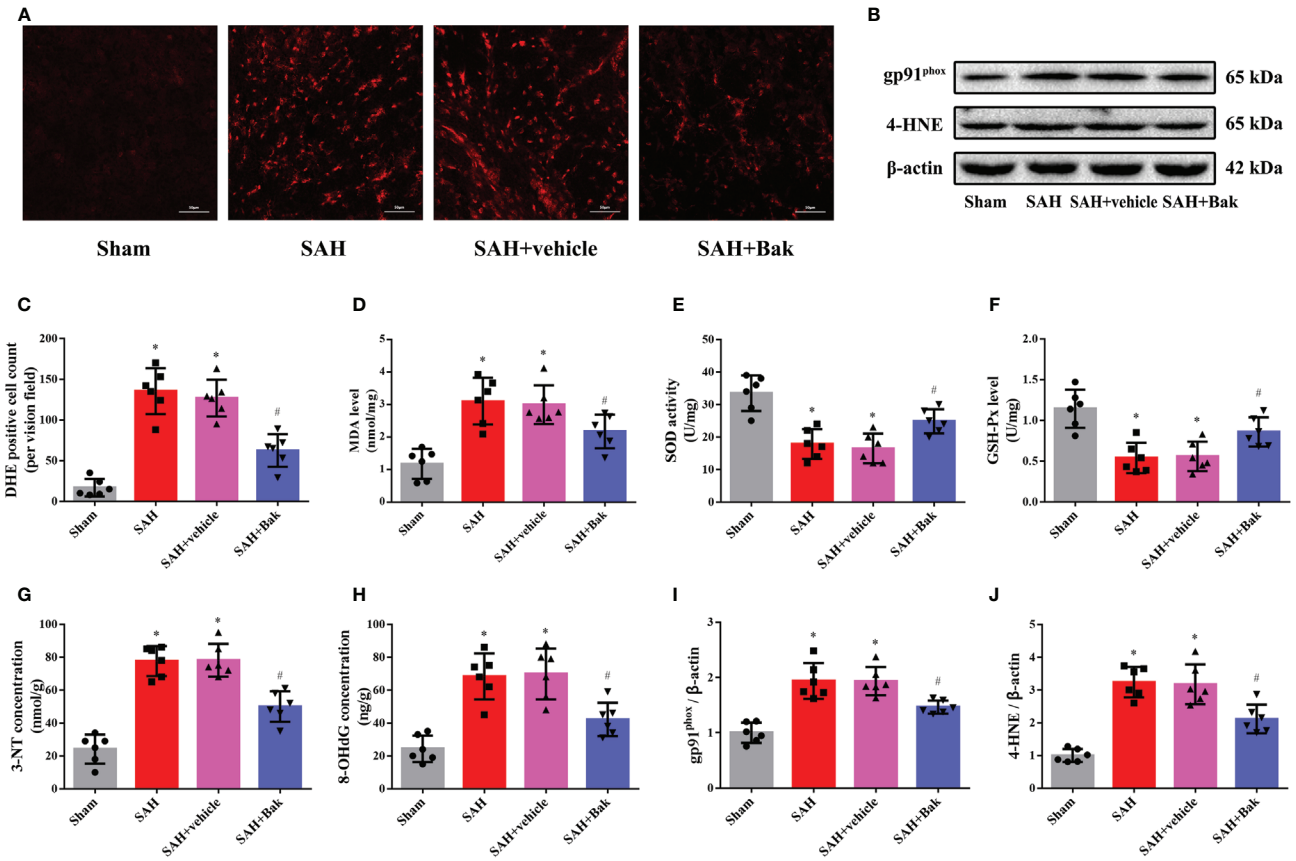

FIGURE 3 | The effect of Bak on the oxidative stress 24 h after SAH. **(A, C)** Representative images and quantitative analyses of DHE staining. Scale bar = 50 μm. **(D–F)** The effect of Bak on the level of MDA, and on the activity of SOD and GSH-Px after SAH. **(G, H)** The effect of Bak on 8-OHdG and 3-NT concentrations after SAH. **(B, I, J)** The effects of Bak on the gp91^{phox} and 4-hydroxynonenal (4-HNE) after SAH. The representative western blot images and statistical analysis of the protein levels of gp91^{phox} and 4-HNE are shown. Values are expressed as mean ± SD, n=6 for each group. $^{*}P < 0.05$ *vs*. sham group, $^{\#}P < 0.05$ *vs*. SAH + vehicle group. Bak, bakuchiol; SAH, subarachnoid hemorrhage; DHE, dihydroethidium; MDA, malondialdehyde; SOD, superoxide dismutase; GSH-Px, glutathione peroxidase; 8-OHdG, 8-hydroxy-2-deoxyguanosine; 3-NT, 3-nitrotyrosine.

of Bax and cleaved caspase-3 were increased 24 h after SAH, which were partially offset by Bak. However, the protein level of Bcl-2 was decreased 24 h after SAH, which was significantly ameliorated by Bak (**Figures 4E–H**).

The Role of Trx/TXNIP and AMPK in the Protective Effects of Bak Against Subarachnoid Hemorrhage

Western blotting was conducted 24 h after SAH to explore the role of Trx, TXNIP, and AMPK in the protective effects of Bak. The protein level of Trx was significantly decreased after SAH and increased after Bak administration. In contrast, the protein level of TXNIP was significantly increased after injury and decreased after Bak administration. In addition, the phosphorylation of AMPK was significantly increased after SAH. Bak administration further increased the level of phosphorylated AMPK (*vs*. the SAH + vehicle group, $P < 0.05$) Besides, an increase of AMPK phosphorylation also observed in the sham + Bak group (*vs*. the sham group, $P < 0.05$) (**Figures 5A–D**).

Then, PX-12, a Trx inhibitor, and CC, an AMPK inhibitor, were used as negative controls to further explore the roles of AMPK and Trx/TXNIP in this mechanism. The neurological score was decreased, and the brain water content and EB extravasation were obviously increased after the administration of PX-12 or CC compared to those in the SAH + Bak group (**Figures 5E–G**). The MDA level was significantly increased by PX-12 and CC (*vs*. the SAH + Bak group, $P < 0.05$). In contrast, the activities of GSH-Px and SOD were downregulated by PX-12 and CC (*vs*. the SAH + Bak group, $P < 0.05$) (**Figures 5H–J**). Meanwhile, transmission electron micrographs were used to observe ultrastructural changes in the mitochondria of neurons. Neurons in the SAH + Bak + PX-12 and SAH + Bak + CC groups were characterized by the loss of mitochondrial cristae, swollen mitochondria, and morphological changes in the endoplasmic reticulum, which was similar to neurons in the SAH group (**Figure 5K**).

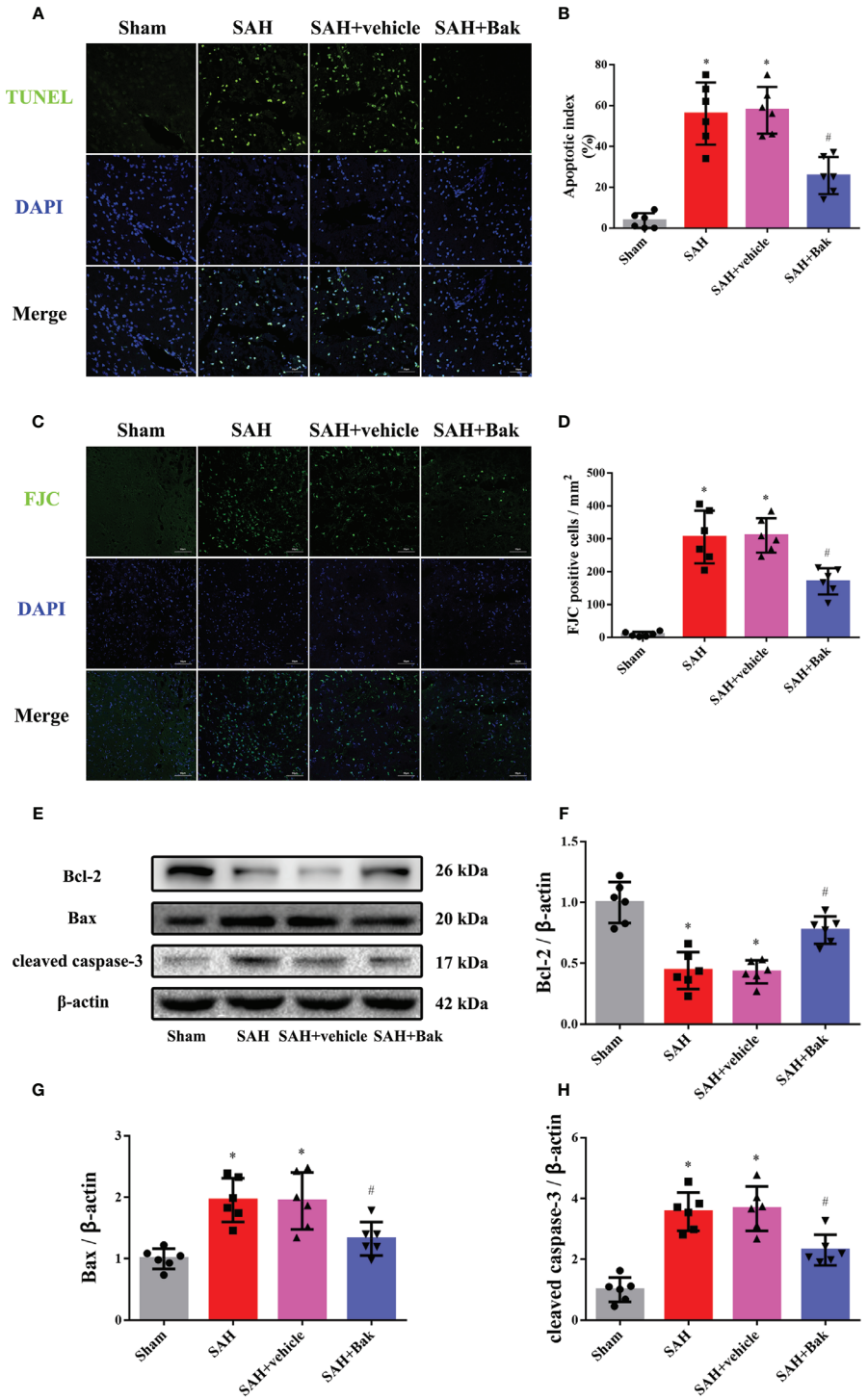

FIGURE 4 | The effects of Bak on cellular apoptosis and neuronal degeneration following SAH. **(A, B)** Representative images of TUNEL staining and quantitative analyses of TUNEL positive cells. Scale bar = 50 μm. **(C, D)** Representative images of FJC staining and quantitative analyses of FJC positive cells. Scale bar = 50 μm. **(E–H)** The effects of Bak on the apoptosis signaling 24 h after SAH. The representative western blot images and statistical analysis of the protein levels of Bcl-2, Bax, and cleaved caspase-3 are shown. Values are expressed as mean ± SD, n=6 for each group. *$P < 0.05$ *vs*. sham group, #$P < 0.05$ *vs*. SAH + vehicle group. Bak, bakuchiol; SAH, subarachnoid hemorrhage; TUNEL, terminal deoxynucleotidyl transferase UTP nick-end labeling; FJC, Fluoro-Jade C.

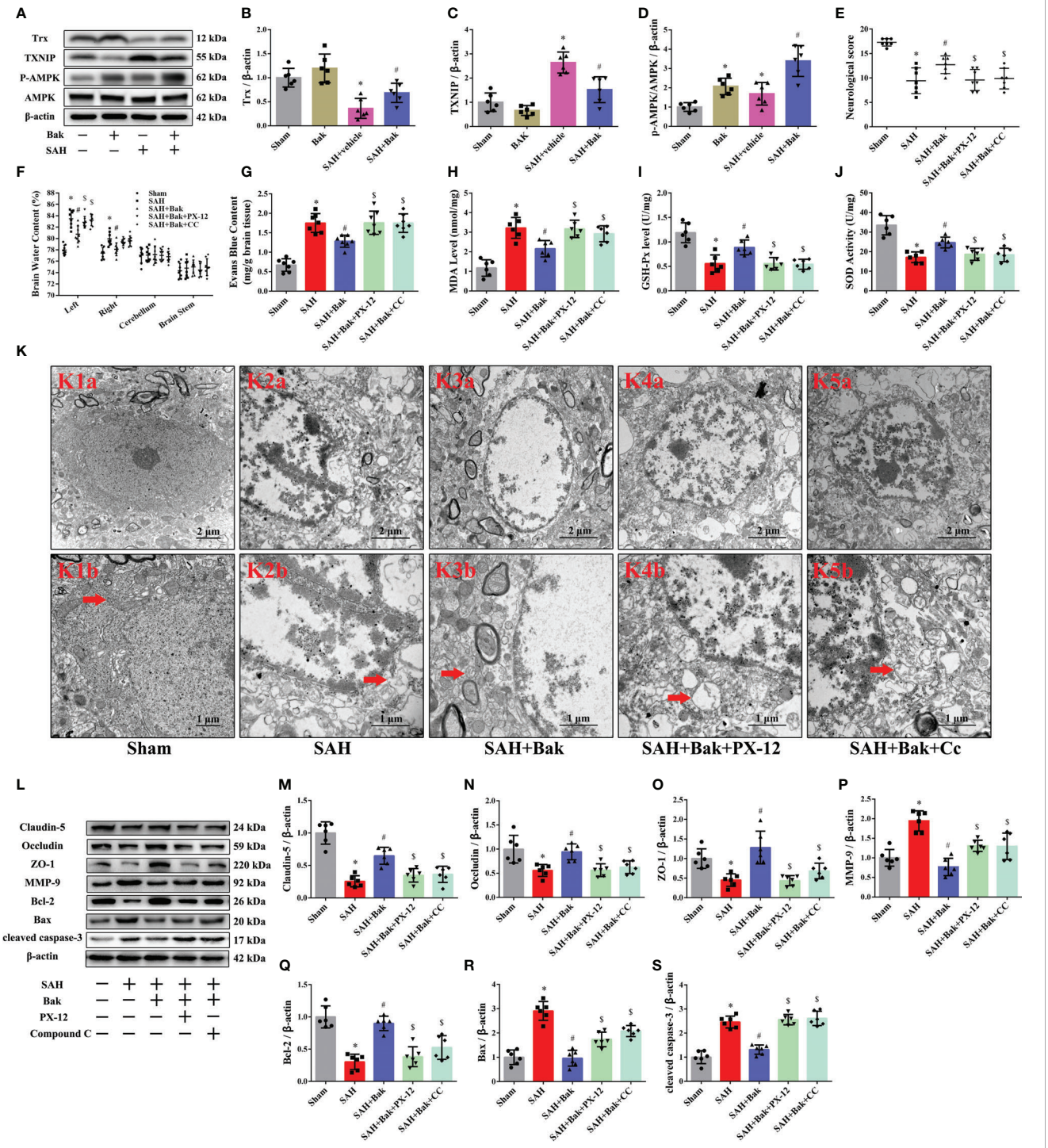

FIGURE 5 | Continued

FIGURE 5 | The role of Trx/TXNIP and AMPK in the protective effect of Bak after SAH. **(A–D)** The representative western blot images and statistical analysis of the protein levels of Trx and TXNIP and the phosphorylation of AMPK at 24 h after SAH. n=6 for each group. The protein levels of Trx and the phosphorylation levels of AMPK are up-regulated significantly by Bak (*vs*. the SAH + vehicle group). Then, the PX-12 and CC were used to identify the role of Trx and AMPK in the protective mechanism of Bak. **(E)** The neurological scores at 24 h. n=7 for each group. Values are expressed as median and 25th–75th percentiles. **(F)** Brain water content at 24 h. n=8 for each group. **(G)** Evans blue (EB) extravasation at 24 h. n=7 for each group. **(H–J)** The level of MDA, and the activity of SOD and GSH-Px in each group. n=6 for each group. **(K)** The ultrastructure of neurons in each group. K1b–K4b are the enlargements representative ultrastructure of neurons in K1a–K4a respectively. Scale bar = 2 μm in K1a–K4a, 1 μm in K1b–K4b. Arrows indicate the mitochondria. **(L–S)** The representative western blot images and statistical analysis of the protein levels of claudin-5, occludin, ZO-1, MMP-9, Bcl-2, Bax, and cleaved caspase-3 at 24 h. n=6 for each group. Values are expressed as mean ± SD except the neurological score, $^{*}P < 0.05$ *vs*. sham group, $^{\#}P < 0.05$ *vs*. SAH + vehicle group, $^{\$}P < 0.05$ *vs*. SAH + Bak group. Bak, bakuchiol; SAH, subarachnoid hemorrhage; Trx, thioredoxin; TXNIP, thioredoxin-interacting protein; AMPK, AMP-activated protein kinase; PX-12, 1-methylpropyl 2-imidazolyl disulfide; CC, compound C; MDA, malondialdehyde; SOD, superoxide dismutase; GSH-Px, glutathione peroxidase; ZO-1, zonula occludens-1; MMP-9, matrix metalloproteinase-9.

BBB integrity and cellular apoptosis were also tested 24 h after injury. The increased protein levels of claudin-5, occludin, ZO-1, and Bcl-2 after Bak administration were significantly reduced by PX-12 or CC. In addition, the levels of MMP-9 and Bax were increased significantly by PX-12 or CC (**Figures 5L–S**).

DISCUSSION

SAH accounts for 5% of all strokes and occurs at a fairly young age (van Gijn et al., 2007). Patients with SAH often have cognitive impairments, which severely affect their ability to work and quality of life (Macdonald and Schweizer, 2017). However, the current SAH treatment strategy does not achieve a satisfactory functional outcome. Thus, the need to find better treatment is urgent.

EBI is the most important cause of disability and death after SAH. The treatment of EBI may successfully attenuate some of the devastating secondary injuries and improve the outcome of SAH patients[5]. Thus, attenuating EBI is the main goal of SAH treatment and a crucial method to reduce disability and mortality (Cahill and Zhang, 2009).

Bak, a prenylated phenolic monoterpene, is used in both traditional Chinese medicine and traditional Indian medicine (Chen et al., 2010). Recently, Bak was demonstrated to have multiorgan protective effects through a variety of pharmacological activities (Xin et al., 2019). In the present study, oral administration of Bak 1) reduced the mortality rate and improved the neurological function of animals after SAH, 2) attenuated disruption to the BBB and brain edema caused by SAH, 3) reduced the superoxide production, alleviated oxidative stress, and protected the mitochondrial ultrastructure during EBI, 4) attenuated SAH-induced cellular apoptosis and neuron damage, and 5) regulated the protein levels of Trx and TXNIP and the phosphorylation of AMPK. Moreover, both PX-12, a selective Trx inhibitor (Ji et al., 2019), and CC, a selective AMPK inhibitor (Oliveira et al., 2012; Guo et al., 2018), reversed the protective effects of Bak. To summarize, the present study confirmed that Bak can inhibit oxidative stress, attenuate cellular apoptosis, and ameliorate BBB disruption *via* regulating the protein level of Trx and the activity of AMPK after SAH (**Figure 6**).

The pathological mechanisms of EBI include oxidative stress, inflammation, cellular apoptosis, disruption of the BBB, and microvascular dysfunction (Cahill et al., 2006; Sehba et al., 2012). Intercellular contacts between cerebral microvessel endothelial cells participate in the formation of the BBB and are critical to maintaining the brain's structure and function (Keep et al., 2018). These intercellular contacts include tight junctions, the stability of which is maintained by complex networks of occludin, claudin-5, ZO-1 and junctional adhesion molecule (JAM), and adherens junctions, which consist of vascular endothelial (VE) cadherins (Altay et al., 2012; Keep et al., 2018). Proteins in the MMP family are involved in the breakdown of extracellular matrix in the pathological processes of intracerebral hemorrhage (Zhao et al., 2006; Cao et al., 2016). Disruption of the BBB induces vasogenic edema, allows leukocyte extravasation, and allows neurotoxic and vasoactive compounds to leak into the brain (Keep et al., 2018). The BBB disruption and brain edema in EBI after SAH were alleviated by Bak in the present study.

Additionally, the excessive production and release of free radicals, with a weakened scavenger system, disrupt the BBB, leading to brain edema (Park et al., 2004). Reactive oxygen species (ROS) are chemically reactive chemical species containing oxygen including peroxides, superoxide, hydroxyl radical, singlet oxygen, and alpha-oxygen (Hayyan et al., 2016). It is produced in mitochondria by the electron transport chain under physiological conditions. The overload of ROS not only induces oxidative stress damage but also mediates inflammation and apoptosis (Bolanos et al., 2009; Forrester et al., 2018). EBI induces oxidative damage through inhibiting intrinsic antioxidant systems and increasing the production of ROS (Zhang et al., 2016; Liu H. et al., 2017). The production of ROS leads to serious tissue damage by promoting lipid peroxidation, DNA damage, and protein modification (Liu H. et al., 2017). The superoxide anion, as a representative of ROS, was detected by DHE staining to reflect the oxidant stress levels in the tissue in the present study.

Lipid peroxidation is a consequence of free radical-mediated injury in the brain. MDA, 3-NT, and 4-HNE are products of the lipid peroxidation chain reaction and markers which reflect the degree of tissue lipid peroxidation (Gutteridge and Halliwell, 1990; Ayala et al., 2014). 8-OHdG is widely used as a sensitive marker of DNA damage (Di Minno et al., 2016). $gp91^{phox}$, a member of the NADPH oxidase (NOX) family, is the primary catalytic subunit of NADPH oxidase which produces reactive oxygen species (Hasegawa et al., 2017). SOD is a member of the

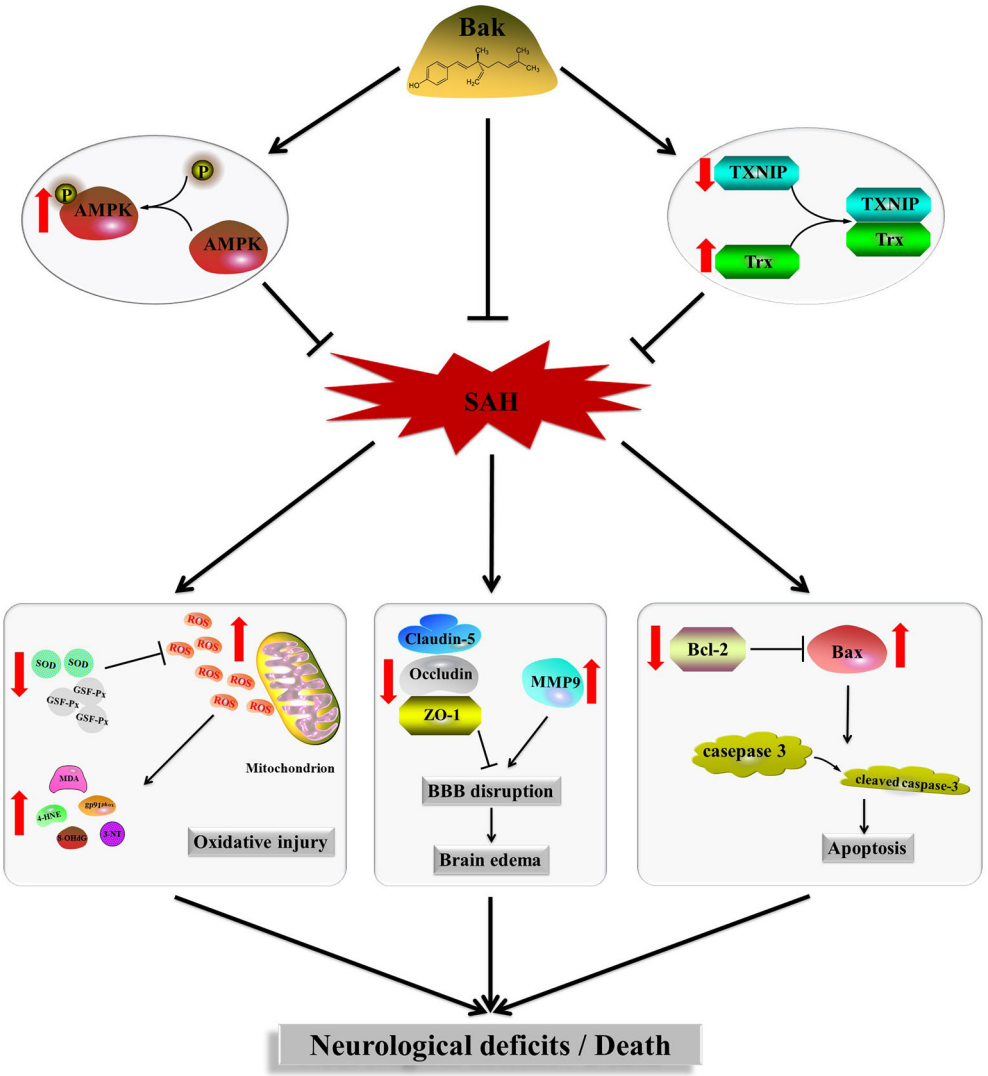

FIGURE 6 | Signaling pathway of Bak's neuroprotective effect against SAH injury which is suggested in the present study. Bak promotes the phosphorylation of AMPK, upregulates the protein level of Trx, and downregulated the protein level of TXNIP, thus alleviates the oxidative stress, cellular apoptosis, brain edema, and neurological deficits after SAH. Bak, bakuchiol; SAH, subarachnoid hemorrhage; Trx, thioredoxin; TXNIP, thioredoxin-interacting protein; AMPK, AMP-activated protein kinase.

enzymatic antioxidative pathway by which the dismutation of superoxide anions into hydrogen peroxide (H_2O_2) and oxygen (O_2) is catalyzed. GSH-Px also has notable antioxidative stress effects. Under physiological conditions, SOD, GSH-Px, and other antioxidant molecules comprise the intrinsic antioxidant system and fight against harmful reactive oxygen species (Wu et al., 2004; Poprac et al., 2017). The protective effects of Bak are mainly derived from its strong antioxidative properties (Adhikari et al., 2003; Xin et al., 2019). In the present study, Bak simultaneously increased the activities of SOD and GSH-Px and decreased the levels of superoxide production, MDA, 3-NT, 8-OHdG, $gp91^{phox}$, and 4-HNE in EBI.

ROS can be produced in the endoplasmic reticulum, mitochondria, cytoplasm, and peroxisome. The NOX family is one of the important sources of cytoplasmic ROS, a cornerstone of cellular signaling. Mitochondrial ROS are a natural byproduct of electron transfer in the respiratory chain. Proper respiratory chain function in mitochondria requires a delicate balance between the prooxidant and antioxidant systems (Forrester et al., 2018). In our study, the morphology of mitochondria and endoplasmic reticulum in neurons was observed. Mitochondria were found to be badly impaired, characterized by the loss of mitochondrial cristae, mitochondrial swelling, and collapsed cristae, during EBI, which were notably reversed by Bak administration. The normal morphology of the endoplasmic reticulum was also observed after Bak treatment.

The Trx/TXNIP system has been suggested to be an important contributor to enzymatic systems in ROS generation

and oxidative stress (Ji et al., 2019). Trx2, the main ROS-scavenging enzyme in mitochondria, balances ROS levels and maintains mitochondrial function. Trx1, which is located mainly in the cytoplasm, is usually induced as a response to oxidative stresses (Yoshihara et al., 2014). TXNIP, an endogenous inhibitor of the Trx system, directly binds to Trx1/Trx2 and inhibits their activity through disulfide exchange (Yoshihara et al., 2014; Nasoohi et al., 2018). The inhibition or the deletion of TXNIP is found to be neuroprotective in cerebrovascular and neurodegenerative diseases (Nasoohi et al., 2018). In the present study, the Trx/TXNIP system was involved in the antioxidative mechanism of Bak during EBI.

Cytoplasmic ROS also regulate the activity of AMPK (Hinchy et al., 2018), a central regulator of metabolic functions including lipid metabolism and mitochondrial function (Forrester et al., 2018; Herzig and Shaw, 2018). AMPK is activated by its phosphorylation at threonine-172 and plays a neuroprotective role after SAH (Lin and Hardie, 2018; Enkhjargal et al., 2019). In the present study, an increase in AMPK phosphorylation was observed after Bak administration. Besides, the upregulation of AMPK phosphorylation occurs after SAH in the present study, which has also been reported previously (Osuka et al., 2009; Xu et al., 2019; Xu et al., 2020). In our opinion, this phenomenon may be caused by the compensation mechanism during which the self-protecting signal pathways have been activated to tolerate the stress. In the present study, this mechanism was further enhanced by Bak. More importantly, the protective effects of Bak against BBB disruption, mitochondrial impairment, oxidative stress, and cellular apoptosis were reversed by CC and PX-12.

Cellular apoptosis is the result of oxidative stress-associated lipid peroxidation, protein breakdown, and DNA damage in neurons and endothelial cells during EBI, which leads to neurological deficits (Yuksel et al., 2012; Zhang et al., 2015b). The Bcl-2 family proteins mediate the mitochondrial apoptotic pathway by regulating the release of cytochrome C. The overexpression of Bcl-2 protects cells from apoptosis, whereas the upregulation of Bax reduces the protective effects of Bcl-2 and promotes cell death (Li et al., 2016). We evaluated the expressions of Bcl-2 and Bax and the activity of caspase-3 after SAH. In the present study, as shown by TUNEL staining and western blotting, Bak protected against apoptosis, which strongly contributed to the alleviation of neurological deficits after SAH.

Previously, it was believed that the apoptosis mainly occurred on neurons after stroke. However, the latest research showed that the apoptosis and cell loss also occurred on glial cells (Chen et al., 2017; Ma et al., 2017; Ning et al., 2017; Sekerdag et al., 2018). Strictly, TUNEL staining alone could not reflect the entire destruction of neurons. However, the FJC staining, detecting the overall neurodegeneration, could reflect the degree of neuron damage more comprehensively. It has been reported that the distribution and degree of FJC-positive cells after SAH were remarkably larger than TUNEL-positive cells (Xie et al., 2015).

The oxidative stress and BBB disruption begin within a few minutes to several hours after stroke and peaks quickly during EBI. By contrast, an important feature of SAH is that there is a delayed phase of brain injury at 3–14 days after hemorrhage in about a third of patients (Macdonald and Schweizer, 2017). The neuronal destruction continues from the EBI phase to the delayed injury phase, resulting in the continuous neurological deterioration (Coulibaly and Provencio, 2020). Considering that neurons are hard to regenerate, this persistent neuronal irreversible structural damage and loss of neurological functions worsen the SAH patients' poor neurological functional outcomes. Therefore, the FJC staining and electron microscopy were conducted at 72 h after SAH to further evaluate the degree of neuron damage in the present study. Whereas, the long-term changes after 3 days in neuronal structure and neurological functions were not observed, which is a limitation.

With numerous pharmacological properties, Bak exerts a multiorgan protective effect to alleviate damage to the brain (Xin et al., 2019), liver, cardiovascular system, skin, and retina (Kim et al., 2013; Kim S. et al., 2016; Xin et al., 2019). Previous studies have demonstrated that Bak could play anti-neuroinflammatory effects on activated microglia by the inhibition of the p38 mitogen-activated protein kinases (MAPK)/extracellular signal-regulated kinase 1/2 (ERK) pathways (Lim et al., 2019). ERK could inhibit the activity of AMPK[18]. This evidence is consistent with our findings. Moreover, Bak is proved to be able to suppress lipopolysaccharide (LPS)-stimulated nitric oxide production in LPS-treated BV-2 microglia and shows potent inhibitory activity against hydrogen peroxide-induced cell death in HT22 hippocampal cells (Kim Y. et al., 2016). Bak also has estrogen-like effects (Lim et al., 2011; Weng et al., 2015). Estrogens are strong neuroprotectants that play a protective role in the oxidative stress, mitochondria damage, neuroinflammation, neurodegeneration, and other injury mechanisms in central nervous system (CNS) disease (Miller and Duckles, 2008; Villa et al., 2016; Engler-Chiurazzi et al., 2017). This evidence also suggests that Bak has a strong neuroprotective effect. However, no study about Bak's direct effects on cerebrovascular disease has been reported previously.

In the present study, the protective effects of Bak against SAH injury have been demonstrated for the first time. The previously demonstrated antioxidative stress and anti-apoptosis effects of Bak have also been further validated in our study. Besides, it has also been confirmed in the present study that AMPK and Trx/TXNIP play a pivotal role in the antioxidative effect and neuroprotective effect of Bak. The protein kinase activity of AMPK plays a pivotal role in a variety of intracellular biological processes such as the growth of the cell, the metabolism of glucose and lipid, the oxidative stress, the maintenance of mitochondrial function and mitochondrial homeostasis, and the autophagy (Garcia and Shaw, 2017). The Trx system is a main intracellular antioxidant system, which detoxifies ROS and protects cells from oxidative damage (Cheng et al., 2011). While, TXNIP, as an intersection of oxidative stress and inflammasome activation, is essential in both of the oxidative damage and inflammatory injury (Zhou et al., 2010). Therefore, AMPK, Trx, and TXNIP might play a central role in the mechanism of Bak's neuroprotective effect.

Our findings suggest that Bak has great potential for clinical application in the CNS system. However, the direct molecule target and its particular intracellular signal transduction mechanism of Bak still needs to be further revealed before Bak can be transformed for clinical use. The effects of Bak on other CNS diseases also need to be explored.

The present study was focused on the pretreatment effects of Bak. This route of drug administration is usually used to explore the preventive strategies of diseases. Thus, the findings in the present study can be applied in some clinical occasions. For example, patients are at a high risk of hemorrhage during the neurosurgical procedures dealing with intracranial diseases such as intracranial aneurysms and intracranial arteriovenous malformations. The pretreatment of Bak before surgery might improve patients' tolerance to the possible hemorrhage injury. Besides, periprocedural aneurysm re-rupture is an extremely serious complication of endovascular treatment dealing with aneurysmal SAH. The mortality of patients with aneurysm re-rupture is as high as about 70% (Dmytriw et al., 2014; van Lieshout et al., 2019). The pretreatment of Bak might be a novel preventive therapeutic strategy against the re-rupture of cerebral aneurysms. In addition, patients with unruptured intracranial aneurysms and arteriovenous malformations are at a high risk of stroke when the lesion remains untreated. The preventive taking of Bak could be very beneficial for patients if the stroke occurs. Of course, urgent treatment after SAH is the most difficult problem in clinical practice. However, the effects of Bak post-treatment on SAH injury remain unclear. We will continue to explore this effect in the future.

Limitations still exist in the present study. The direct receptor and signal transduction pathways of Bak have not been fully explored. In subsequent studies, we will continue to explore the upstream and downstream regulators of TRX/TXNIP and AMPK. The effects of Bak on other injury mechanisms after SAH, such as neuroinflammation and autophagy, have not been observed. Thus, there is still a long way to go before the clinical application of Bak.

Another limitation is the measurement method of brain water content. The highest brain water contents in most of the studies using the same animal model did not reach 84%. However, the highest tested brain water content in the present study is about 85%. After careful reflection of our experimental protocol, we believe that the following factors might be the cause of this discrepancy. First, the sutures were advanced approximately 3 more millimeters after feeling the resistance to make sure the vascular was ruptured which might cause more serious traumatic brain injury than the operation in other studies. Second, the bloodstains and clots were not totally removed from the brain tissue before weighing in the present study. Third, the brains were handled on ice and might be stained with water released from the ice melt. Other unknown factors may also exist, which should be found out in our future study. Besides, the data in the present study cannot be used to compare the degree of cerebral edema at different time points post SAH, which is of great significance in the evolution process of SAH injury.

In conclusion, the present study confirms the protective effects of Bak against EBI after SAH in mice. These effects are mediated through alleviating BBB impairment, oxidative stress, and apoptosis by regulating Trx/TXNIP and AMPK phosphorylation. The powerful effects of Bak make it a promising novel drug for the treatment of EBI after SAH.

DATA AVAILABILITY STATEMENT

All datasets generated for this study are included in the article/supplementary material.

ETHICS STATEMENT

The animal study was reviewed and approved by Ethics Committee of the Fourth Military Medical University.

AUTHOR CONTRIBUTIONS

YQ conducted this project and supported the research. HL designed the study and drafted the manuscript. HL, WG, HG, LZ, LY, and XL performed the experiments and acquired the primary data. JL, XW, and WC completed the statistics and interpreted the data. DF revised the manuscript.

FUNDING

This study was supported by grants from the National Natural Science Foundation of China (81571215, 81630027).

ACKNOWLEDGMENTS

The authors thank the editors from American Journal Experts for their help with professional language editing.

REFERENCES

Adhikari, S., Joshi, R., Patro, B. S., Ghanty, T. K., Chintalwar, G. J., Sharma, A., et al. (2003). Antioxidant activity of bakuchiol: experimental evidences and theoretical treatments on the possible involvement of the terpenoid chain. *Chem. Res. Toxicol.* 16 (9), 1062–1069. doi: 10.1021/tx034082r

Altay, O., Suzuki, H., Hasegawa, Y., Caner, B., Krafft, P. R., Fujii, M., et al. (2012). Isoflurane attenuates blood-brain barrier disruption in ipsilateral hemisphere after subarachnoid hemorrhage in mice. *Stroke* 43 (9), 2513–2516. doi: 10.1161/STROKEAHA.112.661728

Ayala, A., Munoz, M. F., and Arguelles, S. (2014). Lipid peroxidation: production, metabolism, and signaling mechanisms of malondialdehyde and 4-hydroxy-2-nonenal. *Oxid. Med. Cell Longev.* 2014, 360438. doi: 10.1155/2014/360438

Bai, H., Zhao, L., Liu, H., Guo, H., Guo, W., Zheng, L., et al. (2018). Adiponectin confers neuroprotection against cerebral ischemia-reperfusion injury through

activating the cAMP/PKA-CREB-BDNF signaling. *Brain Res. Bull.* 143, 145–154. doi: 10.1016/j.brainresbull.2018.10.013

Bolanos, J. P., Moro, M. A., Lizasoain, I., and Almeida, A. (2009). Mitochondria and reactive oxygen and nitrogen species in neurological disorders and stroke: Therapeutic implications. *Adv. Drug Delivery Rev.* 61 (14), 1299–1315. doi: 10.1016/j.addr.2009.05.009

Cahill, J., and Zhang, J. H. (2009). Subarachnoid hemorrhage: is it time for a new direction? *Stroke* 40 (3 Suppl), S86–S87. doi: 10.1161/STROKEAHA.108.533315

Cahill, J., Calvert, J. W., and Zhang, J. H. (2006). Mechanisms of early brain injury after subarachnoid hemorrhage. *J. Cereb. Blood Flow Metab.* 26 (11), 1341–1353. doi: 10.1038/sj.jcbfm.9600283

Cao, S., Zhu, P., Yu, X., Chen, J., Li, J., Yan, F., et al. (2016). Hydrogen sulfide attenuates brain edema in early brain injury after subarachnoid hemorrhage in rats: Possible involvement of MMP-9 induced blood-brain barrier disruption and AQP4 expression. *Neurosci. Lett.* 621, 88–97. doi: 10.1016/j.neulet.2016.04.018

Chaudhuri, R. K., and Bojanowski, K. (2014). Bakuchiol: a retinol-like functional compound revealed by gene expression profiling and clinically proven to have anti-aging effects. *Int. J. Cosmet. Sci.* 36 (3), 221–230. doi: 10.1111/ics.12117

Chen, Z., Jin, K., Gao, L., Lou, G., Jin, Y., Yu, Y., et al. (2010). Anti-tumor effects of bakuchiol, an analogue of resveratrol, on human lung adenocarcinoma A549 cell line. *Eur. J. Pharmacol.* 643 (2-3), 170–179. doi: 10.1016/j.ejphar.2010.06.025

Chen, X., Lu, M., He, X., Ma, L., Birnbaumer, L., and Liao, Y. (2017). TRPC3/6/7 Knockdown Protects the Brain from Cerebral Ischemia Injury via Astrocyte Apoptosis Inhibition and Effects on NF-small ka, CyrillicB Translocation. *Mol. Neurobiol.* 54 (10), 7555–7566. doi: 10.1007/s12035-016-0227-2

Cheng, Z., Zhang, J., Ballou, D. P., and Williams, C. H.Jr. (2011). Reactivity of thioredoxin as a protein thiol-disulfide oxidoreductase. *Chem. Rev.* 111 (9), 5768–5783. doi: 10.1021/cr100006x

Choi, S. Y., Lee, S., Choi, W. H., Lee, Y., Jo, Y. O., and Ha, T. Y. (2010). Isolation and anti-inflammatory activity of Bakuchiol from Ulmus davidiana var. japonica. *J. Med. Food* 13 (4), 1019–1023. doi: 10.1089/jmf.2009.1207

Coulibaly, A. P., and Provencio, J. J. (2020). Aneurysmal Subarachnoid Hemorrhage: an Overview of Inflammation-Induced Cellular Changes. *Neurotherapeutics*. doi: 10.1007/s13311-019-00829-x

Di Minno, A., Turnu, L., Porro, B., Squellerio, I., Cavalca, V., Tremoli, E., et al. (2016). 8-Hydroxy-2-Deoxyguanosine Levels and Cardiovascular Disease: A Systematic Review and Meta-Analysis of the Literature. *Antioxid. Redox Signal* 24 (10), 548–555. doi: 10.1089/ars.2015.6508

Dmytriw, A. A., Pickett, G. E., and Shankar, J. J. (2014). Rupture of aneurysms in the immediate post-coiling period. *J. Neurointerv. Surg.* 6 (1), 16–18. doi: 10.1136/neurintsurg-2012-010588

Engler-Chiurazzi, E. B., Brown, C. M., Povroznik, J. M., and Simpkins, J. W. (2017). Estrogens as neuroprotectants: Estrogenic actions in the context of cognitive aging and brain injury. *Prog. Neurobiol.* 157, 188–211. doi: 10.1016/j.pneurobio.2015.12.008

Enkhjargal, B., Malaguit, J., Ho, W. M., Jiang, W., Wan, W., Wang, G., et al. (2019). Vitamin D attenuates cerebral artery remodeling through VDR/AMPK/eNOS dimer phosphorylation pathway after subarachnoid hemorrhage in rats. *J. Cereb. Blood Flow Metab.* 39 (2), 272–284. doi: 10.1177/0271678X17726287

Feng, J., Yang, Y., Zhou, Y., Wang, B., Xiong, H., Fan, C., et al. (2016). Bakuchiol attenuates myocardial ischemia reperfusion injury by maintaining mitochondrial function: the role of silent information regulator 1. *Apoptosis* 21 (5), 532–545. doi: 10.1007/s10495-016-1225-6

Forrester, S. J., Kikuchi, D. S., Hernandes, M. S., Xu, Q., and Griendling, K. K. (2018). Reactive Oxygen Species in Metabolic and Inflammatory Signaling. *Circ. Res.* 122 (6), 877–902. doi: 10.1161/CIRCRESAHA.117.311401

Fujii, M., Yan, J., Rolland, W. B., Soejima, Y., Caner, B., and Zhang, J. H. (2013). Early brain injury, an evolving frontier in subarachnoid hemorrhage research. *Transl. Stroke Res.* 4 (4), 432–446. doi: 10.1007/s12975-013-0257-2

Garcia, D., and Shaw, R. J. (2017). AMPK: Mechanisms of Cellular Energy Sensing and Restoration of Metabolic Balance. *Mol. Cell* 66 (6), 789–800. doi: 10.1016/j.molcel.2017.05.032

Garcia, J. H., Wagner, S., Liu, K. F., and Hu, X. J. (1995). Neurological deficit and extent of neuronal necrosis attributable to middle cerebral artery occlusion in rats. Statistical validation. *Stroke* 26 (4), 627–634; discussion 635. doi: 10.1161/01.str.26.4.627

Guo, H., Zhao, L., Wang, B., Li, X., Bai, H., Liu, H., et al. (2018). Remote limb ischemic postconditioning protects against cerebral ischemia-reperfusion injury by activating AMPK-dependent autophagy. *Brain Res. Bull.* 139, 105–113. doi: 10.1016/j.brainresbull.2018.02.013

Gutteridge, J. M., and Halliwell, B. (1990). The measurement and mechanism of lipid peroxidation in biological systems. *Trends Biochem. Sci.* 15 (4), 129–135. doi: 10.1016/0968-0004(90)90206-q

Haraguchi, H., Inoue, J., Tamura, Y., and Mizutani, K. (2000). Inhibition of mitochondrial lipid peroxidation by Bakuchiol, a meroterpene from Psoralea corylifolia. *Planta Med.* 66 (6), 569–571. doi: 10.1055/s-2000-8605

Hasegawa, Y., Nakagawa, T., Matsui, K., and Kim-Mitsuyama, S. (2017). Renal Denervation in the Acute Phase of Ischemic Stroke Provides Brain Protection in Hypertensive Rats. *Stroke* 48 (4), 1104–1107. doi: 10.1161/STROKEAHA.116.015782

Hayyan, M., Hashim, M. A., and AlNashef, I. M. (2016). Superoxide Ion: Generation and Chemical Implications. *Chem. Rev.* 116 (5), 3029–3085. doi: 10.1021/acs.chemrev.5b00407

Herzig, S., and Shaw, R. J. (2018). AMPK: guardian of metabolism and mitochondrial homeostasis. *Nat. Rev. Mol. Cell Biol.* 19 (2), 121–135. doi: 10.1038/nrm.2017.95

Hinchy, E. C., Gruszczyk, A. V., Willows, R., Navaratnam, N., Hall, A. R., Bates, G., et al. (2018). Mitochondria-derived ROS activate AMP-activated protein kinase (AMPK) indirectly. *J. Biol. Chem.* 293 (44), 17208–17217. doi: 10.1074/jbc.RA118.002579

Ji, L., Wang, Q., Huang, F., An, T., Guo, F., Zhao, Y., et al. (2019). FOXO1 Overexpression Attenuates Tubulointerstitial Fibrosis and Apoptosis in Diabetic Kidneys by Ameliorating Oxidative Injury via TXNIP-TRX. *Oxid. Med. Cell Longev.* 2019, 3286928. doi: 10.1155/2019/3286928

Jin, W. N., Shi, S. X., Li, Z., Li, M., Wood, K., Gonzales, R. J., et al. (2017). Depletion of microglia exacerbates postischemic inflammation and brain injury. *J. Cereb. Blood Flow Metab.* 37 (6), 2224–2236. doi: 10.1177/0271678X17694185

Keep, R. F., Andjelkovic, A. V., Xiang, J., Stamatovic, S. M., Antonetti, D. A., Hua, Y., et al. (2018). Brain endothelial cell junctions after cerebral hemorrhage: Changes, mechanisms and therapeutic targets. *J. Cereb. Blood Flow Metab.* 38 (8), 1255–1275. doi: 10.1177/0271678X18774666

Kim, K. A., Shim, S. H., Ahn, H. R., and Jung, S. H. (2013). Protective effects of the compounds isolated from the seed of Psoralea corylifolia on oxidative stress-induced retinal damage. *Toxicol. Appl. Pharmacol.* 269 (2), 109–120. doi: 10.1016/j.taap.2013.03.017

Kim, S. J., Oh, H. C., Kim, Y. C., Jeong, G. S., and Lee, S. (2016). Selective Inhibition of Bakuchicin Isolated from Psoralea corylifolia on CYP1A in Human Liver Microsomes. *Evid Based Complement Alternat. Med.* 2016, 5198743. doi: 10.1155/2016/5198743

Kim, Y. J., Lim, H. S., Lee, J., and Jeong, S. J. (2016). Quantitative Analysis of Psoralea corylifolia Linne and its Neuroprotective and Anti-Neuroinflammatory Effects in HT22 Hippocampal Cells and BV-2 Microglia. *Molecules* 21 (8), E1076. doi: 10.3390/molecules21081076

Kooijman, E., Nijboer, C. H., van Velthoven, C. T., Kavelaars, A., Kesecioglu, J., and Heijnen, C. J. (2014). The rodent endovascular puncture model of subarachnoid hemorrhage: mechanisms of brain damage and therapeutic strategies. *J. Neuroinflammation* 11, 2. doi: 10.1186/1742-2094-11-2

Krenisky, J. M., Luo, J., Reed, M. J., and Carney, J. R. (1999). Isolation and antihyperglycemic activity of bakuchiol from Otholobium pubescens (Fabaceae), a Peruvian medicinal plant used for the treatment of diabetes. *Biol. Pharm. Bull.* 22 (10), 1137–1140. doi: 10.1248/bpb.22.1137

Li, J., Chen, J., Mo, H., Chen, J., Qian, C., Yan, F., et al. (2016). Minocycline Protects Against NLRP3 Inflammasome-Induced Inflammation and P53-Associated Apoptosis in Early Brain Injury After Subarachnoid Hemorrhage. *Mol. Neurobiol.* 53 (4), 2668–2678. doi: 10.1007/s12035-015-9318-8

Li, L., Liu, C. C., Chen, X., Xu, S., Hernandez Cortes-Manno, S., and Cheng, S. H. (2017). Mechanistic Study of Bakuchiol-Induced Anti-breast Cancer Stem Cell and in Vivo Anti-metastasis Effects. *Front. Pharmacol.* 8, 746. doi: 10.3389/fphar.2017.00746

Li, X., Guo, H., Zhao, L., Wang, B., Liu, H., Yue, L., et al. (2017). Adiponectin attenuates NADPH oxidase-mediated oxidative stress and neuronal damage

induced by cerebral ischemia-reperfusion injury. *Biochim. Biophys. Acta Mol. Basis Dis.* 1863 (12), 3265–3276. doi: 10.1016/j.bbadis.2017.08.010

Lim, S. H., Ha, T. Y., Ahn, J., and Kim, S. (2011). Estrogenic activities of Psoralea corylifolia L. seed extracts and main constituents. *Phytomedicine* 18 (5), 425–430. doi: 10.1016/j.phymed.2011.02.002

Lim, H. S., Kim, Y. J., Kim, B. Y., and Jeong, S. J. (2019). Bakuchiol Suppresses Inflammatory Responses Via the Downregulation of the p38 MAPK/ERK Signaling Pathway. *Int. J. Mol. Sci.* 20 (14), E3574. doi: 10.3390/ijms20143574

Lin, S. C., and Hardie, D. G. (2018). AMPK: Sensing Glucose as well as Cellular Energy Status. *Cell Metab.* 27 (2), 299–313. doi: 10.1016/j.cmet.2017.10.009

Liu, H., Zhao, L., Yue, L., Wang, B., Li, X., Guo, H., et al. (2017). Pterostilbene Attenuates Early Brain Injury Following Subarachnoid Hemorrhage via Inhibition of the NLRP3 Inflammasome and Nox2-Related Oxidative Stress. *Mol. Neurobiol.* 54 (8), 5928–5940. doi: 10.1007/s12035-016-0108-8

Liu, L., Kawakita, F., Fujimoto, M., Nakano, F., Imanaka-Yoshida, K., Yoshida, T., et al. (2017). Role of Periostin in Early Brain Injury After Subarachnoid Hemorrhage in Mice. *Stroke* 48 (4), 1108–1111. doi: 10.1161/STROKEAHA.117.016629

Lucke-Wold, B. P., Logsdon, A. F., Manoranjan, B., Turner, R. C., McConnell, E., Vates, G. E., et al. (2016). Aneurysmal Subarachnoid Hemorrhage and Neuroinflammation: A Comprehensive Review. *Int. J. Mol. Sci.* 17 (4), 497. doi: 10.3390/ijms17040497

Ma, Y. L., Zhang, L. X., Liu, G. L., Fan, Y., Peng, Y., and Hou, W. G. (2017). N-Myc Downstream-Regulated Gene 2 (Ndrg2) Is Involved in Ischemia-Hypoxia-Induced Astrocyte Apoptosis: a Novel Target for Stroke Therapy. *Mol. Neurobiol.* 54 (5), 3286–3299. doi: 10.1007/s12035-016-9814-5

Macdonald, R. L., and Schweizer, T. A. (2017). Spontaneous subarachnoid haemorrhage. *Lancet* 389 (10069), 655–666. doi: 10.1016/S0140-6736(16)30668-7

Macdonald, R. L. (2014). Delayed neurological deterioration after subarachnoid haemorrhage. *Nat. Rev. Neurol.* 10 (1), 44–58. doi: 10.1038/nrneurol.2013.246

Miller, V. M., and Duckles, S. P. (2008). Vascular actions of estrogens: functional implications. *Pharmacol. Rev.* 60 (2), 210–241. doi: 10.1124/pr.107.08002

Nasoohi, S., Ismael, S., and Ishrat, T. (2018). Thioredoxin-Interacting Protein (TXNIP) in Cerebrovascular and Neurodegenerative Diseases: Regulation and Implication. *Mol. Neurobiol.* 55 (10), 7900–7920. doi: 10.1007/s12035-018-0917-z

Ning, B., Guo, G., Liu, H., Ning, L., Sun, B. L., Li, Z., et al. (2017). MSK1 downregulation is associated with neuronal and astrocytic apoptosis following subarachnoid hemorrhage in rats. *Oncol. Lett.* 14 (3), 2940–2946. doi: 10.3892/ol.2017.6496

Oliveira, S. M., Zhang, Y. H., Solis, R. S., Isackson, H., Bellahcene, M., Yavari, A., et al. (2012). AMP-activated protein kinase phosphorylates cardiac troponin I and alters contractility of murine ventricular myocytes. *Circ. Res.* 110 (9), 1192–1201. doi: 10.1161/CIRCRESAHA.111.259952

Osuka, K., Watanabe, Y., Usuda, N., Atsuzawa, K., Yoshida, J., and Takayasu, M. (2009). Modification of endothelial nitric oxide synthase through AMPK after experimental subarachnoid hemorrhage. *J. Neurotrauma* 26 (7), 1157–1165. doi: 10.1089/neu.2008-0836

Park, S., Yamaguchi, M., Zhou, C., Calvert, J. W., Tang, J., and Zhang, J. H. (2004). Neurovascular protection reduces early brain injury after subarachnoid hemorrhage. *Stroke* 35 (10), 2412–2417. doi: 10.1161/01.STR.0000141162.29864.e9

Poprac, P., Jomova, K., Simunkova, M., Kollar, V., Rhodes, C. J., and Valko, M. (2017). Targeting Free Radicals in Oxidative Stress-Related Human Diseases. *Trends Pharmacol. Sci.* 38 (7), 592–607. doi: 10.1016/j.tips.2017.04.005

Sehba, F. A., Hou, J., Pluta, R. M., and Zhang, J. H. (2012). The importance of early brain injury after subarachnoid hemorrhage. *Prog. Neurobiol.* 97 (1), 14–37. doi: 10.1016/j.pneurobio.2012.02.003

Sekerdag, E., Solaroglu, I., and Gursoy-Ozdemir, Y. (2018). Cell Death Mechanisms in Stroke and Novel Molecular and Cellular Treatment Options. *Curr. Neuropharmacol.* 16 (9), 1396–1415. doi: 10.2174/1570159X16666180302115544

Seo, E., Oh, Y. S., Kim, D., Lee, M. Y., Chae, S., and Jun, H. S. (2013). Protective Role of Psoralea corylifolia L. Seed Extract against Hepatic Mitochondrial Dysfunction Induced by Oxidative Stress or Aging. *Evid Based Complement Alternat. Med.* 2013, 678028. doi: 10.1155/2013/678028

Sozen, T., Tsuchiyama, R., Hasegawa, Y., Suzuki, H., Jadhav, V., Nishizawa, S., et al. (2009). Role of interleukin-1beta in early brain injury after subarachnoid hemorrhage in mice. *Stroke* 40 (7), 2519–2525. doi: 10.1161/STROKEAHA.109.549592

Sugawara, T., Ayer, R., Jadhav, V., and Zhang, J. H. (2008). A new grading system evaluating bleeding scale in filament perforation subarachnoid hemorrhage rat model. *J. Neurosci. Methods* 167 (2), 327–334. doi: 10.1016/j.jneumeth.2007.08.004

van Gijn, J., Kerr, R. S., and Rinkel, G. J. (2007). Subarachnoid haemorrhage. *Lancet* 369 (9558), 306–318. doi: 10.1016/S0140-6736(07)60153-6

van Lieshout, J. H., Verbaan, D., Donders, R., van den Berg, R., Vandertop, P. W. P., Klijn, C. J. M., et al. (2019). Periprocedural aneurysm rerupture in relation to timing of endovascular treatment and outcome. *J. Neurol. Neurosurg. Psychiatry* 90 (3), 363–365. doi: 10.1136/jnnp-2018-318090

Villa, A., Vegeto, E., Poletti, A., and Maggi, A. (2016). Estrogens, Neuroinflammation, and Neurodegeneration. *Endocr. Rev.* 37 (4), 372–402. doi: 10.1210/er.2016-1007

Weng, Z. B., Gao, Q. Q., Wang, F., Zhao, G. H., Yin, F. Z., Cai, B. C., et al. (2015). Positive skeletal effect of two ingredients of Psoralea corylifolia L. @ on estrogen deficiency-induced osteoporosis and the possible mechanisms of action. *Mol. Cell Endocrinol.* 417, 103–113. doi: 10.1016/j.mce.2015.09.025

Wu, L., Noyan Ashraf, M. H., Facci, M., Wang, R., Paterson, P. G., Ferrie, A., et al. (2004). Dietary approach to attenuate oxidative stress, hypertension, and inflammation in the cardiovascular system. *Proc. Natl. Acad. Sci. U. S. A* 101 (18), 7094–7099. doi: 10.1073/pnas.0402004101

Xi, G., Hua, Y., Bhasin, R. R., Ennis, S. R., Keep, R. F., and Hoff, J. T. (2001). Mechanisms of edema formation after intracerebral hemorrhage: effects of extravasated red blood cells on blood flow and blood-brain barrier integrity. *Stroke* 32 (12), 2932–2938. doi: 10.1161/hs1201.099820

Xie, Y., Liu, W., Zhang, X., Wang, L., Xu, L., Xiong, Y., et al. (2015). Human Albumin Improves Long-Term Behavioral Sequelae After Subarachnoid Hemorrhage Through Neurovascular Remodeling. *Crit. Care Med.* 43 (10), e440–e449. doi: 10.1097/CCM.0000000000001193

Xin, Z., Wu, X., Ji, T., Xu, B., Han, Y., Sun, M., et al. (2019). Bakuchiol: A newly discovered warrior against organ damage. *Pharmacol. Res.* 141, 208–213. doi: 10.1016/j.phrs.2019.01.001

Xu, W., Li, T., Gao, L., Zheng, J., Yan, J., Zhang, J., et al. (2019). Apelin-13/APJ system attenuates early brain injury via suppression of endoplasmic reticulum stress-associated TXNIP/NLRP3 inflammasome activation and oxidative stress in a AMPK-dependent manner after subarachnoid hemorrhage in rats. *J. Neuroinflammation* 16 (1), 247. doi: 10.1186/s12974-019-1620-3

Xu, W., Mo, J., Ocak, U., Travis, Z. D., Enkhjargal, B., Zhang, T., et al. (2020). Activation of Melanocortin 1 Receptor Attenuates Early Brain Injury in a Rat Model of Subarachnoid Hemorrhage viathe Suppression of Neuroinflammation through AMPK/TBK1/NF-kappaB Pathway in Rats. *Neurotherapeutics* 17 (1), 294–308. doi: 10.1007/s13311-019-00772-x

Yoshihara, E., Masaki, S., Matsuo, Y., Chen, Z., Tian, H., and Yodoi, J. (2014). Thioredoxin/Txnip: redoxisome, as a redox switch for the pathogenesis of diseases. *Front. Immunol.* 4, 514. doi: 10.3389/fimmu.2013.00514

Yuksel, S., Tosun, Y. B., Cahill, J., and Solaroglu, I. (2012). Early brain injury following aneurysmal subarachnoid hemorrhage: emphasis on cellular apoptosis. *Turk Neurosurg.* 22 (5), 529–533. doi: 10.5137/1019-5149.JTN.5731-12.1

Zhang, X. S., Zhang, X., Zhou, M. L., Zhou, X. M., Li, N., Li, W., et al. (2014). Amelioration of oxidative stress and protection against early brain injury by astaxanthin after experimental subarachnoid hemorrhage. *J. Neurosurg.* 121 (1), 42–54. doi: 10.3171/2014.2.JNS13730

Zhang, Z. Y., Sun, B. L., Yang, M. F., Li, D. W., Fang, J., and Zhang, S. (2015a). Carnosine attenuates early brain injury through its antioxidative and anti-apoptotic effects in a rat experimental subarachnoid hemorrhage model. *Cell Mol. Neurobiol.* 35 (2), 147–157. doi: 10.1007/s10571-014-0106-1

Zhang, Z. Y., Yang, M. F., Wang, T., Li, D. W., Liu, Y. L., Zhang, J. H., et al. (2015b). Cysteamine alleviates early brain injury via reducing oxidative stress and apoptosis in a rat experimental subarachnoid hemorrhage model. *Cell Mol. Neurobiol.* 35 (4), 543–553. doi: 10.1007/s10571-014-0150-x

Zhang, L., Wu, J., Duan, X., Tian, X., Shen, H., Sun, Q., et al. (2016). NADPH Oxidase: A Potential Target for Treatment of Stroke. *Oxid. Med. Cell Longev.* 2016, 5026984. doi: 10.1155/2016/5026984

Zhang, X., Chang, N., Zhang, Y., Ye, M., Han, Z., Li, J., et al. (2017). Bakuchiol Protects Against Acute Lung Injury in Septic Mice. *Inflammation* 40 (2), 351–359. doi: 10.1007/s10753-016-0481-5

Zhao, B. Q., Wang, S., Kim, H. Y., Storrie, H., Rosen, B. R., Mooney, D. J., et al. (2006). Role of matrix metalloproteinases in delayed cortical responses after stroke. *Nat. Med.* 12 (4), 441–445. doi: 10.1038/nm1387

Zhao, L., Liu, H., Yue, L., Zhang, J., Li, X., Wang, B., et al. (2017). Melatonin Attenuates Early Brain Injury via the Melatonin Receptor/Sirt1/NF-kappaB Signaling Pathway Following Subarachnoid Hemorrhage in Mice. *Mol. Neurobiol.* 54 (3), 1612–1621. doi: 10.1007/s12035-016-9776-7

Zhou, R., Tardivel, A., Thorens, B., Choi, I., and Tschopp, J. (2010). Thioredoxin-interacting protein links oxidative stress to inflammasome activation. *Nat. Immunol.* 11 (2), 136–140. doi: 10.1038/ni.1831

Conflict of Interest: The authors declare that the research was conducted in the absence of any commercial or financial relationships that could be construed as a potential conflict of interest.

frontiers in Molecular Neuroscience

REVIEW
published: 02 July 2020
doi: 10.3389/fnmol.2020.00116

Neuroprotection Against Oxidative Stress: Phytochemicals Targeting TrkB Signaling and the Nrf2-ARE Antioxidant System

Md. Abdul Hannan[1,2], Raju Dash[1], Abdullah Al Mamun Sohag[2], Md. Nazmul Haque[3†] and Il Soo Moon[1]**

[1] *Department of Anatomy, Dongguk University College of Medicine, Gyeongju, South Korea,* [2] *Department of Biochemistry and Molecular Biology, Bangladesh Agricultural University, Mymensingh, Bangladesh,* [3] *Department of Fisheries Biology and Genetics, Patuakhali Science and Technology University, Patuakhali, Bangladesh*

OPEN ACCESS

Edited by:
Nady Braidy, University of New South Wales, Australia

Reviewed by:
Anthony Robert White, The University of Queensland, Australia
Francisca C. Bronfman, Andres Bello University, Chile

***Correspondence:**
Md. Abdul Hannan
hannanbmb@bau.edu.bd
Il Soo Moon
moonis@dongguk.ac.kr

†ORCID:
Md. Nazmul Haque
orcid.org/0000-0002-8539-8905

Received: *24 February 2020*
Accepted: *04 June 2020*
Published: *02 July 2020*

Citation:
Hannan MA, Dash R, Sohag AAM, Haque MN and Moon IS (2020) Neuroprotection Against Oxidative Stress: Phytochemicals Targeting TrkB Signaling and the Nrf2-ARE Antioxidant System. Front. Mol. Neurosci. 13:116. doi: 10.3389/fnmol.2020.00116

Oxidative stress (OS) plays a critical role in the pathophysiology of several brain-related disorders, including neurodegenerative diseases and ischemic stroke, which are the major causes of dementia. The Nrf2-ARE (nuclear factor erythroid 2-related factor 2/antioxidant responsive element antioxidant) system, the primary cellular defense against OS, plays an essential role in neuroprotection by regulating the expressions of antioxidant molecules and enzymes. However, simultaneous events resulting in the overproduction of reactive oxygen species (ROS) and deregulation of the Nrf2-ARE system damage essential cell components and cause loss of neuron structural and functional integrity. On the other hand, TrkB (tropomyosin-related kinase B) signaling, a classical neurotrophin signaling pathway, regulates neuronal survival and synaptic plasticity, which play pivotal roles in memory and cognition. Also, TrkB signaling, specifically the TrkB/PI3K/Akt (TrkB/phosphatidylinositol 3 kinase/protein kinase B) pathway promotes the activation and nuclear translocation of Nrf2, and thus, confers neuroprotection against OS. However, the TrkB signaling pathway is also known to be downregulated in brain disorders due to lack of neurotrophin support. Therefore, activations of TrkB and the Nrf2-ARE signaling system offer a potential approach to the design of novel therapeutic agents for brain disorders. Here, we briefly overview the development of OS and the association between OS and the pathogenesis of neurodegenerative diseases and brain injury. We propose the cellular antioxidant defense and TrkB signaling-mediated cell survival systems be considered pharmacological targets for the treatment of neurodegenerative diseases, and review the literature on the neuroprotective effects of phytochemicals that can co-activate these neuronal defense systems.

Keywords: neuroprotection, oxidative stress, Nrf2-ARE system, TrkB/PI3K signaling, phytochemicals, neurodegeneration

INTRODUCTION

Oxidative stress (OS) is a pathological condition resulting from an imbalance between ROS generation and cellular antioxidant capacity. Factors contributing to OS in the brain include excitotoxicity, cellular antioxidant system depletion, lipid-rich membranes, susceptibility to lipid peroxidation, and high oxygen demand (Sivandzade et al., 2019). Excess ROS causes structural and functional modifications of cellular biomolecules, including proteins, DNA, and lipids, and thus potentially limits neuronal function and survival. The mechanisms underlying the pathobiologies of neurodegenerative diseases (NDDs) remain elusive; however, evidence strongly suggests a significant relationship between OS and NDDs, such as Alzheimer's disease (AD) and Parkinson's disease (PD) (Niedzielska et al., 2016). In addition, OS is known to contribute to the pathogeneses of secondary damage after cerebral ischemia and other brain injuries (Rodrigo et al., 2013; Rodríguez-Rodríguez et al., 2014).

The deposition of misfolded proteins, as is evident in major NDDs, can also induce inflammatory responses, which promote ROS generation and result in OS (Liu et al., 2017). Furthermore, OS causes and is caused by mitochondrial dysfunction (Wang et al., 2014). Given the central role mitochondria play in energy metabolism and the regulation of redox homeostasis, this dysfunction could contribute to the pathobiologies of brain disorders. Howsoever caused, when encountered, cells compensate for the damaging effect of OS by activating the intracellular antioxidant defense system, which is unfortunately compromised in a background of NDD. Therefore, it would appear triggering this endogenous defense system by activating Nrf2 might provide a means of suppressing OS-mediated cellular damage. However, although OS damages neuronal cytoarchitecture, minimizing the detrimental effect of ROS alone may not suffice to prevent/reverse OS-mediated cellular damage, which suggests approaches that help regenerate damaged neuronal structures should also be considered. Physiologically, neuronal growth and survival are maintained via the neurotrophic signaling pathway, but an alteration in the regulation of specific neurotrophic factors and their receptors ensued in the degenerating and aging brains (Sampaio et al., 2017). In particular, the brain-derived neurotrophic factor (BDNF)-dependent TrkB pathway, which is an essential signaling pathway for the survival and normal functioning of mature neurons, is compromised due to lack of BDNF (Gupta et al., 2013; Mitre et al., 2017). These relationships suggest the TrkB pathway and the Nrf2 signaling system are potential targets for promoting neuronal survival and initiating the regeneration of damaged neuronal structures and synaptic connectivity.

Phytochemicals and other natural products can directly scavenge oxygen free radicals and enhance the expressions of cellular antioxidant enzymes and molecules (Amato et al., 2019), and thus, protect against OS-mediated cellular injury (Son et al., 2008; Lee et al., 2014; Naoi et al., 2017; Hannan et al., 2020b). These bioactive compounds and their natural sources have been demonstrated to have neuritogenic potentials (Jang et al., 2010; Hannan et al., 2013, 2014, 2019) and to aid the reconstruction of synaptic connectivity by regenerating damaged neuronal processes (Moosavi et al., 2015; Venkatesan et al., 2015; Tohda, 2016). In fact, several studies have described a number of natural pharmacological modulators that can co-activate antioxidant defense and neurotrophin signaling-mediated cell survival systems (Gao et al., 2015; Kwon et al., 2015; Zhang et al., 2017; Cui et al., 2018; Fang et al., 2018; Hui et al., 2018), and suggested that these compounds have therapeutic potential for the treatment of OS-mediated brain disorders. Targeting both of these signaling systems with a single compound offers some benefits over that with combination. For example, the first strategy could bypass the possible drug–drug interactions that could be either synergistic or antagonistic. Instead, if a single compound can activate both the signaling system, it would be more convenient to establish it as a therapeutic agent concerning pharmacokinetics and drug delivery. However, we did not ignore the dual targeting with a combination that has also some other pharmacological benefits. While there is a sizable quantity of natural products that independently activate either TrkB signaling or Nrf2 pathway (Moosavi et al., 2015; Murphy and Park, 2017), we limited our review only to those reports that describe co-activation of TrkB signaling and Nrf2-ARE antioxidant pathways.

In this review, we provide a brief overview of the causes of OS development and its involvement in the pathobiology of NDD and brain injury. We then present the cellular antioxidant defense system and TrkB signaling pathway as pharmacological targets for the treatment of NDDs. Finally, we review recent literature on the neuroprotective effects and underlying pharmacological mechanisms of bioactive phytochemicals that co-activate these neuronal defense systems.

OXIDATIVE STRESS

The metabolisms of all eukaryotes essentially require oxygen to maintain their physiological functions and meet energy demands, but this life-sustaining element can sometimes damage cells, particularly high oxygen consuming cells. Different tissues have different oxygen demands, which are largely determined by metabolic needs. In mammals, the brain, which is a metabolically demanding organ, accounts for around 20% of total oxygen utilization (Halliwell, 2006), and neurons and astrocytes are principally responsible for this oxygen consumption. This huge oxygen turnover often results in the generation of excess ROS [superoxide ($O_2^{\cdot-}$), the hydroxyl radical (·OH), and hydrogen peroxide (H_2O_2)]. Moreover, high susceptibility to lipid peroxidation and relatively weaker antioxidant defense leave the lipid-rich brain vulnerable to OS. The unpaired valence electrons of ROS indicate they are highly reactive and capable of damaging to cellular biomolecules (Kim et al., 2015). Although $O_2^{\cdot-}$ has been suggested to play a central role in the production of ROS, ·OH is mainly responsible for its cytotoxic effects (Bolisetty and Jaimes, 2013).

ROS in brain may be of exogenous origin, for example, produced by xenobiotic metabolism or radiation, or of endogenous origin resulting from the activities of ROS-generating enzymes (Kim et al., 2015). The primary sources of

ROS are mitochondrial oxidative phosphorylation, particularly by complex I and several redox enzymes (Zorov et al., 2014). Physiologically, a certain amount of ROS is essential for cell signaling and pro-survival pathways (Patten et al., 2010), but when ROS production overwhelms the cellular antioxidant defense system, cells are exposed to the pathological condition termed OS (Gao et al., 2018), which may lead to mitochondrial dysfunction and further ROS generation (Stelmashook et al., 2019). The endoplasmic reticulum, the primary site of protein folding, also involved in ROS generation (Chaudhari et al., 2014), and resulting protein misfolding causes ER stress and additional ROS overproduction (Lindholm et al., 2006).

ROS damages cells by compromising the structures and functions of biomolecules, such as by peroxidizing lipids, oxidizing proteins, and damaging DNA (Kim et al., 2015), and eventually causing neurodegeneration (Gandhi and Abramov, 2012). Oxidative metabolites such as lipid peroxidation products [4-hydroxynonenal, 4-HNE, and malondialdehyde (MDA)], protein oxidation products (protein carbonyl moieties), and the DNA oxidation product (8-hydroxy-2′-deoxyguanosine, 8-OHdG) are the biomarkers that are elevated in the patients with NDDs (Zou et al., 2008; Rani et al., 2017; Haque et al., 2019) (**Figure 1**).

OXIDATIVE STRESS IN CASES OF NEURODEGENERATIVE DISEASES OR BRAIN INJURY

Dementia disorders, including NDDs, and complications arising from ischemic stroke or traumatic brain injury (TBI), are major public health concerns that are intimately associated with OS. Preclinical and clinical studies have revealed that brain and peripheral tissues and body fluids from patients with these brain disorders contain significantly higher concentrations of OS biomarkers and lower amounts of antioxidant biomarkers (Gandhi and Abramov, 2012).

Alzheimer's Disease

Alzheimer's disease is the most common progressive NDD and the major cause of dementia (Butterfield and Halliwell, 2019). The main pathological hallmarks of AD, include extracellular deposition of amyloid plaque, intraneuronal aggregation of neurofibrillary tangles (NFTs), and brain atrophy (van der Kant et al., 2020). Furthermore, OS has been shown to provoke Aβ deposition (plaque formation), tau hyperphosphorylation (NFT formation), and the subsequent degenerations of synaptic connectivity and neurons by impairing the protein degradation system (Butterfield and Halliwell, 2019). Several studies have reported elevated levels of ROS-mediated changes in AD brains, which supports the notion that OS is implicated in the pathobiology of AD (Wojsiat et al., 2018; Youssef et al., 2018). For example, levels of MDA and 4-HNE (measures of lipid peroxidation) are higher than normal in the brain tissues and cerebrospinal fluid samples of AD patients (Di Domenico et al., 2017; Butterfield and Boyd-Kimball, 2018). Although 4-HNE levels remained unchanged, the levels of antioxidant enzymes, such as superoxide dismutase (SOD), glutathione peroxidase (GPx), catalase (CAT), and peroxiredoxin (Prdx) were altered in the affected areas of the brain (Youssef et al., 2018). High plasma levels of protein carbonyls and advanced glycation end products (carboxymethyllysine and carboxyethyllysine) have been detected in male AD patients (Sharma et al., 2020). Moreover, 3-nitrotyrosine (3-NT), a protein nitration product, was found to be increased in $CD3^+$ T-cells from AD patients (Tramutola et al., 2018). In AD patients, reductions in the activities of antioxidant enzymes result in a significant decline in plasma levels of antioxidants (e.g., uric acid and bilirubin) (Kim et al., 2006). Redox proteomics studies have also reported oxidation of protein moieties in AD models (Di Domenico et al., 2016; Butterfield and Boyd-Kimball, 2019).

Oxidative stress leads to mitochondrial dysfunction and cellular atrophy (Singh et al., 2019) as pathological aggregations of proteins such as Aβ and tau have been reported to target mitochondria and augment ROS production (Buendia et al., 2016). OS also retards synaptic plasticity, and thus, contributes to progressive memory impairment, which is a characteristic clinical symptom of AD (Tönnies and Trushina, 2017). This relationship between OS and AD strongly suggests that strategies linked to antioxidant or antioxidant defense system could play important roles in the future management of AD.

Parkinson's Disease

In terms of its prevalence, PD is second only to AD and is characterized by dopaminergic neuron degeneration in the substantia nigra (Gandhi and Abramov, 2012). The intraneuronal aggregation of α-synuclein and the formation of Lewy bodies is a major pathological hallmark of PD (Singh et al., 2019). Although the exact mechanisms underlying the pathophysiology of this disease remains elusive, convincing evidence suggests the crucial involvement of OS (Gaki and Papavassiliou, 2014). Numerous studies have reported elevated levels of oxidative damage markers and low levels of glutathione (GSH) in the substantia nigra of PD patients (Singh et al., 2019). Furthermore, MDA plasma levels (de Farias et al., 2016) and protein carbonyl and 8-OHdG (markers of oxidative damage to protein and DNA, respectively) in brain tissues (Beal, 2002) have been reported to be elevated. A meta-analysis reported elevated levels of 8-OHdG and MDA and reduced levels of catalase, uric acid, and GSH in the blood of PD patients (Wei et al., 2018). These findings support the involvement of OS in the pathobiology of PD and suggest that targeting OS offers a potential therapeutic strategy for addressing this devastating brain disorder.

Ischemic Stroke

Stroke is the second leading cause of death (Donkor, 2018) and an important cause of permanent disability in adults worldwide (Feigin et al., 2017), and is caused by a sudden interruption in brain blood supply due to vascular occlusion. As a consequence, a portion of the brain experiences oxygen and nutrient insufficiencies, which cause depolarization of neuronal membranes and glutamate surge into synapses, resulting in a cascade of events, including calcium overload, dissipation of mitochondrial membrane potentials, OS, and inflammation

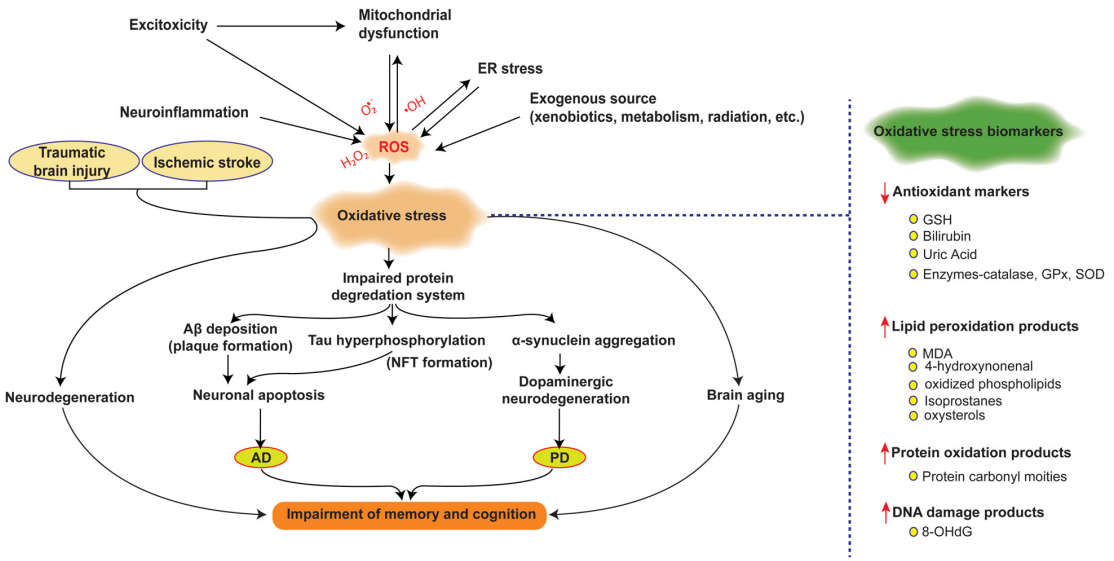

FIGURE 1 | Oxidative stress and its implications in the pathobiologies of neurodegeneration in NDDs and after ischemia or TBI. ROS are produced by multiple sources: endogenously, result from excitotoxic insults, neuroinflammation, ER stress, or mitochondrial dysfunction, whereas exogenously ROS are generated by radiation or xenobiotics. When the production of ROS overwhelms intracellular antioxidant defense, brain cells are exposed to oxidative stress (OS), which may lead to mitochondrial dysfunction and further ROS production. OS impairs the protein degradation system, and thus, hinders the clearance and results in the subsequent deposition of misfolded protein, which in turn, result in lipid peroxidation, protein oxidation, and DNA damage, leading to neuronal death. These events constitute the pathological basis of neurodegenerative diseases (NDDs) and brain aging. OS also contributes to the pathogeneses of secondary damage after cerebral ischemia or other brain injuries. Oxidative metabolites such as the lipid peroxidation products (4-HNE and MDA), protein oxidation products (protein carbonyl moieties), DNA oxidation product (8-OHdG) and antioxidant components such as GSH, bilirubin, uric acid, and antioxidative enzymes (CAT, GPx and SOD) are potential oxidative biomarkers and are elevated in patients with NDDs. OS, oxidative stress; ER, endoplasmic reticulum; NFT, neurofibrillary tangle; AD, Alzheimer's disease; PD, Parkinson's disease; GSH, glutathione; GPx, glutathione peroxidase; SOD; superoxide dismutase; CAT, catalase; MDA, malondialdehyde; 8-OHdG, 8-hydroxy-2′-deoxyguanosine, NDD, neurodegenerative disease.

(Sivandzade et al., 2019; Hannan et al., 2020a). Inappropriate levels of antiapoptotic proteins [e.g., Bcl-2 (B-cell lymphoma 2)] and proapoptotic proteins [e.g., Bax (Bcl-2-associated X protein)] contribute to mitochondrial dysfunction and OS-induced apoptosis (Wu et al., 2019). In addition, the re-establishment of blood supply immediately after ischemia exposes brain tissue to excess oxygen, which exacerbates ROS production, which, in turn, induces further OS-associated injury, lipid peroxidation, protein oxidation, and intracellular DNA damage (Kishimoto et al., 2019; Sivandzade et al., 2019). Several *in vivo* investigations of OS biomarkers in patients after ischemic stroke suggest that oxidative damage follows the ischemic shock, as blood levels of NO and MDA have been reported to be elevated after ischemic stroke (Dogan et al., 2018). These findings indicate targeting OS offers a promising therapeutic strategy to reduce secondary brain injury after ischemic stroke and to improve outcomes (Sivandzade et al., 2019).

Traumatic Brain Injury

Traumatic brain injury (TBI) is also a major cause of death and disability worldwide, particularly in countries with high traffic densities. Non-fatal TBI may lead to neurological deficits due to direct tissue damage (primary injury) or subsequent biochemical changes (secondary injury) (Lozano et al., 2015). Primary injuries cause immediate neuronal death, whereas secondary damage leads to progressive neuronal degeneration driven by biochemical factors such as excitotoxicity, inflammation, mitochondrial dysfunction, and OS (Khatri et al., 2018). Thus, it is important that these secondary changes be targeted to reduce further damage. Following TBI, OS markers such as oxidized protein moieties, lipid peroxidation products, and products of DNA damage accumulate in the brain, whereas levels of antioxidant molecules and enzymes, such as GSH, GPx, glutathione reductase (GR), glutathione *S*-transferase (GST), SOD, and CAT decline, which indicates TBI results in OS (Rodríguez-Rodríguez et al., 2014). Neuroprotective strategies directed at salvaging injured brain tissue soon after injury and that promote regeneration during the recovery stage are advantageous (Wurzelmann et al., 2017). The therapeutic potentials of BDNF and its mimics have been reported in the contexts of several neurological conditions, including TBI (Wurzelmann et al., 2017; Houlton et al., 2019). Therefore, it appears targeting cellular antioxidant defense and the BDNF/TrkB signaling pathway might improve cognitive deficits secondary to TBI.

CELLULAR DEFENSE AGAINST OXIDATIVE STRESS: THE Nrf2-ARE ANTIOXIDANT SYSTEM

Cells are equipped with an antioxidant defense system comprised of antioxidant enzymes and other molecules that attenuate

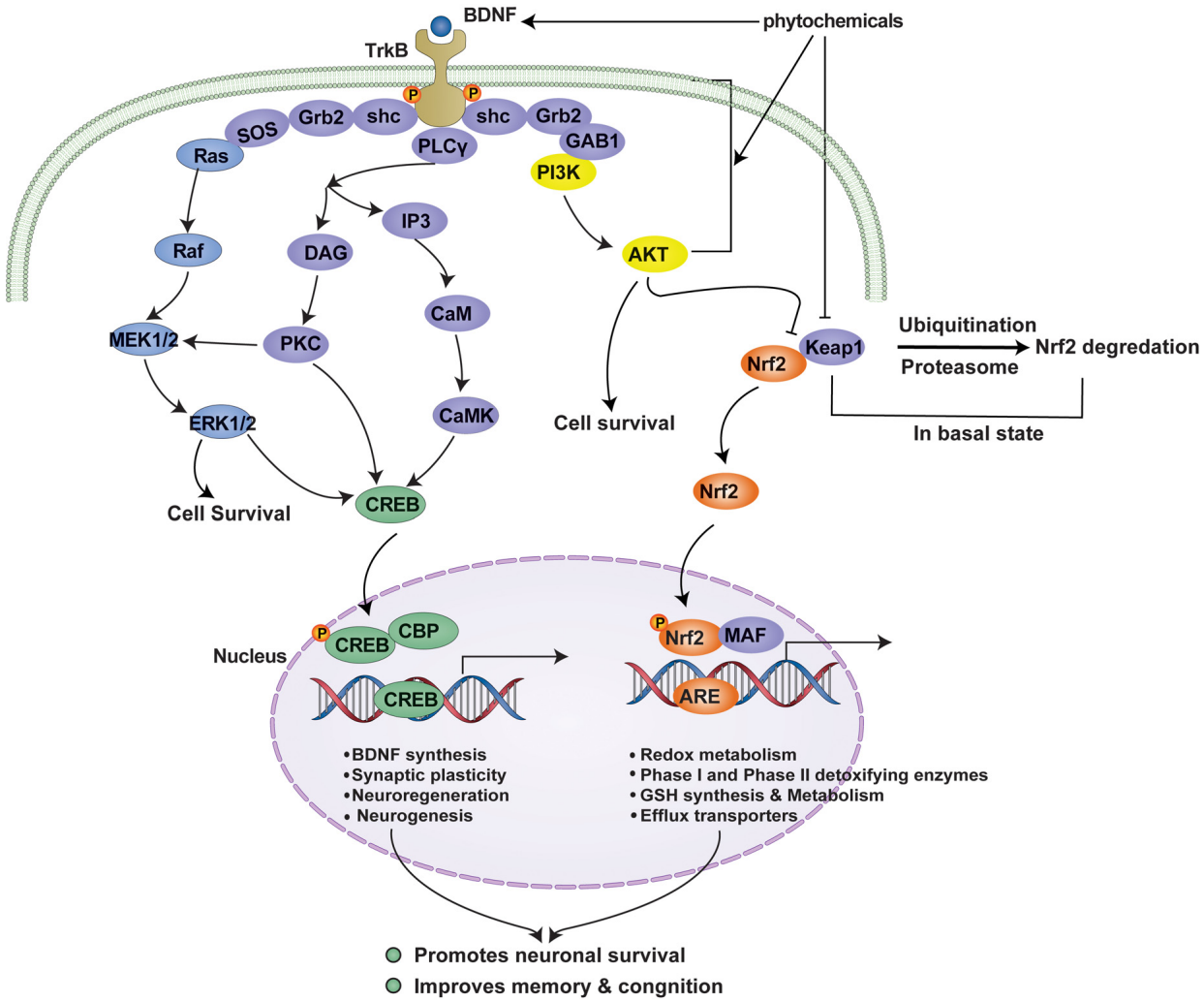

FIGURE 2 | TrkB signaling-mediated cell survival and the Nrf2-ARE antioxidant system. Neurons maintain survival and connectivity through neurotrophin signaling pathway such as the PI3K/Akt, MAPK (Ras/ref/Erk), and PLCγ (PKC or CaMK) pathways. The PI3K/Akt pathway destabilizes Nrf2-Keap1 complex, which under basal conditions leads to the ubiquitination and degradation of Nrf2 by proteasomal system, and thus, promotes the nuclear translocation of Nrf2. This, in turn, activates the Nrf2-ARE antioxidant system and results in the expressions of multiple genes that encode antioxidant enzymes responsible for redox metabolism and GSH synthesis and metabolism. Activated Akt also regulates cell survival by maintaining a balance between pro-apoptotic and anti-apoptotic proteins. Furthermore, MAPK and PLCγ signaling pathways regulate neuronal survival and the transcriptions of CREB-dependent genes that encode BDNF and other proteins required for synaptic plasticity and neurogenesis. Phytochemicals may promote cell survival by activating TrkB signaling by functioning as BDNF mimetics or by promoting Akt phosphorylation or inhibiting Nrf2-Keap1 complex, and thus, activating the antioxidant defense system. TrkB signaling and the Nrf2-ARE antioxidant system are complementary to each other and simultaneous activation of these pathways has been shown to confer neuroprotection against OS and to attenuate memory and cognition impairments in patients with NDDs or brain injury. BDNF, brain-derived neurotrophic factor; PI3K, phosphatidyl inositol-3 kinase; Akt, protein kinase B; MEK1/2, mitogen-activated protein kinase kinase; ERK1/2, extracellular signal-regulated kinase 1/2; PLCγ, phospholipase C-γ; DAG, diacylglycerol; PKC, protein kinase C; IP3, inositol 1,4,5-trisphosphate; CaM, calmodulin; CaMK, Ca^{2+}/calmodulin-dependent protein kinase; CREB, cAMP response element-binding protein); CBP, CREB binding protein; CRE, cAMP response elements; Nrf2, nuclear factor erythroid 2-related factor 2; Keap1, Kelch-like ECH-associated protein 1; MAF, small musculoaponeurotic fibrosarcoma; ARE, antioxidant response elements.

OS-mediated injury. The Keap1-Nrf2 pathway is the principal cellular pathway that regulates the antioxidant defense system. Nrf2 (encoded by *NFE2L2*) is a master regulator of cellular redox homeostasis, and its activity is regulated in various ways. Under resting conditions, Nrf2 is sequestered by Keap1 (Kelch-like ECH-associated protein) in the cytoplasm (Itoh et al., 1999), where it is polyubiquitinated and targeted for proteasomal degradation (McMahon et al., 2003). However, under OS or in a background of pharmacological intervention, the Nrf2-Keap1 complex is disrupted, which leads to the release of Nrf2 and its nuclear translocation (Joshi and Johnson, 2012). Once in the nucleus, Nrf2 forms heterodimers with small musculoaponeurotic fibrosarcoma (MAF) proteins, and these Nrf2-MAF heterodimers recognize an enhancer sequence termed ARE present in the regulatory regions of over 250 genes (Ma, 2013) (**Figure 2**).

Activation of the Nrf2-ARE pathway via Keap1-Nrf2 disruption results in the expressional up-regulation of multiple genes encoding a network of cooperating enzymes that constitute an antioxidant defense system (Joshi and Johnson, 2012; Dinkova-Kostova et al., 2018). The roles of this antioxidant system include redox homeostasis, involving SOD, CAT, sulfaredoxin (Srx), thioredoxin (Trx), and Prdx; GSH synthesis and metabolism, involving Gpx, GR, γ-glutamine cysteine ligase (GCL) and synthase (GCS); quinone recycling, involving NAD(P)H quinone oxidoreductase (Nqo1), and iron homeostasis- heme oxygenase 1 (HO-1).

Superoxide dismutases mediate the conversion of $O_2 \cdot^-$ to H_2O_2, which is subsequently neutralized to H_2O. SOD2 (Mn-SOD) is primarily found in mitochondria, where it acts to minimize oxidative damage by $O_2 \cdot^-$ (Murphy, 2009). Knockout of SOD2 increased amyloid plaque burden and exacerbated cognitive deficits in mice (Li et al., 2004; Esposito et al., 2006; Lee et al., 2012), and conversely, SOD2 overexpression reduced oxidative markers, amyloid deposition, and cognitive deficit in transgenic AD mice (Dumont et al., 2009). Peroxisomal catalase and GPx both catalyze the conversion of H_2O_2 to water and oxygen. GSH is generated from glutamate, cysteine, and glycine by γ-GCS, GCL, and glutathione synthetase (GS) (Murphy and Park, 2017). Furthermore, HO-1, in combination with cytochrome p450 and NADPH, catalyzes the degradation of heme to biliverdin, which is subsequently converted to bilirubin by biliverdin reductase, and both biliverdin and biliverdin reductase have antioxidant and anti-inflammatory effects (Joshi and Johnson, 2012; Murphy and Park, 2017). HO-1 overexpression has been reported in NDD (Schipper, 2004), presumably to compensate for oxidative damage (Cuadrado and Rojo, 2008).

In the degenerative brain, Nrf2 is primarily localized in cytoplasm (Ramsey et al., 2007), which suggests Nrf2 activity is insufficient to mediate a competent antioxidant response. This shortfall in Nrf2 activity might explain why oxidative damage is commonly observed in NDDs despite the presence of an antioxidant defense system (Ramsey et al., 2007). Evidence shows that Nrf2 knockdown left neurons more susceptible to OS, whereas Nrf2 overexpression reversed the effect (Lee and Johnson, 2004). In an amyloid protein precursor/presenilin 1 (APP/PS1) mouse model, Nrf2 knockout aggravated oxidative damage (Joshi et al., 2015), whereas activation or overexpression of Nrf2 protected APP/PS1 mice from Aβ toxicity (Kanninen et al., 2008). Moreover, in rat stroke model, Nrf2 overexpression rescued neurons from ischemic shock (Shih et al., 2005). Pharmacological modulators of Nrf2 have also shown therapeutic promise in experimental models of NDD (Dinkova-Kostova et al., 2018). Therefore, it is believed activation of the antioxidant defense system based on the targeting of Nrf2 signaling offers potential means of treating NDDs and brain injuries.

CELL SURVIVAL SYSTEM: THE TrkB SIGNALING PATHWAY

Neurotrophin signaling plays an essential role in maintaining neuronal survival and synaptic plasticity as well as learning and memory (Bothwell, 2019). BDNF is predominant among the several neurotrophins in the adult central nervous system. BDNF binds TrkB and helps maintain neuronal survival and synaptic plasticity by activating canonical signaling pathways, that is, the PI3K/Akt pathway, the mitogen-activated protein kinase (MAPK) pathway, and the phospholipase C-γ (PLCγ) pathway (Kowiański et al., 2018). The PI3K/Akt signaling pathway is the major TrkB-mediated survival pathway that promotes neuronal survival and protects against apoptosis (Wu et al., 2019). Activated Akt also controls cell survival by maintaining a balance between pro-apoptotic and anti-apoptotic proteins (Sussman, 2009). The MAPK and PLCγ pathways regulate neuronal growth and survival by expressing multiple genes in a CREB (cAMP response element binding protein)-dependent pathway, which encodes BDNF and other proteins associated with synaptic plasticity (Cunha et al., 2010; Numakawa et al., 2018) (**Figure 2**).

BDNF heterozygous knockout mice (BDNF ± mice) exhibit fear learning deficits (Meis et al., 2017). Moreover, in AD, alterations in BDNF level and its receptor were observed in the frontal cortex and the entorhinal cortex, which control spatial memory and higher cognitive functions (Weissmiller and Wu, 2012). Also, in *in situ* hybridization of the patient sample, the protein and mRNA levels of BDNF were found to be decreased in dopaminergic neurons of the substantia nigra (Mogi et al., 1999), in which the neurons are most vulnerable in PD. A line of evidence from experimental studies and metanalysis further showed a close correlation between decreased BDNF levels and neuronal loss in neurological disorders (Ventriglia et al., 2013; Siuda et al., 2017; Jiang et al., 2019). These observations suggest that the BDNF/TrkB signaling pathway plays an essential role in neuronal growth, survival and synaptic plasticity. Several natural compounds have been reported to activate the TrkB signaling pathway and promote cell survival (Obianyo and Ye, 2013), and therefore, have been suggested as possible treatments for NDD and brain injury.

CROSS-TALK BETWEEN TrkB SIGNALING PATHWAY AND Nrf2-ARE ANTIOXIDANT SYSTEM

Neurons maintain survival and connectivity through neurotrophin signaling pathways such as the PI3K/Akt, MAPK (Ras/ref/Erk), and PLCγ (PKC or CaMK) pathways. A piece of evidence suggests that the TrkB signaling pathway, the dominant neurotrophin pathway in mature neurons, may act upstream of the Nrf2-ARE system. For example, phosphorylation of Akt mediates the nuclear translocation of Nrf2, which, in turn, activates the Nrf2-ARE system resulting in the transcriptions of multiple genes encoding antioxidant enzymes (Qi et al., 2017). Moreover, PI3K/Akt pathway regulates hemeoxygenase-1 (HO-1), which is involved in the maintenance of cellular homeostasis (Pischke et al., 2005). Besides, growing evidence suggests a possible cross-talk between the TrkB signaling pathway and the Nrf2-ARE antioxidant system. For instance, the MAPK (ERK/p38 MAPK) pathway, another downstream signaling of TrkB pathway, was shown to regulate Nrf2 transcriptional

activity (Singh et al., 2010; Tufekci et al., 2011). TrkB signaling pathway and the Nrf2-ARE antioxidant system are, therefore, complementary to each other and simultaneous activation of these pathways has been shown to confer neuroprotection against OS and to attenuate memory and cognition impairments in patients with NDDs or brain injury.

Brain-derived neurotrophic factor-dependent $p75^{NTR}$ signaling is associated with TrkB and may also activate Nrf2 pathway. The primary receptor of BDNF, TrkB, has two functional isoforms-TrkB.FL (full-length) and TrkB.T1 (truncated) receptors. TrkB.FL inhibits ceramide generation through its low-affinity receptor, $p75^{NTR}$, via its tyrosine kinase activity. Conversely, TrkB.T1, lacking the intracellular tyrosine kinase domain, promotes ceramide generation following activation by BDNF. The $p75^{NTR}$ signaling pathway may act as a double-edged sword (Ishii and Mann, 2018). The overstimulation of $p75^{NTR}$ results in excess ceramide generation and was known to be associated with apoptosis (Ibáñez and Simi, 2012; Shen et al., 2019). Whereas, TrkB.FL receptor tyrosine kinase activity inhibits sphingomyelinase protecting cells from ceramide toxicity along with restricting the $p75^{NTR}$-mediated prodeath signaling pathway (Ishii et al., 2018). Moreover, the BDNF-TrkB.T1-$p75^{NTR}$ signaling complex generates physiological concentrations of ceramide to activate protein kinase Cζ (PKCζ) leading to activation of casein kinase 2 (CK2) and Nrf2, thereby modulating antioxidant capacity of cells (Ishii et al., 2018).

Neurons express both TrkB.FL and TrkB.T1 receptors but the ratio of these receptor levels changes based on the neuronal activity (Gomes et al., 2012). The excitotoxic stimulation of cultured rat hippocampal neurons results in the downregulation of TrkB.FL, while upregulation of TrkB.T1 expression caused a significant alternation in the ratio of the two receptors (Gomes et al., 2012), which allows BDNF to induce Nrf2 activation in the presence of $p75^{NTR}$ (Ishii and Mann, 2018). This mechanism protects neurons from oxidative damage during excitotoxic stimulation with glutamate, an event that frequently encountered in neural injury, stroke, and NDDs (Ishii and Mann, 2018). Moreover, BDNF-TrkB.T1-$p75^{NTR}$-Nrf2-mediated neuroprotection is context-dependent (Bothwell, 2019), i.e., it depends on the degree of activation. However, there is no evidence, so far, demonstrating the association of the neuroprotective phytochemicals with this signaling pathway suggesting further investigation.

PHYTOCHEMICALS THAT ACTIVATE NEURONAL ANTIOXIDANT DEFENSE AND SURVIVAL

Many plant-derived bioactive molecules neutralize ROS and reportedly, potentiate the cellular antioxidant system. This latter mode of inducing an antioxidant effect by promoting adaptive cellular stress response using phytochemicals is substantially supported (Son et al., 2008; Lee et al., 2014). Furthermore, these molecules can promote cellular survival by activating the growth signaling pathway. Here, we reviewed the literature over the past 5 years for phytochemicals that have been shown to protect neurons from OS by activating TrkB signaling pathways and the Nrf2-ARE system; two excellent reviews appropriately addressed preceding reports (Moosavi et al., 2015; Murphy and Park, 2017). Specific targets, experimental and disease models, research outcomes, and pharmacological markers of these phytochemicals are summarized in **Tables 1–3**.

Phenolic Compounds

Several phenolics have been reported to exhibit neuroprotective effects against OS in models of AD and other neurodegenerative disorders (**Table 1**). For example, sulfuretin, a flavonoid glycoside isolated from the stem bark of *Albizia julibrissin* and heartwood of *Rhus verniciflua*, protected SH-SY5Y cells and primary hippocampal neurons from Aβ-induced neurotoxicity (Kwon et al., 2015). The PI3K/Akt and Nrf2/HO-1 signaling pathways have been proposed to contribute to sulfuretin-mediated neuroprotection. Sulfuretin is considered to inhibit cell death by suppressing ROS production and enhancing PI3K/Akt pathway and the nuclear translocation of Nrf2. Resveratrol, a polyphenol found in grapes, and anthocyanins, derived from Korean black beans, protected PC12 cells (Hui et al., 2018) and HT22 cells (Ali et al., 2018), respectively from Aβ-induced toxicity by activating the PI3K/Akt/Nrf2 pathway. In Aβ-induced toxicity, resveratrol inhibited cell death and suppressed OS markers such as MDA and ROS by increasing the phosphorylations of PI3K and Akt, the nuclear translocation of Nrf2, and the protein levels of SOD, HO-1, and GSH (Hui et al., 2018). Anthocyanins attenuate cell death by suppressing the expressions of pro-apoptotic markers (e.g., cleaved caspase-3) and stress markers (MDA, H_2O_2, 8-OHdG) and enhancing the phosphorylations of PI3K, Akt, glycogen synthase kinase-3 beta (GSK3β), the nuclear translocation of Nrf2, the expression of HO-1, and GSH levels (Ali et al., 2018). Tea polyphenols (TPs) attenuated OS in H_2O_2-stimulated SH-SY5Y cells by activating the Keap1-Nrf2 signaling pathway and the TrkB/CREB/BDNF pathway (Qi et al., 2017). TPs attenuated H_2O_2-induced cell death and mitochondrial dysfunction and elevated ROS and H_2O_2 levels (Qi et al., 2017). Moreover, TPs enhanced the nuclear translocation of Nrf2 and the TrkB/CREB/BDNF signaling pathway by activating the PI3K/Akt pathway, and thus, transcriptionally regulated the downstream expressions of HO-1, NQO1, SOD, GPx, and CAT in SH-SY5Y cells (Qi et al., 2017). 8-Hydroxydaidzein (8-OHD), an isoflavone of fermented soy, protected against neuroinflammation in LPS-stimulated BV2 microglial cells (Wu et al., 2018) by activating Nrf2-antioxidant and Akt/NF-κB-inflammatory signaling pathways. In BV2 microglial cells, 8-OHD inhibited the LPS-stimulated productions of NO, TNF-α, and IL-6 by suppressing gene expression (Wu et al., 2018). Moreover, 8-OHD quenches ROS and promotes the nuclear translocation of Nrf2, and thus, upregulates the expressions of Phase II enzymes, such as HO-1, NQO1, and GCL (Wu et al., 2018). 8-OHD also suppresses the LPS-stimulated phosphorylations of Akt and NF-κB-p65, and attenuates LPS-induced prostaglandin E_2 (PGE_2) production without affecting COX-2 expression (Wu et al., 2018). Rutin, a flavonoid found in buckwheat, protected male albino SD rats from acrylamide or γ-radiation-induced neurotoxicity by activating

TABLE 1 | Neuroprotection afforded by phytochemicals targeting the PI3K/Akt/Nrf2 signaling pathway against AD and other neurodegenerative disorders.

Modulator	Specific target pathway	Chemical class and natural sources	Experimental model	Disease model	Pathobiology involved	Major research outcomes	Molecular markers	References
Phenolic compounds								
Sulfuretin	PI3K/Akt and Nrf2/HO-1 signaling pathways	Flavonoid glycosides; stem bark of *Albizzia julibrissin* and heartwood of *Rhus verniciflua*	Aβ-induced neurotoxicity in SH-SY5Y cells and primary hippocampal neurons	AD	Oxidative stress	Neuroprotection (antioxidation and increased cell survival)	↓ROS, ↑HO-1 ↑PI3K/Akt ↑Nrf2	Kwon et al. (2015)
Resveratrol	PI3K/Akt/Nrf2 pathway	Polyphenol; grapes	Aβ1–42-induced cytotoxicity in PC12 cells	AD	Oxidative stress	Neuroprotection (antioxidant and anti-apoptosis); amelioration of memory impairment	↓MDA, ROS ↑SOD, HO-1, GSH, Nrf2 ↑PI3K, Akt	Hui et al. (2018)
Anthocyanins	PI3K/Akt/Nrf2 signaling	Anthocyanins; Korean black beans	APP/PS1 mouse model of AD; AβO-induced neurotoxicity in HT22 cells	AD	Oxidative stress	Neuroprotection (antioxidant)	↑p-PI3K, p-Akt, pGSK3β (Ser9) ↑Nrf2 ↑HO-1, GCLM ↓MDA, H_2O_2, 8-OxoG ↑GSH ↓cleaved caspase 3 ↓PARP1	Ali et al. (2018)
Tea polyphenols	TrkB/CREB/BDNF pathway and Keap1/Nrf2 signaling pathway	Tea flavonoids	H_2O_2-treated SH-SY5Y neuronal cells; shift work disruption model of C57BL/6J male mice	NDD	Oxidative stress	Neuroprotection (antioxidation, anti-apoptosis, attenuates mitochondrial dysfunction); amelioration of memory impairment	↓Bax, cytochrome c, caspase-3 activation, PARP cleavage, ↑Bcl-2 ↑p-TrkB, pCREB, BDNF ↑MMP, ↓H_2O_2 ↓IκB, NF-κB ↑ERK, pAkt, pERK ↓pJNK, pP38 ↑HO-1, NQO-1 c, Nrf2, Keap1 ↑γGCS, MnSOD, GPx1, GSH, SOD, CAT	Qi et al. (2017)
8-Hydroxydaidzein	Nrf2-antioxidant and Akt/NF-κB-inflammatory signaling pathways	Isoflavone; fermented soy food	LPS-stimulated BV2 microglial cells	NDD	Neuroinflammation and oxidative stress	Anti-inflammation and antioxidation	↓NO ↓TNF-α, IL-6, IL-1β ↓ROS, ↑Nrf2 ↑HO-1, NQO1 ↓NF-κB-p65 ↓PGE2	Wu et al. (2018)
Rutin	PI3K/Akt/GSK-3β/NRF-2 signaling pathway	Flavonoid; buckwheat	Acrylamide or γ-radiation-induced neurotoxicity in male albino SD rats	NDD	Oxidative stress	Neuroprotection (antioxidant and anti-inflammatory)	↑p-PI3K, p-Akt, p-GSK-3β ↑NRF-2, ↓MDA ↓GST ↓IL-1b, IL-6 ↑IGF1, NGF	Thabet and Moustafa (2018)

(Continued)

TABLE 1 | Continued

Modulator	Specific target pathway	Chemical class and natural sources	Experimental model	Disease model	Pathobiology involved	Major research outcomes	Molecular markers	References
Non-phenolic compounds								
Brassicaphenanthrene A	Nrf2-mediated HO-1 expression by PI3K/Akt and JNK regulatory pathways	Phenanthrene derivative; *Brassica rapa* ssp. campestris (Brassicaceae) (Turnip)	Glutamate-induced excitotoxicity in HT-22 neuronal cells	AD	Oxidative stress	Neuroprotection (antioxidation)	↑HO-1, Nrf2 ↑GSH ↑Glutamine- cysteine ligase ↑Nrf2 nuclear translocation and ARE promoter activity ↑pAkt	Lee et al. (2020)
Acerogenin A	PI3K/Akt/Nrf2/HO-1 pathway	Stem bark of Japanese folk medicine *Acer nikoense*	Glutamate-induced oxidative neurotoxicity in HT22 cell line	NDD	Oxidative stress	Neuroprotection (antioxidant)	↓ROS ↑HO-1 ↑Nrf2 ↑pAkt	Lee et al. (2015)
TMC-256C1	PI3K/Akt/Nrf2 pathway	Marine-derived fungus *Aspergillus* sp. SF6354	LPS-stimulated BV2 microglial cells and glutamate-induced neurotoxicity in mouse hippocampal HT22 cells	NDD	Oxidative stress and neuroinflammation	Neuroprotection (anti-inflammatory and antioxidant)	↑HO-1, Nrf2 ↓ROS ↓TNF-α, IL-1β, IL-6, IL-12 ↓I PEG_2, NO ↓Cox2, iNOS ↓NF-κB, plκBα, p65, p50 ↑pAkt	Kim et al. (2016)
Polysaccharide extracts	PI3K/Akt and Nrf2-mediated HO-1/NQO1 pathways	Polysaccharide; *Perilla frutescens*	H_2O_2-induced oxidative stress in HT22 hippocampus cells	NDD	Oxidative stress	Neuroprotection (antioxidant and anti-inflammatory)	↓Bax, cytochrome c ↓caspases-3, -8, and -9 ↑PARP, ↑Bcl-2 ↑SOD, ↓MDA ↓p MAPKs (p38, ERK, JNK), ↓NF-κB ↑HO-1, ↑p-PI3K, ↑pAkt, p65	Byun et al. (2018)
3,3'-Diindolylmethane	TrkB/Akt pathway and antioxidant enzyme system	Metabolite of indole-3-carbinol; Brassicaceae vegetables	Glutamate-treated HT-22 cells; scopolamine-treated ICR mice	NDD	Oxidative stress	Neuroprotection (antioxidant and anti-apoptosis); amelioration of memory impairment	↓ROS, ↑GSH ↓Bax, cytochrome c, cleaved caspase-3, AIF ↑Bcl-2 ↑p-TrkB, p-CREB, BDNF, p-Akt ↑HO-1, GCLC, NQO-1 ↓MDA ↓AChE, ↑ChAT ↑GR, Gpx	Lee et al. (2019)
N-Acetyl serotonin	BDNF/TrkB/CREB signaling and Akt/Nrf2/antioxidant enzyme pathway	Naturally occurring precursor and intermediate in the melatonin biosynthesis	Glutamate or H_2O_2-induced oxidative stress in HT-22 cells; scopolamine-treated memory impairment in Swiss CD-1 mice	AD	Oxidative stress	Neuroprotection (antioxidation and anti-apoptosis); amelioration of memory impairment	↓AIF, Bax, calpain, cytochrome c and cleaved caspase-3 ↑Bcl-2 ↑pTrkB, pCREB, BDNF ↓ROS, ↑GSH ↑Nrf2, HO-1, GCLC	Yoo et al. (2017)

TABLE 2 | Neuroprotection afforded by phytochemicals targeting the PI3K/Akt/Nrf2 signaling pathway against ischemic stroke and other neuronal injuries.

Modulator	Specific target pathway	Chemical class and natural sources	Experimental model	Disease model	Pathobiology involved	Major research outcomes	Molecular markers	References
Phenolic compounds								
Totarol	Akt/HO-1 pathway	Phenolic diterpenoid; sap of *Podocarpus totara*	Glutamate and OGD-induced injury in rat cerebellar granule neurons and cerebral cortical neurons; MCAO model of acute cerebral ischemic injury in adult male SD rats	Ischemic stroke	Oxidative stress	Neuroprotection (antioxidant)	↑pAkt, pGSK-3β ↑Nrf2 ↑HO-1, SOD ↑GSH	Gao et al. (2015)
Rosmarinic acid	PI3K/Akt/Nrf2 signaling pathway	Phenolic compound; commercial source	Right middle cerebral artery occlusion in CD-1 mice	Ischemic stroke	Oxidative stress	Neuroprotection (anti-oxidative and anti-apoptotic properties)	↑Bcl-2, ↓Bax ↑HO-1, ↑Nrf2 ↑SOD, ↓MDA ↓pAkt	Cui et al. (2018)
Baicalin	Akt/Nrf2 pathway	Flavone; radix of *Scutellaria baicalensis*	TBI mice model	TBI	Oxidative stress	Neuroprotection (anti-oxidative and anti-apoptotic properties); attenuates neurological deficits and brain edema	↑Bcl-2, ↓Bax, ↓MDA ↑GPx, SOD, NQO-1, HO-1 ↓cleaved caspase 3 ↑pAkt	Fang et al. (2018)
Non-phenolic compounds								
Diallyl trisulfide	PI3K/Akt -mediated Nrf2/HO-1 signaling pathway	Organosulfur compound of garlic oil	OGD-induced neuronal injury in B35 rat neuroblastoma cells	Ischemic stroke	Oxidative stress	Neuroprotection (antioxidant)	↓ROS ↓MDA ↑Nrf2 ↑HO-1 ↓Cleaved caspase-3 ↑pAkt	Xu et al. (2015)
Oxymatrine	Akt/GSK3β/HO-1/Nrf-2 signaling pathway	Quinolizidine alkaloid; Chinese herb *Sophora flavescens*	Hypoxic-ischemic brain injury model of P7 SD rats	Ischemic stroke	Oxidative stress	Neuroprotection (anti-oxidative and anti-apoptotic properties); attenuates neurological deficits and reduces infarct volume	↑p-Akt ↑p-GSK3β ↑Nrf-2 ↑HO1	Ge et al. (2018)

(Continued)

TABLE 2 | Continued

Modulator	Specific target pathway	Chemical class and natural sources	Experimental model	Disease model	Pathobiology involved	Major research outcomes	Molecular markers	References
6′-*O*-galloylpaeoniflorin	PI3K/Akt/Nrf2 activation	Galloylated derivative of paeoniflorin; peony root	OGD-induced ischemic model of PC12 cells; CIRI model of male Wistar rats	Ischemic stroke	Neuroinflammation and oxidative stress	Neuroprotection (antioxidant and anti-inflammatory); reduces infarct volume and improves neurological deficits	↑p-Akt, Nrf2 ↓MDA, SOD ↓TNF-α, IL-1β ↓Caspase 3	Wen et al. (2018)
Diterpene ginkgolides (ginkgolides A, B and C)	Akt/Nrf2 and Akt/CREB signaling pathways	Ginkgolide terpenoid lactones; *Ginkgo biloba* L	MCAO model of acute cerebral ischemic injury in adult male SD rats; OGD/R-induced ischemic injury in PC12 cells	Ischemic stroke	Oxidative stress	Neuroprotection (antioxidant)	↑pAkt, pNrf2, pCREB ↑HO-1 ↓cleaved caspase 3, Bax	Zhang et al. (2018)
Ginkgolides (ginkgolide A, ginkgolide B, ginkgolide K) and bilobalide	Akt/Nrf2 signaling pathway	Ginkgolide terpenoid lactones; *Ginkgo biloba* L	OGD-induced ischemic model of SH-SY5Y cells; MCAO model of cerebral ischemic injury in male SD rats	Ischemic stroke	Oxidative stress	Neuroprotection (antioxidation)	↑HO-1, Nqo1, SOD ↑p-Akt ↑p-Nrf2, Nrf2 ↓ROS	Liu Q. et al. (2019)
Protodioscin	PI3K/Akt/Nrf2 pathway	Steroidal saponin	OGD/reperfusion-induced neuronal injury in PC12 cells	Ischemic stroke	Oxidative stress	Neuroprotection (antioxidant, anti-apoptotic effects)	↓ROS, MDA ↑HIF-1α, SOD, GPx HSP70, HO-1, PI3K, pAkt ↑Nuclear Nrf2 ↑miR-124	Shu and Zhang (2019)
Matrine	PI3K/Akt-mediated NF-κB inhibition and Keap1/Nrf2-dependent HO-1 induction	Quinolizidine alkaloid derived from the herb *Radix sophorae* Flavescentis	Subarachnoid hemorrhage in rat	Brain injury	Oxidative stress (secondary effects)	Attenuates neurological deficit, brain edema, and BBB disruption	↓TNF-α, IL-1β ↓Bax, caspase-3 ↑Bcl-2 ↑pAkt, plκB-α ↓NF-kB P65 ↑Keap1, Nrf2, and HO-1 ↓MMP-9	Liu et al. (2016)
Panax notoginseng saponins	PI3K/Akt/Nrf2 antioxidant signaling pathway	Saponins; *P. notoginseng*	LPS-stimulated cerebral microvascular endothelial cells (bEnd.3)	BBB injury (hemorrhagic stroke)	Oxidative stress	Protection of BBB	↓IL−1β, TNF−α ↓ROS ↑Nrf2, HO−1 ↓NF−κB ↑pAkt	Hu et al. (2019)

TABLE 3 | Anti-aging potentials of phytochemicals that target the PI3K/Akt/Nrf2 signaling pathway.

Modulator	Specific target pathway	Chemical class and natural sources	Experimental model	Disease model	Pathobiology involved	Major research outcomes	Molecular markers	References
Naringenin	PI3K/Akt/Nrf2 Pathway	Polyphenol	D-Galactose-induced brain aging model of male ICR mice	Brain aging	Oxidative stress	Neuroprotection (antioxidant)	↑Nrf2 ↑HO−1, NQO1, SOD, CAT ↑pPI3K, pAkt	Zhang et al. (2017)
Maltol	PI3K/Akt-mediated Nrf2/HO-1 signaling pathway	Maillard reaction product from ginseng	D-Galactose-induced brain aging model of male ICR mice	Brain aging	Oxidative stress	Antiaging (antioxidation)	↑ChAT, ↓AChE ↓ROS, MDA ↑pPI3K, pAkt, ↑pNrf2 ↑HO-1, CAT ↑GSH	Sha et al. (2019)

the PI3K/Akt/GSK-3β/NRF-2 signaling pathway (Thabet and Moustafa, 2018). Here, rutin increased the phosphorylations of PI3K, Akt, and GSK-3β and the nuclear translocation of Nrf2, suppressed MDA levels, GST activity, and the expressions of IL-1b and IL-6, and increased IGF1 and NGF levels (Thabet and Moustafa, 2018).

Three phenolics have been shown to have neuroprotective effects against OS in ischemic stroke and other brain injury models (**Table 2**). Totarol is a phenolic diterpenoid isolated from the sap of *Podocarpus totara* and protected rat cerebellar granule neurons and cerebral cortical neurons from glutamate and OGD (oxygen-glucose deprivation)-induced injury in a manner involving the Akt/HO-1 pathway (Gao et al., 2015). Totarol increased the nuclear translocation of Nrf2, the expressions of HO-1 and SOD, GSH levels, and the phosphorylations of Akt and GSK-3β (Gao et al., 2015). In CD-1 right middle cerebral artery occlusion (MCAO) mouse model, rosmarinic acid protected against ischemic stroke (Cui et al., 2018) by activating the PI3K/Akt/Nrf2 signaling pathway. In this ischemic model, rosmarinic acid improved ischemic outcomes, attenuated neuronal apoptosis, upregulated the protein and mRNA levels of Bcl-2, HO-1, and Nrf2, downregulated Bax expression, increased SOD activity and Akt phosphorylation, and lowered MDA levels (Cui et al., 2018). Baicalin is a flavone isolated from the radix of *Scutellaria baicalensis*, and in a TBI mouse model protected from oxidative injury by activating the Akt/Nrf2 pathway (Fang et al., 2018). Baicalin reduced Bax and cleaved caspase-3 levels but enhanced Bcl-2 expression and increased the nuclear translocation of Nrf2, the expressions of GPx, SOD, NQO-1, and HO-1, and the phosphorylation of Akt (Fang et al., 2018). Baicalin also improved neurological deficits (Fang et al., 2018).

Non-phenolic Compounds

Several non-phenolics have been reported to exhibit neuroprotective effects against OS in models of AD and other neurodegenerative disorders (**Table 1**). For instance, brassicaphenanthrene A isolated from *Brassica rapa* protected HT-22 neuronal cells from glutamate-induced excitotoxicity and upregulated Nrf2-mediated HO-1 expression via PI3K/Akt and JNK regulatory pathways (Lee et al., 2020). Acerogenin A isolated from the stem bark of *Acer nikoense* (a traditional Japanese medicine) protected HT22 cells from glutamate-induced oxidative injury (Lee et al., 2015 activating the PI3K/Akt/Nrf2/HO-1 pathway. Acerogenin A attenuated cell death by suppressing the production of ROS and increasing the nuclear translocation of Nrf2, the expression of HO-1, and the phosphorylation of Akt (Lee et al., 2015). TMC-256C1 isolated from a marine-derived fungus (*Aspergillus* sp. SF6354) protected BV2 microglial cells from LPS-induced inflammatory response and mouse hippocampal HT22 cells from glutamate-induced neurotoxicity (Kim et al., 2016). The PI3K/Akt/Nrf2 pathway has been implicated in the neuroprotective effect of TMC-256C1. TMC-256C1 suppressed the expressions of pro-inflammatory markers (NF-κB (nuclear factor-kappa B), pIκBα (phosphorylated inhibitor of NF-κB alpha), p65, and p50) and inflammatory cytokines (TNF-α (tumor necrosis

factor), interleukin (IL)-1β, IL-6, IL-12), and increased the nuclear translocation of Nrf2 and the expression of HO-1 (Kim et al., 2016). TMC-256C1 also suppressed the expression of IPEG2, NO (nitric oxide), COX2 (cyclooxygenase 2), and iNOS (induced nitric oxide synthase) and increased the phosphorylation of Akt (Kim et al., 2016). Polysaccharide extracts (PPE) of *Perilla frutescens* activated PI3K/Akt and Nrf2-mediated HO-1/NQO1 pathways and protected against H_2O_2-induced OS in HT22 cells (Byun et al., 2018). PPE attenuated cell injury by suppressing the expressions of Bax, cytochrome C, and caspases-3,-8, and -9, and enhancing the expressions Bcl-2 and Poly [ADP-ribose] polymerase (PARP) (Byun et al., 2018). PPE also increased the phosphorylations of MAPKs (p38, ERK, JNK), PI3K, Akt and p65, decreased NF-κB level and enhanced the nuclear translocation of Nrf2 and the expressions of HO-1 and SOD (Byun et al., 2018). 3,3′-Diindolylmethane is a metabolite of indole-3-carbinol found in Brassicaceae family and was found to attenuate OS in glutamate-induced HT-22 cells by activating the TrkB/Akt pathway (Lee et al., 2019). 3,3′-Diindolylmethane metabolite attenuated the expressions of Bax, cytochrome c, cleaved caspase-3, and AIF (apoptosis-inducing factor), and increased Bcl-2 expression, the phosphorylations of TrkB, Akt, and CREB, and the expressions of HO-1, GCLC, NQO-1, and GPx (Lee et al., 2019). 3,3′-Diindolylmethane also improved cognitive deficits in scopolamine-treated mice (Lee et al., 2019). *N*-Acetyl serotonin (NAS), a melatonin precursor (non-phytochemical) with a stronger antioxidant effect than 3,3′-diindolylmethane, protected neurons from glutamate or H_2O_2-induced-OS (Yoo et al., 2017). NAS-mediated neuroprotection was found to involve BDNF/TrkB/CREB signaling and the Akt/Nrf2/antioxidant system (Yoo et al., 2017). NAS inhibited neuronal death by suppressing the expressions of pro-apoptotic markers (e.g., AIF, Bax, calpain, cytochrome c, and cleaved caspase-3, by enhancing pro-survival markers (e.g., Bcl-2), and by increasing the nuclear translocation of Nrf2 and the expressions of antioxidant enzymes (e.g., HO-1 and GCLC) (Yoo et al., 2017). In addition, NAS also ameliorated scopolamine-induced memory impairment and attenuated cell death in CA1 and CA3 brain regions in mice (Yoo et al., 2017).

Several non-phenolics have been reported to have neuroprotective effects against OS in ischemic stroke models (**Table 2**). For example, in B35 rat neuroblastoma cells, diallyl trisulfide, an organosulfur compound in garlic oil, activated the PI3K/Akt -mediated Nrf2/HO-1 signaling pathway and protected against OGD-induced neuronal injury (Xu et al., 2015). Diallyl trisulfide inhibited the expressions of pro-apoptotic markers (e.g., cleaved caspase-3), OS markers (ROS and MDA), and increased the nuclear translocation of Nrf2, the expression of antioxidant enzymes (e.g., HO-1), and the phosphorylation of Akt (Xu et al., 2015). Oxymatrine, isolated from the Chinese herb *Sophora flavescens* protected P7 SD rats from hypoxic-ischemic brain injury (Ge et al., 2018), activating the Akt/GSK3β/HO-1/Nrf-2 signaling pathway. In experimental rats, oxymatrine increased the nuclear translocation of Nrf2, the phosphorylations of Akt and GSK3β, and HO-1 expression and attenuated neurological deficits (Ge et al., 2018). 6′-*O*-Galloylpaeoniflorin, a galloylated derivative of paeoniflorin isolated from peony root, protected an OGD-induced ischemic PC12 cell model and a CIRI male Wistar rat model against ischemic stroke by activating PI3K/Akt/Nrf2 (Wen et al., 2018). In this study, 6′-*O*-galloylpaeoniflorin attenuated OS and neuroinflammation, improved neurological deficits, inhibited apoptosis by suppressing the expressions of pro-apoptotic markers (e.g., cleaved caspase-3), inhibited inflammatory cytokine (TNF-α, IL-1β), and MDA levels, and increased the nuclear translocation of Nrf2 and SOD expression by increasing Akt phosphorylation (Wen et al., 2018). Ginkgolides A, B and C are diterpene ginkgolides isolated from *Ginkgo biloba* L. and protected PC12 cells from OGD/R-induced ischemic injury and adult male SD rats subjected to MCAO-induced acute cerebral ischemic injury (Zhang et al., 2018) by activating Akt/Nrf2 and Akt/CREB signaling pathways. These ginkgolides inhibit cell death by suppressing the expressions of Bax and cleaved caspase-3, enhancing the phosphorylations of Akt and pCREB, and increasing the nuclear translocation of Nrf2 and HO-1 expression (Zhang et al., 2018). Liu et al. demonstrated ginkgolides protected against ischemic stroke using an OGD-induced SH-SY5Y cell ischemic model and MCAO-induced model of cerebral ischemic injury in male SD rats (Liu Q. et al., 2019). Ginkgolides inhibited ROS production and increased Akt phosphorylation, the nuclear translocation and phosphorylation of Nrf2, and the expressions of HO-1, Nqo1, and SOD (Liu Q. et al., 2019). Protodioscin protected PC12 cells against OGD/R-induced neuronal injury by activating the PI3K/Akt/Nrf2 pathway by increasing the expressions of HIF-1α, SOD, GPx, HSP70, and HO-1, the phosphorylations of PI3K and Akt, the nuclear translocation of Nrf2, and upregulating miR-124, and thus, attenuating OS (Shu and Zhang, 2019).

Non-phenolics also attenuate other brain injuries by targeting the PI3K/Akt/Nrf2 signaling pathway (**Table 2**). For example, matrine, a quinolizidine alkaloid derived from the herb Radix *Sophorae flavescentis*, protected rats from subarachnoid hemorrhage (Liu et al., 2016) via PI3K/Akt-mediated NF-κB inhibition and Keap1/Nrf2-dependent HO-1 induction. Matrine suppressed the expressions of inflammatory cytokines (TNF-α, IL-1β) and pro-apoptotic markers (Bax and cleaved caspase-3) and enhanced the pro-survival marker Bcl-2 (Liu et al., 2016). Matrine increased nuclear translocation of Nrf2 and HO-1 expression and lowered NF-kB P65 expression by increasing the phosphorylations of Keap1, Akt, and IκB-α (Liu et al., 2016). *Panax notoginseng* saponins were observed to protect against blood–brain barrier (BBB) injury (Hu et al., 2019) by activating the PI3K/Akt/Nrf2 antioxidant signaling pathway. In LPS-stimulated cerebral microvascular endothelial cells of this BBB injury model, saponins attenuated the productions of ROS and inflammatory cytokines (IL−1β, TNF−α), decreased NF−κB levels, and increased the nuclear translocation of Nrf2 HO-1 expression, and the phosphorylation of Akt (Hu et al., 2019).

Phytochemicals have also been reported to confer neuroprotection against OS-induced brain aging by activating the

PI3K/Akt/Nrf2 pathway. For instance, naringenin, a polyphenol, protected against OS-induced aging in a D-galactose-induced male ICR mouse model of brain aging by activating the PI3K/Akt/Nrf2 pathway and increasing the nuclear translocation of Nrf2, the expressions of HO−1, NQO1, SOD, and CAT, and the phosphorylations of PI3K and Akt (Zhang et al., 2017). A similar study showed that maltol, a Maillard reaction product of ginseng, protected against brain aging (Sha et al., 2019), activating the PI3K/Akt-mediated Nrf2/HO-1 signaling pathway. In a D-galactose-induced male ICR mouse model of brain aging, maltol inhibited cell death and suppressed the productions of OS markers (ROS and MDA) by enhancing the phosphorylations of PI3K and Akt and increasing the nuclear translocation and phosphorylation of Nrf2 and the expression of antioxidative enzymes, such as HO-1, CAT, and GSH (Sha et al., 2019). Maltol also suppressed AChE and increased ChAT production (Sha et al., 2019).

In addition to the aforementioned reports, Murphy and Park (2017) reviewed the neuroprotective effects of several phytochemicals, such as luteolin (Lin et al., 2010), apigenin (Han et al., 2012; Zhao et al., 2013), 7,8-dihydroxyflavone (Jang et al., 2010), harpagoside (Li et al., 2015), and allicin (Li et al., 2010; Zhu et al., 2015), which all target antioxidant defense and neurotrophic signaling systems (Murphy and Park, 2017). Several natural compounds have been shown to have neuroprotective potential by either activating the antioxidant defense system (Sun et al., 2017), for example, pinocembrin (Jin et al., 2015; Wang et al., 2016), naringenin (Lou et al., 2014), ginsenoside Re (Liu M. et al., 2019), genistein (Wang et al., 2013), orientin (Yu et al., 2015), tiliroside (Velagapudi et al., 2018), or by activating the neurotrophin-mediated cell survival system (Moosavi et al., 2015), for example, curcumin (Zhang et al., 2015), topiramate (Mao et al., 2015), 3β,23,28-trihydroxy-12-oleanene 3β-caffeate (Cheng et al., 2019), and icariside II (Yin et al., 2018).

CONCLUSION AND FUTURE DIRECTIONS

Oxidative stress has been implicated in the pathogeneses of degenerative brain disorders, and hence, its targeting offers a means of developing a viable strategy to treat these chronic brain diseases. Cells are equipped with an antioxidant defense system to combat the effects of OS, and Nrf2 is the master regulator of redox homeostasis and does so by activating the antioxidant enzyme system. Accordingly, targeting Nrf2 appears to offer a means of controlling OS. However, attenuating OS alone may not confer sufficient protection against these diseases, in which case, targeting the classical cell survival pathway, that is, the TrkB/PI3K/Akt pathway would be required to restore cellular function, as these signaling pathways upregulate prosurvival factors but suppress their pro-apoptotic counterparts. Pharmacological modulators that can coactivate TrkB signaling-mediated cell survival and Nrf2-ARE antioxidant systems offer promise for the treatment of diseases associated with OS-associated brain degeneration. In this context, several phytochemicals have been reported to protect against neuronal injury by activating TrkB/PI3K/Akt and Nrf2 signaling systems, which suggests they could be utilized to design novel therapeutic agents for NDD, ischemic stroke, TBI, and brain aging.

In addition, being antioxidants, several vitamins such as vitamins E and C and the related compounds have also shown to confer neuroprotection in preclinical studies (Boccardi et al., 2016; Alzoubi et al., 2019). However, the majority of the human trials with these antioxidant vitamins failed to provide compelling evidence of clinical efficacy to improve AD outcomes (NCT00040378; Galasko et al., 2012; Farina et al., 2017; Kryscio et al., 2017). Although the causes are multifactorial, these vitamins only are only suggested to limit OS via directly scavenging reactive free radicals, thus acting as non-specific protective chemical shields (Behl, 1999). No evidence is, so far, suggestive of their capacity to enhance regeneration of damaged neuronal networks that occurred in neurodegenerative disorders and brain injury. On the contrary, phytochemicals (for example, resveratrol, tea polyphenols, and some other compounds mentioned earlier) that were shown to promote the regeneration capacity of neurons along with their protection by dual targeting TrkB/PI3K and Nrf2-ARE signaling (Qi et al., 2017; Hui et al., 2018) may have a better chance of succeeding in the clinical trial with AD subjects.

Although the neuroprotective actions of these phytochemicals are encouraging, their effects have only been reported in preclinical studies. No clinical evidence investigating the neuroprotective potential of phytochemicals that involve TrkB/Nrf2 signaling pathways has, so far, been reported. The attempt to clinical studies may fail to succeed, even if a phytochemical in preclinical investigations responds significantly. The reasons for these outcomes might include the poor bioavailability and the discrepancy between the doses used for the preclinical investigation and those used in clinical trials. Resveratrol, for example, is a potent neuroprotective agent that activates PI3K/Akt/Nrf2 pathway in the cell culture system, but shows poor bioavailability (due to chemical instability, BBB, low absorption, rapid metabolism, and clearance) and thus requires improved drug delivery systems, such as nanoparticle-mediated drug delivery along with the appropriate drug dose regimen. Moreover, the in-depth molecular cross-section of the neuroprotective effects of phytochemicals is essential to identify which cellular defense system between TrkB signaling and Nrf2 pathways is particularly involved in this effect and to elucidate pharmacodynamics.

AUTHOR CONTRIBUTIONS

MAH contributed to the design of this review, manuscript writing, table, and figure construction. RD contributed to manuscript writing and figure drawing. AAMS contributed to manuscript writing, revision, and summary table preparation. MNH contributed to manuscript writing and revision. ISM contributed to review planning, supervision, and manuscript revision. All authors contributed to the article and approved the submitted version.

FUNDING

Our research work and publications have been supported by Korea Research Fellowship Program (#2018H1D3A1A01074712 to MAH), and by the Basic Science Research Program (#2018R1A2B6002232 to ISM) through the National Research Foundation of Korea (NRF) funded by the Ministry of Science, ICT and Future Planning.

REFERENCES

Ali, T., Kim, T., Rehman, S. U., Khan, M. S., Amin, F. U., Khan, M., et al. (2018). Natural dietary supplementation of anthocyanins via PI3K/Akt/Nrf2/HO-1 pathways mitigate oxidative stress, neurodegeneration, and memory impairment in a mouse model of Alzheimer's disease. *Mol. Neurobiol.* 55, 6076–6093. doi: 10.1007/s12035-017-0798-6

Alzoubi, K. H., Halboup, A. M., Alomari, M. A., and Khabour, O. F. (2019). The neuroprotective effect of vitamin E on waterpipe tobacco smoking-induced memory impairment: the antioxidative role. *Life Sci.* 222, 46–52. doi: 10.1016/j.lfs.2019.02.050

Amato, A., Terzo, S., and Mulè, F. (2019). Natural compounds as beneficial antioxidant agents in neurodegenerative disorders: a focus on Alzheimer's disease. *Antioxidants (Basel, Switzerland)* 8:608. doi: 10.3390/antiox8120608

Beal, M. F. (2002). Oxidatively modified proteins in aging and disease. *Free Radic. Biol. Med.* 32, 797–803. doi: 10.1016/s0891-5849(02)00780-3

Behl, C. (1999). Vitamin E and other antioxidants in neuroprotection. *Int. J. Vitam. Nutr. Res.* 69, 213–219. doi: 10.1024/0300-9831.69.3.213

Boccardi, V., Baroni, M., Mangialasche, F., and Mecocci, P. (2016). Vitamin E family: role in the pathogenesis and treatment of Alzheimer's disease. *Alzheimers Dement. (N. Y.)* 2, 182–191. doi: 10.1016/j.trci.2016.08.002

Bolisetty, S., and Jaimes, E. A. (2013). Mitochondria and reactive oxygen species: physiology and pathophysiology. *Int. J. Mol. Sci.* 14, 6306–6344. doi: 10.3390/ijms14036306

Bothwell, M. (2019). Recent advances in understanding context-dependent mechanisms controlling neurotrophin signaling and function. *Version 1 F1000Res* 8:F1000FacultyRev-1658.

Buendia, I., Michalska, P., Navarro, E., Gameiro, I., Egea, J., and León, R. (2016). Nrf2–ARE pathway: an emerging target against oxidative stress and neuroinflammation in neurodegenerative diseases. *Pharmacol. Ther.* 157, 84–104. doi: 10.1016/j.pharmthera.2015.11.003

Butterfield, D. A., and Boyd-Kimball, D. (2018). Oxidative stress, amyloid-β peptide, and altered key molecular pathways in the pathogenesis and progression of Alzheimer's disease. *J. Alzheimers Dis.* 62, 1345–1367. doi: 10.3233/jad-170543

Butterfield, D. A., and Boyd-Kimball, D. (2019). Redox proteomics and amyloid β-peptide: insights into Alzheimer disease. *J. Neurochem.* 151, 459–487. doi: 10.1111/jnc.14589

Butterfield, D. A., and Halliwell, B. (2019). Oxidative stress, dysfunctional glucose metabolism and Alzheimer disease. *Nat. Rev. Neurosci.* 20, 148–160. doi: 10.1038/s41583-019-0132-6

Byun, E.-B., Cho, E.-J., Kim, Y.-E., Kim, W. S., and Byun, E.-H. (2018). Neuroprotective effect of polysaccharide separated from *Perilla frutescens* Britton var. acuta Kudo against H(2)O(2)-induced oxidative stress in HT22 hippocampus cells. *Biosci. Biotechnol. Biochem.* 82, 1344–1358. doi: 10.1080/09168451.2018.1460572

Chaudhari, N., Talwar, P., Parimisetty, A., Lefebvre D'hellencourt, C., and Ravanan, P. (2014). A molecular web: endoplasmic reticulum stress, inflammation, and oxidative stress. *Front. Cell. Neurosci.* 8:231. doi: 10.3389/fncel.2014.00213

Cheng, L., Muroi, M., Cao, S., Bian, L., Osada, H., Xiang, L., et al. (2019). 3β,23,28-Trihydroxy-12-oleanene 3β-caffeate from desmodium sambuense-induced neurogenesis in PC12 cells mediated by ER stress and BDNF-TrkB signaling pathways. *Mol. Pharm.* 16, 1423–1432. doi: 10.1021/acs.molpharmaceut.8b00939

Cuadrado, A., and Rojo, A. I. (2008). Heme oxygenase-1 as a therapeutic target in neurodegenerative diseases and brain infections. *Curr. Pharm. Des.* 14, 429–442. doi: 10.2174/138161208783597407

Cui, H.-Y., Zhang, X.-J., Yang, Y., Zhang, C., Zhu, C.-H., Miao, J.-Y., et al. (2018). Rosmarinic acid elicits neuroprotection in ischemic stroke via Nrf2 and heme oxygenase 1 signaling. *Neural Regen. Res.* 13, 2119–2128.

Cunha, C., Brambilla, R., and Thomas, K. (2010). A simple role for BDNF in learning and memory? *Front. Mol. Neurosci.* 3:1. doi: 10.3389/neuro.02.001.2010

de Farias, C. C., Maes, M., Bonifácio, K. L., Bortolasci, C. C., De Souza Nogueira, A., Brinholi, F. F., et al. (2016). Highly specific changes in antioxidant levels and lipid peroxidation in Parkinson's disease and its progression: disease and staging biomarkers and new drug targets. *Neurosci. Lett.* 617, 66–71. doi: 10.1016/j.neulet.2016.02.011

Di Domenico, F., Pupo, G., Giraldo, E., Badìa, M. C., Monllor, P., Lloret, A., et al. (2016). Oxidative signature of cerebrospinal fluid from mild cognitive impairment and Alzheimer disease patients. *Free Radic. Biol. Med.* 91, 1–9. doi: 10.1016/j.freeradbiomed.2015.12.004

Di Domenico, F., Tramutola, A., and Butterfield, D. A. (2017). Role of 4-hydroxy-2-nonenal (HNE) in the pathogenesis of Alzheimer disease and other selected age-related neurodegenerative disorders. *Free Radic. Biol. Med.* 111, 253–261. doi: 10.1016/j.freeradbiomed.2016.10.490

Dinkova-Kostova, A. T., Kostov, R. V., and Kazantsev, A. G. (2018). The role of Nrf2 signaling in counteracting neurodegenerative diseases. *FEBS J.* 285, 3576–3590. doi: 10.1111/febs.14379

Dogan, O., Kisa, U., Erdemoglu Ali, K., Kacmaz, M., Caglayan, O., and Kurku, H. (2018). Oxidative and nitrosative stress in patients with ischemic stroke. *LaboratoriumsMedizin* 42, 195–200. doi: 10.1515/labmed-2018-0036

Donkor, E. S. (2018). Stroke in the 21(st) century: a snapshot of the burden, epidemiology, and quality of life. *Stroke Res. Treat.* 2018:3238165.

Dumont, M., Wille, E., Stack, C., Calingasan, N. Y., Beal, M. F., and Lin, M. T. (2009). Reduction of oxidative stress, amyloid deposition, and memory deficit by manganese superoxide dismutase overexpression in a transgenic mouse model of Alzheimer's disease. *FASEB J.* 23, 2459–2466. doi: 10.1096/fj.09-132928

Esposito, L., Raber, J., Kekonius, L., Yan, F., Yu, G.-Q., Bien-Ly, N., et al. (2006). Reduction in mitochondrial superoxide dismutase modulates Alzheimer's disease-like pathology and accelerates the onset of behavioral changes in human amyloid precursor protein transgenic mice. *J. Neurosci.* 26, 5167–5179. doi: 10.1523/jneurosci.0482-06.2006

Fang, J., Wang, H., Zhou, J., Dai, W., Zhu, Y., Zhou, Y., et al. (2018). Baicalin provides neuroprotection in traumatic brain injury mice model through Akt/Nrf2 pathway. *Drug Des. Dev. Ther.* 12, 2497–2508. doi: 10.2147/dddt.s163951

Farina, N., Llewellyn, D., Isaac, M., and Tabet, N. (2017). Vitamin E for Alzheimer's dementia and mild cognitive impairment. *Cochrane Database Syst. Rev.* 4:Cd002854.

Feigin, V. L., Norrving, B., and Mensah, G. A. (2017). Global burden of stroke. *Circ. Res.* 120, 439–448.

Gaki, G. S., and Papavassiliou, A. G. (2014). Oxidative stress-induced signaling pathways implicated in the pathogenesis of Parkinson's disease. *Neuro Mol. Med.* 16, 217–230. doi: 10.1007/s12017-014-8294-x

Galasko, D. R., Peskind, E., Clark, C. M., Quinn, J. F., Ringman, J. M., Jicha, G. A., et al. (2012). Antioxidants for Alzheimer disease: a randomized clinical trial with cerebrospinal fluid biomarker measures. *Arch. Neurol.* 69, 836–841.

Gandhi, S., and Abramov, A. Y. (2012). Mechanism of oxidative stress in neurodegeneration. *Oxid. Med. Cell. Longev.* 2012:428010.

Gao, J., Liu, S., Xu, F., Liu, Y., Lv, C., Deng, Y., et al. (2018). Trilobatin protects against oxidative injury in neuronal PC12 cells through regulating mitochondrial ROS homeostasis mediated by AMPK/Nrf2/Sirt3 signaling pathway. *Front. Mol. Neurosci.* 11:267. doi: 10.3389/fnmol.2018.00267

Gao, Y., Xu, X., Chang, S., Wang, Y., Xu, Y., Ran, S., et al. (2015). Totarol prevents neuronal injury in vitro and ameliorates brain ischemic stroke: potential roles of Akt activation and HO-1 induction. *Toxicol. Appl. Pharmacol.* 289, 142–154. doi: 10.1016/j.taap.2015.10.001

Ge, X.-H., Shao, L., and Zhu, G.-J. (2018). Oxymatrine attenuates brain hypoxic-ischemic injury from apoptosis and oxidative stress: role of

p-Akt/GSK3β/HO-1/Nrf-2 signaling pathway. *Metabol. Brain Dis.* 33, 1869–1875. doi: 10.1007/s11011-018-0293-4

Gomes, J. R., Costa, J. T., Melo, C. V., Felizzi, F., Monteiro, P., Pinto, M. J., et al. (2012). Excitotoxicity downregulates TrkB.FL signaling and upregulates the neuroprotective truncated TrkB receptors in cultured hippocampal and striatal neurons. *J. Neurosci.* 32, 4610–4622. doi: 10.1523/jneurosci.0374-12.2012

Gupta, V. K., You, Y., Gupta, V. B., Klistorner, A., and Graham, S. L. (2013). TrkB receptor signalling: implications in neurodegenerative, psychiatric and proliferative disorders. *Int. J. Mol. Sci.* 14, 10122–10142. doi: 10.3390/ijms140510122

Halliwell, B. (2006). Oxidative stress and neurodegeneration: where are we now? *J. Neurochem.* 97, 1634–1658. doi: 10.1111/j.1471-4159.2006.03907.x

Han, J.-Y., Ahn, S.-Y., Kim, C.-S., Yoo, S.-K., Kim, S.-K., Kim, H.-C., et al. (2012). Protection of apigenin against kainate-induced excitotoxicity by anti-oxidative effects. *Biol. Pharm. Bull.* 35, 1440–1446. doi: 10.1248/bpb.b110686

Hannan, M. A., Dash, R., Sohag, A. A. M., and Moon, I. S. (2019). Deciphering molecular mechanism of the neuropharmacological action of fucosterol through integrated system pharmacology and in silico analysis. *Mar. Drugs* 17:639. doi: 10.3390/md17110639

Hannan, M. A., Haque, M. N., Mohibbullah, M., Dash, R., Hong, Y. K., and Moon, I. S. (2020a). Gelidium amansii attenuates hypoxia/reoxygenation-induced oxidative injury in primary hippocampal neurons through suppressing GluN2B expression. *Antioxidants (Basel)* 9:223. doi: 10.3390/antiox9030223

Hannan, M. A., Kang, J. Y., Hong, Y. K., Lee, H., Choi, J. S., Choi, I. S., et al. (2013). The marine alga *Gelidium amansii* promotes the development and complexity of neuronal cytoarchitecture. *Phytother. Res.* 27, 21–29. doi: 10.1002/ptr.4684

Hannan, M. A., Kang, J. Y., Mohibbullah, M., Hong, Y. K., Lee, H., Choi, J. S., et al. (2014). Moringa oleifera with promising neuronal survival and neurite outgrowth promoting potentials. *J. Ethnopharmacol.* 152, 142–150. doi: 10.1016/j.jep.2013.12.036

Hannan, M. A., Sohag, A. A. M., Dash, R., Haque, M. N., Mohibbullah, M., Oktaviani, D. F., et al. (2020b). Phytosterols of marine algae: insights into the potential health benefits and molecular pharmacology. *Phytomedicine* 69:153201. doi: 10.1016/j.phymed.2020.153201

Haque, M. M., Murale, D. P., Kim, Y. K., and Lee, J.-S. (2019). Crosstalk between oxidative stress and tauopathy. *Int. J. Mol. Sci.* 20:1959. doi: 10.3390/ijms20081959

Houlton, J., Abumaria, N., Hinkley, S. F. R., and Clarkson, A. N. (2019). Therapeutic potential of neurotrophins for repair after brain injury: a helping hand from biomaterials. *Front. Neurosci.* 13:790. doi: 10.3389/fnins.2019.00790

Hu, S., Liu, T., Wu, Y., Yang, W., Hu, S., Sun, Z., et al. (2019). Panax notoginseng saponins suppress lipopolysaccharide-induced barrier disruption and monocyte adhesion on bEnd.3 cells via the opposite modulation of Nrf2 antioxidant and NF-κB inflammatory pathways. *Phytother. Res.* 33, 3163–3176. doi: 10.1002/ptr.6488

Hui, Y., Chengyong, T., Cheng, L., Haixia, H., Yuanda, Z., and Weihua, Y. (2018). Resveratrol attenuates the cytotoxicity induced by amyloid-β(1-42) in PC12 cells by upregulating heme oxygenase-1 via the PI3K/Akt/Nrf2 pathway. *Neurochem. Res.* 43, 297–305. doi: 10.1007/s11064-017-2421-7

Ibáñez, C. F., and Simi, A. (2012). p75 neurotrophin receptor signaling in nervous system injury and degeneration: paradox and opportunity. *Trends Neurosci.* 35, 431–440. doi: 10.1016/j.tins.2012.03.007

Ishii, T., and Mann, G. E. (2018). When and how does brain-derived neurotrophic factor activate Nrf2 in astrocytes and neurons? *Neural Regen. Res.* 13, 803–804.

Ishii, T., Warabi, E., and Mann, G. E. (2018). Circadian control of p75 neurotrophin receptor leads to alternate activation of Nrf2 and c-Rel to reset energy metabolism in astrocytes via brain-derived neurotrophic factor. *Free Radic. Biol. Med.* 119, 34–44. doi: 10.1016/j.freeradbiomed.2018.01.026

Itoh, K., Wakabayashi, N., Katoh, Y., Ishii, T., Igarashi, K., Engel, J. D., et al. (1999). Keap1 represses nuclear activation of antioxidant responsive elements by Nrf2 through binding to the amino-terminal Neh2 domain. *Genes Dev.* 13, 76–86. doi: 10.1101/gad.13.1.76

Jang, S.-W., Liu, X., Yepes, M., Shepherd, K. R., Miller, G. W., Liu, Y., et al. (2010). A selective TrkB agonist with potent neurotrophic activities by 7,8-dihydroxyflavone. *Proc. Natl. Acad. Sci. U.S.A.* 107, 2687–2692. doi: 10.1073/pnas.0913572107

Jiang, L., Zhang, H., Wang, C., Ming, F., Shi, X., and Yang, M. (2019). Serum level of brain-derived neurotrophic factor in Parkinson's disease: a meta-analysis. *Prog. Neuropsychopharmacol. Biol. Psychiatry* 88, 168–174. doi: 10.1016/j.pnpbp.2018.07.010

Jin, X., Liu, Q., Jia, L., Li, M., and Wang, X. (2015). Pinocembrin attenuates 6-OHDA-induced neuronal cell death through Nrf2/ARE pathway in SH-SY5Y cells. *Cell. Mol. Neurobiol.* 35, 323–333. doi: 10.1007/s10571-014-0128-8

Joshi, G., Gan, K. A., Johnson, D. A., and Johnson, J. A. (2015). Increased Alzheimer's disease-like pathology in the APP/ PS1ΔE9 mouse model lacking Nrf2 through modulation of autophagy. *Neurobiol. Aging* 36, 664–679. doi: 10.1016/j.neurobiolaging.2014.09.004

Joshi, G., and Johnson, J. A. (2012). The Nrf2-ARE pathway: a valuable therapeutic target for the treatment of neurodegenerative diseases. *Recent Pat. CNS Drug Discov.* 7, 218–229. doi: 10.2174/157488912803252023

Kanninen, K., Malm, T. M., Jyrkkänen, H.-K., Goldsteins, G., Keksa-Goldsteine, V., Tanila, H., et al. (2008). Nuclear factor erythroid 2-related factor 2 protects against beta amyloid. *Mol. Cell. Neurosci.* 39, 302–313. doi: 10.1016/j.mcn.2008.07.010

Khatri, N., Thakur, M., Pareek, V., Kumar, S., Sharma, S., and Datusalia, A. K. (2018). Oxidative stress: major threat in traumatic brain injury. *CNS Neurol. Disord. Drug Targets* 17, 689–695. doi: 10.2174/1871527317666180627120501

Kim, D.-C., Cho, K.-H., Ko, W., Yoon, C.-S., Sohn, J. H., Yim, J. H., et al. (2016). Anti-inflammatory and cytoprotective effects of TMC-256C1 from marine-derived fungus *Aspergillus* sp. SF-6354 via up-regulation of heme oxygenase-1 in murine hippocampal and microglial cell lines. *Int. J. Mol. Sci.* 17:529. doi: 10.3390/ijms17040529

Kim, G. H., Kim, J. E., Rhie, S. J., and Yoon, S. (2015). The role of oxidative stress in neurodegenerative diseases. *Exp. Neurobiol.* 24, 325–340.

Kim, T.-S., Pae, C.-U., Yoon, S.-J., Jang, W.-Y., Lee, N. J., Kim, J.-J., et al. (2006). Decreased plasma antioxidants in patients with Alzheimer's disease. *Int. J. Geriatr. Psychiatry* 21, 344–348.

Kishimoto, M., Suenaga, J., Takase, H., Araki, K., Yao, T., Fujimura, T., et al. (2019). Oxidative stress-responsive apoptosis inducing protein (ORAIP) plays a critical role in cerebral ischemia/reperfusion injury. *Sci. Rep.* 9:13512.

Kowiański, P., Lietzau, G., Czuba, E., Waśkow, M., Steliga, A., and Moryś, J. (2018). BDNF: a key factor with multipotent impact on brain signaling and synaptic plasticity. *Cell. Mol. Neurobiol.* 38, 579–593. doi: 10.1007/s10571-017-0510-4

Kryscio, R. J., Abner, E. L., Caban-Holt, A., Lovell, M., Goodman, P., Darke, A. K., et al. (2017). Association of antioxidant supplement use and dementia in the prevention of Alzheimer's disease by vitamin E and selenium trial (PREADViSE). *JAMA Neurol.* 74, 567–573.

Kwon, S. H., Ma, S. X., Hwang, J. Y., Lee, S. Y., and Jang, C. G. (2015). Involvement of the Nrf2/HO-1 signaling pathway in sulfuretin-induced protection against amyloid beta25-35 neurotoxicity. *Neuroscience* 304, 14–28. doi: 10.1016/j.neuroscience.2015.07.030

Lee, B. D., Yoo, J.-M., Baek, S. Y., Li, F. Y., Sok, D.-E., and Kim, M. R. (2019). 3,3'-Diindolylmethane promotes BDNF and antioxidant enzyme formation via TrkB/Akt pathway activation for neuroprotection against oxidative stress-induced apoptosis in hippocampal neuronal cells. *Antioxidants* 9:3. doi: 10.3390/antiox9010003

Lee, D.-S., Cha, B.-Y., Woo, J.-T., Kim, Y.-C., and Jang, J.-H. (2015). Acerogenin a from acer nikoense maxim prevents oxidative stress-induced neuronal cell death through Nrf2-mediated heme oxygenase-1 expression in mouse hippocampal HT22 cell line. *Molecules (Basel, Switzerland)* 20, 12545–12557. doi: 10.3390/molecules200712545

Lee, H., Ko, W., Chowdhury, A., Li, B., Kim, S. C., Oh, H., et al. (2020). Brassicaphenanthrene A from *Brassica rapa* protects HT22 neuronal cells through the regulation of Nrf2-mediated heme oxygenase-1 expression. *Mol. Med. Rep.* 21, 493–500.

Lee, H.-P., Pancholi, N., Esposito, L., Previll, L. A., Wang, X., Zhu, X., et al. (2012). Early induction of oxidative stress in mouse model of Alzheimer disease with reduced mitochondrial superoxide dismutase activity. *PLoS One* 7:e28033. doi: 10.1371/journal.pone.0028033

Lee, J., Jo, D.-G., Park, D., Chung, H. Y., and Mattson, M. P. (2014). Adaptive cellular stress pathways as therapeutic targets of dietary phytochemicals: focus on the nervous system. *Pharmacol. Rev.* 66, 815–868. doi: 10.1124/pr.113.007757

Lee, J.-M., and Johnson, J. A. (2004). An important role of Nrf2-ARE pathway in the cellular defense mechanism. *J. Biochem. Mol. Biol.* 37, 139–143. doi: 10.5483/bmbrep.2004.37.2.139

Li, F., Calingasan, N. Y., Yu, F., Mauck, W. M., Toidze, M., Almeida, C. G., et al. (2004). Increased plaque burden in brains of APP mutant MnSOD heterozygous knockout mice. *J. Neurochem.* 89, 1308–1312. doi: 10.1111/j.1471-4159.2004.02455.x

Li, J., Ding, X., Zhang, R., Jiang, W., Sun, X., Xia, Z., et al. (2015). Harpagoside ameliorates the amyloid-β-induced cognitive impairment in rats via up-regulating BDNF expression and MAPK/PI3K pathways. *Neuroscience* 303, 103–114. doi: 10.1016/j.neuroscience.2015.06.042

Li, X.-H., Li, C.-Y., Xiang, Z.-G., Zhong, F., Chen, Z.-Y., and Lu, J.-M. (2010). Allicin can reduce neuronal death and ameliorate the spatial memory impairment in Alzheimer's disease models. *Neurosciences (Riyadh, Saudi Arabia)* 15, 237–243.

Lin, C.-W., Wu, M.-J., Liu, I. Y. C., Su, J.-D., and Yen, J.-H. (2010). Neurotrophic and cytoprotective action of luteolin in PC12 cells through ERK-dependent induction of Nrf2-driven HO-1 expression. *J. Agric. Food Chem.* 58, 4477–4486. doi: 10.1021/jf904061x

Lindholm, D., Wootz, H., and Korhonen, L. (2006). ER stress and neurodegenerative diseases. *Cell Death Differ.* 13, 385–392. doi: 10.1038/sj.cdd.4401778

Liu, M., Bai, X., Yu, S., Zhao, W., Qiao, J., Liu, Y., et al. (2019). Ginsenoside re inhibits ROS/ASK-1 dependent mitochondrial apoptosis pathway and activation of Nrf2-antioxidant response in beta-amyloid-challenged SH-SY5Y cells. *Molecules (Basel, Switzerland)* 24:2687. doi: 10.3390/molecules24152687

Liu, Q., Jin, Z., Xu, Z., Yang, H., Li, L., Li, G., et al. (2019). Antioxidant effects of ginkgolides and bilobalide against cerebral ischemia injury by activating the Akt/Nrf2 pathway in vitro and in vivo. *Cell Stress Chaperones* 24, 441–452. doi: 10.1007/s12192-019-00977-1

Liu, X., Zhang, X., Ma, K., Zhang, R., Hou, P., Sun, B., et al. (2016). Matrine alleviates early brain injury after experimental subarachnoid hemorrhage in rats: possible involvement of PI3K/Akt-mediated NF-κB inhibition and Keap1/Nrf2-dependent HO-1 induction. *Cell. Mol. Biol. (Noisy-le-Grand, France)* 62, 38–44.

Liu, Z., Zhou, T., Ziegler, A. C., Dimitrion, P., and Zuo, L. (2017). Oxidative stress in neurodegenerative diseases: from molecular mechanisms to clinical applications. *Oxid. Med. Cell. Longev.* 2017, 2525967–2525967.

Lou, H., Jing, X., Wei, X., Shi, H., Ren, D., and Zhang, X. (2014). Naringenin protects against 6-OHDA-induced neurotoxicity via activation of the Nrf2/ARE signaling pathway. *Neuropharmacology* 79, 380–388. doi: 10.1016/j.neuropharm.2013.11.026

Lozano, D., Gonzales-Portillo, G. S., Acosta, S., De La Pena, I., Tajiri, N., Kaneko, Y., et al. (2015). Neuroinflammatory responses to traumatic brain injury: etiology, clinical consequences, and therapeutic opportunities. *Neuropsychiatr. Dis. Treat.* 11, 97–106.

Ma, Q. (2013). Role of nrf2 in oxidative stress and toxicity. *Annu. Rev. Pharmacol. Toxicol.* 53, 401–426. doi: 10.1146/annurev-pharmtox-011112-140320

Mao, X.-Y., Cao, Y.-G., Ji, Z., Zhou, H.-H., Liu, Z.-Q., and Sun, H.-L. (2015). Topiramate protects against glutamate excitotoxicity via activating BDNF/TrkB-dependent ERK pathway in rodent hippocampal neurons. *Prog. Neuro Psychopharmacol. Biol. Psychiatry* 60, 11–17. doi: 10.1016/j.pnpbp.2015.01.015

McMahon, M., Itoh, K., Yamamoto, M., and Hayes, J. D. (2003). Keap1-dependent proteasomal degradation of transcription factor Nrf2 contributes to the negative regulation of antioxidant response element-driven gene expression. *J. Biol. Chem.* 278, 21592–21600. doi: 10.1074/jbc.m300931200

Meis, S., Endres, T., Munsch, T., and Lessmann, V. (2017). The relation between long-term synaptic plasticity at glutamatergic synapses in the amygdala and fear learning in adult heterozygous BDNF-knockout mice. *Cereb. Cortex* 28, 1195–1208. doi: 10.1093/cercor/bhx032

Mitre, M., Mariga, A., and Chao, M. V. (2017). Neurotrophin signalling: novel insights into mechanisms and pathophysiology. *Clin. Sci. (London, England 1979)* 131, 13–23. doi: 10.1042/cs20160044

Mogi, M., Togari, A., Kondo, T., Mizuno, Y., Komure, O., Kuno, S., et al. (1999). Brain-derived growth factor and nerve growth factor concentrations are decreased in the substantia nigra in Parkinson's disease. *Neurosci. Lett.* 270, 45–48. doi: 10.1016/s0304-3940(99)00463-2

Moosavi, F., Hosseini, R., Saso, L., and Firuzi, O. (2015). Modulation of neurotrophic signaling pathways by polyphenols. *Drug Des. Dev. Ther.* 10, 23–42.

Murphy, K. E., and Park, J. J. (2017). Can Co-activation of Nrf2 and neurotrophic signaling pathway slow Alzheimer's disease? *Int. J. Mol. Sci.* 18:1168. doi: 10.3390/ijms18061168

Murphy, M. P. (2009). How mitochondria produce reactive oxygen species. *Biochem. J.* 417, 1–13. doi: 10.1042/bj20081386

Naoi, M., Inaba-Hasegawa, K., Shamoto-Nagai, M., and Maruyama, W. (2017). Neurotrophic function of phytochemicals for neuroprotection in aging and neurodegenerative disorders: modulation of intracellular signaling and gene expression. *J. Neural Transm. (Vienna, Austria 1996)* 124, 1515–1527. doi: 10.1007/s00702-017-1797-5

Niedzielska, E., Smaga, I., Gawlik, M., Moniczewski, A., Stankowicz, P., Pera, J., et al. (2016). Oxidative stress in neurodegenerative diseases. *Mol. Neurobiol.* 53, 4094–4125.

Numakawa, T., Odaka, H., and Adachi, N. (2018). Actions of brain-derived neurotrophin factor in the neurogenesis and neuronal function, and its involvement in the pathophysiology of brain diseases. *Int. J. Mol. Sci.* 19:3650. doi: 10.3390/ijms19113650

Obianyo, O., and Ye, K. (2013). Novel small molecule activators of the Trk family of receptor tyrosine kinases. *Biochim. Biophys. Acta* 1834, 2213–2218. doi: 10.1016/j.bbapap.2012.08.021

Patten, D. A., Germain, M., Kelly, M. A., and Slack, R. S. (2010). Reactive oxygen species: stuck in the middle of neurodegeneration. *J. Alzheimers Dis.* 20(Suppl, 2), S357–S367.

Pischke, S. E., Zhou, Z., Song, R., Ning, W., Alam, J., Ryter, S. W., et al. (2005). Phosphatidylinositol 3-kinase/Akt pathway mediates heme oxygenase-1 regulation by lipopolysaccharide. *Cell. Mol. Biol. (Noisy-le-grand)* 51, 461–470.

Qi, G., Mi, Y., Wang, Y., Li, R., Huang, S., Li, X., et al. (2017). Neuroprotective action of tea polyphenols on oxidative stress-induced apoptosis through the activation of the TrkB/CREB/BDNF pathway and Keap1/Nrf2 signaling pathway in SH-SY5Y cells and mice brain. *Food Funct.* 8, 4421–4432. doi: 10.1039/c7fo00991g

Ramsey, C. P., Glass, C. A., Montgomery, M. B., Lindl, K. A., Ritson, G. P., Chia, L. A., et al. (2007). Expression of Nrf2 in neurodegenerative diseases. *J. Neuropathol. Exp. Neurol.* 66, 75–85.

Rani, P., Krishnan, S., and Rani Cathrine, C. (2017). Study on analysis of peripheral biomarkers for Alzheimer's disease diagnosis. *Front. Neurol.* 8:328. doi: 10.3389/fneur.2017.00328

Rodrigo, R., Fernández-Gajardo, R., Gutiérrez, R., Matamala, J. M., Carrasco, R., Miranda-Merchak, A., et al. (2013). Oxidative stress and pathophysiology of ischemic stroke: novel therapeutic opportunities. *CNS Neurol. Disord. Drug Targets* 12, 698–714. doi: 10.2174/18715273113120500015

Rodríguez-Rodríguez, A., Egea-Guerrero, J. J., Murillo-Cabezas, F., and Carrillo-Vico, A. (2014). Oxidative stress in traumatic brain injury. *Curr. Med. Chem.* 21, 1201–1211.

Sampaio, T., Savall, A., Gutierrez, M., and Pinton, S. (2017). Neurotrophic factors in Alzheimer's and Parkinson's diseases: implications for pathogenesis and therapy. *Neural Regen. Res.* 12, 549–557.

Schipper, H. M. (2004). Heme oxygenase expression in human central nervous system disorders. *Free Radic. Biol. Med.* 37, 1995–2011.

Sha, J.-Y., Zhou, Y.-D., Yang, J.-Y., Leng, J., Li, J.-H., Hu, J.-N., et al. (2019). Maltol (3-Hydroxy-2-methyl-4-pyrone) slows d-galactose-induced brain aging process by damping the Nrf2/HO-1-mediated oxidative stress in mice. *J. Agric. Food Chem.* 67, 10342–10351.

Sharma, A., Weber, D., Raupbach, J., Dakal, T. C., Fließbach, K., Ramirez, A., et al. (2020). Advanced glycation end products and protein carbonyl levels in plasma reveal sex-specific differences in Parkinson's and Alzheimer's disease. *Redox Biol.* 34:101546.

Shen, L. L., Li, W. W., Xu, Y. L., Gao, S. H., Xu, M. Y., Bu, X. L., et al. (2019). Neurotrophin receptor p75 mediates amyloid β-induced tau pathology. *Neurobiol. Dis.* 132:104567.

Shih, A. Y., Imbeault, S., Barakauskas, V., Erb, H., Jiang, L., Li, P., et al. (2005). Induction of the Nrf2-driven antioxidant response confers neuroprotection during mitochondrial stress in vivo. *J. Biol. Chem.* 280, 22925–22936.

Shu, K., and Zhang, Y. (2019). Protodioscin protects PC12 cells against oxygen and glucose deprivation-induced injury through miR-124/AKT/Nrf2 pathway. *Cell Stress Chaperones* 24, 1091–1099.

Singh, A., Kukreti, R., Saso, L., and Kukreti, S. (2019). Oxidative stress: a key modulator in neurodegenerative diseases. *Molecules (Basel, Switzerland)* 24:1583.

Singh, S., Vrishni, S., Singh, B. K., Rahman, I., and Kakkar, P. (2010). Nrf2-ARE stress response mechanism: a control point in oxidative stress-mediated dysfunctions and chronic inflammatory diseases. *Free Radic. Res.* 44, 1267–1288.

Siuda, J., Patalong-Ogiewa, M., Żmuda, W., Targosz-Gajniak, M., Niewiadomska, E., Matuszek, I., et al. (2017). Cognitive impairment and BDNF serum levels. *Neurol. Neurochir. Pol.* 51, 24–32.

Sivandzade, F., Prasad, S., Bhalerao, A., and Cucullo, L. (2019). NRF2 and NF-κB interplay in cerebrovascular and neurodegenerative disorders: molecular mechanisms and possible therapeutic approaches. *Redox Biol.* 21:101059.

Son, T. G., Camandola, S., and Mattson, M. P. (2008). Hormetic dietary phytochemicals. *Neuromol. Med.* 10, 236–246.

Stelmashook, E. V., Isaev, N. K., Genrikhs, E. E., and Novikova, S. V. (2019). Mitochondria-targeted antioxidants as potential therapy for the treatment of traumatic brain injury. *Antioxidants* 8:124.

Sun, Y., Yang, T., Leak, R. K., Chen, J., and Zhang, F. (2017). Preventive and protective roles of dietary Nrf2 activators against central nervous system diseases. *CNS Neurol. Disord. Drug Targets* 16, 326–338.

Sussman, M. A. (2009). Mitochondrial integrity: preservation through Akt/Pim-1 kinase signaling in the cardiomyocyte. *Exp. Rev. Cardiovasc. Ther.* 7, 929–938.

Thabet, N. M., and Moustafa, E. M. (2018). Protective effect of rutin against brain injury induced by acrylamide or gamma radiation: role of PI3K/AKT/GSK-3β/NRF-2 signalling pathway. *Arch. Physiol. Biochem.* 124, 185–193.

Tohda, C. (2016). New age therapy for Alzheimer's disease by neuronal network reconstruction. *Biol. Pharm. Bull.* 39, 1569–1575.

Tönnies, E., and Trushina, E. (2017). Oxidative stress, synaptic dysfunction, and Alzheimer's disease. *J. Alzheimers Dis.* 57, 1105–1121.

Tramutola, A., Abate, G., Lanzillotta, C., Triani, F., Barone, E., Iavarone, F., et al. (2018). Protein nitration profile of CD3(+) lymphocytes from Alzheimer disease patients: novel hints on immunosenescence and biomarker detection. *Free Radic. Biol. Med.* 129, 430–439.

Tufekci, K. U., Civi Bayin, E., Genc, S., and Genc, K. (2011). The Nrf2/are pathway: a promising target to counteract mitochondrial dysfunction in Parkinson's disease. *Parkinsons Dis.* 2011:314082.

van der Kant, R., Goldstein, L. S. B., and Ossenkoppele, R. (2020). Amyloid-β-independent regulators of tau pathology in Alzheimer disease. *Nat. Rev. Neurosci.* 21, 21–35.

Velagapudi, R., El-Bakoush, A., and Olajide, O. A. (2018). Activation of Nrf2 pathway contributes to neuroprotection by the dietary flavonoid tiliroside. *Mol. Neurobiol.* 55, 8103–8123.

Venkatesan, R., Ji, E., and Kim, S. Y. (2015). Phytochemicals that regulate neurodegenerative disease by targeting neurotrophins: a comprehensive review. *BioMed Res. Int.* 2015:814068.

Ventriglia, M., Zanardini, R., Bonomini, C., Zanetti, O., Volpe, D., Pasqualetti, P., et al. (2013). Serum brain-derived neurotrophic factor levels in different neurological diseases. *Biomed Res. Int.* 2013:901082.

Wang, R., Tu, J., Zhang, Q., Zhang, X., Zhu, Y., Ma, W., et al. (2013). Genistein attenuates ischemic oxidative damage and behavioral deficits via eNOS/Nrf2/HO-1 signaling. *Hippocampus* 23, 634–647.

Wang, X., Wang, W., Li, L., Perry, G., Lee, H.-G., and Zhu, X. (2014). Oxidative stress and mitochondrial dysfunction in Alzheimer's disease. *Biochim. Biophys. Acta* 1842, 1240–1247.

Wang, Y., Miao, Y., Mir, A. Z., Cheng, L., Wang, L., Zhao, L., et al. (2016). Inhibition of beta-amyloid-induced neurotoxicity by pinocembrin through Nrf2/HO-1 pathway in SH-SY5Y cells. *J. Neurol. Sci.* 368, 223–230.

Wei, Z., Li, X., Li, X., Liu, Q., and Cheng, Y. (2018). Oxidative stress in Parkinson's disease: a systematic review and meta-analysis. *Front. Mol. Neurosci.* 11:236. doi: 10.3389/fnmol.2018.00236

Weissmiller, A. M., and Wu, C. (2012). Current advances in using neurotrophic factors to treat neurodegenerative disorders. *Trans. Neurodegener.* 1:14.

Wen, Z., Hou, W., Wu, W., Zhao, Y., Dong, X., Bai, X., et al. (2018). 6'-O-Galloylpaeoniflorin attenuates cerebral ischemia reperfusion-induced neuroinflammation and oxidative stress via PI3K/Akt/Nrf2 activation. *Oxid. Med. Cell. Longev.* 2018:8678267.

Wojsiat, J., Zoltowska, K. M., Laskowska-Kaszub, K., and Wojda, U. (2018). Oxidant/antioxidant imbalance in Alzheimer's disease: therapeutic and diagnostic prospects. *Oxid. Med. Cell. Longev.* 2018: 6435861.

Wu, C.-H., Chen, C.-C., Hung, T.-H., Chuang, Y.-C., Chao, M., Shyue, S.-K., et al. (2019). Activation of TrkB/Akt signaling by a TrkB receptor agonist improves long-term histological and functional outcomes in experimental intracerebral hemorrhage. *J. Biomed. Sci.* 26:53.

Wu, P.-S., Ding, H.-Y., Yen, J.-H., Chen, S.-F., Lee, K.-H., and Wu, M.-J. (2018). Anti-inflammatory activity of 8-hydroxydaidzein in LPS-stimulated BV2 microglial cells via activation of Nrf2-antioxidant and attenuation of Akt/NF-κB-inflammatory signaling pathways, as well as inhibition of COX-2 activity. *J. Agric. Food Chem.* 66, 5790–5801.

Wurzelmann, M., Romeika, J., and Sun, D. (2017). Therapeutic potential of brain-derived neurotrophic factor (BDNF) and a small molecular mimics of BDNF for traumatic brain injury. *Neural Regen. Res.* 12, 7–12.

Xu, X. H., Li, G. L., Wang, B. A., Qin, Y., Bai, S. R., Rong, J., et al. (2015). Diallyl trisufide protects against oxygen glucose deprivation -induced apoptosis by scavenging free radicals via the PI3K/Akt -mediated Nrf2/HO-1 signaling pathway in B35 neural cells. *Brain Res.* 1614, 38–50.

Yin, C., Deng, Y., Liu, Y., Gao, J., Yan, L., and Gong, Q. (2018). Icariside II ameliorates cognitive impairments induced by chronic cerebral hypoperfusion by inhibiting the amyloidogenic pathway: involvement of BDNF/TrkB/CREB signaling and up-regulation of PPARα and PPARγ in rats. *Front. Pharmacol.* 9:1211. doi: 10.3389/fphar.2018.01211

Yoo, J.-M., Lee, B. D., Sok, D.-E., Ma, J. Y., and Kim, M. R. (2017). Neuroprotective action of N-acetyl serotonin in oxidative stress-induced apoptosis through the activation of both TrkB/CREB/BDNF pathway and Akt/Nrf2/Antioxidant enzyme in neuronal cells. *Redox Biol.* 11, 592–599.

Youssef, P., Chami, B., Lim, J., Middleton, T., Sutherland, G. T., and Witting, P. K. (2018). Evidence supporting oxidative stress in a moderately affected area of the brain in Alzheimer's disease. *Sci. Rep.* 8:11553.

Yu, L., Wang, S., Chen, X., Yang, H., Li, X., Xu, Y., et al. (2015). Orientin alleviates cognitive deficits and oxidative stress in Aβ1-42-induced mouse model of Alzheimer's disease. *Life Sci.* 121, 104–109.

Zhang, L., Fang, Y., Xu, Y., Lian, Y., Xie, N., Wu, T., et al. (2015). Curcumin improves amyloid β-peptide (1-42) induced spatial memory deficits through BDNF-ERK signaling pathway. *PLoS One* 10:e0131525. doi: 10.1371/journal.pone.0131525

Zhang, W., Song, J.-K., Yan, R., Li, L., Xiao, Z.-Y., Zhou, W.-X., et al. (2018). Diterpene ginkgolides protect against cerebral ischemia/reperfusion damage in rats by activating Nrf2 and CREB through PI3K/Akt signaling. *Acta Pharmacol. Sin.* 39, 1259–1272.

Zhang, Y., Liu, B., Chen, X., Zhang, N., Li, G., Zhang, L.-H., et al. (2017). Naringenin ameliorates behavioral dysfunction and neurological deficits in a d-galactose-induced aging mouse model through activation of PI3K/Akt/Nrf2 Pathway. *Rejuvenation Res.* 20, 462–472.

Zhao, L., Wang, J.-L., Liu, R., Li, X.-X., Li, J.-F., and Zhang, L. (2013). Neuroprotective, anti-amyloidogenic and neurotrophic effects of apigenin in an Alzheimer's disease mouse model. *Molecules (Basel, Switzerland)* 18, 9949–9965.

Zhu, Y.-F., Li, X.-H., Yuan, Z.-P., Li, C.-Y., Tian, R.-B., Jia, W., et al. (2015). Allicin improves endoplasmic reticulum stress-related cognitive deficits via PERK/Nrf2 antioxidative signaling pathway. *Eur. J. Pharmacol.* 762, 239–246.

Zorov, D. B., Juhaszova, M., and Sollott, S. J. (2014). Mitochondrial reactive oxygen species (ROS) and ROS-induced ROS release. *Physiol. Rev.* 94, 909–950.

Zou, Y., Qian, Z. J., Li, Y., Kim, M. M., Lee, S. H., and Kim, S. K. (2008). Antioxidant effects of phlorotannins isolated from Ishige okamurae in free radical mediated oxidative systems. *J. Agric. Food Chem.* 56, 7001–7009.

Conflict of Interest: The authors declare that the research was conducted in the absence of any commercial or financial relationships that could be construed as a potential conflict of interest.

frontiers in Aging Neuroscience

ORIGINAL RESEARCH
published: 22 July 2020
doi: 10.3389/fnagi.2020.00223

Blood-Based Biomarkers for Predictive Diagnosis of Cognitive Impairment in a Pakistani Population

Ghazala Iqbal[1], *Nady Braidy*[2] *and Touqeer Ahmed*[1]*

[1]Neurobiology Laboratory, Department of Healthcare Biotechnology, Atta-ur-Rahman School of Applied Biosciences, National University of Sciences & Technology (NUST), Islamabad, Pakistan, [2]Centre for Healthy Ageing, School of Psychiatry, Faculty of Medicine, University of New South Wales, Sydney, NSW, Australia

Numerous studies have identified an association between age-related cognitive impairment (CI) and oxidative damage, accumulation of metals, amyloid levels, tau, and deranged lipid profile. There is a concerted effort to establish the reliability of these blood-based biomarkers for predictive diagnosis of CI and its progression. We assessed the serum levels of high-density lipoprotein (HDL) cholesterol, low-density lipoprotein (LDL) cholesterol, triglycerides, total cholesterol, selected metals (Cu, Al, Zn, Pb, Mn, Cad), and total-tau and amyloid beta-42 protein in mild (n = 71), moderate (n = 86) and severe (n = 25) cognitively impaired patients and compared them with age-matched healthy controls (n = 90) from Pakistan. We found that a decrease in HDL cholesterol (correlation coefficient r = 0.467) and amyloid beta-42 (r = 0.451) were associated with increased severity of CI. On the other hand, an increase in cholesterol ratio (r = −0.562), LDL cholesterol (r = −0.428), triglycerides, and total-tau (r = −0.443) were associated with increased severity of CI. Increases in cholesterol ratio showed the strongest association and correlated with increases in tau concentration (r = 0.368), and increased triglycerides were associated with decreased amyloid beta-42 (r = −0.345). Increased Cu levels showed the strongest association with tau increase and increased Zn and Pb levels showed the strongest association with reduced amyloid beta-42 levels. Receiver Operating Characteristic (ROC) showed the cutoff values of blood metals (Al, Pb, Cu, Cad, Zn, and Mn), total-tau, and amyloid beta-42 with sensitivity and specificity. Our data show for the first time that blood lipids, metals (particularly Cu, Zn, Pb, and Al), serum amyloid-beta-42/tau proteins modulate each other's levels and can be collectively used as a predictive marker for CI.

Keywords: biomarkers, oxidative stress, cognitive impairment, amyloid-beta, serum, tau, metals, lipids

OPEN ACCESS

Edited by:
Franc Llorens,
Center for Biomedical Research on Neurodegenerative Diseases (CIBERNED), Spain

Reviewed by:
Dennis Qing Wang,
Southern Medical University, China
Davide Chiasserini,
University of Perugia, Italy

***Correspondence:**
Touqeer Ahmed
touqeer.aahmed@gmail.com;
touqeer.ahmed@asab.nust.edu.pk

Received: *16 March 2020*
Accepted: *22 June 2020*
Published: *22 July 2020*

Citation:
Iqbal G, Braidy N and Ahmed T (2020) Blood-Based Biomarkers for Predictive Diagnosis of Cognitive Impairment in a Pakistani Population. Front. Aging Neurosci. 12:223. doi: 10.3389/fnagi.2020.00223

INTRODUCTION

Cognitive impairment (CI) is characterized by short and long term memory loss, deterioration of language, inability to execute motor functions, and/or poor recognition of objects, and impairments in executive abilities (American Psychiatric Association, 1996). Timely diagnosis of CI in old age is very important because CI is likely to progress to the development of dementias (Ritchie et al., 2014, 2017; Tang et al., 2020). Improved diagnoses of CI can help in better management of

the disease and might delay dementias in these subjects. CI is the major component of the aging process and is associated with a variety of risk factors, such as smoking, high drug, and alcohol consumption, fewer years of formal education, low-income status, various metabolic diseases like hypertension and diabetes (Freedman et al., 2001; Raz and Rodrigue, 2006), elevated levels of metals (Iqbal et al., 2018), brain shrinkage with age (Raz et al., 2004), genetic factors such as APOE copies (Deary et al., 2009) and oxidative stress (Raz and Daugherty, 2018; Gandhi and Abramov, 2012).

Reliable biomarkers for prediction of early CI are needed, although there has been little success in this aspect. Here, we investigated the role of blood-based lipids, amyloid beta-42, tau and metals, and their correlations as potential biomarkers for improved diagnosis of CI. Lipids play an important role in neurodegeneration by promoting oxidative stress and influencing amyloid plaques formation, thus playing a contributory role in CI (Bodovitz and Klein, 1996; Xicoy et al., 2019). Higher blood cholesterol level leads to lipid peroxidation and reduced levels of several antioxidant enzymes (including superoxide dismutase) have been reported (Sparks et al., 1994). Lipids have also been recently used to distinguish between elderly subjects with small vessel disease and "healthy" age-matched controls (Liu et al., 2020). The association of low-density lipoprotein (LDL) cholesterol, high-density lipoprotein (HDL) cholesterol and total cholesterol with cognitive function has been previously reported but remains inconclusive (Postiglione et al., 1989; Wieringa et al., 1997) due to limited availability of data and varied techniques of assessment of lipid profiles (Anstey et al., 2008; Segatto et al., 2014; Zanchetti et al., 2014). It has also been well established that redox-active metals can disturb the equilibrium between free radical generation and antioxidant potential of cells by increasing the levels of reactive oxygen species (Singh et al., 2019).

Amyloid beta-42 as a biomarker in cerebrospinal fluid (CSF) and/or plasma has been extensively studied in Alzheimer's disease (AD; Vos et al., 2013) and other neurocognitive disorders (Ritchie et al., 2014, 2017). Amyloid beta-42 is a proteolytic fragment of amyloid precursor protein (APP), which is selectively cleaved by beta and gamma-secretase enzymes to yield the toxic amyloid beta-42 peptide (Selkoe, 1994) and its fibrils damage synapses (Chen et al., 2017) and causes oxidative stress (Ferrera et al., 2008). There is contradictory evidence on whether the levels of amyloid-beta in the CSF and/or plasma are clinically relevant biomarkers in AD, since published results are difficult to interpret, and there are variations in study design and methodologies used. For instance, some studies have reported increased levels of amyloid-beta (Vos et al., 2013; Petersen and O'Bryant, 2019; Tang et al., 2020) while others have reported lower levels (Song et al., 2011; Ruiz et al., 2013; Mizoi et al., 2014). However, both of these above-mentioned types of studies concluded that amyloid-beta cannot be an accurate biomarker, suggesting that levels of amyloid beta are certainly modulated by other factors (possibly metals, lipids, and tau) and further studies are required.

Tau proteins are abundant in the central nervous system (CNS) and are mainly active in the distal portion of axons hence stabilizing microtubules (Billingsley and Kincaid, 1997). As compared to the amyloid-beta, tau seems to be a reliable marker. Several studies have reported that elevated levels of total-tau and phosphorylated tau in the CSF correlate well with CI and progressing to dementias (Hansson et al., 2006; Diniz et al., 2008; Mattsson et al., 2009; Monge-Argilés et al., 2010; Olsson et al., 2016). As CI is associated with several neurological disorders establishing selective and specific blood-based biomarkers is challenging (Grundke-Iqbal et al., 1986).

Blood-based biomarkers for CI offer ease of access, and in some cases, plasma markers (plasma tau for AD particularly) show better correlation (Zetterberg et al., 2013). CSF based biomarkers can be reliable, however, CSF acquisition is invasive and difficult to obtain, and sometimes data has to be supported by neuro-imaging scans (Jia et al., 2019), which are expensive and time-consuming (Mapstone et al., 2014). A large amount of CSF is absorbed in the blood, suggesting that proteins present in the serum have the potential to act as biomarkers in the neurodegenerative diseases. Therefore, proteins associated with the axonal injury and damage of the blood-brain barrier may be measured in the serum (Zetterberg et al., 2013). Keeping in view all these factors, we studied selected plasma/sera biomarkers for CI in Pakistani health. The key goal of this study was to observe the association between total and fractional cholesterol with the extent of CI and its correlation with amyloid beta-42 and total tau. Furthermore, we estimated the association between serum total-tau and amyloid beta-42 with various metals in the blood and the stages of cognitively impaired subjects and compared the data with age matched healthy controls. Finally receiver operating characteristic (ROC) analysis was performed to evaluate the specificity and sensitivity of amyloid beta-42, tau protein, and various metals as potential biomarkers for diagnosis of mild, moderate, and severe CI.

MATERIALS AND METHODS

Ethics

This study protocol was approved by the Internal Review Board (IRB) of the Atta-ur-Rahman School of Applied Biosciences, National University of Sciences and Technology (approval letter number 35IRB). The procedures were performed following the code of ethics of the World Medical Association (Declaration of Helsinki). Written informed consent was obtained from all subjects and/or caregivers included in the study.

Subjects

A total of 273 subjects aged more than 50 years were included in this study. A well-defined inclusion criterion was practiced. Subjects having proper evidence of the CI as reported by neuro physicians or psychiatrists and with more than 50 years of age were included. The patients under any kind of therapies (including the lipid-lowering medications) were excluded from the study. Detailed information was obtained from all subjects through an approved questionnaire. The questionnaire includes the date of birth, occupation, medical history, medications, and

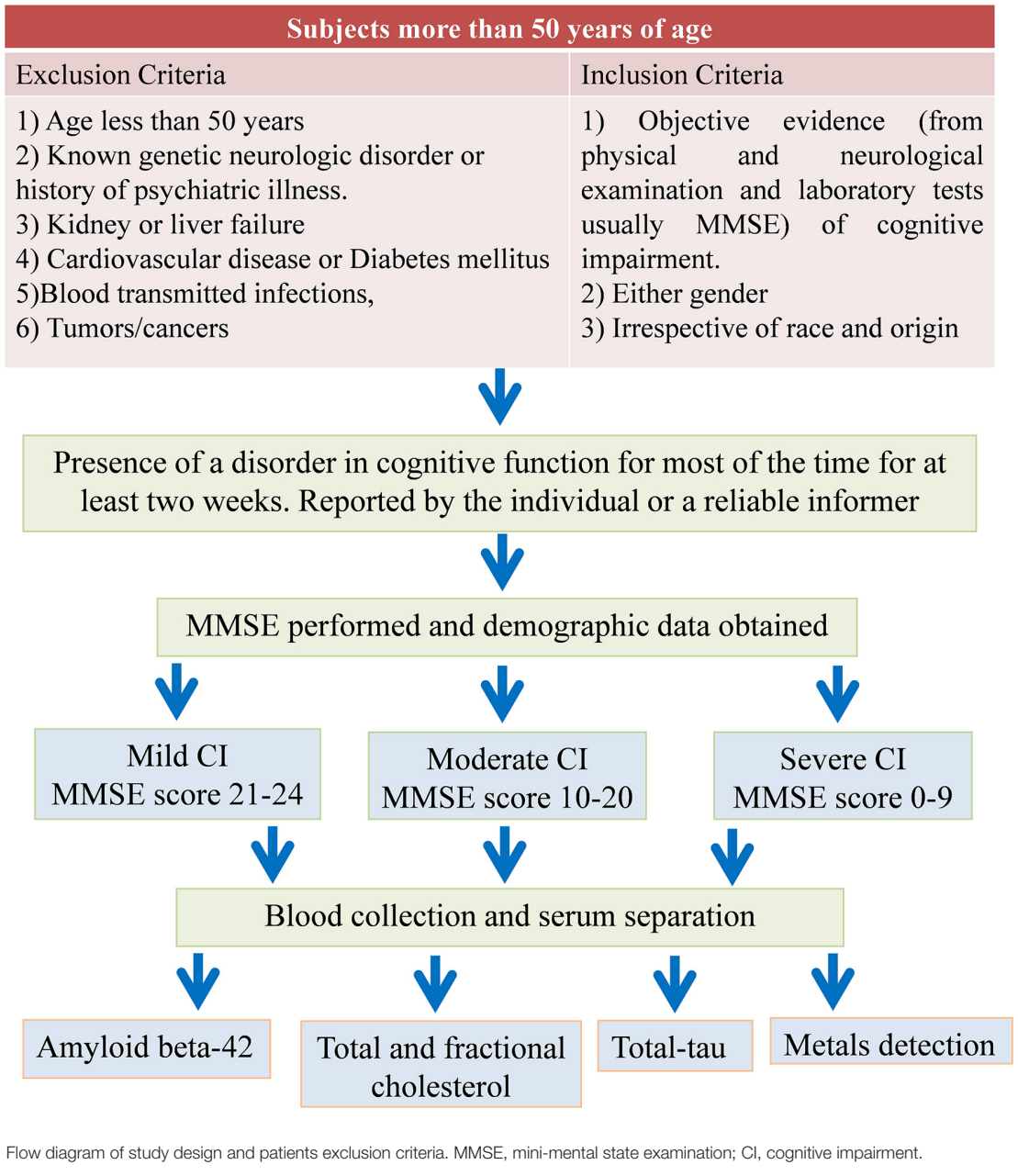

FIGURE 1 | Flow diagram of study design and patients exclusion criteria. MMSE, mini-mental state examination; CI, cognitive impairment.

lifestyle of the subjects. The study design and the patient's exclusion criteria are shown in **Figure 1**.

Cognitive Function Assessment and Classification of Subjects

Screening of cognitive function was performed using a standard and widely used and accepted 30 point questionnaire test known as the Folstein test or mini-mental state examination (MMSE; Folstein et al., 1975; Ferrante et al., 2019; Nardes et al., 2020). The MMSE was administered by an independent health care provider to evaluate overall cognitive function. The subjects were classified based on MMSE score into mild, moderate, and severe CI (**Table 1**). In this study of 273 subjects, 72 patients with mild CI, 86 with moderate CI, 25 with severe CI and 90 age-matched healthy control were examined for lipids profiling, total-tau and amyloid beta-42 in serum and correlation of these biomarkers with metals (Al, Pb, Zn, Cu, Cd, and Mn) concentrations were studied. Metals levels in these subjects are reported earlier (Iqbal et al., 2018). All cognitively impaired subjects with co-morbidities were excluded from the study. Older "healthy" individuals aged 50 years, with overall good health and with normal MMSE score were used as age-matched healthy controls in this study.

TABLE 1 | Demographic data of the study subjects.

Variables/parameters measured		Age matched healthy control (n = 90)	Mild cognitive impairment (n = 71)	Moderate cognitive impairment (n = 86)	Severe cognitive impairment (n = 25)
MMSE score		28.67 ± 1.3	22.7 ± 1	15.7 ± 2.2	5.96 ± 2
Gender	Male	48	33	51	10
	Female	42	39	35	15
Age years (SD)		58.1 ± 6.6	61.7 ± 9	65.1 ± 10.9	79.68 ± 7
Weight kg (SD)		73.07 ± 7.5	71.25 ± 7.2	72.2 ± 7	74.7 ± 5.1
Living standard	Rural	76	59	74	18
	Urban	14	12	12	7
Education	Primary (0–5 yeras)	26	34	43	17
	Secondary level	49	32	39	8
	Higher secondary level	3	3	3	0
	Bachelors and above	12	2	1	0
Marital status	Married	86	64	74	19
	Unmarried	4	8	12	6
Smoking	Smokers	11	21	39	10
	No smokers	89	50	47	15

Serum Collection

All the procedure was performed under aseptic conditions. Five milliliters of blood was collected by vein puncture from each subject using a sterile needle. Two milliliters was transferred to EDTA vacutainer tubes for metal detection while three milliliters of blood in the other vacutainer was left to clot at room temperature for about 20 min. After that, vacutainers were centrifuged at 3,000 rpm for 10 min to separate the serum from clotted blood. This serum was then immediately transferred to labeled Eppendorf tubes and stored at −80°C for further use.

Lipid Profile Measurements

Triglycerides, HDL cholesterol, and total cholesterol were measured from serum by Merck Microlab 300 apparatus. Triglycerides were measured by the Abcam triglyceride kit (Catalogue Number: ab65336), total cholesterol was estimated by Merck kit (Catalogue Number: 428901) and cholesterol was calculated by Abcam human ELISA kit (Catalogue number: ab12561). All procedures were carried out according to the manufacturer's instructions. LDL cholesterol was estimated using the Friedenwald equation i.e.,

$$\text{LDL cholesterol} = \text{total cholesterol} - \text{HDL cholesterol—(triglycerides/2.2)}$$

Cholesterol ratio was calculated by the formula

$$\text{Cholesterol ratio} = \text{Total cholesterol/HDL cholesterol}$$

Total-Tau Level Measurement

Serum Total-tau was estimated using the human tau ELISA kit (catalog number ab210972 and lot: GR302657-1) purchased from Abcam, Cambridge, UK. All the procedures were performed according to the manufacturer's instructions.

Amyloid Beta-42 Level Measurement

Measurement of serum amyloid beta-42 was carried out using human amyloid beta-42 ELISA kit (E-El-H0543; lot: AK0017JAN11029) purchased from Elabscience (Hubei, China). The assay was performed according to the manufacturer's instructions.

Quantification of Metal Levels and Their ROC Analyses

Blood was digested by a microwave-assisted acid digestion method as previously described (Iqbal et al., 2018). Heavy metals were analyzed in digested blood samples by double-beam Perkin Elmer atomic absorption spectrometer model 700 (Perkin Elmer, USA). Metals levels are reported earlier (Iqbal et al., 2018) and their ROC was analyzed here to find out their diagnostic significance.

Statistical Analysis

The data were statistically analyzed using GraphPad prism software and variables were compared using one-way ANOVA followed by Bonferroni *post hoc* test. Data were expressed as mean ± standard error of the mean (SEM) and considered significant only if the p-value was less than 0.05. Correlation analysis among the two variables was calculated using Pearson's correlation by GraphPad prism. ROC analyses were carried out to find the cutoff concentration of total-tau, amyloid beta-42, Cu, Al, Zn, Pb, Mn, and Cd.

RESULTS

Demographic Data of Subjects

The demographic data obtained from all subject groups i.e., age-matched healthy control, mild CI, moderate CI, and severe CI patients are summarized in **Table 1**. There were more females compared to the number of males in diseased groups. Most of the subjects were from urban areas. There was less number of individuals with higher education in the case of moderate and severe CI groups. An increasing trend in percent of smokers from mild to severe cognitively impaired groups was observed.

Lipid Profile Measurement in Blood Samples of CI Subjects

The LDL cholesterol concentrations in mild CI (100.5 ± 3.67 mg/dl), moderate CI (107.8 ± 3.01 mg/dl) and severe CI groups (125.8 ± 5.22 mg/dl) were significantly

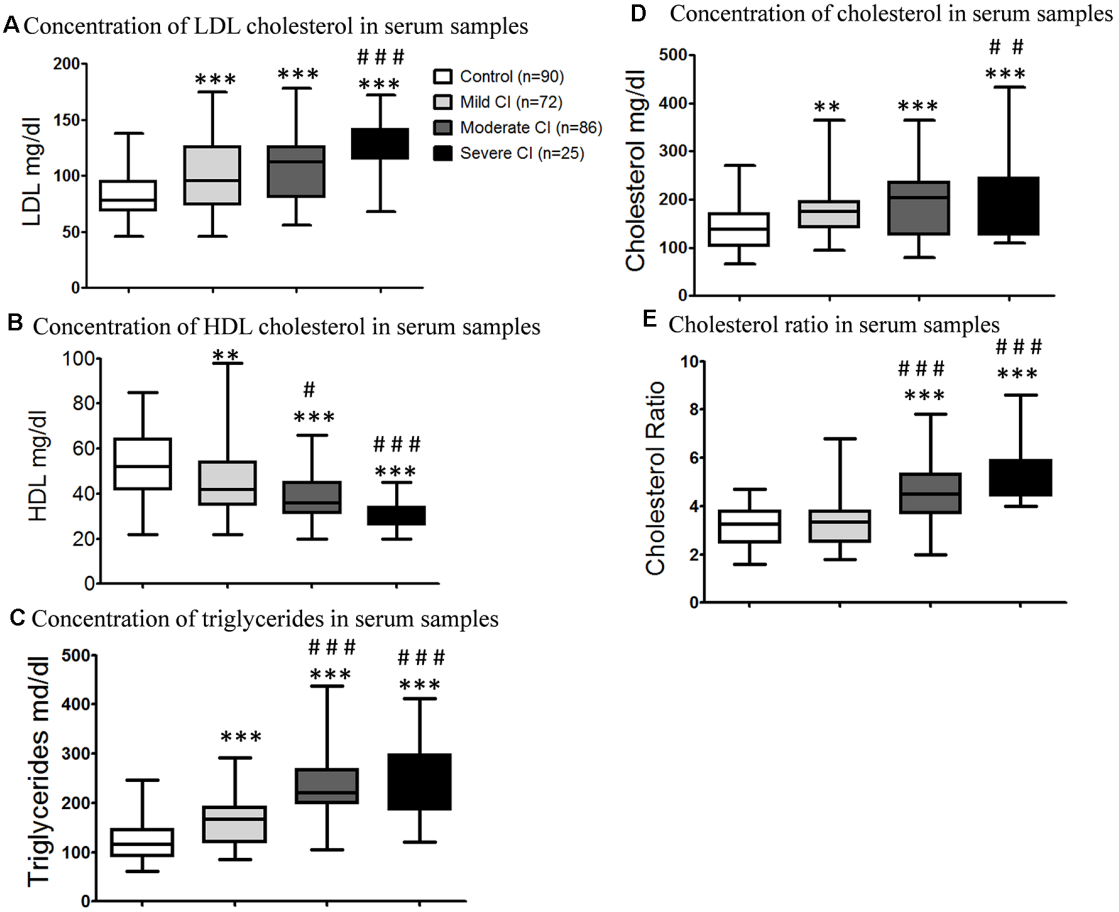

FIGURE 2 | Bar graph showing the total and fractional cholesterol in serum samples of age-matched healthy control, mild CI, moderate CI and severe cognitively impaired subjects. **(A)** Low-density lipoprotein (LDL) cholesterol in serum samples. **(B)** High-density lipoprotein (HDL) cholesterol level in serum samples. **(C)** Triglycerides level in serum samples. **(D)** Total cholesterol concentration in serum samples. **(E)** Cholesterol ratio in serum samples. $^{**}p < 0.01$, $^{***}p < 0.001$ compared with age-matched healthy control group; $^{\#}p < 0.05$, $^{\#\#}p < 0.01$, $^{\#\#\#}p < 0.001$ comparison with mild cognitive impaired group; n, samples size.

($^{***}p < 0.001$) higher than the age matched healthy control group (**Figure 2A**). The level of HDL cholesterol in serum samples of age matched healthy controls (51.9 ± 1.41 mg/dl) were significantly higher than mild (44.56 ± 1.67 mg/dl; $^{**}p < 0.01$), moderate (38.26 ± 1.31 mg/dl; $^{***}p < 0.001$) and severe (30.68 ± 1.28 mg/dl; $^{***}p < 0.001$) cognitively impaired subjects (**Figure 2B**). It was found that triglycerides levels in serum were significantly higher in mild CI (161.5 ± 5.65 mg/dl; $^{**}p < 0.01$), moderate CI (230.3 ± 8.1 mg/dl; $^{***}p < 0.001$) and severe CI groups (248.5 ± 15 mg/dl; $^{***}p < 0.001$) comparative to age matched healthy controls (30.68 ± 1.28 mg/dl; **Figure 2C**). The total cholesterol levels were significantly lower in age matched healthy control group (138.9 ± 4.49 mg/dl) compared to those diagnosed with mild CI (172.5 ± 5.79 mg/dl; $^{***}p < 0.01$), moderate CI (195.8 ± 6.73 mg/dl; $^{***}p < 0.001$) and severe CI (217.1 ± 17.48 mg/dl; $^{***}p < 0.001$). However there was no significant difference observed among mild CI and moderate CI group and also among moderate CI and severe CI groups (**Figure 2D**). Cholesterol ratio was significant ($^{***}p < 0.001$) increased in subjects diagnosed with moderate CI (4.51 ± 0.13 mg/dl) and severe CI (5.28 ± 0.24 mg/dl) when compared to age matched healthy controls. Moreover there was no significant difference among subjects with mild CI (3.43 ± 0.13 mg/dl) and age matched healthy controls (**Figure 2E**).

Correlation Between Lipids Profile and MMSE

Correlation analysis was performed in order to observe the association of concentrations of LDL cholesterol, HDL cholesterol, triglycerides, total cholesterol and cholesterol ratio with the extent of CI. Correlation test revealed that the strongest negative correlation was observed with cholesterol ratio ($r = -0.562$; $^{***}p < 0.001$) followed by LDL cholesterol ($r = -0.428$; $^{***}p < 0.001$), total cholesterol ($r = -0.39$; $^{***}p < 0.001$) and triglycerides ($r = -0.329$; $^{***}p < 0.001$), respectively (**Figures 3A–E**). A strong positive correlation

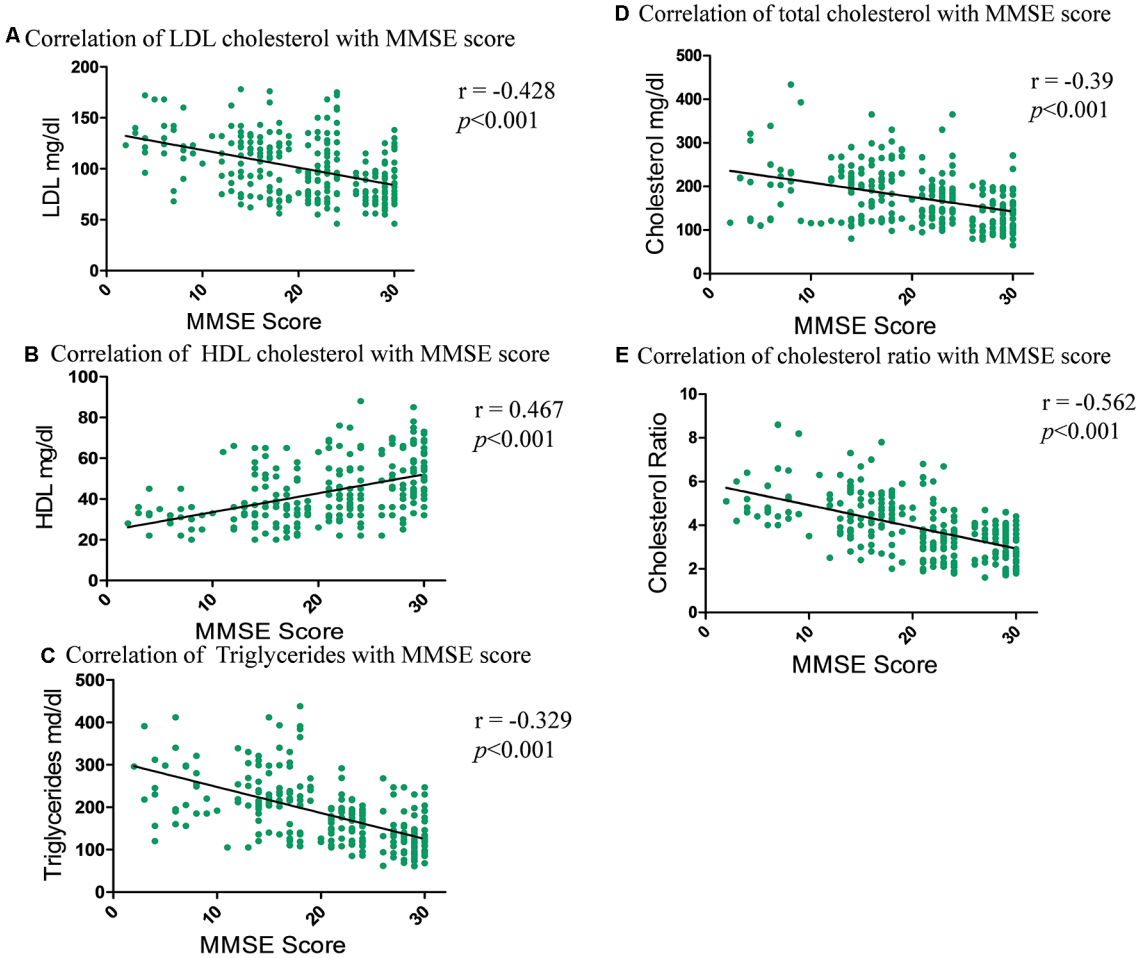

FIGURE 3 | Correlation graph showing the relationship between the total and fractional cholesterol in serum samples and subjects MMSE score. **(A)** Correlation of LDL cholesterol with MMSE scores. **(B)** Correlation of HDL cholesterol with MMSE scores. **(C)** Correlation of triglycerides with MMSE scores. **(D)** Correlation of total cholesterol with MMSE scores. **(E)** Correlation of cholesterol ratio with MMSE scores.

was observed with HDL cholesterol concentration (r = 0.467; $^{***}p < 0.001$) and MMSE score.

Tau Levels in Serum, ROCs in CI Severity and Its Correlation With MMSE, Lipids Profile, and Metals Levels

The concentration of serum total-tau levels increased with increasing severity of CI (**Figure 4A**). The total-tau concentration in subjects with severe CI (50.05 ± 3.68 pg/ml; $^{**}p < 0.01$) and moderate CI (44.94 ± 3.19 pg/ml; $^{*}p < 0.05$) were significantly higher than the age-matched healthy control (31.8 ± 2.79 pg/ml). There were significantly low levels of tau in subjects with mild CI (34.4 ± 3.76 pg/ml; $^{**}p < 0.01$) in comparison to severe CI group. No significant difference was observed among mild CI group and age-matched healthy control (**Figure 4A**). A significant and downhill linear correlation was found between total-tau levels and MMSE score ($r = -0.443$; $^{***}p < 0.001$; **Figure 4B**).

ROC analysis revealed that tau levels showed the best results in moderate CI followed by severe CI, but not very accurate in mild CI (**Supplementary Figure S1**). In the case of moderate CI vs. control, the AUC for tau was 0.80 and the cutoff value was 47.37 pg/ml; with a sensitivity of 55% and specificity of 90% to detect moderate CI patients (**Figure 4C**). While, in case of severe CI vs. control, the AUC was 0.75, the cutoff concentration was 46.79 pg/ml; with a sensitivity of 50% and specificity of 90% to detect severe CI (**Figure 4D**).

Correlation analysis of tau concentration and cholesterol fractions showed the strongest positive correlation with cholesterol ratio ($r = 0.368$; $^{***}p < 0.001$) followed by triglyceride ($r = 0.32$; $^{**}p < 0.01$) and least with LDL cholesterol ($r = -0.251$; $^{*}p < 0.05$; **Figures 5A–C**). A negative correlation between the HDL cholesterol ($r = -0.245$; $^{*}p < 0.05$) and tau concentration whereas no correlation with total cholesterol was shown (**Supplementary Figures S2A,B**).

Metal concentrations were correlated with tau levels to determine any association among the elevated levels of metals

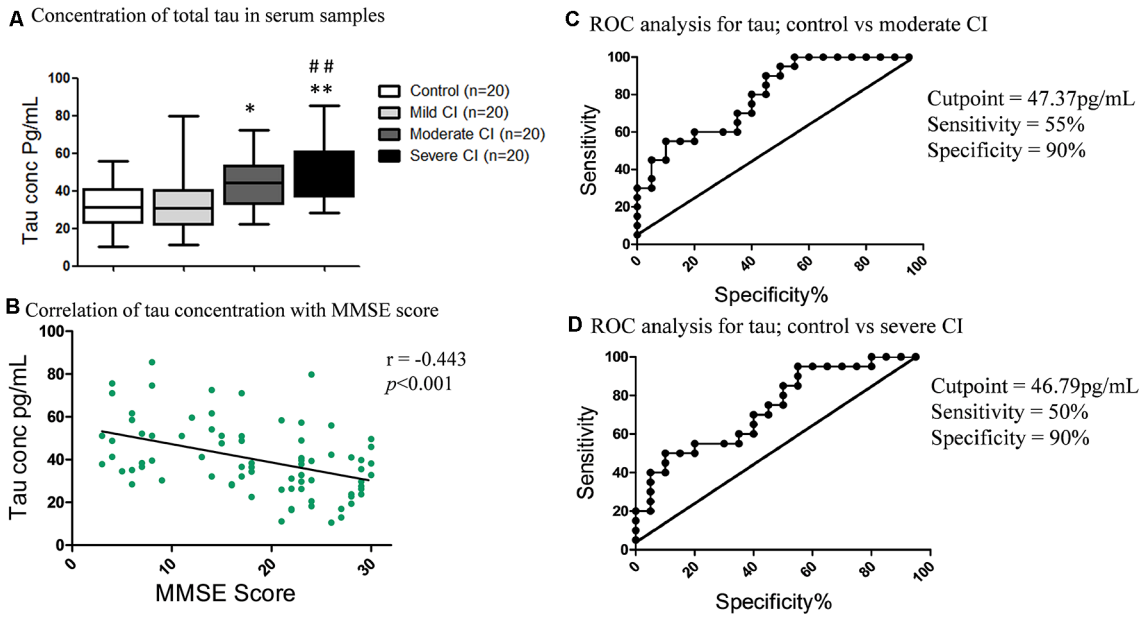

FIGURE 4 | Serum tau levels and its correlation with MMSE and Receiver Operating Characteristic (ROC) curves. **(A)** Concentration of total-tau in serum samples in studied subjects. $^{*}p < 0.05$, $^{**}p < 0.01$ compared with age-matched healthy control group; $^{\#\#}p < 0.01$ comparison with mild cognitive impaired group; *n* = sample size. **(B)** Correlation of tau concentration with MMSE scores. ROC analysis of serum tau proteins between **(C)** Control vs. moderate CI and **(D)** Control vs. severe CI groups.

with the levels of serum tau proteins. Pearson's correlation demonstrated significant correlation of tau with Cu ($r = 0.32$; $^{**}p < 0.01$), followed by Zn ($r = 0.28$; $^{*}p < 0.05$), Al ($r = 0.26$; $^{*}p < 0.05$) as shown in **Figures 5D–F**. While Mn ($r = 0.23$; $^{*}p < 0.05$) was weakly correlated and Pb ($r = -0.251$; ns) and Cd ($r = -0.251$; ns) were non-significant (**Supplementary Figures S2C–E**).

Amyloid Beta-42 Levels in Serum, ROCs in CI Severity and Its Correlation With MMSE, Lipids Profile and Metals Levels

The amyloid beta-42 levels declined with the increase in CI (**Figure 6A**). The amyloid beta-42 concentration was low in subjects diagnosed with severe CI (17.05 ± 1.68 pg/ml) compared to mild CI (23.52 ± 1.36; $^{**}p < 0.01$ pg/ml) and age matched healthy controls (24.68 ± 1.68 pg/ml; $^{***}p < 0.001$). Correlation analyses revealed significant positive correlation of amyloid beta-42 levels and MMSE score ($r = 0.451$; $^{***}p < 0.001$; **Figure 6B**).

ROC analyses revealed that amyloid beta-42 did now show promising results for mild CI vs. control (**Supplementary Figure S3**). In case of moderate CI vs. control, the AUC was 0.74, the cutoff value was 22.68 pg/ml; with sensitivity 80% and specificity 70% (**Figure 6C**). While in case of severe CI vs. control, the AUC was 0.79, the cutoff value of amyloid beta-42 was 22.57 pg/ml; with a sensitivity of 90% and specificity of 70% to detect severe cognitively impaired patients (**Figure 6D**).

Furthermore amyloid beta-42 correlation with cholesterol fractions was evaluated and a negative correlation was seen in the order of triglyceride ($r = -0.345$; $^{**}p < 0.01$), LDL cholesterol ($r = -0.34$; $^{**}p < 0.01$) and cholesterol ratio ($r = -0.323$; $^{**}p < 0.01$; **Figures 7A–C**). A positive correlation with HDL cholesterol ($r = 0.292$; $^{**}p < 0.01$) and amyloid beta-42 concentration, whereas weak negative correlation of total cholesterol ($r = -0.28$; $^{*}p < 0.05$) with amyloid beta-42 was seen (**Supplementary Figures S4A,B**).

When amyloid beta-42 concentration was correlated with metals, it was found that amyloid beta-42 is negatively correlated with the concentration of Zn ($r = -0.32$; $^{**}p < 0.01$), followed by Pb ($r = -0.31$; $^{**}p < 0.01$) and Cu ($r = -0.26$; $^{**}p < 0.01$) as shown in **Figures 7D–F**. Al was marginally negatively associated ($r = -0.25$; $^{*}p < 0.05$) whereas Mn ($r = -0.21$; ns) and Cd ($r = -0.20$; ns) showed non-significant correlation (**Supplementary Figures S4C–E**).

ROC Analysis of Metals to Detect Mild CI, Moderate CI and Severe CI

Metals levels were estimated in these subjects (Iqbal et al., 2018) and their ROC analyses for diagnostic value were evaluated here. It was found that Cu showed the best diagnostic value (**Figures 8A–C**), followed by Zn (**Figures 8D–F**), Al (**Figures 8G–I**), and Pb (**Figures 8J–L**). ROC analyses of Mn and Cd were also analyzed (**Supplementary Figures S5A–F**).

Finally, we added amyloid beta-42 and total tau concentration and ROC analysis was performed. The results did not show very promising ROC values of these combined biomarkers (**Supplementary Figure S6**).

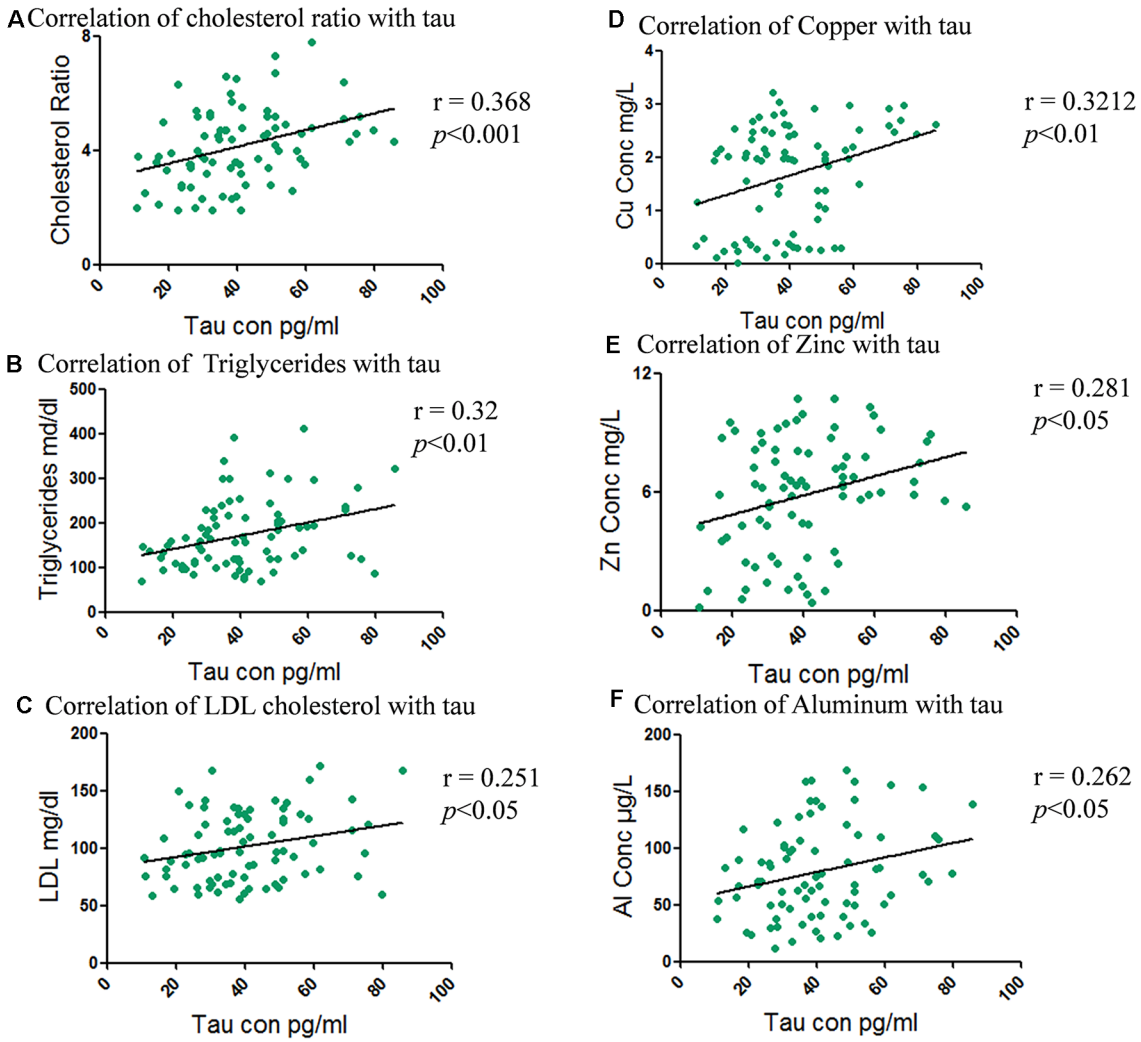

FIGURE 5 | Correlation between total and fractional serum cholesterol levels with total tau concentration and metals levels with tau. **(A)** Correlation of cholesterol ratio with tau. **(B)** Correlation of triglycerides with tau. **(C)** Correlation of LDL cholesterol with tau. **(D)** Correlation of total tau with Copper. **(E)** Correlation of total tau with Zinc. **(F)** Correlation of total tau with Aluminum.

DISCUSSION

The decline in both physical and cognitive function has been associated with increased aging. A physiological link exists between physical frailty and cognitive decline. These underlying processes include chronic inflammation, impaired hypothalamic-pituitary axis stress response, imbalanced energy metabolism, mitochondrial dysfunction, oxidative stress, and neuroendocrine dysfunction (Freitas et al., 2019; Adams et al., 2019; Yang et al., 2019; Ma and Chan, 2020). Blood-based biomarkers for CI are very important and can be effectively used to promote healthy brain aging, for screening and diagnosis at every stage of the dementias, assessment of risk to the disease, and may also be helpful in drug discovery approaches. In many cases, blood-based biomarkers lack specificity and sensitivity; hence their clinical application is limited. Tau proteins that are associated with axonal damage and amyloid proteins linked with plaque formation have been used in clinical trials as CSF based diagnostic markers for certain neurological diseases (Cummings, 2011). Interestingly, the present study showed that the concentration of both serum tau and amyloid beta-42 were significantly different in cases of moderate and severe CI compared to mild CI and age-matched healthy controls. These findings add further evidence that serum amyloid and tau levels may improve prediction of CI, are associated with various manifestations of CI, and may represent a useful biomarker for evaluating at-risk individuals in CI prevention trials.

A recent study reported that high levels of plasma tau was associated with a decrease in logical memory, volume of gray matter, and hippocampus (Chiu et al., 2014). Our study also showed similar results that patients of severe CI have increased levels of serum tau and tau protein levels are negatively correlated with the MMSE score. The ROC analysis

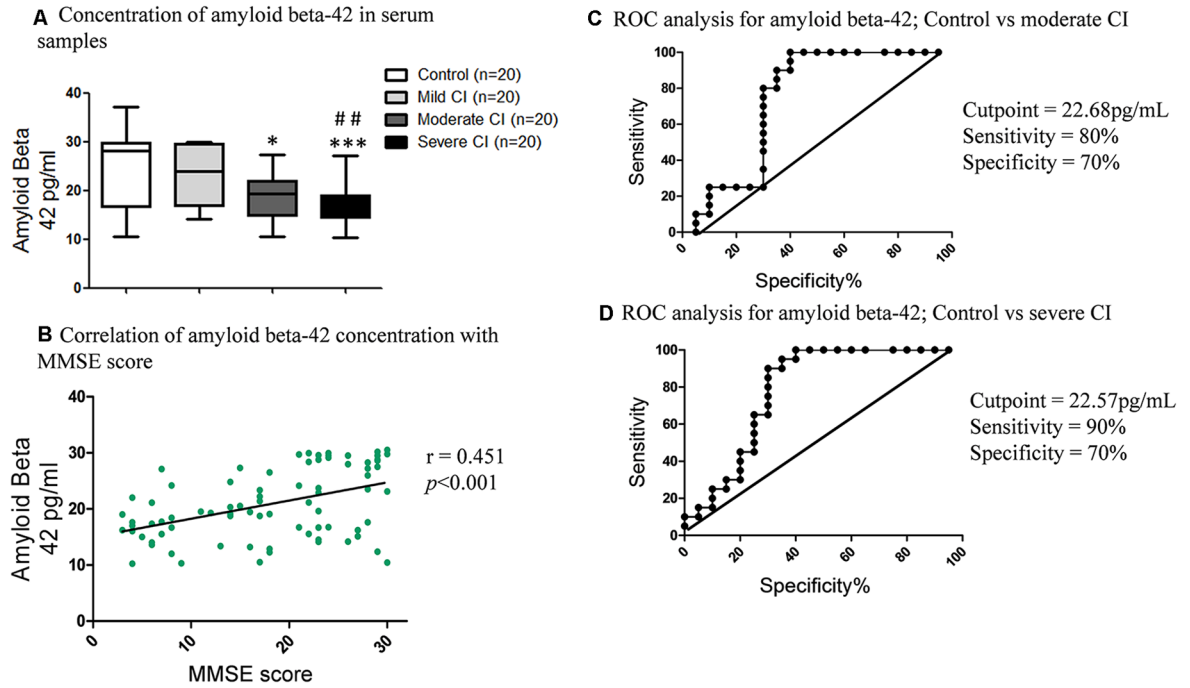

FIGURE 6 | Serum amyloid beta-42 levels and its correlation with MMSE, and ROC curves. **(A)** Concentration of serum amyloid beta-42 in serum samples in studied subjects. $^{*}p < 0.05$, $^{***}p < 0.001$ compared with age-matched healthy control group; $^{\#\#}p < 0.01$ comparison with mild cognitive impaired group; n = sample size. **(B)** Correlation of serum amyloid beta-42 concentration with MMSE scores. ROC curves of **(C)** Control vs. moderate CI and **(D)** Control vs. severe CI.

determined the cutoff concentrations which were highly sensitive and specific to differentiate mild, moderate, and severe CI from age-matched healthy controls. The cutoff values from ROC analysis have depicted that tau concentration can be efficiently used to detect severe CI. Metals contribute to the pathology of CI by aggregating amyloid-beta and tau phosphorylation (Kim et al., 2018). The hyper-phosphorylation of tau leads to oxidative stress (Mandelkow and Mandelkow, 1998). Cu and Zn add to the tau pathology by directly binding with tau proteins (Ma et al., 2006; Huang et al., 2014) while Pb and Al contribute to apoptosis (Zhang et al., 2012; Brown et al., 2019). Our results show that tau concentration and metals are directly correlated, where increasing metals concentration was directly affecting tau increases, and this was found in the order of Cu, Zn, and Al, suggesting the modulatory roles of these metals.

Amyloid-beta levels are in dynamic equilibrium at the peripheral and cerebral level (Wang et al., 2006). The deposition of amyloid beta-42 in the brain might reduce plasma levels of amyloid beta-42 (Iadecola, 2003). The accumulation of extracellular amyloid beta-42 can induce the formation of intracellular NFTs that causes organelle stress leading to neurodegeneration and CI in AD. This phenomenon is termed the "snowball hypothesis" (Bi et al., 2019). The beta and gamma secretases enzyme that is involved in the amyloid beta-42 formation is dominantly localized in cholesterol-rich domains of the plasma membrane (Ehehalt et al., 2003). Studies have also shown that the cellular concentration of cholesterol might regulate the concentration and production of amyloid-beta peptides. Increased levels of cellular cholesterol shift the metabolism towards the amyloidogenic pathway however decreased cholesterol results in the non-amyloidogenic pathway (Bodovitz and Klein, 1996; Kojro et al., 2001). Different lipid-lowering therapies have been shown to interfere indirectly with amyloid-beta protofibrils by either cholesterol-dependent or cholesterol independent pathways (Shakour et al., 2019). Lipid-lowering therapy has been shown to ameliorate asymptomatic intracranial atherosclerosis, which is a risk factor for vascular CI and dementia (Xie et al., 2018; Zou et al., 2018; Miao et al., 2019; Shetty et al., 2019). Atorvastatin treatment also improved cognitive outcomes and induced anti-inflammatory response in a rat model for a chronic subdural hematoma and intracerebral hemorrhage (Quan et al., 2019).

In the current study, we reported that the levels of serum amyloid-beta decreased with the progression of the disease from mild to severe. There was a positive correlation observed between levels of amyloid beta-42 and the MMSE score. The ROC cutoff value revealed that amyloid beta-42 is more sensitive and specific to determine the different stages of disease compared to tau. The high sensitivity and specificity of serum tau and amyloid beta-42 might be useful to diagnose the CI with high accuracy. Al, Cu, and Zn were found in large quantities in aggregates of amyloid beta-42 (Mantyh et al., 1993) and were strongly associated with amyloid beta-42 levels in our study. Cu is required for normal brain function and Cu metabolism is dysregulated in brain aging (Braidy et al., 2017). Alterations in copper fluxes have also been reported in murine brain

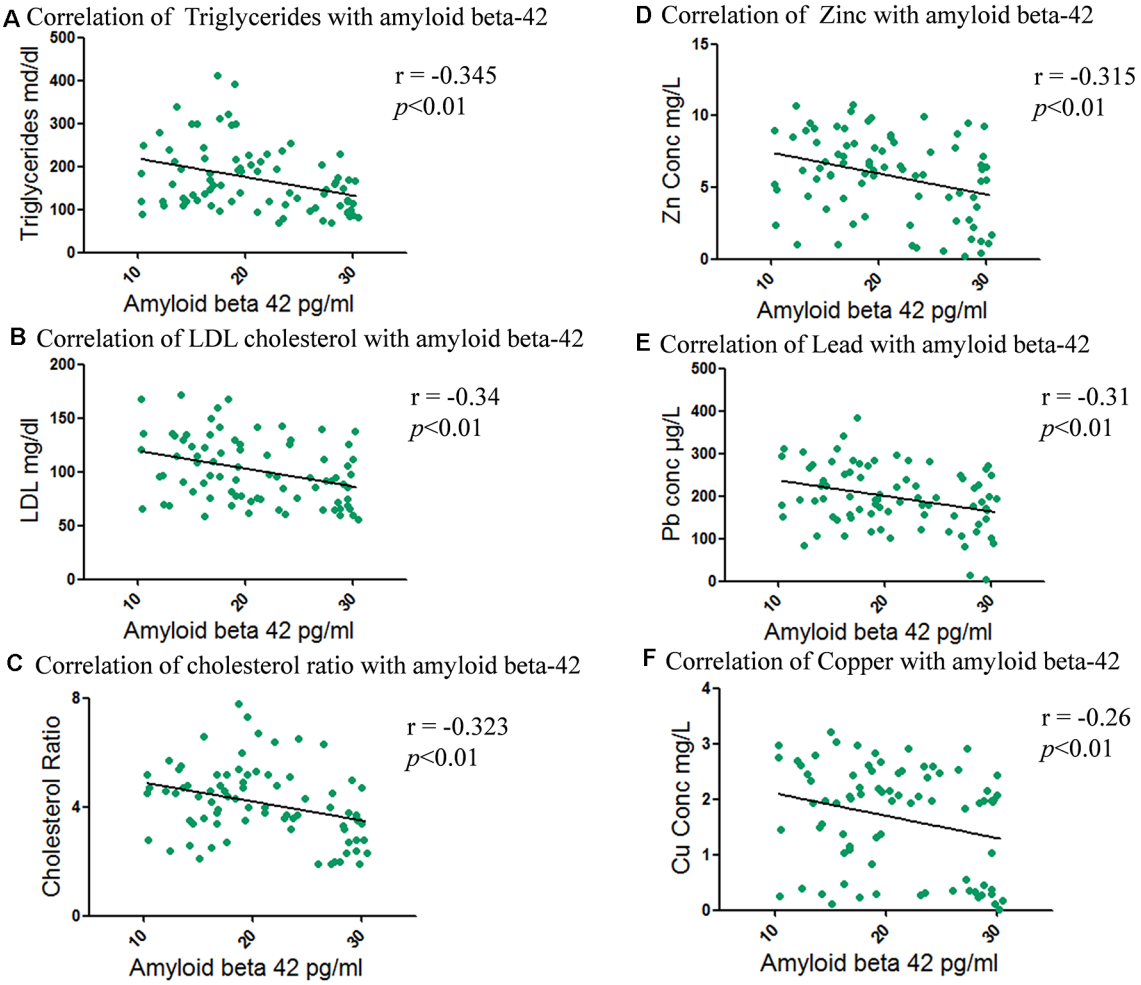

FIGURE 7 | Correlation between total and fractional serum cholesterol levels with amyloid beta-42 and metals levels with amyloid beta-42. **(A)** Correlation of triglycerides with amyloid beta-42. **(B)** Correlation of LDL cholesterol with amyloid beta-42. **(C)** Correlation of cholesterol ratio with amyloid beta-42. **(D)** Correlation of amyloid beta-42 with Zinc. **(E)** Correlation of amyloid beta-42 with Lead. **(F)** Correlation of amyloid beta-42 with Copper.

aging using $^{64}CuCl_2$ as a radiotracer ($^{64}CuCl_2$-PET/CT; Peng et al., 2018). Metals, including Cu and redox metals, are directly involved in the generation of amyloid plaques and indirectly by inducing oxidative stress/damage (Smith et al., 2006; Liguori et al., 2018). High Mn concentration also induces the amyloid-beta related cognitive decline in previous studies (Tong et al., 2014). Our study revealed a similar finding that metals increased the amyloid-beta aggregates and ultimately leading to decreed amyloid-beta levels in blood serum.

This study also explored the association between adverse lipid profiles and CI. We found that a low serum concentration of HDL cholesterol was linked to CI. Serum concentrations of total cholesterol, triglycerides, and LDL cholesterol showed association with CI therefore we can conclude that alteration in cholesterol metabolism in the brain might contribute to the pathology of CI. The subjects included in this study did not have cardiovascular disease or hypertension. The association of these parameters was not confounded by living standards or education status.

An association between high levels of total cholesterol, LDL cholesterol, triglycerides; and a low concentration of HDL cholesterol are risk factors for cardiovascular disease that have been previously documented (Sacco et al., 2001). Lipoprotein-associated phospholipase A2 and superoxide dismutase are linked to regulating neuroinflammation (Zhu et al., 2019). Lipoprotein cholesterol and high sensitivity C-reactive protein have also been shown to correlate with Parkinson's disease severity (Yang et al., 2020). LDL cholesterol and plasma cystatin—a protein produced by nucleated cells—has been shown to differentiate progressive supranuclear palsy from healthy subjects and predict disease severity (Weng et al., 2018). Our study reported similar results with the risk of CI and its propagation. In this study, HDL cholesterol was highly correlated with the CI as compared to LDL cholesterol, triglycerides, and total cholesterol. HDL cholesterol is the predominant lipoprotein

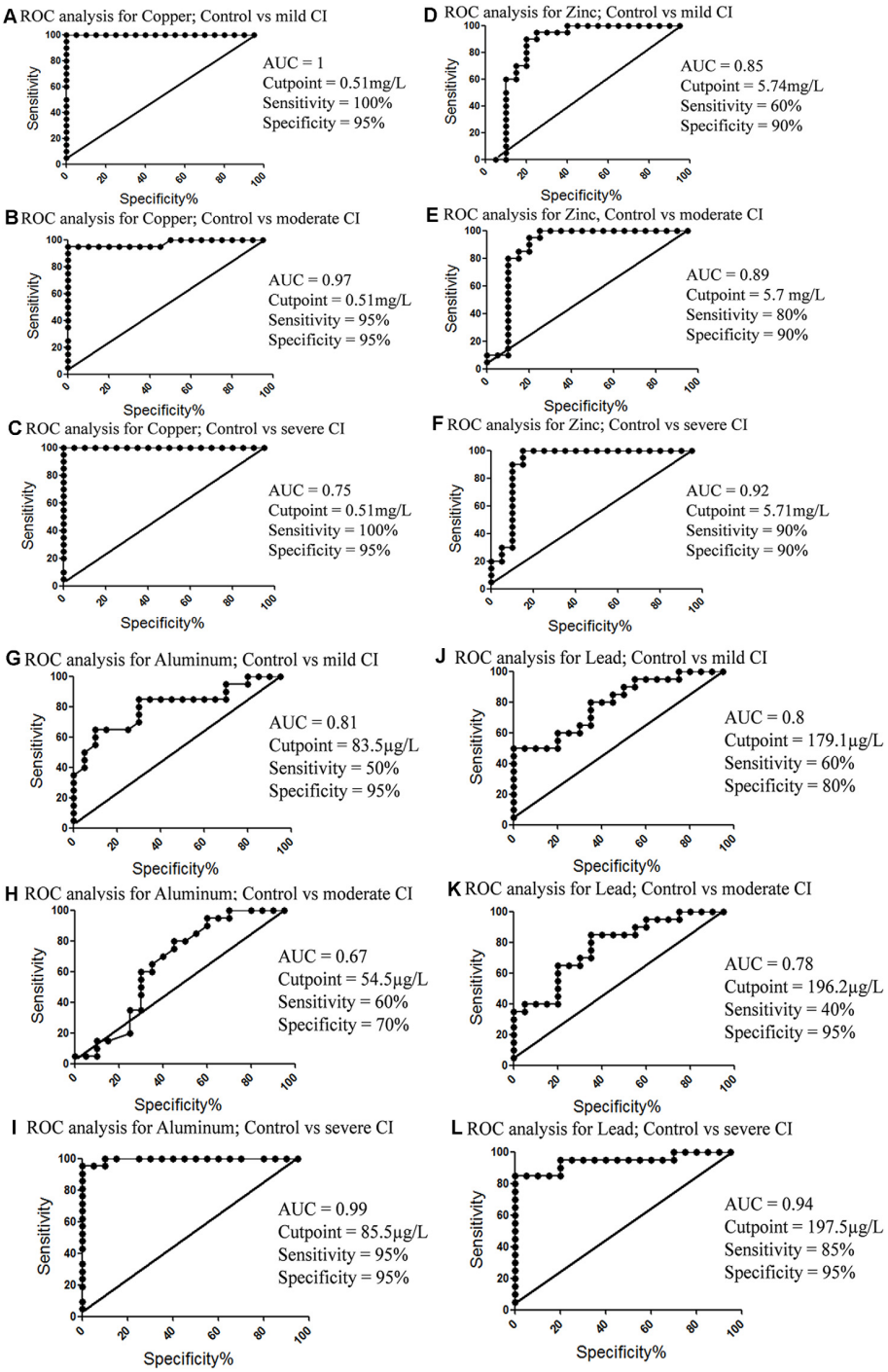

FIGURE 8 | ROC analysis of metals concentrations in different groups. **(A)** Copper concentration; control vs. mild CI. **(B)** Copper concentration; control vs. moderate CI. **(C)** Copper concentration; control vs. severe CI. **(D)** Zinc concentration; control vs. mild CI. **(E)** Zinc concentration; control vs. moderate CI. **(F)** Zinc concentration; control vs. severe CI. **(G)** Aluminum concentration; control vs. mild CI. **(H)** Aluminum concentration; control vs. moderate CI. **(I)** Aluminum concentration; control vs. severe CI. **(J)** Lead concentration; control vs. moderate CI. **(K)** Lead concentration; control vs. severe CI. **(L)** Lead concentration; control vs. mild CI.

in the human brain (Olesen and Dagø, 2000) and prevents aggregation of amyloid proteins (Koudinov et al., 1998), and may prevent the development and progression of the disease. The association between low levels of HDL cholesterol and progression of CI was irrespective of the presence of stroke, hypertension, and cardiovascular disease. HDL cholesterol

has anti-inflammatory properties (Cockerill et al., 1995), and inflammation is considered to play a contributory if not causal role in neurodegenerative processes (Grundke-Iqbal et al., 1986; McGeer and McGeer, 1998).

Our study has also shown that individuals with high concentrations of LDL cholesterol were diagnosed with severe CI. The stronger correlation was demonstrated with LDL cholesterol followed by HDL cholesterol. Previous studies have also reported that individuals with AD have significantly higher LDL cholesterol and lower HDL cholesterol hence influencing AD pathology (Kuo et al., 1998; Moroney et al., 1999). High levels of LDL cholesterol and total cholesterol leads to microglial activation and amyloid-beta formation and may be directly involved in the pathobiology of dementia (Streit and Sparks, 1997). High serum total cholesterol may be a risk factor for CI and its progression. Total cholesterol was positively correlated with the MMSE score. One study revealed that total cholesterol is an independent risk factor for dementia and AD (Notkola et al., 1998). As well, Anstey et al showed an association between high midlife total cholesterol and cognitive decline (Anstey et al., 2008).

Triglycerides mediate CI, possibly by impairing maintenance of the *N*-methyl-D-aspartate component of hippocampal long-term potentiation and increasing oxidative stress (Razay et al., 2007; Farr et al., 2008). Our study is also consistent with previous findings, since serum triglyceride levels increased, in line with increased CI. There was a negative correlation observed between triglycerides and MMSE scores. Hence lipid-lowering therapy can improve neurological outcome (Quan et al., 2019).

This study provides insights on aging and mechanisms of CI as these are critical for novel therapies that might prevent or cure multiple age-related diseases. Among metals, Cu and Al were found to be significantly correlated with amyloid and tau. Whereas ROC analysis has also shown that Cu, Zn, and Al levels can be used as diagnostic markers for CI. Blood-based amyloid beta-42 and tau proteins might be used as specific biomarkers to evaluate the extent of cognitive deficits. Whereas, lipid and metal dyshomeostasis may contribute to the pathology of CI and its progression.

CONCLUSION

In conclusion, the low serum concentration of HDL cholesterol, high LDL cholesterol, total cholesterol, and triglycerides was associated with the progression of CI and clinical diagnosis of CI. The serum proteins, total-tau, and amyloid beta-42 may be practical to diagnose CI with high sensitivity and specificity. These findings are of clinical importance because they suggest that increasing HDL and lowering LDL cholesterol, total cholesterol, triglycerides, and metals might prevent the development and progression of CI and quantifying total-tau, Cu, Zn, Al and amyloid beta-42 may collectively represent a useful diagnostic tool.

DATA AVAILABILITY STATEMENT

All datasets generated for this study are included in the article/**Supplementary Material**.

ETHICS STATEMENT

The studies involving human participants were reviewed and approved by Internal Review Board (IRB) ASAB NUST. The patients/participants provided their written informed consent to participate in this study.

AUTHOR CONTRIBUTIONS

TA: project supervisor. TA, NB, and GI: study design. GI: data collection. GI: laboratory work/experimental. GI and TA: data analysis. TA, NB, and GI: manuscript preparation.

ACKNOWLEDGMENTS

We are thankful to the Atta-ur-Rahman School of Applied Biosciences, National University of Sciences and Technology, Pakistan, and the Higher Education Commission (HEC) of Pakistan for supporting this study and providing the technical research facilities. There are no financial or contractual agreements or obligations linked to the article. This research did not receive any specific grant from funding agencies in the public, commercial, or not-for-profit sectors.

SUPPLEMENTARY MATERIAL

The Supplementary Material for this article can be found online at: https://www.frontiersin.org/articles/10.3389/fnagi.2020.00223/full#supplementary-material.

REFERENCES

Adams, B., Nunes, J. M., Page, M. J., Roberts, T., Carr, J., Nell, T. A., et al. (2019). Parkinson's disease: a systemic inflammatory disease accompanied by bacterial inflammagens. *Front. Aging Neurosci.* 11:210. doi: 10.3389/fnagi.2019.00210

American Psychiatric Association, A. P. (1996). *DSM-IV: Manual de Diagnóstico e Estatística das Perturbações Mentais.* Portugal: Catalogação na publicação: Ana Paula M. Magnus CRB 10/2052.

Anstey, K. J., Lipnicki, D. M., and Low, L.-F. (2008). Cholesterol as a risk factor for dementia and cognitive decline: a systematic review of prospective studies with meta-analysis. *Am. J. Geriatr. Psychiatry* 16, 343–354. doi: 10.1097/JGP.0b013e31816b72d4

Bi, C., Bi, S., and Li, B. (2019). Processing of mutant β-amyloid precursor protein and the clinicopathological features of familial Alzheimer's disease. *Aging Dis.* 10:383. doi: 10.2210/pdb1jl0/pdb

Billingsley, M. L., and Kincaid, R. L. (1997). Regulated phosphorylation and dephosphorylation of tau protein: effects on microtubule interaction, intracellular trafficking and neurodegeneration. *Biochem. J.* 323, 577–591. doi: 10.1042/bj3230577

Bodovitz, S., and Klein, W. L. (1996). Cholesterol modulates-secretase cleavage of amyloid precursor protein. *J. Biol. Chem.* 271, 4436–4440. doi: 10.1074/jbc.271.8.4436

Braidy, N., Poljak, A., Marjo, C., Rutlidge, H., Rich, A., Jugder, B.-E., et al. (2017). Identification of cerebral metal ion imbalance in the brain of aging Octodon degus. *Front. Aging Neurosci.* 9:66. doi: 10.3389/fnagi.2017.00066

Brown, E. E., Shah, P., Pollock, B. G., Gerretsen, P., and Graff-Guerrero, A. (2019). Lead (Pb) in Alzheimer's dementia: a systematic review of human case-control studies. *Curr. Alzheimer Res.* 16, 353–361. doi: 10.2174/1567205016666190311101445

Chen, G.-F., Xu, T.-H., Yan, Y., Zhou, Y.-R., Jiang, Y., Melcher, K., et al. (2017). Amyloid beta: structure, biology and structure-based therapeutic development. *Acta Pharmacol. Sin.* 38, 1205–1235. doi: 10.1038/aps.2017.28

Chiu, M. J., Chen, Y. F., Chen, T. F., Yang, S. Y., Yang, F. P. G., Tseng, T. W., et al. (2014). Plasma tau as a window to the brain—negative associations with brain volume and memory function in mild cognitive impairment and early Alzheimer's disease. *Hum. Brain Mapp.* 35, 3132–3142. doi: 10.1002/hbm.22390

Cockerill, G. W., Rye, K.-A., Gamble, J. R., Vadas, M. A., and Barter, P. J. (1995). High-density lipoproteins inhibit cytokine-induced expression of endothelial cell adhesion molecules. *Arterioscler. Thromb. Vascu. Biol.* 15, 1987–1994. doi: 10.1161/01.atv.15.11.1987

Cummings, J. L. (2011). Biomarkers in Alzheimer's disease drug development. *Alzheimers Dement.* 7, e13–e44. doi: 10.1016/j.jalz.2010.06.004

Deary, I. J., Corley, J., Gow, A. J., Harris, S. E., Houlihan, L. M., Marioni, R. E., et al. (2009). Age-associated cognitive decline. *Br. Med. Bull.* 92, 135–152. doi: 10.1093/bmb/ldp033

Diniz, B. S., Pinto, J. A. Jr., and Forlenza, O. V. (2008). Do CSF total tau, phosphorylated tau and β-amyloid 42 help to predict progression of mild cognitive impairment to Alzheimer's disease? A systematic review and meta-analysis of the literature. *World J. Biol. Psychiatry* 9, 172–182. doi: 10.1080/15622970701535502

Ehehalt, R., Keller, P., Haass, C., Thiele, C., and Simons, K. (2003). Amyloidogenic processing of the Alzheimer β-amyloid precursor protein depends on lipid rafts. *J. Cell Biol.* 160, 113–123. doi: 10.1083/jcb.200207113

Farr, S. A., Yamada, K. A., Butterfield, D. A., Abdul, H. M., Xu, L., Miller, N. E., et al. (2008). Obesity and hypertriglyceridemia produce cognitive impairment. *Endocrinology* 149, 2628–2636. doi: 10.1210/en.2007-1722

Ferrante, L. E., Murphy, T. E., Leo-Summers, L. S., Gahbauer, E. A., Pisani, M. A., and Gill, T. M. (2019). The combined effects of frailty and cognitive impairment on post-ICU disability among older ICU survivors. *Am. J. Respir. Crit. Care Med.* 200, 107–110. doi: 10.1164/rccm.201806-1144le

Ferrera, P., Mercado-Gómez, O., Silva-Aguilar, M., Valverde, M., and Arias, C. (2008). Cholesterol potentiates β-amyloid-induced toxicity in human neuroblastoma cells: involvement of oxidative stress. *Neurochem. Res.* 33, 1509–1517. doi: 10.1007/s11064-008-9623-y

Folstein, M. F., Folstein, S. E., and McHugh, P. R. (1975). "Mini-mental state": a practical method for grading the cognitive state of patients for the clinician. *J. Psychiatr. Res.* 12, 189–198. doi: 10.1016/0022-3956(75)90026-6

Freedman, V. A., Aykan, H., and Martin, L. G. (2001). Aggregate changes in severe cognitive impairment among older Americans: 1993 and 1998. *J. Gerontol. B Psychol. Sci. Soc. Sci.* 56, S100–S111. doi: 10.1093/geronb/56.2.s100

Freitas, G. R. R., da Luz Fernandes, M., Agena, F., Jaluul, O., Silva, S. C., Lemos, F. B. C., et al. (2019). Aging and end stage renal disease cause a decrease in absolute circulating lymphocyte counts with a shift to a memory profile and diverge in treg population. *Aging Dis.* 10, 49–61. doi: 10.14336/ad.2018.0318

Gandhi, S., and Abramov, A. Y. (2012). Mechanism of oxidative stress in neurodegeneration. *Oxid. Med. Cell. Longev.* 2012:428010. doi: 10.1155/2012/428010

Grundke-Iqbal, I., Iqbal, K., Tung, Y.-C., Quinlan, M., Wisniewski, H. M., and Binder, L. I. (1986). Abnormal phosphorylation of the microtubule-associated protein tau (tau) in Alzheimer cytoskeletal pathology. *Proc. Natl. Acad. Sci. U S A* 83, 4913–4917. doi: 10.1073/pnas.83.13.4913

Hansson, O., Zetterberg, H., Buchhave, P., Londos, E., Blennow, K., and Minthon, L. (2006). Association between CSF biomarkers and incipient Alzheimer's disease in patients with mild cognitive impairment: a follow-up study. *Lancet Neurol.* 5, 228–234. doi: 10.1016/S1474-4422(06)70355-6

Huang, Y., Wu, Z., Cao, Y., Lang, M., Lu, B., and Zhou, B. (2014). Zinc binding directly regulates tau toxicity independent of tau hyperphosphorylation. *Cell Rep.* 8, 831–842. doi: 10.1016/j.celrep.2014.06.047

Iadecola, C. (2003). Cerebrovascular effects of amyloid-ßpeptides: mechanisms and implications for Alzheimer's dementia. *Cell. Mol. Neurobiol.* 23, 681–689. doi: 10.1023/a:1025092617651

Iqbal, G., Zada, W., Mannan, A., and Ahmed, T. (2018). Elevated heavy metals levels in cognitively impaired patients from Pakistan. *Environ. Toxicol. Pharmacol.* 60, 100–109. doi: 10.1016/j.etap.2018.04.011

Jia, X., Wang, Z., Yang, T., Li, Y., Gao, S., Wu, G., et al. (2019). Entorhinal cortex atrophy in early, drug-naive Parkinson's disease with mild cognitive impairment. *Aging Dis.* 10, 1221–1232. doi: 10.14336/AD.2018.1116

Kim, A. C., Lim, S., and Kim, Y. K. (2018). Metal ion effects on Aβ and tau aggregation. *Int. J. Mol. Sci.* 19:128. doi: 10.3390/ijms19010128

Kojro, E., Gimpl, G., Lammich, S., März, W., and Fahrenholz, F. (2001). Low cholesterol stimulates the nonamyloidogenic pathway by its effect on the α-secretase ADAM 10. *Proc. Natl. Acad. Sci. U S A* 98, 5815–5820. doi: 10.1073/pnas.081612998

Koudinov, A. R., Berezov, T. T., Kumar, A., and Koudinova, N. V. (1998). Alzheimer's amyloid β interaction with normal human plasma high density lipoprotein: association with apolipoprotein and lipids. *Clin. Chim. Acta* 270, 75–84. doi: 10.1016/s0009-8981(97)00207-6

Kuo, Y.-M., Emmerling, M. R., Bisgaier, C. L., Essenburg, A. D., Lampert, H. C., Drumm, D., et al. (1998). Elevated low-density lipoprotein in Alzheimer's disease correlates with brain Aβ 1–42 levels. *Biochem. Biophys. Res. Commun.* 252, 711–715. doi: 10.1006/bbrc.1998.9652

Liguori, I., Russo, G., Curcio, F., Bulli, G., Aran, L., Della-Morte, D., et al. (2018). Oxidative stress, aging and diseases. *Clin. Interv. Aging* 13, 757–772. doi: 10.2147/CIA.S158513

Liu, Y., Ky Chan, D., Thalamuthu, A., Wen, W., Jiang, J., Paradise, M., et al. (2020). Plasma lipidomic biomarker analysis reveals distinct lipid changes in vascular dementia. *Comput. Struct. Biotechnol. J.* 18, 1613–1624. doi: 10.1016/j.csbj.2020.06.001

Ma, L., and Chan, P. (2020). Understanding the physiological links between physical frailty and cognitive decline. *Aging Dis.* 11, 405–418. doi: 10.14336/ad.2019.0521

Ma, Q., Li, Y., Du, J., Liu, H., Kanazawa, K., Nemoto, T., et al. (2006). Copper binding properties of a tau peptide associated with Alzheimer's disease studied by CD, NMR and MALDI-TOF MS. *Peptides* 27, 841–849. doi: 10.1016/j.peptides.2005.09.002

Mandelkow, E.-M., and Mandelkow, E. (1998). Tau in Alzheimer's disease. *Trends Cell Biol.* 8, 425–427. doi: 10.1016/s0962-8924(98)01368-3

Mantyh, P. W., Ghilardi, J. R., Rogers, S., DeMaster, E., Allen, C. J., Stimson, E. R., et al. (1993). Aluminum, iron and zinc ions promote aggregation of physiological concentrations of β-amyloid peptide. *J. Neurochem.* 61, 1171–1174. doi: 10.1111/j.1471-4159.1993.tb03639.x

Mapstone, M., Cheema, A. K., Fiandaca, M. S., Zhong, X., Mhyre, T. R., MacArthur, L. H., et al. (2014). Plasma phospholipids identify antecedent memory impairment in older adults. *Nature Medicine* 20, 415–418. doi: 10.1038/nm.3466

Mattsson, N., Zetterberg, H., Hansson, O., Andreasen, N., Parnetti, L., Jonsson, M., et al. (2009). CSF biomarkers and incipient Alzheimer disease in patients with mild cognitive impairment. *JAMA* 302, 385–393. doi: 10.1001/jama.2009.1064

McGeer, E. G., and McGeer, P. L. (1998). The importance of inflammatory mechanisms in Alzheimer disease. *Exp. Gerontol.* 33, 371–378. doi: 10.1016/s0531-5565(98)00013-8

Miao, H., Yang, Y., Wang, H., Huo, L., Wang, M., Zhou, Y., et al. (2019). Intensive lipid-lowering therapy ameliorates asymptomatic intracranial atherosclerosis. *Aging Dis.* 10, 258–266. doi: 10.14336/ad.2018.0526

Mizoi, M., Yoshida, M., Saiki, R., Waragai, M., Uemura, K., Akatsu, H., et al. (2014). Distinction between mild cognitive impairment and Alzheimer's disease by CSF amyloid β40 and β42 and protein-conjugated acrolein. *Clin. Chim. Acta* 430, 150–155. doi: 10.1016/j.cca.2014.01.007

Monge-Argilés, J., Sanchez-Paya, J., Munoz-Ruiz, C., Pampliega-Perez, A., Montoya-Gutierrez, J., and Leiva-Santana, C. (2010). Biomarkers in the cerebrospinal fluid of patients with mild cognitive impairment: a meta-analysis of their predictive capacity for the diagnosis of Alzheimer's disease. *Rev. Neurol.* 50, 193–200. doi: 10.33588/rn.5004.2009163

Moroney, J. T., Tang, M.-X., Berglund, L., Small, S., Merchant, C., Bell, K., et al. (1999). Low-density lipoprotein cholesterol and the risk of dementia with stroke. *JAMA* 282, 254–260. doi: 10.1001/jama.282.3.254

Nardes, F., Araújo, A. P. Q. C., Ribeiro, M. G., Bittar, M., and Gomes, H. F. (2020). The mini-mental state examination (MMSE) as a cognitive screening tool in duchenne muscular dystrophy. *Ann. Child Neurol.* 28, 57–65. doi: 10.26815/acn.2020.00052

Notkola, I. L., Sulkava, R., Pekkanen, J., Erkinjuntti, T., Ehnholm, C., Kivinen, P., et al. (1998). Serum total cholesterol, apolipoprotein E FC12e4 allele and Alzheimer's disease. *Neuroepidemiology* 17, 14–20. doi: 10.1159/000026149

Olesen, O. F., and Dagø, L. (2000). High density lipoprotein inhibits assembly of amyloid β-peptides into fibrils. *Biochem. Biophys. Res. Commun.* 270, 62–66. doi: 10.1006/bbrc.2000.2372

Olsson, B., Lautner, R., Andreasson, U., Öhrfelt, A., Portelius, E., Bjerke, M., et al. (2016). CSF and blood biomarkers for the diagnosis of Alzheimer's disease: a systematic review and meta-analysis. *Lancet Neurol.* 15, 673–684. doi: 10.1016/S1474-4422(16)00070-3

Peng, F., Xie, F., and Muzik, O. (2018). Alteration of copper fluxes in brain aging: a longitudinal study in rodent using 64CuCl2-PET/CT. *Aging Dis.* 9, 109–118. doi: 10.14336/ad.2017.1025

Petersen, M. E., and O'Bryant, S. E. (2019). Blood-based biomarkers for Down syndrome and Alzheimer's disease: a systematic review. *Dev. Neurobiol.* 79, 699–710. doi: 10.1002/dneu.22714

Postiglione, A., Cortese, C., Fischetti, A., Cicerano, U., Gnasso, A., Gallotta, G., et al. (1989). Plasma lipids and geriatric assessment in a very aged population of south Italy. *Atherosclerosis* 80, 63–68. doi: 10.1016/0021-9150(89)90069-5

Quan, W., Zhang, Z., Li, P., Tian, Q., Huang, J., Qian, Y., et al. (2019). Role of regulatory T cells in atorvastatin induced absorption of chronic subdural hematoma in rats. *Aging Dis.* 10, 992–1002. doi: 10.14336/ad.2018.0926

Raz, N., and Daugherty, A. M. (2018). Pathways to brain aging and their modifiers: free-radical-induced energetic and neural decline in senescence (FRIENDS) model - a mini-review. *Gerontology* 64, 49–57. doi: 10.1159/000479508

Raz, N., and Rodrigue, K. M. (2006). Differential aging of the brain: patterns, cognitive correlates and modifiers. *Neurosci. Biobehav. Rev.* 30, 730–748. doi: 10.1016/j.neubiorev.2006.07.001

Raz, N., Rodrigue, K. M., Head, D., Kennedy, K. M., and Acker, J. D. (2004). Differential aging of the medial temporal lobe. *Neurology* 62, 433–438. doi: 10.1212/01.wnl.0000106466.09835.46

Razay, G., Vreugdenhil, A., and Wilcock, G. (2007). The metabolic syndrome and Alzheimer disease. *Arch. Neurol.* 64, 93–96. doi: 10.1001/archneur.64.1.93

Ritchie, C., Smailagic, N., Noel-Storr, A. H., Takwoingi, Y., Flicker, L., Mason, S. E., et al. (2014). Plasma and cerebrospinal fluid amyloid beta for the diagnosis of Alzheimer's disease dementia and other dementias in people with mild cognitive impairment (MCI). *Cochrane Database Syst. Rev.* 6:CD008782. doi: 10.1002/14651858.cd008782.pub4

Ritchie, C., Smailagic, N., Noel-Storr, A. H., Ukoumunne, O., Ladds, E. C., and Martin, S. (2017). CSF tau and the CSF tau/Aβ ratio for the diagnosis of Alzheimer's disease dementia and other dementias in people with mild cognitive impairment (MCI). *Cochrane Database Syst. Rev.* 3:CD010803. doi: 10.1002/14651858.cd010803.pub2

Ruiz, A., Pesini, P., Espinosa, A., Pérez-Grijalba, V., Valero, S., Sotolongo-Grau, O., et al. (2013). Blood amyloid beta levels in healthy, mild cognitive impairment and Alzheimer's disease individuals: replication of diastolic blood pressure correlations and analysis of critical Covariates. *PLoS One* 8:e81334. doi: 10.1371/journal.pone.0081334

Sacco, R. L., Benson, R. T., Kargman, D. E., Boden-Albala, B., Tuck, C., Lin, I.-F., et al. (2001). High-density lipoprotein cholesterol and ischemic stroke in the elderly: the Northern Manhattan Stroke Study. *JAMA* 285, 2729–2735. doi: 10.1001/jama.285.21.2729

Segatto, M., Leboffe, L., Trapani, L., and Pallottini, V. (2014). Cholesterol homeostasis failure in the brain: implications for synaptic dysfunction and cognitive decline. *Curr. Med. Chem.* 21, 2788–2802. doi: 10.2174/0929867321666140303142902

Selkoe, D. J. (1994). Normal and abnormal biology of the beta-amyloid precursor protein. *Annu. Rev. Neurosci.* 17, 489–517. doi: 10.1146/annurev.ne.17.030194.002421

Shakour, N., Bianconi, V., Pirro, M., Barreto, G. E., Hadizadeh, F., and Sahebkar, A. (2019). *In silico* evidence of direct interaction between statins and β-amyloid. *J. Cell. Biochem.* 120, 4710–4715. doi: 10.1002/jcb.27761

Shetty, A. K., Upadhya, R., Madhu, L. N., and Kodali, M. (2019). Novel insights on systemic and brain aging, stroke, amyotrophic lateral sclerosis, and Alzheimer's disease. *Aging Dis.* 10, 470–482. doi: 10.14336/ad.2019.0330

Singh, A., Kukreti, R., Saso, L., and Kukreti, S. (2019). Oxidative stress: a key modulator in neurodegenerative diseases. *Molecules* 24:1583. doi: 10.3390/molecules24081583

Smith, D. P., Smith, D. G., Curtain, C. C., Boas, J. F., Pilbrow, J. R., Ciccotosto, G. D., et al. (2006). Copper-mediated amyloid-β toxicity is associated with an intermolecular histidine bridge. *J. Biol. Chem.* 281, 15145–15154. doi: 10.1074/jbc.M600417200

Song, F., Poljak, A., Valenzuela, M., Mayeux, R., Smythe, G. A., and Sachdev, P. S. (2011). Meta-analysis of plasma amyloid-β levels in Alzheimer's disease. *J. Alzheimers Dis.* 26, 365–375. doi: 10.3233/JAD-2011-101977

Sparks, D. L., Scheff, S. W., Hunsaker, J. C. III., Liu, H., Landers, T., and Gross, D. R. (1994). Induction of Alzheimer-like β-amyloid immunoreactivity in the brains of rabbits with dietary cholesterol. *Exp. Neurol.* 126, 88–94. doi: 10.1006/exnr.1994.1044

Streit, W., and Sparks, D. L. (1997). Activation of microglia in the brains of humans with heart disease and hypercholesterolemic rabbits. *J. Mol. Med.* 75, 130–138. doi: 10.1007/s001090050097

Tang, W., Wang, Y., Cheng, J., Yao, J., Yao, Y.-Y., Zhou, Q., et al. (2020). CSF sAPPα and sAPPβ levels in Alzheimer's disease and multiple other neurodegenerative diseases: a network meta-analysis. *Neuromolecular Med.* 22, 45–55. doi: 10.1007/s12017-019-08561-7

Tong, Y., Yang, H., Tian, X., Wang, H., Zhou, T., Zhang, S., et al. (2014). High manganese, a risk for Alzheimer's disease: high manganese induces amyloid-β related cognitive impairment. *J. Alzheimers Dis.* 42, 865–878. doi: 10.3233/jad-140534

Vos, S. J. B., van Rossum, I. A., Verhey, F., Knol, D. L., Soininen, H. and Wahlund, L.-O.. (2013). Prediction of Alzheimer Disease in subjects with amnestic and nonamnestic MCI. *Neurology* 80, 1124–1132. doi: 10.1212/WNL.0b013e318288690c

Wang, Y.-J., Zhou, H.-D., and Zhou, X.-F. (2006). Clearance of amyloid-beta in Alzheimer's disease: progress, problems and perspectives. *Drug Discov. Today* 11, 931–938. doi: 10.1016/j.drudis.2006.08.004

Weng, R., Wei, X., Yu, B., Zhu, S., Yang, X., Xie, F., et al. (2018). Combined measurement of plasma cystatin C and low-density lipoprotein cholesterol: a valuable tool for evaluating progressive supranuclear palsy. *Parkinsonism Relat. Disord.* 52, 37–42. doi: 10.1016/j.parkreldis.2018.03.014

Wieringa, G. E., Burlinson, S., Rafferty, J. A., Gowland, E., and Burns, A. (1997). Apolipoprotein E genotypes and serum lipid levels in Alzheimer's disease and multi-infarct dementia. *Int. J. Geriatr. Psychiatry* 12, 359–362. doi: 10.1002/(sici)1099-1166(199703)12:3<359::aid-gps506>3.0.co;2-x

Xicoy, H., Wieringa, B., and Martens, G. J. (2019). The role of lipids in Parkinson's disease. *Cells* 8:27. doi: 10.3390/cells8010027

Xie, F., Gao, X., Yang, W., Chang, Z., Yang, X., Wei, X., et al. (2018). Advances in the research of risk factors and prodromal biomarkers of Parkinson's disease. *ACS Chem. Neurosci.* 10, 973–990. doi: 10.1021/acschemneuro.8b00520

Yang, Q., Huang, Z., Luo, Y., Zheng, F., Hu, Y., Liu, H., et al. (2019). Inhibition of Nwd1 activity attenuates neuronal hyperexcitability and GluN2B phosphorylation in the hippocampus. *EBioMedicine* 47, 470–483. doi: 10.1016/j.ebiom.2019.08.050

Yang, W., Chang, Z., Que, R., Weng, G., Deng, B., Wang, T., et al. (2020). Contra-directional expression of plasma superoxide dismutase with lipoprotein cholesterol and high-sensitivity c-reactive protein as important markers of Parkinson's disease severity. *Front. Aging Neurosci.* 12:53. doi: 10.3389/fnagi.2020.00053

Zanchetti, A., Liu, L., Mancia, G., Parati, G., Grassi, G., Stramba-Badiale, M., et al. (2014). Blood pressure and low-density lipoprotein-cholesterol lowering for prevention of strokes and cognitive decline: a review of available trial evidence. *J. Hypertens.* 32, 1741–1750. doi: 10.1097/HJH.0000000000000253

Zetterberg, H., Wilson, D., Andreasson, U., Minthon, L., Blennow, K., Randall, J., et al. (2013). Plasma tau levels in Alzheimer's disease. *Alzheimers Res. Ther.* 5:9. doi: 10.1186/alzrt163

Zhang, J., Cai, T., Zhao, F., Yao, T., Chen, Y., Liu, X., et al. (2012). The role of α-synuclein and tau hyperphosphorylation-mediated autophagy and apoptosis in lead-induced learning and memory injury. *Int. J. Biol. Sci.* 8, 935–944. doi: 10.7150/ijbs.4499

Zhu, S., Wei, X., Yang, X., Huang, Z., Chang, Z., Xie, F., et al. (2019). Plasma lipoprotein-associated phospholipase A2 and superoxide dismutase are independent predicators of cognitive impairment in cerebral small vessel disease patients: diagnosis and assessment. *Aging Dis.* 10, 834–846. doi: 10.14336/AD.2019.0304

Zou, J., Chen, Z., Liang, C., Fu, Y., Wei, X., Lu, J., et al. (2018). Trefoil factor 3, cholinesterase and homocysteine: potential predictors for Parkinson's disease dementia and vascular parkinsonism dementia in advanced stage. *Aging Dis.* 9, 51–65. doi: 10.14336/ad.2017.0416

Conflict of Interest: The authors declare that the research was conducted in the absence of any commercial or financial relationships that could be construed as a potential conflict of interest.

frontiers in Aging Neuroscience

MINI REVIEW
published: 27 July 2020
doi: 10.3389/fnagi.2020.00231

Early Detection and Prevention of Alzheimer's Disease: Role of Oxidative Markers and Natural Antioxidants

Jamshed Arslan[1]*, *Humaira Jamshed*[2] and *Humaira Qureshi*[2]

[1]Department of Basic Medical Sciences, Faculty of Pharmacy, Barrett Hodgson University, Karachi, Pakistan, [2]Department of Integrated Sciences and Mathematics, Dhanani School of Science and Engineering, Habib University, Karachi, Pakistan

Oxidative stress (OS) contributes to Alzheimer's disease (AD) pathology. OS can be a result of increased reactive oxygen/nitrogen species, reduced antioxidants, oxidatively damaged molecules, and/or a combination of these factors. Scientific literature is scarce for the markers of OS-specific for detecting AD at an early stage. The first aim of the current review is to provide an overview of the potential OS markers in the brain, cerebrospinal fluid (CSF), blood and/or urine that can be used for early diagnosis of human AD. The reason for exploring OS markers is that the proposed antioxidant therapies against AD appear to start too late to be effective. The second aim is to evaluate the evidence for natural antioxidants currently proposed to prevent or treat AD symptoms. To address these two aims, we critically evaluated the studies on humans in which various OS markers for detecting AD at an early stage were presented. Non-invasive OS markers that can detect mild cognitive impairment (MCI) and AD at an early stage in humans with greater specificity and sensitivity are primarily related to lipid peroxidation. However, a combination of OS markers, family history, and other biochemical tests are needed to detect the disease early on. We also report that the long-term use of vitamins (vitamin E as in almonds) and polyphenol-rich foods (curcumin/curcuminoids of turmeric, ginkgo biloba, epigallocatechin-3-gallate in green tea) seem justified for ameliorating AD symptoms. Future research on humans is warranted to justify the use of natural antioxidants.

Keywords: reactive oxygen species, mild cognitive impairment, lipid peroxidation, tocopherols, polyphenols

OPEN ACCESS

Edited by:
Nady Braidy,
University of New South Wales, Australia

Reviewed by:
Amandine Grimm,
University of Basel, Switzerland
Antonina Luca,
University of Catania, Italy

***Correspondence:**
Jamshed Arslan
jamshed.arslan@bhu.edu.pk;
jamshed.arslan@gmail.com

Received: *01 April 2020*
Accepted: *01 July 2020*
Published: *27 July 2020*

Citation:
Arslan J, Jamshed H and Qureshi H (2020) Early Detection and Prevention of Alzheimer's Disease: Role of Oxidative Markers and Natural Antioxidants. Front. Aging Neurosci. 12:231. doi: 10.3389/fnagi.2020.00231

INTRODUCTION

Alzheimer's disease (AD) is the most common dementia of the elderly (Fattoretti et al., 2018). The discovery that memory decline often precedes other neuropathological signs of AD (Thomas et al., 2020) has ignited an interest in the pathology of AD, especially the translational state between normal aging and AD called mild cognitive impairment (MCI). Oxidative stress (OS) underlies MCI (Cervellati et al., 2014a; Di Domenico et al., 2016) and neurodegenerative diseases including AD (Dong et al., 2018). Various antioxidants have been suggested to prevent or even cure AD (Boasquivis et al., 2018; Mohamed et al., 2018; Popli et al., 2018). Major biomarkers of oxidative

damage in AD have been identified (Smith et al., 1997; Nourooz-Zadeh et al., 1999; Lauderback et al., 2001; Halliwell, 2006; Dizdaroglu et al., 2015; Milne et al., 2015; Wang et al., 2015; Di Domenico et al., 2016, 2017; Dai et al., 2018; Ishii et al., 2018), but only a limited data on the usefulness of these biomarkers in the early detection of AD is available (Garcia-Blanco et al., 2017). Several antioxidants have been proposed for ameliorating oxidative damage in humans and non-human models of AD (Butterfield and Halliwell, 2019). Among these, some are preventive while others are touted to have a curative effect in AD. A discussion on the rigor of the evidence favoring the purported antioxidants in preventing or treating human AD is scarce.

Therefore, our objective is to highlight potential oxidative markers that can be used for early diagnosis of human AD and to evaluate the evidence for the natural antioxidants currently proposed to prevent or treat AD in humans. Primary research on OS and antioxidants in the context of human MCI and/or AD was analyzed. The studies on early detection of AD, preclinical AD, or MCI in humans in terms of oxidative damage and the research on antioxidants useful in these conditions were selected for review. It should be noted that the animal studies, the discussion on effects of any non-dietary intervention like exercise on MCI/AD (Suridjan et al., 2017), trials on synthetic compounds with antioxidant anti-AD potential like statins (Chu et al., 2018), data on novel or synthetic antioxidant supplements for AD (Tadokoro et al., 2020), OS-biometal association in MCI/AD (Balmus et al., 2017), and studies on patients with comorbidities (Zheng et al., 2016) were deemed outside the scope of this article.

OXIDATIVE STRESS MARKERS FOR EARLY DETECTION OF AD

Studies have reported various products derived from proteins, lipids, DNA, or RNA that indicate OS in the brain. For example, OS damage to the protein can be determined by measuring 3-nitrotyrosine, protein carbonyls, methionine sulfoxide or highly reactive aldehydes; lipid damage by determining isoprostanes and lipid and cyclic peroxides; DNA damage by estimating 8-hydroxy-deoxyguanosine (8OHdG); and RNA damage has been determined by measuring 8-hydroxyguanine (8OHG; Butterfield and Halliwell, 2019).

Oxidative Damage to Proteins

Elevated levels of protein carbonyls and 3-nitrotyrosine in the MCI lymphocyte mitochondria (Sultana et al., 2013) and in the frontal cortex (Ansari and Scheff, 2010) and hippocampus of MCI and AD (Scheff et al., 2016) indicate that OS damage to proteins is an early sign of AD. Oxidative inactivation of several proteins in the hippocampus leads to the progression of AD from MCI (Butterfield et al., 2006a). The oxidatively modified proteins in the cerebrospinal fluid (CSF) of MCI, as determined by redox proteomics, remain oxidized in the disease progression to AD (Di Domenico et al., 2016). Both MCI and AD patients show increased plasma levels of advanced oxidation protein products (Chico et al., 2013). Increased carbonyl groups content in the plasma of early AD subjects have been reported (Puertas et al., 2012). Carbonyl proteins in the plasma can be roughly three times higher in MCI/AD relative to the age-matched healthy controls (Greilberger et al., 2010; **Table 1**).

The specificity of plasma carbonyl proteins is still questionable since one cannot differentiate between AD and other dementias like vascular dementia based on carbonyl proteins alone (Polidori et al., 2004). Likewise, caloric restriction itself reduces oxidative damage to the brain proteins, measured by protein carbonyl levels (Forster et al., 2000). Further investigations are warranted that record patient's dietary habits whilst evaluating the link between plasma carbonyl proteins and early AD.

Role of Lipid Peroxidation

The plasma, CSF, and urine of MCI subjects exhibit higher levels of isoprostane 8,12-iso-iPF(2alpha)-VI, a marker of *in vivo* lipid peroxidation, as compared to cognitively normal elderly controls (Pratico et al., 2002). Plasma and whole blood levels of thiobarbituric acid reactive substances, an index of lipid peroxidation, are likewise high in early AD (Puertas et al., 2012; Martinez de Toda et al., 2019). Lipid hydroperoxides are the unstable products of lipid peroxidation that undergo non-enzymatic decomposition to generate aldehydes like malondialdehyde (MDA) and 4-hydroxynonenal (4-HNE); latter form covalent adducts to alter physiological proteins. High serum hydroperoxide levels are associated with MCI and AD (Cervellati et al., 2013, 2014a). The OS detected in the serum (high hydroperoxides with low residual antioxidant power) is more pronounced in MCI and AD as compared to vascular dementia (Cervellati et al., 2014b; **Table 1**), highlighting the specificity of certain lipid peroxidation outcomes in early detection of AD.

Elevated levels of MDA and 4-HNE have been reported in the brains of subjects with MCI or early AD (Keller et al., 2005; Butterfield et al., 2006b; Greilberger et al., 2008; Reed et al., 2008; Lopez et al., 2013; Scheff et al., 2016). Mitochondria isolated from MCI lymphocytes show increased levels of HNE-bound proteins (Sultana et al., 2013). Plasma production of MDA shows a gradation: AD > MCI > healthy controls (Torres et al., 2011) and blood MDA levels have been correlated with the progression of MCI into AD (Baldeiras et al., 2010; **Table 1**). It should be noted that covalent adducts of 4-HNE are elevated in the brain and body fluids of other neurodegenerative diseases as well including Parkinson's disease and amyotrophic lateral sclerosis (Di Domenico et al., 2017), necessitating future research on the patterns of MDA and 4-HNE that could distinguish AD from other dementias and neurodegenerative diseases.

The level of F2-isoprostanes, indicating lipid peroxidation, is enhanced in the brain and CSF of MCI and AD patients, but plasma and urinary isoprostanes are normal in AD (Markesbery et al., 2005; Irizarry et al., 2007). A prospective population-based study failed to confirm the association between systemic isoprostanes and the risk of AD (Sundelöf et al., 2009). Despite being touted as "gold standard" biomarker of lipid peroxidation (Butterfield and Halliwell, 2019), the diagnostic

TABLE 1 | Oxidative markers for early detection of Alzheimer's disease.

Author, year	Groups	Sample	Key result
Ansari and Scheff (2010)	HC = (*n* = 10) MCI (*n* = 8) Mild-to-moderate AD (*n* = 4) Late-stage AD (*n* = 9).	Brain tissue	Elevated levels of protein carbonyls and 3-nitrotyrosine in the frontal cortex of MCI and AD in a disease-dependent manner.
Arce-Varas et al. (2017)	HC (*n* = 44) MCI (*n* = 43) AD (*n* = 53)	Plasma and peripheral mononuclear cells	Decreased SOD is observed in MCI and AD, pointing to the importance of considering extracellular and intracellular blood compartments in evaluating oxidative stress
Baldeiras et al. (2010)	MCI (*n* = 70)	Serum	MDA levels have been correlated with the progression of MCI into AD
Cervellati et al. (2013)	HC (*n* = 99) MCI (*n* = 134) AD (*n* = 101)	Serum	High hydroperoxides levels associated with MCI and AD
Cervellati et al. (2014a)	HC (*n* = 118) MCI (*n* = 111) AD (*n* = 105)	Serum	High hydroperoxide levels associated with MCI and AD. Antioxidant capacity in AD and MCI is lower than that of HC
Cervellati et al. (2014b)	HC (*n* = 48) MCI (*n* = 103) AD (*n* = 89)	Serum	High hydroperoxides with low residual antioxidant capacity are more pronounced in MCI and AD as compared to HC.
Chico et al. (2013)	HC (*n* = 63) MCI (*n* = 34) AD (*n* = 85)	Plasma	Both MCI and AD patients have increased levels of advanced oxidation protein products. APOE4 carriers MCI have reduced plasma SOD activity relative to non-APOE4 carriers. Plasma reducing capacity AD < MCI < HC
Di Domenico et al. (2016)	HC (*n* = 6) MCI (*n* = 6) AD (*n* = 6)	CSF	Oxidatively modified proteins in the CSF of MCI remain oxidized in disease progression to AD
Du et al. (2019)	HC (*n* = 832) MCI (*n* = 113)	Serum	IMA is a potential biomarker for oxidative stress in MCI
Greilberger et al. (2010)	HC (*n* = 15) MCI (*n* = 6) AD (*n* = 10)	Plasma	Carbonyl proteins in plasma can be roughly three times higher in MCI/AD relative to HC.
Lopez et al. (2013)	HC (*n* = 33) MCI (*n* = 18) AD (*n* = 36)	Blood	MDA levels MCI > HC SOD activity AD < HC
Mangialasche et al. (2013)	HC (*n* = 86) MCI (*n* = 86) AD (*n* = 81)	Serum	Higher levels of gamma-tocopherol, beta-tocotrienol, total tocotrienols, and gamma-tocopherol/cholesterol ratio are associated with a lower risk of MCI or AD in the older adults
Martinez de Toda et al. (2019)	HC (*n* = 30) MCI (*n* = 20) AD (*n* = 20)	Blood	Higher TBARS and lower glutathione peroxidase and reductase activities in both sexes can be a marker for prodromal AD
Nunomura et al. (2012)	HC (*n* = 5) MCI (*n* = 6) AD (*n* = 5)	Brain tissue	Oxidized RNA nucleoside 8OHG in the neurons of the cerebral cortex is an age-associated phenomenon, but a more prominent RNA damage correlates with MCI and AD
Picco et al. (2014)	HC (*n* = 23) MCI (*n* = 28) AD (*n* = 34)	Brain and plasma	SOD activity and brain glucose metabolism AD < MCI < HC
Puertas et al. (2012)	HC (*n* = 46) MCI (*n* = 46)	Plasma	Carbonyl groups content, thiobarbituric acid reactive substances (index of lipid peroxidation) MCI > HC Plasma glutathione levels and antioxidant enzymes such as glutathione peroxidase, catalase, and superoxide dismutase (SOD) HC > MCI
Rita Cardoso et al. (2014)	HC (*n* = 29) MCI (*n* = 31) AD (*n* = 28)	Red blood cells and plasma	Antioxidant selenium levels HC > MCI > AD
Scheff et al. (2016)	HC (*n* = 48) MCI (*n* = 15)	Brain	Increased protein carbonyls, 4-hydroxynonenal and 3-nitrotyrosine in hippocampus enhances the likelihood of AD-like pathology
Sultana et al. (2013)	HC (*n* = 10) MCI (*n* = 12)	Blood	Elevated levels of protein carbonyls and 3-nitrotyrosine, and 4-hydroxy-2-nonenal-bound proteins in MCI lymphocyte mitochondria relative to HC
Torres et al. (2011)	HC (*n* = 26) MCI (*n* = 33) AD (*n* = 29)	Red blood cells and plasma	Plasma production of MDA and catalase activity AD > MCI > HC Glutathione reductase/glutathione peroxidase ratio HC > MCI > AD

AD, Alzheimer's disease; APOE4, Apolipoprotein E4; CSF, Cerebrospinal fluid; HC, Healthy control with no cognitive impairment; IMA, Ischemia-modified albumin; MCI, Mild cognitive impairment; MDA, malondialdehyde; 8OHG, 8-hydroxyguanosine; SOD, superoxide dismutase; TBARS, thiobarbituric acid-reactive substances.

use of isoprostanes is tricky because of their non-specificity: isoprostanes have been potential biomarkers for many diseases including obesity, genetic disorders and cancers (Irizarry et al., 2007; Milne et al., 2015).

Oxidative Damage to Nucleic Acids

Nucleic acid damage also occurs early in AD. Significantly elevated levels of 8OHG and 4,6-diamino-5-formamidopyrimidine have been reported in the post-mortem MCI brains relative to the age-matched controls (Wang et al., 2006). Oxidized RNA nucleoside 8OHG in the neurons of the cerebral cortex is an age-associated phenomenon, but a more prominent RNA damage correlates with MCI and AD (Nunomura et al., 2012). Peripheral leukocytes from MCI and AD patients show enhanced oxidative DNA damage including higher amounts of oxidized purines and pyrimidines relative to the healthy controls (Migliore et al., 2005). Certain nuclear (but not mitochondrial) oxidative phosphorylation genes are upregulated in the hippocampus of MCI patients relative to both AD and normal controls (Mastroeni et al., 2017). What pattern of oxidative damage and gene expression can best distinguish AD at an early stage from other dementia is an open question.

Reduced Antioxidant Defenses

In addition to oxidative damage, reduced antioxidant defenses have been reported in MCI and early AD (Rinaldi et al., 2003; Baldeiras et al., 2010; Chico et al., 2013). Plasma glutathione levels and antioxidant enzymes such as glutathione peroxidase, catalase, and superoxide dismutase (SOD) are significantly decreased in early AD (Torres et al., 2011; Puertas et al., 2012). Apolipoprotein E4 (APOE4) is the major genetic risk factor in AD. The E4 carriers MCI exhibit significantly reduced plasma SOD activity relative to non-APOE4 carriers (Chico et al., 2013). Plasma SOD activity follows gradation: healthy controls > MCI > AD (Picco et al., 2014). Decreased SOD has also been reported in blood peripheral mononuclear cells of MCI and AD patients (Arce-Varas et al., 2017; **Table 1**). In other words, reduced antioxidant potential can be detected in both the extracellular and intracellular blood compartments.

Serum analysis of MCI and AD patients have revealed a low residual antioxidant power (Cervellati et al., 2014b). Albumin is considered a major endogenous antioxidant in serum because of its free radical-trapping ability. OS in MCI and AD can increase the serum levels of ischemia-modified albumin (IMA), a form of albumin in which the N-terminal is structurally changed (Du et al., 2019). The levels of selenium, an essential trace element, were found to be lower in both MCI and AD relative to the controls, but plasma selenium was the lowest in the AD group (Rita Cardoso et al., 2014; **Table 1**). Higher serum levels of gamma-tocopherol, beta-tocotrienol, total tocotrienols, and gamma-tocopherol/cholesterol ratio are associated with a lower risk of MCI or AD in the older adults (Mangialasche et al., 2013). Levels of 5-nitro-gamma-tocopherol, a marker of vitamin E damage, show a significant positive correlation with protein carbonyls, protein-conjugated HNE, and protein-bound 3-nitrotyrosine (Sultana et al., 2013) in MCI and AD (**Table 1**).

The limited specificity of OS and antioxidant markers must be kept in view. The serum, urine, or CSF concentrations of these biomolecules are associated with several cardiometabolic conditions (Vona et al., 2019) as well. Therefore, OS markers must always be combined with family history and other imaging techniques to detect AD at early stages.

NATURAL ANTIOXIDANTS FOR ALZHEIMER'S DISEASE PREVENTION AND TREATMENT

Vitamins

Plasma antioxidant defenses are depleted in MCI and AD (Rinaldi et al., 2003). So, antioxidant intake may be a reliable strategy to prevent or even reverse MCI/AD symptoms. In this regard, vitamin E (tocopherols/tocotrienols) and vitamin C (ascorbate) is considered the scavenging and chain-breaking molecules called direct antioxidants (Mecocci and Polidori, 2012; Polidori and Nelles, 2014). Dietary vitamin E can dictate OS outcomes (Dong et al., 2018). Although vitamin E supplementation cannot stop the progression from MCI to AD, it does delay the onset of AD symptoms (Dysken et al., 2014). Combining vitamin E with vitamin C is better at decreasing F2-isoprostane in the CSF in mild-to-moderate AD than the vitamin E alone (Galasko et al., 2012). The therapeutic importance of the latter observation is yet to be explored.

The risk of AD appears to be decreased in elderly subjects with high plasma levels of vitamin E (tocopherols and tocotrienols; Mecocci and Polidori, 2012; Polidori and Nelles, 2014), but this could be due to a good overall diet rather than vitamin E alone. Almond supplementation on an empty stomach has been found to enhanced memory in animal models of AD (Arslan et al., 2017; Batool et al., 2018). This can partly be explained by high amounts of antioxidants like vitamin E and selenium in almonds (Yada et al., 2011; Arslan et al., 2017). However, a clinical study reported that supplementation with vitamin E and selenium does not ameliorate human dementia (Kryscio et al., 2017). The result of this underpowered study (Kryscio et al., 2017) can be explained by the inclusion of only one gender (men), high loss to follow-up, and short exposure time.

Polyphenols

Polyphenolic agents, such as curcuminoids found in turmeric, work through multiple pathways and have shown improvements in AD symptoms in animal models (Ahmed and Gilani, 2009, 2014; Ahmed et al., 2014; Khalid et al., 2017), but results of human trials are conflicting (Chen et al., 2018). Gingko Biloba extract contains antioxidant flavonoids among other chemicals. Meta-analyses of human studies have shown promise in AD (Wang et al., 2010; Hashiguchi et al., 2015), but the results of Gingko biloba are far from conclusive (Vellas et al., 2012; Hashiguchi et al., 2015). Like curcumin, the neuroprotection by flavonoid-rich foods may not entirely be due to antioxidant effects since only a limited amount enters the brain. The additional mechanism behind neuroprotection includes flavonoid-induced improvement in brain vascular function (Schaffer and Halliwell, 2012).

Catechins flavonoids are considered the active, therapeutic components of green tea. The ester of epigallocatechin and gallic acid called epigallocatechin-3-gallate (EGCG) is the main bioactive polyphenol in green tea extract that has neuroprotective effects partly owing to its antioxidant activities (Mandel et al., 2011; Mori et al., 2019). Green tea consumption seems to improve cognitive performance in the healthy (Kuriyama et al., 2006) as well as cognitively challenged elderly (Ide et al., 2014). However, the results of a long-term clinical trial of EGCG in the early stages of AD are yet to be published (ClinicalTrials.gov Identifier: NCT00951834). The EGCG dose and frequency needed for AD prevention and/or reversal must be explored further.

Other natural antioxidants tested extensively in animal models but only limitedly in humans for AD include: resveratrol, a polyphenol in grapes and red wine (Rege et al., 2014; Turner et al., 2015); blueberry extract (Papandreou et al., 2009); tannic acid (Mori et al., 2012); and lipoic acid (Siedlak et al., 2009).

CONCLUSION

Biomolecules predicting oxidative damage before the onset of clinical systems in AD can help in the diagnosis of this dreaded neurodegenerative disease. AD cannot be detected at an early stage based on oxidative markers alone because of the limited sensitivity and specificity of available options. Among the non-invasive choices, lipid peroxidation (high serum peroxides) holds the most promise in the early detection of AD. It is unlikely, however, that a single non-invasive and cheap biomarker could detect AD at early stages. AD is a complex disease involving multiple pathways. OS is a part of normal aging, but a high OS can be one of the earliest signs of AD. The antioxidants offered to tackle oxidative damage in AD have limited efficacy partly because of the dose, duration, unbalanced monotherapy, and the presence of blood-brain-barrier that does not allow liberal amounts of antioxidants to enter the brain. By the time antioxidants are prescribed in humans, it is already too late. So, a balanced diet and lifestyle modifications can be the only long-term solution to prevent or reverse cognitive impairments associated with the heterogeneous disease that we call AD.

AUTHOR CONTRIBUTIONS

JA conceived the idea and wrote the first draft of the manuscript with equal inputs from HJ and HQ.

FUNDING

The article processing charges were generously provided by Habib University, Karachi, Pakistan.

REFERENCES

Ahmed, E. M., EL-Maraghy, S. A., Teleb, Z. A., and Shaheen, A. A. (2014). Pretreatment with turmeric modulates the inhibitory influence of cisplatin and paclitaxel on CYP2E1 and CYP3A1/2 in isolated rat hepatic microsomes. *Chem. Biol. Interact.* 220, 25–32. doi: 10.1016/j.cbi.2014.05.007

Ahmed, T., and Gilani, A. H. (2009). Inhibitory effect of curcuminoids on acetylcholinesterase activity and attenuation of scopolamine-induced amnesia may explain medicinal use of turmeric in Alzheimer's disease. *Pharmacol. Biochem. Behav.* 91, 554–559. doi: 10.1016/j.pbb.2008.09.010

Ahmed, T., and Gilani, A. H. (2014). Therapeutic potential of turmeric in Alzheimer's disease: curcumin or curcuminoids? *Phytother. Res.* 28, 517–525. doi: 10.1002/ptr.5030

Ansari, M. A., and Scheff, S. W. (2010). Oxidative stress in the progression of Alzheimer disease in the frontal cortex. *J. Neuropathol. Exp. Neurol.* 69, 155–167. doi: 10.1097/nen.0b013e3181cb5af4

Arce-Varas, N., Abate, G., Prandelli, C., Martinez, C., Cuetos, F., Menendez, M., et al. (2017). Comparison of extracellular and intracellular blood compartments highlights redox alterations in Alzheimer's and mild cognitive impairment patients. *Curr. Alzheimer Res.* 14, 112–122. doi: 10.2174/1567205013666161010125413

Arslan, J., Ahmed, T., and Gilani, A.-H. (2017). Soaked almonds exhibit vitamin e-dependent memory protective effect in rodent models. *Int. J. Pharmacol.* 13, 448–456. doi: 10.3923/ijp.2017.448.456

Baldeiras, I., Santana, I., Proenca, M. T., Garrucho, M. H., Pascoal, R., Rodrigues, A., et al. (2010). Oxidative damage and progression to Alzheimer's disease in patients with mild cognitive impairment. *J. Alzheimers Dis.* 21, 1165–1177. doi: 10.3233/jad-2010-091723

Balmus, I. M., Strungaru, S. A., Ciobica, A., Nicoara, M. N., Dobrin, R., Plavan, G., et al. (2017). Preliminary data on the interaction between some biometals and oxidative stress status in mild cognitive impairment and Alzheimer's disease patients. *Oxid. Med. Cell. Longev.* 2017:7156928. doi: 10.1155/2017/7156928

Batool, Z., Tabassum, S., Siddiqui, R. A., and Haider, S. (2018). Dietary supplementation of almond prevents oxidative stress by advocating antioxidants and attenuates impaired aversive memory in male rats. *Plant. Foods Hum. Nutr.* 73, 7–12. doi: 10.1007/s11130-018-0655-4

Boasquivis, P. F., Silva, G. M. M., Paiva, F. A., Cavalcanti, R. M., Nunez, C. V., and de Paula Oliveira, R. (2018). Guarana (*Paullinia cupana*) extract protects caenorhabditis elegans models for alzheimer disease and huntington disease through activation of antioxidant and protein degradation pathways. *Oxid. Med. Cell. Longev.* 2018:9241308. doi: 10.1155/2018/9241308

Butterfield, D. A., and Halliwell, B. (2019). Oxidative stress, dysfunctional glucose metabolism and Alzheimer disease. *Nat. Rev. Neurosci.* 20, 148–160. doi: 10.1038/s41583-019-0132-6

Butterfield, D. A., Poon, H. F., St Clair, D., Keller, J. N., Pierce, W. M., Klein, J. B., et al. (2006a). Redox proteomics identification of oxidatively modified hippocampal proteins in mild cognitive impairment: insights into the development of Alzheimer's disease. *Neurobiol. Dis.* 22, 223–232. doi: 10.1016/j.nbd.2005.11.002

Butterfield, D. A., Reed, T., Perluigi, M., De Marco, C., Coccia, R., Cini, C., et al. (2006b). Elevated protein-bound levels of the lipid peroxidation product, 4-hydroxy-2-nonenal, in brain from persons with mild cognitive impairment. *Neurosci. Lett.* 397, 170–173. doi: 10.1016/j.neulet.2005.12.017

Cervellati, C., Cremonini, E., Bosi, C., Magon, S., Zurlo, A., Bergamini, C. M., et al. (2013). Systemic oxidative stress in older patients with mild cognitive impairment or late onset alzheimer's disease. *Curr. Alzheimer Res.* 10, 365–372. doi: 10.2174/1567205011310040003

Cervellati, C., Romani, A., Seripa, D., Cremonini, E., Bosi, C., Magon, S., et al. (2014a). Systemic oxidative stress and conversion to dementia of elderly patients with mild cognitive impairment. *Biomed. Res. Int.* 2014:309507. doi: 10.14257/astl.2014.68.02

Cervellati, C., Romani, A., Seripa, D., Cremonini, E., Bosi, C., Magon, S., et al. (2014b). Oxidative balance, homocysteine and uric acid levels in older patients with Late onset alzheimer's disease or vascular dementia. *J. Neurol. Sci.* 337, 156–161. doi: 10.1016/j.jns.2013.11.041

Chen, M., Du, Z. Y., Zheng, X., Li, D. L., Zhou, R. P., and Zhang, K. (2018). Use of curcumin in diagnosis, prevention and treatment of Alzheimer's disease. *Neural Regen. Res.* 13, 742–752. doi: 10.4103/1673-5374.230303

Chico, L., Simoncini, C., Lo Gerfo, A., Rocchi, A., Petrozzi, L., Carlesi, C., et al. (2013). Oxidative stress and APO E polymorphisms in Alzheimer's disease and in mild cognitive impairment. *Free Radic Res.* 47, 569–576. doi: 10.3109/10715762.2013.804622

Chu, C. S., Tseng, P. T., Stubbs, B., Chen, T. Y., Tang, C. H., Li, D. J., et al. (2018). Use of statins and the risk of dementia and mild cognitive impairment: a systematic review and meta-analysis. *Sci. Rep.* 8:5804. doi: 10.1016/j.jalz.2018.06.690

Dai, D. P., Gan, W., Hayakawa, H., Zhu, J. L., Zhang, X. Q., Hu, G. X., et al. (2018). Transcriptional mutagenesis mediated by 8-oxoG induces translational errors in mammalian cells. *Proc. Natl. Acad. Sci. U S A* 115, 4218–4222. doi: 10.1073/pnas.1718363115

Di Domenico, F., Pupo, G., Giraldo, E., Badìa, M.-C., Monllor, P., Lloret, A., et al. (2016). Oxidative signature of cerebrospinal fluid from mild cognitive impairment and Alzheimer disease patients. *Free Radic. Biol. Med.* 91, 1–9. doi: 10.1016/j.freeradbiomed.2015.12.004

Di Domenico, F., Tramutola, A., and Butterfield, D. A. (2017). Role of 4-hydroxy-2-nonenal (HNE) in the pathogenesis of alzheimer disease and other selected age-related neurodegenerative disorders. *Free Radic. Biol. Med.* 111, 253–261. doi: 10.1016/j.freeradbiomed.2016.10.490

Dizdaroglu, M., Coskun, E., and Jaruga, P. (2015). Measurement of oxidatively induced DNA damage and its repair, by mass spectrometric techniques. *Free Radic Res.* 49, 525–548. doi: 10.3109/10715762.2015.1014814

Dong, S., Huang, X., Zhen, J., Van Halm-Lutterodt, N., Wang, J., Zhou, C., et al. (2018). Dietary vitamin E status dictates oxidative stress outcomes by modulating effects of fish oil supplementation in alzheimer disease model APPswe/PS1dE9 mice. *Mol. Neurobiol.* 55, 9204–9219. doi: 10.1007/s12035-018-1060-6

Du, L., Ma, J., He, D., and Zhang, X. (2019). Serum ischaemia-modified albumin might be a potential biomarker for oxidative stress in amnestic mild cognitive impairment. *Psychogeriatrics* 19, 150–156. doi: 10.1111/psyg.12377

Dysken, M. W., Sano, M., Asthana, S., Vertrees, J. E., Pallaki, M., Llorente, M., et al. (2014). Effect of vitamin E and memantine on functional decline in Alzheimer disease: the TEAM-AD VA cooperative randomized trial. *JAMA* 311, 33–44. doi: 10.1001/jama.2013.282834

Fattoretti, P., Malavolta, M., Fabbietti, P., Papa, R., Giacconi, R., Costarelli, L., et al. (2018). Oxidative stress in elderly with different cognitive status: my mind project. *J. Alzheimers Dis.* 63, 1405–1414. doi: 10.3233/jad-171117

Forster, M. J., Sohal, B. H., and Sohal, R. S. (2000). Reversible effects of long-term caloric restriction on protein oxidative damage. *J. Gerontol. A Biol. Sci. Med. Sci.* 55, B522–529. doi: 10.1093/gerona/55.11.b522

Galasko, D. R., Peskind, E., Clark, C. M., Quinn, J. F., Ringman, J. M., Jicha, G. A., et al. (2012). Antioxidants for Alzheimer disease: a randomized clinical trial with cerebrospinal fluid biomarker measures. *Arch. Neurol.* 69, 836–841. doi: 10.1001/archneurol.2012.85

Garcia-Blanco, A., Baquero, M., Vento, M., Gil, E., Bataller, L., and Chafer-Pericas, C. (2017). Potential oxidative stress biomarkers of mild cognitive impairment due to Alzheimer disease. *J. Neurol. Sci.* 373, 295–302. doi: 10.1016/j.jns.2017.01.020

Greilberger, J., Fuchs, D., Leblhuber, F., Greilberger, M., Wintersteiger, R., and Tafeit, E. (2010). Carbonyl proteins as a clinical marker in Alzheimer's disease and its relation to tryptophan degradation and immune activation. *Clin. Lab* 56, 441–448.

Greilberger, J., Koidl, C., Greilberger, M., Lamprecht, M., Schroecksnadel, K., Leblhuber, F., et al. (2008). Malondialdehyde, carbonyl proteins and albumin-disulphide as useful oxidative markers in mild cognitive impairment and Alzheimer's disease. *Free Radic. Res.* 42, 633–638. doi: 10.1080/10715760802255764

Halliwell, B. (2006). Oxidative stress and neurodegeneration: where are we now?. *J. Neurochem.* 97, 1634–1658. doi: 10.1111/j.1471-4159.2006.03907.x

Hashiguchi, M., Ohta, Y., Shimizu, M., Maruyama, J., and Mochizuki, M. (2015). Meta-analysis of the efficacy and safety of Ginkgo biloba extract for the treatment of dementia. *J. Pharm. Health Care Sci.* 1:14. doi: 10.1186/isrctn02262139

Ide, K., Yamada, H., Takuma, N., Park, M., Wakamiya, N., Nakase, J., et al. (2014). Green tea consumption affects cognitive dysfunction in the elderly: a pilot study. *Nutrients* 6, 4032–4042. doi: 10.3390/nu6104032

Irizarry, M. C., Yao, Y., Hyman, B. T., Growdon, J. H., and Pratico, D. (2007). Plasma F2A isoprostane levels in Alzheimer's and Parkinson's disease. *Neurodegener. Dis.* 4, 403–405. doi: 10.1159/000107699

Ishii, T., Hayakawa, H., Igawa, T., Sekiguchi, T., and Sekiguchi, M. (2018). Specific binding of PCBP1 to heavily oxidized RNA to induce cell death. *Proc. Natl. Acad. Sci. U S A* 115, 6715–6720. doi: 10.1073/pnas.1806912115

Keller, J. N., Schmitt, F. A., Scheff, S. W., Ding, Q., Chen, Q., Butterfield, D. A., et al. (2005). Evidence of increased oxidative damage in subjects with mild cognitive impairment. *Neurology* 64, 1152–1156. doi: 10.1212/01.WNL.0000156156.13641.BA

Khalid, A., Shakeel, R., Justin, S., Iqbal, G., Shah, S. A. A., Zahid, S., et al. (2017). Pharmacological effects of turmeric on learning, memory and expression of muscarinic receptor genes (M1, M3 and M5) in stress-induced mouse model. *Curr. Drug Targets* 18, 1545–1557. doi: 10.2174/1389450118666170315120627

Kryscio, R. J., Abner, E. L., Caban-Holt, A., Lovell, M., Goodman, P., Darke, A. K., et al. (2017). Association of antioxidant supplement use and dementia in the prevention of Alzheimer's disease by vitamin E and selenium trial (PREADViSE). *JAMA Neurol.* 74, 567–573. doi: 10.1001/jamaneurol.2016.5778

Kuriyama, S., Hozawa, A., Ohmori, K., Shimazu, T., Matsui, T., Ebihara, S., et al. (2006). Green tea consumption and cognitive function: a cross-sectional study from the Tsurugaya Project 1. *Am. J. Clin. Nutr.* 83, 355–361. doi: 10.1093/ajcn/83.2.355

Lauderback, C. M., Hackett, J. M., Huang, F. F., Keller, J. N., Szweda, L. I., Markesbery, W. R., et al. (2001). The glial glutamate transporter, GLT-1, is oxidatively modified by 4-hydroxy-2-nonenal in the Alzheimer's disease brain: the role of Abeta1–42. *J. Neurochem.* 78, 413–416. doi: 10.1046/j.1471-4159.2001.00451.x

Lopez, N., Tormo, C., De Blas, I., Llinares, I., and Alom, J. (2013). Oxidative stress in Alzheimer's disease and mild cognitive impairment with high sensitivity and specificity. *J. Alzheimers Dis.* 33, 823–829. doi: 10.3233/jad-2012-121528

Mandel, S. A., Amit, T., Weinreb, O., and Youdim, M. B. (2011). Understanding the broad-spectrum neuroprotective action profile of green tea polyphenols in aging and neurodegenerative diseases. *J. Alzheimers Dis.* 25, 187–208. doi: 10.3233/jad-2011-101803

Mangialasche, F., Solomon, A., Kareholt, I., Hooshmand, B., Cecchetti, R., Fratiglioni, L., et al. (2013). Serum levels of vitamin E forms and risk of cognitive impairment in a Finnish cohort of older adults. *Exp. Gerontol.* 48, 1428–1435. doi: 10.1016/j.exger.2013.09.006

Markesbery, W. R., Kryscio, R. J., Lovell, M. A., and Morrow, J. D. (2005). Lipid peroxidation is an early event in the brain in amnestic mild cognitive impairment. *Ann. Neurol.* 58, 730–735. doi: 10.1002/ana.20629

Martinez de Toda, I., Miguelez, L., Vida, C., Carro, E., and De la Fuente, M. (2019). Altered redox state in whole blood cells from patients with mild cognitive impairment and Alzheimer's disease. *J. Alzheimers Dis.* 71, 153–163. doi: 10.3233/jad-190198

Mastroeni, D., Khdour, O. M., Delvaux, E., Nolz, J., Olsen, G., Berchtold, N., et al. (2017). Nuclear but not mitochondrial-encoded oxidative phosphorylation genes are altered in aging, mild cognitive impairment, and Alzheimer's disease. *Alzheimers Dement.* 13, 510–519. doi: 10.1016/j.jalz.2016.09.003

Mecocci, P., and Polidori, M. C. (2012). Antioxidant clinical trials in mild cognitive impairment and Alzheimer's disease. *Biochim. Biophys. Acta* 1822, 631–638. doi: 10.1016/j.bbadis.2011.10.006

Migliore, L., Fontana, I., Trippi, F., Colognato, R., Coppede, F., Tognoni, G., et al. (2005). Oxidative DNA damage in peripheral leukocytes of mild cognitive impairment and AD patients. *Neurobiol. Aging* 26, 567–573. doi: 10.1016/j.neurobiolaging.2004.07.016

Milne, G. L., Dai, Q., and Roberts, L. J. 2nd. (2015). The isoprostanes—25 years later. *Biochim. Biophys. Acta* 1851, 433–445. doi: 10.1016/j.neurobiolaging.2004.07.016

Mohamed, H. E., Abo, E. D. M., Mesbah, N. M., Saleh, S. M., Ali, A. A., and Sakr, A. T. (2018). Raspberry ketone preserved cholinergic activity and antioxidant defense in obesity induced Alzheimer disease in rats. *Biomed Pharmacother* 107, 1166–1174. doi: 10.1016/j.biopha.2018.08.034

Mori, T., Koyama, N., Tan, J., Segawa, T., Maeda, M., and Town, T. (2019). Combined treatment with the phenolics (-)-epigallocatechin-3-gallate and ferulic acid improves cognition and reduces Alzheimer-like pathology in mice. *J. Biol. Chem.* 294, 2714–2731. doi: 10.1074/jbc.ra118.004280

Mori, T., Rezai-Zadeh, K., Koyama, N., Arendash, G. W., Yamaguchi, H., Kakuda, N., et al. (2012). Tannic acid is a natural beta-secretase inhibitor that prevents cognitive impairment and mitigates Alzheimer-like pathology in transgenic mice. *J. Biol. Chem.* 287, 6912–6927. doi: 10.1074/jbc.m111.294025

Nourooz-Zadeh, J., Liu, E. H., Yhlen, B., Änggård, E. E., and Halliwell, B. (1999). F4-isoprostanes as specific marker of docosahexaenoic acid peroxidation in Alzheimer's disease. *J. Neurochem.* 72, 734–740. doi: 10.1046/j.1471-4159.1999.0720734.x

Nunomura, A., Tamaoki, T., Motohashi, N., Nakamura, M., McKeel, D. W. Jr., Tabaton, M., et al. (2012). The earliest stage of cognitive impairment in transition from normal aging to Alzheimer disease is marked by prominent RNA oxidation in vulnerable neurons. *J. Neuropathol. Exp. Neurol.* 71, 233–241. doi: 10.1097/nen.0b013e318248e614

Papandreou, M. A., Dimakopoulou, A., Linardaki, Z. I., Cordopatis, P., Klimis-Zacas, D., Margarity, M., et al. (2009). Effect of a polyphenol-rich wild blueberry extract on cognitive performance of mice, brain antioxidant markers and acetylcholinesterase activity. *Behav. Brain Res.* 198, 352–358. doi: 10.1016/j.bbr.2008.11.013

Picco, A., Polidori, M. C., Ferrara, M., Cecchetti, R., Arnaldi, D., Baglioni, M., et al. (2014). Plasma antioxidants and brain glucose metabolism in elderly subjects with cognitive complaints. *Eur. J. Nucl. Med. Mol. Imaging* 41, 764–775. doi: 10.1007/s00259-013-2638-x

Polidori, M. C., Mattioli, P., Aldred, S., Cecchetti, R., Stahl, W., Griffiths, H., et al. (2004). Plasma antioxidant status, immunoglobulin g oxidation and lipid peroxidation in demented patients: relevance to Alzheimer disease and vascular dementia. *Dement. Geriatr. Cogn. Disord.* 18, 265–270. doi: 10.1159/000080027

Polidori, M. C., and Nelles, G. (2014). Antioxidant clinical trials in mild cognitive impairment and Alzheimer's disease—challenges and perspectives. *Curr. Pharm. Des.* 20, 3083–3092. doi: 10.2174/13816128113196660706

Popli, D., Anil, V., Subramanyam, A. B., M, N. N., V, R. R., Rao, S. N., et al. (2018). Endophyte fungi, Cladosporium species-mediated synthesis of silver nanoparticles possessing *in vitro* antioxidant, anti-diabetic and anti-Alzheimer activity. *Artif. Cells Nanomed. Biotechnol.* 46, 676–683. doi: 10.1080/21691401.2018.1434188

Pratico, D., Clark, C. M., Liun, F., Rokach, J., Lee, V. Y., and Trojanowski, J. Q. (2002). Increase of brain oxidative stress in mild cognitive impairment: a possible predictor of Alzheimer disease. *Arch. Neurol.* 59, 972–976. doi: 10.1001/archneur.59.6.972

Puertas, M. C., Martinez-Martos, J. M., Cobo, M. P., Carrera, M. P., Mayas, M. D., and Ramirez-Exposito, M. J. (2012). Plasma oxidative stress parameters in men and women with early stage Alzheimer type dementia. *Exp. Gerontol.* 47, 625–630. doi: 10.1016/j.exger.2012.05.019

Reed, T., Perluigi, M., Sultana, R., Pierce, W. M., Klein, J. B., Turner, D. M., et al. (2008). Redox proteomic identification of 4-hydroxy-2-nonenal-modified brain proteins in amnestic mild cognitive impairment: insight into the role of lipid peroxidation in the progression and pathogenesis of Alzheimer's disease. *Neurobiol. Dis.* 30, 107–120. doi: 10.1016/j.nbd.2007.12.007

Rege, S. D., Geetha, T., Griffin, G. D., Broderick, T. L., and Babu, J. R. (2014). Neuroprotective effects of resveratrol in Alzheimer disease pathology. *Front. Aging Neurosci.* 6:218. doi: 10.3389/fnagi.2014.00218

Rinaldi, P., Polidori, M. C., Metastasio, A., Mariani, E., Mattioli, P., Cherubini, A., et al. (2003). Plasma antioxidants are similarly depleted in mild cognitive impairment and in Alzheimer's disease. *Neurobiol. Aging* 24, 915–919. doi: 10.1016/s0197-4580(03)00031-9

Rita Cardoso, B., Silva Bandeira, V., Jacob-Filho, W., and Franciscato Cozzolino, S. M. (2014). Selenium status in elderly: relation to cognitive decline. *J. Trace Elem. Med. Biol.* 28, 422–426. doi: 10.1016/j.jtemb.2014.08.009

Schaffer, S., and Halliwell, B. (2012). Do polyphenols enter the brain and does it matter? Some theoretical and practical considerations. *Genes Nutr.* 7, 99–109. doi: 10.1007/s12263-011-0255-5

Scheff, S. W., Ansari, M. A., and Mufson, E. J. (2016). Oxidative stress and hippocampal synaptic protein levels in elderly cognitively intact individuals with Alzheimer's disease pathology. *Neurobiol. Aging* 42, 1–12. doi: 10.1016/j.neurobiolaging.2016.02.030

Siedlak, S. L., Casadesus, G., Webber, K. M., Pappolla, M. A., Atwood, C. S., Smith, M. A., et al. (2009). Chronic antioxidant therapy reduces oxidative stress in a mouse model of Alzheimer's disease. *Free Radic Res.* 43, 156–164. doi: 10.1080/10715760802644694

Smith, M. A., Harris, P. L. R., Sayre, L. M., Beckman, J. S., and Perry, G. (1997). Widespread peroxynitrite-mediated damage in Alzheimer's disease. *J. Neurosci.* 17, 2653–2657. doi: 10.1523/jneurosci.17-08-02653.1997

Sultana, R., Baglioni, M., Cecchetti, R., Cai, J., Klein, J. B., Bastiani, P., et al. (2013). Lymphocyte mitochondria: toward identification of peripheral biomarkers in the progression of Alzheimer disease. *Free Radic. Biol. Med.* 65, 595–606. doi: 10.1016/j.freeradbiomed.2013.08.001

Sundelöf, J., Kilander, L., Helmersson, J., Larsson, A., Ronnemaa, E., Degerman-Gunnarsson, M., et al. (2009). Systemic tocopherols and F2-isoprostanes and the risk of Alzheimer's disease and dementia: a prospective population-based study. *J. Alzheimers Dis.* 18, 71–78. doi: 10.3233/jad-2009-1125

Suridjan, I., Herrmann, N., Adibfar, A., Saleem, M., Andreazza, A., Oh, P. I., et al. (2017). Lipid Peroxidation markers in coronary artery disease patients with possible vascular mild cognitive impairment. *J. Alzheimers Dis.* 58, 885–896. doi: 10.3233/jad-161248

Tadokoro, K., Ohta, Y., Inufusa, H., Loon, A. F. N., and Abe, K. (2020). Prevention of cognitive decline in Alzheimer's disease by novel antioxidative supplements. *Int. J. Mol. Sci.* 21:1974. doi: 10.3390/ijms21061974

Thomas, K. R., Bangen, K. J., Weigand, A. J., Edmonds, E. C., Wong, C. G., Cooper, S., et al. (2020). Objective subtle cognitive difficulties predict future amyloid accumulation and neurodegeneration. *Neurology* 94, e397–e406. doi: 10.1212/WNL.0000000000008838

Torres, L. L., Quaglio, N. B., de Souza, G. T., Garcia, R. T., Dati, L. M., Moreira, W. L., et al. (2011). Peripheral oxidative stress biomarkers in mild cognitive impairment and Alzheimer's disease. *J. Alzheimers Dis.* 26, 59–68. doi: 10.3233/JAD-2011-110284

Turner, R. S., Thomas, R. G., Craft, S., van Dyck, C. H., Mintzer, J., Reynolds, B. A., et al. (2015). A randomized, double-blind, placebo-controlled trial of resveratrol for Alzheimer disease. *Neurology* 85, 1383–1391. doi: 10.1212/wnl.0000000000002206

Vellas, B., Coley, N., Ousset, P. J., Berrut, G., Dartigues, J. F., Dubois, B., et al. (2012). Long-term use of standardised Ginkgo biloba extract for the prevention of Alzheimer's disease (GuidAge): a randomised placebo-controlled trial. *Lancet Neurol.* 11, 851–859. doi: 10.1016/s1474-4422(12)70206-5

Vona, R., Gambardella, L., Cittadini, C., Straface, E., and Pietraforte, D. (2019). Biomarkers of oxidative stress in metabolic syndrome and associated diseases. *Oxid. Med. Cell. Longev.* 2019:8267234. doi: 10.1155/2019/8267234

Wang, J.-X., Gao, J., Ding, S.-L., Wang, K., Jiao, J.-Q., Wang, Y., et al. (2015). Oxidative modification of miR-184 enables it to target Bcl-xL and Bcl-w. *Mol. cell* 59, 50–61. doi: 10.1016/j.molcel.2015.05.003

Wang, J., Markesbery, W. R., and Lovell, M. A. (2006). Increased oxidative damage in nuclear and mitochondrial DNA in mild cognitive impairment. *J. Neurochem.* 96, 825–832. doi: 10.1111/j.1471-4159.2005.03615.x

Wang, B. S., Wang, H., Song, Y. Y., Qi, H., Rong, Z. X., Wang, B. S., et al. (2010). Effectiveness of standardized ginkgo biloba extract on cognitive symptoms of dementia with a six-month treatment: a bivariate random effect meta-analysis. *Pharmacopsychiatry* 43, 86–91. doi: 10.1055/s-0029-1242817

Yada, S., Lapsley, K., and Huang, G. (2011). A review of composition studies of cultivated almonds: macronutrients and micronutrients. *J. Food Comp. Analy.* 24, 469–480. doi: 10.1016/j.jfca.2011.01.007

Zheng, T., Qin, L., Chen, B., Hu, X., Zhang, X., Liu, Y., et al. (2016). Association of plasma DPP4 activity with mild cognitive impairment in elderly patients with type 2 diabetes: results from the GDMD study in china. *Diabetes Care* 39, 1594–1601. doi: 10.2337/dc16-0316

Conflict of Interest: The authors declare that the research was conducted in the absence of any commercial or financial relationships that could be construed as a potential conflict of interest.

frontiers in Neuroscience

ORIGINAL RESEARCH
published: 06 August 2020
doi: 10.3389/fnins.2020.00730

Bergapten Improves Scopolamine-Induced Memory Impairment in Mice *via* Cholinergic and Antioxidative Mechanisms

*Joanna Kowalczyk[1,2], Łukasz Kurach[2], Anna Boguszewska-Czubara[3], Krystyna Skalicka-Woźniak[4], Marta Kruk-Słomka[5], Jacek Kurzepa[3], Małgorzata Wydrzynska-Kuźma[5], Grażyna Biała[5], Adrianna Skiba[4] and Barbara Budzyńska[2]**

[1] Chair and Department of Applied Pharmacy, Medical University of Lublin, Lublin, Poland, [2] Independent Laboratory of Behavioral Studies, Medical University of Lublin, Lublin, Poland, [3] Chair and Department of Medicinal Chemistry, Medical University of Lublin, Lublin, Poland, [4] Chair and Department of Pharmacognosy with Medicinal Plant Unit, Medical University of Lublin, Lublin, Poland, [5] Chair and Department of Pharmacology and Pharmacodynamics, Medical University of Lublin, Lublin, Poland

OPEN ACCESS

Edited by:
Maria Javier Ramirez, University of Navarra, Spain

Reviewed by:
Patrizio Blandina, University of Florence, Italy
Mariela Fernanda Perez, National University of Córdoba, Argentina

***Correspondence:**
Barbara Budzyńska
basia.budzynska@umlub.pl

Specialty section:
This article was submitted to Neuropharmacology, a section of the journal Frontiers in Neuroscience

Received: *26 March 2020*
Accepted: *18 June 2020*
Published: *06 August 2020*

Citation:
Kowalczyk J, Kurach Ł, Boguszewska-Czubara A, Skalicka-Woźniak K, Kruk-Słomka M, Kurzepa J, Wydrzynska-Kuźma M, Biała G, Skiba A and Budzyńska B (2020) Bergapten Improves Scopolamine-Induced Memory Impairment in Mice via Cholinergic and Antioxidative Mechanisms. Front. Neurosci. 14:730. doi: 10.3389/fnins.2020.00730

Bergapten is a furanocoumarin naturally occurring in the *Apiaceae* family *and* it is a well-known photosensitizing agent used in photochemotherapy. In this study, we investigated the influence of bergapten on cognitive function and mechanism underlying these effects in scopolamine-induced memory impairment in male Swiss mice. The passive avoidance test was used to evaluate the efficiency of memory acquisition and consolidation. The results demonstrated that both single and repeated administration of bergapten improved not only the acquisition but also consolidation of memory. The behavioral tests showed that bergapten prevented memory impairment induced by administration of scopolamine. Observed effects may result from the inhibition of acetylcholinesterase activity in the hippocampus and prefrontal cortex. Also, bergapten caused significant anti-oxidative effects. These new findings provide pharmacological and biochemical support for the development of the coumarin's potential in cognitive deficits.

Keywords: acetylcholine, oxidative stress, coumarins, memory, passive avoidance

INTRODUCTION

Dementia, a group of symptoms with memory deficits and losing social abilities, have become increasingly significant worldwide. They are especially problematic in developed countries. Memory loss in dementia has different causes, e.g., alteration of cholinergic transmission, oxidative stress, inflammation, or monoaminergic disturbances. These effects contribute to neuronal apoptosis and therefore to memory impairments (Deng et al., 2019). Alzheimer's disease (AD) is considered as the most common cause of dementia in older people. Increased level of acetylcholinesterase (AChE) is one of the mechanisms underlying cognitive dysfunction

in AD patients. This enzyme is responsible for acetylcholine (ACh) degradation. ACh is a neurotransmitter crucial for memory and learning processes. The increased amount of AChE is a consequence of AD rather than the main cause of the disease. AD patients experience neurodegeneration of cholinergic neurons especially in the basal nucleus of Meynert [responsible for about 90% ACh production in the central nervous system (CNS)], cerebral cortex, hippocampus, and amygdala (Wszelaki, 2009; Budzyñska et al., 2015). As a result, the level of ACh decreases, and neuronal transmission is ameliorated. Also, amyloid-beta (Aβ) aggregates cumulated in the brain can increase the production of AChE. Furthermore, the more advanced the disease is, the more butyrylcholinesterase (BChE) is produced. BChE is another form of cholinesterase and catalyzes the hydrolysis of ACh. When neuronal cells are destroyed, the level of BChE automatically becomes higher (Bukowska et al., 2017).

Acetylcholinesterase inhibitors (AChEIs) increase the level of ACh causing improvement of patient's learning and memory functions. Procognitive medicines are commonly prescribed to people with AD. However, the use of AChEIs is limited by their hepatotoxicity and the side effects resulting from activation of the cholinergic system (Deng et al., 2019). The other limitation is the low bioavailability of the drug. However, cognitive functions are dependent not only on the level of ACh in the human brain but also on other neurotransmitters and factors (Parihar and Brewer, 2010).

It is well established that the CNS is especially susceptible to oxidants due to its specific construction and functions, such as high consumption of oxygen with a simultaneously high content of unsaturated lipids and weak antioxidant protection (Kruk-Slomka et al., 2012). Therefore, reactive oxygen species (ROS) overproduced in CNS cause dysfunction in membrane fluidity and decrease membrane potential, which in turn increases calcium permeability, especially in the regions of the brain such as the hippocampus, substantia nigra, and the striatum (Phaniendra et al., 2015). The oxidative mechanisms and affected brain regions are strictly connected with the pathology of several neurodegenerative diseases, including AD. Moreover, the mechanism underlying AD is also associated with increased ROS production, due to transition metal ions chelation [Cu, Zn, and Fe (III)] by neurofibrillary tangles. Aβ plaques, which are electron donors in Fenton or Haber–Weiss reactions can also be the source of ROS (Phaniendra et al., 2015). Therefore, antioxidant therapy is recommended as preventive care and effective support for the main therapy.

The current study is a continuation of our previous research regarding the activity of furanocoumarins in CNS (Budzyñska et al., 2015, 2016; Skalicka-Wozniak et al., 2018). Previously, we revealed the procognitive activity of xanthotoxin [8-methoxypsoralen; 9-methoxy-7H-furo(3,2-g)chromen-7-one], as well as its ability to prevent memory deficits induced by scopolamine (Skalicka-Wozniak et al., 2018). In the present study bergapten (5-methoxypsoralen), a structural analog of xanthotoxin was used. Bergapten was isolated from plants belonging to *the Apiaceae* family *and* is a well-known photosensitizing agent used in photochemotherapy (Tanew et al., 1999). It also shows anticancer (Panno et al., 2012), antioxidative (Liu et al., 2012), and anti-inflammatory properties (Bose et al., 2011). It was shown that bergapten was also the most potent inhibitor of CYP3A4 (Ho et al., 2001). Our studies revealed that bergapten prolongs antidepressant and procognitive effects of nicotine (Budzyñska et al., 2016; Skalicka-Wozniak et al., 2016). Also bergapten causes the increase of Ach in the brain by inhibiting the BChE and AChE activity (Senol et al., 2011, 2015; Wszelaki et al., 2011; Rohini and Srikumar, 2014). Bergapten was shown to be an effective inhibitor of monoamine oxidase (MAO), which resulted in the antidepressant effect (Huong et al., 1999).

Taking into account all the above, the current study aimed to evaluate the influence of bergapten on consolidation and acquisition of memory processes impaired by scopolamine administration in male Swiss mice. Subsequently, the level of AChE was measured in the prefrontal cortex and hippocampus, the structures important for cognitive functions, to check the mechanism underlying bergapten activity in memory impairments. Finally, to find out if the antioxidant mechanism is also engaged in neuroprotective action of bergapten, the oxidative stress markers in the aforementioned brain structures were determined.

MATERIALS AND METHODS

Animals

Male Swiss mice weighing 20–25 g were maintained under the conditions of 12 h light/dark cycle, room temperature 21 ± 1°C, no limited tap water and laboratory chow (Agropol, Poland). Animals were becoming accustomed to the laboratory environment for one week. Experimental groups had 8–10 individuals. The National Institute of Health Guidelines for the Care and Use of Laboratory Animals and to the European Community Council Directive for the Care and Use of Laboratory Animals of September 22, 2010 (2010/63/EU) was kept during the whole experiment. The study was approved by the 1st Local Ethics Committee, Lublin, Poland. Different mice were used for each drug treatment.

Drugs

Bergapten (5-methoxypsoralen) was extracted from fruits of *Heracleum leskovii* L using the method described previously by Budzyñska et al. (2016). The solution of scopolamine (Sigma-Aldrich, St. Louis, MO, United States) was prepared using 0.9% NaCl. The suspension of bergapten in a1% solution of Tween 80 (Sigma-Aldrich, St. Louis, MO, United States) and 0.9% NaCl solution was prepared as described previously by Budzyñska et al. (2016). Solutions were prepared daily and injected intraperitoneally (i.p., 10 ml/kg) Control groups were injected with an equal volume of the 0.9% NaCl solution.

Experimental Procedure

The doses of bergapten and scopolamine were chosen based on literature data (Luszczki et al., 2010; Zhou et al., 2017), our recently published articles (Budzyñska et al., 2016), as well as on preliminary studies.

The Task for the Assessment of Memory-Related Responses

Memory-related responses were measured by the passive avoidance (PA) task (Venault et al., 1986). The apparatus used for the PA task comprized of an acrylic box divided into two compartments: a light compartment (10 × 13 × 15 cm) and a dark compartment (25 × 20 × 15 cm).The procedure was applied according to the description of Allami et al. (2011) and Javadi-Paydar et al. (2012) with minor modifications.

The experiment consisted of a pre-test and test. As was described previously by Budzyñska et al. (2016), in the pre-test after 30 s of habituation in the light compartment, the door was open and mice were allowed to enter into the dark space. Subsequently, the door was closed and the impulse of 0.15 mA (2 s) was generated. On the second day, the test was performed according to the same procedure but without electroshock. The time from opening the door to the entrance into the dark room was measured (pre-test – TL1, test – TL2). Depending on the used procedure, the time of drug administration, and the period between training and the test, PA allows examining different stages of memory. Drug administration before the first trial (pretest) should affect the acquisition of information, while drug administration immediately after the pretest should affect the consolidation of information.

Spontaneous Locomotor Activity

For spontaneous locomotor activity evaluation, an Opto-Varimex-4 Auto-Track (Columbus Instruments, United States) was chosen and used according to the procedure of Budzyñska et al. (2016). After subsequent injections of saline, bergapten (12.5, 25 mg/kg), scopolamine (1 mg/kg) or saline, or bergapten (12.5, 25 mg/kg) co-administered with scopolamine mice were placed separately in the apparatus for 15 min.

Rota-Rod Procedure

The ability of mice to maintain balance on a spinning rod was tracked by the Rota-rod procedure (Dunham and Miya, 1957). An animal was placed on a metal rod spinning at a constant velocity of 18 rpm. The parameter measured during the test was the period of time the mouse can stay on the spinning rod. However, a time limitation of 60 s per session applies.

Each experiment was preceded by a 3-min training session during which the mouse had an unlimited number of trails. Those rodents which were capable of maintaining balance the whole duration of the experiment passed the test.

Treatment

The first step of the experiment was designed to estimate the influence of an acute and sub-chronic administration of bergapten on the acquisition and consolidation of memory in mice, using the PA test.

During the acute treatment bergapten (12.5, 25, 50, and 100 mg/kg, i.p.) or saline (control group) were administered 30 min before the first trial (memory acquisition) or immediately after the first trial (memory consolidation) and re-tested after 24 h.

During the sub-chronic administration bergapten (12.5 and 25 mg/kg, i.p.) or saline (control group) were administered twice daily (8.00 a.m., 8.00 p.m.) for 6 days. On the seventh day bergapten (12.5 and 25 mg/kg, i.p.) or saline were administered only once (8.00 a.m), 30 min before the first trial (memory acquisition) or immediately after the first trial (memory consolidation) and re-tested after 24 h.

The next step of experiment was to evaluate the impact of an acute and sub-chronic administration of bergapten on the memory impairment induced by an acute administration of scopolamine in mice, using the PA test.

During the acute treatment bergapten (25 mg/kg, i.p.) or saline (control group) were administered 10 min before injection of scopolamine (1 mg/kg, i.p.) or saline. Pre-test was conducted 20 min after scopolamine administration (memory acquisition) or before appropriate injections (memory consolidation).

During the sub-chronic administration bergapten (12.5 mg/kg, i.p.) or saline (control group) were administered twice daily (8.00 a.m., 8.00 p.m.) for 6 days. On the seventh day bergapten (12.5 mg/kg, i.p.) or saline were administered only once (8.00 a.m) 10 min before saline or scopolamine (1 mg/kg) injection. Twenty minutes after scopolamine or saline administration (memory acquisition) or before appropriate injections (memory consolidation) the pre-test was conducted. Twenty-four hours later the mice were re-tested.

Biochemical Procedures

Brain Tissue Dissection and Preparation

Immediately after the behavioral tests, mice were decapitated. As soon as the whole brains were taken out, they were immediately flushed with ice-cold saline to remove excessive blood. Then prefrontal cortex and hippocampus were resected. The isolated structures were homogenized in ice-cold saline for AChE determination or in 10% Tris buffer (pH 7.4) on ice for determination of oxidative stress markers. The homogenates were centrifuged at 10,000 *g* to separate nuclear debris.

Measurement of Acetylcholinesterase Activity

The activity of AChE was carried out using mouse AChE ELISA Kit from MyBio Source (MBS260553) according to the manufacturer's instructions. The absorbance was read at 412 nm. The intensity of obtained color was proportional to the activity of AChE in the sample and it was expressed as enzymatic activity units (U).

Measurement of Total Antioxidant Capacity – TAC

Total antioxidant capacity (TAC) of tissue homogenates was determined spectrophotometrically by ferric-reducing ability of plasma (FRAP) method with modifications for tissue homogenates supernatants. A chromophore was produced by addition of 200 μl of working reagent [acetate buffer (pH 3.6), 2,4,6-tri-pyridyl-s-triazine (10 mmol/l) in 40 mmol/l HCl and aqueous solution of $FeCl_3$ (20 mmol/l) in the ratio of 10:1:1] to 10 μl of samples diluted with 20 μl of deionized water at 96-well plate. The absorbance was measured at 593 nm after 30 min at 37°C and the

results were evaluated from the standard curve prepared of $FeSO_4$ at concentrations from 0 to 1000 μmol/l. The experiment was performed in triplicate and the final results are mean values of them.

Statistical Analysis

The statistical analysis were performed using one- or two-way ANOVA for the factors of pretreatment, treatment and pretreatment/treatment interactions.

Post hoc comparison of means was carried out with the Tukey's test (for one-way ANOVA) or with the Bonferroni's test (for two-way ANOVA, scopolamine pretreatment, bergapten treatment and interaction between scopolamine and bergapten administration) for multiple comparisons, when appropriate. The data were considered statistically significant at confidence limit of $p < 0.05$. ANOVA analysis with Tukey's or Bonferroni's post tests were performed using GraphPad Prism version 5.00 for Windows, GraphPad Software, San Diego California USA[1].

The results obtained in **the spontaneous locomotor activity** test were presented as an arithmetic average distance (cm) covered by a mouse ± SEM for each experimental group.

For the evaluation of memory-related behavior, a latency index (LI) was calculated as a difference between entrance latencies (TL2 and TL1) were calculated and depicted as a ratio:

$$LI = TL2 - TL1/TL1$$

TL1 – the time taken to enter the dark compartment during the training; TL2 – the time taken to re-enter the dark compartment during the retention (Chimakurthy and Talasila, 2010).

RESULTS

The Influence of an Acute Administration of Bergapten on the Memory Acquisition and Consolidation in the PA Test in Mice

Acquisition of Memory

One-way ANOVA revealed that administration of acute i.p. doses of bergapten (12.5, 25, 50, and 100 mg/kg) had a statistically significant effect on LI values for memory acquisition [$F(4,43) = 18.09$; $p < 0.0001$). The *post hoc* Tukey's test confirmed that the treatment with bergapten (25, 50, and 100 mg/kg) significantly increased LI values in mice compared to those in the saline-treated control group ($p < 0.001$) (**Figure 1A**), indicating that bergapten at these used doses improved acquisition of memory and learning.

Consolidation of Memory

One-way ANOVA revealed that administration of acute i.p. doses of bergapten (12.5, 25, 50, and 100 mg/kg) had a statistically significant effect on LI values for memory acquisition [$F(4,48) = 14.45$; $p < 0.0001$). The *post hoc* Tukey's test confirmed that the treatment with bergapten significantly increased LI values in mice compared to those in the saline-treated control group [$p < 0.001$ – for the doses of bergapten: 25 and 100 mg/kg (**Figure 1B**)], indicating that bergapten, at these used doses, improved consolidation of memory and learning.

The Influence of Sub-Chronic Administration of Bergapten on the Memory Acquisition and Consolidation in the PA Test in Mice

Acquisition of Memory

One-way ANOVA revealed that administration of both sub-chronic i.p. doses of bergapten (12.5 and 25 mg/kg) had a statistically significant effect on LI values for memory acquisition [$F(2,19) = 11.86$; $p = 0.0005$]. The *post hoc* Tukey's test confirmed that the treatment with bergapten significantly increased LI values in mice compared to those in the saline-treated control group ($p < 0.001$ – for the dose of 12.5 mg/kg and $p < 0.05$ for the dose of 25 mg/kg (**Figure 2A**), indicating that bergapten, at the used doses, improved acquisition of memory and learning.

Consolidation of Memory

One-way ANOVA revealed that administration of both sub-chronic i.p. doses of bergapten (12.5 and 25 mg/kg) had a statistically significant effect on LI values for memory acquisition [$F(2,24) = 9.986$; $p = 0.0007$]. The *post hoc* Tukey's test confirmed that the treatment with bergapten significantly increased LI values in mice compared to those in the saline-treated control group ($p < 0.05$ – for the dose of 12.5 mg/kg and $p < 0.001$ for the dose of 25 mg/kg (**Figure 2B**), indicating that bergapten, at these used doses, improved acquisition of memory and learning.

The Influence of an Acute Administration of Bergapten on the Memory Impairment Induced by an Acute Injection of Scopolamine

Acquisition of Memory

For memory acquisition, two-way ANOVA analyses revealed that there was statistically significant effect caused by bergapten (25 mg/kg) pretreatment [$F(1,51) = 1.90$; $p = 0.1745$] as well as by scopolamine (1 mg/kg) treatment [$F(2,51) = 7,08$; $p = 0.0019$]) but there is no statistically significant effect caused by interactions between bergapten pretreatment and scopolamine treatment [$F(2,51) = 3.81$; $p = 0.0287$]. The *post hoc* Bonferroni's test confirmed that scopolamine at the dose of 1 mg/kg significantly decreased LI values in mice in the PA test in comparison to the saline/saline-treated mice, suggesting the amnesic effect of this drug ($p < 0.05$). The *post hoc* Bonferroni's test also confirmed that bergapten, at these doses of 25 mg/kg, improved acquisition of memory and learning ($p < 0.001$). Additionally, bergapten (25 mg/kg) attenuated this amnesic effect of scopolamine (1 mg/kg) ($p < 0.05$) as compared with scopolamine-treated (1 mg/kg) mice (**Figure 3A**).

Consolidation of Memory

For memory consolidation, two-way ANOVA analyses revealed that there was statistically significant effect caused by bergapten

[1] www.graphpad.com

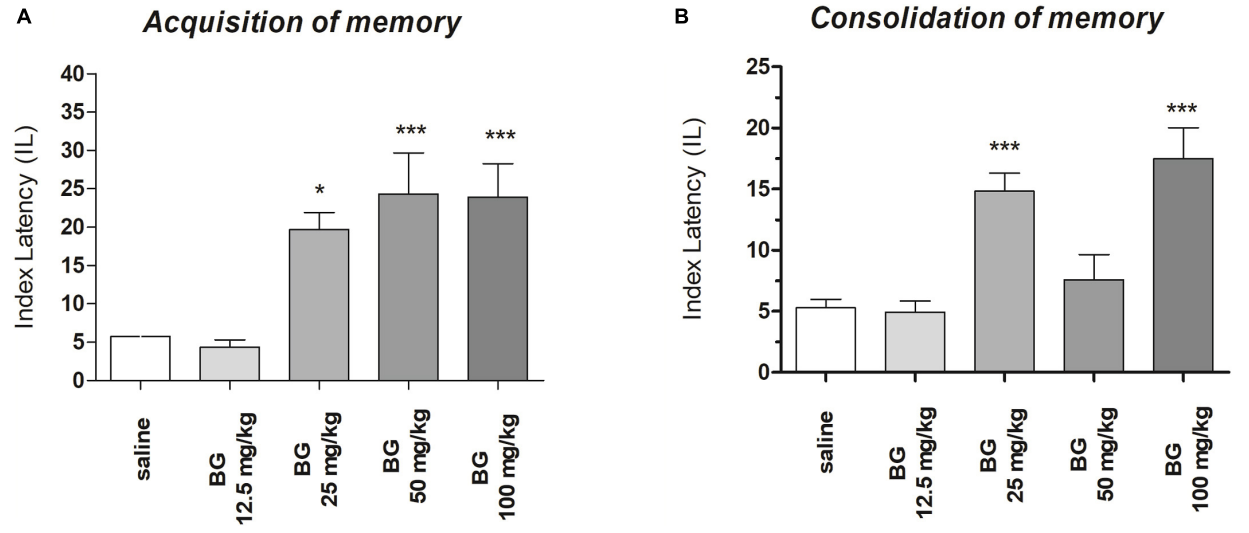

FIGURE 1 | Effects of an acute bergapten or saline administration on the latency index (LI) during the acquisition trial **(A)** and consolidation trial **(B)**, using the PA test in mice. Bergapten (12.5, 25, 50, and 100 mg/kg, i.p.) or saline were injected 30 min before the first trial **(A)** or immediately after first trial **(B)** and mice were re-tested 24 h later; n = 8–10; the means ± SEM; $^{*}p < 0.05$, $^{***}p < 0.001$ vs. saline-treated control group; Tukey's test.

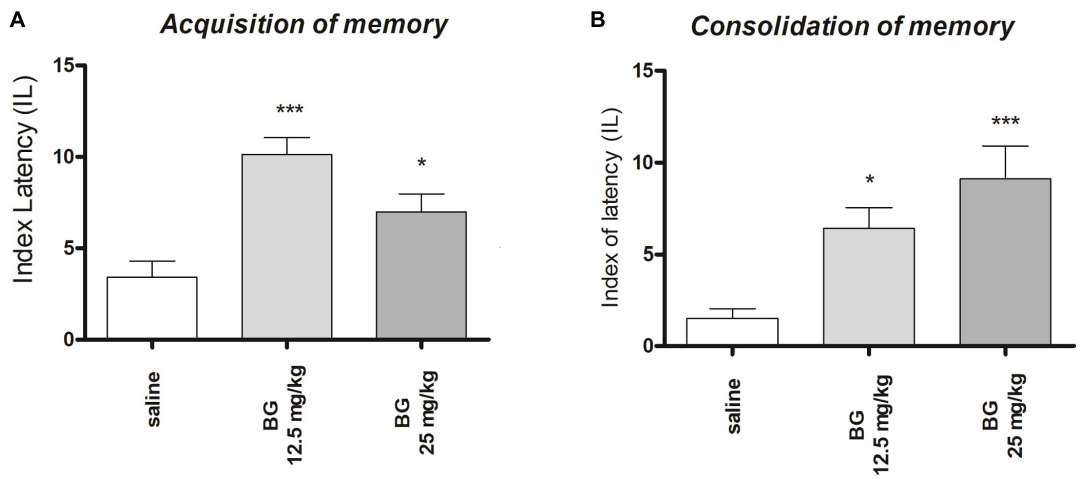

FIGURE 2 | Effects of sub-chronic bergapten or saline administration on the latency index (LI) during the acquisition trial **(A)** and consolidation trial **(B)**, using the PA test in mice. Bergapten (12.5 and 25 mg/kg, i.p.) or saline were administered for the 6 days. On the seventh day bergapten was administered 30 min before the first trial **(A)** or immediately after first trial **(B)** and mice were re-tested 24 h later; n = 8–10; the means ± SEM; $^{*}p < 0.05$; $^{***}p < 0.001$ vs. saline-treated control group; Tukey's test.

pretreatment [$F(1,32) = 7.02$; $p = 0.012$, $F(2,51) = 7.08$; $p = 0.00194$] as well as by interactions between bergapten pretreatment and scopolamine treatment [$F(2,51) = 3.81$; $p = 0.0287$] but there is no statistically significant effect caused by scopolamine (1 mg/kg) treatment [$F(1,51) = 1.90$; $p = 0.1745$]. The *post hoc* Bonferroni's test showed that scopolamine at the dose of 1 mg/kg significantly decreased LI values in mice in the PA test in comparison to the saline-treated mice, suggesting the amnesic effect of this drug ($p < 0.05$). The *post hoc* Bonferroni's test also confirmed that bergapten, at these doses of 25 mg/kg, improved consolidation of memory and learning ($p < 0.001$). Additionally, bergapten (25 mg/kg) attenuated this amnesic effect of scopolamine (1 mg/kg) ($p < 0.05$) as compared with scopolamine-treated (1 mg/kg) mice (**Figure 3B**).

Repeated Bergapten Injection Effects on Memory-Related Processes Induced by Scopolamine in the PA Test in Mice

In order to check the influence of subchronic bergapten administration on acquisition and consolidation of the memory processes the doses of 12.5 mg/kg as the inactive in PA test was selected. **Figure 4A** indicates the effects of repeated injections of bergapten on memory acquisition impaired by

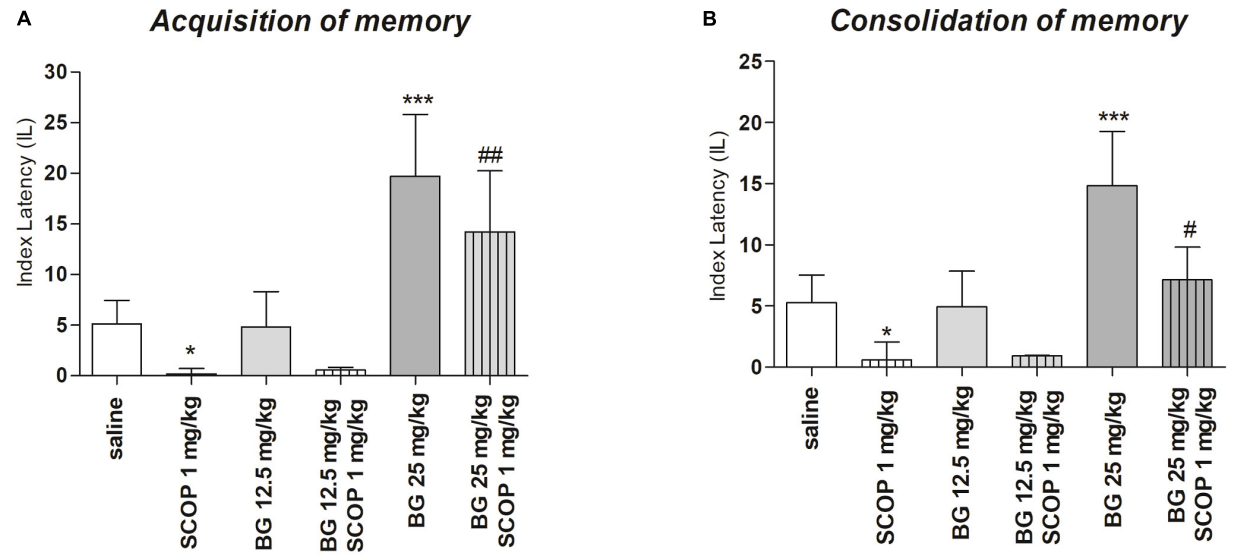

FIGURE 3 | Effects of acute administration of bergapten (BG) on scopolamine-induced impairment of memory acquisition trial **(A)** and consolidation trial **(B)** using the PA test in mice. Bergapten (12.5 and 25 mg/kg, i.p.) was administered 30 min and scopolamine (SCOP, 1 mg/kg, i.p.) 20 min before the first trial **(A)** or bergapten was administered immediately after first trial and scopolamine 10 min after bergapten injection **(B)** and animals were re-tested 24 h after the last injection; n = 8–12; the means ± SEM; $^{*}p < 0.05$; $^{***}p < 0.001$ vs. saline-treated control group, $^{\#}p < 0.05$, $^{\#\#\#}p < 0.01$ vs. scopolamine-treated group; Bonferroni's test.

scopolamine during the retention trial in the PA task [two-way ANOVA: pre-treatment ($F(1,32) = 14.70$; $p = 0.0006$), treatment ($F(1, 32) = 41.77$; $p < 0.0001$) and interactions effect ($F(1, 32) = 13.74$; $p = 0.0008$)]. The *post hoc* Bonferroni's test revealed that bergapten given repeatedly, at the doses of 12.5 mg/kg significantly increased IL value, as compared with the saline-treated mice, thus indicating that subchronic administration of bergapten improved acquisition of the memory and learning processes during the retention trial ($p < 0.001$). In contrast, when mice were treated subchronically with saline and with scopolamine (1 mg/kg) on the seventh day, the impairment of memory acquisition was observed ($p < 0.05$) as compared with saline-treated group. Furthermore, we did not observe improvement in memory and learning processes in the animals injected repeatedly with bergapten (12.5 mg/kg). Also on the seventh day of injection, we did not observe improvement in memory and learning processes in animals injected with bergapten in combination with scopolamine when compared to the mice treated exclusively with scopolamine.

The changes of IL values, indicated by two-way ANOVA, were noticed at the consolidation trial [treatment ($F(1,30) = 1.64$; $p = 0.2107$), and without pre-treatment effect ($F(1,30) = 33.91$; $p < 0.0001$) and interactions effect ($F(1,30) = 1.64$; $p = 0.2107$)] (**Figure 4B**). The *post hoc* Bonferroni's test showed that repeated injection of bergapten (12.5 mg/kg) improved the cognitive processes ($p < 0.001$), compared to the saline-treated mice. Additionally, mice subchronically treated with saline and on the seventh day with scopolamine, exhibited the impairment of memory consolidation ($p < 0.05$). It was also revealed that repeated administration of bergapten at the doses of 12.5 mg/kg significantly decreased impairment of memory and learning processes induced by an acute injection of scopolamine ($p < 0.01$), as compared with subchronically saline-treated group and on the seventh day scopolamine-treated mice (**Figure 4b**).

Effect of Acute Administration of Bergapten on Motor Coordination in Rota-Rod in Mice

In the rota-rod test no changes in motor coordination were observed [one-way ANOVA ($F(3,26) = 3.067$; $p = 0.0536$)]. Value on time on rotating rod (s) ± SEM: vehicle 60.00 ± 0.00; bergapten 12.5 mg/kg 58.25 ± 1.750; bergapten 25 mg/kg 60.00 ± 0.00; bergapten 50 mg/kg 50.71 ± 4.91

Single Injection of Bergapten, Scopolamine and Co-administration of Both Drugs on Locomotor Activity in Mice

Table 1 shows the influence of an acute administration of bergapten and scopolamine on locomotor activity. Two-way ANOVA analyses revealed that there was statistically significant effect caused by as well as by scopolamine (1 mg/kg) treatment [$F(2,42) = 14.45$; $p = 0.0005$] but there is no statistically significant effect caused by bergapten pretreatment [$F(1,42) = 2.20$; $p = 0.1236$] as well as interactions between bergapten pretreatment and scopolamine treatment [$F(2,51) = 3.81$; $p = 0.0287$]. The *post hoc* Bonferroni's test confirmed that scopolamine at the dose of 1 mg/kg significantly increased locomotor activity in mice in comparison with the saline-treated mice ($p < 0.01$). The *post hoc* Bonferroni's test also confirmed that co-administration of scopolamine with bergapten, at these doses of 12.5 mg/kg ($p < 0.05$) and 25 mg/kg ($p < 0.01$)

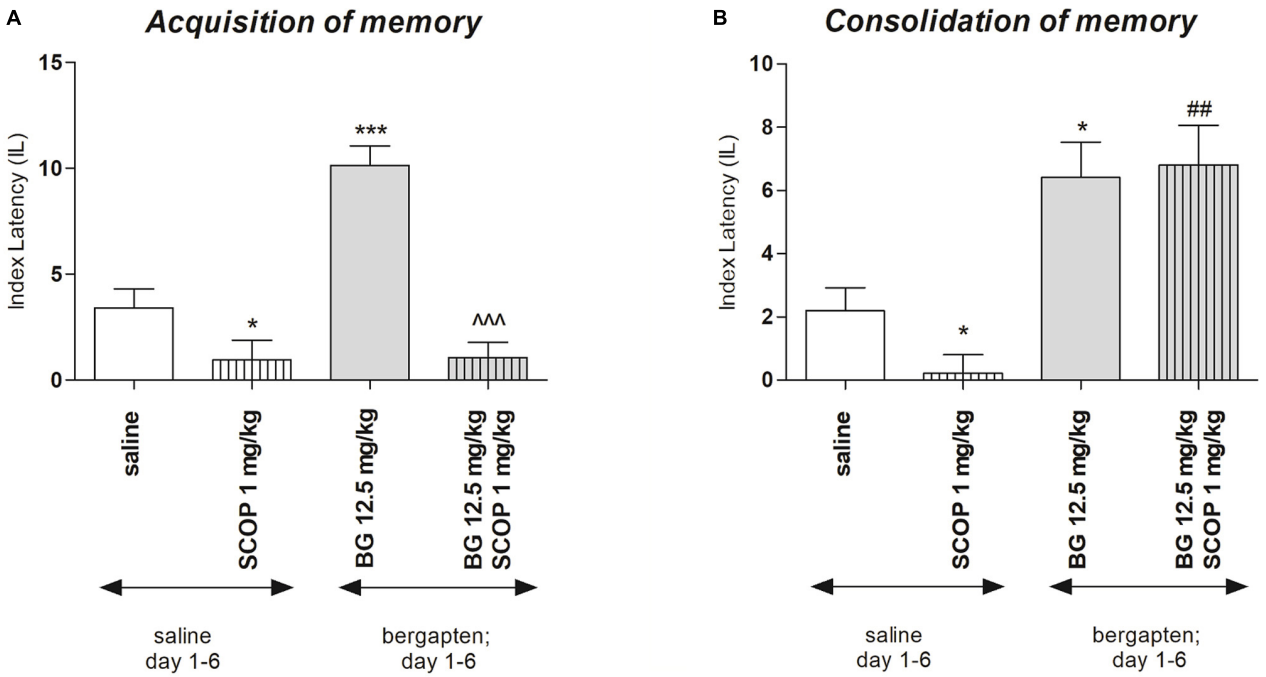

FIGURE 4 | Effects of subchronic administration of bergapten (BG) on scopolamine-induced impairment of memory acquisition trial **(A)** and consolidation trial **(B)** using the PA test in mice. Bergapten (12.5 mg/kg, i.p.) was administered 6 days twice daily. On the seventh day bergapten was administered 30 min and scopolamine (SCOP, 1 mg/kg, i.p.) 20 min before the first trial **(A)** or bergapten was administered immediately after first trial and scopolamine 10 min after bergapten injection **(B)** and animals were re-tested 24 h after the last injection; n = 8–12; the means ± SEM; $^{*}p < 0.05$; $^{***}p < 0.01$ vs. saline-treated control group, $^{\#\#}p < 0.01$ vs. scopolamine-treated control group; $^{\wedge\wedge\wedge}p < 0.001$ vs. bergapten-treated (12.5 mg/kg) group; Bonferroni's test.

increased locomotor activity as compared with bergapten-treated mice (**Table 1**). Bergapten at the doses of 50 mg/kg (458.10 ± 41.41) and 100 mg/kg (385.90 ± 42.15) mg/kg did not influenced on observed parameter when compared with saline-treated mice.

Biochemical Studies

Figure 5A indicates the effects of bergapten (12.5 and 25 mg/kg) administered alone or in combination with scopolamine on AChE level measured in the prefrontal cortex [pretreatment ($F(1,50) = 33.58$, $p = 0.0352$), interactions effect ($F(1,50) = 4.08$, $p = 0.0229$), treatment ($F(1,50) = 37.21$, $p < 0.0001$); two-way ANOVA]. *Post hoc* Bonferroni's test confirmed the significant increasing of the AChE concentration in the prefrontal cortex after single injection of scopolamine ($p < 0.001$). No changes were noticed after single acute injection of bergapten (12.5 and 25 mg/kg), however, combination of bergapten at both doses and scopolamine decreased the level of AChE in the prefrontal cortex (12.5 mg/kg – $p < 0.001$; 25 mg/kg – $p < 0.01$) in comparison with scopolamine-treated group (**Figure 5A**).

Figure 5B indicates the effects of subchronic bergapten (12.5 and 25 mg/kg) administered alone or in combination with acute injection of scopolamine on AChE level measured in the prefrontal cortex [pretreatment ($F(2,35) = 24.28$, $p < 0.0001$), interactions effect ($F(1,35) = 4.51$, $p = 0.0409$), treatment ($F(1,35) = 76.40$, $p < 0.0001$); two-way ANOVA]. *Post hoc* Bonferroni's test confirmed the significant increase of the AChE concentration in the prefrontal cortex after single injection of scopolamine ($p < 0.01$). No changes were noticed after single subchronic injection of bergapten (12.5 mg/kg), however, we observed attenuation of enzyme level in the prefrontal cortex ($p < 0.05$) in comparison with scopolamine- and saline treated group (**Figure 5B**).

Figure 6A presents the effect of single dose of bergapten (12.5, 25, 50, 100 mg/kg) on TAC measured in the prefrontal cortex [$F(4,25) = 7.791$, $p = 0.0003$; one-way ANOVA]. *Post hoc* Tukey test confirmed significant increase in TAC level after single injection of bergapten in doses 25 and 50 mg/kg ($p < 0.05$) and 100 mg/kg ($p < 0.01$).

Figure 6B presents the effect of subchronic bergapten (12.5, 25 mg/kg) on TAC measured in the prefrontal cortex [$F(2,15) = 6.794$, $p = 0.0079$; one-way ANOVA]. *Post hoc* Tukey test confirmed significant increase in TAC level after single injection of bergapten in dose 25 mg/kg ($p < 0.01$) in comparison with saline-treated group.

Figure 7A indicates the effect of single dose of bergapten (12.5, 25 mg/kg) administered alone or in combination with scopolamine (1 mg/kg) on TAC determined in the prefrontal cortex [pretreatment ($F(2,54) = 21.35$, $p < 0.0001$), treatment ($F(1,54) = 51.61$, $p < 0.0001$) without interactions ($F(2, 54) = 0.6146$, $p = 0.5446$); two-way ANOVA]. *Post hoc* Tukey's test confirmed statistically significant decrease in TAC level in the prefrontal cortex after single injection of scopolamine ($p < 0.05$). Administration of bergapten caused dose-dependent increase in

TABLE 1 | Effect of bergapten (BG, 12.5, 25 mg/kg, i.p.) and scopolamine (SCOP, 1 mg/kg, i.p.) on spontaneous locomotor activity in mice.

	Saline	SCOP	BG 12.5 mg/kg	BG 25 mg/kg	BG 12.5 mg/kg + SCOP	BG 25 mg/kg + SCOP
Photocell beam breaks ± SEM (30 min)	402.30 ± 31.01	863.30 ± 188.70***	439.50 ± 30.31	398.10 ± 24.54	534.25 ± 68.45###	657.12 ± 56.19$$$,###

*Drugs were administered separately or in combination. Animals were injected with bergapten 15 min before scopolamine administration and then immediately placed in actimeters for the 30 min. Data are presented as the means ± SEM. n = 8–12; ***p < 0.001, vs. saline-treated group; ###p < 0.001 vs. scopolamine-treated group; $$$p < 0.001, vs. bergapten (25 mg/kg)-treated group, Bonferroni's test.*

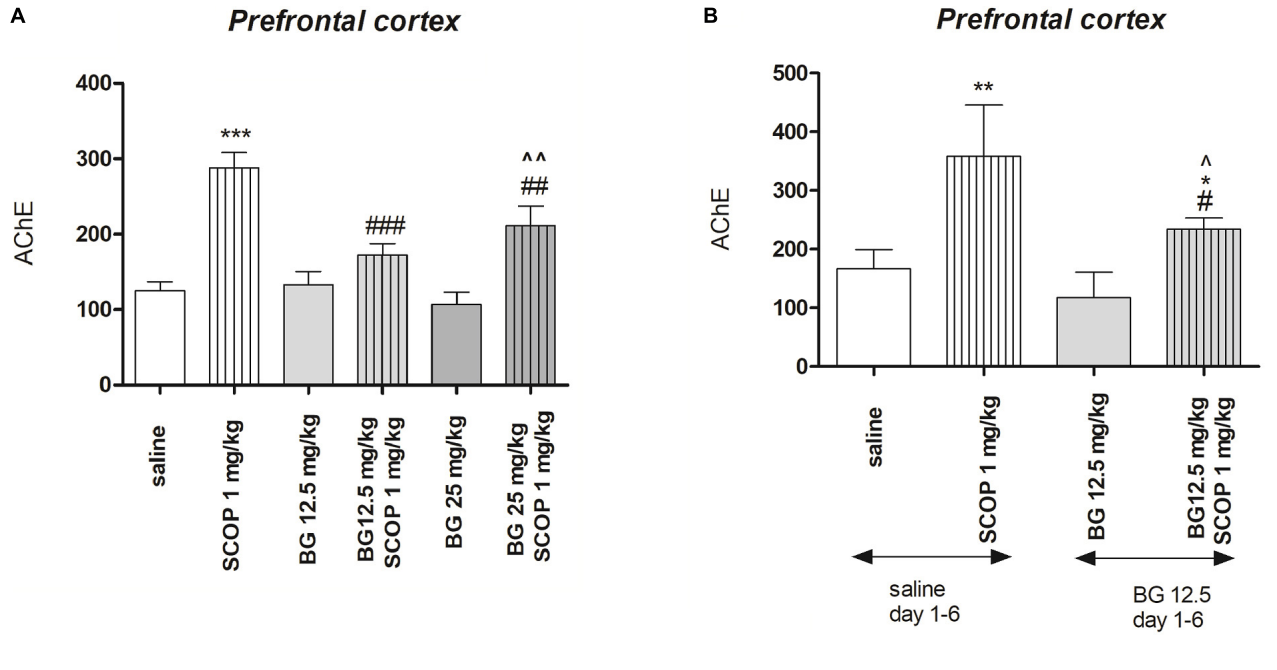

FIGURE 5 | Effects of acute **(A)** or subchronic **(B)** administration of bergapten (BG) on AChE level increased by scopolamine administration in the prefrontal cortex in mice. BG was administered 30 min and scopolamine (SCOP, 1 mg/kg, i.p.) *n* = 8–12; the means ± SEM; *$p < 0.05$, **$p < 0.01$, ***$p < 0.001$ *vs.* saline-treated control group, #$p < 0.05$, ##$p < 0.01$, ###$p < 0.001$ vs. scopolamine-treated control group, ^$p < 0.05$, ~$p < 0.01$ vs. bergapten-treated group; Bonferroni's test.

TAC level, being statistically significant for the highest dose of bergapten (25 mg/kg, $p < 0.05$) in comparison to scopolamine-treated group (**Figure 7A**).

Figure 7B indicates the effect of subchronic bergapten (12.5 mg/kg) administered alone or in combination with scopolamine (1 mg/kg) on TAC determined in the prefrontal cortex [pretreatment ($F(1,36) = 18.44$, $p = 0.0001$), treatment ($F(1,36) = 38.61$, $p < 0.0001$) without interactions ($F(1,36) = 3.433$, $p = 0.0721$); two-way ANOVA]. *Post hoc* Tukey's test confirmed statistically significant decrease in TAC level after single injection of scopolamine ($p < 0.01$). Administration of bergapten caused increase in TAC level, being statistically significant in the prefrontal cortex ($p < 0.05$) in comparison to scopolamine-treated group (**Figure 7B**).

DISCUSSION

In the present study, we revealed for the first time the procognitive effects of bergapten on memory processes, consolidation, and acquisition, in the scopolamine model of memory impairment in male Swiss mice. We also evaluated the presumable mechanisms underlying these effects. Our previous findings showed that xanthotoxin improved scopolamine-impaired consolidation and acquisition of memory. This effect resulted from decreased AChE activity and attenuation of oxidative stress processes (Skalicka-Wozniak et al., 2018). Consequently, in the present study, scopolamine was used as a tool substance for the induction of memory deficits in rodents. It was revealed that this compound induces cognitive disorders in various paradigms: radial maze (Buresová and Bures, 1982; Rahimzadegan and Soodi, 2018), object recognition and spatial tasks (Sambeth et al., 2007), Morris water maze, and PA test (Cozzolino et al., 1994). It is suggested that muscarinic receptors' blockade is crucial for memory impairment induced by scopolamine. Also, (Jang et al., 2013) apoptosis (Jahanshahi et al., 2013) and inflammatory responses (Ahmad et al., 2014) in brain tissue may play a role in these effects. One of the mechanisms responsible for scopolamine-induced amnesia is oxidative stress. Scopolamine was reported to exert pro-oxidative effects as it decreased activities of antioxidant enzymes such as superoxide dismutase, catalase, and glutathione peroxidase

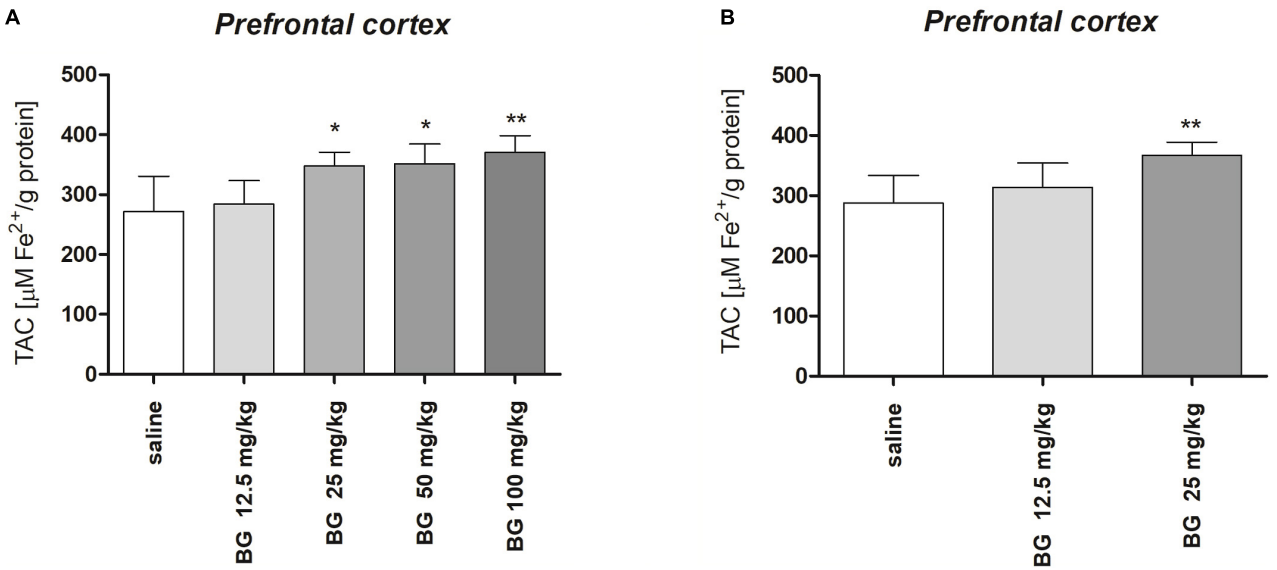

FIGURE 6 | Total antioxidant capacity (TAC) of the prefrontal cortex of mice brain after single **(A)** or subchronic **(B)** administration of bergapten (BG). The results are expressed as micromoles per gram protein and presented as the means ± SD; $n = 10$; $^{*}p < 0.05$, $^{**}p < 0.01$ vs. saline-treated control group; Tukey's test.

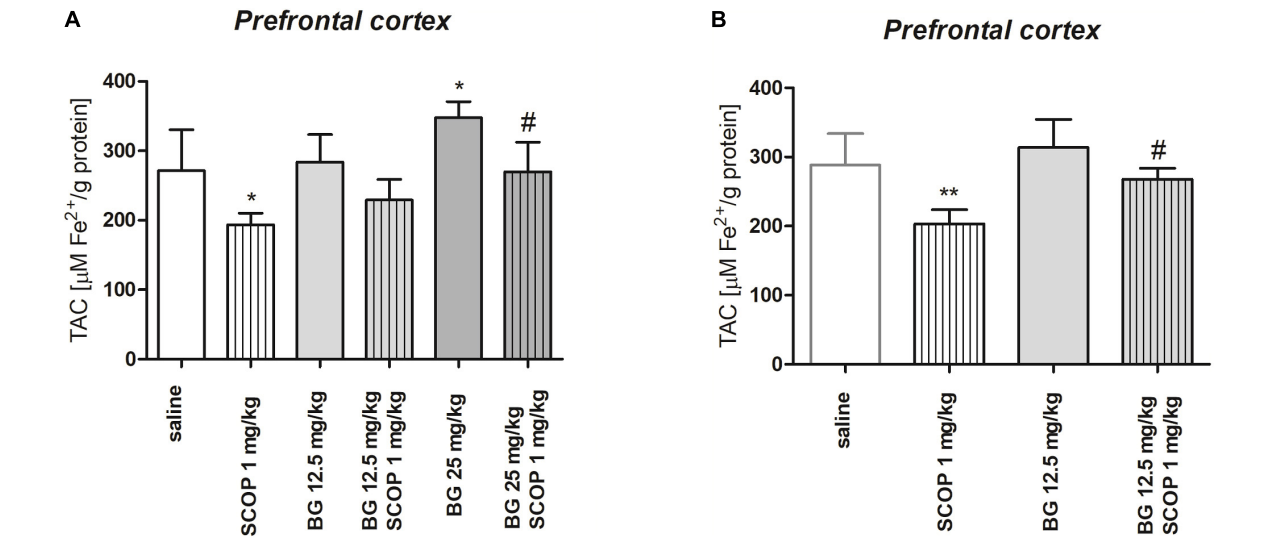

FIGURE 7 | Total antioxidant capacity (TAC) of the prefrontal cortex of mice brain after single **(A)** or subchronic **(B)** administration of bergapten (BG) or saline with or without scopolamine (1 mg/kg) administered 1 h before the decapitation. The results are expressed as micromoles per gram protein and presented as the means ± SD; $n = 10$; $^{*}p < 0.05$, $^{**}p < 0.01$ vs. saline-treated control group; $^{\#}p < 0.05$ vs. scopolamine-treated group; Bonferroni's test.

(Uma and Maheswari, 2014), and increased the concentration of malondialdehyde (MDA), which is the main marker of lipids peroxidation (Abd-El-Fattah et al., 2014). Moreover, several studies proved procognitive effects of antioxidant compounds in scopolamine-induced memory impairment, probably through attenuating the markers of oxidative stress (Harrison et al., 2009; Hritcu et al., 2015). Therefore, oxidative stress seems to play a crucial role in memory deficits caused by scopolamine.

The PA test was used as a validated paradigm for evaluation of the influence of different compounds on memory processes. PA is considered to be an aversive conditioning paradigm in which rodents learn to associate a specific compartment with the appearance of an unpleasant/aversive stimulus (e.g., electric shock). It is well established that administration of scopolamine as a nonselective muscarinic receptor antagonist before PA training induces impairment of acquisition of memory processes, whereas administration of scopolamine immediately after PA training disrupts consolidation of memory processes (Skalicka-Wozniak et al., 2018). Subsequent studies showed that the administration of cholinomimetic drugs

such as rivastigmine antagonized memory deficits induced by scopolamine (Bejar et al., 1999).

In our studies, we examined the acute and subchronic effects of bergapten. First, we evaluated if one dose of compound affects memory and learning processes. Subsequently, we assessed if any changes in behavioral processes and biochemical parameters occurred during subchronic administration. Since all of the current anti-dementia therapies are long-lasting, it was recommended to test the procognitive activity of bergapten also in the subchronic model of administration. The changes after acute and subchronic injections were compared with each other. Our behavioral study revealed that bergapten administered acutely at the doses of 25 mg/kg and 100 mg/kg improved acquisition as well as the consolidation of memory. Administered acutely at the dose of 50 mg/kg bergapten improved only the acquisition of memory. Furthermore, the coumarin at the lowest dose (12.5 mg/kg) did not show the influence on cognitive function. Subchronic administration improved both acquisition and consolidation (12.5 and 25 mg/kg) of memory processes, however, the effect is not dose-dependent. Additionally, acute administration of bergapten (25 mg/kg) decreased scopolamine-induced impairment of memory, whereas the dose of 12.5 mg/kg did not prevent amnesic effects of scopolamine. Furthermore, the subchronic administration of bergapten (12.5 mg/kg) improved only the consolidation of memory processes impaired by scopolamine. Interestingly, both acute and chronic injections of tested coumarin deceased the level of AChE elevated by scopolamine administration but TAC level was increased after the subchronic, not acute, model of drugs administration. Thus, we may speculate that cholinergic mechanisms (AChE level) together with antioxidative processes enhance procognitive effects induced by bergapten. However, other molecular and adaptive receptor changes may underlay these effects.

Importantly, bergapten at the used doses did not influence the motor coordination and locomotor activity. However, we cannot rule out adverse effects at other levels, such as anxiety, hepatotoxicity, or other characteristics for cholinomimetic drugs. Although we observed an increase of locomotor activity in the groups treated with scopolamine and bergapten (at both doses) when compared to scopolamine-injected mice, these results did not affect the acquisition and consolidation of memory as these processes were evaluated 24 h after the last injection. The next step in our study was to evaluate possible mechanisms underlying the procognitive effects of bergapten as well as the reason for the amelioration of cognitive deficits induced by scopolamine administration. Thus, the level of AChE and oxidative stress markers were examined. Biochemical analyses were performed on selected brain structures: the prefrontal cortex and hippocampus. The hippocampus is a part of the limbic system responsible for long-term and spatial memory. It is considered to be a structure that transfers information from short-term memory into long-term memory. It leads to the occurrence of various memories and learning processes (Abraham et al., 2019). Working (operational) memory is located in the prefrontal cortex (Anand and Dhikav, 2012). The cholinergic system is primarily involved in memory and attention-related functions. The age-related memory impairment, among others, results from a dysfunction of cholinergic transmission. ACh activates the neurons of the neocortex and hippocampus thereby facilitating the stimulation related to reward and associative learning (Rezayof et al., 2008; Yousefi et al., 2012; Zarrindast et al., 2012; Khakpai et al., 2013; Piri et al., 2013). ACh exerts its effects by activation of the muscarinic or nicotinic cholinergic receptors. Afterward, AChE and BuChE, enzymes synthesized in the postsynaptic membrane, break down ACh into choline and acetic acid. Physiologically, this mechanism prevents excessive activation of the neuronal system. However, the excessive degradation of ACh by AChE and BuChE leads to deterioration of cognitive functions. Thus, it is reasonable to introduce cholinesterase inhibitors as anti-dementia drugs. Many natural products or whole extracts from natural products inhibit AChE activity (Vallejo et al., 2007, 2009, 2017). Also, inhibitory activities of bergapten toward cholinesterase were investigated *in vitro*. It was revealed that bergapten, even at the lowest tested doses (12.5 $\mu g/mL^{-1}$), inhibited BChE more than AChE (37.77 and 84.82%, respectively), which is even more potent than galantamine (98.97 and 80.31% at 100 $\mu g/mL^{-1}$) (Senol et al., 2011).

Thus, our study was undertaken to evaluate bergapten activity as an AChE inhibitor in *ex vivo* study. We showed for the first time, that administration of bergapten either subchronically or acutely, did not change the level of AChE in the hippocampus and prefrontal cortex. In light of the in vitro experiments, further research concerning inhibition of BuChE should be undertaken *ex vivo*. Interestingly, bergapten diminished the level of the enzyme increased previously by scopolamine administration and these results comply with our previous study. Our previous experiments showed that acute and subchronic administration of xanthotoxin (1 mg/kg) did not influence the level of AChE in both tested brain structures, although it prevented the increase of the AChE activity caused by a single dose of scopolamine. Also, no improvement of memory and learning functions in the PA test after co-administration xanthotoxin and scopolamine was observed.

Memory improvement noticed after acute and subchronic administration of bergapten seems to be independent of AChE activity. Thus, other mechanisms may underlie these effects. On the other hand, bergapten decreased AChE activity when the level of the enzyme was altered by scopolamine application.

Additionally, as it was mentioned previously (Skalicka-Wozniak et al., 2018), processes connected with oxidative stress may underlie the improvement of cognitive function induced by coumarins. Our study proved that oxidative stress is involved in scopolamine-induced dementia as we observed a decrease in TAC as well as an increase in MDA (**Supplementary Material**) concentration. It can be the reason for long- and short-term memory's interferences too. Furthermore, our study revealed antioxidant properties of bergapten as well as its antioxidant activity against scopolamine-induced oxidative stress in a single dose and subchronic models of administration. Interestingly, the prefrontal cortex was more affected by bergapten than the hippocampus. This effect probably comes from the specific

functions of these regions in memory and cognitive functions. The prefrontal cortex is responsible for filtration, interpretation, and moderation of emerging stimuli (through sense organs) and thoughts that come into the brain. In other words, the prefrontal part is involved in slowing down aggression and fear, and blocking curiosity, which allows remembering emotions accompanying the events. The hippocampus is mainly responsible for declarative memory (regarding various events and situations), as well as for spatial memory and long-term memory. This means that it is in the "second line" of cognitive processes and probably it is less susceptible to temporary changes because it maintains its internal homeostasis (Tyng et al., 2017). The prefrontal cortex is also phylogenetically the youngest brain structure, therefore it is also the most susceptible to damage (Passingham and Wise, 2012). The coumarins can act as antioxidants to protect cells against free radicals.

Similarly to our findings, it was also revealed that Ishige foliacea extract (Kim et al., 2020) and *Elaeagnus umbellata* fruit extract improved memory processes in the scopolamine model of dementia in mice. Both of them showed antioxidant activity in the brain as well as AChE inhibition. Nazir et al. (2020) found out that *E. umbellata* fruit extract administered orally decreased the level of the highly active free radical, DPPH, in the hippocampus and frontal cortex. This antioxidant effect was associated with AChE inhibition and the procognitive effect in the novel object recognition test and Y-Maze test (Nazir et al., 2020). The study of Roshanbakhsh et al. (2020) revealed that another natural compound, piperine, improved memory impairments in rats by diminishing the iNOS level and increasing TAC in the hippocampus. This effect was associated with spatial memory improvement in the Morris water maze test (Roshanbakhsh et al., 2020). The scopolamine model of dementia was used by Ngoupaye et al. (2017) to prove the antioxidative effect of Gladiolus dalenii lyophilisate in the process of working and spatial memory improvement. In this study, the levels of malondialdehyde and AChE were decreased (Ngoupaye et al., 2017). We reported a similar result in our project. Due to the above, we suggest that antioxidant activity together with AChE inhibition in the hippocampus and prefrontal cortex might be significant in the improvement of memory processes.

Moreover, it was revealed that bergapten can inhibit MAO activity involved in regulation, e.g., depressive behaviors (Huong et al., 1999). This compound also shows anti-inflammatory properties associated with inhibition of interleukin 8, interleukin 6, and tumor necrosis factor (TNF). Oxidative stress and the neurotransmitter abnormalities underlie neurodegenerative diseases associated with memory impairments. Consequently, coumarins such as bergapten may become the basis for prophylaxis as well as therapies for these diseases (Budzyñska et al., 2015; Skalicka-Wozniak et al., 2018).

CONCLUSION

In summary, bergapten might be able to improve the acquisition and consolidation of memory. At the same time, it can effectively alleviate the cognitive symptoms of scopolamine-induced amnesia in the mouse. The mechanism of these effects seems unrevealed as bergapten did not change the level of AChE by itself but decreased the level of enzyme changed as a consequence of scopolamine administration. These new findings provide pharmacological and biochemical support for the development of the potential of coumarin in cognitive deficits. This hypothesis will form a new direction for our future research. Also, further studies concerning the administration of bergapten after scopolamine injection, to observe whether this compound can reverse established cognitive deficits, and not only propose them as prophylactic agents should be considered.

DATA AVAILABILITY STATEMENT

The raw data supporting the conclusions of this article will be made available by the authors, without undue reservation.

ETHICS STATEMENT

The animal study was reviewed and approved by Local Ethics Committee in Lublin, Poland.

AUTHOR CONTRIBUTIONS

JK, MW-K, and BB performed behavioral experiments. KS-W and AS performed phytochemical isolation. AB-C and JK performed biochemical study. JK, BB, MK-S, and AB-C analyzed data. KS-W, BB, AB-C, and JK wrote the manuscript. GB checked the manuscript. KS-W provided research materials. All authors contributed to the article and approved the submitted version.

FUNDING

This work was supported by the National Science Centre, Poland (2014/13/B/NZ4/01249).

SUPPLEMENTARY MATERIAL

The Supplementary Material for this article can be found online at: https://www.frontiersin.org/articles/10.3389/fnins.2020.00730/full#supplementary-material

REFERENCES

Abd-El-Fattah, M. A., Abdelakader, N. F., and Zaki, H. F. (2014). Pyrrolidine dithiocarbamate protects against scopolamine-induced cognitive impairment in rats. *Eur. J. Pharmacol.* 723, 330–338. doi: 10.1016/j.ejphar.2013.11.008

Abraham, W. C., Jones, O. D., and Glanzman, D. L. (2019). Is plasticity of synapses the mechanism of long-term memory storage? *npj Sci. Learn.* 4:9.

Ahmad, A., Ramasamy, K., Jaafar, S. M., Majeed, A. B., and Mani, V. (2014). Total isoflavones from soybean and tempeh reversed scopolamine-induced amnesia,

improved cholinergic activities and reduced neuroinflammation in brain. *Food Chem. Toxicol.* 65, 120–128. doi: 10.1016/j.fct.2013.12.025

Allami, N., Javadi-Paydar, M., Rayatnia, F., Sehhat, K., Rahimian, R., Norouzi, A., et al. (2011). Suppression of nitric oxide synthesis by L-NAME reverses the beneficial effects of pioglitazone on scopolamine-induced memory impairment in mice. *Eur. J. Pharmacol.* 650, 240–248. doi: 10.1016/j.ejphar.2010.10.007

Anand, K. S., and Dhikav, V. (2012). Hippocampus in health and disease: an overview. *Ann. Indian Acad. Neurol.* 15, 239–246. doi: 10.4103/0972-2327.104323

Bejar, C., Wang, R. H., and Weinstock, M. (1999). Effect of rivastigmine on scopolamine-induced memory impairment in rats. *Eur. J. Pharmacol.* 383, 231–240. doi: 10.1016/s0014-2999(99)00643-3

Bose, S. K., Dewanjee, S., Sahu, R., and Dey, S. P. (2011). Effect of bergapten from Heracleum nepalense root on production of proinflammatory cytokines. *Nat. Prod. Res.* 25, 1444–1449. doi: 10.1080/14786410902800665

Budzyñska, B., Boguszewska-Czubara, A., Kruk-Slomka, M., Skalicka-Wozniak, K., Michalak, A., Musik, I., et al. (2015). Effects of imperatorin on scopolamine-induced cognitive impairment and oxidative stress in mice. *Psychopharmacology* 232, 931–942. doi: 10.1007/s00213-014-3728-6

Budzyñska, B., Skalicka-Wozniak, K., Kruk-Slomka, M., Wydrzynska-Kuzma, M., and Biala, G. (2016). In vivo modulation of the behavioral effects of nicotine by the coumarins xanthotoxin, bergapten, and umbelliferone. *Psychopharmacology* 233, 2289–2300. doi: 10.1007/s00213-016-4279-9

Bukowska, B., Pajak, A., Koceva-Chyla, A., Pietras, T., Nizinkowski, P., Gorski, P., et al. (2017). Decreased activity of butyrylcholinesterase in blood plasma of patients with chronic obstructive pulmonary disease. *Arch. Med. Sci.* 13, 645–651. doi: 10.5114/aoms.2016.60760

Buresová, O., and Bures, J. (1982). Radial maze as a tool for assessing the effect of drugs on the working memory of rats. *Psychopharmacology* 77, 268–271. doi: 10.1007/bf00464578

Chimakurthy, J., and Talasila, M. (2010). Effects of curcumin on pentylenetetrazole-induced anxiety-like behaviors and associated changes in cognition and monoamine levels. *Psychol. Neurosci.* 3, 238–244. doi: 10.3922/j.psns.2010.2.013

Cozzolino, R., Guaraldi, D., Giuliani, A., Ghirardi, O., Ramacci, M. T., and Angelucci, L. (1994). Effects of concomitant nicotinic and muscarinic blockade on spatial memory disturbance in rats are purely additive: evidence from the Morris water task. *Physiol. Behav.* 56, 111–114. doi: 10.1016/0031-9384(94)90267-4

Deng, G., Wu, C., Rong, X., Li, S., Ju, Z., Wang, Y., et al. (2019). Ameliorative effect of deoxyvasicine on scopolamine-induced cognitive dysfunction by restoration of cholinergic function in mice. *Phytomedicine* 63:153007. doi: 10.1016/j.phymed.2019.153007

Dunham, N. W., and Miya, T. S. (1957). A note on a simple apparatus for detecting neurological deficit in rats and mice. *J. Am. Pharm. Assoc. Am. Pharm Assoc.* 46, 208–209. doi: 10.1002/jps.3030460322

Harrison, F. E., Hosseini, A. H., Dawes, S. M., Weaver, S., and May, J. M. (2009). Ascorbic acid attenuates scopolamine-induced spatial learning deficits in the water maze. *Behav. Brain Res.* 205, 550–558. doi: 10.1016/j.bbr.2009.08.017

Ho, P. C., Saville, D. J., and Wanwimolruk, S. J. (2001). Inhibition of human CYP3A4 activity by grapefruit flavonoids, furanocoumarins and related compounds. *J. Pharm. Pharm. Sci.* 4, 217–227.

Hritcu, L., Stefan, M., Brandsch, R., and Mihasan, M. (2015). Enhanced behavioral response by decreasing brain oxidative stress to 6-hydroxy-l-nicotine in Alzheimer's disease rat model. *Neurosci. Lett.* 591, 41–47. doi: 10.1016/j.neulet.2015.02.014

Huong, D. T., Choi, H. C., Rho, T. C., Lee, H. S., Lee, M. K., and Kim, Y. H. (1999). Inhibitory activity of monoamine oxidase by coumarins from Peucedanum japonicum. *Arch. Pharm. Res.* 22, 324–326. doi: 10.1007/bf02976373

Jahanshahi, M., Nickmahzar, E. G., and Babakordi, F. (2013). Effect of Gingko biloba extract on scopolamine-induced apoptosis in the hippocampus of rats. *Anat. Sci. Int.* 88, 217–222. doi: 10.1007/s12565-013-0188-8

Jang, Y. J., Kim, J., Shim, J., Kim, C. Y., Jang, J. H., Lee, K. W., et al. (2013). Decaffeinated coffee prevents scopolamine-induced memory impairment in rats. *Behav. Brain Res.* 245, 113–119. doi: 10.1016/j.bbr.2013.02.003

Javadi-Paydar, M., Zakeri, M., Norouzi, A., Rastegar, H., Mirazi, N., and Dehpour, A. R. (2012). Involvement of nitric oxide in granisetron improving effect on scopolamine-induced memory impairment in mice. *Brain Res.* 1429, 61–71. doi: 10.1016/j.brainres.2011.08.006

Khakpai, F., Zarrindast, M. R., Nasehi, M., Haeri-Rohani, A., and Eidi, A. (2013). The role of glutamatergic pathway between the septum and hippocampus in the memory formation. *EXCLI J.* 12, 41–51.

Kim, T. E., Son, H. J., Lim, D. W., Yoon, M., Lee, J., and Kim, Y. T. (2020). Memory-enhancing effects of Ishige foliacea extract: in vitro and in vivo study. *J. Food Biochem.* 4;e13162. doi: 10.1111/jfbc.13162

Kruk-Slomka, M., Budzyñska, B., and Biala, G. (2012). Involvement of cholinergic receptors in the different stages of memory measured in the modified elevated plus maze test in mice. *Pharmacol. Rep.* 64, 1066–1080. doi: 10.1016/s1734-1140(12)70904-0

Liu, W. X., Jia, F. L., He, Y. Y., and Zhang, B. X. (2012). Protective effects of 5-methoxypsoralen against acetaminophen-induced hepatotoxicity in mice. *World J. Gastroenterol.* 18, 2197–2202. doi: 10.3748/wjg.v18.i18.2197

Luszczki, J. J., Andres-Mach, M., Glensk, M., and Skalicka-Wozniak, K. (2010). Anticonvulsant effects of four linear furanocoumarins, bergapten, imperatorin, oxypeucedanin, and xanthotoxin, in the mouse maximal electroshock-induced seizure model: a comparative study. *Pharmacol. Rep.* 62, 1231–1236. doi: 10.1016/s1734-1140(10)70387-x

Nazir, N., Zahoor, M., Nisar, M., Karim, N., Latif, A., and Ahmad, S. (2020). Evaluation of neuroprotective and anti-amnesic effects of *Elaeagnus umbellata* Thunb. on scopolamine-induced memory impairment in mice. *BMC Complement Med Ther.* 20:143. doi: 10.1186/s12906-020-02942-3

Ngoupaye, G. T., Pahaye, D. B., Ngondi, J., Moto, F. C. O., and Bum, E. N. (2017). Gladiolus dalenii lyophilisate reverses scopolamine-induced amnesia and reduces oxidative stress in rat brain. *Biomed. Pharmacother.* 91, 350–357. doi: 10.1016/j.biopha.2017.04.061

Panno, M. L., Giordano, F., Rizza, P., Pellegrino, M., Zito, D., Giordano, C., et al. (2012). Bergapten induces ER depletion in breast cancer cells through SMAD4-mediated ubiquitination. *Breast Cancer Res. Treat.* 136, 443–455. doi: 10.1007/s10549-012-2282-3

Parihar, M. S., and Brewer, G. J. (2010). Amyloid Beta as a Modulator of Synaptic Plasticity. *J. Alzheimers. Dis.* 22, 741–763. doi: 10.3233/JAD-2010-101020

Passingham, R. E., and Wise, S. P. (2012). *The Neurobiology of the Prefrontal Cortex: Anatomy, Evolution, and the Origin of Insight*. Oxford: Oxford University Press.

Phaniendra, A., Jestadi, D. B., and Periyasamy, L. (2015). Free radicals: properties, sources, targets, and their implication in various diseases. *Indian J. Clin. Biochem.* 30, 11–26. doi: 10.1007/s12291-014-0446-0

Piri, M., Rostampour, M., Nasehi, M., and Zarrindast, M. R. (2013). Blockade of the dorsal hippocampal dopamine D1 receptors inhibits the scopolamine-induced state-dependent learning in rats. *Neuroscience* 252, 460–467. doi: 10.1016/j.neuroscience.2013.08.003

Rahimzadegan, M., and Soodi, M. (2018). Comparison of memory impairment and oxidative stress following single or repeated doses administration of scopolamine in rat hippocampus. *Basic clin. Neurosci.* 9, 5–14. doi: 10.29252/NIRP.BCN.9.1.5

Rezayof, A., Darbandi, N., and Zarrindast, M. R. (2008). Nicotinic acetylcholine receptors of the ventral tegmental area are involved in mediating morphine-state-dependent learning. *Neurobiol. Learn. Mem.* 90, 255–260. doi: 10.1016/j.nlm.2008.03.004

Rohini, K., and Srikumar, P. S. (2014). Therapeutic role of coumarins and coumarin-related compounds. *J. Thermodyn. Catal.* 5:2. doi: 10.4172/2157-7544.1000130

Roshanbakhsh, H., Elahdadi, S. M., Dehghan, S., Nazari, A., Javan, M., and Pourabdolhossein, F. (2020). Piperine ameliorated memory impairment and myelin damage in lysolecethin induced hippocampal demyelination. *Life Sci.* 253:117671. doi: 10.1016/j.lfs.2020.117671

Sambeth, A., Riedel, W. J., Smits, L. T., and Blokland, A. (2007). Cholinergic drugs affect novel object recognition in rats: relation with hippocampal EEG? *Eur. J. Pharmacol.* 572, 151–159. doi: 10.1016/j.ejphar.2007.06.018

Senol, F. S., Orhan, I. E., Erdem, S. A., Kartal, M., Sener, B., Kan, Y., et al. (2011). Evaluation of cholinesterase inhibitory and antioxidant activities of wild and cultivated samples of sage (Salvia fruticosa) by activity-guided fractionation. *Med. Food* 14, 1476–1483. doi: 10.1089/jmf.2010.0158

Senol, F. S., Orhan, I. E., and Ustun, O. (2015). In vitro cholinesterase inhibitory and antioxidant effect of selected coniferous tree species. *Asian Pac. J. Trop. Med.* 8, 269–275. doi: 10.1016/S1995-7645(14)60329-1

Skalicka-Wozniak, K., Budzynska, B., Biala, G., and Boguszewska-Czubara, A. (2018). Scopolamine-induced memory impairment is alleviated by xanthotoxin: role of acetylcholinesterase and oxidative stress processes. *ACS Chem. Neurosci.* 9, 1184–1194. doi: 10.1021/acschemneuro.8b00011

Skalicka-Wozniak, K., Orhan, I. E., Cordell, G. A., Nabavi, S. M., and Budzynska, B. (2016). Implication of coumarins towards central nervous system disorders. *Pharmacol. Res.* 103, 188–203. doi: 10.1016/j.phrs.2015.11.023

Tanew, A., Radakovic-Fijan, S., Schemper, M., and Hönigsmann, H. (1999). Narrowband UV-B phototherapy vs photochemotherapy in the treatment of chronic plaque-type psoriasis: a paired comparison study. *Arch. Dermatol.* 135, 519–524.

Tyng, C. M., Amin, H. U., Saad, M. N. M., and Malik, A. S. (2017). The influences of emotion on learning and memory. *Front. Psychol.* 8:1454.

Uma, G., and Maheswari, S. U. (2014). Neuroprotective effects of polyherbal formulation (Indian) on noni scopolamineinduced memory impairment in mice. *Int. J. Pharm. Pharm. Sci.* 6, 354–357.

Vallejo, M., Carlini, V., Gabach, L., Ortega, M. G., Cabrera, L. J., de Barioglio, S. R., et al. (2017). Sauroxine reduces memory retention in rats and impairs hippocampal long-term potentiation generation. *Biomed. Pharmacother.* 91, 155–161. doi: 10.1016/j.biopha.2017.04.016

Vallejo, M. G., Ortega, M. G., Cabrera, J. L., Carlini, V. P., de Barioglio, S. R., and Agnese, A. M. (2007). Huperzia saururus increases memory retention in rats. *J. Ethnopharmacol.* 111, 685–687. doi: 10.1016/j.jep.2007.01.012

Vallejo, M. G., Ortega, M. G., Cabrera, J. L., Carlini, V. P., de Barioglio, S. R., Almirón, R. S., et al. (2009). Sauroine, an alkaloid from *Huperzia saururus* with activity in wistar rats in electrophysiological and behavioral assays related to memory retention. *J. Nat. Prod.* 72, 156–158. doi: 10.1021/np800151v

Venault, P., Chapouthier, G., de Carvalho, L. P., Simiand, J., Morre, M., Dodd, R. H., et al. (1986). Benzodiazepine impairs and beta-carboline enhances performance in learning and memory tasks. *Nature* 321, 864–866. doi: 10.1038/321864a0

Wszelaki, N. (2009). Plants as a source of acetylcholinesterase and butyrylcholinesterase inhibitors. *Postêpy Fitoterapii.* 10, 24–38.

Wszelaki, N., Paradowska, K., Jamróz, M. K., Granica, S., and Kiss, A. K. (2011). Bioactivity-guided fractionation for the butyrylcholinesterase inhibitory activity of furanocoumarins from Angelica archangelica L. roots and fruits. *J. Agric. Food Chem.* 59, 9186–9193. doi: 10.1021/jf201971s

Yousefi, B., Nasehi, M., Khakpai, F., and Zarrindast, M. R. (2012). Possible interaction of cholinergic and GABAergic systems between MS and CA1 upon memory acquisition in rats. *Behav. Brain Res.* 235, 231–243. doi: 10.1016/j.bbr.2012.08.006

Zarrindast, M. R., Ardjmand, A., Ahmadi, S., and Rezayof, A. (2012). Activation of dopamine D1 receptors in the medial septum improves scopolamine-induced amnesia in the dorsal hippocampus. *Behav. Brain Res.* 229, 68–73. doi: 10.1016/j.bbr.2011.12.033

Zhou, Y., Wang, J., Yang, W., Qi, X., Lan, L., Luo, L., et al. (2017). Bergapten prevents lipopolysaccharide-induced inflammation in RAW264.7 cells through suppressing JAK/STAT activation and ROS production and increases the survival rate of mice after LPS challenge. *Int. Immunopharmacol.* 48, 159–168. doi: 10.1016/j.intimp.2017.04.026

Conflict of Interest: The authors declare that the research was conducted in the absence of any commercial or financial relationships that could be construed as a potential conflict of interest.

frontiers in Behavioral Neuroscience

ORIGINAL RESEARCH
published: 21 August 2020
doi: 10.3389/fnbeh.2020.00152

The Reversal of Memory Deficits in an Alzheimer's Disease Model Using Physical and Cognitive Exercise

*Leticia R. Dare[1], Alexandre Garcia[1], Caroline B. Soares[1], Luiza Lopes[1], Ben-Hur S. Neves[1], Daniel V. Dias[2] and Pâmela B. Mello-Carpes[1]**

[1]Physiology Research Group, Federal University of Pampa, Uruguaiana, Brazil, [2]Department of Structural Biology, Federal University of Triangulo Mineiro, Uberaba, Brazil

Alzheimer's disease (AD) is the leading cause of dementia in the world, accounting for 50–75% of cases. Currently, there is limited treatment for AD. The current pharmacological therapy minimizes symptom progression but does not reverse brain damage. Studies focused on nonpharmacological treatment for AD have been developed to act on brain plasticity and minimize the neurotoxicity caused by the amyloid-beta (Aβ) peptide. Using a neurotoxicity model induced by Aβ in rats, the present study shows that physical (PE) and cognitive exercise (CE) reverse recognition memory deficits (with a prominent effect of long-term object recognition memory), decrease hippocampal lipid peroxidation, restore the acetylcholinesterase activity altered by Aβ neurotoxicity, and seems to reverse, at least partially, hippocampal tissue disorganization.

Keywords: Alzheimer's disease, physical exercise, cognitive exercise, oxidative damage, Aβ neurotoxicity

OPEN ACCESS

Edited by:
Nady Braidy, University of New South Wales, Australia

Reviewed by:
Joaquim Pereira Brasil-Neto, Unieuro, Brazil
Igor Klyubin, Trinity College Dublin, Ireland

****Correspondence:***
Pâmela B. Mello-Carpes
pamelacarpes@unipampa.edu.br

Specialty section:
This article was submitted to Learning and Memory, a section of the journal Frontiers in Behavioral Neuroscience

Received: *07 March 2020*
Accepted: *03 August 2020*
Published: *21 August 2020*

Citation:
Dare LR, Garcia A, Soares CB, Lopes L, Neves B-HS, Dias DV and Mello-Carpes PB (2020) The Reversal of Memory Deficits in an Alzheimer's Disease Model Using Physical and Cognitive Exercise. Front. Behav. Neurosci. 14:152. doi: 10.3389/fnbeh.2020.00152

INTRODUCTION

According to the World Health Organization, Alzheimer's disease (AD) is a global public health priority (Lane et al., 2018). This neurodegenerative disease is the most common form of dementia, accounting for 50–75% of cases (Prince et al., 2015). AD is related to aging, and every 5 years after 65 years of age, its prevalence doubles (Prince et al., 2015).

The formation and aggregation of abnormal amyloid-beta (Aβ) peptides in the extracellular space, hyperphosphorylated tau protein, and brain oxidative stress are some of the pathological alterations found in AD (Grundke-Iqbal et al., 1986; Selkoe, 1999; Lee et al., 2001; Moneim, 2015). These alterations lead to a gradual loss of cognitive function, usually starting with short-term memory (STM) dysfunction, impaired judgment and reasoning, and disorientation and culminating in total memory loss and personality alterations (Martins et al., 2018).

In addition to the high prevalence of AD, there are limited options for treatment for this disease. Furthermore, the current pharmacological therapies only minimize the progression of the symptoms; they do not reverse brain damage (Habtemariam, 2019). In this sense, research focused on nonpharmacological treatment has been developed (Zucchella et al., 2018). Among the possible nonpharmacological strategies is physical exercise (PE).

PE improves cerebral blood circulation, thereby increasing the supply of oxygen and energetic substrates to the brain (Black et al., 1991). The effects of aerobic exercises, such as running on a treadmill, can also be related to its effect on reducing the formation of amyloid plaques and the hyperphosphorylation of tau and on reducing neuroinflammation and oxidative stress (Dao et al., 2014; Koo et al., 2017; Lu et al., 2017).

Another potential nonpharmacological treatment is cognitive exercise (CE). Cognitive training contributes to maintaining neural functions, promoting cognitive flexibility, decreasing oxidative stress, and improving the quality of life in patients. Evidence suggests that CE produces long-lasting improvements in the memory performance of older adults who experience a normal cognitive decline (Winocur et al., 2007). Previous studies have demonstrated that cognitive stimulation programs are effective in maintaining cognition and quality of life in AD patients with mild to moderate dementia (Woods et al., 2012; Epperly et al., 2017). Despite these positive observations, the mechanisms by which CE acts in the AD brain are not yet well described. Recently, using an animal model of Aβ neurotoxicity, we showed that CE is effective in protecting against memory deficits when it is performed before neurotoxicity induction (Rossi Dare et al., 2019). In this case, we observed that CE was able to avoid the brain oxidative imbalance induced by Aβ.

One of the main properties of the brain is neuroplasticity. The term "neuroplasticity" refers to the ability of the organ to change according to external stimuli, altering its function and morphology through neural mechanisms such as synaptogenesis and neurogenesis (Lövdén et al., 2013; Calabrese et al., 2014). Learning and memory are examples of functions that are highly dependent on hippocampal neuroplasticity; deficits in this process, as occur in AD, lead to memory impairments (Yau et al., 2015). Cognitive plasticity may be strengthened *via* aerobic (Foster et al., 2011) and cognitive training (Greenwood and Parasuraman, 2010).

It is important to highlight that our group has already demonstrated that CE is as good as PE as a preventive strategy for memory deficits related to Aβ neurotoxicity (Rossi Dare et al., 2019). Despite the well-demonstrated preventive effects of PE and CE, we investigated whether the same strategies could be used to treat memory deficits. In the present case, PE and CE training were introduced after the induction of Aβ neurotoxicity, when cognitive deficits were already established. Our results demonstrate that PE and CE can reverse memory deficits, hippocampal oxidative imbalance, and some hippocampal morphological alterations related to Aβ neurotoxicity.

MATERIALS AND METHODS

Animals and Experimental Design

All experiments were carried out according to the Principles of Laboratory Animal Care and in agreement with the guidelines established by the Local Institutional Animal Care and Use Committee (approved protocol n. 14/2017). Adult male Wistar rats were purchased from the Federal University of Santa Maria (RS/Brazil) and were housed at the institute's vivarium under controlled temperature (23 ± 2°C) in a 12-h light-dark cycle, with food and water available *ad libitum*.

Initially, the animals were divided into two large groups and were subjected to stereotaxic surgery for intrahippocampal infusion of Aβ protein or saline (vehicle), followed by 10 days of recovery from surgery and Aβ aggregation. After this period, animals were subdivided according to the treatments (PE training, CE training, or no treatment), resulting in six groups (n = 12/group): sham surgery (Control); Aβ-induced neurotoxicity model (Aβ); sham surgery and PE training (PE); sham surgery and CE training (CE); Aβ and PE training (Aβ + PE); and Aβ and CE training (Aβ + CE). After that, the animals were subjected to behavioral tests to evaluate recognition memory and to monitor control parameters. Finally, the rats were euthanized, and brain tissue was collected for biochemical testing (n = 8) or histological analyses (n = 4; **Figure 1**).

Aβ-Induced Neurotoxicity Model

Aβ peptide 25–35 (A4559; Sigma–Aldrich) was dissolved in saline solution (i.e., vehicle) at a concentration of 100 μM and incubated at 37°C for 4 days to induce Aβ 25–35 aggregation initiation. A total volume of 2.0 μl of Aβ protein was injected into each hippocampus based on the Paxinos and Watson brain atlas coordinates (anterior-posterior = −4.2 mm; lateral–lateral, ± 3.0 mm; ventral-medial, −3.0 mm) by stereotaxic microinjection using a Hamilton syringe and an infusion pump. After surgery, rats were returned to their home cages and were monitored for 10 days.

Treatments

Physical Exercise (PE)

Before PE training, the rats were habituated to a treadmill built for rodents (Insight Limited, São Paulo, Brazil) to avoid stress effects. The habituation was conducted for 3 days (on the first day, the animals were placed on the treadmill turned off for 10 min; on the second and third days, they were put in the treadmill at a velocity of 2–5 m/min for 10 min).

After the rats were subjected to the "good runner protocol," which consists of placing the animals on the treadmill without inclination for three consecutive days (velocity 8 m/min for 10 min), the level of trainability was evaluated with a score ranging from 1 to 5 points (1: refuses to run; 2: below the average of the runners—runs and stops or runs in the wrong direction; 3: average runner; 4: above the average—runs well, with sporadic stops; 5: good runner—runs and always stays in the front part of the treadmill). In the end, the animals that maintained an average of three or more points were included in the exercise group.

On the last day, an indirect oxygen consumption (VO_2) running test was performed to determine the individual intensity of exercise. For this, the rats started running at a low velocity, which was increased 5 m/min every 3 min until the rat was unable to keep running. The time to fatigue (min) and the work volume (m/min) were considered indirect measures of maximal indirect VO_2 (Brooks and White, 1978).

The PE started in the following week and was performed at an intensity of 60–70% of the maximal indirect VO_2 (Cechetti et al., 2012; Malek et al., 2013), three times a week, once a day for 30 min, for 4 weeks, without treadmill inclination.

Cognitive Exercise (CE)

The CE was based on the adaptation of the Barnes maze memory task (Barnes, 1979) as proposed by Rossi Dare et al. (2019). The Barnes maze is a circular platform with 20 potential escape holes,

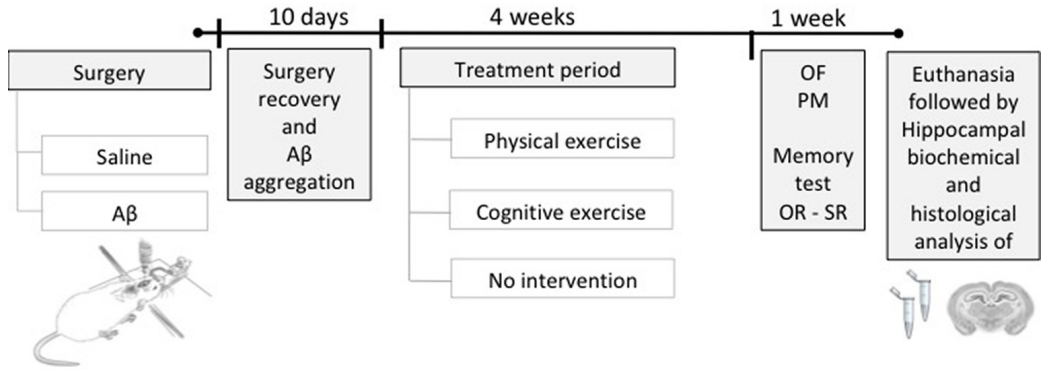

FIGURE 1 | Experimental design. Rats were submitted to a stereotaxic surgery with the injection of Aβ or saline solution (sham surgery) in the hippocampus. Ten days after surgery, the time required for surgery recovery and Aβ aggregation, the training period started, being: physical exercise (PE), cognitive exercise (CE), or none (no intervention), during 4 weeks. Afterward, behavioral tests were performed to evaluate the object and social recognition memory and to monitor the general behavioral; after, the euthanasia was performed to brain tissue collection for histological and biochemical analyses. OR, object recognition memory test; SR, social recognition memory test; OF, open field; PM, plus maze.

equally spaced in the periphery, only one of which leads to an escape cage. Negative reinforcement (bright lights) is used to motivate the animal to escape to a dark cage hidden underneath one of the holes. Visual cues surrounding the maze are used to make spatial learning possible.

To perform the CE, the animals were trained every day in the Barnes maze for 4 weeks, and each day, they were able to perform the CE more efficiently, i.e., they found the escape hole more quickly using the spatial cues. Therefore, every 10 days, the escape cage was altered to another place; consequently, the animals had to form a new spatial memory, which required cognitive flexibility (Rossi Dare et al., 2019).

Control Behavioral Tasks

The open field (OF) and elevated plus maze (PM) were used to analyze exploratory and locomotor activities and to evaluate anxiety state, respectively.

In the OF, the rats were placed in the left quadrant of a 50 × 50 × 39 cm open field made with wood painted white, with a frontal glass wall. Black lines were drawn on the floor to divide it into 12 equal quadrants. Crossing and rearing, as measures of locomotor and exploratory activities, respectively, were measured over 5 min (Bonini et al., 2006).

In the PM, the rats were placed in the center of the maze. The maze consists of two open arms (50 × 10 cm) and two enclosed arms (50 × 10 × 40 cm), with an open roof, arranged such that the two open arms were opposite to each other. The maze is elevated to a height of 50 cm. The total number of entries and the time spent in the four arms were recorded over a 5-min session (Pellow et al., 1985).

Memory Tests

Object Recognition (OR)

Rats were first habituated individually to the OR memory task apparatus and left to freely explore it for 20 min during four consecutive days before the training session. On the fifth day, OR memory training was performed. In the training, two different novel objects were placed in the apparatus, and rats were allowed to freely explore them for 5 min. Three hours and 24 h later, STM and long-term memory (LTM) were evaluated, respectively (Broadbent et al., 2010). In each testing session, one of the objects was randomly replaced by a novel/unfamiliar object, and the rats were reintroduced into the apparatus for an additional 5 min period of free exploration. The time spent exploring the familiar and novel objects was recorded. Additionally, the discrimination index (DI) on STM and LTM tests was determined by the difference of time spent exploring the new (T novel) and the familiar (T familiar) objects: DI = [(T novel − T familiar)/(T novel + T familiar) × 100 (%)], and used as a memory parameter.

Social Recognition (SR)

The SR memory task is an adaptation of the social interaction test proposed by Kaidanovich-Beilin et al. (2011). The task was completed in 3 days. First, the rats were placed in an arena with two small cages for 20 min for habituation to the apparatus. On the following day, a training session was performed with the inclusion of one unfamiliar rat in one of the cages for 10 min of free exploration. After 24 h, a testing session was performed when the same rat from the training (now a familiar rat) and a new/unfamiliar rat was placed for exploration for 10 min. The time spent exploring the familiar and novel rats was recorded. Exploration of the conspecific animal was defined as sniffing or touching the small cages with the nose and/or forepaws. Additionally, the DI was determined by the difference of time spent exploring the unfamiliar (T novel) and the familiar (T familiar) rat: DI = [(T unfamiliar − T familiar)/(T unfamiliar + T familiar) × 100 (%)], and used as a memory parameter.

Biochemical Testing

After euthanasia, the brain tissues of some animals (n = 8) were quickly removed, and then the hippocampal tissues were immediately isolated from the brain and cleaned using ice-cold

saline. Tissue samples were frozen in liquid nitrogen and stored at −80°C until biochemical analysis was performed.

For biochemical experiments, the tissue samples were homogenized in 50 mM Tris-HCl, pH 7.4. The homogenates were centrifuged at 2,400 *g* for 20 min at 4°C to obtain supernatants that were used for the analysis of all biochemical variables.

Hippocampal reactive oxygen species (ROS) levels were measured by a spectrofluorometric method using 20,70-dichlorofluorescein diacetate (DCFH-DA; Loetchutinat et al., 2005). The sample was incubated in darkness with 5 μl of DCFH-DA (1 mM). The oxidation of DCHF-DA to fluorescent dichlorofluorescein (DCF) was measured for the detection of intracellular ROS. The formation of the oxidized fluorescent derivative (i.e., DCF), measured by DCF fluorescence intensity, was recorded at 520 nm (480-nm excitation) 30 min after the addition of DCFH-DA to the medium. The results are expressed as arbitrary units.

The hippocampal lipid peroxidation level was evaluated by the TBARS test (Ohkawa et al., 1979). The samples were incubated with a 0.8% thiobarbituric acid solution, acetic acid buffer (pH 3.2), and SDS solution (8%) at 95°C for 2 h and the color reaction was measured at 532 nm. The results were expressed as nanomoles of malondialdehyde per milligram of protein.

The total antioxidant capacity was measured by FRAP (ferric reducing/antioxidant power) assay. The working FRAP reagent was prepared by mixing 25 ml acetate buffer, 2.5 ml TPTZ solution, and 2.5 ml $FeCl_3 \cdot 6H_2O$ solution. The homogenate (10 μl) was added to 300 μl of working FRAP reagent in a microplate (Benzie and Strain, 1996). Additionally, a standard curve with 10 μl Trolox concentrations (15, 30, 60, 120, and 240 mM) and 300 μl working FRAP reagent was used. The microplate was incubated at 37°C for 15 min before reading in a SpectraMax M5 Microplate Reader at 593 nm.

Acetylcholinesterase (AChE) activity is a marker of the loss of cholinergic neurons in the forebrain. The AChE activity was assessed by the Ellman method (Ellman et al., 1961). The reaction mixture was composed of 100 mM phosphate buffer, pH 7.4, and 1 mM 5,5′-dithio-bis-2-nitrobenzoic acid. The method is based on the formation of a yellow anion, 4,4′-dithio-bis nitrobenzoic acid, after the addition of 0.8 mM acetylthiocholine iodide. The change in absorbance was measured for 2 min at 30-s intervals at 412 nm (SpectraMax M5; Molecular Devices). The results were expressed as micromoles of acetylthiocholine iodide hydrolyzed per minute per milligram of protein.

Histological Analysis

Some rats ($n = 4$) were anesthetized and transcardially perfused with phosphate-buffered saline (PBS) solution followed by 4% formaldehyde. Brains were removed, postfixed for 24 h in 4% formaldehyde, and cryopreserved in 30% sucrose overnight at 4°C. Then, the brains were frozen, and coronal brain sections (12 μm thickness) were cut in a Cryostat (LEICA CM3050S). The sections were stained by hematoxylin-eosin (HE), and a qualitative analysis of the morphological parameters were observed under an optical microscope (Olympus CX21).

Statistical Analysis

First, the data normality was evaluated by the Shapiro–Wilk test. Behavioral results are expressed as the mean ± the SD. Object exploration time in the OR memory task and rat exploration time in the SR memory task were converted to a percentage of total exploration time, and a one-sample *t*-test was used to compare the percentage of the total time of exploration spent on each object/rat with a theoretical mean of 50%. The OR STM DI and the SR DI data were compared between the groups using one-way ANOVA. The OR LTM DI data were compared between the groups using one-way Kruskal–Wallis followed by the Mann–Whitney test. The OF and PM data were analyzed by one-way ANOVA.

Biochemical results that followed a normal distribution (DCFH and TBARS) were compared using ANOVA followed by Tukey's *post hoc* test and are expressed as the mean ± the SD. For non-normal variables, AChE and FRAP, a Kruskal–Wallis test was performed, followed by Dunn's *post hoc* test; these data are expressed as the median ± the interquartile range.

The significance level was set at 0.05 for all variables.

RESULTS

Control Behavioral Tasks

There were no differences between the groups in the number of rearings ($F_{(5,64)} = 1.171$; $P = 0.33$; **Table 1**) and crossings ($F_{(5,64)} = 3.279$; $P = 0.36$; **Table 1**) during the free exploration session in the OF, showing that treatments and surgery did not affect rats' exploratory and locomotor behavior. In the same way, the procedures did not affect anxiety behavior, since no differences were observed among groups in the PM test ($F_{(5,64)} = 0.7539$; $P = 0.58$). These data are important since they guarantee that the results observed on memory tasks are related to procedures

TABLE 1 | Different training and surgery procedures do not alter the locomotor and exploratory activities evaluated in the open field, and the anxiety behavior evaluated in the elevated plus maze.

	Control	Aβ	PE	Aβ + PE	CE	Aβ + CE	*P*-value
Open field							
Rearings (*n*)	33.4 ± 9.58	33.2 ± 6.85	39.4 ± 12.13	40.4 ± 10.24	37.6 ± 7.39	39.0 ± 11.30	0.33
Crossings (*n*)	98.5 ± 27.73	108.0 ± 16.43	98.9 ± 18.13	124.2 ± 24.10	125.3 ± 20.36	118.0 ± 17.25	0.09
Plus maze							
Time in open arms (s)	194.9 ± 45.37	221.1 ± 41.07	200.6 ± 32.36	197.5 ± 48.16	213.8 ± 37.74	211.7 ± 39.56	0.58

Data are expressed as mean ± SD of the number of crossings and rearings on the OF, and of the percentage of time spent in the open arms of the PM (n = 12 per group; P > 0.05; one-way ANOVA).

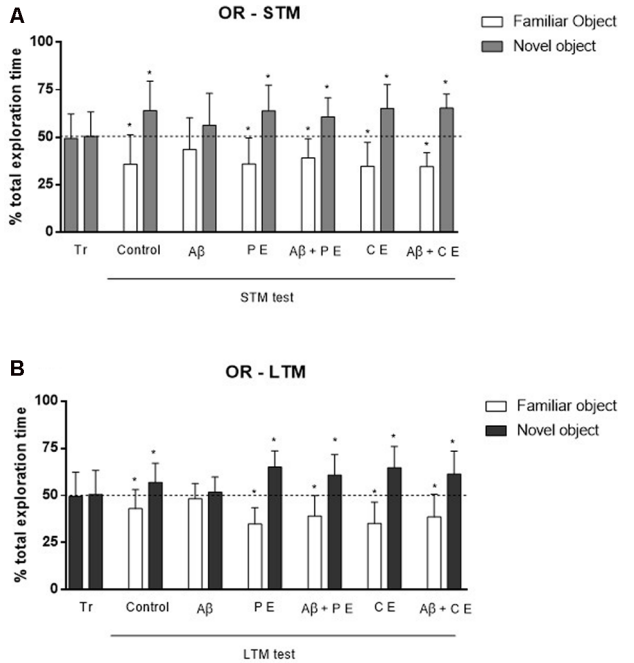

FIGURE 2 | The hippocampal Aβ infusion promotes Object Recognition (OR) memory deficit. PEs and CEs can revert the OR memory deficit caused by hippocampal Aβ infusion. **(A)** OR short-term memory (STM). **(B)** OR long-term memory (LTM). *$P < 0.05$; one-sample Student's t-test (theoretical mean 50%). Data are presented as mean ± SD (n = 11–12/group). Tr, training.

influencing learning and memory processes and not to other behavioral alterations.

Memory Tasks

Object Recognition (OR)

In the OR memory training session, the rats explored each object for a similar percentage of total exploration time (in the graphs, the data are presented as the mean of all groups: object A = 51.24 ± 10.75%, B = 48.76 ± 10.75%; $P > 0.05$ for all groups; Control: $t_{(10)} = 2.11$, $P = 0.06$; Aβ: $t_{(11)} = 1.08$, $P = 0.30$; PE: $t_{(11)} = 0.70$, $P = 0.49$; Aβ + PE: $t_{(10)} = 1.61$, $P = 0.14$; CE: $t_{(11)} = 0.21$, $P = 0.83$; Aβ + CE: $t_{(11)} = 1.42$, $P = 0.18$; **Figures 2A,B**, tr). This result was expected, since both objects were new to the animals.

In the STM test, the control animals spent more time exploring the novel object (Control: $t_{(10)} = 0.30$, $P = 0.0127$; **Figure 2A**), showing that they remembered familiar objects. The same was observed in the PE and CE groups, which spent more time exploring the novel object (PE: $t_{(11)} = 3.56$, $P = 0.0045$; CE: $t_{(11)} = 4.18$, $P = 0.0015$; **Figure 2A**). The Aβ infusion impaired STM, since the rats spent a similar percentage of time exploring both objects, familiar and novel (Aβ: $t_{(11)} = 1.32$, $P = 0.21$; **Figure 2A**). The 4 weeks of treatment reversed the deficits caused by Aβ neurotoxicity; the animals subjected to Aβ infusion and to PE or CE training were able to form OR STM, i.e., they explored the novel object more than 50% of the total exploration time (Aβ + PE: $t_{(10)} = 3.59$, $P = 0.0049$; Aβ + CE: $t_{(11)} = 7.22$, $P = 0.001$; **Figure 2A**).

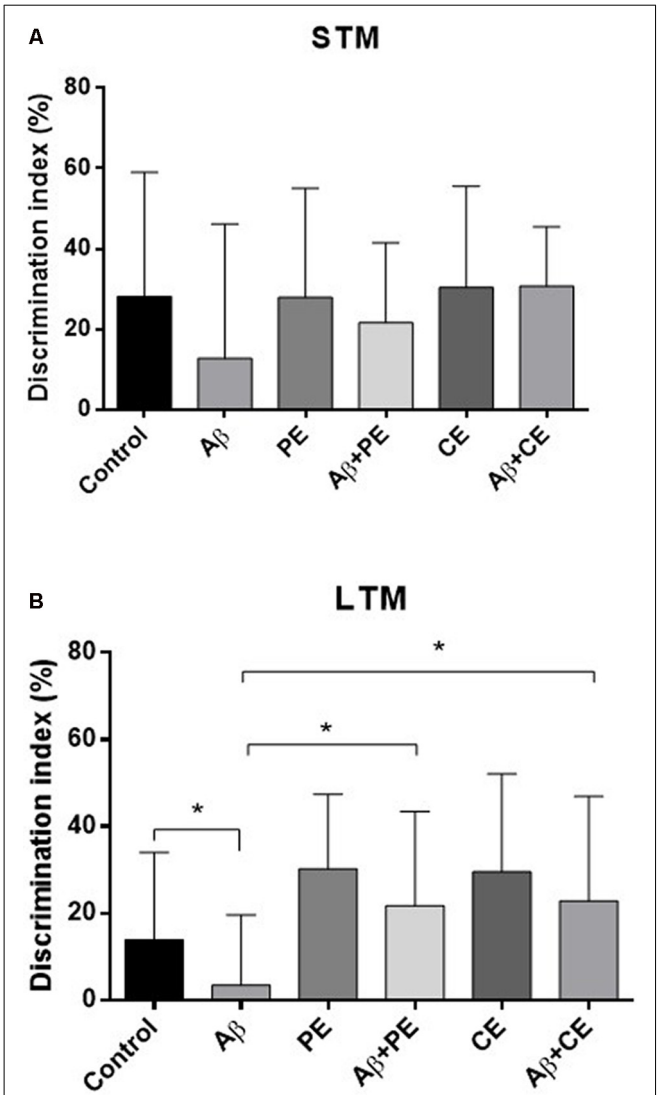

FIGURE 3 | The PE and CE interventions overcome OR LTM, but not STM, memory discrimination index (DI) deficit induced by Aβ protein. *$P < 0.05$, Kruskal–Wallis followed by Mann–Whitney test. **(A)** STM DI. **(B)** LTM DI. Data are presented as mean ± SD (n = 11–12/group).

Twenty-four hours after the training, rats in the Control, PE and CE groups explored the novel object for more than 50% of the total exploration time (Control: $t_{(10)} = 2.28$, $P = 0.04$; PE: $t_{(11)} = 6.08$, $P = 0.0001$; CE: $t_{(11)} = 4.54$, $P = 0.0008$; LTM; **Figure 2B**). The animals in the Aβ group presented impaired LTM since they spent approximately 50% of the total exploration time on each object (LTM; Aβ: $t_{(11)} = 0.74$, $P = 0.47$; **Figure 2B**). PE and CE were able to reverse the damage induced by the Aβ protein since the Aβ + PE and Aβ + CE groups spent more than 50% of the total exploration time exploring the novel object (Aβ + PE: $t_{(10)} = 3.34$, $P = 0.0075$; Aβ + CE: $t_{(11)} = 3.28$, $P = 0.007$; **Figure 2B**).

Considering the DI, used for comparison between the groups, no differences were found in STM test ($F_{(5,64)} = 0.85$; $P = 0.51$; **Figure 3A**). In contrast, significant differences were found in

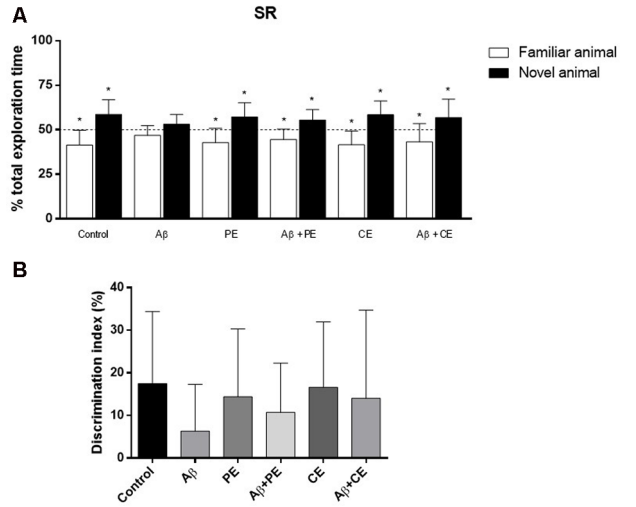

FIGURE 4 | Effects of hippocampal Aβ infusion, physical and CEs on social recognition (SR) memory. **(A)** The hippocampal Aβ infusion promotes SR memory deficit. PE and CE can promote SR memory consolidation in rats that received intrahippocampal Aβ infusion. **(B)** There are no differences on SR DI between the groups. *$P < 0.05$; one-sample Student's *t*-test (theoretical mean 50%). Data are presented as mean ± SD (n = 11–12/group).

LTM test ($H_{(6)} = 13.93$; $P = 0.016$; **Figure 3B**). The animals of Aβ group presented lower DI compared to Control group ($U = 30$, $P = 0.026$). The interventions overcome memory deficits induced by Aβ protein (Aβ + PE vs. Aβ: $U = 30$, $P = 0.026$; Aβ + CE vs. Aβ: $U = 32$, $P = 0.0204$; **Figure 3B**). No differences were found between Control and PE group ($U = 36$; $P = 0.06$) and between Control and CE group ($U = 40$; $P = 0.116$).

Social Recognition (SR)

In the SR memory test session, Control, PE and CE rats explored the novel rat for a longer percentage of time than the familiar rat (Control: $t_{(10)} = 3.43$, $P = 0.0064$; PE: $t_{(11)} = 3.19$, $P = 0.0098$; CE: $t_{(11)} = 3.77$, $P = 0.0031$; **Figure 4A**). Animals in the Aβ group, however, explored each rat for ∼50% of the total exploration time (Aβ: $t_{(11)} = 1.97$, $P = 0.07$; **Figure 4A**). PE and CE reversed the deleterious effect of Aβ protein on SR memory, since the treated animals spent more than 50% of the total exploration time exploring the new rat (Aβ + PE: $t_{(10)} = 3.11$, $P = 0.011$; Aβ + CE: $t_{(11)} = 2.29$, $P = 0.042$; **Figure 4A**).

Considering the DI, used for comparison between the groups, no differences were found ($F_{(5,64)} = 0.822$; $P = 0.538$; **Figure 4B**).

Biochemical Results

We found differences between the groups in ROS levels, as measured by the DCFH test ($F_{(5,42)} = 2.767$, $P = 0.03$; **Figure 5A**). Aβ rats presented higher ROS levels than the control group ($P = 0.033$; **Figure 5A**). No significant differences in hippocampal ROS levels were observed among the other groups.

Differences among the groups were found ($F_{(5,42)} = 4.464$; $P = 0.002$; **Figure 5B**) in hippocampal lipid peroxidation (TBARS). The infusion of Aβ protein increased hippocampal lipid peroxidation in comparison to the control group ($P = 0.004$; **Figure 5B**). PE and CE reversed the lipid peroxidation increase induced by Aβ ($P = 0.031$ for Aβ vs. Aβ + PE; $P = 0.012$ for Aβ vs. Aβ + CE; **Figure 5B**).

Differences in total antioxidant capacity (i.e., ferric reducing/antioxidant power—FRAP) were observed among the groups ($H_{(6)} = 16.44$, $P = 0.0057$; **Figure 5C**). The infusion of Aβ resulted in lower total antioxidant capacity than that observed in the control group ($P = 0.0144$; **Figure 5C**). No significant differences were observed among the other groups.

The AChE activity was different between the groups ($H_{(6)} = 18.70$, $P = 0.0022$; **Figure 5C**). Aβ rats presented decreased acetylcholinesterase activity compared to the control group ($P = 0.0080$; **Figure 5D**). Aβ rats subjected to PE and CE presented higher AChE activity than Aβ rats not subjected to any intervention ($P = 0.0321$ for Aβ vs. Aβ + PE; $P = 0.0092$ for Aβ vs. Aβ + CE; **Figure 5D**).

Histological Results

Morphological differences in hippocampal tissue were observed among the groups. The control group presented a normal structure with the standard organization (**Figure 6A**). PE and CE training groups showed a normal structure, similar to the control group (**Figures 6C,E**). The infusion of the Aβ peptide promoted the formation of vacuole-like structures (indicated by arrows in **Figure 6B**), significant tissue disorganization, and clear neuronal tissue loss (indicated by triangles in **Figure 6B**). Aβ rats treated with physical and cognitive training showed improvements in hippocampal tissue disorganization due to Aβ infusion (**Figures 6D,F**).

DISCUSSION

The present results show that physical and CEs can promote recognition, short and LTM consolidation in animals with memory deficits induced by Aβ neurotoxicity. Also, physical and CEs were able to reverse long-term object recognition memory, decrease hippocampal lipid peroxidation, and restore hippocampal acetylcholinesterase activity altered by Aβ neurotoxicity. Still, PE and CE seem to promote a better morphological organization of the hippocampal tissue, which was altered after Aβ infusion.

It is difficult to study AD in humans since a precise diagnosis of this pathology is not simple or definitive. On the other hand, there are many available experimental models of AD, each one with benefits and limitations (Drummond and Wisniewski, 2017). An ideal model needs to mimic the lesions and symptoms of the disease in a way that is similar to the real situation (Duyckaerts et al., 2008). However, currently, no animal model reproduces all of the characteristics of AD. As the deposition of extracellular Aβ is one of the main AD features (Braak and Braak, 1988), brain infusion of Aβ protein is an important model that can contribute to the understanding of key aspects of AD biology since it mimics both the cognitive and the oxidative imbalance characteristics of AD.

It is important to consider that between the main regions where the Aβ deposits are in the AD patient brain are

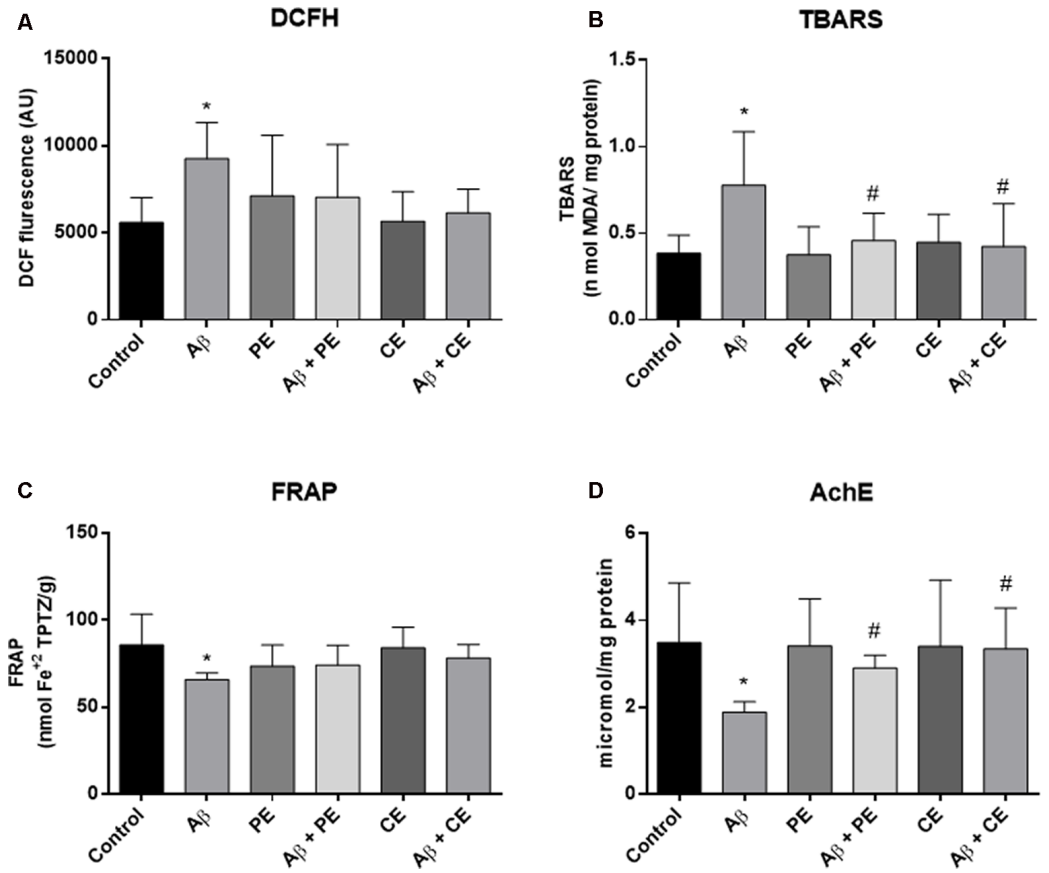

FIGURE 5 | Aβ hippocampal infusion promotes reactive oxygen species (ROS; DCFH, **A**) and lipid peroxidation increase (TBARS, **B**); and promotes total antioxidant capacity **(C)** and acetylcholinesterase activity decrease **(D)**. The PE and the CE performed during 4 weeks reverted the lipid peroxidation **(B)**, and AchE activity **(D)** alterations. Data from ROS (DCFH, **A**) and TBARS **(B)** are presented as mean ± SD and were analyzed by ANOVA followed by Tukey's test. Data from FRAP **(C)** and Acetylcholinesterase (AChE; **D**) are presented as median ± interquartile range and were analyzed by Kruskal–Wallis test followed by Dunn's test. $^{*}P < 0.05$, compared to control. $^{\#}P < 0.05$, compared to Aβ.

the hippocampus and cortex, structures that are associated with learning and memory function (Jing et al., 2009). Previous studies found increased hippocampal and cortical lipid peroxidation and protein oxidation in AD patients (Butterfield and Lauderback, 2002). In the same way, in this study, the hippocampal infusion of $A\beta_{25–35}$ promoted hippocampal oxidative stress and damage (increased ROS levels and lipid peroxidation) and decreased the total antioxidant capacity and acetylcholinesterase activity in the hippocampus, leading to STM and LTM recognition deficits. Also, in a previous study, our group performed the histopathological analysis of the cerebral cortex of the rats submitted to the same Aβ hippocampal infusion model and we observed that the cerebral cortex of these rats presented intense deposition of amyloid plaques (Martinez-Oliveria et al., 2018).

The neuroprotective influence of PE on dementia is widely studied. Individuals who practice regular physical activity have a 30–40% reduced risk of AD development in comparison to physically inactive individuals (Aarsland et al., 2010; Williams et al., 2010). Several studies have demonstrated that aerobic PE, such as running or swimming exercise, improved memory in rats with Aβ-induced AD (Kim et al., 2014; Özbeyli et al., 2017; Prado Lima et al., 2018; Rossi Dare et al., 2019). Exercise-induced factors, including neurogenesis, synaptic plasticity, and increased cerebral blood flow, seem to promote beneficial effects on the brain (Tari et al., 2019). Following this literature, our results showed that PE was able to promote STM and LTM consolidation in Aβ rats, reversing oxidative stress disruption, and altering AChE activity.

As impressively as PE training, cognitive training also promoted short and long-term learning in Aβ rats. There is clinically significant evidence to support the effectiveness of CE (Cui et al., 2018), but little evidence about the possible mechanisms involved. In general, this type of intervention aims to maintain cognitive brain function as long as possible, reducing disabilities and improving patients' quality of life (Zucchella et al., 2018). However, our results showed a direct effect of CE on cognition through its influence on hippocampal oxidative balance and AChE activity. A previous experimental study by our group showed that cognitive training was able to prevent the oxidative damage induced by the Aβ peptide

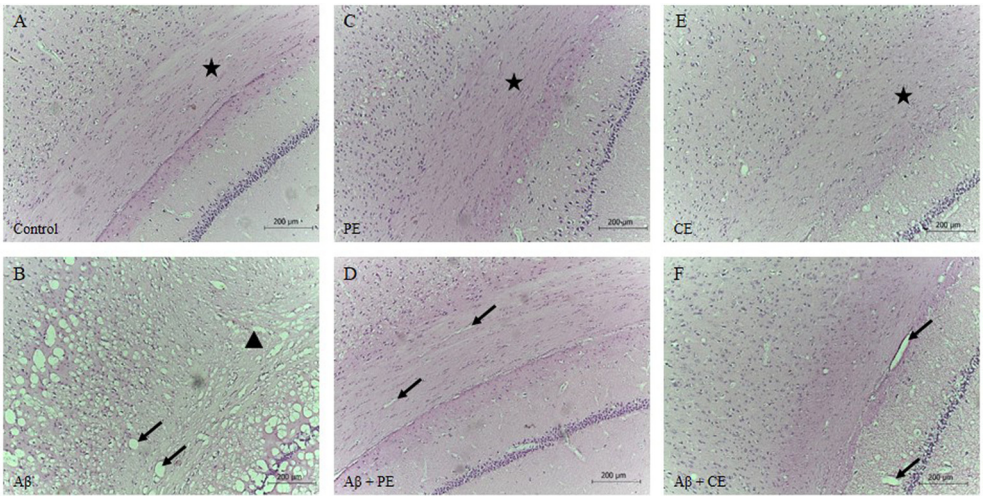

FIGURE 6 | Control **(A)**, PE **(C)** and CE **(E)** groups presented standard hippocampal morphology with tissue organization. Infusion of Aβ promotes hippocampal disorganization, vacuoles formation, and neuronal tissue loss **(B)**. PE **(D)** and CE **(F)** improved hippocampal tissue morphology. Brain stained by hematoxylin-eosin (HE; magnification 10×). The arrows indicated vacuoles; the stars indicated tissue with normal organization, with cells in a parallel and layered position; and, the triangle indicated atrophy and tissue disorganization **(A)**: Control group; **(B)**: Aβ group; **(C)**: PE group; **(D)**: Aβ + PE group; **(E)**: CE group; **(F)**: Aβ + CE group.

in the same animal model (Rossi Dare et al., 2019); here, we demonstrated that CE can also have an important role after Aβ deposition.

It is important to highlight that both the physical and the cognitive training had a more prominent effect of LTM object recognition memory, since, for this type of memory, in addition to the ability to learn the task, it is noteworthy that the animals that received the Aβ infusion and underwent the different training had a significantly higher object DI than those that received beta-amyloid but did not perform any type of exercise. The same difference between the groups was not observed in STM OR. It is important to consider that STM and LTM consolidation involve different neurobiological mechanisms, as the increase of hippocampal protein and gene expression, that is observed in LTM consolidation but is not required for STM (Izquierdo et al., 1998). In this sense, the fact that these different types of memory involve some distinct neurobiological processes can justify the different effects observed.

Neurodegeneration related to AD is most pronounced in hippocampal cholinergic neurons, which are directly related to cognitive function (Gold, 2003; Kumar and Singh, 2015). In rat models of AD that present impairments in learning and memory, a loss of and damage to cholinergic neurons are observed (Klinkenberg and Blokland, 2010; Haider et al., 2015; Zhang et al., 2019). The degeneration of cholinergic neurons in AD promotes cholinergic hypofunction, which can result in a decrease in choline acetyltransferase and AChE activity in the hippocampus (Francis et al., 1999; Kaushal et al., 2019). Our data showed that Aβ promoted hippocampal tissue disorganization, vacuole formation, and neuronal loss, in addition to promoting a decrease in AChE activity. On the other hand, PE and CE were able to reverse the cholinergic hypofunction caused by Aβ infusion and to restore hippocampal tissue morphology.

Many studies address protection and prevention strategies to avoid AD. The most effective type of strategy seems to act before the pathology. However, we also need to think about treatment for patients who already have the disease, and currently, the alternatives are few. Since the symptoms of AD start to appear approximately 20 years after the onset of pathophysiological hallmarks (Dubois et al., 2014), when the patient discovers the disease, the biochemical changes are already advanced. Currently, pharmacological therapies available for AD contribute only to the temporary reduction of symptoms and slowing the progression of the disease (Habtemariam, 2019). Thus, strategies for treating the disease are important. Here, we present two interesting nonpharmacological options that are effective by acting on oxidative balance and cholinergic function.

In summary, the model of intrahippocampal Aβ infusion used in this study caused hippocampal oxidative stress and damage, decreased antioxidant capacity, altered hippocampal tissue morphology, and promoted short- and long-term deficits in recognition memory that mimic those described or suggested to occur in AD. Surprisingly, both PE and CE induced memory consolidation in animals that received Aβ infusion, which normally presents deficits. The effect of PE and CE is more prominent in long-term object recognition memory. Still, PE and CE reversed the lipid peroxidation and acetylcholinergic activity alterations induced by hippocampal Aβ. Therefore, both PE and CE have the potential to be included in the treatment of AD, since both interventions could be used in humans.

DATA AVAILABILITY STATEMENT

The datasets generated for this study are available on request to the corresponding author.

ETHICS STATEMENT

The animal study was reviewed and approved by Animal Care and Use Committee from Federal University of Pampa—protocol n. 14/2017.

AUTHOR CONTRIBUTIONS

LD, AG, CS, LL, B-HN, and DD performed the experiments, analyzed the data, and wrote the manuscript. PM-C was responsible for the conceptualization of the study and supervision, analyzed the data, and wrote the manuscript.

FUNDING

This study was financed in part by the Coordenação de Aperfeiçoamento de Pessoal de Nível Superior (CAPES)—finance code 001 and PROCAD program (Grant No. 88881.068493/2014-01) and by the Federal University of Pampa (Universidade Federal do Pampa). AG is supported by Conselho Nacional de Pesquisa (Conselho Nacional de Desenvolvimento Científico e Tecnológico; CNPq/Brazil). CS is supported by Fundação de Amparo à Pesquisa do Rio Grande do Sul (FAPERGS). B-HN is supported by CAPES/Brazil. PM-C is supported by CNPq/Brazil and IBRO/IBE-UNESCO Science of Learning Program.

REFERENCES

Aarsland, D., Sardahaee, F. S., Anderssen, S., and Ballard, C. (2010). Is physical activity a potential preventive factor for vascular dementia? A systematic review. *Aging Ment. Health* 14, 386–395. doi: 10.1080/13607860903586136

Barnes, C. A. (1979). Memory deficits associated with senescence: a neurophysiological and behavioral study in the rat. *J. Comp. Physiol. Psychol.* 93, 74–104. doi: 10.1037/h0077579

Benzie, I. F., and Strain, J. J. (1996). The ferric reducing ability of plasma (FRAP) as a measure of "antioxidant power": the FRAP assay. *Anal. Biochem.* 239, 70–76. doi: 10.1006/abio.1996.0292

Black, J. E., Isaacs, K. R., and Greenough, W. T. (1991). Usual vs. successful aging: some notes on experiential factors. *Neurobiol. Aging* 12, 325–328; discussion 352–325. doi: 10.1016/0197-4580(91)90009-9

Bonini, J. S., Bevilaqua, L. R., Zinn, C. G., Kerr, D. S., Medina, J. H., Izquierdo, I., et al. (2006). Angiotensin II disrupts inhibitory avoidance memory retrieval. *Horm. Behav.* 50, 308–313. doi: 10.1016/j.yhbeh.2006.03.016

Braak, H., and Braak, E. (1988). Neuropil threads occur in dendrites of tangle-bearing nerve cells. *Neuropathol. Appl. Neurobiol.* 14, 39–44. doi: 10.1111/j.1365-2990.1988.tb00864.x

Broadbent, N. J., Gaskin, S., Squire, L. R., and Clark, R. E. (2010). Object recognition memory and the rodent hippocampus. *Learn. Mem.* 17, 5–11. doi: 10.1101/lm.1650110

Brooks, G. A., and White, T. P. (1978). Determination of metabolic and heart rate responses of rats to treadmill exercise. *J. Appl. Physiol. Respir. Environ. Exerc. Physiol.* 45, 1009–1015. doi: 10.1152/jappl.1978.45.6.1009

Butterfield, D. A., and Lauderback, C. M. (2002). Lipid peroxidation and protein oxidation in Alzheimer's disease brain: potential causes and consequences involving amyloid beta-peptide-associated free radical oxidative stress. *Free Radic. Biol. Med.* 32, 1050–1060. doi: 10.1016/s0891-5849(02)00794-3

Calabrese, F., Rossetti, A. C., Racagni, G., Gass, P., Riva, M. A., and Molteni, R. (2014). Brain-derived neurotrophic factor: a bridge between inflammation and neuroplasticity. *Front. Cell. Neurosci.* 8:430. doi: 10.3389/fncel.2014.00430

Cechetti, F., Worm, P. V., Elsner, V. R., Bertoldi, K., Sanches, E., Ben, J., et al. (2012). Forced treadmill exercise prevents oxidative stress and memory deficits following chronic cerebral hypoperfusion in the rat. *Neurobiol. Learn. Mem.* 97, 90–96. doi: 10.1016/j.nlm.2011.09.008

Cui, M. Y., Lin, Y., Sheng, J. Y., Zhang, X., and Cui, R. J. (2018). Exercise intervention associated with cognitive improvement in Alzheimer's disease. *Neural Plast.* 2018:9234105. doi: 10.1155/2018/9234105

Dao, A. T., Zagaar, M. A., Salim, S., Eriksen, J. L., and Alkadhi, K. A. (2014). Regular exercise prevents non-cognitive disturbances in a rat model of Alzheimer's disease. *Int. J. Neuropsychopharmacol.* 17, 593–602. doi: 10.1017/s1461145713001351

Drummond, E., and Wisniewski, T. (2017). Alzheimer's disease: experimental models and reality. *Acta Neuropathol.* 133, 155–175. doi: 10.1007/s00401-016-1662-x

Dubois, B., Feldman, H. H., Jacova, C., Hampel, H., Molinuevo, J. L., Blennow, K., et al. (2014). Advancing research diagnostic criteria for Alzheimer's disease: the IWG-2 criteria. *Lancet Neurol.* 13, 614–629. doi: 10.1016/S1474-4422(14)70090-0

Duyckaerts, C., Potier, M. C., and Delatour, B. (2008). Alzheimer disease models and human neuropathology: similarities and differences. *Acta Neuropathol.* 115, 5–38. doi: 10.1007/s00401-007-0312-8

Ellman, G. L., Courtney, K. D., Andres, V. Jr., and Featherstone, R. M. (1961). A new and rapid colorimetric determination of acetylcholinesterase activity. *Biochem. Pharmacol.* 7, 88–95. doi: 10.1016/0006-2952(61)90145-9

Epperly, T., Dunay, M. A., and Boice, J. L. (2017). Alzheimer disease: pharmacologic and nonpharmacologic therapies for cognitive and functional symptoms. *Am. Fam. Physician* 95, 771–778.

Foster, P. P., Rosenblatt, K. P., and Kuljis, R. O. (2011). Exercise-induced cognitive plasticity, implications for mild cognitive impairment and Alzheimer's disease. *Front. Neurol.* 2:28. doi: 10.3389/fneur.2011.00028

Francis, P. T., Palmer, A. M., Snape, M., and Wilcock, G. K. (1999). The cholinergic hypothesis of Alzheimer's disease: a review of progress. *J. Neurol. Neurosurg. Psychiatry* 66, 137–147. doi: 10.1136/jnnp.66.2.137

Gold, P. E. (2003). Acetylcholine modulation of neural systems involved in learning and memory. *Neurobiol. Learn. Mem.* 80, 194–210. doi: 10.1016/j.nlm.2003.07.003

Greenwood, P. M., and Parasuraman, R. (2010). Neuronal and cognitive plasticity: a neurocognitive framework for ameliorating cognitive aging. *Front. Aging Neurosci.* 2:150. doi: 10.3389/fnagi.2010.00150

Grundke-Iqbal, I., Iqbal, K., Tung, Y. C., Quinlan, M., Wisniewski, H. M., and Binder, L. I. (1986). Abnormal phosphorylation of the microtubule-associated protein tau (tau) in Alzheimer cytoskeletal pathology. *Proc. Natl. Acad. Sci. U S A* 83, 4913–4917. doi: 10.1073/pnas.83.13.4913

Habtemariam, S. (2019). Natural products in Alzheimer's disease therapy: would old therapeutic approaches fix the broken promise of modern medicines? *Molecules* 24:1519. doi: 10.3390/molecules24081519

Haider, S., Liaquat, L., Shahzad, S., Sadir, S., Madiha, S., Batool, Z., et al. (2015). A high dose of short term exogenous D-galactose administration in young male rats produces symptoms simulating the natural aging process. *Life Sci.* 124, 110–119. doi: 10.1016/j.lfs.2015.01.016

Izquierdo, I., Barros, D. M., Mello e Souza, T., Souza, M. M., Izquierdo, L. A., and Medina, J. H. (1998). Mechanisms for memory types differ. *Nature* 393, 635–636. doi: 10.1038/31371

Jing, W., Guo, F., Cheng, L., Zhang, J. F., and Qi, J. S. (2009). Arginine vasopressin prevents amyloid beta protein-induced impairment of long-term potentiation in rat hippocampus *in vivo*. *Neurosci. Lett.* 450, 306–310. doi: 10.1016/j.neulet.2008.11.053

Kaidanovich-Beilin, O., Lipina, T., Vukobradovic, I., Roder, J., and Woodgett, J. R. (2011). Assessment of social interaction behaviors. *J. Vis. Exp.* 48:2473. doi: 10.3791/2473

Kaushal, A., Wani, W. Y., Bal, A., Gill, K. D., and Kaur, J. (2019). Okadaic acid and hypoxia induced dementia model of Alzheimer's type in rats. *Neurotox. Res.* 35, 621–634. doi: 10.1007/s12640-019-0005-9

Kim, B. K., Shin, M. S., Kim, C. J., Baek, S. B., Ko, Y. C., and Kim, Y. P. (2014). Treadmill exercise improves short-term memory by enhancing neurogenesis in amyloid beta-induced Alzheimer disease rats. *J. Exerc. Rehabil.* 10, 2–8. doi: 10.12965/jer.140086

Klinkenberg, I., and Blokland, A. (2010). The validity of scopolamine as a pharmacological model for cognitive impairment: a review of animal

behavioral studies. *Neurosci. Biobehav. Rev.* 34, 1307–1350. doi: 10.1016/j.neubiorev.2010.04.001

Koo, J. H., Kang, E. B., Oh, Y. S., Yang, D. S., and Cho, J. Y. (2017). Treadmill exercise decreases amyloid-beta burden possibly *via* activation of SIRT-1 signaling in a mouse model of Alzheimer's disease. *Exp. Neurol.* 288, 142–152. doi: 10.1016/j.expneurol.2016.11.014

Kumar, A., Singh, A., and Ekavali. (2015). A review on Alzheimer's disease pathophysiology and its management: an update. *Pharmacol. Rep.* 67, 195–203. doi: 10.1016/j.pharep.2014.09.004

Lane, C. A., Hardy, J., and Schott, J. M. (2018). Alzheimer's disease. *Eur. J. Neurol.* 25, 59–70. doi: 10.1111/ene.13439

Lee, V. M., Goedert, M., and Trojanowski, J. Q. (2001). Neurodegenerative tauopathies. *Annu. Rev. Neurosci.* 24, 1121–1159. doi: 10.1146/annurev.neuro.24.1.1121

Loetchutinat, C., Kothan, S., Dechsupa, S., Meesungnoen, J., Jay-Gerin, J.-P., and Mankhetkorn, S. (2005). Spectrofluorometric determination of intracellular levels of reactive oxygen species in drug-sensitive and drug-resistant cancer cells using the 2′,7′-dichlorofluorescein diacetate assay. *Radiat. Phys. Chem.* 72, 323–331. doi: 10.1016/j.radphyschem.2004.06.011

Lövdén, M., Wenger, E., Martensson, J., Lindenberger, U., and Backman, L. (2013). Structural brain plasticity in adult learning and development. *Neurosci. Biobehav. Rev.* 37, 2296–2310. doi: 10.1016/j.neubiorev.2013.02.014

Lu, Y., Dong, Y., Tucker, D., Wang, R., Ahmed, M. E., Brann, D., et al. (2017). Treadmill exercise exerts neuroprotection and regulates microglial polarization and oxidative stress in a streptozotocin-induced rat model of sporadic Alzheimer's disease. *J. Alzheimers Dis.* 56, 1469–1484. doi: 10.3233/jad-160869

Malek, M. H., Huttemann, M., Lee, I., and Coburn, J. W. (2013). Similar skeletal muscle angiogenic and mitochondrial signalling following 8 weeks of endurance exercise in mice: discontinuous versus continuous training. *Exp. Physiol.* 98, 807–818. doi: 10.1113/expphysiol.2012.070169

Martinez-Oliveria, P. M., Oliveira, M. F., Alves, N., Coelho, R. P., Pilar, B. C., Gullich, A. A., et al. (2018). Yacon leaf extract supplementation demonstrates neuroprotective effect against memory deficit related to β-amyloid-induced neurotoxicity. *J. Funct. Foods* 48, 665–675. doi: 10.1016/j.jff.2018.08.004

Martins, R. N., Villemagne, V., Sohrabi, H. R., Chatterjee, P., Shah, T. M., Verdile, G., et al. (2018). Alzheimer's disease: a journey from amyloid peptides and oxidative stress, to biomarker technologies and disease prevention strategies-gains from AIBL and DIAN cohort studies. *J. Alzheimers Dis.* 62, 965–992. doi: 10.3233/jad-171145

Moneim, A. E. (2015). Oxidant/antioxidant imbalance and the risk of Alzheimer's disease. *Curr. Alzheimer Res.* 12, 335–349. doi: 10.2174/1567205012666150325182702

Ohkawa, H., Ohishi, N., and Yagi, K. (1979). Assay for lipid peroxides in animal tissues by thiobarbituric acid reaction. *Anal. Biochem.* 95, 351–358. doi: 10.1016/0003-2697(79)90738-3

Özbeyli, D., Sari, G., Özkan, N., Karademir, B., Yüksel, M., Çilingir Kaya, O. T., et al. (2017). Protective effects of different exercise modalities in an Alzheimer's disease-like model. *Behav. Brain Res.* 328, 159–177. doi: 10.1016/j.bbr.2017.03.044

Pellow, S., Chopin, P., File, S. E., and Briley, M. (1985). Validation of open:closed arm entries in an elevated plus-maze as a measure of anxiety in the rat. *J. Neurosci. Methods* 14, 149–167. doi: 10.1016/0165-0270(85)90031-7

Prado Lima, M. G., Schimidt, H. L., Garcia, A., Dare, L. R., Carpes, F. P., Izquierdo, I., et al. (2018). Environmental enrichment and exercise are better than social enrichment to reduce memory deficits in amyloid beta neurotoxicity. *Proc. Natl. Acad. Sci. U S A* 115, E2403–E2409. doi: 10.1073/pnas.1718435115

Prince, M., Wimo, A., Guerchet, M., Ali, G., Wu, Y., and Prina, M. (2015). The global impact of dementia: an analysis of prevalence, incidence, cost and trends. *World Alzheimer Rep.* 2015, 10–28. Available online at https://www.alz.co.uk/research/WorldAlzheimerReport2015.pdf.

Rossi Dare, L., Garcia, A., Alves, N., Ventura Dias, D., de Souza, M. A., and Mello-Carpes, P. B. (2019). Physical and cognitive training are able to prevent recognition memory deficits related to amyloid beta neurotoxicity. *Behav. Brain Res.* 365, 190–197. doi: 10.1016/j.bbr.2019.03.007

Selkoe, D. J. (1999). Translating cell biology into therapeutic advances in Alzheimer's disease. *Nature* 399, A23–A31. doi: 10.1038/399a023

Tari, A. R., Norevik, C. S., Scrimgeour, N. R., Kobro-Flatmoen, A., Storm-Mathisen, J., Bergersen, L. H., et al. (2019). Are the neuroprotective effects of exercise training systemically mediated? *Prog. Cardiovasc. Dis.* 62, 94–101. doi: 10.1016/j.pcad.2019.02.003

Williams, J. W., Plassman, B. L., Burke, J., and Benjamin, S. (2010). Preventing Alzheimer's disease and cognitive decline. *Evid. Rep. Technol. Assess.* 193, 1–727.

Winocur, G., Craik, F. I., Levine, B., Robertson, I. H., Binns, M. A., Alexander, M., et al. (2007). Cognitive rehabilitation in the elderly: overview and future directions. *J. Int. Neuropsychol. Soc.* 13, 166–171. doi: 10.1017/s1355617707070191

Woods, B., Aguirre, E., Spector, A. E., and Orrell, M. (2012). Cognitive stimulation to improve cognitive functioning in people with dementia. *Cochrane Database Syst. Rev.* 2:CD005562. doi: 10.1002/14651858.CD005562.pub2

Yau, S., Li, A., and So, K.-F. (2015). Involvement of adult hippocampal neurogenesis in learning and forgetting. *Neural Plast.* 2015:717958. doi: 10.1155/2015/717958

Zhang, X., Wang, X., Hu, X., Chu, X., Li, X., and Han, F. (2019). Neuroprotective effects of a Rhodiola crenulata extract on amyloid-β peptides ($A\beta_{1-42}$)—induced cognitive deficits in rat models of Alzheimer's disease. *Phytomedicine* 57, 331–338. doi: 10.1016/j.phymed.2018.12.042

Zucchella, C., Sinforiani, E., Tamburin, S., Federico, A., Mantovani, E., Bernini, S., et al. (2018). The multidisciplinary approach to Alzheimer's disease and dementia. A narrative review of non-pharmacological treatment. *Front. Neurol.* 9:1058. doi: 10.3389/fneur.2018.01058

Conflict of Interest: The authors declare that the research was conducted in the absence of any commercial or financial relationships that could be construed as a potential conflict of interest.

frontiers in Pharmacology

ORIGINAL RESEARCH
published: 21 August 2020
doi: 10.3389/fphar.2020.01220

A Potent Antioxidant Endogenous Neurohormone Melatonin, Rescued MCAO by Attenuating Oxidative Stress-Associated Neuroinflammation

Li Ling[1], Abdullah Alattar[2], Zhen Tan[3], Fawad Ali Shah[4], Tahir Ali[5], Reem Alshaman[2], Phil Ok Koh[6] and Shupeng Li[7]**

[1] Department of Endocrinology, Shenzhen Nanshan People's Hospital and the 6th Affiliated Hospital of Shenzhen University Health Science Center, Shenzhen, China, [2] Department of Pharmacology and Toxicology, Faculty of Pharmacy, University of Tabuk, Tabuk, Saudi Arabia, [3] Health Management Center, Shenzhen University General Hospital, Shenzhen University Clinical Medical Academy, Shenzhen University, Shenzhen, China, [4] Riphah Institute of Pharmaceutical Sciences, Riphah International University, Islamabad, Pakistan, [5] Department of Comparative Biology and Experimental Medicine, Faculty of Veterinary Medicine, Hotchkiss Brain Institute, Cumming School of Medicine, University of Calgary, Calgary, AB, Canada, [6] Department of Anatomy, College of Veterinary Medicine, Research Institute of Life Science, Gyeongsang National University, Jinju, South Korea, [7] State Key Laboratory of Oncogenomics, School of Chemical Biology and Biotechnology, Shenzhen Graduate School, Peking University, Shenzhen, China

OPEN ACCESS

Edited by:
Touqeer Ahmed,
National University of Sciences & Technology, Pakistan

Reviewed by:
Javier Egea,
Institute of Health Research of the University Hospital of La Princesa, Spain
Ignacio Bejarano
University of Seville, Spain

***Correspondence:**
Fawad Ali Shah
fawad.shah@riphah.edu.pk
Shupeng Li
lisp@pkusz.edu.cn

Specialty section:
This article was submitted to Neuropharmacology, a section of the journal Frontiers in Pharmacology

Received: *01 April 2020*
Accepted: *27 July 2020*
Published: *21 August 2020*

Citation:
Ling L, Alattar A, Tan Z, Shah FA, Ali T, Alshaman R, Koh PO and Li S (2020) A Potent Antioxidant Endogenous Neurohormone Melatonin, Rescued MCAO by Attenuating Oxidative Stress-Associated Neuroinflammation. Front. Pharmacol. 11:1220. doi: 10.3389/fphar.2020.01220

Ischemic stroke is an acute neurological syndrome either due to permanent or temporary obstruction of blood. Such obstruction immediately triggers abrupt pathological cascading processes, which collectively lead to neuronal cell death. Oxidative stress and neuroinflammation in ischemic stroke are critical regulating events that ultimately lead to neuronal death. Complicated interplay exists between the two processes which occur through several stages. Most often, oxidative stress precedes the inflammatory mechanisms and includes several interconnected cascades that underlie the ischemic stroke pathology. In continuation of the previously published data, here, we further ruled out the protective role of melatonin in focal cerebral ischemic injury model. Administration of 5 mg/kg dose of melatonin 30 min prior to ischemia reduced brain infarction associated with sequentially rescued neuronal apoptosis. Furthermore, melatonin attenuated neuroinflammatory markers and reactive oxygen species (ROS), induced by ischemic stroke, *via* halting the key players of mitogen stress family (p38/JNK). Besides, melatonin modulated the endogenously produced antioxidant enzyme, thioredoxin (Trx) pathway. These broader therapeutic efficacies of melatonin suggest that melatonin could be further investigated for its diverse therapeutic actions with multiple targets in recovering, preventing and halting the detrimental outcomes of MCAO, such as elevated oxidative stress, neuroinflammation, and neurodegeneration.

Keywords: melatonin, middle cerebral artery occlusion, neuroinflammation, antioxidant, ischemic stroke

INTRODUCTION

Globally, ischemic stroke is the most devastating human health condition and the major leading cause of impaired health and death in these modern technologically advanced and industrialized era (Feigin et al., 2014). Ischemic stroke results in severe physiological and neurological impairment (Boden-Albala et al., 2019). The pathophysiological complication of ischemic stroke depends largely on the area and type of occlusion, which can be either permanent or transient. Such occlusion can obstruct the supply of oxygenated blood to the brain. Furthermore, the supply of essential micro molecules is also affected by this impediment (Firan et al., 2020; Hui et al., 2020). The characteristic pathological attributes include loss of ionic gradient, as a result of reduced adenosine triphosphate (ATP) supply, which ultimately provokes membrane depolarization and calcium surge. Glutamate amassing further augments calcium release along with inflammatory and apoptotic mediators (Bruno et al., 2001). This metabolic crisis is followed by the prompt activation of several cytotoxic and pathological cascading events. The subsequent disturbances of cellular dysregulation further incorporate secondary tissue damage such as neuroinflammatory reactions. The inflammatory mediators have a significant role in stroke pathophysiology, due to the instant release of neuroinflammatory markers within the first hour of ischemic stroke (Tuttolomondo et al., 2012; Wang et al., 2013). Subsequent activation of glia cells further creates a vicious cycle of inflammatory cascades, in which release of inflammatory cytokines (tumor necrotic factor/TNF-α) from microglia further bolster the glia cell architecture towards inflammation. Furthermore, a secondary surge of proinflammatory cytokines such as interleukin-1 (IL-1β), and interleukin-6 (IL-6), contributes to a higher infarct volume in humans and thus further complicates the clinical prognosis. Antithrombotics are the first-line therapeutic agents against this life-threatening condition and include activase and tenecteplase (TNKase) (Melandri et al., 2009). The associated short therapeutic window, however, is largely considered as the potential limiting factor for these thrombolytic agents.

The impairment in the endogenous hormones has been implicated in several diseases such as cancer, cardiovascular, and age-associated neurodegenerative diseases. It has been widely reported that stroke mainly affect the older population, which may be associated with a deficiency of endogenous hormones, such as estrogens, progesterone, and melatonin (Singh et al., 2008; Dodda et al., 2019). Among these the most promising is melatonin as the people become older, the melatonin level declined, which might be associated with the risk factor of ischemic stroke and make the people more vulnerable towards the stroke. A significant consideration is given to multiple synthetic compounds that mimic the endogenously produced hormones such as estrogens, progesterone, and melatonin due to their promising biological activities. Several studies reiterated the neuroprotective effects of melatonin, which is an indoleamine secreted mainly from the pineal gland, and other tissues (Messner et al., 2001; Stefulj et al., 2001; Venegas et al., 2012). Furthermore, the neuroprotective effects of melatonin in the ischemic brain model have been observed a long time ago, but still different studies suggest different molecular mechanisms for melatonin. Currently proposed mechanisms include including maintaining Ca2+ homeostasis (Onaolapo et al., 2019), suppressing inflammatory response (Azedi et al., 2019), decreasing oxidative stress, modulating stem cell survival (Watson et al., 2016), attenuating endoplasmic reticulum stress (Lin et al., 2018) and by modulation of microglia phenotypic responses (Liu et al., 2019). These beneficial effects of melatonin could be attributed mainly to its lipophilic nature that facilitates its rapid transportation to the brain (Yeleswaram et al., 1997). Second, the ubiquitous distribution of melatonin receptors in the brain leads to extensive interaction with some important intracellular proteins including nuclear receptor ROR/RZR, quinone reductase 2 (MT3), and calmodulin which participate in the regulation of circadian and seasonal rhythms (Benitez-King et al., 1993; Tan et al., 2007). ROR/RZR are nuclear receptor superfamily involved in the immunomodulatory and anti-tumor effects (Karasek et al., 2002; Winczyk et al., 2002). These effects are further supplemented by the large therapeutic window of melatonin, which makes this neurohormone an appropriate therapeutic option not only in brain disorders but also in other conditions. In this context, Ramos et al. demonstrated a detailed neuroprotective profile of melatonin in cerebral ischemia by targeting several signaling pathways, such as the pro-survival PI3K/Akt, mitogen-activated protein kinases (MAPKs), oxidative stress-related erythroid 2-related factor 2 (Nrf2), endothelin-1, and the N-methyl-D-aspartate receptor2A (NR2a)-dependent pathway (Shah et al., 2014; Shah et al., 2018b; Shah et al., 2019).

Current trends of drug development research have changed significantly due to repetitive failures of clinical trials. Several preclinical strategies have been demonstrated to inhibit delayed inflammatory response, but none of them were translated into effective clinical findings (Sughrue et al., 2004). Therefore, the underlying molecular and cellular mechanisms of oxidative stress-induced inflammation should be further delineated. Although several studies have investigated the favorable effects of melatonin against ischemic stroke, very few reports demonstrated the effect of melatonin on oxidative stress-induced inflammation and the role of the NF-κB/Trx pathway in an ischemic stroke model. Therefore, the current study was undertaken to evaluate the role of melatonin in cellular protection against oxidative stress-associated neuroinflammation in ischemic stroke.

MATERIALS AND METHODS

Animal Housing, Grouping, and Drug Treatment

Sprague-Dawley (SD) male rats weighing between 250–300 g and approximately 8-10 weeks old were acquired from an institutional breeding facility and were kept under a controlled

environment, Peking University Shenzhen Graduate School. The animals were maintained in plastic cages, under equal light/dark period at room temperature with free access to food to facilitate experimental procedures and extra care was practiced to avoid unnecessary stressful events. All experimental procedures were pre-approved from the Institutional Animal Care and Use Committee of Peking University Shenzhen Graduate School (Approval number: AP0013002) and as such were strictly adhered to, in addition, to ARRIVE guidelines with few exceptions. We did not apply human endpoints for euthanizing the rats as the permanent MCAO model (24 h) is the most stressful invasive procedure and in which limited mobility with severe suffering is an established documented protocol, and by this our group was more interested in rats that survive this period. By this, we did not euthanize any rats until 24 h of the ischemic period. 4 groups of rats were designed, each with n=12 (**Figure 1**): 1. Sham group, rats in this group were administered saline as a vehicle; 2. MCAO group, rats in this group were exposed to invasive permanent middle cerebral artery occlusion; 3. Mela + MCAO group, rats in this group received melatonin prior to MCAO surgery; 4. Mela + Sham group, Melatonin was administered to sham rats.

We previously optimized the dosage regimen of melatonin (Sigma, St. Louis, MO, U.S.A) (Shah et al., 2014). Herein, we administered melatonin (dissolved in saline) or a vehicle at 5 mg/kg intraperitoneal dose prior to ischemia. A total of 7 animals have died, 4 from the ischemic group, 3 from melatonin treated groups, which we further adjusted by supplementing more animals. The reported reason for this mortality is edema formation, BBB leakage, and hypothalamic shutdown. The ethics committee is mostly aware of the mortality in experimental setup particularly in this model, as we constantly engaged for our work with this committee.

MCAO Surgery

MCAO surgery was performed as per our previously published data (Sughrue et al., 2004; Shah et al., 2016; Shah et al., 2018a). Briefly, the animals were anesthetized by a cocktail of xylazine (9 mg/kg) and ketamine (91 mg/kg) and were placed in a heated cloth in a ventral position under a lamp. A central surgical incision was made, keeping the incision towards the right quadrant. The superficial muscle tissue was dissected out to probe for the right common carotid artery (CCA). Moreover, the whitish vagus nerve is carefully separated from the lining of CCA until the bifurcating point is reached. At this point, the two divergent branches of CCA, the external and internal carotid arteries (ECA and ICA) were identified and set free from surrounding tissues. Superior thyroid artery and the occipital artery which are small protrusions of ECA were identified and knotted with a thin black (6/0) silk (Sterile braided non-absorb SK-61, AILEE.CO, South Korea) and eventually ligated to allow free movement of the ECA. The ECA was then permanently tied with silk (6/0) near the hyoid bone located above the ligated superior thyroid artery. Throughout this procedure, extra care was exercised to avoid excessive bleeding. To induce the symptoms of ischemic stroke, the ECA was pierced, and

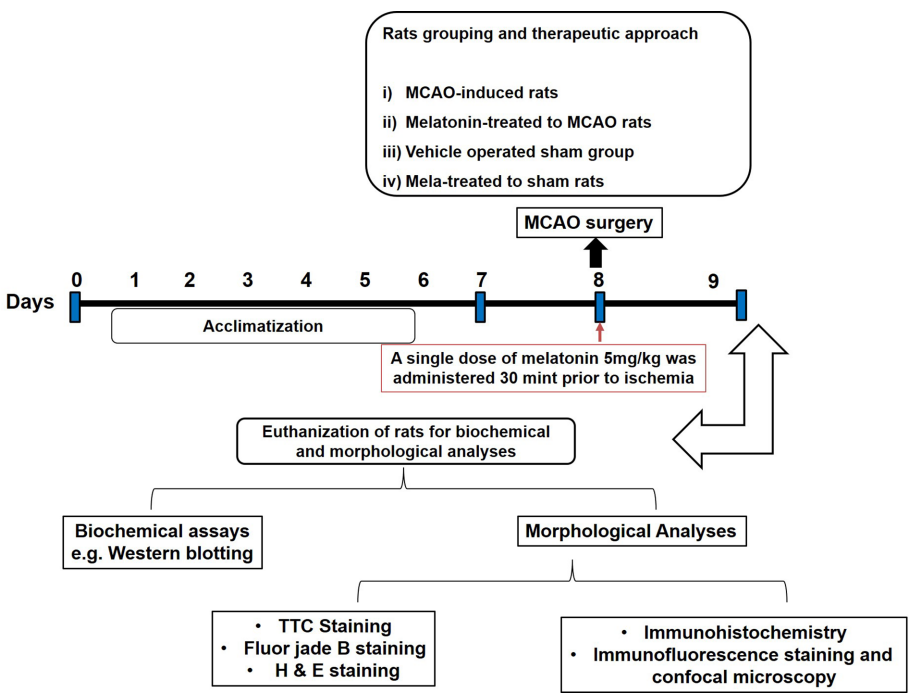

FIGURE 1 | After 1 week of acclimatization, randomly selected male Sprague-Dawley were divided into the following groups: (1) Vehicle-treated sham rats; (2) MCAO rats; (3) Pre-melatonin administration to rats undergoing MCAO; (4) Pre-melatonin administration to sham rats. Melatonin or vehicle was administered as a single dose (5 mg/kg), all rats brain was isolated for further biochemical and immunohistochemical analyses.

subsequently, blue nylon silk (3/0, Sterile braided non-absorb NB319, AILEE.CO, South Korea) of 3 cm with a bulging tip, was introduced from the opening of the ECA and proceeds to the ICA and until finally to the opening of the middle cerebral artery (MCA). 24 h after occlusion, all animals were subjected to carbon dioxide (CO2) euthanasia. No insertion was made in the sham group, although the sham group was subjected to the same stressful setup. The only disadvantage in this method is the lack of Doppler effect and relative blood flow measurement, though we constantly do the occlusion with suitable experimental skills.

Triphenyl Tetrazolium Chloride (TTC) Staining and Histological Preparation

All rats were sacrificed under the same condition of anesthesia, and brain tissue was collected. Three-millimeter thick coronal slices were cut starting from the frontal lobe or occipital lobe. The slices were stained by incubating in freshly prepared TTC solution (2% in PBS) in a water bath until a demarcation of white-red was noticed. The slices were fixed in 4% paraformaldehyde solution and photographed for percent infarct area determination (Shah et al., 2019). ImageJ program was used for infarct area determination and presented as percent total area. To compensate for the false reading of edema, the following formula was applied:

Corrected infarct area

= left hemisphere area of the brain

– (hemisphere area from the right brain

– the area of infarction)

These sections were then processed for paraffin blocks preparation using an embedding machine and rotary microtome n=6/group.

Haematoxylin Eosin (H& E) Staining

Tissue slides were subjected to deparaffinization protocol, which started from three different xylene treatments for 10 min and then rehydrated in graded alcohol preparation (commencing from 100% to 70%, each wash for 5-10 min). These slides were subsequently rinsed with distilled water to clear ethanol remaining and immersed in hematoxylin for 10 min at room temperature. After due time, the slides were washed with distilled water and observed under the microscope to ensure nuclear staining, otherwise, incubation time with hematoxylin was increased, followed by 1% HCl solution treatment for a short interval, rinsed with distilled water and immediately treated with 1% ammonia water, followed by rinsing with water. The slides were then stained with pinkish eosin solution for the appropriate time and were then rinsed in water and kept under room temperature for air-drying. This step was followed by gradient ethanolic dehydration and fixation in absolute xylene (reverse deparaffinization protocol) and mounted with a glass coverslip. By using an Olympus light microscope at 40x magnification scale, slides were analyzed for the extent of neuronal death and survival using an ImageJ program.

Immunohistochemical Staining (IHC) and Microscopic Analysis

IHC was achieved according to our previously published report (Sung et al., 2012). Briefly, after deparaffinization protocol as demonstrated above, slides were processed for antigen retrieval with proteinase K and washed with 0.1 M PBS. The peroxidase activity was quenched by applying a diluted hydrogen peroxide solution (3% in methanol). After washing with 0.1 M PBS, slides were treated with normal goat serum (NGS). Slides were then incubated for a whole night with primary antibodies such as mouse anti-phosphorylated-c-Jun N-terminal kinase (p-JNK), rabbit anti-interleukin (IL-1β), mouse anti-tumor necrotic factor (TNF-α) and rabbit anti-p-NF-κB, (Santa Cruz Biotechnology, Inc) at 1:100 dilution. The next morning, slides were incubated subsequently with biotinylated tagged secondary antibody (dilution 1:50), with ABC Elite kit (Santa Cruz Biotechnology) and stained in DAB solution. This step was followed by gradient ethanolic dehydration and fixation in absolute xylene (reverse deparaffinization protocol) and mounted with a glass coverslip. By using an Olympus light microscope at 40x magnification scale, slides were analyzed for hyperactivated p-JNK, IL-1β, p-NF-κB, and TNF-α using an ImageJ program.

Immunofluorescence Staining and Confocal Microscopy

Same deparaffinization and antigen retrieval protocol were adopted, followed by PBS rinsing. Immuno-slides were incubated with 5% normal serum depending upon secondary antibody employed, followed by whole night incubation at 40C with primary antibodies. The antibodies used were, glial fibrillary acidic protein (GFAP), cyclooxygenase-2 (COX-2), nitric oxide synthase-2 (NOS-2), p-NF-κB, and thioredoxin (Trx) from (Santa Cruz Biotechnology, Inc) with dilution factor 1:100. The following morning, slides were treated with secondary antibodies that were tagged with a fluorescent dye (Santa Cruz Biotechnology) for 1.5 h avoiding the light source. Commercially available Ultra Cruz mounting max (consisting of DAPI and mounting media) were used for coverslipping and were photoshoot by a confocal microscope (Flouview FV 1000 Japan) with appropriate scale and analyzed by ImageJ software.

Fluoro-Jade B (FJB) Staining

After deparaffinization, slides were immersed in 1% NaOH, followed by diluted graded ethanolic solution (starting from 80% to 70%), subsequently with distilled water and were transferred to Coplin jar containing 0.06% KMNO4, rinsed with distilled water and immediately treated with 0.1% acetic acid solution and 0.01% FJB. After rinsing, slides were mounted using DPX mounting medium and then photoshoot by confocal microscopy and quantified by Image. Although, the exact mechanism by which FJB binds to degenerative neurons is not well understood. Schmued et al. stated that FJB, an anionic derivative of fluorescein, possibly interacts with intracellular

polyamines and thereby stains degenerative neurons (Schmued and Hopkins, 2000). Furthermore, FJB has an advantage over its predecessor Fluoro-Jade, due to its greater specific affinity for degenerating neurons.

Western Blot Analysis

For relative protein expression, we followed the same methodological protocols of western blot as our previously published data (Gim et al., 2013). The whole tissue extract was centrifuged and resulted supernatant was carefully isolated. Bicinchoninic acid (BCA) kit (Pierce, Rockford, IL, USA) was utilized to determine protein concentration according to the guidelines provided by the manufacturer. 30 μg per sample of protein were electrophoresed and were transferred to polyvinylidene fluoride (PVDF) membranes (Millipore, Billerica, MA, USA). After blocking, the membrane PVDF was incubated with primary antibodies for the whole night at the refrigerator. The next morning secondary antibodies were applied, and the ECL detection reagent was used for x-ray bands. The antibodies used include anti-TNF-α, anti-p-JNK, Anti-JNK, anti-COX2, anti-IL-1β, anti-NOS2, anti-nuclear factor erythroid 2-related factor 2 (Nrf2), anti-p-NF-κB, anti-heme oxygenase-1 (HO-1), anti-Trx, and anti-β-actin (Santa Cruz, Biotechnology, CA, USA). The anti-mitogen activated protein kinase phosphorylated-P38 (MAPKp-P38) and anti-total-P38 were purchased from (Cell Signaling Technology, CST), and were used at dilutions 1:1000.

Data and Statistical Analysis

All the data are shown as means ± standard error of the mean (SEM) and were analyzed either by one-way or two-way ANOVA followed by Bonferroni Multiple Comparison as post-hoc *via* prism-7. ImageJ software was used for the analysis of protein bands and morphological data.

RESULTS

Pre-Treatment Effect of Melatonin on Brain Infarction and Neuronal Cell Loss

Ischemic brain injury produces a significant distortion of a neuronal cell in the core and penumbral region, which includes striatum and frontal cortex respectively. TTC staining was used to distinguish between intact and infarcted tissue (**Figure 2A**, n=6/group). Melatonin significantly reduced infarction size induced by MCAO ($p<0.05$, **Figure 2A**). The neuronal damage in ischemic injury could be due to necrosis in the infarcted core due to severe depletion of blood flow and ATP supply or due to apoptosis in the penumbral region that surrounds the core. Depending on brain location, broad crosstalk exists between necrotic and apoptotic cell death, due to analogous triggering agents such as glutamate and ROS. We, therefore, selected the peri-infarct regions as indicated by number 1 for the frontal cortex and number 4 for the striatum, as regions of interest (ROIs) (**Figure 2A**) for all further morphological analysis.

The H & E staining revealed the extent of neuronal injury provoked in the frontal cortex and the striatum. The neuropil of the ischemic cortex exhibited considerable aberrant morphological features relative to the sham group. However, melatonin treatment attenuated this damage to a significant extent (**Figure 2B**, $p<0.05$). The characteristic alteration observed in the ipsilateral cortex and striatum included scalloped neuronal structure accompanied by slight changes in color staining, vacuole formation, and neutrophil infiltration (**Figure 2B**). Moreover, FJB staining was performed to observe the anti-apoptotic effect of melatonin, which demonstrated a relative attenuated level of FJB-positive cells in (**Figure 2C**, $p<0.01$) relative to MCAO (**Figure 2C**, $p<0.001$).

Pre-Treatment Effect of Melatonin on Outcomes of MCAO-Mediated Stress-Associated MAPK p-P38/p-JNK Pathways

The MAPK-p38/p-JNK pathway is predominantly activated due to oxidative stress. Besides, inflammatory mediators such as p-NF-κB and Toll-like receptor ligands could also activate p-JNK which suggested a close association of MAPK p-p38/p-JNK pathway in inflammation (Tu et al., 2010; Yao et al., 2013). Moreover, previous reports reiterated the pro-apoptotic role of MAPK such as p-JNK and p-p38. To examine the neuroprotective effects of melatonin on P38/JNK expression, we did Western blotting, and the results demonstrated higher p-JNK and p-P38 expression following permanent MCAO injury in comparison to sham. The pre-treatment dosage regimen of melatonin attenuated MCAO-mediated stress associated MAPK p-P38/p-JNK pathways (**Figure 3A**). Moreover, immunohistochemical results validated our Western findings (**Figure 3B**).

Pre-Treatment Effect of Melatonin on Endogenous Antioxidant Nrf2/HO-1/Trx Pathways

Nrf2 acts as a master cellular homeostasis and stress response element in many neurodegenerative diseases. Nrf2 is an established endogenous antioxidant protein, that executes important protective effects by modulating the expression of several downstream antioxidant proteins. The inactive Nrf2 is localized to cytoplasm in a complex with Keap1, and upon dissociation of the dimer, Nrf2 translocates to the nucleus and activates potential endogenous antioxidant including downstream HO-1, superoxide dismutase (SOD) and glutathione (GSH) (Itoh et al., 2004; Kobayashi and Yamamoto, 2005; Vasconcelos et al., 2019; Yuan et al., 2020). Herein, we were interested in analyzing the effect of melatonin on Nrf2 and its downstream target HO-1. Furthermore, the effect of melatonin on Trx, a key member of the thioredoxin-peroxiredoxin family was also evaluated in the ischemic brain. The western blot images and corresponding histograms showed a relatively higher expression of Nrf2 and HO-1 24 h of permanent MCAO in comparison to the sham group (**Figure 4**). Interestingly, Trx was downregulated in the ischemic brain, while melatonin treatment significantly restored the expression level of Trx. Noticeably, we did not observe any effect on Nrf2 level (90-120 kDa) in the melatonin-treated groups (**Figure 4**).

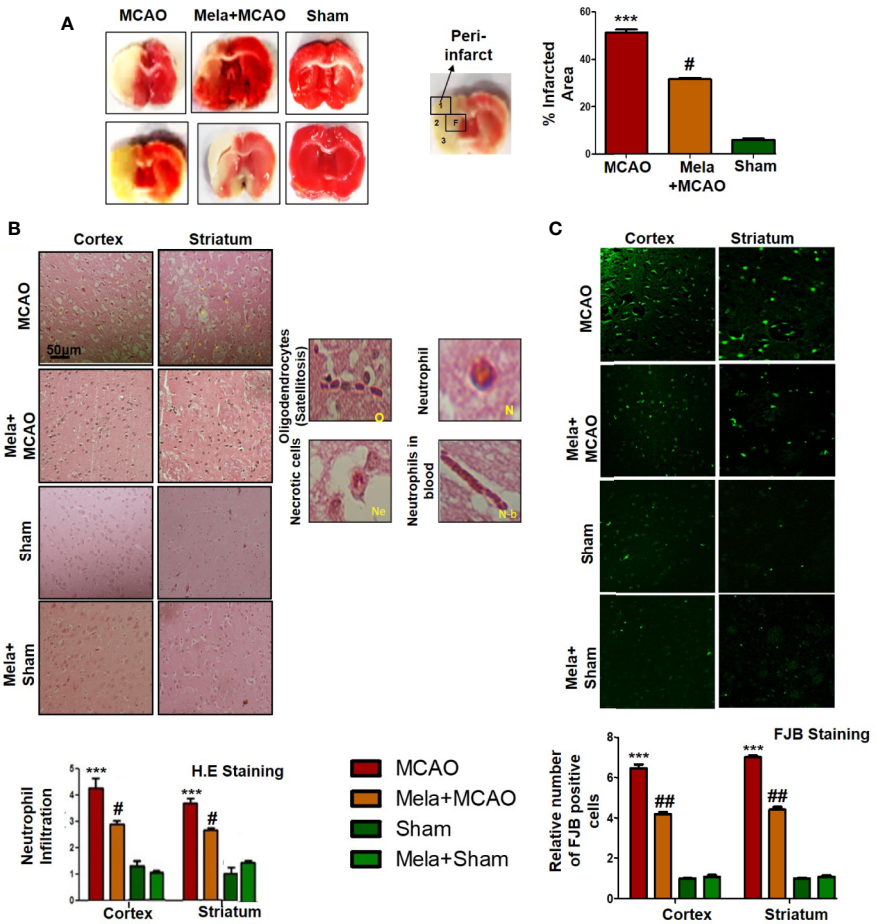

FIGURE 2 | (A) TTC staining was done to demarcate between ischemic and non-ischemic areas and to evaluate the neuroprotective effects of melatonin (n=5/group). The regions of interest (ROIs) selected were indicated by 1 and 4, respectively showing the frontal cortex and striatum. The parietal cortex is shown by 2, and the piriform cortex by 3. TTC staining was analyzed by one ANOVA followed by a non-parametric test (as Kruskal-Wallis test). Significance $^{***}p < 0.001$ showing significant difference relative to vehicle operated sham group, and $^{\#}p < 0.05$ showing significant difference relative to MCAO group **(B)** Representative images of H&E staining showing the degree of neutrophil infiltration in cortical and striatal tissue after ischemic insult, scale bar = 50 μm, magnification 40× and (n = 5/group). These tissue slides were processed from the stained TTC coronal sections after fixation in 4% paraformaldehyde. Infiltrated oligodendrocytes (O), neutrophils (N), and neutrophils in blood (N.b) are shown. Necrotic cells (Ne) with scalloped appearance are shown. Data were analyzed by two ways ANOVA followed by post-hoc Bonferroni Multiple Comparison test using graph-pad prism-5 software **(C)** Representative images of FJB staining, scale bar = 30 μm. These tissue slides were processed from the stained TTC coronal sections after fixation in 4% paraformaldehyde, and the analyzed area is frontal cortex and striatum.). Symbol *** showing significant difference relative to vehicle operated sham group and the value is $p < 0.001$ or $p < 0.01$, respectively, while # or ## showing significant difference values of $p < 0.05$ or $p < 0.01$, respectively, relative to MCAO group. TTC, 2,3,5-Triphenyltetrazolium chloride; FJB, Fluoro-Jade B; H&E, hemotoxylin and eosin.

The Pre-Treatment Dosage Regimen of Melatonin Downregulates Ischemia Stress-Associated Neuroinflammation

Resident immune cells such as glial cells play an integral role in the mediation of inflammation. Moreover, the glial cells particularly the microglia cells are involved both to release the cytokines and to release some trophic substances such as brain-derived neurotrophic factor-BDNF (Yu and Lau, 2000). We demonstrated the astrocytes activation by GFAP-reactive cells as astrocytes assume a characteristic appearance which we revealed by immunofluorescence. Likely, we noticed the increase in the pro-inflammatory cytokines (TNF-α and IL-1β), similar to previously reported observations (Davies et al., 1999). Melatonin treatment, on the other hand, attenuated these effects (**Figures 5A, B**), which was further validated by immunohistochemistry findings (**Figure 5C**).

Effect of Pre-Treatment Dosage Regimen Melatonin on Outcomes of MCAO-induced Inflammatory Mediators

The binding of proinflammatory factors TNF-α and IL-1β to respective receptors triggers the sequential activation of downstream molecules such as ASK1, SEK1, and JNK. Collectively, this leads to

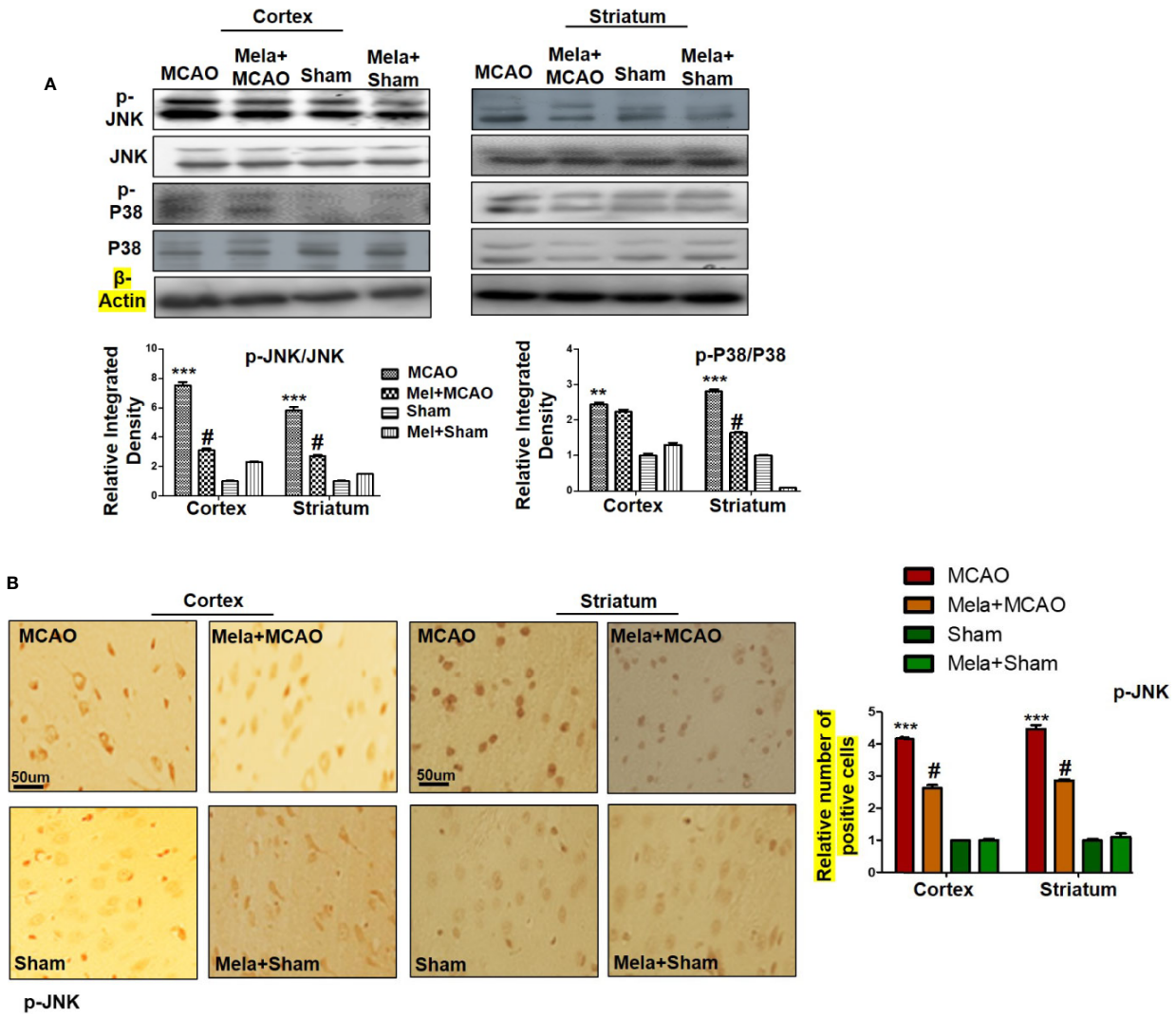

FIGURE 3 | (A) The immunoblot results of p-P38, total P-38, p-JNK, and total JNK from the ipsilateral cortex and striatum following MCAO. The immunoblot bands were quantified using ImageJ software, and the statistical differences are indicated in the corresponding graphs. The data are expressed as the mean ± SEM for n = 6 rats/group, and the number of experiments = 3. β-Actin was used as a control. Data were analyzed by two-way ANOVA followed by post-hoc Bonferroni Multiple Comparison test using graph-pad prism-5 software. The brain tissue for Western blot was collected after 24 h of vehicle or melatonin treatment and stored at −80°C until used. Symbol ∗∗∗ or ∗∗ showing significant difference relative to vehicle operated sham group and their values are $p < 0.001$ or $p < 0.01$ respectively, while # showing significant difference values of $p < 0.05$ relative to MCAO group. **(B)** The presented images indicated Immunoreactivity of p-JNK in the cortical and striatum tissue of rat brain. The p-JNK exhibits cytoplasmic localization. The data are expressed as the mean ± SEM for n = 5 rats/group, and the number of experiments = 3. Scale bar = 50 μm, magnification 40×. The immunohistochemistry slides were processed from the stained TTC coronal sections after fixation in 4% paraformaldehyde. From the thick coronal TTC sections, paraffin blocks were made, and later 4-μm-thin coronal sections were prepared by a rotary microtome. The symbol ∗∗∗ showing significant difference relative to the vehicle operated sham group and the value is $p < 0.00$, while # showing significant difference value of $p<0.05$ relative to the MCAO group. p-JNK, phospho c-Jun N-terminal kinase; JNK, c-Jun N-terminal kinase; p-P38, phospho-P38.

proteasomal dependent IκB dissociation, and nuclear translocation of NF-κB to induce inflammatory transcription types of machinery like NOS2 and COX2 (Popp et al., 2009). These proteins were hyper expressed in western blot finding in the ischemic brain ($p<0.001$, **Figure 6A**). The melatonin pre-treatment dosage regimen significantly alleviated this level ($p<0.05$). Immunostaining was further performed to validate these findings for COX2, NOS2, and p-NF-κB (**Figures 6B, C**).

Effect of Pre-Treatment Dosage Regimen of Melatonin on the p-NF-κB/Trx Pathways

To demonstrate the effect of melatonin on the co-association of p-NF-κB and Trx, we colocalized these proteins by double immunofluorescence (**Figure 7**). As demonstrated, elevated expression of p-NF-κB was observed accompanied by decreased Trx expression. Treatment with melatonin reversed the injury-induced reduction in the level of Trx.

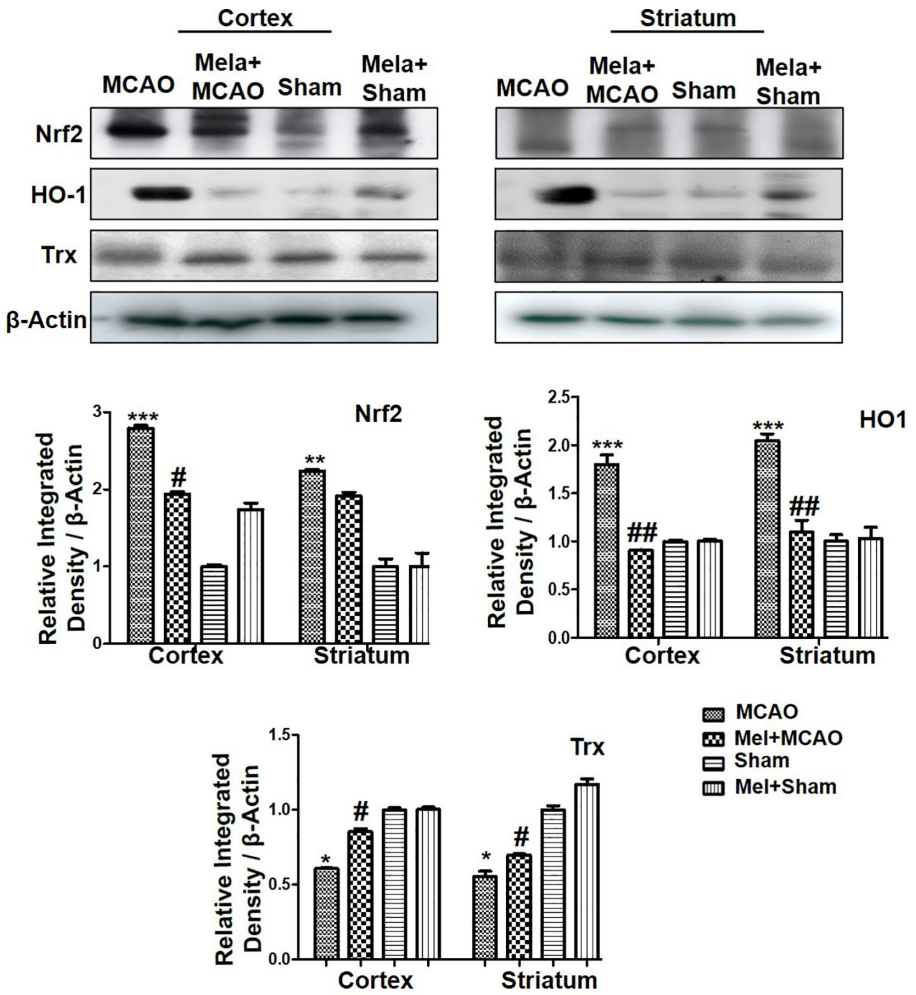

FIGURE 4 | The immunoblot results of Nrf2, HO-1, and Trx in the cortical and striatum tissue of rat ipsilateral brain. The immunoblot bands were quantified using ImageJ software, and the statistical differences are indicated in the relative graphs. The data are expressed as the mean ± SEM for n = 6 rats/group, and the number of experiments = 3. Data were analyzed by two-way ANOVA followed by post-hoc Bonferroni Multiple Comparison test using graph-pad prism-5 software β-Actin was taken as a loading control. Significance = $^{***}p<0.00$, ** or $^{\#\#}p<0.01$, and $^{\#}$ or $^{*}p<0.05$. The brain tissue for Western blot was collected after 24 h of vehicle or melatonin treatment and stored at −80°C until used, Nrf2, nuclear factor erythroid 2-related factor 2; HO-1, heme oxygenase-1; Trx, thioredoxin.

DISCUSSION

Here, we demonstrated that the endogenous neurohormone melatonin attenuates the detrimental outcomes of MCAO-induced ischemic stroke, and the current study is the continuation of our previous studies to further extend the role of melatonin. We previously have shown that melatonin treatment affects the glutamate N-methyl-D-aspartate (NMDA) and alpha-amino-3-hydroxy-5-methyl-4-isoxazole propionic acid (AMPA) receptor signaling in cerebral cortex and striatum 24 h after permanent middle cerebral artery occlusion (MCAO) and attenuated ischemia-induced down-regulation of NMDA receptor 2 (NR2a), postsynaptic density-95 (PSD95) and increases NR2a/PSD95 complex association, which further activates the pro-survival PI3K/Akt/GSK3β pathway with mitigated collapsin response mediator protein 2 (CRMP2) phosphorylation (Shah et al., 2019). Moreover, we have also demonstrated that melatonin may act in a multimechanistic way by modulating the expression of several proteins in the ischemic striatum using a proteomic approach (Shah et al., 2018b). The degree and severity of neuronal injury induced by ischemia largely depend on the occlusion period. The infarct area in the permanent MCAO model frequently involves regions from neocortex and striatum (Lo et al., 2003). Furthermore, necrotic cell death primarily occurs at striatal tissue suggesting a dramatic decrease of blood to this whitish tissue (Fluri et al., 2015).

Our results demonstrated that melatonin mitigated MCAO-mediated neuroinflammation and neurodegeneration *via*

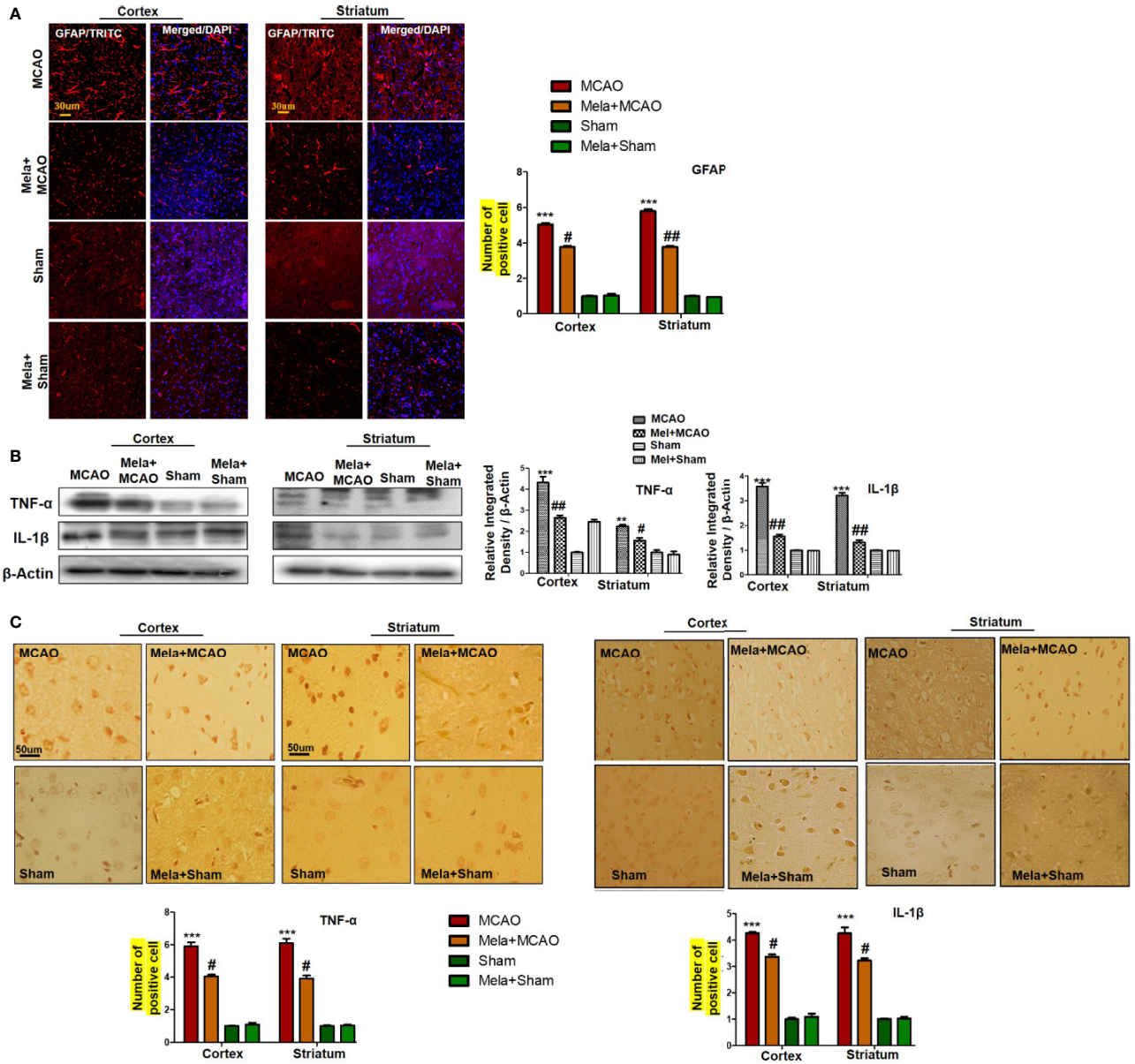

FIGURE 5 | (A) Immunoreactivity of GFAP-positive cells in different groups are shown with magnification 40× and scale bar = 30 μm. The data are expressed as the mean ± SEM for n = 5 rats/group, and the number of experiment s= 3. The immunohistochemistry slides were processed from the stained TTC coronal sections after fixation in 4% paraformaldehyde. From the thick coronal TTC sections, paraffin blocks were made, and later 4-μm-thin coronal sections were prepared by a rotary microtome. The symbol ∗∗∗ showing significant difference relative to the vehicle operated sham group and the value is p<0.00, while # or ## showing significant difference value of $p < 0.05$ and $p < 0.01$, respectively, relative to MCAO group. **(B)** Effect of melatonin on inflammatory cytokines. Western blot results of TNF-α and IL-1β from the ipsilateral brain were analyzed by ImageJ. The statistical differences are indicated in the relative graphs. The data are expressed as the mean ± SEM for n = 6 rats/group, and the number of experiments= 3. β-Actin was used as a control. Data were analyzed by two-way ANOVA followed by post-hoc Bonferroni Multiple Comparison test using graph-pad prism-5 software. The brain tissue for western blot was collected after 24 h of vehicle or melatonin treatment and stored at –80°C until used. The symbol *** or ** showing significant difference relative to the vehicle operated sham group and their values are $p < 0.00$ or $p < 0.01$, respectively, while # or ## showing significant difference value of p<0.05 and p<0.01 respectively relative to MCAO group. Symbol ** showing significant difference relative to vehicle operated sham group and the value is $p < 0.01$. **(C)** Immunohistochemistry results for TNF-α and IL-1β are shown; scale bar = 50 μm; magnification, 40×. Tissue sections show correspondingly elevated expression of TNF-α and IL-1β after 24 h of permanent ischemia and both proteins show cytoplasmic localization. Significance = ***p<0.001 and $^{\#}$p<0.05. All the morphological data are expressed as the mean ± SEM for n = 5 rats/group. The immunohistochemistry slides were processed from the stained TTC coronal sections after fixation in 4% paraformaldehyde. The TTC sections were subjected to embedding and paraffin blocks were made and later 4-μm coronal sections were made by a rotary microtome. GFAP, glial fibrillary acidic protein; TNF-α, tumor necrosis factor; IL-1β, interleukin.

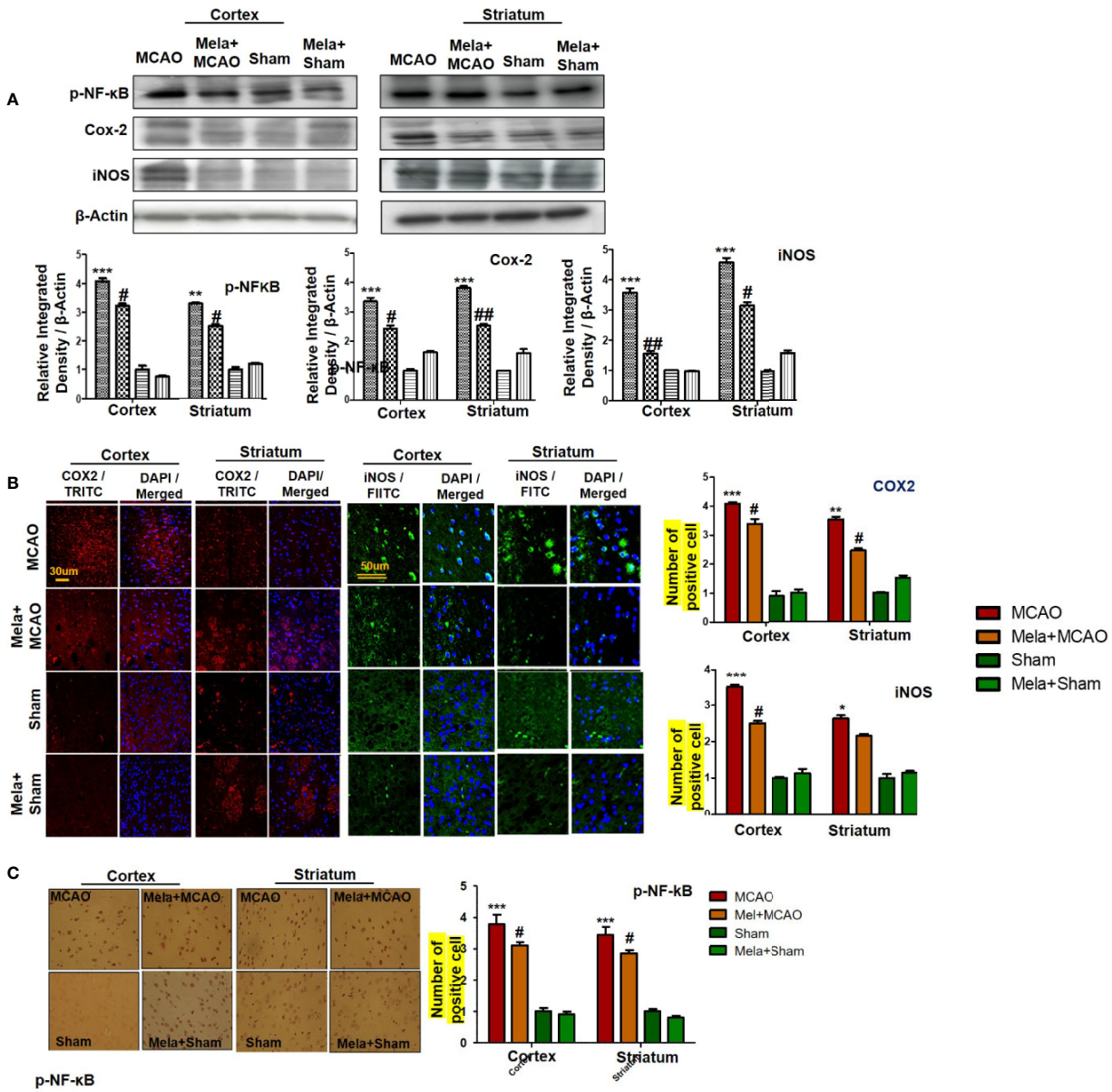

FIGURE 6 | Melatonin downregulated the NF-κB signaling pathway. **(A)** The immunoblot results of p-NF-κB, COX2, and iNOS in the cortical and striatum tissue of rat ipsilateral brain. The immunoblot bands were quantified using ImageJ software, and the statistical differences are indicated in the relative graphs. The data are expressed as the mean ± SEM for n=6 rats/group, and the number of experiments = 3. β-Actin was used as a control. Data were analyzed by two-way ANOVA followed by *post hoc* Bonferroni Multiple Comparison test using graph-pad prism-5 software. The brain tissue for western blot was collected after 24 h of vehicle or melatonin treatment and stored at −80°C until used. The symbol *** showing significant difference relative to the vehicle operated sham group and the value is $p < 0.001$, while # or ## showing significant difference value of $p < 0.05$ and $p < 0.01$ respectively relative to MCAO group. **(B)** Immunofluorescence reactivity of COX2 and iNOS; scale bar = 30 and 50 μm; magnification, 40×. The COX2 and iNOS-positive cells were visualized by TRITC and FITC respectively and showed cytoplasmic localization. The data are expressed as the mean ± SEM for n = 5 rats/group and the number of experiments performed=3. Symbol ** or * showing significant difference relative to vehicle operated sham group and the values are respectively $p < 0.01$ and $p < 0.05$. **(C)** The presented images indicated Immunoreactivity of p-NF-κB in the cortical and striatum tissue of rat brain. The p-NF-κB exhibits nuclear localization, and the number of experiments= 3.; scale bar = 20. Significance = ***$p < 0.001$ ##$p < 0.01$. NF-κb, nuclear factor kappa light chain enhancer of activated B cells; COX2, cyclooxygenase; iNOS, inducible nitric oxide or nitric oxide synthase. Symbol ** or * showing significant difference relative to vehicle operated sham group and the values are respectively $p < 0.01$ and $p < 0.05$.

inhibiting apoptotic cell death, which could be mediated by mitigating inflammation and oxidative stress along with enhanced antioxidant capacity. Furthermore, melatonin had strong pleiotropic effects, both by alleviating ROS mediated neuroinflammation but also through the strengthening of intrinsic antioxidative mechanisms, such as Trx (**Figure 8**). Many studies reiterated that targeting different aspects of stroke injury such as oxidative stress and inflammation could be of

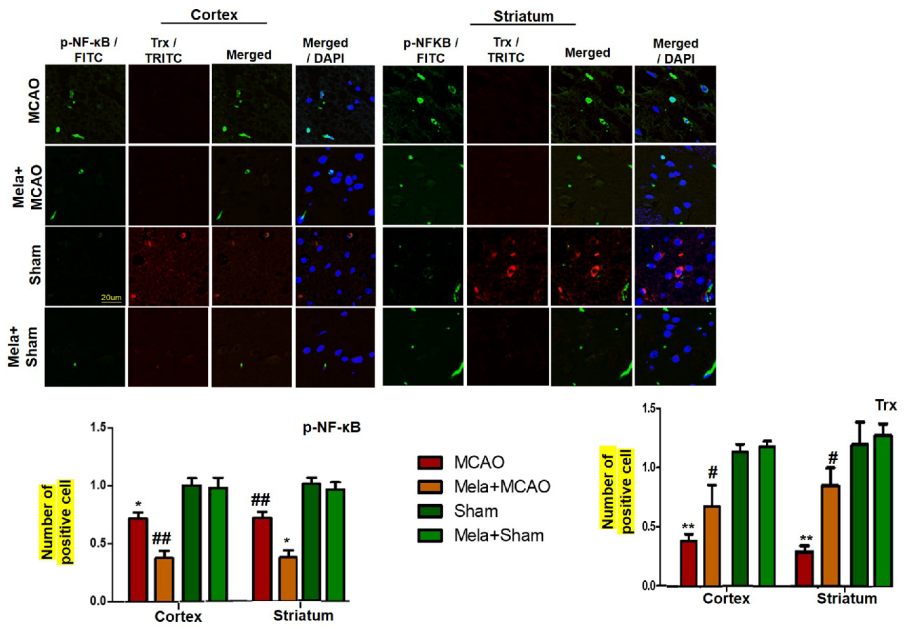

FIGURE 7 | Effect of melatonin (5 mg/kg) on the p-NF-κB/Trx pathways **(A, B)** p-NFκB and Trx were colocalized by double immunofluorescence. Scale bar = 20 μm and (n=5/group). p-NFκB showed higher expression level accompanied with Trx down expression in the MCAO group. p-NF-κB and Trx were visualized by FITC and TRITC, respectively. Significance = * and ** shows significant difference relative to sham operated vehicle group and its value are $p < 0.05$, and $p < 0.01$. $^{\#\#}$ shows significant difference relative to MCAO operated group and its value is $p < 0.01$. Significance = $^{\#}$ or $^{*}p < 0.05$; and ** or $^{\#\#}p < 0.01$. FITC, fluorescein isothiocyanate; TRITC, tetramethylrhodamine.

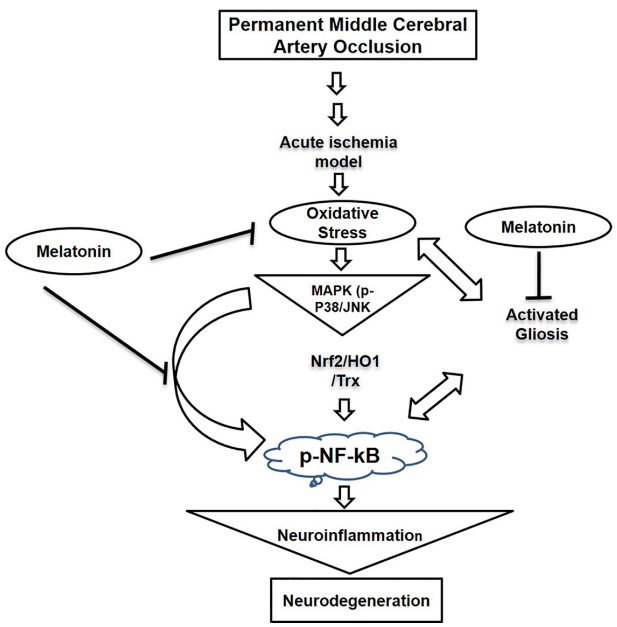

FIGURE 8 | A graphical representation of the underlying neuroprotective mechanisms of melatonin against the MCAO-induced oxidative stress-mediated neuroinflammation and neurodegeneration.

specific therapeutic value. Therefore, more experimental studies are required to unveil such mechanisms (Kacimi et al., 2011).

Consistent studies showed the role of the JNK pathway in mediating inflammatory events. Furthermore, attenuating p-NF-κB expression could also reduce the infarct area by mitigating ROS generation through COX2 and iNOS. JNK and p38 both are implicated in apoptotic cell death by a cross-talk with inflammatory mediators such as elevated p-NF-κB expression. We speculate that melatonin can diminish neuronal susceptibility by negatively affecting mitogen kinase expression, which is further linked to cytokines expression. Inflammation significantly affects the therapeutic outcome of stroke by compromising clinical prognosis. Stroke induces translocation of resident and peripheral cells to the site of injury to contribute to inflammatory pathogenesis (Wang et al., 2013). These cells further release inflammatory mediators to exacerbate neuronal injury by several mechanisms.

Stress-related MAP Kinases including JNK and p38 are activated by TLR-4 agonists located on glial cells (Munoz et al., 2007), which in turn leads to mitochondrial apoptotic activation. Moreover, inflammatory cytokines are released from hypertrophic glial cells such as microglia and astrocytes instantly after the ischemic attack (Rothwell, 1991; Putcha et al., 2003; Caso et al., 2007; Wang et al., 2012). This process is further complicated by activated nuclear transcriptional machinery like NF-κB, which triggers the downstream inflammatory mediators COX-2 and INOS and thus aggravates the damage.

Furthermore, activation of NF-κB by TLR-4 further activates downstream toxic mediators like iNOS/NOS2 and COX-2 (Popp et al., 2009). It has been reported that the activity of COX-2 and NOS2 can be attenuated by inhibiting the TLR-4 receptor on glial cells (Ramos et al., 2017). Results from several other ischemic models suggested the anti-inflammatory potential of melatonin by downregulating the expression of NF-κB, COX-2, and iNOS (Luo et al., 2019). In our study, we examined the expression level of thiol protein Trx, modulates hemostatic redox reactions. Melatonin pre-treatment significantly enhanced the expression level of Trx, further supports the antioxidant notion of melatonin in ischemic injury. Moreover, how melatonin attenuates ischemic induced neuronal toxicities are yet to be explored, though the anti-oxidant nature of melatonin could be ascribed for these effects (Yeligar et al., 2010; Patiño et al., 2016; Guo et al., 2018).

Earlier studies reported the cross-talk of oxidative stress-induced inflammation process (Ali and Kim, 2015; Ali et al., 2018). Thus, therapeutic approaches should aim at regulating and subsiding the neuroinflammation as well as the accumulation of oxidative stress *via* stimulating the antioxidant enzymes. Melatonin acts as an endogenous potent antioxidant, free radical scavenger, and a regulator of endogenous antioxidant enzymes in various pathological and disease conditions (Huang et al., 2015; Yu et al., 2019; Zhang et al., 2019). Melatonin has been associated with the activation of various antioxidant systems and thus helps in maintaining a homeostatic environment in the brain. In particular, melatonin activates SOD GSH, Sirts, and Nrf2/HO-1 pathway. Furthermore, it has been indicated that melatonin plays a vital role in an energy crisis and cellular processes associated with cell survival by activating Sirt1, Sirt3, Sirt6, and other antioxidant pathways and mediators (Ramos et al., 2017). Studies have demonstrated that the antioxidant effects of naturally derived polyphenolic substances involve the activation of the Sirt1-Nrf2 pathway. Similarly, melatonin which acts as a potent antioxidant and endogenous neuroprotective neurohormone also activate the Sirt1-Nrf2 pathway (Hirota et al., 1999; Da Cunha and Arruda, 2017). The Nrf2 is a key endogenous protein and its antioxidant activity is shielded by Keap1 in the cytoplasm. Once stress stimuli trigger Nrf2 activation, its nuclear translocation activates downstream antioxidant machinery including HO-1 and SOD (Jung and Kwak, 2010). In ischemic injury, the activation of this antioxidant machinery starts promptly and continues for 24 h (Yang et al., 2009). Previous studies showed that melatonin activates this machinery in the ischemic model, and thus counteracts the deleterious ischemic effects of oxidative stress (Li and Liu, 2019). In the current study, we did not find a significant overexpression in Nrf2 and HO-1, which could partially be attributed to methodological differences. Consistent studies reiterated the antioxidant potential of melatonin by upregulating the endogenous Nrf2 machinery. A study by Ali et al. showed elevated expression of Nrf2 by melatonin in a neurodegenerative model (Ali et al., 2018). Similarly, Parada et al. demonstrated the upregulation of Nrf2 and HO-1 in the ischemic stroke model (Parada et al., 2014). In our study, we did not notice the overexpression of Nrf2 and its downstream target HO-1. This discrepancy in results may be possibly attributed to species or methodology difference as we used the MCAO rat model, unlikely to photothrombotic mice stroke model by Parada et al. These variations need further exploration to fully understand the potential mechanism of melatonin as a key antioxidant in ischemic conditions. Interestingly, we have found that melatonin stimulates Trx, which has also a key role in the amelioration of oxidative stress associated with ROS and stress kinases, consequently preventing apoptosis and excitotoxicity in ischemic brain injury. Many studies provide evidence for the cross-talk among the endogenous antioxidants and inflammatory mediators, in particular, NF-κB pathways (Schenk et al., 1994). Trx is activated in impaired homeostasis and stress-associated condition and it prevents the neuroinflammation *via* the inhibition of NF-κB nuclear translocation (Schenk et al., 1994). Similarly, our double immunofluorescence and western blot results in this study showed that oxidative stress of ischemic injury (as shown by down expression of Trx) as coupled to the enhanced release of inflammatory cascades (as demonstrated by nuclear p-NF-κB). Interestingly, melatonin pretreatment enhanced the cytoplasmic expression of Trx and down-regulated NF-κB expression, which supports the previous studies and validate the cross-talk between oxidative stress and neuroinflammation (Li and Liu, 2019). It is worth to mention here that melatonin proved a high therapeutic window as the exogenous melatonin dose is most often very high but still, no toxicities and addictive properties have demonstrated with this (Sugden, 1983; Guardiola-Lemaître, 1997), possibly due to its short half-life (20 to 60 min), with a large hepatic first-pass effect and a biphasic elimination pattern (Lane and Moss, 1985). Moreover, the exogenous administration of melatonin elevates both brain Bcl-2 and BDNF levels.

CONCLUSIONS

Our data demonstrated that pretreatment with the endogenous antioxidant and circadian rhythm regulator melatonin rescued the post-MCAO-detrimental outcomes such as oxidative stress-associated MAP kinases, neuroinflammation, and neurodegeneration. Thus, considering our findings, we believe that supplementation with the endogenous antioxidant neurohormone would attenuate the detrimental outcomes of MCAO such as oxidative stress-associated MAPK p-P38/p-JNK, neuroinflammation, and neurodegeneration. The present study revealed the innate immune activation as demonstrated by TNF-α/IL-1 and glial activation, accompanied by oxidative stress signaling (NF-κB/COX2/iNOS) and enhanced anti-oxidative systems such as Nrf2/HO-1/Trx. More interestingly, both systems may work towards the JNK/P38 systems. It is worth mention that our parallel projects screening natural and synthetic compounds targeting JNK/P38 *via* molecular docking also identified melatonin as a potential binding ligand. Moreover, we are also working on the different formulation of melatonin

based nanoparticles in ischemic brain injury. We will continue further studies on melatonin and its formulation in ischemic brain injuries. Thus, future preclinical and clinical investigations may warrant a complete pharmacological profile of melatonin and its formulation along with the lifestyle approach to prevent, rescue, and treat MCAO-associated injuries and morbidities.

DATA AVAILABILITY STATEMENT

The raw data supporting the conclusions of this article will be made available by the authors, without undue reservation, to any qualified researcher.

ETHICS STATEMENT

The animal study was reviewed and approved by Ethical Committee Peking University. Written informed consent was obtained from the owners for the participation of their animals in this study.

AUTHOR CONTRIBUTIONS

Conceptualization: LL and FS. Methodology: FS, PK, and TA. Resources: LL, ZT, and SL. Writing: LL, FS, AA, and RA. Review and editing: FS, AA, RA, and TA. Co-supervision: TA. Funding acquisition: LL and SL. Supervision: SL and FS. All authors contributed to the article and approved the submitted version.

FUNDING

This research work is supported by the research foundation of Huazhong University of Science and Technology Union Shenzhen Hospital No: F202006281838, and Natural Science Foundation of Shenzhen University General Hospital No: SUGH2020QD015.

REFERENCES

Ali, T., and Kim, M. O. (2015). Melatonin ameliorates amyloid beta-induced memory deficits, tau hyperphosphorylation and neurodegeneration via PI 3/Akt/GS k3β pathway in the mouse hippocampus. *J. Pineal Res.* 59, 47–59. doi: 10.1111/jpi.12238

Ali, T., Rehman, S. U., Shah, F. A., and Kim, M. O. (2018). Acute dose of melatonin via Nrf2 dependently prevents acute ethanol-induced neurotoxicity in the developing rodent brain. *J. Neuroinflamm.* 15, 1–19. doi: 10.1186/s12974-018-1157-x

Azedi, F., Mehrpour, M., Talebi, S., Zendedel, A., Kazemnejad, S., Mousavizadehet, K., et al. (2019). Melatonin regulates neuroinflammation ischemic stroke damage through interactions with microglia in reperfusion phase. *Brain Res.* 1723, 146401. doi: 10.1016/j.brainres.2019.146401

Benitez-King, G., Huerto-Delgadillo, L., and Anton-Tay, F. (1993). Binding of 3H-melatonin to calmodulin. *Life Sci.* 53, 201–207. doi: 10.1016/0024-3205(93)90670-X

Boden-Albala, B., Appleton, N., and Schram, B. (2019). "Stroke Epidemiology and Prevention (Chapter 1)," in *Stroke Rehabilitation*. Eds. R. Wilson and P. Raghavan (St. Louis, MO, USA: Elsevier).

Bruno, V., Battaglia, G., Copani, A., D'onofrio, M., Di Iorio, P., De Blasi, A., et al. (2001). Metabotropic glutamate receptor subtypes as targets for neuroprotective drugs. *J. Cerebr. Blood F. Met.* 21, 1013–1033. doi: 10.1097/00004647-200109000-00001

Caso, J. R., Pradillo, J. M., Hurtado, O., Lorenzo, P., Moro, M. A., and Lizasoain, I. (2007). Toll-like receptor 4 is involved in brain damage and inflammation after experimental stroke. *Circulation* 115, 1599. doi: 10.1161/CIRCULATIONAHA.106.603431

Da Cunha, M. D. S. B., and Arruda, S. F. (2017). Tucum-do-Cerrado (Bactris setosa Mart.) may promote anti-aging effect by upregulating SIRT1-Nrf2 pathway and attenuating oxidative stress and inflammation. *Nutrients* 9, 1243. doi: 10.3390/nu9111243

Davies, C. A., Loddick, S. A., Toulmond, S., Stroemer, R. P., Hunt, J., and Rothwell, N. J. (1999). The progression and topographic distribution of interleukin-1β expression after permanent middle cerebral artery occlusion in the rat. *J. Cerebr. Blood F. Met.* 19, 87–98. doi: 10.1097/00004647-199901000-00010

Dodda, B. R., Bondi, C. D., Hasan, M., Clafshenkel, W. P., Gallagher, K. M., Kotlarczyk, M. P., et al. (2019). Co-administering Melatonin with an Estradiol-Progesterone Menopausal Hormone Therapy Represses Mammary Cancer Development in a Mouse Model of HER2-positive Breast Cancer. *Front. Oncol.* 9, 525. doi: 10.3389/fonc.2019.00525

Feigin, V. L., Forouzanfar, M. H., Krishnamurthi, R., Mensah, G. A., Connor, M., Bennett, D. A., et al. (2014). Global and regional burden of stroke during 1990–2010: findings from the Global Burden of Disease Study 2010. *Lancet* 383, 245–255. doi: 10.1016/S0140-6736(13)61953-4

Firan, F. C., Romila, A., and Onose, G. (2020). Current Synthesis and Systematic Review of Main Effects of Calf Blood Deproteinized Medicine (Actovegin®) in Ischemic Stroke. *Int. J. Mol. Sci.* 21, 3181. doi: 10.3390/ijms21093181

Fluri, F., Schuhmann, M. K., and Kleinschnitz, C. (2015). Animal models of ischemic stroke and their application in clinical research. *Drug Des. Devel. Ther.* 9, 3445. doi: 10.2147/DDDT.S56071

Gim, S.-A., Sung, J.-H., Shah, F.-A., Kim, M.-O., and Koh, P.-O. (2013). Ferulic acid regulates the AKT/GSK-3β/CRMP-2 signaling pathway in a middle cerebral artery occlusion animal model. *Lab. Anim.* 29, 63–69. doi: 10.5625/lar.2013.29.2.63

Guardiola-Lemaître, B. (1997). Toxicology of melatonin. *J. Biol. Rhythm.* 12, 697–706. doi: 10.1177/074873049701200627

Guo, Z.-N., Jin, H., Sun, H., Zhao, Y., Liu, J., Ma, H., et al. (2018). Antioxidant melatonin: potential functions in improving cerebral autoregulation after subarachnoid hemorrhage. *Front. Physiol.* 9, 1146. doi: 10.3389/fphys.2018.01146

Hirota, K., Murata, M., Sachi, Y., Nakamura, H., Takeuchi, J., Mori, K., et al. (1999). Distinct roles of thioredoxin in the cytoplasm and in the nucleus a two-step mechanism of redox regulation of transcription factor NF-κB. *J. Biol. Chem.* 274, 27891–27897. doi: 10.1074/jbc.274.39.27891

Huang, K., Chen, C., Hao, J., Huang, J., Wang, S., Liu, P., et al. (2015). Polydatin promotes Nrf2-ARE anti-oxidative pathway through activating Sirt1 to resist AGEs-induced upregulation of fibronetin and transforming growth factor-β1 in rat glomerular messangial cells. *Mol. Cell Endocrinol.* 399, 178–189. doi: 10.1016/j.mce.2014.08.014

Hui, C., Tadi, P., and Patti, L. (2020). "Ischemic stroke," in *StatPearls [Internet]* (StatPearls Publishing).

Itoh, K., Tong, K. I., and Yamamoto, M. (2004). Molecular mechanism activating Nrf2–Keap1 pathway in regulation of adaptive response to electrophiles. *Free Radic. Biol. Med.* 36, 1208–1213. doi: 10.1016/j.freeradbiomed.2004.02.075

Jung, K.-A., and Kwak, M.-K. (2010). The Nrf2 system as a potential target for the development of indirect antioxidants. *Molecules* 15, 7266–7291. doi: 10.3390/molecules15107266

Kacimi, R., Giffard, R. G., and Yenari, M. A. (2011). Endotoxin-activated microglia injure brain derived endothelial cells via NF-κB, JAK-STAT and JNK stress kinase pathways. *Inflammation* 8, 7. doi: 10.1186/1476-9255-8-7

Karasek, M., Carrillo-Vico, A., Guerrero, J. M., Winczyk, K., and Pawlikowski, M. (2002). Expression of melatonin MT(1) and MT(2) receptors, and ROR alpha (1) receptor in transplantable murine Colon 38 cancer. *Neuro Endocrinol. Lett.* 23, 55–60.

Kobayashi, M., and Yamamoto, M. (2005). Molecular mechanisms activating the Nrf2-Keap1 pathway of antioxidant gene regulation. *Antioxid. Redox Sign* 7, 385–394. doi: 10.1089/ars.2005.7.385

Lane, E. A., and Moss, H. B. (1985). Pharmacokinetics of melatonin in man: first pass hepatic metabolism. *J. Clin. Endocrinol. Metab.* 61, 1214–1216. doi: 10.1210/jcem-61-6-1214

Li, S., and Liu, F. (2019). Polydatin attenuates neuronal loss via reducing neuroinflammation and oxidative stress in rat MCAO models. *Front. Pharmacol.* 10, 663. doi: 10.3389/fphar.2019.00663

Lin, Y. U., Chen, T. Y., Hung, C. Y., Tai, S. H., Huang, S. Y., Chang, C. C., et al. (2018). Melatonin protects brain against ischemia/reperfusion injury by attenuating endoplasmic reticulum stress. *Int. J. Mol. Med.* 42, 182–192. doi: 10.3892/ijmm.2018.3607

Liu, Z. J., Ran, Y. Y., Qie, S. Y., Gong, W. J., Gao, F. H., Ding, Z. T., et al. (2019). Melatonin protects against ischemic stroke by modulating microglia/macrophage polarization toward anti-inflammatory phenotype through stat3 pathway. *CNS Neurosci. Ther.* 25, 1353–1362. doi: 10.1111/cns.13261

Lo, E. H., Dalkara, T., and Moskowitz, M. A. (2003). Mechanisms, challenges and opportunities in stroke. *Nat. Rev. Neurosci.* 4, 399–414. doi: 10.1038/nrn1106

Luo, C., Yang, Q., Liu, Y., Zhou, S., Jiang, J., Reiter, R. J., et al. (2019). The multiple protective roles and molecular mechanisms of melatonin and its precursor N-acetylserotonin in targeting brain injury and liver damage and in maintaining bone health. *Free Radic. Biol. Med.* 130, 215–233. doi: 10.1016/j.freeradbiomed.2018.10.402

Melandri, G., Vagnarelli, F., Calabrese, D., Semprini, F., Nanni, S., and Branzi, A. (2009). Review of tenecteplase (TNKase) in the treatment of acute myocardial infarction. *Vasc. Health Risk Manag.* 5, 249. doi: 10.2147/VHRM.S3848

Messner, M., Huether, G., Lorf, T., Ramadori, G., and Schwörer, H. (2001). Presence of melatonin in the human hepatobiliary-gastrointestinal tract. *Life Sci.* 69, 543–551. doi: 10.1016/S0024-3205(01)01143-2

Munoz, L., Ranaivo, H. R., Roy, S. M., Hu, W., Craft, J. M., Mcnamara, L. K., et al. (2007). A novel p38α MAPK inhibitor suppresses brain proinflammatory cytokine up-regulation and attenuates synaptic dysfunction and behavioral deficits in an Alzheimer's disease mouse model. *J. Neuroinflamm.* 4, 21. doi: 10.1186/1742-2094-4-21

Onaolapo, A. Y., Onaolapo, O. J., and Nathaniel, T. I. (2019). Cerebrovascular disease in the young adult: Examining melatonin's possible multiple roles. *J. Exp. Neurosci.* 13, 1179069519827300. doi: 10.1177/1179069519827300

Parada, E., Buendia, I., León, R., Negredo, P., Romero, A., Cuadrado, A., et al. (2014). Neuroprotective effect of melatonin against ischemia is partially mediated by alpha-7 nicotinic receptor modulation and HO-1 overexpression. *J. Pineal Res.* 56, 204–212. doi: 10.1111/jpi.12113

Patiño, P., Parada, E., Farré-Alins, V., Molz, S., Cacabelos, R., Marco-Contelles, J., et al. (2016). Melatonin protects against oxygen and glucose deprivation by decreasing extracellular glutamate and Nox-derived ROS in rat hippocampal slices. *Neurotoxicology* 57, 61–68. doi: 10.1016/j.neuro.2016.09.002

Popp, A., Jaenisch, N., Witte, O. W., and Frahm, C. (2009). Identification of ischemic regions in a rat model of stroke. *PloS One* 4, e4764. doi: 10.1371/journal.pone.0004764

Putcha, G. V., Le, S., Frank, S., Besirli, C. G., Clark, K., Chu, B., et al. (2003). JNK-mediated BIM phosphorylation potentiates BAX-dependent apoptosis. *Neuron* 38, 899–914. doi: 10.1016/S0896-6273(03)00355-6

Ramos, E., Patiño, P., Reiter, R. J., Gil-Martín, E., Marco-Contelles, J., Parada, E., et al. (2017). Ischemic brain injury: new insights on the protective role of melatonin. *Free Radic. Biol. Med.* 104, 32–53. doi: 10.1016/j.freeradbiomed.2017.01.005

Rothwell, N. J. (1991). Functions and mechanisms of interleukin 1 in the brain. *Trends Neurosci.* 12, 430–436. doi: 10.1016/0165-6147(91)90623-Z

Schenk, H., Klein, M., Erdbrügger, W., Dröge, W., and Schulze-Osthoff, K. (1994). Distinct effects of thioredoxin and antioxidants on the activation of transcription factors NF-kappa B and AP-1. *PNAS* 91, 1672–1676. doi: 10.1073/pnas.91.5.1672

Schmued, L. C., and Hopkins, K. J. (2000). Fluoro-Jade B: a high affinity fluorescent marker for the localization of neuronal degeneration. *Brain Res.* 874, 123–130. doi: 10.1016/S0006-8993(00)02513-0

Shah, F.-A., Gim, S.-A., Kim, M.-O., and Koh, P.-O. (2014). Proteomic identification of proteins differentially expressed in response to resveratrol treatment in middle cerebral artery occlusion stroke model. *J. Vet. Med. Sci.* 76, 14–0169. doi: 10.1292/jvms.14-0169

Shah, F.-A., Gim, S.-A., Sung, J.-H., Jeon, S.-J., Kim, M.-O., and Koh, P.-O. (2016). Identification of proteins regulated by curcumin in cerebral ischemia. *J. Surg. Res.* 201, 141–148. doi: 10.1016/j.jss.2015.10.025

Shah, F.-A., Park, D.-J., and Koh, P.-O. (2018a). Identification of proteins differentially expressed by quercetin treatment in a middle cerebral artery occlusion model: a proteomics approach. *Neurochem. Res.* 43, 1608–1623. doi: 10.1007/s11064-018-2576-x

Shah, F. A., Zeb, A., Ali, T., Muhammad, T., Faheem, M., Alam, S. I., et al. (2018b). Identification of proteins differentially expressed in the striatum by melatonin in a middle cerebral artery occlusion rat model—a proteomic and in silico approach. *Front. Neurosci.* 12, 888. doi: 10.3389/fnins.2018.00888

Shah, F. A., Liu, G., Al Kury, L. T., Zeb, A., Koh, P.-O., Abbas, M., et al. (2019). Melatonin protects MCAO-induced neuronal loss via NR2A mediated prosurvival pathways. *Front. Pharmacol.* 10, 297. doi: 10.3389/fphar.2019.00297

Singh, M., Sumien, N., Kyser, C., and Simpkins, J. W. (2008). Estrogens and progesterone as neuroprotectants: what animal models teach us. *Front. Biosci.: J. Virtual Library* 13, 1083.

Stefulj, J., Hortner, M., Ghosh, M., Schauenstein, K., Rinner, I., Wölfler, A., et al. (2001). Gene expression of the key enzymes of melatonin synthesis in extrapineal tissues of the rat. *J. Pineal Res.* 30, 243–247. doi: 10.1034/j.1600-079X.2001.300408.x

Sugden, D. (1983). Psychopharmacological effects of melatonin in mouse and rat. *J. Pharmacol. Exp. Ther.* 227, 587–591.

Sughrue, M., Mehra, A., Connolly, E., and D'ambrosio, A. (2004). Anti-adhesion molecule strategies as potential neuroprotective agents in cerebral ischemia: a critical review of the literature. *J. Inflammation Res.* 53, 497–508. doi: 10.1007/s00011-004-1282-0

Sung, J.-H., Shah, F.-A., Cho, E.-H., Gim, S.-A., Jeon, S.-J., Kim, K.-M., et al. (2012). Ginkgo biloba extract (EGb 761) prevents the ischemic brain injury-induced decrease in parvalbumin expression. *Lab. Anim.* 28, 77–82. doi: 10.5625/lar.2012.28.2.77

Tan, D. X., Manchester, L. C., Terron, M. P., Flores, L. J., Tamura, H., and Reiter, R. J. (2007). Melatonin as a naturally occurring co-substrate of quinone reductase-2, the putative MT3 melatonin membrane receptor: hypothesis and significance. *J. Pineal Res.* 43, 317–320. doi: 10.1111/j.1600-079X.2007.00513.x

Tu, Y.-F., Tsai, Y.-S., Wang, L.-W., Wu, H.-C., Huang, C.-C., and Ho, C.-J. (2010). Overweight worsens apoptosis, neuroinflammation and blood-brain barrier damage after hypoxic ischemia in neonatal brain through JNK hyperactivation. *J. Neuroinflamm.* 8, 40. doi: 10.1186/1742-2094-8-40

Tuttolomondo, A., Di Raimondo, D., Pecoraro, R., Arnao, V., Pinto, A., and Licata, G. (2012). Inflammation in ischemic stroke subtypes. *Curr. Pharm. Des.* 18, 4289–4310. doi: 10.2174/138161212802481200

Vasconcelos, A. R., Dos Santos, N. B., Scavone, C., and Munhoz, C. D. (2019). Nrf2/ARE pathway modulation by dietary energy regulation in neurological disorders. *Front. Pharmacol.* 10, 33. doi: 10.3389/fphar.2019.00033

Venegas, C., Garcia, J. A., Escames, G., Ortiz, F., Lopez, A., Doerrier, C., et al. (2012). Extrapineal melatonin: analysis of its subcellular distribution and daily fluctuations. *J. Pineal Res.* 52, 217–227. doi: 10.1111/j.1600-079X.2011.00931.x

Wang, L.-W., Tu, Y.-F., Huang, C.-C., and Ho, C.-J. (2012). JNK signaling is the shared pathway linking neuroinflammation, blood–brain barrier disruption, and oligodendroglial apoptosis in the white matter injury of the immature brain. *J. Neuroinflamm.* 9, 1–17. doi: 10.1186/1742-2094-9-175

Wang, Q., Tang, X. N., and Yenari, M. A. (2013). The inflammatory response in stroke. *J. Neuroimmunol.* 184, 53–68. doi: 10.1016/j.jneuroim.2006.11.014

Watson, N., Diamandis, T., Gonzales-Portillo, C., Reyes, S., and Borlongan, C. V. (2016). Melatonin as an antioxidant for stroke neuroprotection. *Cell Transplant.* 25, 883–891. doi: 10.3727/096368915X689749

Winczyk, K., Pawlikowski, M., Guerrero, J. M., and Karasek, M. (2002). Possible involvement of the nuclear RZR/ROR-alpha receptor in the antitumor action of melatonin on murine Colon 38 cancer. *Tumour. Biol.* 23, 298–302. doi: 10.1159/000068569

Yang, C., Zhang, X., Fan, H., and Liu, Y. (2009). Curcumin upregulates transcription factor Nrf2, HO-1 expression and protects rat brains against focal ischemia. *Brain Res.* 1282, 133–141. doi: 10.1016/j.brainres.2009.05.009

Yao, L., Kan, E. M., Lu, J., Hao, A., Dheen, S. T., Kaur, C., et al. (2013). Toll-like receptor 4 mediates microglial activation and production of inflammatory mediators in neonatal rat brain following hypoxia: role of TLR4 in hypoxic microglia. *J. Neuroinflamm.* 10, 1–21. doi: 10.1186/1742-2094-10-23

Yeleswaram, K., Mclaughlin, L. G., Knipe, J. O., and Schabdach, D. (1997). Pharmacokinetics and oral bioavailability of exogenous melatonin in

preclinical animal models and clinical implications. *J. Pineal Res.* 22, 45–51. doi: 10.1111/j.1600-079X.1997.tb00302.x

Yeligar, S. M., Machida, K., and Kalra, V. K. (2010). Ethanol-induced HO-1 and NQO1 are differentially regulated by HIF-1α and Nrf2 to attenuate inflammatory cytokine expression. *J. Biol.* 285, 35359–35373. doi: 10.1074/jbc.M110.138636

Yu, A. C. H., and Lau, L. T. (2000). Expression of interleukin-1 alpha, tumor necrosis factor alpha and interleukin-6 genes in astrocytes under ischemic injury. *Neurochem. Int.* 36, 369–377. doi: 10.1016/S0197-0186(99)00145-X

Yu, H., Zhang, J., Ji, Q., Yu, K., Wang, P., Song, M., et al. (2019). Melatonin alleviates aluminium chloride-induced immunotoxicity by inhibiting oxidative stress and apoptosis associated with the activation of Nrf2 signaling pathway. *Ecotoxicol. Environ. Saf.* 173, 131–141. doi: 10.1016/j.ecoenv.2019.01.095

Yuan, J., Lu, Y., Wang, H., Feng, Y., Jiang, S., Gao, X.-H., et al. (2020). Paeoniflorin Resists H2O2-Induced Oxidative Stress in Melanocytes by JNK/Nrf2/HO-1 Pathway. *Front. Pharmacol.* 11, 536. doi: 10.3389/fphar.2020.00536

Zhang, W.-X., He, B.-M., Wu, Y., Qiao, J.-F., and Peng, Z.-Y. (2019). Melatonin protects against sepsis-induced cardiac dysfunction by regulating apoptosis and autophagy via activation of SIRT1 in mice. *Life Sci.* 217, 8–15. doi: 10.1016/j.lfs.2018.11.055

Conflict of Interest: The authors declare that the research was conducted in the absence of any commercial or financial relationships that could be construed as a potential conflict of interest.

frontiers in Molecular Neuroscience

ORIGINAL RESEARCH
published: 12 November 2020
doi: 10.3389/fnmol.2020.557647

Nicotine Prevents Oxidative Stress-Induced Hippocampal Neuronal Injury Through α7-nAChR/Erk1/2 Signaling Pathway

Yun Dong[1]†, Wenchuan Bi[1]†, Kai Zheng[1], Enni Zhu[1], Shaoxiang Wang[1], Yiping Xiong[1], Junlei Chang[2], Jianbing Jiang[1], Bingfeng Liu[2], Zhonghua Lu[2] and Yongxian Cheng[1]*

[1]School of Pharmaceutical Sciences, Health Science Center, Shenzhen University, Shenzhen, China, [2]Shenzhen Institutes of Advanced Technology, Chinese Academy of Sciences, Shenzhen, China

Oxidative stress-induced neuronal damage has been implicated to play a dominant role in neurodegenerative disorders, such as Alzheimer's disease (AD). Nicotine, a principal additive compound for tobacco users, is thought as a candidate to attenuate amyloid-β-mediated neurotoxicity and NMDA-induced excitotoxicity. Previous studies demonstrated that nicotine exerted this neuroprotective action on oxidative stress. However, the mechanisms underlying how nicotine contributes on oxidative injury in immortalized hippocampal HT-22 cells remain largely unknown. Therefore, in this study we investigated that the potential effects of nicotine on hydrogen peroxide (H_2O_2)-induced oxidative injury and underlying mechanisms in HT-22 cells. We found that pretreatment with nicotine at low concentrations markedly recovered the cell cycle that was arrested at the G2/M phase in the presence of H_2O_2 through reduced intracellular ROS generation. Moreover, nicotine attenuated H_2O_2-induced mitochondrial dysfunctions. Mechanistically, the application of nicotine significantly upregulated the levels of phosphorylated Erk1/2. The neuroprotective effects of nicotine, in turn, were abolished by PD0325901, a selective Erk1/2 inhibitor. Further obtained investigation showed that nicotine exerted its neuroprotective effects *via* specifically activating α7 nicotinic acetylcholine receptors (α7-nAChRs). A selective inhibitor of α7-nAChRs, methyllycaconitine citrate (MLA), not only completely prevented nicotine-mediated antioxidation but also abolished expression of p-Erk1/2. Taken together, our findings suggest that nicotine suppresses H_2O_2-induced HT-22 cell injury through activating the α7-nAChR/Erk1/2 signaling pathway, which indicates that nicotine may be a novel strategy for the treatment of neurodegenerative disorders.

Keywords: oxidative stress, nicotine, neuroprotection, ERK1/2, α7-nAChRs

OPEN ACCESS

Edited by:
Touqeer Ahmed, National University of Sciences and Technology, Pakistan

Reviewed by:
Petra Scholze, Medical University of Vienna, Austria
Kelly Dineley, University of Texas Medical Branch at Galveston, United States

***Correspondence:**
Yun Dong
yundong@szu.edu.cn

†*These authors have contributed equally to this work*

Received: *30 April 2020*
Accepted: *01 October 2020*
Published: *12 November 2020*

Citation:
Dong Y, Bi W, Zheng K, Zhu E, Wang S, Xiong Y, Chang J, Jiang J, Liu B, Lu Z and Cheng Y (2020) Nicotine Prevents Oxidative Stress-Induced Hippocampal Neuronal Injury Through α7-nAChR/Erk1/2 Signaling Pathway. Front. Mol. Neurosci. 13:557647. doi: 10.3389/fnmol.2020.557647

INTRODUCTION

Oxidative stress caused by the accumulation of excessive reactive oxygen species (ROS) damages proteins, DNA, and membranes, which thereby disrupts neuronal cell functions and triggers neuronal cell death and eventually leads to neurodegenerative diseases (Cao and Kaufman, 2014; Tasdogan et al., 2016; Debattisti et al., 2017; Valverde et al., 2018). It is well known that

the mammalian brain has a high concentration of oxygen but low levels of antioxidant enzymes (Khan and Black, 2003; Olmez and Ozyurt, 2012), suggesting that neurons are particularly vulnerable to ROS-induced oxidative stress. Moreover, oxidative stress is postulated to be a critical factor associated with pathophysiological progression of Alzheimer's disease (AD; Smith et al., 1996), which, at least in part, contributes to destruction of neurons by amyloid-β (Aβ; Harris et al., 1995).

Hydrogen peroxide (H_2O_2), an inducer of highly reactive ROS, is responsible for the majority of oxidative neuronal damage (Behl et al., 1994; Riley, 1994; Desagher et al., 1997). H_2O_2 has been widely used as a neurotoxic paradigm to mimic *in vitro* oxidative stress in many different cell types. For instance, H_2O_2 caused intracellular ROS generation and repressed mitochondrial membrane potential, which then underwent apoptosis in PC12 cells (Gao J. et al., 2018) and in SK-N-MC cells (Lee and Kim, 2019). Similarly, mitochondrial dysfunctions induced by H_2O_2 occurred in HT-22 cells as well (Dai et al., 2014). Evidence further demonstrated that H_2O_2-induced mitochondrial membrane depolarization, swelling, and fragmentation could be due to the motility of mitochondria accompanied with mitochondrial elongation (Debattisti et al., 2017). Moreover, evidence showed that H_2O_2 could induce autophagic death in dopaminergic SY5Y cells through ROS-dependent endoplasmic reticulum stress and AMPK activation (Gao Z. et al., 2018). Therefore, it is of importance to identify a mechanism that exerts neuroprotective effects against oxidative injury.

Nicotine has been recognized as the principal additive compound of tobacco that causes devastating health problems and even premature death for tobacco users (Hoffmann et al., 1990; Benowitz, 2009; Hatsukami et al., 2008). Nicotine abuse induces oxidative stress, apoptosis, and inflammation in brain cells (Oliveira-da-Silva et al., 2009; Benowitz, 2010; Cardinale et al., 2012; Motaghinejad et al., 2016) and also exacerbates behavioral impairments in mice (Shim et al., 2008). Chronic nicotine administration exacerbates tau pathology in a mouse model of AD (Oddo et al., 2005). Interestingly, frequency of dietary nicotine however has been reported to be inversely associated with Parkinson's disease (PD) risk (Nielsen et al., 2013). These studies suggest that nicotine might exert opposite roles with respect to neurodegeneration and neuroprotection. Indeed, an experimental study showed that nicotine prevents dopaminergic neuron loss in a rodent PD model (Liu Y. et al., 2017). Evidence has also accumulated that nicotine has been linked with decreased risk for AD (Oddo et al., 2005; Echeverria and Zeitlin, 2012; Moreno-Gonzalez et al., 2013; Lombardo and Maskos, 2015). Nicotine could attenuate Aβ peptide-induced neurotoxicity in hippocampal neurons of rats (Liu and Zhao, 2004). Moreover, an *in vitro* study showed that nicotine is neuroprotective against NMDA-induced excitotoxicity (Dajas-Bailador et al., 2000). The actual results indicate the opposite effects of nicotine in the CNS, neuroprotective effects, and neurotoxic effects. Importantly, nicotine has been reported to encourage oxidative impairments in rat's brain (Barr et al., 2007; Benowitz, 2010; Saad et al., 2020); nevertheless, increasing studies *in vitro* and *in vivo* showed the functions of nicotine on oxidative stress (Guan et al., 2003; Liu and Zhao, 2004; Hritcu et al., 2017). For instance, nicotine could neuroprotect against oxidative stress in primary cultures (Liu et al., 2015), in PC12 cells (Slotkin et al., 2015). Moreover, antioxidative functions of nicotine have been indicated in SY5Y cells (Parada et al., 2010). However, the contribution of nicotine on oxidative injury and its underlying mechanisms in mouse hippocampal HT-22 cell remain largely unknown.

In the present study, we investigated whether nicotine could mitigate H_2O_2-induced oxidative damage in HT-22 cells and explored the potential molecular mechanisms. Thereby, a thorough understanding of the potential functions of nicotine on oxidative stress will be revealed, and this could promote the development of effective agents in the treatment of these conditions.

MATERIALS AND METHODS

Reagents and Antibodies

The FITC-labeled Annexin V Apoptosis Detection Kit was obtained from BD Biosciences (Canada). The ROS assay kit (DCFH-DA) was purchased from Meilun (China). The cell culture medium was obtained from HyClone (Utah, USA), and cell-cultured grade fetal bovine serum (FBS), penicillin/streptomycin, and trypsin were purchased from Gibco (Thornton, Australia). The antibodies of p-Erk1/2, Erk1/2, p-Akt, Akt, cleaved-caspase 3, caspase 3, cleaved-caspase 9, caspase 9, β-actin, and horseradish peroxidase (HRP)-conjugated goat anti-rabbit antibody were obtained from Cell Signaling Technology (Danvers, MA, USA). Anti-nicotinic acetylcholine receptor α7 antibody was purchased from Abcam (ab216485, Abcam). The drugs were obtained from the following sources: nicotine, methyllycaconitine citrate (MLA), dihydro-β-erythroidine hydrobromide (DHβE), and PD0325901 from MedChemExpress (MCE, USA) and H_2O_2 and *N*-acetylcysteine (NAC) from Sigma–Aldrich (St. Louis, MO, USA).

Cell Culture

HT-22 cells (a mouse hippocampal cell line) purchased from iCell company in Shanghai, China, were cultured in Dulbecco's modified Eagle's medium (DMEM) with 10% FBS, 100 U/ml penicillin, and 100 U/ml streptomycin. The cells were maintained in a humidified 5% CO_2 atmosphere at 37°C. The cells were plated at a density of 1×10^4/well in 96-well plates and 2×10^5/well in six-well plates, respectively. After 24 h, cells were applied for various treatments and subjected to measurements.

Cell Viability

Cell cytotoxicity was quantified by a Cell Counting Kit (CCK-8, Dojindo Laboratory, Kumamoto, Japan), following the manufacturer's instruction. HT-22 cells were plated in 96-well plates with the application of various drugs. CCK-8 solution (10 μl/well) was added to each well and incubated for an additional 1 h at 37°C in 5% CO_2. Then, the spectrophotometric absorbance at 450 nm was determined by using a microplate reader (BioTek).

Cell-Cycle Analysis

For cell-cycle analysis, HT-22 cells were seeded in six-well plates with the application of different drugs, then the cells were washed twice with cold PBS. The cells were resuspended in 300 μl PI/RNase Staining Buffer (BD Biosciences) and incubated for 15 min at room temperature in the dark. The cells were then analyzed by a FACSCalibur flow cytometer at 480 nm. Data were analyzed with CELLQuest software.

Measurement of Cell Proliferation

HT-22 cell proliferation was determined by EdU incorporation assay *via* EdU cell proliferation Kit with Alexa Fluor 594 following the manufacturer's instructions (Beyotime, China). HT-22 cells were seeded in six-well plates and were allowed to be treated with various drugs for 24 h. Cells were then incubated with 10 μM EdU solution in DMEM medium for 4 h. The cells were washed with washing buffer (PBS containing 3% BSA), followed by fixation of 4% polyformaldehyde for 15 min and then permeabilization with PBS containing 0.3% Triton X-100 for 20 min. After three times washing, cells were incubated with azide-conjugated Alexa Fluor 594 for 30 min in click addictive reactive buffer with 4 mM $CuSO_4$. Cells were then washed three times with washing buffer. DAPI (1:1,000, Beyotime, China) was incubated with cells in PBS solution for 10 min at room temperature. The cells in six different areas of each well were photographed under a fluorescent microscope and analyzed with ImageJ software. The percentage of proliferated cells was calculated as EdU-positive cell number/total cell number × 100%.

Measurement of Mitochondrial Membrane Potential

Mitochondrial membrane potential has been used as an important parameter of mitochondrial function (Liu et al., 2018). To assess the level of mitochondrial membrane potential, a commercial cyanine dye JC-1 assay kit (5,5′,6,6′-tetrachloro-1,1′,3,3′-tetraethyl-imidacarbocyanine iodide, Beyotime, China) was used according to the manufacturer's instructions. Previous studies have described that JC-1 staining for mitochondria, either as red fluorescent J-aggregates or as green fluorescent J-monomers, was used for monitoring the mitochondrial membrane potential (Smiley et al., 1991). J-aggregates at higher mitochondrial concentrations reflected higher mitochondrial potential, and J-monomers at lower mitochondrial concentrations indicated lost membrane potential. Accordingly, the J-aggregate/J-monomer (red/green) fluorescence intensity ratio monitored mitochondrial membrane potential fluctuations. In brief, the cells were collected and washed in PBS and then incubated with 1 ml JC-1 (5 μg/ml) staining solution for 20 min at 37°C in dark. Cell treated with 10 μM carbonyl cyanide m-chlorophenylhydrazone (CCCP) was used as positive control. CCCP is a protonophore which can cause dissipation of mitochondrial membrane potential. Subsequently, the cells were measured using flow cytometry. The red fluorescence was measured at the excitation wavelength of 530 nm and the emission wavelength of 590 nm. The green fluorescence was detected at the excitation wavelength of 485 nm and the emission wavelength of 530 nm. The changes in mitochondrial membrane potential were calculated as the JC-1-stained red/green fluorescence intensity ratio, which were analyzed using FlowJo v7.6 software 41.

Analysis of Apoptosis

HT-22 cells seeded in six-well plates were allowed to be treated with various drugs for 24 h. The apoptosis assay was conducted using Annexin V-FITC/PI apoptosis detection kit (BD Biosciences, Mississauga, ON, Canada) following the manufacturers' instruction. The cells were collected and washed with cold Ca^{2+}-free PBS. Then, the cells were resuspended in 500 μl 1× binding buffer, containing Annexin V/FITC and 5 μl PI for 15 min at room temperature in the dark. Cell apoptosis was analyzed by using a flow cytometer. Data were analyzed using FACSAria equipped with the CellQuest Software.

Measurement of Intracellular ROS

The amount of intracellular ROS was measured by probe 2′,7′-dichlorodihydrofluorescein diacetate (DCFH-DA, ROS assay Kit, Meilun, China) in HT-22 cells. The treated cells were washed twice with PBS and then incubated with 10 μM DCFH-DA at 37°C for 30 min. After washing with fresh DMEM, cells were collected by trypsin. Cells were analyzed using a flow cytometer (cytoFLEX, Beckman Coulter), and the level of ROS was measured as the mean fluorescence intensity. The images of the cells were captured in six different areas of each well under a fluorescent microscope (AxioVert Al, Zeiss, Germany) and measured by using ImageJ (NH) software. The number of ROS-positive cells was calculated as a percentage: positive cell number/total cell number × 100%.

Western Blot Analysis

HT-22 cells were seeded in six-well plates and were allowed to be treated with various drugs for 24 h. The cells were rinsed twice with cold PBS and lysed by homogenization of RIPA buffer (Beyotime Institute of Biotechnology, Shanghai, China), and a phosphatase inhibitor and a protease inhibitor cocktail tablet (1:50, Roche, Germany) were added for 30 min on ice. Then, the collected cell lysates were vortexed and the insoluble cell debris were removed using centrifugation at 12,000× *g* for 10 min at 4°C. The total protein concentrations were measured using a Pierce BCA Protein Assay Kit (Thermo Fisher Scientific, Waltham, MA, USA), and then all lysates were diluted to the same concentration. The cell lysates were boiled in a gel-loading buffer at 95°C for 10 min. The protein extracts of 10 μg were separated in 10% acrylamide gel by electrophoresis and then transferred to polyvinylidene fluoride Immun-Blot PVDF Membranes (Bio-Rad, Hercules, CA, USA). Membranes were blocked with 5% skim milk in a Tris-buffered saline containing 0.05% (v/v) Tween-20 (TBS-T) for 1 h at room temperature before an overnight incubation at 4°C with various primary antibodies. The antibodies were in different dilution as follows: p-Erk1/2, Erk1/2, p-Akt, Akt, cleaved caspase-3, caspase-3, cleaved caspase-9, and caspase-9 in 1:1,000 dilution; nAChR α7 in 1:300 dilution; and β-actin in 1:5,000 dilution. Blots were rinsed with TBS-T and incubated for 1 h at room temperature with an HRP-conjugated

secondary antibody at a 1:5,000 dilution. Reactive bands were visualized by the Quantity One automatic imaging analysis system (Bio-Rad, Hercules, CA, USA) using enhanced chemiluminescence ECL (Millipore, Kankakee, IL, USA). The intensities of the immune-reactive bands were calculated by ImageJ software.

Statistical Analysis

Statistical comparisons were performed using one-way analysis of variance (ANOVA) followed by a *post hoc* test. Data were expressed as the mean ± standard error of the mean (SEM). Statistical significance was taken at $p < 0.05$.

RESULTS

H_2O_2 Inhibits HT-22 Cell Growth

To study the vulnerability of HT-22 cells to oxidative stress, HT-22 cells were exposed to various concentrations of H_2O_2 (200, 400, 600, and 800 μM) for 24 h, and the cell viability was detected following the H_2O_2 challenge using CCK-8 Kit as described previously (Zhang et al., 2018). Increase in H_2O_2 concentrations caused a dose-dependent decrease in cell viability as compared to control (**Figures 1A,B**). Observed results showed that 400 μM H_2O_2 significantly induced a decrease in cell density. To further investigate H_2O_2-induced oxidative injury, flow cytometer assay was performed to analyze cell-cycle distribution, and we found that cell cycle was arrested at the G2/M phase in the presence of H_2O_2 (**Figures 1C,D**), which is in accordance with a previous study (Liu H. et al., 2017). Moreover, exposure to increasing H_2O_2 concentrations resulted in a dose-dependent decrease in EdU incorporation to cells (**Supplementary Figure 1**). These results demonstrated that H_2O_2-mediated oxidative injury significantly inhibits cell proliferation.

H_2O_2 Damages Mitochondria of HT-22 Cells

A previous study demonstrated that cardiac mitochondria are vulnerable to oxidative stress (Kim et al., 2016). In order to evaluate the mitochondrial functions of HT-22 cells in response to H_2O_2, mitochondrial membrane potential was detected by JC-1 staining. As shown in **Figures 2A,B**, H_2O_2 at different concentrations considerably decreased the red/green ratio, indicating that H_2O_2 caused mitochondrial dysfunctions. Since the change in mitochondrial membrane potential is an indicator for apoptosis, we next examined whether H_2O_2 could induce apoptosis of HT-22 cells. Western blot analysis showed that H_2O_2 did not trigger apoptosis, as indicated by the unchanged protein levels of cleaved caspase 3 and caspase 9 (**Figures 2C,D**). Moreover, there was no statistically significant difference of the percentages of apoptotic cells in the H_2O_2-treated group when apoptosis was analyzed by flow cytometer after Annexin V/PI staining (**Figures 2E,F**). These results suggested that the inhibitory effects of H_2O_2 observed in HT-22 cells were not through the induction of apoptosis.

H_2O_2-Induced Oxidative Damage Is Due to Excessive Intracellular ROS Generation in HT-22 Cells

Because H_2O_2 is an ROS inducer, we next investigated the association between H_2O_2-mediated cell growth retardation and ROS generations. We found that exposure of HT-22 cells to H_2O_2 significantly elevated ROS levels (**Figures 3A,B**). Besides, cell loss induced by H_2O_2 (200, 400, 600, and 800 μM) was significantly prevented by the ROS scavenger, *N*-acetylcysteine (NAC, 4 mM, **Figure 3C**).

Since 600 μM H_2O_2 led to almost half HT-22 cell loss, this concentration was applied in the following experiments. HT-22 cells were treated with H_2O_2 in the presence or absence of NAC (4 mM) for 24 h and then the cell cycle was detected. Results showed that NAC apparently reduced the percentage of G2/M phase (**Figures 3D,E**). Together, these results suggested that H_2O_2-induced oxidative injury were mainly mediated by ROS generations.

Nicotine Reduces H_2O_2-Induced Oxidative Damage

Previously, a study showed neuroprotection of nicotine from Aβ-induced neurotoxicity (Rothbard et al., 2018). Here, we examined nicotine effects on HT-22 cell viability after the application of H_2O_2. HT-22 cells were pretreated with different concentrations (1, 2, 5, and 10 μM) of nicotine for 24 h. Afterward, the cells were exposed to 600 μM H_2O_2 for another 24 h. As shown in **Figure 4** and **Supplementary Figure 2**, nicotine remarkably reduced H_2O_2-induced oxidative damage compared to the H_2O_2-treated group. Nicotine (1, 2, 5, and 10 μM) significantly increased the cell viability (**Figures 4A,B**), although the antioxidative functions of 10 μM nicotine showed a reduction. Besides, nicotine remarkably inhibited H_2O_2-stimulated ROS generation (**Figure 4C**). In addition, PI staining assay also showed that nicotine significantly recovered the cell cycle arrested by H_2O_2 (**Figures 4D,E**). Finally, the change in mitochondrial membrane potential was monitored and the results showed that the red/green ratio was significantly reduced by 600 μM of H_2O_2. However, pretreatment with nicotine substantially ameliorated the disruption of mitochondrial membrane potential induced by H_2O_2 (**Figures 4F,G**). Therefore, nicotine exerted its protective effects against H_2O_2 *via* reducing ROS production and restoring mitochondrial function and, as a result, facilitating cell proliferation.

The Antioxidation of Nicotine Involves the Erk1/2 Signaling Pathway

Both Erk1/2 and PI3K/Akt signaling pathways have been demonstrated to mediate neuroprotection from H_2O_2-mediated cell death (Fodero et al., 2004; Liu J. Y. et al., 2017; Wang T. et al., 2018). To investigate the molecular pathways underlying the effects of nicotine against H_2O_2-induced cell damage, the levels of phosphorylated Erk1/2 (p-Erk1/2) and Akt (p-Akt) upon H_2O_2 stimulation were monitored in the presence or absence of nicotine. Western blot analysis showed that phosphorylation of Erk1/2 was downregulated by H_2O_2 incubation in HT-22 cells;

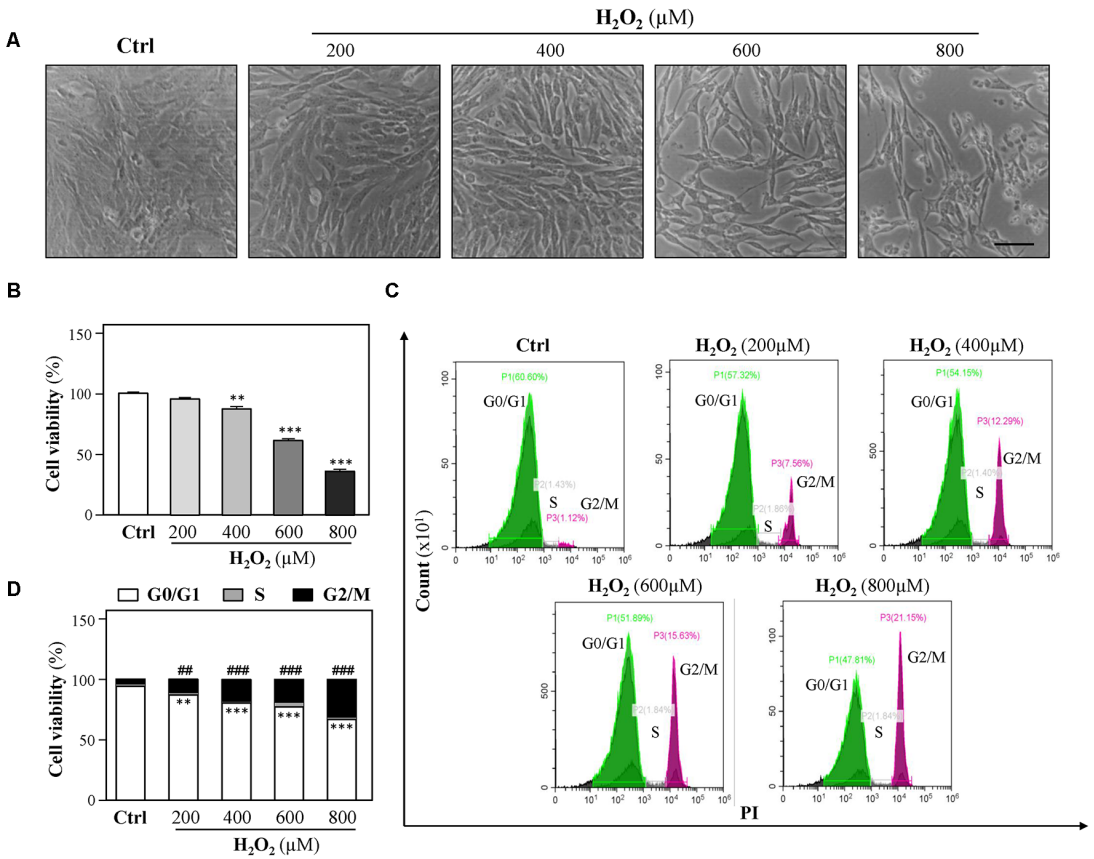

FIGURE 1 | H_2O_2 inhibits HT-22 cell proliferation. Cultured HT-22 cells were incubated with H_2O_2 at different concentrations (200–800 μM) for 24 h; the control group (Ctrl) consists of the untreated cells. **(A)** Representative images of the cell morphology. Bar = 100 μm. **(B)** Cell viability test was performed using CCK-8 kit. **(C)** The cell cycle was detected by a flow cytometer. **(D)** Cell viability was calculated as G2/M phase. Values are shown in percentage as compared to control cells. All data in bar charts represent mean ± SEM, $n = 3$. $^{**}p < 0.01$, $^{***}p < 0.001$ represents G0/G1 phase vs. control group; $^{\#\#}p < 0.01$ and $^{\#\#\#}p < 0.001$ represents G2/M phase vs. control group.

yet, nicotine treatment significantly increased phosphorylation of Erk1/2 (**Figure 5A**). To further explore the relation between H_2O_2 and Erk1/2, CCK8 assay was employed to assess HT-22 cell viability by treating with H_2O_2 and/or nicotine in the presence or absence of a selective Erk1/2 inhibitor (PD0325901). The results showed that the neuroprotection of 2-μM nicotine against H_2O_2 was totally abolished by PD0325901 (**Figure 5B**). Furthermore, we found that NAC also increased the level of p-Erk1/2 (**Figure 5C**), implying that ROS accumulation inactivates the Erk1/2 pathway. Taken together, these data suggested that the activated Erk1/2 pathway accounted for the neuroprotective functions of nicotine against H_2O_2-induced oxidative injury. In addition, our observation showed that p-Akt expression was not significantly influenced by H_2O_2 and nicotine (**Figure 5D**).

α7 Nicotinic Acetylcholine Receptors Play a Dominant Role in the Antioxidation of Nicotine

To further reveal the relationship between nicotine and Erk1/2, methyllycaconitine citrate (MLA), an α7-nAChR inhibitor, was applied to HT-22 cells together with H_2O_2 after the preincubation of nicotine. The neuroprotection of nicotine against ROS generation and cell-cycle arrest was almost prevented by MLA (**Figures 6A,B**, and **Supplementary Figure 4**). Cell viability analysis showed that the proliferation of nicotine against H_2O_2 was significantly inhibited by MLA (**Figure 6C**). Furthermore, we found that MLA fully inhibited p-Erk1/2 upregulation by nicotine (**Figures 6D,E**). Notably, the expression of α7-nAChRs was decreased by H_2O_2 (**Supplementary Figure 3**). These results suggest that α7-nAChRs is critical for nicotine-mediated activation of ERK1/2 signaling and antioxidation. In addition, we also analyzed the potential role of α4β2 nicotinic acetylcholine receptors (α4β2-nAChRs) in nicotine-mediated antioxidation. Our observation showed that α4β2-nAChRs did not influence the antioxidation of nicotine (**Supplementary Figure 5**).

DISCUSSION

Accumulating studies have shown that nicotine *in vitro* and *in vivo* promotes neuronal survival against oxidative stress (Guan et al., 2003; Liu and Zhao, 2004; Hritcu et al., 2017).

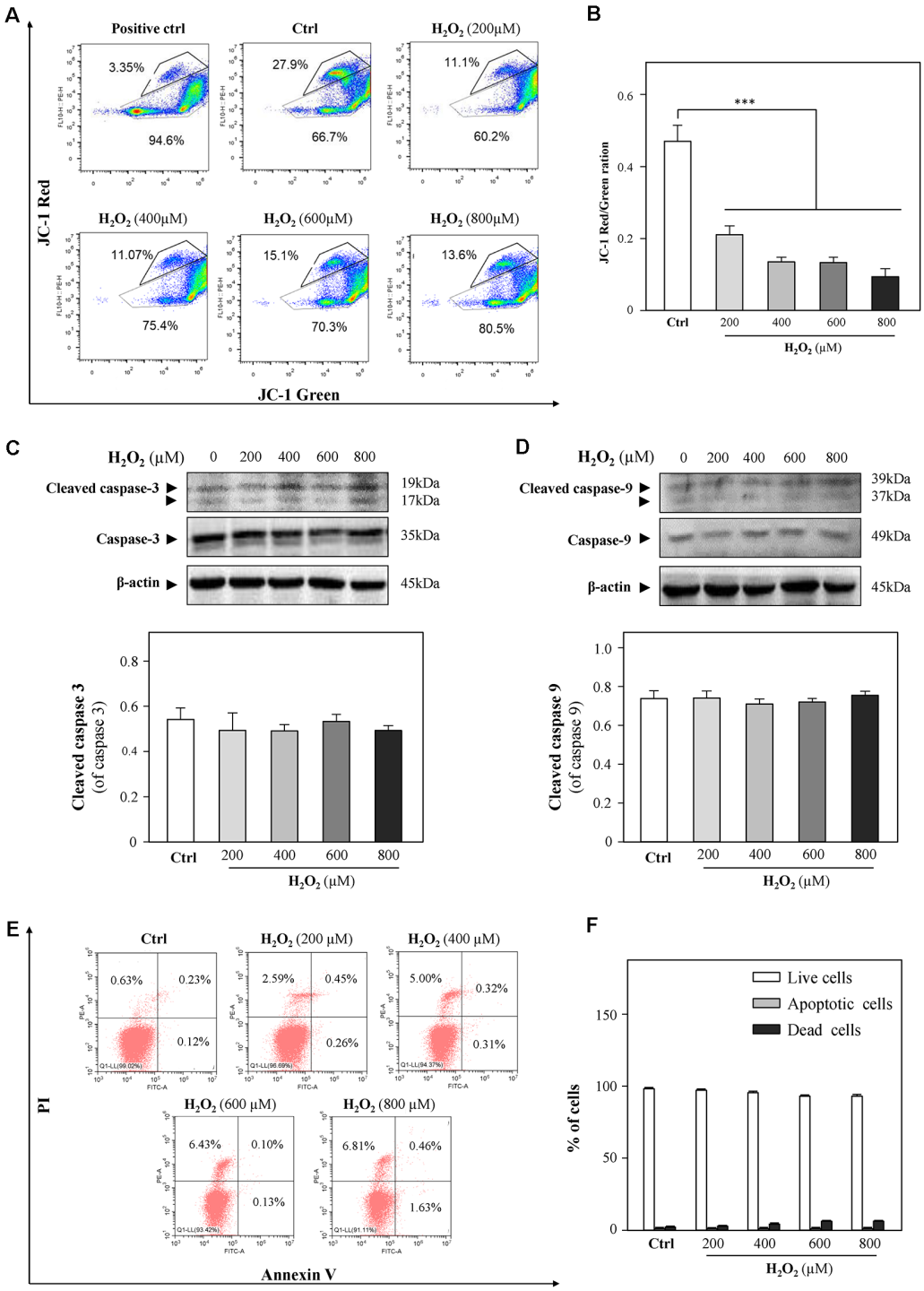

FIGURE 2 | H_2O_2 shows impairment functions to mitochondria, but it cannot induce apoptosis in HT-22 cells. Cultured HT-22 cells were incubated with H_2O_2 at different concentrations (200–800 μM) for 24 h; control group (Ctrl) consists of the untreated cells. **(A)** Representative dot plot of the changed mitochondrial membrane potential using flow cytometry after labeling the fluorescent probe with JC-1. The changes in mitochondrial membrane potential induced by 10 μM CCCP were used as positive control. **(B)** Ratios of JC-1 red/green were shown in histograms. **(C)** Western blot analyses of cleaved-caspase 3 and caspase 3. Expression of β-actin was served as a loading control. Quantification plot of cleaved-caspase 3 was shown in histograms. **(D)** Western blot analyses of cleaved-caspase 9 at and caspase 9. Expression of β-actin served as a loading control. Quantification plot of cleaved-caspase 9 was shown in histograms. **(E)** Cell apoptosis was detected by flow cytometry with Annexin V/PI apoptosis detection kit using a flow cytometer. **(F)** Values are in percentage of apoptotic cell rates of live cells, apoptotic cells, and dead cells, as calibrated from **(E)**. Values are in percentage as compared to control (no drug treatment), and each point represents the mean ± SEM, $n = 3$. $^{***}p < 0.001$ vs. control group. CCCP, carbonyl cyanide m-chlorophenylhydrazone.

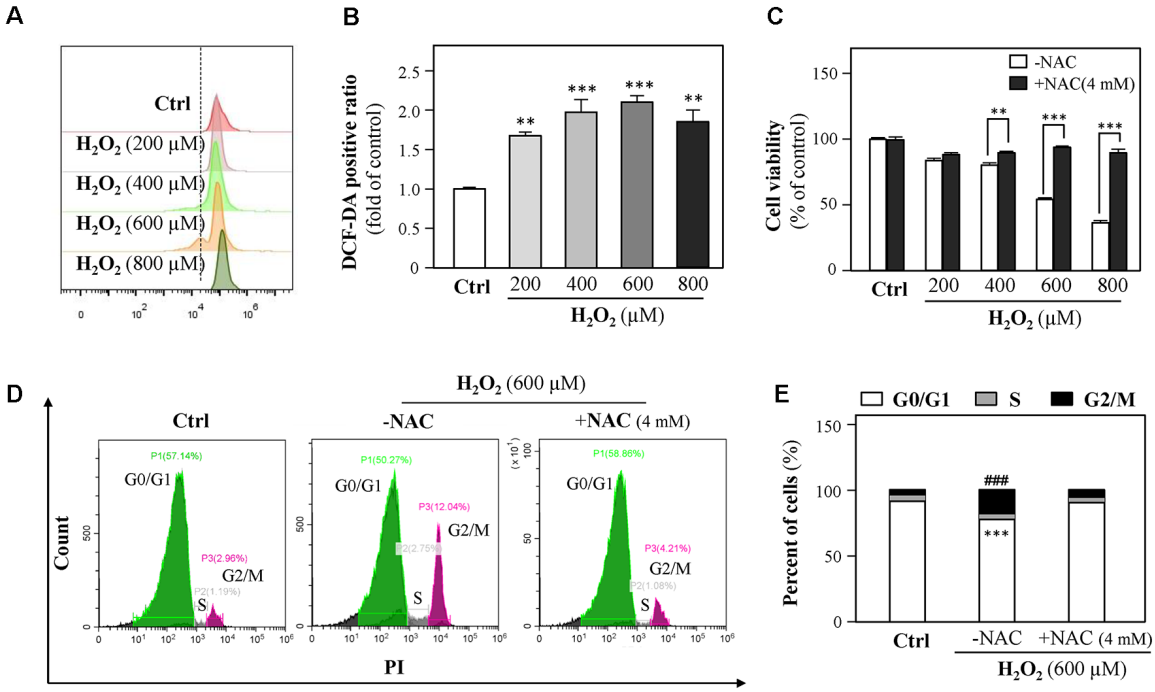

FIGURE 3 | H_2O_2 increases intracellular reactive oxygen species (ROS) formation, thus causing cell-cycle arrest. **(A)** Cultured HT-22 cells were incubated with H_2O_2 at different concentrations (200–800 μM) for 24 h; the control group consists of the untreated cells. The amount of intracellular ROS was detected by DCFH-DA using a flow cytometry. **(B)** Mean fluorescence density of ROS level was calibrated from panel **(A)**. **(C)** Cultured HT-22 cells were treated with or without NAC (4 mM); simultaneously, the cells were treated with H_2O_2 at different concentrations (200–800 μM) for 24 h. The cell viability test was performed using CCK-8 kit, and the changes were shown in histograms as percentage with control. **(D)** Cultured HT-22 cells were seeded in six-well plates and incubated with H_2O_2 (600 μM) in the presence or absence with NAC (4 mM) for 24 h, respectively. The control group consists of the untreated cells. Cell apoptosis was detected by flow cytometry with Annexin V/PI apoptosis detection kit using a flow cytometer. **(E)** Values are in percentage of apoptotic cell rates of live cells, apoptotic cells, and dead cells, as calibrated from panel **(D)**. Values are shown in percentage; each point represents the mean ± SEM, $n = 3$. $^{**}p < 0.01$, $^{***}p < 0.001$ and $^{\#\#\#}p < 0.001$ vs. H_2O_2-treated group. NAC, *N*-acetylcysteine.

Liu and Zhao (2004) previously reported that nicotine prevented Aβ-induced free radical in culture hippocampal neurons of rats. Our work provides a novel molecular link between nicotine and oxidative injury in HT-22 neuronal cells. The obtained results presented in the current study demonstrated that the pretreated nicotine at low concentrations (1, 2, 5, and 10 μM) inhibited H_2O_2-induced oxidative damage *via* activating its α7-nAChRs and subsequent Erk1/2 signaling pathway in HT-22 cells. These findings suggest that nicotine at low concentrations could be developed as a therapeutic agent for neurodegenerative disorders.

Oxidative stress has been implicated in numerous chronic or acute neurodegenerative disorders, such as AD (Behl et al., 1994) and PD (Fahn and Cohen, 1992), as well as neuroexcitotoxicity-related diseases (Coyle and Puttfarcken, 1993; Patel et al., 1996). The cytotoxic events mediated by oxidative stress are mainly due to the excessive ROS generations stimulated by H_2O_2 and the superoxide anion of free radicals. The accumulation of intracellular ROS has been linked to DNA damage, mitochondrial dysfunctions, lipid peroxidation, and protein destruction of neurons (Chen et al., 2012). H_2O_2 has been widely used as an *in vitro* inducer for oxidative stress to investigate neuroprotection in many different cell types (Desagher et al., 1997; Wang S. et al., 2018). In the present study, HT-22 cells were exposed to H_2O_2 for 24 h, and then intracellular ROS levels were remarkably increased, accompanied with a dose-dependent reduction of cell density. Furthermore, our results demonstrated that the decreased cell density mainly resulted from the changes of cell-cycle progression at the G2/M phase and the inhibition of cell proliferation caused by H_2O_2-stimulated ROS overproduction (**Figure 1** and **Supplementary Figure 1**), which is consistent with previous studies that H_2O_2 inhibits cell proliferation in neural stem cells (Kim and Wong, 2009; Richter et al., 2015). Evidence has shown that 500 μM H_2O_2 significantly induced cell-cycle changes at the G2/M phase in neuroblastoma (B65) cells (Pizarro et al., 2009), which verified our results. On the other hand, Chen et al. (2000) reported that H_2O_2 induces human fibroblast cell apoptosis with an S-phase cell-cycle distribution. A possible explanation of the observation is that different cell types in response to oxidative stress could result in multiple characteristics of cell injury. Mitochondria are vulnerable to ROS (Sinha et al., 2013). Excessive ROS causes the loss of mitochondrial membrane potential and activates mitochondria-dependent neuronal cell deficits (Liu et al., 2015). We used the JC-1 probe to show that H_2O_2 induced a

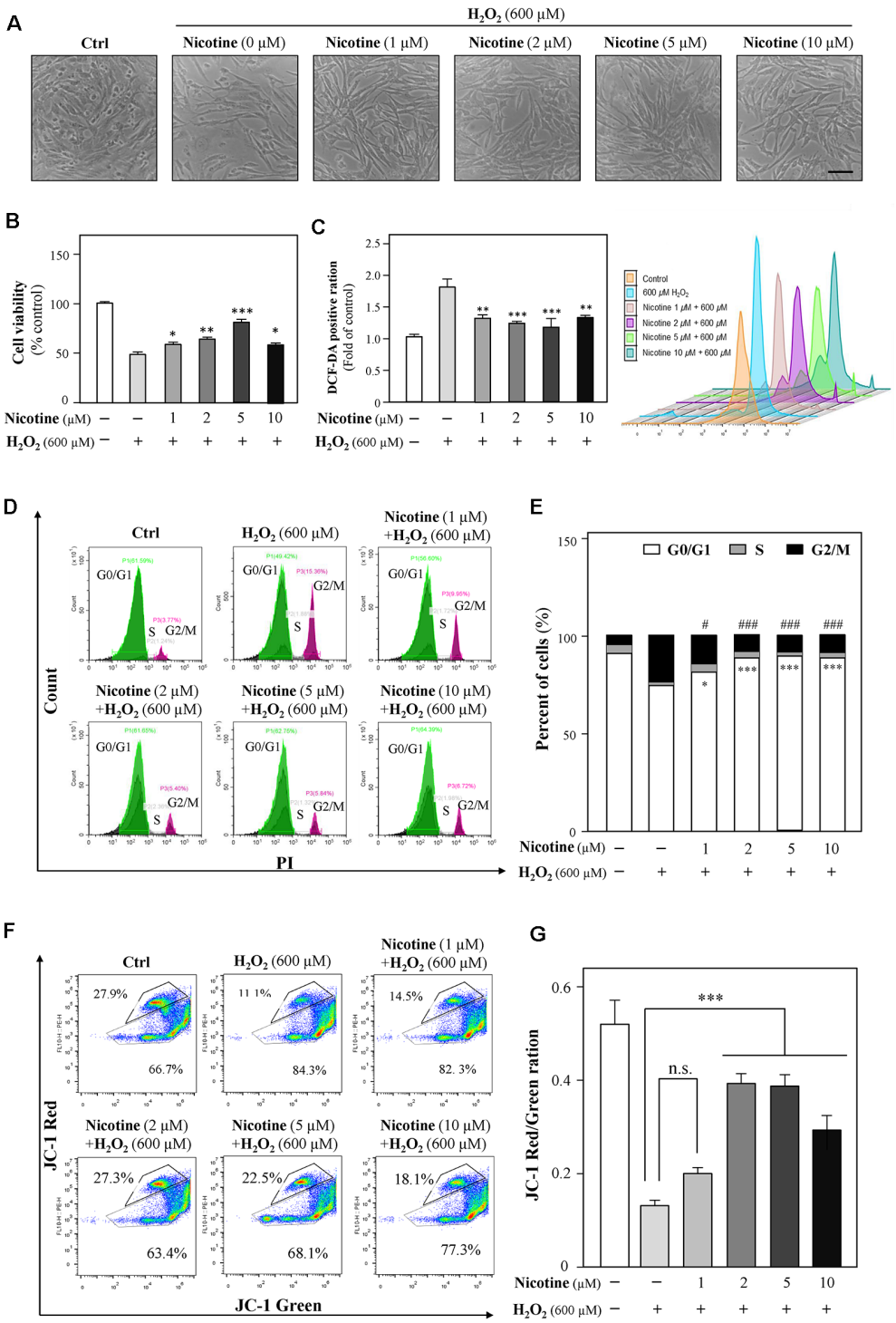

FIGURE 4 | Nicotine suppresses the H_2O_2-induced oxidative injury in HT-22 cells. Cultured HT-22 cells were seeded in six-well plates and incubated in different concentrations of nicotine (1, 2, 5, and 10 μM) for 24 h, followed by the application of H_2O_2 (600 μM) for another 24 h; the control group consists of the untreated cells. **(A)** Representative images of the cell morphology. Bar = 100 μm. **(B)** Cell viability test was performed using CCK-8 kit, and the changes were shown in histograms as percentage with control. **(C)** The amount of intracellular ROS was detected by DCFH-DA using flow cytometry. Mean fluorescence density of the ROS level was calibrated. **(D)** The cell cycle was detected by flow cytometry with Annexin V/PI apoptosis detection kit using a flow cytometer. **(E)** Values are in percentage of apoptotic cell rates of live cells, apoptotic cells, and dead cells, as calibrated from panel **(D)**. **(F)** Representative dot plot of the changed mitochondrial membrane potential using flow cytometry after labeling the fluorescent probe with JC-1. **(G)** Ratios of JC-1 red/green were shown in histograms. All data in the bar charts represent mean ± SEM, $n = 3$. $^{*}p < 0.05$, $^{**}p < 0.01$, $^{***}p < 0.001$, and $^{\#}p < 0.05$, $^{\#\#\#}p < 0.001$ vs. control group. n.s., no significance.

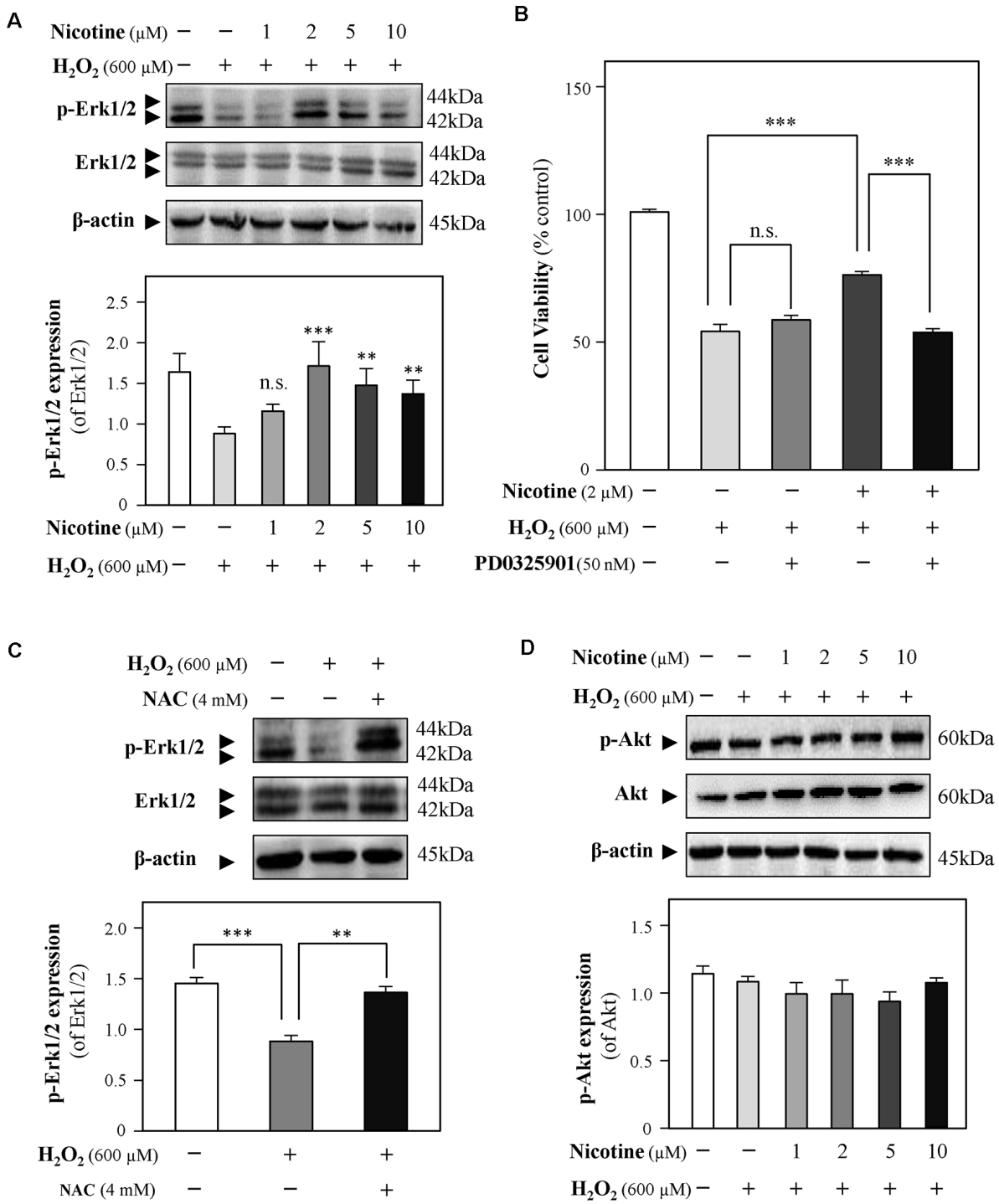

FIGURE 5 | Nicotine reverses H_2O_2-induced oxidative damage through the Erk signaling pathway. Cultured HT-22 cells were treated with or without nicotine (1, 2, 5, and 10 μM) for 24 h, followed by H_2O_2 (600 μM) treatment in the presence or absence of PD0325901 (an inhibitor of Erk1/2, 50 nM) for 24 h or in the presence or absence of NAC (4 mM) for 24 h. The control group consists of the untreated cells. **(A)** The protein expressions of p-Erk1/2 and Erk1/2 were determined by western blotting (upper panel). Expression of β-actin served as loading control. The quantitation of p-Erk1/2 and Erk1/2 expressions was calibrated (lower panel). **(B)** Cell viability test was performed using CCK-8 kit, and the changes were shown in histograms as percentage with control. **(C)** The protein expressions of p-Erk1/2 and Erk1/2 were determined by western blotting (upper panel). Expression of β-actin served as loading control. The quantitation of p-Erk1/2 and Erk1/2 expressions was calibrated (lower panel). **(D)** The protein expressions of p-Akt and Akt were determined by western blotting (upper panel). Expression of β-actin served as loading control. The quantitation of p-Akt and Akt expressions was calibrated (lower panel). All data in bar charts represent mean ± SEM, $n = 3$. $^{**}p < 0.01$, $^{***}p < 0.001$ vs. control group. NAC, *N*-acetylcysteine. n.s., no significance.

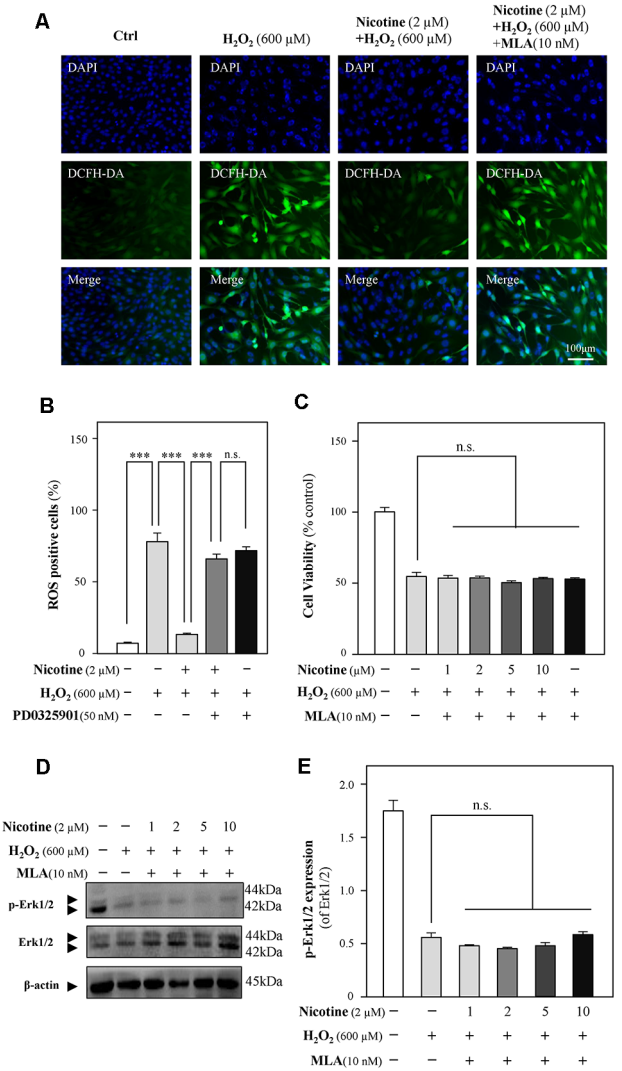

FIGURE 6 | The Erk1/2 signaling pathway is activated by the binding of nicotine to α7-nAChRs. Cultured HT-22 cells were treated with or without nicotine (1, 2, 5, and 10 μM) for 24 h, followed by the application of H_2O_2 (600 μM) in the presence or absence of MLA (an inhibitor of α7-nAChRs, 10 nM) for another 24 h; the control group consists of the untreated cells. **(A)** Cells were stained with DCFH-DA. Cover glasses with cells were fixed and observed under a fluorescent microscope. Bar = 100 μm. **(B)** Mean fluorescence density of ROS level was calibrated. **(C)** Cell viability test was performed using CCK-8 kit, and the changes were shown in histograms as percentage with control. **(D)** The protein expressions of p-Erk1/2 and Erk1/2 were determined by western blotting (upper panel). Expression of β-actin served as loading control. **(E)** The quantitation of p-Erk1/2 and Erk1/2 expressions was calibrated from panel **(D)**. All data in bar charts represent mean ± SEM, $n = 3$. n.s., no significance. $^{***}p < 0.001$ vs. control group. MLA, methyllycaconitine citrate.

significant reduction in mitochondrial membrane potential (**Figure 2A**). Since mitochondrial depolarization has been suggested to be a requirement for cell apoptosis (Ankarcrona et al., 1995; Heiskanen et al., 1999), we further explored whether oxidative injury is related to cell apoptosis. Moreover, we found that apoptosis was not involved in H_2O_2-induced HT-22 cell oxidative injury (**Figures 2C–F**), which is in accordance with the study demonstrated by Xu et al. (2014). On the contrary, evidence clearly demonstrates that oxidative stress induces HT-22 cell injury *via* apoptosis or ferroptosis (Yoo et al., 2017; Yeo et al., 2019). Characteristics of cell injury in response to oxidative stress in HT-22 cells shown in these studies suggest oxidative stress-induced neuronal injury is related to multiple molecular mechanisms. In the current study, we confirmed that H_2O_2-induced oxidative damage mainly changes the cell cycle, inhibits cell proliferation, and triggers mitochondrial depolarization.

Many studies have described the neuroprotective effects of nicotine, including promoting newborn neuron survival in adult olfactory bulb (Mechawar et al., 2004), ameliorating dopamine neuron damage (Liu et al., 2012), decreasing NMDA-mediated neuroexcitotoxicity (Gahring et al., 2003), and preventing Aβ-mediated neurotoxicity (Fodero et al., 2004; Yu et al., 2011). In this study, we explored the potential protective ability of nicotine on H_2O_2-induced oxidative damage in HT-22 cells. We observed that pretreated nicotine at low concentrations (1, 2, 5, and 10 μM) could significantly decrease oxidative damages including increasing cell viability, recovering the cell cycle from G2/M phase arrest, and preventing mitochondrial dysfunctions *via* inhibiting ROS generations (**Figure 4**). However, the antioxidative abilities of 10-μM nicotine against H_2O_2 showed a decrease. The result further indicated that overdose of nicotine might result in side effects on CNS, such as nicotine addiction. Overdose of nicotine has shown a significant decrease in the neuronal densities and the increase in excitotoxicity in the hippocampus (Ferrea and Winterer, 2009). Our results highlight the robust neuroprotection of the application of nicotine at low concentrations.

The underlying mechanisms of nicotine against oxidative damages including alternation of cell cycle, inhibition of cell proliferation, and mitochondrial dysfunctions in HT-22 cells remain to be identified. Therefore, the extracellular signaling pathway by the application of nicotine was investigated. Nicotine exerts its function mainly *via* activating nicotinic acetylcholine receptors (nAChRs; Dani and Heinemann, 1996). Among different nAChRs, the α4/β2 receptors and α7 receptors have been shown to play a dominant role in the CNS (Hsu et al., 1997; Fodero et al., 2004; Liu et al., 2009; Lewis et al., 2018; Xu et al., 2019). Hence, we considered whether the neuroprotective effects of nicotine against oxidative damage could be mediated by the activation of α4/β2-nAChRs or α7-nAChRs, and then antioxidative effects of α4/β2-nAChRs which respond to nicotine in HT-22 cells were determined. As shown in **Supplementary Figure 4**, dihydro-β-erythroidine hydrobromide (DHβE), an antagonist of α4/β2 receptor, hardly influenced the neuroprotective effects of nicotine. However, we found that the antioxidative effects of nicotine could be abolished by the α7-nAChR-selective antagonist MLA, implying that α7-nAChRs play a critical role in HT-22 cell oxidative injury (**Figure 6**). Literatures have documented that nicotine acts its neuroprotective functions on oxidative stress *via* the activation of α7-nAChRs *in vitro* and *in vivo*, for example in astrocytes of mice, hippocampal cells of rats, and PC12 cells

(Guan et al., 2003; Liu and Zhao, 2004; Liu et al., 2015; Hritcu et al., 2017). We first evaluated the potential role of α7-nAChRs in the regulation of oxidative stress in HT-22 cells. An agonist of α7-nAChRs, GTS-21, significantly prevented neuroinflammation in mice (Nullens et al., 2016), which further suggests that the activation of α7-nAChRs plays a key role in neuroprotection. Moreover, the activation of α7-nAChRs promotes neuronal survival against Aβ-induced neurotoxicity *via* suppressing apoptosis in SH-SY5Y cells (Xu et al., 2019). Taken together, these investigations implied that an agonist of α7-nAChRs could be developed as a therapeutic agent against neurodegeneration.

Multiple mechanisms were involved in the neuroprotective effects of nicotine, such as inhibition of astrocyte activation, PI3K signaling pathway, apoptotic signaling pathway, Wnt/β-catenin signaling pathway, and Erk1/2 signaling pathway (Fodero et al., 2004; Yu et al., 2011; Liu et al., 2012; Lombardo and Maskos, 2015). The phosphorylation of Erk1/2 (p-Erk1/2) is known to be induced by nicotine *in vivo* (Brunzell et al., 2003) and *in vitro* (Dajas-Bailador et al., 2002), implying that nicotine might activate α7-nAChRs to initiate the signaling cascade that results in Erk phosphorylation. In the current study, nicotine significantly upregulated p-Erk1/2 in HT-22 cells (**Figure 5**). Upregulated p-Erk1/2 was significantly abolished by the application of an α7-nAChR antagonist, MLA (**Figures 6D,E**). Besides, an Erk1/2 inhibitor, PD0325901, remarkably abolished the neuroprotective effects of nicotine. These findings suggest that the activation of the α7-nAChRs/Erk1/2 signaling pathway contributes to the neuroprotection of nicotine on oxidative injury in HT-22 cells. Previous study showed that the Erk1/2 signaling pathway could be activated by nicotine *via* α7-nAChR activation in SH-SY5Y cells and rat hippocampal cells (Dajas-Bailador et al., 2002), which is consistent with our work. Similarly, α7-nAChR activation protected from 1-methyl-4-phenylpyridinium-induced cell apoptosis *via* the Erk/p53 signaling pathway in SY5Y cells (Xu et al., 2019). Evidence, on the contrary, demonstrated that exposure of α7-nAChRs to nanomolar Aβ42 stimulated Erk2 MAPK cascade in the hippocampus of Tg2576 mice carrying a human APP transgene with K670N-M671L mutation (Dineley et al., 2001), indicating that the α7-nAChRs/Erk2 signaling pathway might mediate neurodegeneration. However, the specific nAChR involved and its potential role in neuroprotective and neurodegenerative effects remain to be clarified.

Additionally, nicotine activated Erk1/2 phosphorylation *via* CaMKII or glutamate receptor rather than binding to its α7-nAChRs in cultured primary cortical neurons (Steiner et al., 2007; Chen et al., 2018). One possible reason leading to such inconsistency might be the profound different distribution of nAChRs in the hippocampus and cortex (Séguéla et al., 1993; Picciotto et al., 1995). Furthermore, it has been reported that α3/β4-nAChR is responsible for Erk1/2 phosphorylation in PC12 cells (Nakayama et al., 2006). However, Rebecca and colleagues showed that α-conotoxin Au1B, a specific antagonist of α3/β4-nAChRs, could not inhibit Erk1/2 phosphorylation (Steiner et al., 2007), indicating that α3/β4-nAChRs might be insufficient to activate Erk1/2. Here, we first found that nicotine could have neuroprotective effects in HT-22 cells from oxidative injury through α7-nAChR activation and then promote the Erk1/2 signaling pathway. In addition, the PI3K/Akt signaling pathway has also been implicated in nicotine-mediated neuroprotection (Steiner et al., 2007; Takeuchi et al., 2009; Huang et al., 2012). However, we found that the PI3K/Akt signaling pathway was not influenced by the application of either H_2O_2 or nicotine (**Figure 5D**). Besides, LY294002, a PI3K/Akt inhibitor, could not inhibit neuroprotection of nicotine (data not shown). Consistent to our data, the PI3K/Akt signaling pathway was not involved in nicotine's neuroprotective activation against 1-methyl-4-phenylpyridinium-induced cell apoptosis in SH-SY5Y cells (Xu et al., 2019).

Nicotine can be physiologically metabolized to nornicotine in CNS in human. Specifically, nornicotine was shown to reduce soluble Aβ peptide aggregation based on alteration of amyloid folding (Dajas-Bailador et al., 2000). This suggests a purported ability of nicotine as a neuroprotective agent. So, the potential efforts of nicotine in the application of oxidative-induced neuronal injury could be further explored.

In conclusion, outcomes show that nicotine exerts its neuroprotection against H_2O_2-induced oxidative injury *via* activating the α7-nAChRs/Erk1/2 signaling pathway in HT-22 cells, which could provide new mechanistic insights into the role of nicotine in oxidative stress. The low dose of nicotine could be developed as a novel therapeutic strategy in oxidative stress-related neurodegenerative disorders, such as AD and PD.

DATA AVAILABILITY STATEMENT

All datasets presented in this study are included in the article/**Supplementary Material**.

AUTHOR CONTRIBUTIONS

YD and WB performed most of the experiments. YD conceived the project and designed the experiments. KZ, SW, YX, and BL participated in data analysis. All authors contributed to the article and approved the submitted version.

FUNDING

This work was supported by the Innovative Research Group Project of the National Natural Science Foundation of China (31700932), Shenzhen Science and Technology Innovation Committee for Basic Research (JCYJ20170307170742519), Shenzhen University funding (C0915), and SZU medical young scientists' program (71201-000001).

SUPPLEMENTARY MATERIAL

The Supplementary Material for this article can be found online at: https://www.frontiersin.org/articles/10.3389/fnmol.2020.557647/full#supplementary-material.

REFERENCES

Ankarcrona, M., Dypbukt, J. M., Bonfoco, E., Zhivotovsky, B., Orrenius, S., Lipton, S. A., et al. (1995). Glutamate-induced neuronal death: a succession of necrosis or apoptosis depending on mitochondrial function. *Neuron* 15, 961–973. doi: 10.1016/0896-6273(95)90186-8

Barr, J., Sharma, C. S., Sarkar, S., Wise, K., Dong, L., Periyakaruppan, A., et al. (2007). Nicotine induces oxidative stress and activates nuclear transcription factor κ B in rat mesencephalic cells. *Mol. Cell. Biochem.* 297, 93–99. doi: 10.1007/s11010-006-9333-1

Behl, C., Davis, J. B., Lesley, R., and Schubert, D. (1994). Hydrogen peroxide mediates amyloidβ protein toxicity. *Cell* 77, 817–827. doi: 10.1016/0092-8674(94)90131-7

Benowitz, N. L. (2009). Pharmacology of nicotine: addiction, smoking-induced disease and therapeutics. *Annu. Rev. Pharmacol. Toxicol.* 49, 57–71. doi: 10.1146/annurev.pharmtox.48.113006.094742

Benowitz, N. L. (2010). Nicotine addiction. *N. Engl. J. Med.* 362, 2295–2303. doi: 10.1056/NEJMra0809890

Brunzell, D. H., Russell, D. S., and Picciotto, M. R. (2003). *In vivo* nicotine treatment regulates mesocorticolimbic CREB and ERK signaling in C57Bl/6J mice. *J. Neurochem.* 84, 1431–1441. doi: 10.1046/j.1471-4159.2003.01640.x

Cao, S. S., and Kaufman, R. J. (2014). Endoplasmic reticulum stress and oxidative stress in cell fate decision and human disease. *Antioxid. Redox Signal.* 21, 396–413. doi: 10.1089/ars.2014.5851

Cardinale, A., Nastrucci, C., Cesario, A., and Russo, P. (2012). Nicotine: specific role in angiogenesis, proliferation and apoptosis. *Crit. Rev. Toxicol.* 42, 68–89. doi: 10.3109/10408444.2011.623150

Chen, X., Guo, C., and Kong, J. (2012). Oxidative stress in neurodegenerative diseases. *Neural Regen. Res.* 7, 376–385. doi: 10.3969/j.issn.1673-5374.2012.05.009

Chen, Q., Liu, J., and Merrett, J. (2000). Apoptosis or senescence-like growth arrest: influence of cell-cycle position, p53, p21 and bax in H_2O_2 response of normal human fibroblasts. *Biochem. J.* 347, 543–551. doi: 10.1042/0264-6021:3470543

Chen, T., Wang, Y., Zhang, T., Zhang, B., Chen, L., Zhao, L., et al. (2018). Simvastatin enhances activity and trafficking of α7 nicotinic acetylcholine receptor in hippocampal neurons through PKC and CaMKII signaling pathways. *Front. Pharmacol.* 9:362. doi: 10.3389/fphar.2018.00362

Coyle, J. T., and Puttfarcken, P. (1993). Oxidative stress, glutamate and neurodegenerative disorders. *Science* 262, 689–695. doi: 10.1126/science.7901908

Dai, S., Chen, T., Wang, Y., Zhu, J., Luo, P., Rao, W., et al. (2014). Sirt3 attenuates hydrogen peroxide-induced oxidative stress through the preservation of mitochondrial function in HT22 cells. *Int. J. Mol. Med.* 34, 1159–1168. doi: 10.3892/ijmm.2014.1876

Dajas-Bailador, F. A., Lima, P. A., and Wonnacott, S. (2000). The α7 nicotinic acetylcholine receptor subtype mediates nicotine protection against NMDA excitotoxicity in primary hippocampal cultures through a Ca^{2+} dependent mechanism. *Neuropharmacology* 39, 2799–2807. doi: 10.1016/s0028-3908(00)00127-1

Dajas-Bailador, F. A., Soliakov, L., and Wonnacott, S. (2002). Nicotine activates the extracellular signal-regulated kinase 1/2 *via* the α7 nicotinic acetylcholine receptor and protein kinase A, in SH-SY5Y cells and hippocampal neurones. *J. Neurochem.* 80, 520–530. doi: 10.1046/j.0022-3042.2001.00725.x

Dani, J. A., and Heinemann, S. (1996). Molecular and cellular aspects of nicotine abuse. *Neuron* 16, 905–908. doi: 10.1016/s0896-6273(00)80112-9

Debattisti, V., Gerencser, A. A., Saotome, M., Das, S., and Hajnóczky, G. (2017). ROS control mitochondrial motility through p38 and the motor adaptor Miro/Trak. *Cell Rep.* 21, 1667–1680. doi: 10.1016/j.celrep.2017.10.060

Desagher, S., Glowinski, J., and Prémont, J. (1997). Pyruvate protects neurons against hydrogen peroxide-induced toxicity. *J. Neurosci.* 17, 9060–9067. doi: 10.1523/JNEUROSCI.17-23-09060.1997

Dineley, K. T., Westerman, M., Bui, D., Bell, K., Ashe, K. H., and Sweatt, J. D. (2001). β-amyloid activates the mitogen-activated protein kinase cascade *via* hippocampal α7 nicotinic acetylcholine receptors: *in vitro* and *in vivo* mechanisms related to Alzheimer's disease. *J. Neurosci.* 21, 4125–4133. doi: 10.1523/JNEUROSCI.21-12-04125.2001

Echeverria, V., and Zeitlin, R. (2012). Cotinine: a potential new therapeutic agent against Alzheimer's disease. *CNS Neurosci Ther.* 18, 517–523. doi: 10.1111/j.1755-5949.2012.00317.x

Fahn, S., and Cohen, G. (1992). The oxidant stress hypothesis in Parkinson's disease: evidence supporting it. *Ann. Neurol.* 32, 804–812. doi: 10.1002/ana.410320616

Ferrea, S., and Winterer, G. (2009). Neuroprotective and neurotoxic effects of nicotine. *Pharmacopsychiatry* 42, 255–265. doi: 10.1055/s-0029-1224138

Fodero, L. R., Mok, S. S., Losic, D., Martin, L. L., Aguilar, M. I., Barrow, C. J., et al. (2004). Small DH. α7-nicotinic acetylcholine receptors mediate an $A\beta_{(1-42)}$-induced increase in the level of acetylcholinesterase in primary cortical neurones. *J. Neurochem.* 88, 1186–1193. doi: 10.1046/j.1471-4159.2003.02296.x

Gahring, L. C., Meyer, E. L., and Rogers, S. W. (2003). Nicotine-induced neuroprotection against *N*-methyl-D-aspartic acid or β-amyloid peptide occur through independent mechanisms distinguished by pro-inflammatory cytokines. *J. Neurochem.* 87, 1125–1136. doi: 10.1046/j.1471-4159.2003.02074.x

Gao, J., Liu, S., Xu, F., Liu, Y., Lv, C., Deng, Y., et al. (2018). Trilobatin protects against oxidative injury in neuronal PC12 cells through regulating mitochondrial ROS homeostasis mediated by AMPK/Nrf2/Sirt3 signaling pathway. *Front. Mol. Neurosci.* 11:267. doi: 10.3389/fnmol.2018.00267

Gao, Z., Wang, H., Zhang, B., Wu, X., Zhang, Y., Ge, P., et al. (2018). Trehalose inhibits H_2O_2-induced autophagic death in dopaminergic SH-SY5Y cells *via* mitigation of ROS-dependent endoplasmic reticulum stress and AMPK activation. *Int. J. Med. Sci.* 15, 1014–1024. doi: 10.7150/ijms.25656

Guan, Z. Z., Yu, W. F., and Nordberg, A. (2003). Dual effects of nicotine on oxidative stress and neuroprotection in PC12 cells. *Neurochem. Int.* 43, 243–249. doi: 10.1016/s0197-0186(03)00009-3

Harris, M. E., Hensley, K., Butterfield, D. A., Leedle, R. A., and Carney, J. M. (1995). Direct evidence of oxidative injury produced by the Alzheimer's β-amyloid peptide (1–40) in cultured hippocampal neurons. *Exp. Neurol.* 131, 193–202. doi: 10.1016/0014-4886(95)90041-1

Hatsukami, D. K., Stead, L. F., and Gupta, P. C. (2008). Tobacco addiction. *Lancet* 371, 2027–2038. doi: 10.1016/S0140-6736(08)60871-5

Heiskanen, K. M., Bhat, M. B., Wang, H. W., Ma, J., and Nieminen, A. L. (1999). Mitochondrial depolarization accompanies cytochrome c release during apoptosis in PC6 cells. *J. Biol. Chem.* 274, 5654–5658. doi: 10.1074/jbc.274.9.5654

Hoffmann, F., Martin, B. A., Sibley, R. B., and Tsay, S. S. (1990). Pollen germination is impeded by tap water. *Environ. Pollut.* 63, 179–187. doi: 10.1016/0269-7491(90)90066-L

Hritcu, L., Ionita, R., Motei, D. E., Babii, C., Stefan, M., and Mihasan, M. (2017). Nicotine versus 6-hydroxy-l-nicotine against chlorisondamine induced memory impairment and oxidative stress in the rat hippocampus. *Biomed. Pharmacother.* 86, 102–108. doi: 10.1016/j.biopha.2016.12.008

Hsu, Y. N., Edwards, S. C., and Wecker, L. (1997). Nicotine enhances the cyclic AMP-dependent protein kinase-mediated phosphorylation of α 4 subunits of neuronal nicotinic receptors. *J. Neurochem.* 69, 2427–2431. doi: 10.1046/j.1471-4159.1997.69062427.x

Huang, X., Cheng, Z., Su, Q., Zhu, X., Wang, Q., Chen, R., et al. (2012). Neuroprotection by nicotine against colchicine-induced apoptosis is mediated by PI3-kinase-Akt pathways. *Int. J. Neurosci.* 122, 324–332. doi: 10.3109/00207454.2012.657377

Khan, J. Y., and Black, S. M. (2003). Developmental changes in murine brain antioxidant enzymes. *Pediatr. Res.* 54, 77–82. doi: 10.1203/01.PDR.0000065736.69214.20

Kim, H. K., Nilius, B., Kim, N., Ko, K. S., Rhee, B. D., and Han, J. (2016). Cardiac response to oxidative stress induced by mitochondrial dysfunction. *Rev. Physiol. Biochem. Pharmacol.* 170, 101–127. doi: 10.1007/112_2015_5004

Kim, J., and Wong, P. K. Y. (2009). Loss of ATM impairs proliferation of neural stem cells through oxidative stress-mediated p38 MAPK signaling. *Stem Cells* 27, 1987–1998. doi: 10.1002/stem.125

Lee, G. W., and Kim, M. S. (2019). Water extract of Samultang reduces apoptotic cell death by H_2O_2-induced oxidative injury in SK-N-MC cells. *Korean J. Physiol. Pharmacol.* 13, 139–145. doi: 10.4196/kjpp.2009.13.3.139

Lewis, A. S., Pittenger, S. T., Mineur, Y. S., Stout, D., Smith, P. H., and Picciotto, M. R. (2018). Bidirectional regulation of aggression in mice by hippocampal α-7 nicotinic acetylcholine receptors. *Neuropsychopharmacology* 43, 1267–1275. doi: 10.1038/npp.2017.276

Liu, J. Y., Guo, F., Wu, H. L., Wang, Y., and Liu, J. S. (2017). Midazolam anesthesia protects neuronal cells from oxidative stress-induced death *via* activation of the JNK-ERK pathway. *Mol. Med. Rep.* 15, 169–179. doi: 10.3892/mmr.2016.6031

Liu, H., Liu, W., Zhou, X., Long, C., Kuang, X., Hu, J., et al. (2017). Protective effect of lutein on ARPE-19 cells upon H_2O_2-induced G2/M arrest. *Mol. Med. Rep.* 16, 2069–2074. doi: 10.3892/mmr.2017.6838

Liu, J., Li, L., and Suo, W. Z. (2009). HT22 hippocampal neuronal cell line possesses functional cholinergic properties. *Life Sci.* 84, 267–271. doi: 10.1016/j.lfs.2008.12.008

Liu, F., Lu, J., Manaenko, A., Tang, J., and Hu, Q. (2018). Mitochondria in ischemic stroke: new insight and implications. *Aging Dis.* 9, 924–937. doi: 10.14336/AD.2017.1126

Liu, Y., Hao, S., Yang, B., Fan, Y., Qin, X., Chen, Y., et al. (2017). Wnt/β-catenin signaling plays an essential role in α7 nicotinic receptor-mediated neuroprotection of dopaminergic neurons in a mouse Parkinson's disease model. *Biochem. Pharmacol.* 140, 115–123. doi: 10.1016/j.bcp.2017.05.017

Liu, Y., Hu, J., Wu, J., Zhu, C., Hui, Y., Han, Y., et al. (2012). α7 nicotinic acetylcholine receptor-mediated neuroprotection against dopaminergic neuron loss in an MPTP mouse model *via* inhibition of astrocyte activation. *J. Neuroinflammation.* 9:98. doi: 10.1186/1742-2094-9-98

Liu, Y., Zeng, X., Hui, Y., Zhu, C., Wu, J., Taylor, D. H., et al. (2015). Activation of α7 nicotinic acetylcholine receptors protects astrocytes against oxidative stress-induced apoptosis: implications for Parkinson's disease. *Neuropharmacology* 91, 87–96. doi: 10.1016/j.neuropharm.2014.11.028

Liu, Q., and Zhao, B. (2004). Nicotine attenuates β-amyloid peptide-induced neurotoxicity, free radical and calcium accumulation in hippocampal neuronal cultures. *Br. J. Pharmacol.* 141, 746–754. doi: 10.1038/sj.bjp.0705653

Lombardo, S., and Maskos, U. (2015). Role of the nicotinic acetylcholine receptor in Alzheimer's disease pathology and treatment. *Neuropharmacology* 96, 255–262. doi: 10.1016/j.neuropharm.2014.11.018

Mechawar, N., Saghatelyan, A., Grailhe, R., Scoriels, L., Gheusi, G., Gabellec, M. M., et al. (2004). Nicotinic receptors regulate the survival of newborn neurons in the adult olfactory bulb. *Proc. Natl. Acad. Sci. U S A* 101, 9822–9826. doi: 10.1073/pnas.0403361101

Moreno-Gonzalez, I., Estrada, L. D., Sanchez-Mejias, E., and Soto, C. (2013). Smoking exacerbates amyloid pathology in a mouse model of Alzheimer's disease. *Nat. Commun.* 4:1495. doi: 10.1038/ncomms2494

Motaghinejad, M., Fatima, S., Karimian, M., and Ganji, S. (2016). Protective effects of forced exercise against nicotine-induced anxiety, depression and cognition impairment in rat. *J. Basic Clin. Physiol. Pharmacol.* 27, 19–27. doi: 10.1515/jbcpp-2014-0128

Nakayama, H., Shimoke, K., Isosaki, M., Satoh, H., Yoshizumi, M., and Ikeuchi, T. (2006). Subtypes of neuronal nicotinic acetylcholine receptors involved in nicotine-induced phosphorylation of extracellular signal-regulated protein kinase in PC12 cells. *Neurosci. Lett.* 392, 101–104. doi: 10.1016/j.neulet.2005.09.003

Nielsen, S. S., Franklin, G. M., Longstreth, W. T., Swanson, P. D., and Checkoway, H. (2013). Nicotine from edible solanaceae and risk of Parkinson disease. *Ann. Neurol.* 74, 472–477. doi: 10.1002/ana.23884

Nullens, S., Staessens, M., Peleman, C., Schrijvers, D. M., Malhotra-Kumar, S., Francque, S., et al. (2016). Effect of GTS-21, an α7 nicotinic acetylcholine receptor agonist, on CLP-induced inflammatory, gastrointestinal motility, and colonic permeability changes in mice. *Shock* 45, 450–459. doi: 10.1097/SHK.0000000000000519

Oddo, S., Caccamo, A., Green, K. N., Liang, K., Tran, L., Chen, Y., et al. (2005). Chronic nicotine administration exacerbates tau pathology in a transgenic model of Alzheimer's disease. *Proc. Natl. Acad. Sci. U S A* 102, 3046–3051. doi: 10.1073/pnas.0408500102

Oliveira-da-Silva, A., Vieira, F. B., Cristina-Rodrigues, F., Filgueiras, C. C., Manhães, A. C., and Abreu-Villaça, Y. (2009). Increased apoptosis and reduced neuronal and glial densities in the hippocampus due to nicotine and ethanol exposure in adolescent mice. *Int. J. Dev. Neurosci.* 27, 539–548. doi: 10.1016/j.ijdevneu.2009.06.009

Olmez, I., and Ozyurt, H. (2012). Reactive oxygen species and ischemic cerebrovascular disease. *Neurochem. Int.* 60, 208–212. doi: 10.1016/j.neuint.2011.11.009

Parada, E., Egea, J., Romero, A., del Barrio, L., García, A. G., and López, M. G. (2010). Poststress treatment with PNU282987 can rescue SH-SY5Y cells undergoing apoptosis *via* α7 nicotinic receptors linked to a Jak2/Akt/HO-1 signaling pathway. *Free Radic. Biol. Med.* 249, 1815–1821. doi: 10.1016/j.freeradbiomed.2010.09.017

Patel, M., Day, B. J., Crapo, J. D., Fridovich, I., and McNamara, J. O. (1996). Requirement for superoxide in excitotoxic cell death. *Neuron* 16, 345–355. doi: 10.1016/s0896-6273(00)80052-5

Picciotto, M. R., Zoli, M., Lena, C., Bessis, A., Lallemand, Y., LeNovere, N., et al. (1995). Abnormal avoidance learning in mice lacking functional high-affinity nicotine receptor in the brain. *Nature* 374, 65–67. doi: 10.1038/374065a0

Pizarro, J. G., Folch, J., Vazquez De la Torre, A., Verdaguer, E., Junyent, F., Jordán, J., et al. (2009). Oxidative stress-induced DNA damage and cell cycle regulation in B65 dopaminergic cell line. *Free Radic. Res.* 43, 985–994. doi: 10.1080/10715760903159188

Richter, M., Nickel, C., Apel, L., Kaas, A., Dodel, R., Culmsee, C., et al. (2015). SK channel activation modulates mitochondrial respiration and attenuates neuronal HT-22 cell damage induced by H_2O_2. *Neurochem. Int.* 81, 63–75. doi: 10.1016/j.neuint.2014.12.007

Riley, P. A. (1994). Free radicals in biology: oxidative stress and the effects of ionizing radiation. *Int. J. Radiat. Biol.* 65, 27–33. doi: 10.1080/09553009414550041

Rothbard, J. B., Rothbard, J. J., Soares, L., Fathman, C. G., and Steinman, L. (2018). Identification of a common immune regulatory pathway induced by small heat shock proteins, amyloid fibrils and nicotine. *Proc. Natl. Acad. Sci. U S A* 115, 7081–7086. doi: 10.1073/pnas.1804599115

Saad, A. B., Rjeibi, I., Brahmi, N., Elaloui, E., and Zouari, N. (2020). Nicotine-induced oxidative stress, testis injury, AChE inhibition and brain damage alleviated by *Mentha spicata*. *Inflammopharmacology* 28, 939–948. doi: 10.1007/s10787-019-00650-0

Séguéla, P., Wadiche, J., Dineley-Miller, K., Dani, J. A., and Patrick, J. W. (1993). Molecular cloning, functional properties and distribution ofrat brain α7: a nicotinic cation channel highly permeable tocalcium. *J. Neurosci.* 13, 596–604. doi: 10.1523/JNEUROSCI.13-02-00596.1993

Shim, S. B., Lee, S. H., Chae, K. R., Kim, C. K., Hwang, D. Y., Kim, B. G., et al. (2008). Nicotine leads to improvements in behavioral impairment and an increase in the nicotine acetylcholine receptor in transgenic mice. *Neurochem. Res.* 33, 1783–1788. doi: 10.1007/s11064-008-9629-5

Sinha, K., Das, J., Pal, P. B., and Sil, P. C. (2013). Oxidative stress: the mitochondria-dependent and mitochondria-independent pathways of apoptosis. *Arch. Toxicol.* 87, 1157–1180. doi: 10.1007/s00204-013-1034-4

Slotkin, T. A., Skavicus, S., Card, J., Levin, E. D., and Seidle, F. J. (2015). Amelioration strategies fail to prevent tobacco smoke effects on neurodifferentiation: nicotinic receptor blockade, antioxidants, methyl donors. *Toxicology* 333, 63–75. doi: 10.1016/j.tox.2015.04.005

Smiley, S. T., Reers, M., Mottola-Hartshorn, C., Lin, M., Chen, A., Smith, T. W., et al. (1991). Intracellular heterogeneity in mitochondrial membrane potentials revealed by a J-aggregate-forming lipophilic cation JC-1. *Proc. Natl. Acad. Sci. U S A* 88, 3671–3675. doi: 10.1073/pnas.88.9.3671

Smith, M. A., Perry, G., Richey, P. L., Sayre, L. M., Anderson, V. E., Beal, M. F., et al. (1996). Oxidative damage in Alzheimer's. *Nature* 382, 120–121. doi: 10.1038/382120b0

Steiner, R. C., Heath, C. J., and Picciotto, M. R. (2007). Nicotine-induced phosphorylation of ERK in mouse primary cortical neurons: evidence for involvement of glutamatergic signaling and CaMKII. *J. Neurochem.* 103, 666–678. doi: 10.1111/j.1471-4159.2007.04799.x

Takeuchi, H., Yanagida, T., Inden, M., Takata, K., Kitamura, Y., Yamakawa, K., et al. (2009). Nicotinic receptor stimulation protects nigral dopaminergic neurons in rotenone-induced Parkinson's disease models. *J. Neurosci. Res.* 87, 576–585. doi: 10.1002/jnr.21869

Tasdogan, A., Kumar, S., Allies, G., Bausinger, J., Beckel, F., Hofemeister, H., et al. (2016). DNA damage-induced HSPC malfunction depends on ROS accumulation downstream of IFN-1 signaling and bid mobilization. *Cell Stem Cell* 19, 752–767. doi: 10.1016/j.stem.2016.08.007

Valverde, M., Lozano-Salgado, J., Fortini, P., Rodriguez-Sastre, M. A., Rojas, E., and Dogliotti, E. (2018). Hydrogen peroxide-induced DNA damage and repair through the differentiation of human adipose-derived mesenchymal stem cells. *Stem Cells Int.* 2018:1615497. doi: 10.1155/2018/1615497

Wang, T., Cheng, J., Wang, S., Wang, X., Jiang, H., Yang, Y., et al. (2018). α-lipoic acid attenuates oxidative stress and neurotoxicity *via* the ERK/Akt-dependent pathway in the mutant hSOD1 related Drosophila model and the NSC34 cell line of amyotrophic lateral sclerosis. *Brain Res. Bull.* 140, 299–310. doi: 10.1016/j.brainresbull.2018.05.019

Wang, S., Huang, L., Zhang, Y., Peng, Y., Wang, X., and Peng, Y. (2018). Protective effects of L-3-n-butylphthalide against H_2O_2-induced injury in neural stem cells by activation of PI3K/Akt and mash1 pathway. *Neuroscience* 393, 164–174. doi: 10.1016/j.neuroscience.2018.10.003

Xu, H., Luo, P., Zhao, Y., Zhao, M., Yang, Y., Chen, T., et al. (2014). Iduna protects HT22 cells from hydrogen peroxide-induced oxidative stress through interfering poly (ADP-ribose) polymerase-1-induced cell death (parthanatos). *Cell. Singal.* 25, 1018–1026. doi: 10.1016/j.cellsig.2013.01.006

Xu, S., Yang, B., Tao, T., Zhang, J., Liu, Y., Hu, J., et al. (2019). Activation of α7-nAChRs protects SH-SY5Y cells from 1-methyl-4-phenylpyridinium-induced apoptotic cell death *via* ERK/p53 signaling pathway. *J. Cell. Physiol.* 234, 18480–18491. doi: 10.1002/jcp.28484

Yeo, H. J., Shina, M. J., Yeo, E. J., Choi, Y. J., Kim, D. W., Kim, D. S., et al. (2019). Tat-CIAPIN1 inhibits hippocampal neuronal cell damage through the MAPK and apoptotic signaling pathways. *Free Radic. Biol. Med.* 135, 68–78. doi: 10.1016/j.freeradbiomed.2019.02.028

Yu, W., Mechawar, N., Krantic, S., and Quirion, R. (2011). α7 Nicotinic receptor activation reduces β-amyloid-induced apoptosis by inhibiting caspase-independent death through phosphatidylinositol 3-kinase signaling. *J. Neurochem.* 119, 848–858. doi: 10.1111/j.1471-4159.2011.07466.x

Yoo, J. M., Lee, B. D., Sok, D. E., Maa, J. Y., and Kim, M. R. (2017). Neuroprotective action of *N*-acetyl serotonin in oxidative stress-induced apoptosis through the activation of both TrkB/CREB/BDNF pathway and Akt/Nrf2/Antioxidant enzyme in neuronal cells. *Redox Biol.* 11, 592–599. doi: 10.1016/j.redox.2016.12.034

Zhang, L., Fang, Y., Cheng, X., Lian, Y., Zeng, Z., Wu, C., et al. (2018). The potential protective effect of curcumin on Amyloid-β-42 induced cytotoxicity in HT-22 cells. *Biomed. Res. Int.* 2018:8134902. doi: 10.1155/2018/8134902

Conflict of Interest: The authors declare that the research was conducted in the absence of any commercial or financial relationships that could be construed as a potential conflict of interest.

Advantages of publishing in Frontiers

OPEN ACCESS
Articles are free to read for greatest visibility and readership

FAST PUBLICATION
Around 90 days from submission to decision

HIGH QUALITY PEER-REVIEW
Rigorous, collaborative, and constructive peer-review

TRANSPARENT PEER-REVIEW
Editors and reviewers acknowledged by name on published articles

Frontiers
Avenue du Tribunal-Fédéral 34
1005 Lausanne | Switzerland

Visit us: www.frontiersin.org
Contact us: frontiersin.org/about/contact

REPRODUCIBILITY OF RESEARCH
Support open data and methods to enhance research reproducibility

DIGITAL PUBLISHING
Articles designed for optimal readership across devices

FOLLOW US
@frontiersin

IMPACT METRICS
Advanced article metrics track visibility across digital media

EXTENSIVE PROMOTION
Marketing and promotion of impactful research

LOOP RESEARCH NETWORK
Our network increases your article's readership